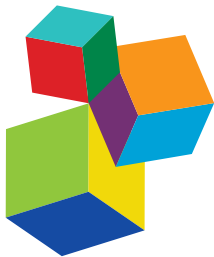


# **MAKING SCIENCE FUN**

## **A TRIBUTE TO OUR COLLEAGUE AND FRIEND**

### **PROF. ANTONIUS G. ROLINK (1953–2017)**

**EDITED BY:** Hermann Eibel, Thomas H. Winkler and Rhodri Ceredig  
**PUBLISHED IN:** Frontiers in Immunology



#### Frontiers Copyright Statement

© Copyright 2007-2019 Frontiers Media SA. All rights reserved.

All content included on this site, such as text, graphics, logos, button icons, images, video/audio clips, downloads, data compilations and software, is the property of or is licensed to Frontiers Media SA ("Frontiers") or its licensees and/or subcontractors. The copyright in the text of individual articles is the property of their respective authors, subject to a license granted to Frontiers.

The compilation of articles constituting this e-book, wherever published, as well as the compilation of all other content on this site, is the exclusive property of Frontiers. For the conditions for downloading and copying of e-books from Frontiers' website, please see the Terms for Website Use. If purchasing Frontiers e-books from other websites or sources, the conditions of the website concerned apply.

Images and graphics not forming part of user-contributed materials may not be downloaded or copied without permission.

Individual articles may be downloaded and reproduced in accordance with the principles of the CC-BY licence subject to any copyright or other notices. They may not be re-sold as an e-book.

As author or other contributor you grant a CC-BY licence to others to reproduce your articles, including any graphics and third-party materials supplied by you, in accordance with the Conditions for Website Use and subject to any copyright notices which you include in connection with your articles and materials.

All copyright, and all rights therein, are protected by national and international copyright laws.

The above represents a summary only. For the full conditions see the Conditions for Authors and the Conditions for Website Use.

ISSN 1664-8714  
ISBN 978-2-88945-751-9  
DOI 10.3389/978-2-88945-751-9

#### About Frontiers

Frontiers is more than just an open-access publisher of scholarly articles: it is a pioneering approach to the world of academia, radically improving the way scholarly research is managed. The grand vision of Frontiers is a world where all people have an equal opportunity to seek, share and generate knowledge. Frontiers provides immediate and permanent online open access to all its publications, but this alone is not enough to realize our grand goals.

#### Frontiers Journal Series

The Frontiers Journal Series is a multi-tier and interdisciplinary set of open-access, online journals, promising a paradigm shift from the current review, selection and dissemination processes in academic publishing. All Frontiers journals are driven by researchers for researchers; therefore, they constitute a service to the scholarly community. At the same time, the Frontiers Journal Series operates on a revolutionary invention, the tiered publishing system, initially addressing specific communities of scholars, and gradually climbing up to broader public understanding, thus serving the interests of the lay society, too.

#### Dedication to Quality

Each Frontiers article is a landmark of the highest quality, thanks to genuinely collaborative interactions between authors and review editors, who include some of the world's best academicians. Research must be certified by peers before entering a stream of knowledge that may eventually reach the public - and shape society; therefore, Frontiers only applies the most rigorous and unbiased reviews.

Frontiers revolutionizes research publishing by freely delivering the most outstanding research, evaluated with no bias from both the academic and social point of view. By applying the most advanced information technologies, Frontiers is catapulting scholarly publishing into a new generation.

#### What are Frontiers Research Topics?

Frontiers Research Topics are very popular trademarks of the Frontiers Journals Series: they are collections of at least ten articles, all centered on a particular subject. With their unique mix of varied contributions from Original Research to Review Articles, Frontiers Research Topics unify the most influential researchers, the latest key findings and historical advances in a hot research area! Find out more on how to host your own Frontiers Research Topic or contribute to one as an author by contacting the Frontiers Editorial Office: [researchtopics@frontiersin.org](mailto:researchtopics@frontiersin.org)

# MAKING SCIENCE FUN

## A TRIBUTE TO OUR COLLEAGUE AND FRIEND PROF. ANTONIUS G. ROLINK (1953–2017)

Topic Editors:

**Hermann Eibel**, University Medical Center, Germany

**Thomas H. Winkler**, Friedrich Alexander University Erlangen, Germany

**Rhodri Ceredig**, National University of Ireland Galway, Ireland



Professor Antonius G. Rolink 1953–2017.  
Image courtesy of the University of Basel.

This Research Topic honors the memory of Prof. Antonius "Ton" G. Rolink (April 19, 1953–August 06, 2017), our colleague, mentor and friend in immunology. It is now over a year since Ton left us. This article collection, authored by many of Ton's friends and colleagues, reflects the huge contribution to cellular and molecular immunology that work emanating directly from Ton's own hands and laboratory have made to the understanding of lymphocyte development. Ton's hard work, expertise, generosity, passion for science and infectious humor were legendary and for all of those lucky enough to have been his colleague, he ensured that science was fun. We take this opportunity of thanking all contributors for submitting their manuscripts; we are sure that Ton would have enjoyed reading and making his own insightful comments on them.

In the form of original research and review articles, these papers cover many of Ton's scientific interests in different aspects of lymphocyte development in mouse and man. In the first section, **Development of hematopoietic cells and lymphocytes**, Klein et al. describe the accumulation of multipotent hematopoietic progenitors in peripheral lymphoid organs of IL-7xFlt3L double transgenic mice and Pang et al. the role of the transcription factor PU.1 on the development of Common Lymphoid Progenitors. In **Early B cell development**, Winkler and Mårtensson review the role of the Pre-B cell receptor in B cell development and papers by Hobeika et al. and Brennecke et al. describe models of inducible B cell development. For **B cell selection, survival and tolerance**, Smulski and Eibel review the role of BAFF and Kowalczyk-Quintans et al. analyse the role of membrane-bound BAFF. The impact of BIM on B cell homeostasis is discussed by Liu et al. The role of the MEK-ERK pathway in B cell tolerance is discussed by Greaves et al. and the transcriptional regulation of germinal center development is reviewed by Song and Matthias. For **Hematological diseases**, Ghia reviews how studies of B cell development help the understanding of Leukemia development, Kim and Schaniel review how iPS technology helps the understanding of hematological diseases and Hellmann et al. describe development of new therapeutic antibody drug conjugates. Finally, in **T cell development, homeostasis and graft vs. host disease**, Heiler et al. describe the therapeutic effects of IL-2/anti-IL-2 immune complexes in GvHD, Calvo-Asensio et al. describe the DNA damage response of thymocyte progenitors and Mori and Pieters review the role of Coronin 1 in T cell survival.

Cover image of GFP+ pro-B cells growing on stromal cells.  
Image courtesy of Dr Julia Merkenschlager, Rockefeller University.

**Citation:** Eibel, H., Winkler, T. H., Ceredig, R., eds. (2019). Making Science Fun – A Tribute to Our Colleague and Friend, Prof. Antonius G. Rolink (1953–2017). Lausanne: Frontiers Media. doi: 10.3389/978-2-88945-751-9

# Table of Contents

- 06 Editorial: Making Science Fun – A Tribute to Our Colleague and Friend, Prof. Antonius G. Rolink (1953–2017)**  
Hermann Eibel, Thomas Winkler and Rhodri Ceredig

## DEVELOPMENT OF HEMATOPOIETIC CELLS AND LYMPHOCYTES

- 19 Accumulation of Multipotent Hematopoietic Progenitors in Peripheral Lymphoid Organs of Mice Over-expressing Interleukin-7 and Flt3-Ligand**  
Fabian Klein, Lilly von Muenchow, Giuseppina Capoferri, Stefan Heiler, Llucia Alberti-Servera, Hannie Rolink, Corinne Engdahl, Michael Rolink, Mladen Mitrovic, Grozdan Cvijetic, Jan Andersson, Rhodri Ceredig, Panagiotis Tsapogas and Antonius Rolink
- 37 PU.1 is Required for the Developmental Progression of Multipotent Progenitors to Common Lymphoid Progenitors**  
Swee Heng Milon Pang, Carolyn A. de Graaf, Douglas J. Hilton, Nicholas D. Huntington, Sebastian Carotta, Li Wu and Stephen L. Nutt

## EARLY B CELL DEVELOPMENT

- 48 The Role of the Pre-B Cell Receptor in B Cell Development, Repertoire Selection, and Tolerance**  
Thomas H. Winkler and Inga-Lill Mårtensson
- 58 Conditional Selection of B Cells in Mice With an Inducible B Cell Development**  
Elias Hobeika, Marcel Dautzenberg, Ella Levit-Zerdoun, Roberta Pelanda and Michael Reth
- 73 Induced B Cell Development in Adult Mice**  
Anne-Margarete Brennecke, Sandra Düber, Bishnudeo Roy, Irene Thomsen, Annette I. Garbe, Frank Klawonn, Oliver Pabst, Karsten Kretschmer and Siegfried Weiss

## B CELL SELECTION, SURVIVAL AND TOLERANCE

- 89 BAFF and BAFF-Receptor in B Cell Selection and Survival**  
Cristian R. Smulski and Hermann Eibel
- 99 Inhibition of Membrane-Bound BAFF by the Anti-BAFF Antibody Belimumab**  
Christine Kowalczyk-Quintas, Dehlia Chevalley, Laure Willen, Camilla Jandus, Michele Vigolo and Pascal Schneider
- 109 Proapoptotic BIM Impacts B Lymphoid Homeostasis by Limiting the Survival of Mature B Cells in a Cell-Autonomous Manner**  
Rui Liu, Ashleigh King, Philippe Bouillet, David M. Tarlinton, Andreas Strasser and Jörg Heierhorst
- 119 Activation of the MEK-ERK Pathway is Necessary but not Sufficient for Breaking Central B Cell Tolerance**  
Sarah A. Greaves, Jacob N. Peterson, Raul M. Torres and Roberta Pelanda

- 133 Corrigendum: Activation of the MEK-ERK Pathway is Necessary but not Sufficient for Breaking Central B Cell Tolerance**  
Sarah A. Greaves, Jacob N. Peterson, Raul M. Torres and Roberta Pelanda
- 134 The Transcriptional Regulation of Germinal Center Formation**  
Shuang Song and Patrick D. Matthias

## HEMATOLOGICAL DISEASES

- 143 From Mice to Men: How B Cell Immunology Helped the Understanding of Leukemia Development**  
Paolo Ghia
- 147 Modeling Hematological Diseases and Cancer With Patient-Specific Induced Pluripotent Stem Cells**  
Huensuk Kim and Christoph Schaniel
- 160 Novel Antibody Drug Conjugates Targeting Tumor-Associated Receptor Tyrosine Kinase ROR2 by Functional Screening of Fully Human Antibody Libraries Using Transpo-mAb Display on Progenitor B Cells**  
Ina Hellmann, Lorenz Waldmeier, Marie-Christine Bannwarth-Escher, Kseniya Maslova, Fabian I. Wolter, Ulf Grawunder and Roger R. Beerli

## T CELL DEVELOPMENT, HOMEOSTASIS AND GRAFT VERSUS HOST DISEASE

- 176 Prophylactic and Therapeutic Effects of Interleukin-2 (IL-2)/Anti-IL-2 Complexes in Systemic Lupus Erythematosus-Like Chronic Graft-Versus-Host Disease**  
Stefan Heiler, Jonas Löttscher, Matthias Kreuzaler, Johanna Rolink and Antonius Rolink
- 191 DN2 Thymocytes Activate a Specific Robust DNA Damage Response to Ionizing Radiation-Induced DNA Double-Strand Breaks**  
Irene Calvo-Asensio, Tara Sugrue, Nabil Bosco, Antonius Rolink and Rhodri Ceredig
- 204 Getting in and Staying Alive: Role for Coronin 1 in the Survival of Pathogenic Mycobacteria and Naïve T Cells**  
Mayumi Mori and Jean Pieters



# Editorial: Making Science Fun – A Tribute to Our Colleague and Friend, Prof. Antonius G. Rolink (1953–2017)

Hermann Eibel<sup>1</sup>, Thomas Winkler<sup>2</sup> and Rhodri Ceredig<sup>3\*</sup>

<sup>1</sup> Center for Chronic Immunodeficiency, University Medical Center Freiburg, Freiburg, Germany, <sup>2</sup> Nikolaus-Fiebiger-Zentrum für Molekulare Medizin, Universität Erlangen-Nürnberg, Erlangen, Germany, <sup>3</sup> Discipline of Physiology, College of Medicine and Nursing Health Science, National University of Ireland, Galway, Ireland

**Keywords:** lymphocyte development and function, B cells, T cells, hemopoiesis, graft versus host disease, BAFF - B-cell activating factor, treg cells, monoclonal antibodies

## Editorial on the Research Topic

### Making Science Fun – A Tribute to Our Colleague and Friend, Prof. Antonius G. Rolink (1953–2017)

## RESEARCH TOPIC CONTENT

This Research Topic was organized to honor the memory of our dear friend Antonius “Ton” Rolink (April 19, 1953–August 06, 2017). The contributions are from his former students, colleagues, and collaborators. In the form of original research and review articles, these papers cover many of Ton’s scientific interests in different aspects of lymphocyte development in mouse and man. Thus, the majority of articles concern B cell biology, ranging from papers by Pang et al. and Kim and Schaniel on stem cells to Klein et al. and Winkler and Mårtensson on B cell precursors, Brennecke et al. and Hobeika et al. on inducible B cell development, Smulski and Eibel and Kowalczyk-Quintans et al. on B cell Activating Factor (BAFF) and the impact of BIM on B cell survival, Greaves et al. on tolerance and Song and Matthias on the formation of germinal centers. However, Ton’s research was also motivated by his continuous interest in T cells and graft-versus-host reactions, lymphoid tumours and in the application of antibody technology to develop novel therapeutic approaches. These subjects are covered by the contributions of Mori and Pieters on T cells, Calvo-Asensio et al. on T cell progenitors, by the article of Ghia on leukemia development, by Heiler et al. on GvH and by Hellmann et al. on human antibody libraries.

## OPEN ACCESS

### Edited and reviewed by:

Barbara L. Kee,  
University of Chicago, United States

### \*Correspondence:

Rhodri Ceredig  
rhodri.ceredig@nuigalway.ie

### Specialty section:

This article was submitted to  
B Cell Biology,  
a section of the journal  
*Frontiers in Immunology*

**Received:** 02 November 2018

**Accepted:** 28 November 2018

**Published:** 19 December 2018

### Citation:

Eibel H, Winkler T and Ceredig R (2018) Editorial: Making Science Fun – A Tribute to Our Colleague and Friend, Prof. Antonius G. Rolink (1953–2017).

*Front. Immunol.* 9:2915.  
doi: 10.3389/fimmu.2018.02915

## TON’S SCIENTIFIC CAREER

Ton Rolink began his scientific career as a PhD student in the group of Ernst Gleichman at the University of Amsterdam focussing on the mechanisms of T cell mediated immunopathology during Graft versus Host Disease (GvHD). This resulted in a remarkable output of 12 publications, including five in the Journal of Experimental Medicine (1–12).

In 1983, he moved to the Basel Institute of Immunology (BII) as a Scientific Member, joining the laboratory of Fritz Melchers. In the following years, the team developed the technologies and skills that led to the discovery of fundamental principles in B cell development (13–16), B cell tolerance (17) and autoimmunity (18–20). Over the years, Ton and his collaborators generated many monoclonal antibodies, some of which, including those to precursor B cells (21), the IL-5 receptor (22), CD40 (23), CD93 (24), and BAFF (25), resulted in numerous novel findings and publications.

One of the key technical advances in which Ton made a significant contribution was the establishment of stroma cell-based *in vitro* system allowing the cultivation of B cell precursors

starting with single hematopoietic stem cells (26). Since Ton indeed had “green fingers” for growing cells, he was naturally gifted at cell culture. Therefore, when Stephen Nutt in Busslinger’s laboratory showed that the transcription factor Pax5 (or BSAP) was essential for B lymphopoiesis (27) the scientific collaboration established with Ton’s laboratory continued. This culminated in 1999 with two seminal articles in *Nature* describing how Pax5-deficient pro B cell lines could proceed along different developmental pathways to become antigen-presenting dendritic cells, osteoclasts, granulocytes or natural killer cells *in vitro* and to T cells following reconstitution of mice *in vivo* (28, 29). The realization that the transcription factor Pax5 was a master regulator of B cell development had a profound influence on the field of haematopoiesis and lymphopoiesis and opened new research avenues allowing in depth analysis of the roles of other transcription factors in the regulation of lymphocyte development (30–36).

By refining the conditions of *in vitro* B cell development, the roles of different chemokines and cytokines implicated in B cell development and homeostasis were also investigated (37–41) including the detailed dissection in mouse and man of the role of the B cell Activating Factor (BAFF) (42, 43) in normal B cell homeostasis and as well as in the development of autoimmunity (44–47). Using emerging molecular technologies, Ton and his group dissected B cell development at the single cell level, analysing their genotypic and transcriptomic profiles (48–50). For this, techniques capable of identifying rearrangement of D<sub>H</sub> and J<sub>H</sub> genes on one immunoglobulin heavy chain allele,

corresponding to one molecule of rearranged DNA, could be detected (51). Without a doubt, Ton’s research contributions were recognized world-wide and he became one of the leaders in studies of mouse and human B cell development.

Having helped to show the multi-lineage differentiation capacity of B220<sup>+</sup>CD117<sup>low</sup>CD19<sup>−</sup> Pax 5 KO pro-B cell lines, Ton became interested in trying to identify a cell type with identical phenotype and equivalent differentiation capacity in the bone marrow of normal mice. This progenitor was indeed identified and referred to as an Early Progenitor with Lymphocyte and Myeloid Potential, or EPLM (52). More recent experiments using additional markers and taking advantage of single cell RNA sequencing, has revealed that the original EPLM population is both phenotypically and genetically heterogeneous with the earliest member being already committed to either lymphoid or myeloid lineages (53, 54).

Seeing that mice could be reconstituted with genetically-modified B cell progenitors grown *in vitro* and that Pax5 KO (29) and EPLM (52) could reconstitute the T cell compartment led Ton to expand his studies to T cell development (55). Realising that therapeutic use of progenitors grown on stromal cells would pose difficulties for clinical approval, he established stromal cell-free culture conditions whereby mouse and human T cell progenitors could be expanded and differentiated without stromal cells. The system developed was affectionately called “the plastic thymus” (56) allowing the dissection of signals involved in T cell commitment (57–59). In recent years, this led to a series of experiments investigating the possible instructive



**FIGURE 1 |** The cartoon has been painted and kindly provided by Professor Daniela Finke, who has been for many years Ton Rolink’s colleague at the Department of Biomedicine, University of Basel.

role of cytokines, in particular IL-7 and Flt3L, on lymphocyte development (53, 60–62).

This T cell work set the foundation for Ton's subsequent studies on T cell autoimmunity. Using T cell progenitors from genetically-modified mice, his group was able to expand and reconstitute the T cell compartment of immunodeficient recipients (63). However, the “plastic thymus” could not replace one of the key functions of the thymus, namely the generation of regulatory T cells (64). Without endogenous regulatory T cells, after a few weeks recipient mice reconstituted with *in vitro* generated T cell progenitors invariably developed immunopathology reminiscent of that seen in GvHD. Addition of regulatory T cells to the T progenitor inoculum was sufficient to prevent disease onset (64), providing Ton with a functional *in vivo* assay for regulatory T cell function.

Ton's interest in autoimmunity associated with GvHD, initiated whilst a PhD student and continued at BII and the University of Basel, interested him until the very end of his career. In his latest publications, he looked at this topic from a T-cell (Heiler et al.) and a B-cell perspective (65). In the first, Heiler et al. analyzed the contribution of the different T cell compartments at various stages of disease, the latter (65) showed the processes by which self-reactive antibodies might arise in aged mice.

## REFERENCES

1. Van der Veen F, Rolink AG, Gleichmann E. Diseases caused by reactions of T lymphocytes to incompatible structures of the major histocompatibility complex. IV. Autoantibodies to nuclear antigens. *Clin Exp Immunol.* (1981) 46:589–96.
2. van der Veen JP, Rolink AG, Gleichmann E. Diseases caused by reactions of T lymphocytes to incompatible structures of the major histocompatibility complex. III. Autoantibodies to thymocytes. *J Immunol.* (1981) 127:1281–6.
3. Van Elven EH, Rolink AG, Veen FV, Gleichmann E. Capacity of genetically different T lymphocytes to induce lethal graft-versus-host disease correlates with their capacity to generate suppression but not with their capacity to generate anti-F1 killer cells. A non-H-2 locus determines the inability to induce lethal graft-versus-host disease. *J Exp Med.* (1981) 153:1474–88.
4. van Elven EH, van der Veen FM, Rolink AG, Issa P, Duin TM, Gleichmann E. Diseases caused by reactions of T lymphocytes to incompatible structures of the major histocompatibility complex. V. High titers of IgG autoantibodies to double-stranded DNA. *J Immunol.* (1981) 127:2435–8.
5. Rolink AG, Radaszkiewicz T, Pals ST, van der Meer WG, Gleichmann E. Allosuppressor and allohelper T cells in acute and chronic graft-vs.-host disease. I. Alloreactive suppressor cells rather than killer T cells appear to be the decisive effector cells in lethal graft-vs.-host disease. *J Exp Med.* (1982) 155:1501–22.
6. van der Veen FM, Rolink AG, Gleichmann E. Autoimmune disease strongly resembling systemic lupus erythematosus (SLE) in F1 mice undergoing graft-versus-host reaction (GVHR). *Adv Exp Med Biol.* (1982) 149:669–77.
7. van Rappard-van der Veen FM, Rolink AG, Gleichmann E. Diseases caused by reactions of T lymphocytes towards incompatible structures of the major histocompatibility complex. VI. Autoantibodies characteristic of systemic lupus erythematosus induced by abnormal T-B cell cooperation across I-E. *J Exp Med.* (1982) 155:1555–60.
8. Rolink AG, Gleichmann E. Allosuppressor- and allohelper-T cells in acute and chronic graft-vs.-host (GVH) disease. III. Different Lyt subsets of donor T cells induce different pathological syndromes. *J Exp Med.* (1983) 158:546–58.
9. Rolink AG, Gleichmann H, Gleichmann E. Diseases caused by reactions of T lymphocytes to incompatible structures of the major histocompatibility complex. VII. Immune-complex glomerulonephritis. *J Immunol.* (1983) 130:209–15.
10. Rolink AG, Pals ST, Gleichmann E. Allosuppressor and allohelper T cells in acute and chronic graft-vs.-host disease. II. F1 recipients carrying mutations at H-2K and/or I-A. *J Exp Med.* (1983) 157:755–71.
11. Rolink AG, Van der Meer W, Melief CJ, Gleichmann E. Intra-H-2 and T cell requirements for the induction of maximal positive and negative allogeneic effects *in vitro*. *Eur J Immunol.* (1983) 13:191–7.
12. Gleichmann E, Pals ST, Rolink AG, Radaszkiewicz T, Gleichmann H. Graft-versus-host reactions: clues to the etiopathology of a spectrum of immunological diseases. *Immunol Tod.* (1984) 5:324–32.
13. Melchers F, Strasser A, Bauer SR, Kudo A, Thalmann P, Rolink A. Cellular stages and molecular steps of murine B-cell development. *Cold Spring Harb Symp Quant Biol.* (1989) 54 (Pt 1):183–9.
14. Strasser A, Rolink A, Melchers F. One synchronous wave of B cell development in mouse fetal liver changes at day 16 of gestation from dependence to independence of a stromal cell environment. *J Exp Med.* (1989) 170:1793–86.
15. Melchers F, Strasser A, Bauer SR, Kudo A, Thalmann P, Rolink A. B cell development in fetal liver. *Adv Exp Med Biol.* (1991) 292:201–5.
16. Rolink A, Melchers F. Molecular and cellular origins of B lymphocyte diversity. *Cell* (1991) 66:1081–94.
17. Tussiwand R, Bosco N, Ceredig R, Rolink AG. Tolerance checkpoints in B-cell development: Johnny B good. *Eur J Immunol.* (2009) 39:2317–24. doi: 10.1002/eji.200939633
18. Rolink AG, Radaszkiewicz T, Melchers F. The autoantigen-binding B cell repertoires of normal and of chronically graft-versus-host-diseased mice. *J Exp Med.* (1987) 165:1675–87.
19. Rolink AG, Radaszkiewicz T, Melchers F. Monoclonal autoantibodies specific for kidney proximal tubular brush border from mice with experimentally induced chronic graft-versus-host disease. *Scand J Immunol.* (1988) 28:29–41.
20. Rolink AG, Thalmann P, Berger C, Radaszkiewicz T, Melchers F. Autoreactive B-cell repertoire in mice with chronic graft versus host disease. *Mol Immunol.* (1988) 25:1217–22.

Ton Rolink's key findings in the field of lymphocyte biology as well as his talent for developing numerous monoclonal antibodies and cell culture systems now used as research tools in many laboratories world-wide, were always complemented by his open, friendly, and generous personality and his infectious good humor. Throughout his scientific career, Ton worked almost daily at the bench. He was always ready to share his ideas, tools and expertise with his colleagues and collaborators, which in times of a steadily growing number of Material Transfer Agreements (MTAs), research contracts and “highly confidential information,” was a rare phenomenon among scientists. Therefore, Ton will not only be remembered for his exceptional work ethic and output, but also, and maybe even more, for his exceptional way of making science fun. He will also be remembered by his colleagues and collaborators through their projects that live and thrive thanks to his reagents and spirit (**Figure 1**).

His complete bibliography can be found in the **Appendix** and the following is a link to Ton's publications on PubMed: <https://www.ncbi.nlm.nih.gov/pubmed/?term=Rolink+A>.

## AUTHOR CONTRIBUTIONS

All authors listed have made a substantial, direct and intellectual contribution to the work, and approved it for publication.

21. Melchers F, Bauer SR, Berger C, Karasuyama H, Kudo A, Rolink A, et al. Precursor B lymphocytes-specific monoclonal antibodies and genes. *Adv Exp Med Biol.* (1989) 254:87–93.
22. Rolink AG, Melchers F, Palacios R. Monoclonal antibodies reactive with the mouse interleukin 5 receptor. *J Exp Med.* (1989) 169:1693–701.
23. Rolink A, Melchers F, Andersson J. The SCID but not the RAG-2 gene product is required for S mu-S epsilon heavy chain class switching. *Immunity* (1996) 5:319–30.
24. Rolink AG, Andersson J, Melchers F. Characterization of immature B cells by a novel monoclonal antibody, by turnover and by mitogen reactivity. *Eur J Immunol.* (1998) 28:3738–48.
25. Rauch M, Tussiwand R, Bosco N, Rolink AG. Crucial role for BAFF-BAFF-R signaling in the survival and maintenance of mature B cells. *PLoS ONE* (2009) 4:e5456. doi: 10.1371/journal.pone.0005456
26. Rolink A, Kudo A, Karasuyama H, Kikuchi Y, Melchers F. Long-term proliferating early pre B cell lines and clones with the potential to develop to surface Ig-positive, mitogen reactive B cells *in vitro* and *in vivo*. *EMBO J.* (1991) 10:327–36.
27. Nutt SL, Urbanek P, Rolink A, Busslinger M. Essential functions of Pax5 (BSAP) in pro-B cell development: difference between fetal and adult B lymphopoiesis and reduced V-to-DJ recombination at the IgH locus. *Genes Dev.* (1997) 11:476–91.
28. Nutt SL, Heavey B, Rolink AG, Busslinger M. Commitment to the B-lymphoid lineage depends on the transcription factor Pax5. *Nature* (1999) 401:556–62.
29. Rolink AG, Nutt SL, Melchers F, Busslinger M. Long-term *in vivo* reconstitution of T-cell development by Pax5-deficient B-cell progenitors. *Nature* (1999) 401:603–6.
30. Schubart DB, Rolink A, Kosco-Vilbois MH, Botteri F, Matthias P. B-cell-specific coactivator OBF-1/OCA-B/Bob1 required for immune response and germinal centre formation. *Nature* (1996) 383:538–42.
31. Schubart DB, Rolink A, Schubart K, Matthias P. Cutting edge: lack of peripheral B cells and severe agammaglobulinemia in mice simultaneously lacking Bruton's tyrosine kinase and the B cell-specific transcriptional coactivator OBF-1. *J Immunol.* (2000) 164:18–22. doi: 10.4049/jimmunol.164.1.18
32. Schubart K, Massa S, Schubart D, Corcoran LM, Rolink AG, Matthias P. B cell development and immunoglobulin gene transcription in the absence of Oct-2 and OBF-1. *Nat Immunol.* (2001) 2:69–74. doi: 10.1038/83190
33. Matthias P, Rolink AG. Transcriptional networks in developing and mature B cells. *Nat Rev Immunol.* (2005) 5:497–508. doi: 10.1038/nri1633
34. Bordon A, Bosco N, Du Roure C, Bartholdy B, Kohler H, Matthias G, et al. Enforced expression of the transcriptional coactivator OBF1 impairs B cell differentiation at the earliest stage of development. *PLoS ONE* (2008) 3:e4007. doi: 10.1371/journal.pone.0004007
35. Choukran MA, Song S, Rolink AG, Burger L, Matthias P. Enhancer repertoires are reshaped independently of early priming and heterochromatin dynamics during B cell differentiation. *Nat Commun.* (2015) 6:8324. doi: 10.1038/ncomms9324
36. Manoharan A, Du Roure C, Rolink AG, Matthias P. *De novo* DNA Methyltransferases Dnmt3a and Dnmt3b regulate the onset of Igkappa light chain rearrangement during early B-cell development. *Eur J Immunol.* (2015) 45:2343–55. doi: 10.1002/eji.201445035
37. Schaniel C, Pardali E, Sallusto F, Speletras M, Ruedl C, Shimizu T, et al. Activated murine B lymphocytes and dendritic cells produce a novel CC chemokine which acts selectively on activated T cells. *J Exp Med.* (1998) 188:451–63.
38. Ghia P, Schaniel C, Rolink AG, Nadler LM, Cardoso AA. Human macrophage-derived chemokine (MDC) is strongly expressed following activation of both normal and malignant precursor and mature B cells. *Curr Top Microbiol Immunol.* (1999) 246:103–10.
39. Melchers F, Rolink AG, Schaniel C. The role of chemokines in regulating cell migration during humoral immune responses. *Cell* (1999) 99:351–4.
40. Schaniel C, Sallusto F, Ruedl C, Sideras P, Melchers F, Rolink AG. Three chemokines with potential functions in T lymphocyte-independent and -dependent B lymphocyte stimulation. *Eur J Immunol.* (1999) 29:2934–47.
41. Schaniel C, Sallusto F, Sideras P, Melchers F, Rolink AG. A novel CC chemokine ABCD-1, produced by dendritic cells and activated B cells, exclusively attracts activated T lymphocytes. *Curr Top Microbiol Immunol.* (1999) 246:95–101.
42. Rolink AG, Melchers F. BAFFed B cells survive and thrive: roles of BAFF in B-cell development. *Curr Opin Immunol.* (2002) 14:266–75. doi: 10.1016/S0952-7915(02)00332-1
43. Rolink AG, Tschopp J, Schneider P, Melchers F. BAFF is a survival and maturation factor for mouse B cells. *Eur J Immunol.* (2002) 32:2004–10. doi: 10.1002/1521-4141(200207)32:7<2004::AID-IMMU2004>3.0.CO;2-5
44. Bossen C, Tardivel A, Willen L, Fletcher CA, Perroud M, Beermann F, et al. Mutation of the BAFF furin cleavage site impairs B-cell homeostasis and antibody responses. *Eur J Immunol.* (2011) 41:787–97. doi: 10.1002/eji.201040591
45. Kreuzaler M, Rauch M, Salzer U, Birmelin J, Rizzi M, Grimbacher B, et al. Soluble BAFF levels inversely correlate with peripheral B cell numbers and the expression of BAFF receptors. *J Immunol.* (2012) 188:497–503. doi: 10.4049/jimmunol.1102321
46. Tussiwand R, Rauch M, Fluck LA, Rolink AG. BAFF-R expression correlates with positive selection of immature B cells. *Eur J Immunol.* (2012) 42:206–16. doi: 10.4049/jimmunol.1102321
47. Fazio G, Turazzi N, Cazzaniga V, Kreuzaler M, Maglia O, Magnani CF, et al. TNFRSF13C (BAFFR) positive blasts persist after early treatment and at relapse in childhood B-cell precursor acute lymphoblastic leukaemia. *Br J Haematol.* (2018) 182:427–456. doi: 10.1111/bjh.14794
48. ten Boekel E, Melchers F, Rolink A. The status of Ig loci rearrangements in single cells from different stages of B cell development. *Int Immunol.* (1995) 7:1013–9.
49. Ghia P, ten Boekel E, Sanz E, de la Hera A, Rolink A, Melchers F. Ordering of human bone marrow B lymphocyte precursors by single-cell polymerase chain reaction analyses of the rearrangement status of the immunoglobulin H and L chain gene loci. *J Exp Med.* (1996) 184:2217–29.
50. ten Boekel E, Melchers F, Rolink AG. Changes in the V(H) gene repertoire of developing precursor B lymphocytes in mouse bone marrow mediated by the pre-B cell receptor. *Immunity* (1997) 7:357–68.
51. ten Boekel E, Melchers F, Rolink AG. Precursor B cells showing H chain allelic inclusion display allelic exclusion at the level of pre-B cell receptor surface expression. *Immunity* (1998) 8:199–207.
52. Balciunaite G, Ceredig R, Massa S, Rolink AG. A B220+ CD117+ CD19-hematopoietic progenitor with potent lymphoid and myeloid developmental potential. *Eur J Immunol.* (2005) 35:2019–30. doi: 10.1002/eji.200526318
53. von Muenchow L, Alberti-Servera L, Klein F, Capoferri G, Finke D, Ceredig R, et al. Permissive roles of cytokines interleukin-7 and Flt3 ligand in mouse B-cell lineage commitment. *Proc Natl Acad Sci USA.* (2016) 113:E8122–30. doi: 10.1073/pnas.1613316113
54. Alberti-Servera L, von Muenchow L, Tsapogas P, Capoferri G, Eschbach K, Beisel C, et al. Single-cell RNA sequencing reveals developmental heterogeneity among early lymphoid progenitors. *EMBO J.* (2017) 36:3619–33. doi: 10.15252/embj.201797105
55. Balciunaite G, Ceredig R, Fehling HJ, Zuniga-Pflucker JC, Rolink AG. The role of Notch and IL-7 signaling in early thymocyte proliferation and differentiation. *Eur J Immunol.* (2005) 35:1292–300. doi: 10.1002/eji.200425822
56. Gehre N, Nusser A, von Muenchow L, Tussiwand R, Engdahl C, Capoferri G, et al. A stromal cell free culture system generates mouse pro-T cells that can reconstitute T-cell compartments *in vivo*. *Eur J Immunol.* (2015) 45:932–42. doi: 10.1002/eji.201444681
57. Balciunaite G, Ceredig R, Rolink AG. The earliest subpopulation of mouse thymocytes contains potent T, significant macrophage, and natural killer cell but no B-lymphocyte potential. *Blood* (2005) 105:1930–6. doi: 10.1182/blood-2004-08-3087
58. Ceredig R, Bosco N, Rolink AG. The B lineage potential of thymus settling progenitors is critically dependent on mouse age. *Eur J Immunol.* (2007) 37:830–7. doi: 10.1002/eji.200636728
59. Ceredig R, Rolink AG, Brown G. Models of haematopoiesis: seeing the wood for the trees. *Nat Rev Immunol.* (2009) 9:293–300. doi: 10.1038/nri2525
60. Ceredig R, Rauch M, Balciunaite G, Rolink AG. Increasing Flt3L availability alters composition of a novel bone marrow lymphoid progenitor compartment. *Blood* (2006) 108:1216–22. doi: 10.1182/blood-2005-10-006643

61. Tsapogas P, Swee LK, Nusser A, Nuber N, Kreuzaler M, Capoferri G, et al. *In vivo* evidence for an instructive role of fms-like tyrosine kinase-3 (FLT3) ligand in hematopoietic development. *Haematologica* (2014) 99:638–46. doi: 10.3324/haematol.2013.089482
62. Tsapogas P, Mooney CJ, Brown G, Rolink A. The Cytokine Flt3-Ligand in Normal and Malignant Hematopoiesis. *Int J Mol Sci.* (2017) 18:E1115. doi: 10.3390/ijms18061115
63. Bosco N, Engdahl C, Benard A, Rolink J, Ceredig R, Rolink AG. TCR- $\beta$  chains derived from peripheral  $\gamma\delta$  T cells can take part in  $\alpha\beta$  T-cell development. *Eur J Immunol.* (2008) 38:3520–9. doi: 10.1002/eji.200838668
64. Benard A, Ceredig R, Rolink AG. Regulatory T cells control autoimmunity following syngeneic bone marrow transplantation. *Eur J Immunol.* (2006) 36:2324–35. doi: 10.1002/eji.200636434
65. Faderl M, Klein F, Wirz OF, Heiler S, Alberti-Servera L, Engdahl C, et al. Two Distinct Pathways in Mice Generate Antinuclear Antigen-Reactive B Cell Repertoires. *Front Immunol.* (2018) 9:16. doi: 10.3389/fimmu.2018.00016

**Conflict of Interest Statement:** The authors declare that the research was conducted in the absence of any commercial or financial relationships that could be construed as a potential conflict of interest.

Copyright © 2018 Eibel, Winkler and Ceredig. This is an open-access article distributed under the terms of the Creative Commons Attribution License (CC BY). The use, distribution or reproduction in other forums is permitted, provided the original author(s) and the copyright owner(s) are credited and that the original publication in this journal is cited, in accordance with accepted academic practice. No use, distribution or reproduction is permitted which does not comply with these terms.

## APPENDIX

### Ton's Complete Bibliography

1. Van der Veen F, Rolink AG, Gleichmann E. Diseases caused by reactions of T lymphocytes to incompatible structures of the major histocompatibility complex. IV. Autoantibodies to nuclear antigens. *Clin Exp Immunol.* 1981;46(3):589-96.
2. van der Veen JP, Rolink AG, Gleichmann E. Diseases caused by reactions of T lymphocytes to incompatible structures of the major histocompatibility complex. III. Autoantibodies to thymocytes. *J Immunol.* 1981;127(4):1281-6.
3. Van Elven EH, Rolink AG, Veen FV, Gleichmann E. Capacity of genetically different T lymphocytes to induce lethal graft-versus-host disease correlates with their capacity to generate suppression but not with their capacity to generate anti-F1 killer cells. A non-H-2 locus determines the inability to induce lethal graft-versus-host disease. *J Exp Med.* 1981;153(6):1474-88.
4. van Elven EH, van der Veen FM, Rolink AG, Issa P, Duin TM, Gleichmann E. Diseases caused by reactions of T lymphocytes to incompatible structures of the major histocompatibility complex. V. High titers of IgG autoantibodies to double-stranded DNA. *J Immunol.* 1981;127(6):2435-8.
5. Rolink AG, Radaszkiewicz T, Pals ST, van der Meer WG, Gleichmann E. Allosuppressor and allohelper T cells in acute and chronic graft-vs-host disease. I. Alloreactive suppressor cells rather than killer T cells appear to be the decisive effector cells in lethal graft-vs.-host disease. *J Exp Med.* 1982;155(5):1501-22.
6. van der Veen FM, Rolink AG, Gleichmann E. Autoimmune disease strongly resembling systemic lupus erythematosus (SLE) in F1 mice undergoing graft-versus-host reaction (GVHR). *Adv Exp Med Biol.* 1982;149:669-77.
7. van Rappard-van der Veen FM, Rolink AG, Gleichmann E. Diseases caused by reactions of T lymphocytes towards incompatible structures of the major histocompatibility complex. VI. Autoantibodies characteristic of systemic lupus erythematosus induced by abnormal T-B cell cooperation across I-E. *J Exp Med.* 1982;155(5):1555-60.
8. Rolink AG, Gleichmann E. Allosuppressor- and allohelper-T cells in acute and chronic graft-vs.-host (GVH) disease. III. Different Lyt subsets of donor T cells induce different pathological syndromes. *J Exp Med.* 1983;158(2):546-58.
9. Rolink AG, Gleichmann H, Gleichmann E. Diseases caused by reactions of T lymphocytes to incompatible structures of the major histocompatibility complex. VII. Immune-complex glomerulonephritis. *J Immunol.* 1983;130(1):209-15.
10. Rolink AG, Pals ST, Gleichmann E. Allosuppressor and allohelper T cells in acute and chronic graft-vs.-host disease. II. F1 recipients carrying mutations at H-2K and/or I-A. *J Exp Med.* 1983;157(2):755-71.
11. Rolink AG, Van der Meer W, Melief CJ, Gleichmann E. Intra-H-2 and T cell requirements for the induction of maximal positive and negative allogeneic effects in vitro. *Eur J Immunol.* 1983;13(3):191-7.
12. Gleichmann E, Pals ST, Rolink AG, Radaszkiewicz T, Gleichmann H. Graft-versus-host reactions: clues to the etiopathology of a spectrum of immunological diseases. *Immunol Today.* 1984;5(11):324-32.
13. Lernhardt W, Karasuyama H, Rolink A, Melchers F. Control of the cell cycle of murine B lymphocytes: the nature of alpha- and beta-B-cell growth factors and of B-cell maturation factors. *Immunol Rev.* 1987;99:241-62.
14. Palacios R, Karasuyama H, Rolink A. Ly1+ PRO-B lymphocyte clones. Phenotype, growth requirements and differentiation in vitro and in vivo. *EMBO J.* 1987;6(12):3687-93.
15. Rolink AG, Radaszkiewicz T, Melchers F. The autoantigen-binding B cell repertoires of normal and of chronically graft-versus-host-diseased mice. *J Exp Med.* 1987;165(6):1675-87.
16. Karasuyama H, Rolink A, Melchers F. Recombinant interleukin 2 or 5, but not 3 or 4, induces maturation of resting mouse B lymphocytes and propagates proliferation of activated B cell blasts. *J Exp Med.* 1988;167(4):1377-90.
17. Rolink AG, Radaszkiewicz T, Melchers F. Monoclonal autoantibodies specific for kidney proximal tubular brush border from mice with experimentally induced chronic graft-versus-host disease. *Scand J Immunol.* 1988;28(1):29-41.
18. Rolink AG, Thalmann P, Berger C, Radaszkiewicz T, Melchers F. Autoreactive B-cell repertoire in mice with chronic graft versus host disease. *Mol Immunol.* 1988;25(11):1217-22.
19. Melchers F, Bauer SR, Berger C, Karasuyama H, Kudo A, Rolink A, et al. Precursor B lymphocytes-specific monoclonal antibodies and genes. *Adv Exp Med Biol.* 1989;254:87-93.
20. Melchers F, Strasser A, Bauer SR, Kudo A, Thalmann P, Rolink A. Cellular stages and molecular steps of murine B-cell development. *Cold Spring Harb Symp Quant Biol.* 1989;54 Pt 1:183-9.
21. Palacios R, Stuber S, Rolink A. The epigenetic influences of bone marrow and fetal liver stroma cells on the developmental potential of Ly-1+ pro-B lymphocyte clones. *Eur J Immunol.* 1989;19(2):347-56.
22. Rolink AG, Melchers F, Palacios R. Monoclonal antibodies reactive with the mouse interleukin 5 receptor. *J Exp Med.* 1989;169(5):1693-701.
23. Strasser A, Rolink A, Melchers F. One synchronous wave of B cell development in mouse fetal liver changes at day 16 of gestation from dependence to independence of a stromal cell environment. *J Exp Med.* 1989;170(6):1973-86.
24. Devos R, Tavernier J, Plaetinck G, Van der Heyden J, Rolink A, Fiers W. Expression of the murine interleukin-5 receptor on *Xenopus laevis* oocytes. *Biochem Biophys Res Commun.* 1990;172(2):570-5.
25. Rolink AG, Thalmann P, Kikuchi Y, Erdei A. Characterization of the interleukin 5-reactive splenic B cell population. *Eur J Immunol.* 1990;20(9):1949-56.
26. Tary-Lehmann M, Rolink AG, Lehmann PV, Nagy ZA, Hurtenbach U. Induction of graft versus host-associated immunodeficiency by CD4+ T cell clones. *J Immunol.* 1990;145(7):2092-8.
27. Devos R, Vandekerckhove J, Rolink A, Plaetinck G, Van der Heyden J, Fiers W, et al. Amino acid sequence analysis of a mouse interleukin 5 receptor protein reveals homology with a mouse interleukin 3 receptor protein. *Eur J Immunol.* 1991;21(5):1315-7.

28. Melchers F, Strasser A, Bauer SR, Kudo A, Thalmann P, Rolink A. B cell development in fetal liver. *Adv Exp Med Biol.* 1991;292:201-5.
29. Mita S, Takaki S, Hitoshi Y, Rolink AG, Tominaga A, Yamaguchi N, et al. Molecular characterization of the beta chain of the murine interleukin 5 receptor. *Int Immunol.* 1991;3(7):665-72.
30. Rolink A, Kudo A, Karasuyama H, Kikuchi Y, Melchers F. Long-term proliferating early pre B cell lines and clones with the potential to develop to surface Ig-positive, mitogen reactive B cells in vitro and in vivo. *EMBO J.* 1991;10(2):327-36.
31. Rolink A, Kudo A, Melchers F. Long-term proliferating early pre-B-cell lines and clones with the potential to develop to surface immunoglobulin-positive, mitogen-reactive B-cells in vitro and in vivo. *Biochem Soc Trans.* 1991;19(2):275-6.
32. Rolink A, Melchers F. Molecular and cellular origins of B lymphocyte diversity. *Cell.* 1991;66(6):1081-94.
33. Rolink A, Streb M, Melchers F. The kappa/lambda ratio in surface immunoglobulin molecules on B lymphocytes differentiating from DHJH-rearranged murine pre-B cell clones in vitro. *Eur J Immunol.* 1991;21(11):2895-8.
34. Rolink A, Streb M, Nishikawa S, Melchers F. The c-kit-encoded tyrosine kinase regulates the proliferation of early pre-B cells. *Eur J Immunol.* 1991;21(10):2609-12.
35. Kudo A, Thalmann P, Sakaguchi N, Davidson WF, Pierce JH, Kearney JF, et al. The expression of the mouse VpreB/lambda 5 locus in transformed cell lines and tumors of the B lineage differentiation pathway. *Int Immunol.* 1992;4(8):831-40.
36. Melchers F, Haasner D, Karasuyama H, Reininger L, Rolink A. Progenitor and precursor B lymphocytes of mice. Proliferation and differentiation in vitro and population, differentiation and turnover in SCID mice in vivo of normal and abnormal cells. *Curr Top Microbiol Immunol.* 1992;182:3-12.
37. Melchers F, Haasner D, Streb M, Rolink A. B-lymphocyte lineage-committed, IL-7 and stroma cell-reactive progenitors and precursors, and their differentiation to B cells. *Adv Exp Med Biol.* 1992;323:111-7.
38. Oltz EM, Yancopoulos GD, Morrow MA, Rolink A, Lee G, Wong F, et al. A novel regulatory myosin light chain gene distinguishes pre-B cell subsets and is IL-7 inducible. *EMBO J.* 1992;11(7):2759-67.
39. Reininger L, Radaszkiewicz T, Kosco M, Melchers F, Rolink AG. Development of autoimmune disease in SCID mice populated with long-term "in vitro" proliferating (NZB x NZW)F1 pre-B cells. *J Exp Med.* 1992;176(5):1343-53.
40. Grawunder U, Haasner D, Melchers F, Rolink A. Rearrangement and expression of kappa light chain genes can occur without mu heavy chain expression during differentiation of pre-B cells. *Int Immunol.* 1993;5(12):1609-18.
41. Grawunder U, Melchers F, Rolink A. Interferon-gamma arrests proliferation and causes apoptosis in stromal cell/interleukin-7-dependent normal murine pre-B cell lines and clones in vitro, but does not induce differentiation to surface immunoglobulin-positive B cells. *Eur J Immunol.* 1993;23(2):544-51.
42. Karasuyama H, Rolink A, Melchers F. A complex of glycoproteins is associated with VpreB/lambda 5 surrogate light chain on the surface of mu heavy chain-negative early precursor B cell lines. *J Exp Med.* 1993;178(2):469-78.
43. Melchers F, Karasuyama H, Haasner D, Bauer S, Kudo A, Sakaguchi N, et al. The surrogate light chain in B-cell development. *Immunol Today.* 1993;14(2):60-8.
44. Rolink A, Grawunder U, Haasner D, Strasser A, Melchers F. Immature surface Ig+ B cells can continue to rearrange kappa and lambda L chain gene loci. *J Exp Med.* 1993;178(4):1263-70.
45. Rolink A, Haasner D, Nishikawa S, Melchers F. Changes in frequencies of clonable pre B cells during life in different lymphoid organs of mice. *Blood.* 1993;81(9):2290-300.
46. Rolink A, Karasuyama H, Grawunder U, Haasner D, Kudo A, Melchers F. B cell development in mice with a defective lambda 5 gene. *Eur J Immunol.* 1993;23(6):1284-8.
47. Rolink A, Melchers F. Generation and regeneration of cells of the B-lymphocyte lineage. *Curr Opin Immunol.* 1993;5(2):207-17.
48. Rolink A, Melchers F. B lymphopoiesis in the mouse. *Adv Immunol.* 1993;53:123-56.
49. Haasner D, Rolink A, Melchers F. Influence of surrogate L chain on DHJH-reading frame 2 suppression in mouse precursor B cells. *Int Immunol.* 1994;6(1):21-30.
50. Karasuyama H, Rolink A, Shinkai Y, Young F, Alt FW, Melchers F. The expression of Vpre-B/lambda 5 surrogate light chain in early bone marrow precursor B cells of normal and B cell-deficient mutant mice. *Cell.* 1994;77(1):133-43.
51. Kirberg J, Baron A, Jakob S, Rolink A, Karjalainen K, von Boehmer H. Thymic selection of CD8+ single positive cells with a class II major histocompatibility complex-restricted receptor. *J Exp Med.* 1994;180(1):25-34.
52. Melchers F, Haasner D, Grawunder U, Kalberer C, Karasuyama H, Winkler T, et al. Roles of IgH and L chains and of surrogate H and L chains in the development of cells of the B lymphocyte lineage. *Annu Rev Immunol.* 1994;12:209-25.
53. Rolink A, Grawunder U, Winkler TH, Karasuyama H, Melchers F. IL-2 receptor alpha chain (CD25, TAC) expression defines a crucial stage in pre-B cell development. *Int Immunol.* 1994;6(8):1257-64.
54. Rolink A, Karasuyama H, Haasner D, Grawunder U, Martensson IL, Kudo A, et al. Two pathways of B-lymphocyte development in mouse bone marrow and the roles of surrogate L chain in this development. *Immunol Rev.* 1994;137:185-201.
55. Rolink AG, Reininger L, Oka Y, Kalberer CP, Winkler TH, Melchers F. Repopulation of SCID mice with long-term in vitro proliferating pre-B-cell lines from normal and autoimmune disease-prone mice. *Res Immunol.* 1994;145(5):353-6.
56. Young F, Ardman B, Shinkai Y, Lansford R, Blackwell TK, Mendelsohn M, et al. Influence of immunoglobulin heavy- and light-chain expression on B-cell differentiation. *Genes Dev.* 1994;8(9):1043-57.
57. Andersson J, Melchers F, Rolink A. Stimulation by T cell independent antigens can relieve the arrest of differentiation

- of immature auto-reactive B cells in the bone marrow. *Scand J Immunol.* 1995;42(1):21-33.
58. Bruno L, Rocha B, Rolink A, von Boehmer H, Rodewald HR. Intra- and extra-thymic expression of the pre-T cell receptor alpha gene. *Eur J Immunol.* 1995;25(7):1877-82.
  59. Ghia P, Gratwohl A, Signer E, Winkler TH, Melchers F, Rolink AG. Immature B cells from human and mouse bone marrow can change their surface light chain expression. *Eur J Immunol.* 1995;25(11):3108-14.
  60. Grawunder U, Leu TM, Schatz DG, Werner A, Rolink AG, Melchers F, et al. Down-regulation of RAG1 and RAG2 gene expression in preB cells after functional immunoglobulin heavy chain rearrangement. *Immunity.* 1995;3(5):601-8.
  61. Grawunder U, Rolink A, Melchers F. Induction of sterile transcription from the kappa L chain gene locus in V(D)J recombinase-deficient progenitor B cells. *Int Immunol.* 1995;7(12):1915-25.
  62. Jessberger R, Riwar B, Rolink A, Rodewald HR. Stimulation of defective DNA transfer activity in recombination deficient SCID cell extracts by a 72-kDa protein from wild-type thymocytes. *J Biol Chem.* 1995;270(12):6788-97.
  63. Melchers F, Rolink A, Grawunder U, Winkler TH, Karasuyama H, Ghia P, et al. Positive and negative selection events during B lymphopoiesis. *Curr Opin Immunol.* 1995;7(2):214-27.
  64. Oka Y, Rolink AG, Suematsu S, Kishimoto T, Melchers F. An interleukin-6 transgene expressed in B lymphocyte lineage cells overcomes the T cell-dependent establishment of normal levels of switched immunoglobulin isotypes. *Eur J Immunol.* 1995;25(5):1332-7.
  65. Rolink A, Ghia P, Grawunder U, Haasner D, Karasuyama H, Kalberer C, et al. In-vitro analyses of mechanisms of B-cell development. *Semin Immunol.* 1995;7(3):155-67.
  66. ten Boekel E, Melchers F, Rolink A. The status of Ig loci rearrangements in single cells from different stages of B cell development. *Int Immunol.* 1995;7(6):1013-9.
  67. Winkler TH, Melchers F, Rolink AG. Interleukin-3 and interleukin-7 are alternative growth factors for the same B-cell precursors in the mouse. *Blood.* 1995;85(8):2045-51.
  68. Winkler TH, Rolink A, Melchers F, Karasuyama H. Precursor B cells of mouse bone marrow express two different complexes with the surrogate light chain on the surface. *Eur J Immunol.* 1995;25(2):446-50.
  69. Ghia P, ten Boekel E, Sanz E, de la Hera A, Rolink A, Melchers F. Ordering of human bone marrow B lymphocyte precursors by single-cell polymerase chain reaction analyses of the rearrangement status of the immunoglobulin H and L chain gene loci. *J Exp Med.* 1996;184(6):2217-29.
  70. Grawunder U, Schatz DG, Leu TM, Rolink A, Melchers F. The half-life of RAG-1 protein in precursor B cells is increased in the absence of RAG-2 expression. *J Exp Med.* 1996;183(4):1731-7.
  71. Karasuyama H, Rolink A, Melchers F. Surrogate light chain in B cell development. *Adv Immunol.* 1996;63:1-41.
  72. Mertsching E, Grawunder U, Meyer V, Rolink T, Ceredig R. Phenotypic and functional analysis of B lymphopoiesis in interleukin-7-transgenic mice: expansion of pro/pre-B cell number and persistence of B lymphocyte development in lymph nodes and spleen. *Eur J Immunol.* 1996;26(1):28-33.
  73. Oka Y, Rolink AG, Andersson J, Kamanaka M, Uchida J, Yasui T, et al. Profound reduction of mature B cell numbers, reactivities and serum Ig levels in mice which simultaneously carry the XID and CD40 deficiency genes. *Int Immunol.* 1996;8(11):1675-85.
  74. Reininger L, Winkler TH, Kalberer CP, Jourdan M, Melchers F, Rolink AG. Intrinsic B cell defects in NZB and NZW mice contribute to systemic lupus erythematosus in (NZB × NZW)F1 mice. *J Exp Med.* 1996;184(3):853-61.
  75. Rolink A, Haasner D, Melchers F, Andersson J. The surrogate light chain in mouse B-cell development. *Int Rev Immunol.* 1996;13(4):341-56.
  76. Rolink A, Melchers F. B-cell development in the mouse. *Immunol Lett.* 1996;54(2-3):157-61.
  77. Rolink A, Melchers F, Andersson J. The SCID but not the RAG-2 gene product is required for S mu-S epsilon heavy chain class switching. *Immunity.* 1996;5(4):319-30.
  78. Rolink A, ten Boekel E, Melchers F, Fearon DT, Krop I, Andersson J. A subpopulation of B220+ cells in murine bone marrow does not express CD19 and contains natural killer cell progenitors. *J Exp Med.* 1996;183(1):187-94.
  79. Schubart DB, Rolink A, Kosco-Vilbois MH, Botteri F, Matthias P. B-cell-specific coactivator OBF-1/OCA-B/Bob1 required for immune response and germinal centre formation. *Nature.* 1996;383(6600):538-42.
  80. Cavelier P, Nato F, Coquilleau I, Rolink A, Rougeon F, Goodhardt M. B lineage-restricted rearrangement of a human Ig kappa transgene. *Eur J Immunol.* 1997;27(7):1626-31.
  81. D'Apuzzo M, Rolink A, Loetscher M, Hoxie JA, Clark-Lewis I, Melchers F, et al. The chemokine SDF-1, stromal cell-derived factor 1, attracts early stage B cell precursors via the chemokine receptor CXCR4. *Eur J Immunol.* 1997;27(7):1788-93.
  82. Kalberer CP, Reininger L, Melchers F, Rolink AG. Priming of helper T cell-dependent antibody responses by hemagglutinin-transgenic B cells. *Eur J Immunol.* 1997;27(9):2400-7.
  83. Melamed D, Kench JA, Grabstein K, Rolink A, Nemazee D. A functional B cell receptor transgene allows efficient IL-7-independent maturation of B cell precursors. *J Immunol.* 1997;159(3):1233-9.
  84. Nutt SL, Urbanek P, Rolink A, Busslinger M. Essential functions of Pax5 (BSAP) in pro-B cell development: difference between fetal and adult B lymphopoiesis and reduced V-to-DJ recombination at the IgH locus. *Genes Dev.* 1997;11(4):476-91.
  85. Siwarski D, Muller U, Andersson J, Notario V, Melchers F, Rolink A, et al. Structure and expression of the c-Myc/Pvt 1 megagene locus. *Curr Top Microbiol Immunol.* 1997;224:67-72.
  86. ten Boekel E, Melchers F, Rolink AG. Changes in the V(H) gene repertoire of developing precursor B lymphocytes in mouse bone marrow mediated by the pre-B cell receptor. *Immunity.* 1997;7(3):357-68.

87. Ceredig R, ten Boekel E, Rolink A, Melchers F, Andersson J. Fetal liver organ cultures allow the proliferative expansion of pre-B receptor-expressing pre-B-II cells and the differentiation of immature and mature B cells in vitro. *Int Immunol.* 1998;10(1):49-59.
88. Colonna M, Samardis J, Cella M, Angman L, Allen RL, O'Callaghan CA, et al. Human myelomonocytic cells express an inhibitory receptor for classical and nonclassical MHC class I molecules. *J Immunol.* 1998;160(7):3096-100.
89. Dinkel A, Warnatz K, Ledermann B, Rolink A, Zipfel PF, Burki K, et al. The transcription factor early growth response 1 (Egr-1) advances differentiation of pre-B and immature B cells. *J Exp Med.* 1998;188(12):2215-24.
90. Engel H, Bogen B, Muller U, Andersson J, Rolink A, Weiss S. Expression level of a transgenic lambda2 chain results in isotype exclusion and commitment to B1 cells. *Eur J Immunol.* 1998;28(8):2289-99.
91. Ghia P, ten Boekel E, Rolink AG, Melchers F. B-cell development: a comparison between mouse and man. *Immunol Today.* 1998;19(10):480-5.
92. Gunthert U, Schwarzer C, Wittig B, Laman J, Ruiz P, Stauder R, et al. Functional involvement of CD44, a family of cell adhesion molecules, in immune responses, tumour progression and haematopoiesis. *Adv Exp Med Biol.* 1998;451:43-9.
93. Kistler B, Rolink A, Marienfeld R, Neumann M, Wirth T. Induction of nuclear factor-kappa B during primary B cell differentiation. *J Immunol.* 1998;160(5):2308-17.
94. Morrison AM, Nutt SL, Thevenin C, Rolink A, Busslinger M. Loss- and gain-of-function mutations reveal an important role of BSAP (Pax-5) at the start and end of B cell differentiation. *Semin Immunol.* 1998;10(2):133-42.
95. Nutt SL, Morrison AM, Dorfler P, Rolink A, Busslinger M. Identification of BSAP (Pax-5) target genes in early B-cell development by loss- and gain-of-function experiments. *EMBO J.* 1998;17(8):2319-33.
96. Osmond DG, Rolink A, Melchers F. Murine B lymphopoiesis: towards a unified model. *Immunol Today.* 1998;19(2):65-8.
97. Rijkers T, Van Den Ouwehand J, Morolli B, Rolink AG, Baarends WM, Van Sloun PP, et al. Targeted inactivation of mouse RAD52 reduces homologous recombination but not resistance to ionizing radiation. *Mol Cell Biol.* 1998;18(11):6423-9.
98. Rolink AG, Andersson J, Melchers F. Characterization of immature B cells by a novel monoclonal antibody, by turnover and by mitogen reactivity. *Eur J Immunol.* 1998;28(11):3738-48.
99. Schaniel C, Pardali E, Sallusto F, Speletras M, Ruedl C, Shimizu T, et al. Activated murine B lymphocytes and dendritic cells produce a novel CC chemokine which acts selectively on activated T cells. *J Exp Med.* 1998;188(3):451-63.
100. ten Boekel E, Melchers F, Rolink AG. Precursor B cells showing H chain allelic inclusion display allelic exclusion at the level of pre-B cell receptor surface expression. *Immunity.* 1998;8(2):199-207.
101. Ceredig R, Andersson J, Melchers F, Rolink A. Effect of deregulated IL-7 transgene expression on B lymphocyte development in mice expressing mutated pre-B cell receptors. *Eur J Immunol.* 1999;29(9):2797-807.
102. Ceredig R, Rolink AG, Melchers F, Andersson J. Fetal liver organ cultures as a tool to study selection processes during B cell development. *Curr Top Microbiol Immunol.* 1999;246:11-7; discussion 8-9.
103. Engel H, Rolink A, Weiss S. B cells are programmed to activate kappa and lambda for rearrangement at consecutive developmental stages. *Eur J Immunol.* 1999;29(7):2167-76.
104. Ghia P, Schaniel C, Rolink AG, Nadler LM, Cardoso AA. Human macrophage-derived chemokine (MDC) is strongly expressed following activation of both normal and malignant precursor and mature B cells. *Curr Top Microbiol Immunol.* 1999;246:103-10.
105. Melchers F, Rolink AG, Schaniel C. The role of chemokines in regulating cell migration during humoral immune responses. *Cell.* 1999;99(4):351-4.
106. Melchers F, ten Boekel E, Yamagami T, Andersson J, Rolink A. The roles of preB and B cell receptors in the stepwise allelic exclusion of mouse IgH and L chain gene loci. *Semin Immunol.* 1999;11(5):307-17.
107. Nutt SL, Heavey B, Rolink AG, Busslinger M. Commitment to the B-lymphoid lineage depends on the transcription factor Pax5. *Nature.* 1999;401(6753):556-62.
108. Nutt SL, Rolink AG, Busslinger M. The molecular basis of B-cell lineage commitment. *Cold Spring Harb Symp Quant Biol.* 1999;64:51-9.
109. Nutt SL, Vambrie S, Steinlein P, Kozmik Z, Rolink A, Weith A, et al. Independent regulation of the two Pax5 alleles during B-cell development. *Nat Genet.* 1999;21(4):390-5.
110. Rolink A, Nutt S, Busslinger M, ten Boekel E, Seidl T, Andersson J, et al. Differentiation, dedifferentiation, and redifferentiation of B-lineage lymphocytes: roles of the surrogate light chain and the Pax5 gene. *Cold Spring Harb Symp Quant Biol.* 1999;64:21-5.
111. Rolink AG, Brocker T, Bluethmann H, Kosco-Vilbois MH, Andersson J, Melchers F. Mutations affecting either generation or survival of cells influence the pool size of mature B cells. *Immunity.* 1999;10(5):619-28.
112. Rolink AG, Melchers F, Andersson J. The transition from immature to mature B cells. *Curr Top Microbiol Immunol.* 1999;246:39-43; discussion 4.
113. Rolink AG, Nutt SL, Melchers F, Busslinger M. Long-term in vivo reconstitution of T-cell development by Pax5-deficient B-cell progenitors. *Nature.* 1999;401(6753):603-6.
114. Rolink AG, ten Boekel E, Yamagami T, Ceredig R, Andersson J, Melchers F. B cell development in the mouse from early progenitors to mature B cells. *Immunol Lett.* 1999;68(1):89-93.
115. Schaniel C, Sallusto F, Ruedl C, Sideras P, Melchers F, Rolink AG. Three chemokines with potential functions in T lymphocyte-independent and -dependent B lymphocyte stimulation. *Eur J Immunol.* 1999;29(9):2934-47.
116. Schaniel C, Sallusto F, Sideras P, Melchers F, Rolink AG. A novel CC chemokine ABCD-1, produced by dendritic cells and activated B cells, exclusively attracts activated T lymphocytes. *Curr Top Microbiol Immunol.* 1999;246:95-101.

117. ten Boekel E, Yamagami T, Andersson J, Rolink AG, Melchers F. The formation and selection of cells expressing preB cell receptors and B cell receptors. *Curr Top Microbiol Immunol.* 1999;246:3-9; discussion -10.
118. Yamagami T, ten Boekel E, Andersson J, Rolink A, Melchers F. Frequencies of multiple IgL chain gene rearrangements in single normal or kappaL chain-deficient B lineage cells. *Immunity.* 1999;11(3):317-27.
119. Yamagami T, ten Boekel E, Schaniel C, Andersson J, Rolink A, Melchers F. Four of five RAG-expressing JCkappa/- small pre-BII cells have no L chain gene rearrangements: detection by high-efficiency single cell PCR. *Immunity.* 1999;11(3):309-16.
120. Yu W, Nagaoka H, Jankovic M, Misulovin Z, Suh H, Rolink A, et al. Continued RAG expression in late stages of B cell development and no apparent re-induction after immunization. *Nature.* 1999;400(6745):682-7.
121. Busslinger M, Nutt SL, Rolink AG. Lineage commitment in lymphopoiesis. *Curr Opin Immunol.* 2000;12(2):151-8.
122. Ceredig R, Rolink AG, Melchers F, Andersson J. The B cell receptor, but not the pre-B cell receptor, mediates arrest of B cell differentiation. *Eur J Immunol.* 2000;30(3):759-67.
123. Ghia P, Melchers F, Rolink AG. Age-dependent changes in B lymphocyte development in man and mouse. *Exp Gerontol.* 2000;35(2):159-65.
124. Melchers F, ten Boekel E, Seidl T, Kong XC, Yamagami T, Onishi K, et al. Repertoire selection by pre-B-cell receptors and B-cell receptors, and genetic control of B-cell development from immature to mature B cells. *Immunol Rev.* 2000;175:33-46.
125. Rolink AG, Melchers F. Precursor B cells from Pax-5-deficient mice—stem cells for macrophages, granulocytes, osteoclasts, dendritic cells, natural killer cells, thymocytes and T cells. *Curr Top Microbiol Immunol.* 2000;251:21-6.
126. Rolink AG, Schaniel C, Busslinger M, Nutt SL, Melchers F. Fidelity and infidelity in commitment to B-lymphocyte lineage development. *Immunol Rev.* 2000;175:104-11.
127. Rolink AG, Winkler T, Melchers F, Andersson J. Precursor B cell receptor-dependent B cell proliferation and differentiation does not require the bone marrow or fetal liver environment. *J Exp Med.* 2000;191(1):23-32.
128. Schaniel C, Melchers F, Rolink AG. The cluster of ABCD chemokines which organizes T cell-dependent B cell responses. *Curr Top Microbiol Immunol.* 2000;251:181-9.
129. Schubart DB, Rolink A, Schubart K, Matthias P. Cutting edge: lack of peripheral B cells and severe agammaglobulinemia in mice simultaneously lacking Bruton's tyrosine kinase and the B cell-specific transcriptional coactivator OBF-1. *J Immunol.* 2000;164(1):18-22.
130. Ghia P, Transidico P, Veiga JP, Schaniel C, Sallusto F, Matsushima K, et al. Chemoattractants MDC and TARC are secreted by malignant B-cell precursors following CD40 ligation and support the migration of leukemia-specific T cells. *Blood.* 2001;98(3):533-40.
131. Nutt SL, Eberhard D, Horcher M, Rolink AG, Busslinger M. Pax5 determines the identity of B cells from the beginning to the end of B-lymphopoiesis. *Int Rev Immunol.* 2001;20(1):65-82.
132. Rolink AG, Schaniel C, Andersson J, Melchers F. Selection events operating at various stages in B cell development. *Curr Opin Immunol.* 2001;13(2):202-7.
133. Schaniel C, Rolink AG, Melchers F. Attractions and migrations of lymphoid cells in the organization of humoral immune responses. *Adv Immunol.* 2001;78:111-68.
134. Schubart K, Massa S, Schubart D, Corcoran LM, Rolink AG, Matthias P. B cell development and immunoglobulin gene transcription in the absence of Oct-2 and OBF-1. *Nat Immunol.* 2001;2(1):69-74.
135. Seidl T, Rolink A, Melchers F. The VpreB protein of the surrogate light-chain can pair with some mu heavy-chains in the absence of the lambda 5 protein. *Eur J Immunol.* 2001;31(7):1999-2006.
136. Terszowski G, Jankowski A, Hendriks WJ, Rolink AG, Kisielow P. Within the hemopoietic system, LAR phosphatase is a T cell lineage-specific adhesion receptor-like protein whose phosphatase activity appears dispensable for T cell development, repertoire selection and function. *Eur J Immunol.* 2001;31(3):832-40.
137. Bruno L, Schaniel C, Rolink A. Plasticity of Pax-5(-/-) pre-B I cells. *Cells Tissues Organs.* 2002;171(1):38-43.
138. Hoffmann R, Seidl T, Neeb M, Rolink A, Melchers F. Changes in gene expression profiles in developing B cells of murine bone marrow. *Genome Res.* 2002;12(1):98-111.
139. Martensson IL, Rolink A, Melchers F, Mundt C, Licence S, Shimizu T. The pre-B cell receptor and its role in proliferation and Ig heavy chain allelic exclusion. *Semin Immunol.* 2002;14(5):335-42.
140. Rolink AG, Melchers F. BAFFled B cells survive and thrive: roles of BAFF in B-cell development. *Curr Opin Immunol.* 2002;14(2):266-75.
141. Rolink AG, Schaniel C, Bruno L, Melchers F. In vitro and in vivo plasticity of Pax5-deficient pre-B I cells. *Immunol Lett.* 2002;82(1-2):35-40.
142. Rolink AG, Schaniel C, Melchers F. Stability and plasticity of wild-type and Pax5-deficient precursor B cells. *Immunol Rev.* 2002;187:87-95.
143. Rolink AG, Tschopp J, Schneider P, Melchers F. BAFF is a survival and maturation factor for mouse B cells. *Eur J Immunol.* 2002;32(7):2004-10.
144. Schaniel C, Bruno L, Melchers F, Rolink AG. Multiple hematopoietic cell lineages develop in vivo from transplanted Pax5-deficient pre-B I-cell clones. *Blood.* 2002;99(2):472-8.
145. Schaniel C, Gottar M, Roosnek E, Melchers F, Rolink AG. Extensive in vivo self-renewal, long-term reconstitution capacity, and hematopoietic multipotency of Pax5-deficient precursor B-cell clones. *Blood.* 2002;99(8):2760-6.
146. Ceredig R, Bosco N, Maye PN, Andersson J, Rolink A. In interleukin-7-transgenic mice, increasing B lymphopoiesis increases follicular but not marginal zone B cell numbers. *Eur J Immunol.* 2003;33(9):2567-76.
147. Duber S, Engel H, Rolink A, Kretschmer K, Weiss S. Germline transcripts of immunoglobulin light chain variable regions

- are structurally diverse and differentially expressed. *Mol Immunol.* 2003;40(8):509-16.
148. Felix K, Rolink A, Melchers F, Janz S. Bcl-2 reduces mutant rates in a transgenic lacZ reporter gene in mouse pre-B lymphocytes. *Mutat Res.* 2003;522(1-2):135-44.
  149. Hoffmann R, Bruno L, Seidl T, Rolink A, Melchers F. Rules for gene usage inferred from a comparison of large-scale gene expression profiles of T and B lymphocyte development. *J Immunol.* 2003;170(3):1339-53.
  150. Rolink AG. B-cell development and pre-B-1 cell plasticity in vitro. *Methods Mol Biol.* 2004;271:271-81.
  151. Rolink AG, Andersson J, Melchers F. Molecular mechanisms guiding late stages of B-cell development. *Immunol Rev.* 2004;197:41-50.
  152. Tardivel A, Tinel A, Lens S, Steiner QG, Sauberli E, Wilson A, et al. The anti-apoptotic factor Bcl-2 can functionally substitute for the B cell survival but not for the marginal zone B cell differentiation activity of BAFF. *Eur J Immunol.* 2004;34(2):509-18.
  153. Ardouin L, Rolink AG, Mura AM, Gommeaux J, Melchers F, Busslinger M, et al. Rapid in vivo analysis of mutant forms of the LAT adaptor using Pax5-Lat double-deficient pro-B cells. *Eur J Immunol.* 2005;35(3):977-86.
  154. Balciunaite G, Ceredig R, Fehling HJ, Zuniga-Pflucker JC, Rolink AG. The role of Notch and IL-7 signaling in early thymocyte proliferation and differentiation. *Eur J Immunol.* 2005;35(4):1292-300.
  155. Balciunaite G, Ceredig R, Massa S, Rolink AG. A B220+ CD117+ CD19- hematopoietic progenitor with potent lymphoid and myeloid developmental potential. *Eur J Immunol.* 2005;35(7):2019-30.
  156. Balciunaite G, Ceredig R, Rolink AG. The earliest subpopulation of mouse thymocytes contains potent T, significant macrophage, and natural killer cell but no B-lymphocyte potential. *Blood.* 2005;105(5):1930-6.
  157. Harfst E, Andersson J, Grawunder U, Ceredig R, Rolink AG. Homeostatic and functional analysis of mature B cells in lambda5-deficient mice. *Immunol Lett.* 2005;101(2):173-84.
  158. Matthias P, Rolink AG. Transcriptional networks in developing and mature B cells. *Nat Rev Immunol.* 2005;5(6):497-508.
  159. Benard A, Ceredig R, Rolink AG. Regulatory T cells control autoimmunity following syngeneic bone marrow transplantation. *Eur J Immunol.* 2006;36(9):2324-35.
  160. Bosco N, Agenes F, Rolink AG, Ceredig R. Peripheral T cell lymphopenia and concomitant enrichment in naturally arising regulatory T cells: the case of the pre-Talpha gene-deleted mouse. *J Immunol.* 2006;177(8):5014-23.
  161. Ceredig R, Rauch M, Balciunaite G, Rolink AG. Increasing Flt3L availability alters composition of a novel bone marrow lymphoid progenitor compartment. *Blood.* 2006;108(4):1216-22.
  162. Maerki S, Ceredig R, Rolink A. Induction of chemokine receptor expression during early stages of T cell development. *Immunol Lett.* 2006;104(1-2):110-7.
  163. Massa S, Balciunaite G, Ceredig R, Rolink AG. Critical role for c-kit (CD117) in T cell lineage commitment and early thymocyte development in vitro. *Eur J Immunol.* 2006;36(3):526-32.
  164. Melchers F, Rolink AR. B cell tolerance—how to make it and how to break it. *Curr Top Microbiol Immunol.* 2006;305:1-23.
  165. Rolink AG, Balciunaite G, Demoliere C, Ceredig R. The potential involvement of Notch signaling in NK cell development. *Immunol Lett.* 2006;107(1):50-7.
  166. Rolink AG, Massa S, Balciunaite G, Ceredig R. Early lymphocyte development in bone marrow and thymus. *Swiss Med Wkly.* 2006;136(43-44):679-83.
  167. Aschenbrenner K, D'Cruz LM, Vollmann EH, Hinterberger M, Emmerich J, Swee LK, et al. Selection of Foxp3+ regulatory T cells specific for self antigen expressed and presented by Aire+ medullary thymic epithelial cells. *Nat Immunol.* 2007;8(4):351-8.
  168. Brown G, Hughes PJ, Michell RH, Rolink AG, Ceredig R. The sequential determination model of hematopoiesis. *Trends Immunol.* 2007;28(10):442-8.
  169. Ceredig R, Bosco N, Rolink AG. The B lineage potential of thymus settling progenitors is critically dependent on mouse age. *Eur J Immunol.* 2007;37(3):830-7.
  170. Chappaz S, Flueck L, Farr AG, Rolink AG, Finke D. Increased TSLP availability restores T- and B-cell compartments in adult IL-7 deficient mice. *Blood.* 2007;110(12):3862-70.
  171. Hoffmann R, Lottaz C, Kuhne T, Rolink A, Melchers F. Neutrality, compensation, and negative selection during evolution of B-cell development transcriptomes. *Mol Biol Evol.* 2007;24(12):2610-8.
  172. Melchers F, Yamagami T, Rolink A, Andersson J. Rules for the rearrangement events at the L chain gene loci of the mouse. *Adv Exp Med Biol.* 2007;596:63-70.
  173. Rolink AG, Massa S, Balciunaite G, Ceredig R. Early lymphocyte development in bone marrow and thymus. *Swiss Med Wkly.* 2007;137 Suppl 155:20S-4S.
  174. Bordon A, Bosco N, Du Roure C, Bartholdy B, Kohler H, Matthias G, et al. Enforced expression of the transcriptional coactivator OBF1 impairs B cell differentiation at the earliest stage of development. *PLoS One.* 2008;3(12):e4007.
  175. Bosco N, Ceredig R, Rolink A. Transient decrease in interleukin-7 availability arrests B lymphopoiesis during pregnancy. *Eur J Immunol.* 2008;38(2):381-90.
  176. Bosco N, Engdahl C, Benard A, Rolink J, Ceredig R, Rolink AG. TCR-beta chains derived from peripheral gammadelta T cells can take part in alphabeta T-cell development. *Eur J Immunol.* 2008;38(12):3520-9.
  177. Fazio G, Palmi C, Rolink A, Biondi A, Cazzaniga G. PAX5/TEL acts as a transcriptional repressor causing down-modulation of CD19, enhances migration to CXCL12, and confers survival advantage in pre-BI cells. *Cancer Res.* 2008;68(1):181-9.
  178. Mueller P, Massner J, Jayachandran R, Combaluzier B, Albrecht I, Gatfield J, et al. Regulation of T cell survival through coronin-1-mediated generation of inositol-1,4,5-trisphosphate and calcium mobilization after T cell receptor triggering. *Nat Immunol.* 2008;9(4):424-31.
  179. Tiao JY, Bradaia A, Biermann B, Kaupmann K, Metz M, Haller C, et al. The sushi domains of secreted GABA(B1) isoforms

- selectively impair GABA(B) heteroreceptor function. *J Biol Chem.* 2008;283(45):31005-11.
180. Ceredig R, Rolink AG, Brown G. Models of haematopoiesis: seeing the wood for the trees. *Nat Rev Immunol.* 2009;9(4):293-300.
  181. Rauch M, Tussiwand R, Bosco N, Rolink AG. Crucial role for BAFF-BAFF-R signaling in the survival and maintenance of mature B cells. *PLoS One.* 2009;4(5):e5456.
  182. Schmutz S, Bosco N, Chappaz S, Boyman O, Acha-Orbea H, Ceredig R, et al. Cutting edge: IL-7 regulates the peripheral pool of adult ROR gamma+ lymphoid tissue inducer cells. *J Immunol.* 2009;183(4):2217-21.
  183. Swee LK, Bosco N, Malissen B, Ceredig R, Rolink A. Expansion of peripheral naturally occurring T regulatory cells by Fms-like tyrosine kinase 3 ligand treatment. *Blood.* 2009;113(25):6277-87.
  184. Tussiwand R, Bosco N, Ceredig R, Rolink AG. Tolerance checkpoints in B-cell development: Johnny B good. *Eur J Immunol.* 2009;39(9):2317-24.
  185. Bosco N, Swee LK, Benard A, Ceredig R, Rolink A. Auto-reconstitution of the T-cell compartment by radioresistant hematopoietic cells following lethal irradiation and bone marrow transplantation. *Exp Hematol.* 2010;38(3):222-32 e2.
  186. Cassani B, Poliani PL, Marrella V, Schena F, Sauer AV, Ravanini M, et al. Homeostatic expansion of autoreactive immunoglobulin-secreting cells in the Rag2 mouse model of Omenn syndrome. *J Exp Med.* 2010;207(7):1525-40.
  187. Santiago-Raber ML, Amano H, Amano E, Fossati-Jimack L, Swee LK, Rolink A, et al. Evidence that Yaa-induced loss of marginal zone B cells is a result of dendritic cell-mediated enhanced activation. *J Autoimmun.* 2010;34(4):349-55.
  188. Swee LK, Tardivel A, Schneider P, Rolink A. Rescue of the mature B cell compartment in BAFF-deficient mice by treatment with recombinant Fc-BAFF. *Immunol Lett.* 2010;131(1):40-8.
  189. Bossen C, Tardivel A, Willen L, Fletcher CA, Perroud M, Beermann F, et al. Mutation of the BAFF furin cleavage site impairs B-cell homeostasis and antibody responses. *Eur J Immunol.* 2011;41(3):787-97.
  190. Tussiwand R, Engdahl C, Gehre N, Bosco N, Ceredig R, Rolink AG. The preTCR-dependent DN3 to DP transition requires Notch signaling, is improved by CXCL12 signaling and is inhibited by IL-7 signaling. *Eur J Immunol.* 2011;41(11):3371-80.
  191. Ceredig R, Rolink AG. The key role of IL-7 in lymphopoiesis. *Semin Immunol.* 2012;24(3):159-64.
  192. Kreuzaler M, Rauch M, Salzer U, Birmelin J, Rizzi M, Grimbacher B, et al. Soluble BAFF levels inversely correlate with peripheral B cell numbers and the expression of BAFF receptors. *J Immunol.* 2012;188(1):497-503.
  193. Tussiwand R, Rauch M, Fluck LA, Rolink AG. BAFF-R expression correlates with positive selection of immature B cells. *Eur J Immunol.* 2012;42(1):206-16.
  194. Fazio G, Cazzaniga V, Palmi C, Galbiati M, Giordan M, te Kronnie G, et al. PAX5/ETV6 alters the gene expression profile of precursor B cells with opposite dominant effect on endogenous PAX5. *Leukemia.* 2013;27(4):992-5.
  195. Kyaw T, Cui P, Tay C, Kanellakis P, Hosseini H, Liu E, et al. BAFF receptor mAb treatment ameliorates development and progression of atherosclerosis in hyperlipidemic ApoE(-/-) mice. *PLoS One.* 2013;8(4):e60430.
  196. Kraus H, Kaiser S, Aumann K, Bonelt P, Salzer U, Vestweber D, et al. A feeder-free differentiation system identifies autonomously proliferating B cell precursors in human bone marrow. *J Immunol.* 2014;192(3):1044-54.
  197. Nusser A, Nuber N, Wirz OF, Rolink H, Andersson J, Rolink A. The development of autoimmune features in aging mice is closely associated with alterations of the peripheral CD4(+) T-cell compartment. *Eur J Immunol.* 2014;44(10):2893-902.
  198. Okujava R, Guye P, Lu YY, Mistl C, Polus F, Vayssier-Taussat M, et al. A translocated effector required for Bartonella dissemination from derma to blood safeguards migratory host cells from damage by co-translocated effectors. *PLoS Pathog.* 2014;10(6):e1004187.
  199. Pieper K, Rizzi M, Speletras M, Smulski CR, Sic H, Kraus H, et al. A common single nucleotide polymorphism impairs B-cell activating factor receptor's multimerization, contributing to common variable immunodeficiency. *J Allergy Clin Immunol.* 2014;133(4):1222-5.
  200. Swee LK, Nusser A, Curti M, Kreuzaler M, Rolink H, Terracciano L, et al. The amount of self-antigen determines the effector function of murine T cells escaping negative selection. *Eur J Immunol.* 2014;44(5):1299-312.
  201. Tsapogas P, Swee LK, Nusser A, Nuber N, Kreuzaler M, Capoferri G, et al. In vivo evidence for an instructive role of fms-like tyrosine kinase-3 (FLT3) ligand in hematopoietic development. *Haematologica.* 2014;99(4):638-46.
  202. Venhoff N, Niessen L, Kreuzaler M, Rolink AG, Hassler F, Rizzi M, et al. Reconstitution of the peripheral B lymphocyte compartment in patients with ANCA-associated vasculitides treated with rituximab for relapsing or refractory disease. *Autoimmunity.* 2014;47(6):401-8.
  203. Vigano MA, Ivanek R, Balwierz P, Berninger P, van Nimwegen E, Karjalainen K, et al. An epigenetic profile of early T-cell development from multipotent progenitors to committed T-cell descendants. *Eur J Immunol.* 2014;44(4):1181-93.
  204. von Burg N, Chappaz S, Baerenwaldt A, Horvath E, Bose Dasgupta S, Ashok D, et al. Activated group 3 innate lymphoid cells promote T-cell-mediated immune responses. *Proc Natl Acad Sci U S A.* 2014;111(35):12835-40.
  205. von Muenchow L, Engdahl C, Karjalainen K, Rolink AG. The selection of mature B cells is critically dependent on the expression level of the co-receptor CD19. *Immunol Lett.* 2014;160(2):113-9.
  206. Bessa J, Boeckle S, Beck H, Buckel T, Schlicht S, Ebeling M, et al. The immunogenicity of antibody aggregates in a novel transgenic mouse model. *Pharm Res.* 2015;32(7):2344-59.
  207. Bornancin F, Renner F, Touil R, Sic H, Kolb Y, Touil-Allaoui I, et al. Deficiency of MALT1 paracaspase activity results in unbalanced regulatory and effector T and B cell responses leading to multiorgan inflammation. *J Immunol.* 2015;194(8):3723-34.
  208. Brown G, Mooney CJ, Alberti-Servera L, Muenchow L, Toellner KM, Ceredig R, et al. Versatility of stem and

- progenitor cells and the instructive actions of cytokines on hematopoiesis. *Crit Rev Clin Lab Sci.* 2015;52(4):168–79.
209. Choukallah MA, Song S, Rolink AG, Burger L, Matthias P. Enhancer repertoires are reshaped independently of early priming and heterochromatin dynamics during B cell differentiation. *Nat Commun.* 2015;6:8324.
210. Gehre N, Nusser A, von Muenchow L, Tussiwand R, Engdahl C, Capoferri G, et al. A stromal cell free culture system generates mouse pro-T cells that can reconstitute T-cell compartments *in vivo*. *Eur J Immunol.* 2015;45(3):932–42.
211. Harmeier A, Obermueller S, Meyer CA, Revel FG, Buchy D, Chaboz S, et al. Trace amine-associated receptor 1 activation silences GSK3beta signaling of TAAR1 and D2R heteromers. *Eur Neuropsychopharmacol.* 2015;25(11):2049–61.
212. Manoharan A, Du Roure C, Rolink AG, Matthias P. De novo DNA Methyltransferases Dnmt3a and Dnmt3b regulate the onset of Igκ light chain rearrangement during early B-cell development. *Eur J Immunol.* 2015;45(8):2343–55.
213. Nobs SP, Schneider C, Dietrich MG, Brocker T, Rolink A, Hirsch E, et al. PI3-Kinase-gamma Has a Distinct and Essential Role in Lung-Specific Dendritic Cell Development. *Immunity.* 2015;43(4):674–89.
214. Baerenwaldt A, von Burg N, Kreuzaler M, Sitte S, Horvath E, Peter A, et al. Flt3 Ligand Regulates the Development of Innate Lymphoid Cells in Fetal and Adult Mice. *J Immunol.* 2016;196(6):2561–71.
215. von Muenchow L, Alberti-Servera L, Klein F, Capoferri G, Finke D, Ceredig R, et al. Permissive roles of cytokines interleukin-7 and Flt3 ligand in mouse B-cell lineage commitment. *Proc Natl Acad Sci U S A.* 2016;113(50):E8122–E830.
216. Alberti-Servera L, von Muenchow L, Tsapogas P, Capoferri G, Eschbach K, Beisel C, et al. Single-cell RNA sequencing reveals developmental heterogeneity among early lymphoid progenitors. *EMBO J.* 2017;36(24):3619–33.
217. Fazio G, Turazzi N, Cazzaniga V, Kreuzaler M, Maglia O, Magnani CF, et al. TNFRSF13C (BAFFR) positive blasts persist after early treatment and at relapse in childhood B-cell precursor acute lymphoblastic leukaemia. *Br J Haematol.* 2017.
218. Smulski CR, Kury P, Seidel LM, Staiger HS, Edinger AK, Willen L, et al. BAFF- and TACI-Dependent Processing of BAFFR by ADAM Proteases Regulates the Survival of B Cells. *Cell Rep.* 2017;18(9):2189–202.
219. Tsapogas P, Mooney CJ, Brown G, Rolink A. The Cytokine Flt3-Ligand in Normal and Malignant Hematopoiesis. *Int J Mol Sci.* 2017;18(6).
220. von Muenchow L, Tsapogas P, Alberti-Servera L, Capoferri G, Doelz M, Rolink H, et al. Pro-B cells propagated in stromal cell-free cultures reconstitute functional B-cell compartments in immunodeficient mice. *Eur J Immunol.* 2017;47(2):394–405.
221. Calvo-Asensio I, Sugrue T, Bosco N, Rolink A, Ceredig R. DN2 Thymocytes Activate a Specific Robust DNA Damage Response to Ionizing Radiation-Induced DNA Double-Strand Breaks. *Front Immunol.* 2018;9:1312.
222. Faderl M, Klein F, Wirz OF, Heiler S, Alberti-Servera L, Engdahl C, et al. Two Distinct Pathways in Mice Generate Antinuclear Antigen-Reactive B Cell Repertoires. *Front Immunol.* 2018;9:16.
223. Heiler S, Lotscher J, Kreuzaler M, Rolink J, Rolink A. Prophylactic and Therapeutic Effects of Interleukin-2 (IL-2)/Anti-IL-2 Complexes in Systemic Lupus Erythematosus-Like Chronic Graft-Versus-Host Disease. *Front Immunol.* 2018;9:656.
224. Kim M, von Muenchow L, Le Meur T, Kueng B, Gapp B, Weber D, et al. DPP9 enzymatic activity in hematopoietic cells is dispensable for mouse hematopoiesis. *Immunol Lett.* 2018;198:60–5.
225. Turazzi N, Fazio G, Rossi V, Rolink A, Cazzaniga G, Biondi A, et al. Engineered T cells towards TNFRSF13C (BAFFR): a novel strategy to efficiently target B-cell acute lymphoblastic leukaemia. *Br J Haematol.* 2018.
226. Vigolo M, Chambers MG, Willen L, Chevalley D, Maskos K, Lammens A, et al. A loop region of BAFF controls B cell survival and regulates recognition by different inhibitors. *Nat Commun.* 2018;9(1):1199.
227. Wilhelmson AS, Lantero Rodriguez M, Stubelius A, Fogelstrand P, Johansson I, Buechler MB, et al. Testosterone is an endogenous regulator of BAFF and splenic B cell number. *Nat Commun.* 2018;9(1):2067.



# Accumulation of Multipotent Hematopoietic Progenitors in Peripheral Lymphoid Organs of Mice Over-expressing Interleukin-7 and Flt3-Ligand

Fabian Klein<sup>1</sup>, Lilly von Muenchow<sup>1</sup>, Giuseppina Capoferri<sup>1</sup>, Stefan Heiler<sup>1</sup>, Llucia Alberti-Servera<sup>1</sup>, Hannie Rolink<sup>1</sup>, Corinne Engdahl<sup>1</sup>, Michael Rolink<sup>1</sup>, Mladen Mitrovic<sup>1</sup>, Grozdan Cvijetic<sup>1</sup>, Jan Andersson<sup>1</sup>, Rhodri Ceredig<sup>2</sup>, Panagiotis Tsapogas<sup>1\*</sup> and Antonius Rolink<sup>1†</sup>

## OPEN ACCESS

### Edited by:

Barbara L. Kee,  
University of Chicago, United States

### Reviewed by:

Rodney P. DeKoter,  
University of Western Ontario, Canada  
John D. Colgan,  
University of Iowa, United States

### \*Correspondence:

Panagiotis Tsapogas  
panagiotis.tsapogas@unibas.ch

<sup>†</sup>These authors have contributed  
equally to this work

### Specialty section:

This article was submitted to  
B Cell Biology,  
a section of the journal  
*Frontiers in Immunology*

Received: 22 June 2018

Accepted: 11 September 2018

Published: 10 October 2018

### Citation:

Klein F, von Muenchow L, Capoferri G, Heiler S, Alberti-Servera L, Rolink H, Engdahl C, Rolink M, Mitrovic M, Cvijetic G, Andersson J, Ceredig R, Tsapogas P and Rolink A (2018)  
Accumulation of Multipotent Hematopoietic Progenitors in Peripheral Lymphoid Organs of Mice Over-expressing Interleukin-7 and Flt3-Ligand. *Front. Immunol.* 9:2258.  
doi: 10.3389/fimmu.2018.02258

<sup>1</sup> Department of Biomedicine, Developmental and Molecular Immunology, University of Basel, Basel, Switzerland, <sup>2</sup> Discipline of Physiology, College of Medicine & Nursing Health Science, National University of Ireland, Galway, Ireland

Interleukin-7 (IL-7) and Flt3-ligand (FL) are two cytokines important for the generation of B cells, as manifested by the impaired B cell development in mice deficient for either cytokine or their respective receptors and by the complete block in B cell differentiation in the absence of both cytokines. IL-7 is an important survival and proliferation factor for B cell progenitors, whereas FL acts on several early developmental stages, prior to B cell commitment. We have generated mice constitutively over-expressing both IL-7 and FL. These double transgenic mice develop splenomegaly and lymphadenopathy characterized by tremendously enlarged lymph nodes even in young animals. Lymphoid, myeloid and dendritic cell numbers are increased compared to mice over-expressing either of the two cytokines alone and the effect on their expansion is synergistic, rather than additive. B cell progenitors, early progenitors with myeloid and lymphoid potential (EPLM), common lymphoid progenitors (CLP) and lineage<sup>-</sup>, Sca1<sup>+</sup>, kit<sup>+</sup> (LSK) cells are all increased not only in the bone marrow but also in peripheral blood, spleen and even lymph nodes. When transplanted into irradiated wild-type mice, lymph node cells show long-term multilineage reconstitution, further confirming the presence of functional hematopoietic progenitors therein. Our double transgenic mouse model shows that sustained and combined over-expression of IL-7 and FL leads to a massive expansion of most bone marrow hematopoietic progenitors and to their associated presence in peripheral lymphoid organs where they reside and potentially differentiate further, thus leading to the synergistic increase in mature lymphoid and myeloid cell numbers. The present study provides further *in vivo* evidence for the concerted action of IL-7 and FL on lymphopoiesis and suggests that extramedullary niches, including those in lymph nodes, can support the survival and maintenance of hematopoietic progenitors that under physiological conditions develop exclusively in the bone marrow.

**Keywords:** IL-7, Flt3-ligand, hematopoiesis, cytokines, B cell development

## INTRODUCTION

Cytokines are important regulators for the development and function of immune cells. Apart from influencing the survival, expansion and effector function of mature immune cells in peripheral lymphoid organs, cytokines also have a crucial role in the continuous generation of all blood cell lineages (hematopoiesis), which occurs in the bone marrow and thymus. During hematopoiesis cytokines can influence the lineage output of hematopoietic progenitors by selectively promoting their survival, proliferation or developmental potential (1–3). Two of the most important cytokines for the generation of lymphoid cells are Flt3-ligand (FL) and Interleukin-7 (IL-7).

FL is produced by many cell types, but within the hematopoietic system it acts mainly on early, multipotent progenitors, which are the ones expressing its receptor, CD135 (Flt3) (4–6). CD135 is the only known receptor for FL and belongs to the type-III tyrosine kinase receptor family, which also includes CD117 (kit) and platelet-derived growth factor receptor (PDGF-R). CD135 expression within the lineage<sup>−</sup>, Sca1<sup>+</sup>, kit<sup>+</sup> (LSK) compartment of hematopoietic progenitors is associated with loss of self-renewal capacity and preservation of multilineage developmental potential (7). Oligopotent myeloid and lymphoid progenitors retain CD135 expression until they become committed to their respective lineages. From that point on, they down-regulate expression of the receptor, with the exception of dendritic cells (DC), which remain CD135<sup>+</sup> after maturation. The importance of FL in B cell development is manifested by the reduced capacity of *Flt3l*<sup>−/−</sup> and *Flt3*<sup>−/−</sup> hematopoietic progenitors to reconstitute the B cell compartment of lymphopenic mice (8, 9). In addition, B cell regeneration after irradiation or chemically induced myeloablation is dependent on FL (10). Since CD135 is down-regulated in committed B cell progenitors after Pax5 expression (11), the effect of FL signaling on B cell development is attributed to its role in maintaining normal numbers of oligopotent CD135<sup>+</sup> common lymphoid progenitors (CLP) and early progenitors with lymphoid and myeloid potential (EPLM) (12, 13).

CLP are phenotypically defined by the expression of CD127, the α-subunit of the receptor for IL-7 (14). CD127 expression is initiated at the CLP stage and remains expressed throughout the early stages of B cell development until the progenitors start to rearrange their light chain immunoglobulin genes (small pre-B stage). IL-7 was initially identified as a growth factor for B cells (15) and its essential role in lymphoid development has been proven both by its ability to maintain and expand lymphoid cells *in vitro* (16) and by the severe defect in B and T cell development observed in *Il7*<sup>−/−</sup> and *Il7ra*<sup>−/−</sup> mice (17, 18). Early T cell progenitors require IL-7 mainly for their survival, since over-expression of the anti-apoptotic protein Bcl2 can significantly rescue T cell development in *Il7ra*<sup>−/−</sup> mice (19, 20). IL-7 is also important for the survival and homeostatic expansion of mature T cells in the periphery (21). The fact that B cell development in *Il7ra*<sup>−/−</sup> mice cannot be rescued by Bcl2 over-expression (22, 23), together with the absence of early B-cell factor 1 (Ebf1) expression in *Il7ra*<sup>−/−</sup> CLP (24) has led to the hypothesis that

by initiating Ebf1 expression, IL-7 might act as an instructive cytokine for B cell commitment. However, this could also be explained by a survival role of IL-7 on CLP, since the Ebf1-expressing Ly6D<sup>+</sup> compartment of CLP is severely reduced in *Il7*<sup>−/−</sup> mice (25). Furthermore, B cell commitment in the absence of IL-7 signaling can be restored by over-expressing Bcl2 in mice lacking the IL-7 signaling mediator STAT5 (26) and by over-expressing FL in *Il7*<sup>−/−</sup> mice (13), therefore indicating that the role of this cytokine in commitment of progenitors to the B cell lineage is permissive, rather than instructive. Following Pax5 expression and lineage commitment, B cell progenitors require IL-7 for their survival and expansion. This has been clearly manifested in mice expressing high, sustained levels of IL-7, which resulted in expansion of pre-B cell progenitors in the bone marrow and in some cases in the development of B cell tumors (27–29). This increase in pro-B and pre-B cell numbers resulted in their accumulation in secondary lymphoid organs, such as spleen and lymph nodes.

As evident from the above, both FL and IL-7 are pivotal for the generation of normal B cell numbers, a fact highlighted by the complete absence of B cells in mice lacking both cytokines (30). Their combined effect is mostly exerted at different stages of B cell development, with FL being crucial for the generation of early multipotent progenitors and IL-7 for their survival and expansion after B cell commitment (13). However, they also act synergistically at the CLP/EPLM stage, where the receptors for both cytokines are simultaneously expressed, possibly through activation of separate signaling pathways (31). We have previously generated mice expressing high, sustained levels of human FL (hereafter FLtg) (32), which, when crossed to *Il7*<sup>−/−</sup> mice, showed a complete rescue of Ly6D<sup>+</sup> CLP/EPLM numbers (13). Interestingly, however, we have observed that mice over-expressing FL have reduced pre-B cell numbers compared to their wild-type (WT) counterparts (32). This could not be a direct effect of FL on pre-B cells, as they do not express CD135. Since pre-B cells are highly dependent on IL-7 for their expansion, we hypothesized that IL-7 availability might be reduced in FLtg bone marrow, due to the high number of CD127<sup>+</sup> CLP and EPLM progenitors, which might consume a large part of the available IL-7. Binding of IL-7 to its receptor on CD127<sup>+</sup> target cells has been proposed as a mechanism that regulates the abundance of the cytokine in different tissues (33).

In order to test this hypothesis, and to further study the synergy between FL and IL-7 in promoting lymphoid development *in vivo*, we bred FLtg mice with transgenic mice expressing high amounts of IL-7 (hereafter IL7tg) and analyzed the F<sub>1</sub> generation. Double transgenic mice (hereafter FLtgxIL7tg) had a phenotype that combined features of the single transgenic phenotypes and in terms of expansion of lymphoid cells, revealed synergy between the two cytokines. Thus, double transgenic mice exhibited splenomegaly and abnormally enlarged lymph nodes (LN), in which B and T cell numbers were increased more than in the single transgenic mice. Moreover, large numbers of B cell progenitors as well as CD19<sup>−</sup> multipotent progenitors were found in the LN of FLtgxIL7tg mice. Transplantation of LN FLtgxIL7tg cells into myelo-ablated recipients showed that they contained

hematopoietic progenitors with long-term multilineage developmental potential, suggesting that the LN niche can support the survival and maintenance of early hematopoietic progenitors.

## MATERIALS AND METHODS

### Mice

C57BL/6 (CD45.1<sup>+</sup> and CD45.2<sup>+</sup>), FLtg, IL7tg, FLtgxIL7tg and NOD/SCID/*Il2r $\gamma$* <sup>-/-</sup> mice were bred and maintained in our animal facility unit under specific pathogen-free conditions. All mice used were 5–9 weeks old. All animal experiments were carried out within institutional guidelines (authorization numbers 1886 and 1888 from cantonal veterinarian office, Canton Basel-Stadt).

### Antibodies, Flow Cytometry and Sorting

For analysis, cells were flushed from femurs and tibias of the two hind legs of mice or single-cell suspensions of spleen and lymph node (inguinal and axillary) cells were made. For blood analysis, blood was taken from the heart of euthanized animals or from the tail vein of live ones and white blood cells were isolated after separation with Ficoll. Stainings were performed in PBS containing 0.5% BSA and 5 mM EDTA. For intra-cellular Foxp3 staining, cells were fixed and permeabilized after cell-surface staining using the Foxp3 Fix/Perm buffer set (eBioscience), and subsequently stained with PE-conjugated anti-Foxp3. The following antibodies were used for flow cytometry (from BD Pharmingen, eBioscience, BioLegend, or produced in house): anti-B220 (RA3-6B2), anti-CD117 (2B8), anti-CD19 (1D3), anti-NK1.1 (PK136), anti-SiglecH (551), anti-CD11c (HL3), anti-Ly6D (49-H4), anti-CD127 (SB/199), anti-Scal (D7), anti-IgM (M41), anti-Foxp3 (FJK-16s), anti-CD4 (GK1.5), anti-CD8 (53.6.7), anti-Gr1 (RB6-8C5), anti-CD11b (M1.7015), anti-MHC-II (M5/114.15.2), anti-XCR1 (ZET), anti-CD93 (PB493), anti-CD48 (HM48-1), anti-CD150 (TC15-12F12.2), anti-Ter119 (TER-119), anti-CD3 (145-2C11), anti-CD41 (MWReg30), anti-CD105 (MJ7/18), anti-CD16/32 (2.4G2), anti-S1PR1 (713412), anti-CD44 (IM7), anti-CXCR4 (L276F12), anti-CD5 (53-7.3), and anti-Ki67 (B56). Lineage cocktail included antibodies against: CD4, CD8, CD11b, CD11c, Gr1, B220, CD19, Ter119, and NK1.1. Flow cytometry was done using a BD LSRFortessa (BD Biosciences) and data were analyzed using FlowJo Software (Treestar). For cell sorting, a FACSAria IIu (BD Biosciences) was used (>98% purity).

### Flt3-Ligand And IL-7 Quantification

Sera were collected from mice of all genotypes and ELISA was performed using the Invitrogen human Flt3-ligand and mouse IL-7 ELISA kits, following the provider's instructions.

### Quantitative PCR

Spleens were homogenized using the FastPrep<sup>®</sup> homogenizer (MP Biomedicals) and RNA was extracted with Trizol (Invitrogen) following the provider's protocol. Five hundred micrograms of total RNA was used to synthesize cDNA using the GoScript reverse transcriptase (Promega). Quantitative

PCR for the detection of *Il7* transcripts was performed using SYBR<sup>TM</sup> Green (Promega). Primers used: *Hprt*-Forw: atcagtcaacggggcacataaa; *Hprt*-Rev: tgcccgtactgcttaacc; *Il7*-Forw: GATAGTAATTGCCGAATAATGAACCA; *Il7*-Rev: GTTTGTGTGCCTTGTGATACTGTTAG.

### In vitro Limiting Dilution B Cell Generation Assay

Experiments were performed as previously described (34). Briefly, OP9 stromal cells were plated on flat-bottom 96-well plates 1 day before the initiation of co-cultures, at a concentration of 3,000 cells per well. The following day stromal cells were  $\gamma$ -irradiated (3000 rad) and the sorted EPLM cells were added at different concentrations. Cultures were maintained in IMDM medium supplemented with  $5 \times 10^{-5}$  M  $\beta$ -mercaptoethanol, 1 mM glutamine, 0.03% (wt/vol) primateone, 100 U/mL penicillin, 100  $\mu$ g/mL streptomycin, 5% FBS and 10% IL-7-conditioned medium. After 10 days in culture all wells were inspected under an inverted microscope and wells containing colonies of more than 50 cells were scored as positive.

### In vivo Hematopoietic Reconstitution Assays

Ten million BM or LN cells from FLtgxIL7tg mice were injected intravenously into CD45.1<sup>+</sup> recipient mice, which had been sub-lethally irradiated (400 rad) ~2 h before injection. Mice were euthanized 12–16 weeks after cell transfer and their spleen, thymus and bone marrow was analyzed for the presence of donor cells. For secondary transplants,  $6 \times 10^6$  BM cells from recipient mice were injected intravenously into sub-lethally irradiated CD45.1<sup>+</sup> recipients, in the same way. Secondary recipient spleens were analyzed after 9 weeks. For assessment of the *in vivo* B cell potential of EPLM,  $6 \times 10^4$  Ly6D<sup>+</sup> EPLM sorted from the BM or LN of FLtgxIL7tg mice were intravenously injected into NOD/SCID/*Il2r $\gamma$* <sup>-/-</sup> lymphopenic mice. Recipient spleens were analyzed for the presence of CD19<sup>+</sup>IgM<sup>+</sup> cells 3 weeks after cell transfer.

### Statistical Analysis

One-way ANOVA followed by a Tukey-test to correct for multiple comparisons between mouse genotypes was used. Statistical significance is indicated with asterisks in graphs. Non-significant differences are not indicated in the figures.

## RESULTS

### Expansion of Hematopoietic Cells in Secondary Lymphoid Organs of FLtgxIL7tg Mice

FLtg and IL7tg mice heterozygous for the corresponding transgenes were crossed, resulting in mice carrying both transgenes (FLtgxIL7tg), as well as wild-type (WT) and single-transgenic littermates, which were used as controls (Figure 1A). FLtgxIL7tg mice were viable but at around 5–6 weeks after birth, they developed large, clearly visible inguinal lymph nodes (LN), which continued to grow and therefore mice had to be

euthanized at the age of 9–10 weeks. None of the littermate controls exhibited this phenotype. All analyses of FLtgxIL7tg mice and their WT and single transgenic counterparts presented herein were done in 6–9 week old mice. We detected a massive increase in the amount of FL in the serum of FLtg and FLtgxIL7tg mice, which reached 22 and 18 ug/ml, respectively (**Figure 1B**). Even though IL-7 could not be detected in the serum of FLtgxIL7tg mice, as shown previously by *in situ* hybridization in IL7tg mice (35), a significant increase in *Il7* mRNA transcripts was observed in spleens of both IL7tg and FLtgxIL7tg mice (**Figure 1C**). Macroscopically, double transgenic mice exhibited a profound splenomegaly, with spleen size and average cellularity significantly larger than in single transgenic mice, in which the spleen was already increased compared to WT (**Figures 1D,E**). LN enlargement was even more striking, as shown in **Figure 1D**, with the average number of nucleated cells in all four inguinal and axillary LN reaching almost  $10^9$  cells, compared to  $3.4 \times 10^6$  for WT,  $45.4 \times 10^6$  for FLtg and  $145 \times 10^6$  for IL7tg mice (**Figure 1F**). All other LN examined macroscopically (brachial, mediastinal) showed similar enlargement compared to WT and single transgenic mice. FLtgxIL7tg BM cellularity was somewhat increased compared to WT (less than 2-fold and not statistically significant) and similar to the single transgenic controls (**Figure 1G**). On the contrary, thymus cellularity was slightly decreased in single and double transgenic mice compared to their WT littermates (**Figure 1H**).

Analysis of the enlarged spleens and LN of FLtgxIL7tg mice showed that several mature hematopoietic cells, which normally reside in these secondary lymphoid tissues, were remarkably increased. Thus, spleen and LN Gr1<sup>+</sup>CD11b<sup>+</sup> cells, including neutrophils and macrophages, were clearly increased in response to elevated FL levels (**Supplementary Figure 1A**). Also, and in agreement with what has been described previously in single FLtg mice (32), DC populations, including conventional DC of both types (CD11c<sup>+</sup>MHC-II<sup>+</sup>XCR1<sup>+</sup> cDC1 and CD11c<sup>+</sup>MHC-II<sup>+</sup>XCR1<sup>-</sup> cDC2), as well as B220<sup>+</sup>SiglecH<sup>+</sup> plasmacytoid DC (pDC), were all dramatically increased in response to FL over-expression (**Supplementary Figures 1B–E**), although the statistical analysis did not show a significant effect on LN cDC1 and cDC2. A clear effect of over-expressing both cytokines was also observed on splenic and LN T cells. FLtgxIL7tg mice had increased numbers of both CD4<sup>+</sup> and CD8<sup>+</sup> T cells in spleen (4.4- and 13-fold increase compared to WT, respectively) and LN (11- and 30-fold increase compared to WT, respectively) (**Supplementary Figures 2A,B**). This effect was also seen in the numbers of the CD4<sup>+</sup>Foxp3<sup>+</sup> regulatory T cell (Treg) fraction of CD4<sup>+</sup> T cells, particularly in the LN (**Supplementary Figures 2A,B**), as shown before under conditions of high FL availability (36). This increase in peripheral T cell numbers was probably not due to increased thymic output, since analysis of T cell developmental stages in the thymi of FLtgxIL7tg mice showed that over-expression of both cytokines did not significantly affect the numbers of T cell progenitors, including CD4<sup>+</sup> and CD8<sup>+</sup> single positive and CD4/CD8 double positive pro-T cells. Interestingly, FL over-expression resulted in a reduction in the numbers of the earliest double negative T cell progenitors (**Supplementary Figures 2C–E**).

We next examined B cell populations in the peripheral lymphoid organs of FLtgxIL7tg and single transgenic mice. Analysis of peritoneal B cells showed that IL-7 over-expression significantly increased the percent of B2 cells, whereas the frequency of the IL-7-independent (37) CD19<sup>+</sup>CD5<sup>+</sup>CD11b<sup>low</sup> B1a population was decreased by over-expression of both cytokines (**Supplementary Figures 3A,B**). Even though FL has been shown to be critical for the generation of B1a cells (30, 38), their relative frequency was not significantly increased upon FL over-expression, but rather slightly decreased, possibly due to the large expansion of myeloid cells in the peritoneal cavity (**Supplementary Figure 3B**). Mature, recirculating IgM<sup>+</sup>CD93<sup>-</sup> B cells were significantly increased in the LN of FLtgxIL7tg mice compared to WT (21-fold), whereas over-expressing either cytokine alone resulted in increased mature B cell numbers compared to WT, but to a smaller extent (**Figure 2A**). Mature IgM<sup>+</sup> B cells do not express CD135 and, unlike peripheral T cells, they are also CD127<sup>-</sup> and hence do not respond to either FL or IL-7. We therefore reasoned that the observed increase in their numbers in the periphery was the result of increased B cell progenitor numbers in the BM, as shown previously in IL7tg mice (29). Analysis of BM B cell progenitor populations showed a moderate 1.6-fold increase in the numbers of IgM<sup>+</sup>CD93<sup>+</sup> immature B cells, the population that exits the BM to recirculate in the periphery (**Figures 2B,C**). IgM<sup>-</sup> B cell progenitors showed a more pronounced increase compared to WT controls: 7.4-fold for CD19<sup>+</sup>CD117<sup>+</sup>IgM<sup>-</sup> pro-B cells, 3.7-fold for CD19<sup>+</sup>CD117<sup>-</sup>IgM<sup>-</sup>CD127<sup>+</sup>FSC<sup>large</sup> large pre-B and 2.3-fold for CD19<sup>+</sup>CD117<sup>-</sup>IgM<sup>-</sup>CD127<sup>-</sup>FSC<sup>small</sup> small pre-B cells (**Figures 2B,C**). This increase in BM CD19<sup>+</sup> B cell progenitors was mainly an effect of elevated IL-7 levels, since FL over-expression seemed to have a negative outcome on the numbers of pre-B and immature B cells (~2-fold decreased in FLtgxIL7tg mice compared to IL7tg). Thus, the reduction in pre-B and immature B cell numbers observed in FLtg mice (32) is also present when IL-7 is abundantly available (in FLtgxIL7tg mice) and is therefore unlikely to be caused by decreased IL-7 availability, as previously hypothesized.

## Accumulation of Lymphoid Progenitors in Peripheral Lymphoid Organs of FLtgxIL7tg Mice

Previous analysis of IL7tg mice has shown an abundance of immature B cell progenitors in the spleen and LN, where these populations are normally not found in significant numbers (29). We therefore analyzed spleen and LN of FLtgxIL7tg mice for the presence of early B cell progenitors. Indeed, in both spleen and LN of IL7tg mice, all stages of CD19<sup>+</sup> committed B cell progenitors were detected (**Figures 3A,B**). Contrary to what was observed in the BM, however, additional FL over-expression, in FLtgxIL7tg mice, further increased the numbers of pro-B (4.6-fold in spleen and 16-fold in LN), large pre-B (1.8-fold in spleen and 11-fold in LN), small pre-B (2-fold in spleen and 12-fold in LN) and immature B (1.9-fold in spleen and 9.8-fold in LN) cells. Thus, FL and IL-7 seem to act synergistically in promoting the accumulation of immature B cell progenitors in

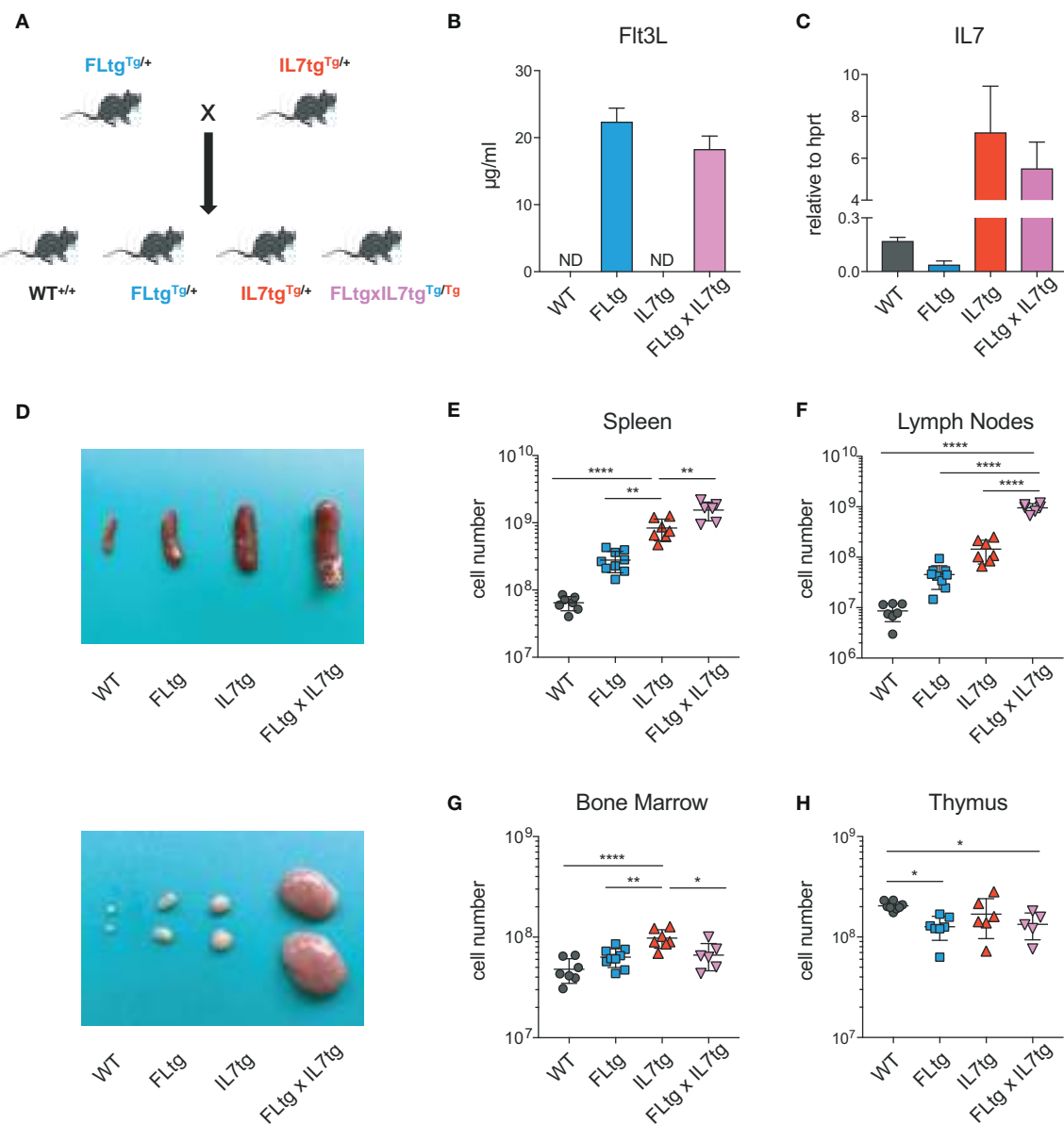


**FIGURE 1 |** Increased cellularity of FLtgxIL7tg lymphoid organs. **(A)** Scheme of the breeding applied to obtain FLtgxIL7tg mice. **(B)** ELISA for human FL protein quantification in the serum of WT, FLtg, IL7tg, and FLtgxIL7tg mice ( $n = 4$ ). **(C)** Quantitative PCR for the detection of *IL7* mRNA in the spleen of WT, FLtg, IL7tg, and FLtgxIL7tg mice ( $n = 3$ ). Bars in **(B,C)** represent mean  $\pm$  standard deviation. **(D)** Representative spleens (top) and lymph nodes (bottom) of WT, FLtg, IL7tg and FLtgxIL7tg mice. **(E–H)** Total numbers of live, nucleated cells in the spleen **(E)**, lymph nodes (axillary and inguinal) **(F)**, bone marrow (femurs and tibias) **(G)**, and thymus **(H)** of WT, FLtg, IL7tg, and FLtgxIL7tg mice. \* $p < 0.05$ , \*\* $p < 0.01$ , and \*\*\* $p < 0.0001$ . Error bars indicate standard deviation.

the peripheral lymphoid organs of mice over-expressing both cytokines.

Since CD135 is not detectable on CD19<sup>+</sup> B cell progenitors, this additional rise in their numbers in spleen and LN upon simultaneous FL and IL-7 over-expression is unlikely to be a direct effect of FL on their survival and/or proliferation. However, their immediate precursors, Ly6D<sup>+</sup> EPLM, are CD135<sup>+</sup> and have been shown to increase dramatically in response to elevated FL levels (13, 34, 39).

Therefore, we assessed their numbers in the BM and periphery of FLtgxIL7tg mice. As shown in Figures 4A,B, CD11c<sup>-</sup>NK1.1<sup>-</sup>SiglecH<sup>-</sup>CD19<sup>+</sup>B220<sup>int</sup>CD117<sup>int</sup>Ly6D<sup>+</sup> EPLM were indeed dramatically increased upon FL over-expression in the BM, whereas IL-7 over-expression did not increase their numbers and even reduced them when in combination with high FL expression (Figure 4B, FLtg compared to FLtgxIL7tg). Ly6D<sup>+</sup> EPLM were clearly detected in spleens of FLtg and FLtgxIL7tg mice, whereas in LN they were strikingly expanded

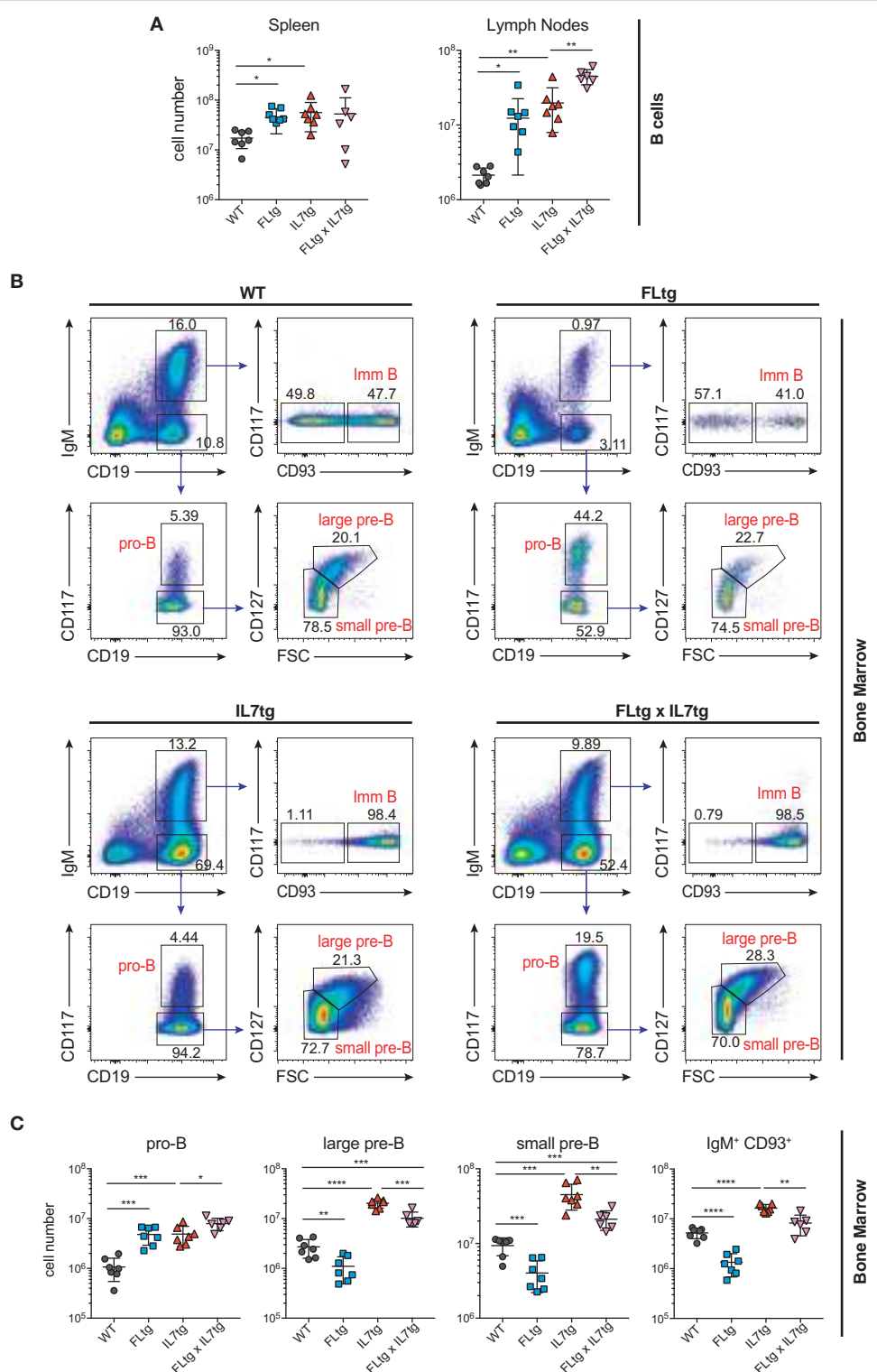
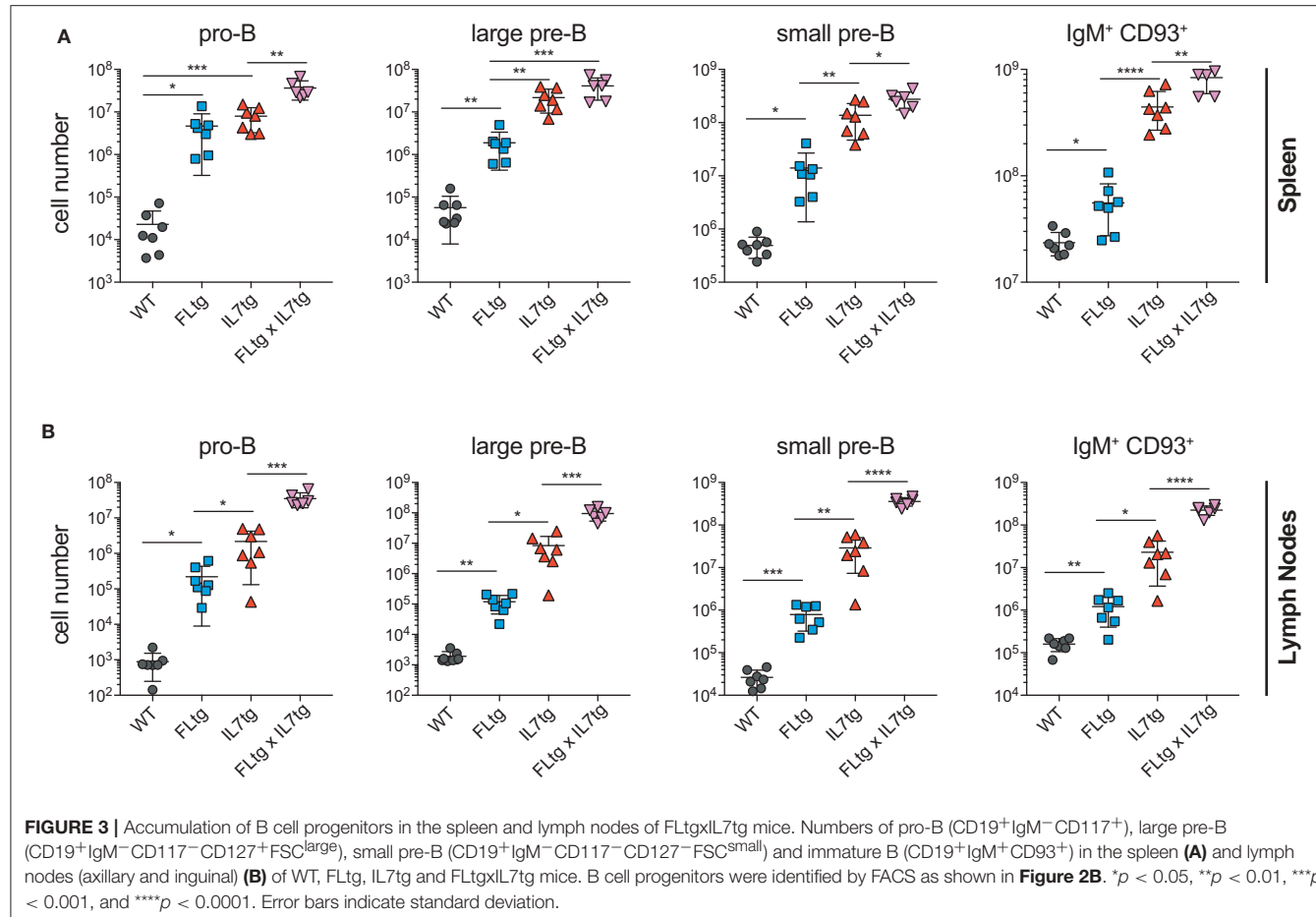


**FIGURE 2 |** Expansion of B cell populations in lymphoid organs of FLtgxIL7tg mice. **(A)** Numbers of IgM<sup>+</sup> CD93<sup>-</sup> mature recirculating B cells in the spleen (left) and lymph nodes (axillary and inguinal) (right) of WT, FLtg, IL7tg, and FLtgxIL7tg mice. **(B)** Representative FACS plots for the identification of B cell progenitor stages in the bone marrow of WT (upper left), FLtg (upper right), IL7tg (lower left), and FLtgxIL7tg (lower right) mice. Gate numbers indicate frequencies of parent gate. **(C)** Numbers of pro-B (CD19<sup>+</sup>IgM<sup>-</sup>CD117<sup>+</sup>), large pre-B (CD19<sup>+</sup>IgM<sup>-</sup>CD117<sup>-</sup>CD127<sup>+</sup>FSC<sup>large</sup>), small pre-B (CD19<sup>+</sup>IgM<sup>-</sup>CD117<sup>-</sup>CD127<sup>-</sup>FSC<sup>small</sup>) and immature B (CD19<sup>+</sup>IgM<sup>+</sup>CD93<sup>+</sup>) in the bone marrow of WT, FLtg, IL7tg, and FLtgxIL7tg mice. B cell populations were identified as indicated in B. \* $p < 0.05$ , \*\* $p < 0.01$ , \*\*\* $p < 0.001$ , \*\*\*\* $p < 0.0001$ . Error bars indicate standard deviation.



mainly upon over-expression of both cytokines. FLtg and IL7tg LN also had higher numbers of Ly6D<sup>+</sup> EPLM compared to WT, in which they were barely detectable. However, this increase was not statistically significant and was proportional to the corresponding overall increase in LN total cellularity (Figure 1F), whereas FLtgxIL7tg LN Ly6D<sup>+</sup> EPLM were 120- and 137-fold increased compared to their FLtg and IL7tg counterparts, respectively. This expansion is  $\sim 10$  times higher than the corresponding LN cellularity difference between these mouse genotypes, indicating that FL and IL-7 synergistically promote the accumulation and/or expansion of Ly6D<sup>+</sup> EPLM in the LN of FLtgxIL7tg mice. Since Ly6D<sup>+</sup> EPLM are not yet committed to the B cell lineage (39, 40), we assessed the ability of these spleen- and LN-residing FLtgxIL7tg progenitors to generate B cells *in vitro* and *in vivo*. Sorting and plating FLtgxIL7tg Ly6D<sup>+</sup> EPLM on OP9 stromal cells together with IL-7 under limiting dilution conditions showed that these cells were able to give rise to CD19<sup>+</sup> B cells *in vitro* (Figure 4C). We noticed that the frequency of LN-derived Ly6D<sup>+</sup> EPLM that could generate B cells under these conditions was slightly reduced compared to their BM counterparts, which showed a frequency similar to WT BM-derived Ly6D<sup>+</sup> EPLM (13, 39). However, after transplantation into NOD/SCID/ $Il2r\gamma^{-/-}$

lymphopenic mice, LN-derived FLtgxIL7tg Ly6D<sup>+</sup> EPLM were as capable as their BM-derived counterparts at generating IgM<sup>+</sup> B cells *in vivo* (Figure 4D). Thus, under conditions of simultaneous increase in FL and IL-7 availability, functional CD19<sup>-</sup>Ly6D<sup>+</sup> EPLM progenitors can reside and accumulate in the spleens and LN of mice.

### Hematopoietic Progenitors With Long-Term, Multilineage Reconstitution Capacity Reside in the LN of FLtgxIL7tg Mice

Apart from Ly6D<sup>+</sup> EPLM, CLP and LSK cells are greatly expanded in FLtg mice (32). We therefore investigated their potential expansion in the BM and presence in the spleen and LN of FLtgxIL7tg mice. Under conditions of high *in vivo* FL availability, CD135 becomes undetectable by flow cytometry (32), possibly due to the continuous binding of the ligand to its receptor. Thus, we identified CLP using the original Lin<sup>-</sup>CD117<sup>int</sup>Sca1<sup>int</sup>CD127<sup>+</sup> phenotype (14) (Figure 5B). We found CLP numbers to be significantly increased in the BM of mice over-expressing FL, whereas IL-7 over-expression did not have any effect (Figure 5A). This was also the case in the spleen,

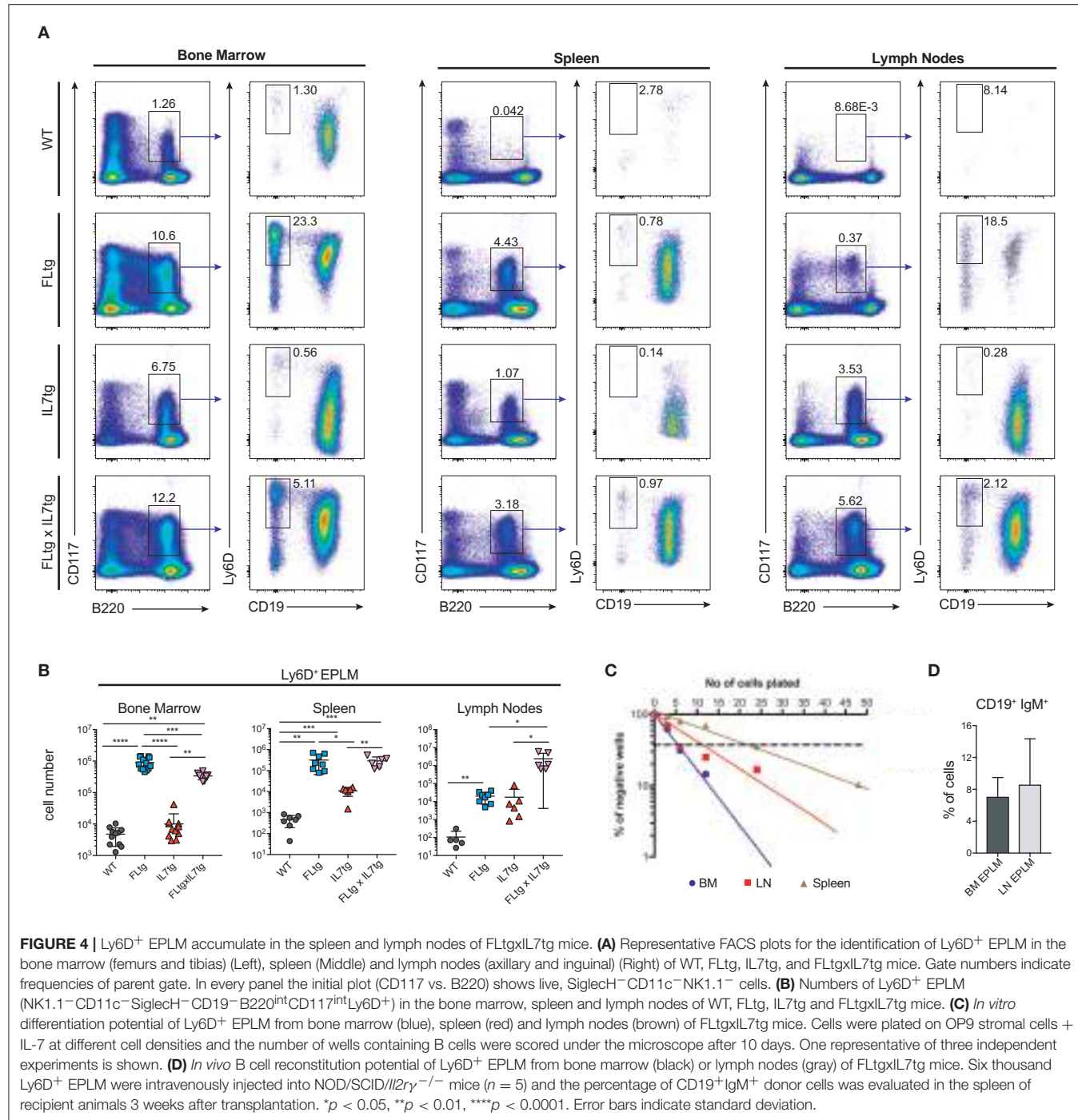


**FIGURE 4 |** Ly6D<sup>+</sup> EPLM accumulate in the spleen and lymph nodes of FLtgxIL7tg mice. **(A)** Representative FACS plots for the identification of Ly6D<sup>+</sup> EPLM in the bone marrow (femurs and tibias) (Left), spleen (Middle) and lymph nodes (axillary and inguinal) (Right) of WT, FLtg, IL7tg, and FLtgxIL7tg mice. Gate numbers indicate frequencies of parent gate. In every panel the initial plot (CD117 vs. B220) shows live, SiglecH<sup>-</sup>CD11c<sup>-</sup>NK1.1<sup>-</sup> cells. **(B)** Numbers of Ly6D<sup>+</sup> EPLM (NK1.1<sup>-</sup>CD11c<sup>-</sup>SiglecH<sup>-</sup>CD19<sup>-</sup>B220<sup>int</sup>CD117<sup>int</sup>Ly6D<sup>+</sup>) in the bone marrow, spleen and lymph nodes of WT, FLtg, IL7tg and FLtgxIL7tg mice. **(C)** *In vitro* differentiation potential of Ly6D<sup>+</sup> EPLM from bone marrow (blue), spleen (red) and lymph nodes (brown) of FLtgxIL7tg mice. Cells were plated on OP9 stromal cells + IL-7 at different cell densities and the number of wells containing B cells were scored under the microscope after 10 days. One representative of three independent experiments is shown. **(D)** *In vivo* B cell reconstitution potential of Ly6D<sup>+</sup> EPLM from bone marrow (black) or lymph nodes (gray) of FLtgxIL7tg mice. Six thousand Ly6D<sup>+</sup> EPLM were intravenously injected into NOD/SCID//*I2rγ*<sup>-/-</sup> mice ( $n = 5$ ) and the percentage of CD19<sup>+</sup>IgM<sup>+</sup> donor cells was evaluated in the spleen of recipient animals 3 weeks after transplantation. \* $p < 0.05$ , \*\* $p < 0.01$ , \*\*\* $p < 0.0001$ . Error bars indicate standard deviation.

where splenic FLtgxIL7tg CLP were increased compared to WT (Figure 5C). Similarly to EPLM, we observed a greater than 10-fold increase in LN FLtgxIL7tg CLP numbers compared to their single transgenic counterparts, which were already increased compared to WT (Figures 5E,F). CD127<sup>-</sup> LSK cell analysis showed a similar picture, with LSK being greatly increased in the BM and found in significant numbers in the spleen and LN of FLtgxIL7tg mice. Within the LSK compartment, the CD48<sup>-</sup>CD150<sup>+</sup> phenotype can be used to enrich for hematopoietic stem cells (HSC) with multilineage developmental

potential and self-renewal capacity (41). As shown in Figure 5A (bottom), CD48<sup>-</sup>CD150<sup>+</sup> LSK cells were significantly reduced in the BM of FLtg mice and this was also the case in FLtgxIL7tg BM (6-fold decreased compared to WT). These cells were detected at very low frequency in the spleen of FLtgxIL7tg mice (Figure 5C), and we could not detect them in the LN of any of the mouse genotypes analyzed (data not shown).

Taken together, our analysis shows that over-expression of both FL and IL-7 leads to a dramatic increase in all BM CD135<sup>+</sup> and CD127<sup>+</sup> progenitors and to their migration to

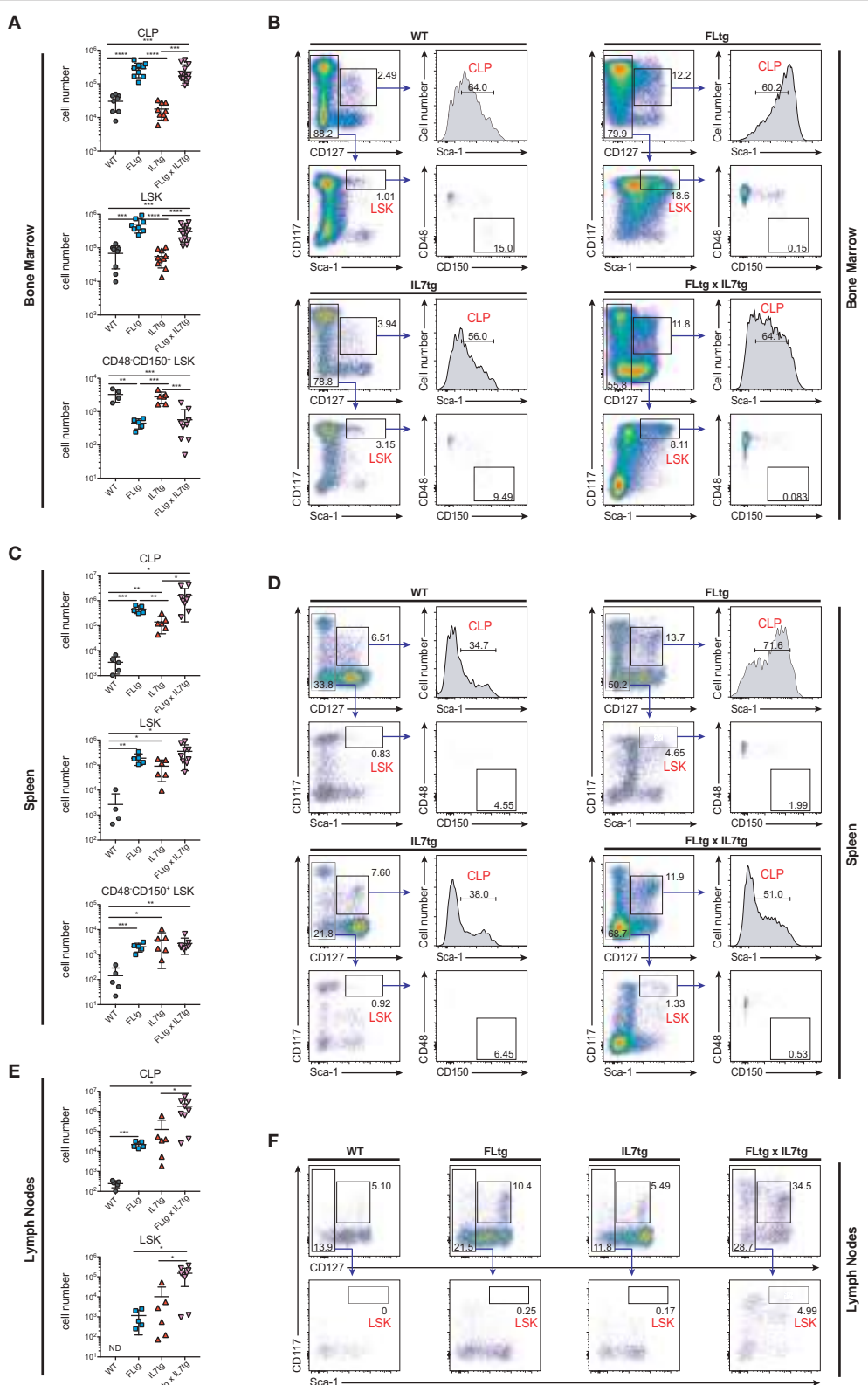


**FIGURE 5 |** Increased numbers of CLP and LSK in the spleen and lymph nodes of FLtgxIL7tg mice. **(A)** Numbers of Lin<sup>-</sup>CD117<sup>int</sup>Sca1<sup>int</sup>CD127<sup>+</sup> (CLP), Lin<sup>-</sup>CD127<sup>-</sup>CD117<sup>+</sup>Sca1<sup>+</sup> (LSK) and Lin<sup>-</sup>CD127<sup>-</sup>CD117<sup>+</sup>Sca1<sup>+</sup>CD48<sup>-</sup>CD150<sup>+</sup> LSK in the bone marrow of WT, FLtg, IL7tg, and FLtgxIL7tg mice.

(Continued)

**FIGURE 5 | (B)** Representative FACS plots for the identification of CLP, LSK, and CD48<sup>-</sup>CD150<sup>+</sup> LSK in the bone marrow (femurs and tibias) of WT, FLtg, IL7tg, and FLtgxIL7tg mice. Gate numbers indicate frequencies of parent gate. In every panel the upper left plot (CD117 vs. CD127) shows live, Lineage<sup>-</sup> cells. **(C)** Numbers of CLP, LSK and CD48<sup>-</sup>CD150<sup>+</sup> LSK in the spleens of WT, FLtg, IL7tg, and FLtgxIL7tg mice. **(D)** Representative FACS plots for the identification of CLP, LSK, and CD48<sup>-</sup>CD150<sup>+</sup> LSK in the spleens of WT, FLtg, IL7tg, and FLtgxIL7tg mice. Gate numbers indicate frequencies of parent gate. In every panel the upper plot (CD117 vs. CD127) shows live, Lin<sup>-</sup> cells. **(E)** Numbers of CLP and LSK in the LN of WT, FLtg, IL7tg, and FLtgxIL7tg mice. **(F)** Representative FACS plots for the identification of LSK in the LN of WT, FLtg, IL7tg, and FLtgxIL7tg mice. Gate numbers indicate frequencies of parent gate. In every panel the upper plot (CD117 vs. CD127) shows live, Lin<sup>-</sup> cells. \* $p < 0.05$ , \*\* $p < 0.01$ , \*\*\* $p < 0.001$ , and \*\*\*\* $p < 0.0001$ . Error bars indicate standard deviation.

the periphery, presumably due to space constraints in the BM. In support of this hypothesis, all CD19<sup>+</sup> B cell progenitor stages were found significantly increased in the peripheral blood of FLtgxIL7tg mice (**Figures 6A,D**). Strikingly, the same was true for CD135<sup>+</sup> Ly6D<sup>+</sup> EPLM, CLP and LSK progenitors, which were increased in the blood mainly in response to FL over-expression (**Figures 6B,C,E**). This effect of FL and IL-7 simultaneous over-expression in promoting the migration of cells from the BM to the periphery was seen mainly on progenitors, since mature B and T cell frequencies in the blood of FLtgxIL7tg mice were not dramatically changed, whereas the relative frequencies of cDC and NK cells were significantly increased in the blood of FLtg animals (**Supplementary Figure 4**). Thus, the synergistic effect of FL and IL-7 over-expression in expanding BM hematopoietic progenitors leads to their exit from the BM and accumulation not only in the spleen but also in LN, where some of these progenitors are undetectable in WT mice.

We next sought to evaluate whether these multipotent hematopoietic progenitors identified by flow cytometry in the LN of FLtgxIL7tg mice were functional, i.e., if they had the ability to generate multiple hematopoietic lineages upon transplantation. To this end, we infused  $10 \times 10^6$  unfractionated LN cells from CD45.2<sup>+</sup> FLtgxIL7tg, into sub-lethally irradiated congenic CD45.1<sup>+</sup> WT mice. FLtgxIL7tg BM cells were used as a positive control for the long-term reconstitution of hematopoietic lineages, since they contain functional hematopoietic progenitors. Recipient mice were analyzed 12–16 weeks after transplantation for the contribution of CD45.2<sup>+</sup> donor cells to the different hematopoietic lineages. As expected, overall engraftment of donor cells in the BM, spleen and thymus of recipient mice was significantly lower in LN-transplanted recipients compared to BM transplanted ones (**Supplementary Figures 5A,B**). Thus, in the FLtgxIL7tg LN transplanted hosts, 20% splenic, 5.4% BM and 6.8% thymic cells were of donor origin. Analysis of the spleen of FLtgxIL7tg LN-reconstituted mice showed that 21.8% CD19<sup>+</sup> B cells, 13.8% CD3<sup>+</sup> T cells, 16.3% NK1.1<sup>+</sup> NK cells, 14.7% SiglecH<sup>-</sup>CD11b<sup>-</sup>CD11c<sup>+</sup> DC, 4.5% CD11b<sup>+</sup>CD11c<sup>-</sup> myeloid cells and 15% Ter119<sup>+</sup> erythroid cells were of donor origin, with more than 80% of the transplanted mice showing donor-derived reconstitution in all the above lineages (**Figures 7A–D**). Donor contribution was also evaluated in the thymus of recipient mice, where we found small but clearly detectable populations of FLtgxIL7tg LN-derived CD4<sup>+</sup>, CD8<sup>+</sup>, and CD4/CD8 double positive T cell progenitors (**Figures 7E–G**). Furthermore, BM analysis showed that a significant fraction of CD19<sup>+</sup> B cell progenitors were of FLtgxIL7tg LN donor origin, with the average percent ranging from 5.6% for large pre-B to 13% for

immature IgM<sup>+</sup>CD93<sup>+</sup> B cells (**Supplementary Figures 5C,D**). Remarkably, we also found small but clearly detectable populations of donor-derived CLP (5%) and LSK (3.5%) 12 weeks after transplantation. Thus, FLtgxIL7tg LN contain progenitors with the long-term capacity to generate multiple hematopoietic lineages.

The presence of early hematopoietic progenitors in the host BM 12 weeks after transfer of FLtgxIL7tg LN cells, prompted us to assess their self-renewal capacity by re-transplanting them into secondary recipients. Six million unfractionated BM cells from FLtgxIL7tg LN-reconstituted mice and FLtgxIL7tg BM-reconstituted controls were intravenously injected into congenic CD45.1<sup>+</sup> irradiated WT hosts 12 weeks after the first transplantation. Nine weeks after secondary transfer, we could detect FLtgxIL7tg-derived donor cells in the secondary recipients' spleen. Importantly, CD45.2<sup>+</sup> cells were found in multiple hematopoietic lineages. Thus, FLtgxIL7tg LN donor-derived cells were found in: 0.1% CD19<sup>+</sup> B cells, 0.25% CD3<sup>+</sup> T cells, 0.6% CD11c<sup>+</sup> DC and 0.07% Ter119<sup>+</sup> erythroid cells (**Figures 8A–D**). These results indicate that there are FLtgxIL7tg LN-residing multipotent hematopoietic progenitors with self-renewal capacity. Overall, considering the significant multilineage contribution of FLtgxIL7tg LN-derived donor cells in host hematopoietic reconstitution more than 12 weeks after transfer, as well as their presence in secondary transplanted hosts after another 9 weeks, we conclude that the LN of FLtgxIL7tg mice contain hematopoietic progenitors with *in vivo* long-term multi-lineage reconstitution ability, some of which have self-renewal capacity.

## DISCUSSION

We have previously generated and analyzed mice with increased, sustained *in vivo* levels of either IL-7 (28, 29) or FL (13, 32, 39), which provided important insights to the roles of the two cytokines at different stages of the various lineages of hematopoiesis. In the present study we over-expressed both cytokines in order to evaluate the concerted action of both FL and IL-7 on the regulation of hematopoiesis in an *in vivo* setting. We find a synergistic effect of the two cytokines in promoting the generation and expansion of lymphoid cells, resulting in a profound enlargement of secondary lymphoid organs, such as spleen and LN, significantly more than what can be seen in single transgenic mice (**Figure 1**). Both spleen and LN of FLtgxIL7tg mice were populated by significant numbers of multipotent hematopoietic progenitors, which in WT mice are generally confined to the BM.

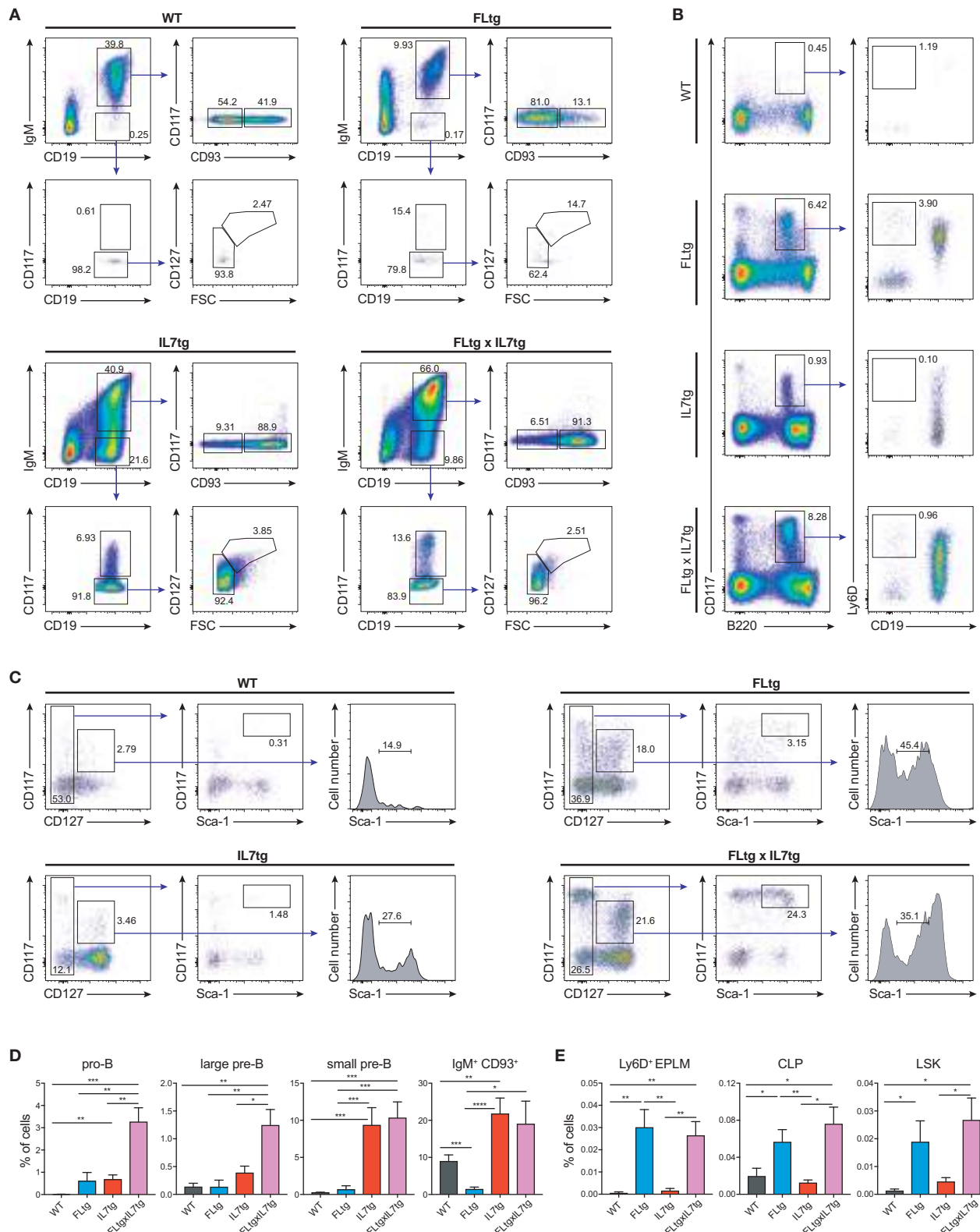


**FIGURE 6 |** Hematopoietic progenitors in the blood of FLtgxIL7tg mice. **(A)** Representative FACS plots for the identification of B cell progenitor stages in the blood of WT (upper left), FLtg (upper right), IL7tg (lower left) and FLtgxIL7tg (lower right) mice. Gate numbers indicate frequencies of parent gate. **(B)** Representative FACS (Continued)

**FIGURE 6 |** plots for the identification of Ly6D<sup>+</sup> EPLM in the blood of WT (upper left), FLtg (upper right), IL7tg (lower left), and FLtgxIL7tg (lower right) mice. Gate numbers indicate frequencies of parent gate. In every panel the left plot (CD117 vs. B220) shows live, NK1.1<sup>-</sup>CD11c<sup>-</sup>SiglecH<sup>-</sup> cells. **(C)** Representative FACS plots for the identification of LSK and CLP in the blood of WT (upper left), FLtg (upper right), IL7tg (lower left), and FLtgxIL7tg (lower right) mice. Gate numbers indicate frequencies of parent gate. In every panel the left plot (CD117 vs. CD127) shows live, Lin<sup>-</sup> cells. **(D)** Percentages of pro-B (CD19<sup>+</sup>IgM<sup>-</sup>CD117<sup>+</sup>), large pre-B (CD19<sup>+</sup>IgM<sup>-</sup>CD117<sup>-</sup>CD127<sup>+</sup>FSC<sup>large</sup>), small pre-B (CD19<sup>+</sup>IgM<sup>-</sup>CD117<sup>-</sup>CD127<sup>-</sup>FSC<sup>small</sup>) and immature B cell (CD19<sup>+</sup>IgM<sup>+</sup>CD93<sup>+</sup>) progenitors in the blood of WT ( $n = 9$ ), FLtg ( $n = 11$ ), IL7tg ( $n = 8$ ), and FLtgxIL7tg ( $n = 11$ ) mice. B cell progenitors were identified by FACS as shown in **(A)**. **(E)** Percentages of Ly6D<sup>+</sup> EPLM (CD11c<sup>-</sup>NK1.1<sup>-</sup>SiglecH<sup>-</sup>B220<sup>int</sup>CD117<sup>int</sup>Ly6D<sup>+</sup>CD19<sup>-</sup>), CLP (Lin<sup>-</sup>CD117<sup>int</sup>Sca1<sup>int</sup>CD127<sup>+</sup>) and LSK (Lin<sup>-</sup>CD117<sup>+</sup>Sca1<sup>+</sup>CD127<sup>-</sup>) progenitors in the blood of WT ( $n = 6$ ), FLtg ( $n = 6$ ), IL7tg ( $n = 7$ ), and FLtgxIL7tg ( $n = 10$ ) mice. The y-axis on all plots indicates % of live, nucleated blood cells. \* $p < 0.05$ , \*\* $p < 0.01$ , \*\*\* $p < 0.001$ , and \*\*\*\* $p < 0.0001$ . Error bars indicate standard deviation.

The enlarged spleens and LN of FLtgxIL7tg mice contained significantly increased populations of myeloid cells (**Supplementary Figure 1A**). This probably reflected the expansion in BM myeloid progenitors that FL over-expression induces (32). Indeed, when assessing early myelo-erythroid progenitor stages in FLtgxIL7tg BM, we observed a significant increase in the earliest identified myeloid progenitors, pre-GM and GMP (42), whereas early erythroid/megakaryocyte progenitors were decreased (**Supplementary Figure 6**), in accordance with the anemia and thrombocytopenia caused by elevated FL (32). Generation of DC is known to depend on FL and we indeed found all splenic and some LN DC populations significantly increased (**Supplementary Figure 1**). This could be the result of DC expansion in peripheral lymphoid organs, since these cells are CD135<sup>+</sup>, or could be due to FL-mediated expansion of their progenitors. Due to the inability to stain for CD135<sup>+</sup> in mice over-expressing FL (32) we were not able to assess the numbers of cDC and pDC progenitors (43–45).

Peripheral T cells were also increased dramatically in spleens and LN of FLtgxIL7tg mice, even though thymic size and T cell output was not increased. Thus, this seems to be mainly an effect of IL-7, which is known to regulate homeostasis of peripheral T cells, particularly of CD8<sup>+</sup> (46) which was the T cell population with the biggest expansion in FLtgxIL7tg mice (**Supplementary Figures 2A,B**). Interestingly, FL over-expression alone also resulted in some increase in mature T cell numbers. Since these cells are CD135<sup>-</sup>, we postulate that this is an indirect effect of high FL levels. Previous experiments, showing expansion of regulatory T cells upon increased FL availability, suggested that this is mediated by IL-2 produced by the expanded DC (36), thus providing a potential explanation for the observed increase in peripheral T cells when FL is over-expressed. The somewhat reduced thymopoiesis observed in FLtgxIL7tg mice might be a direct or secondary result of high FL expression by thymic stromal cells, since IL-7 over-expression alone in the IL7tg mouse model used herein did not affect T cell development (35). Since thymus seeding progenitors that migrate from the BM are multipotent and express CD135 (47, 48), it is conceivable that under the influence of increased FL levels a larger fraction of them differentiates toward myeloid or DC fates, thus resulting in somewhat reduced CD4/CD8 double-negative numbers.

The synergistic effect of FL and IL-7 is clearly manifested in the generation of B cells. Expression of the receptors for the two cytokines on B cell generating progenitors occurs at

slightly different developmental stages: CD135 is expressed on early progenitors (LSK, CLP, EPLM) and is down-regulated upon Pax5/CD19 expression and commitment to the B cell lineage, whereas CD127 is expressed from the CLP up to the small pre-B stage. Accordingly, both receptors are co-expressed during the CLP/EPLM developmental stage, in which a potential synergy between the two cytokines in promoting B cell development can occur. FL is mainly acting as a proliferative factor for CLP/EPLM progenitors, whereas IL-7 supports their survival, rather than expanding them (13). Thus, we find the number of these progenitors greatly expanded in the BM of FLtg and FLtgxIL7tg mice, while IL-7 over-expression does not further increase their numbers but rather decreases them slightly (**Figures 4B, 5A**). IL-7 acts as a proliferative factor for CD19<sup>+</sup> B cell progenitors in the BM, leading to a 5- to 9-fold increase in their numbers upon over-expression (when comparing IL7tg to WT or FLtgxIL7tg to FLtg). This effect of the two cytokines on the proliferation of hematopoietic progenitors was confirmed in the present study, since we found a significant increase in the percentage of cycling LSK in the BM of mice over-expressing FL, whereas IL-7 had a proliferative effect mainly on CD19<sup>+</sup> B cell progenitors (**Supplementary Figure 7**). This vast expansion of CD19<sup>+</sup> cells upon IL-7 over-expression could explain the slight reduction in FLtgxIL7tg Ly6D<sup>+</sup> EPLM numbers compared to FLtg mice, since the expanded progenitor populations have to compete for limited space in the BM. By contrast, in peripheral lymphoid tissues, such as the spleen and LN, which can enlarge to accommodate more cells, the synergistic effect of FL and IL-7 can be clearly seen, as FLtgxIL7tg spleen and LN contain significantly more CLP/EPLM and CD19<sup>+</sup> B cell progenitors of all stages compared to their single transgenic counterparts. Interestingly, the proliferative effect of the two cytokines observed in the BM was also seen in the LN (**Supplementary Figure 7**), indicating that progenitors continue to expand in response to the two cytokines after their migration to the periphery. The space restrictions imposed on cells in the BM might also be the reason for the observed reduction in the number of BM pre-B and immature cells when FL is over-expressed. We have previously hypothesized that this might be the result of reduced IL-7 availability in the BM of FLtg mice, but as the same effect seems to occur in FLtgxIL7tg mice, this is unlikely to be the reason. It is still possible that other trophic signals required for the expansion and/or survival of pre-B cells become limiting in the BM when CD135<sup>+</sup> progenitors expand massively, as is the case in FLtg and FLtgxIL7tg mice. However, this does not happen in the periphery, where the FL-mediated expansion of CLP/EPLM results in a corresponding

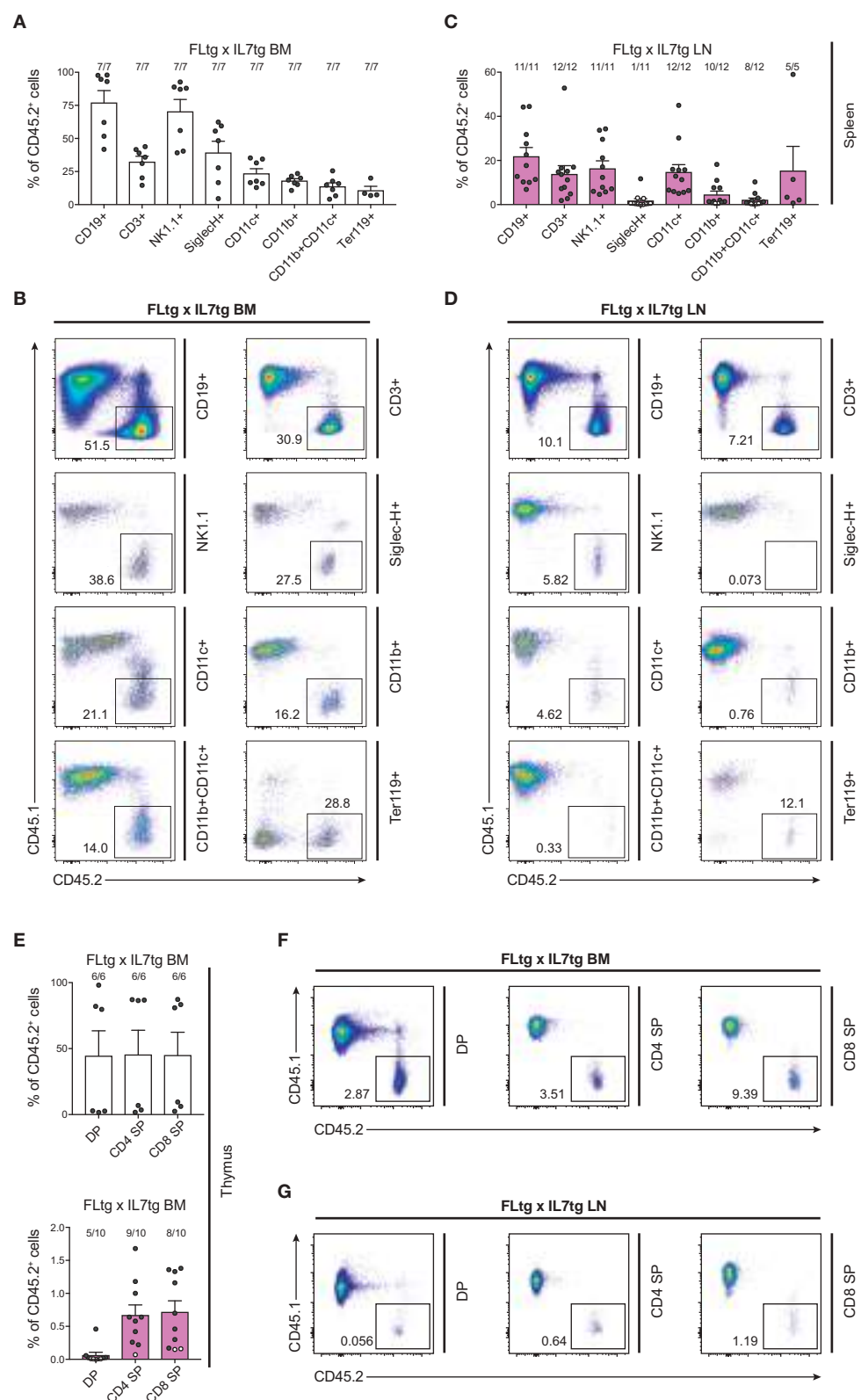


**FIGURE 7 |** Hematopoietic reconstitution potential of FLtgxIL7tg LN cells. **(A,C)** Percentage of CD45.2<sup>+</sup> donor cells within the indicated lineages in spleens of mice reconstituted with FLtgxIL7tg BM **(A)** or FLtgxIL7tg LN **(C)**. Results from four independently performed experiments are shown. Bars indicate mean  $\pm$  standard error (Continued)

**FIGURE 7 |** of the mean. Black circles represent mice where the corresponding lineage was scored as positive for the presence of donor-derived cells (>50 cells in the CD45.2<sup>+</sup> gate) and white circles mice with no reconstitution (<50 cells in the CD45.2<sup>+</sup> gate). The fraction of positive-to-total mice analyzed for each lineage is indicated above the corresponding bar. Lineages were defined as follows: CD19<sup>+</sup>: CD11b<sup>-</sup>CD11c<sup>-</sup>CD3<sup>-</sup>CD19<sup>+</sup>; CD3<sup>+</sup>: CD11b<sup>-</sup>CD11c<sup>-</sup>CD19<sup>-</sup>CD3<sup>+</sup>; NK1.1<sup>+</sup>: CD3<sup>-</sup>CD11c<sup>-</sup>B220<sup>-</sup>SiglecH<sup>-</sup>NK1.1<sup>+</sup>; SiglecH<sup>+</sup>: CD11b<sup>-</sup>NK1.1<sup>-</sup>B220<sup>+</sup>SiglecH<sup>+</sup>; CD11c<sup>+</sup>: NK1.1<sup>-</sup>SiglecH<sup>-</sup>B220<sup>-</sup>CD11b<sup>-</sup>CD11c<sup>+</sup>; CD11b<sup>+</sup>: NK1.1<sup>-</sup>SiglecH<sup>-</sup>B220<sup>-</sup>CD11c<sup>-</sup>CD11b<sup>+</sup>; CD11b<sup>+</sup>CD11c<sup>+</sup>: NK1.1<sup>-</sup>SiglecH<sup>-</sup>B220<sup>-</sup>CD11b<sup>+</sup>CD11c<sup>+</sup>; Ter119<sup>+</sup>: Ter119<sup>+</sup>. **(B,D)** Representative FACS plots showing the CD45.2<sup>+</sup> donor population identified within the lineages shown in **(A,C)**. Left: recipients transplanted with FLtgxIL7tg BM; Right: recipients transplanted with FLtgxIL7tg LN. **(E)** Percentage of CD45.2<sup>+</sup> donor cells within the indicated T cell populations in thymi of mice reconstituted with FLtgxIL7tg BM (upper) and FLtgxIL7tg LN (lower). Results from three independently performed experiments are shown. For FLtgxIL7tg BM:  $n = 6$ ; for FLtgxIL7tg LN:  $n = 10$ . Bars indicate mean  $\pm$  standard error of the mean. Black circles represent mice where the corresponding lineage was scored as positive for the presence of donor-derived cells (>50 cells in the CD45.2<sup>+</sup> gate) and white circles mice with no reconstitution (<50 cells in the CD45.2<sup>+</sup> gate). The ratio of positive-to-total mice analyzed for each lineage is indicated above the corresponding bar. Cells were identified as follows: DP: CD3<sup>+</sup>CD4<sup>+</sup>CD8<sup>+</sup>; CD4 SP: CD3<sup>+</sup>CD8<sup>-</sup>CD4<sup>+</sup>; CD8 SP: CD3<sup>+</sup>CD4<sup>-</sup>CD8<sup>+</sup>. **(F,G)** Representative FACS plots showing the CD45.2<sup>+</sup> donor population identified within the indicated thymic T cell populations. Upper: recipients transplanted with FLtgxIL7tg BM; lower: recipients transplanted with FLtgxIL7tg LN.

increase in pro-B and pre-B cell numbers. Taken together, FL and IL-7 act in concert to promote B cell development, FL by providing sufficient numbers of CLP/EPLM progenitors and IL-7 by promoting their survival and further expansion after commitment to the B cell fate.

FL over-expression resulted in a major expansion of LSK cells, which are largely CD135<sup>+</sup>. When IL-7 was additionally over-expressed, this resulted in the detection of significant LSK numbers in the spleen and LN of FLtgxIL7tg mice. Since LSK are CD127<sup>-</sup>, we hypothesize that the reason for their increase mainly in FLtgxIL7tg LN is again related to confined space and/or resources in the FLtgxIL7tg BM, thus leading to their migration to peripheral lymphoid organs when expanded by FL over-expression. In support of this hypothesis, LSK can also be detected in the blood of FLtgxIL7tg mice (**Figures 6C,E**). Expression of molecules associated with progenitor migration from the BM, such as S1PR<sub>1</sub>, CD44, and CXCR4 was not dramatically different between genotypes, with the exception of an FL-mediated increase in the CXCR4<sup>+</sup> fraction of B cell progenitors, which might be an indirect effect of FL, as these cells are CD135<sup>-</sup> (**Supplementary Figure 8**). This indicates that it is mainly competition for BM space/resources that leads to their accumulation in peripheral lymphoid organs. LSK are mostly comprised of multipotent progenitors with mixed lineage potentials and biases, but which are not considered to possess self-renewal capacity (7). Self-renewing HSC within the LSK compartment can be enriched for by staining with the SLAM markers CD48 and CD150, and are contained within the CD48<sup>-</sup>CD150<sup>+</sup> LSK fraction (41). We were not able to detect CD48<sup>-</sup>CD150<sup>+</sup> LSK cells in the LN of FLtgxIL7tg mice. However, as reported previously (32), and seen in **Figure 5A**, the CD48<sup>-</sup>CD150<sup>+</sup> fraction of LSK in the BM is severely reduced in numbers upon FL over-expression. These cells are CD135<sup>-</sup> when identified by flow cytometry, although some of them express mRNA for the receptor (49). Therefore we do not know if this reduction is a direct effect of FL-signaling. In addition, we cannot exclude that high FL availability might affect the expression of SLAM markers, thus resulting in some HSC losing the CD48<sup>-</sup>CD150<sup>+</sup> phenotype in FLtg and FLtgxIL7tg mice. The expression level of other important markers for the identification of progenitor stages, such as CD117 and Sca1, might also be changed upon FL over-expression. As shown in **Figures 5B,D**, Sca1 expression in the majority of FLtg and FLtgxIL7tg CLP is

relatively higher than the one of their WT and IL7tg counterparts. The same is true for CD117 expression in pro-B (**Figure 2B**). This might be the result of altered marker expression or a selective expansion of the (few in WT mice) cells expressing high levels of the corresponding proteins.

In order to functionally assess the precursor activity of hematopoietic progenitors found in the LN of FLtgxIL7tg mice, we transplanted LN cells from these mice into myelo-ablated WT recipients and assessed their long-term multilineage reconstitution capacity. We found a significant contribution of FLtgxIL7tg donor cells in lymphoid, myeloid, dendritic and erythroid lineages 12–16 weeks after transplantation. This is indicative of the presence of multipotent progenitors in the double transgenic LN, since myeloid and dendritic cells are not long-lived and therefore these donor cells could not be mature myeloid/dendritic cells transferred from the FLtgxIL7tg LN. In addition, we found donor contribution in all stages of recipient T cell development, suggesting that the FLtgxIL7tg LN contain progenitors with thymus-seeding potential. The exact nature of these precursors is not known, but they are known to have multilineage developmental capacity (47, 48). Furthermore, we detected donor progenitor cells in the BM of recipient animals, which upon transplantation into secondary recipients showed a small but clearly detectable contribution in the regeneration of different lineages. We conclude from this data that the LN of FLtgxIL7tg mice contain hematopoietic progenitors with long-term multilineage hematopoietic regeneration capacity. These could be HSC, which do not display the CD48<sup>-</sup>CD150<sup>+</sup> phenotype due to alterations in SLAM marker expression, or downstream multipotent progenitors that have acquired self-renewal capacity under conditions of high FL availability – possibly by an autocrine FL effect.

Irrespective of the precise nature of the multipotent hematopoietic progenitor that resides in FLtgxIL7tg LN, it is clear from our data that not only the spleen but also the LN of these double transgenic mice can support the survival of immature precursors, such as LSK, CLP, EPLM, and pre-B cells, which are normally only found in the BM. Extra-medullary hematopoiesis has been described in patients and has been mostly associated either with bone marrow failure or with myeloproliferative disease (50, 51). Similarly, disruption of hematopoiesis in mice caused by drug treatment (52), mutations

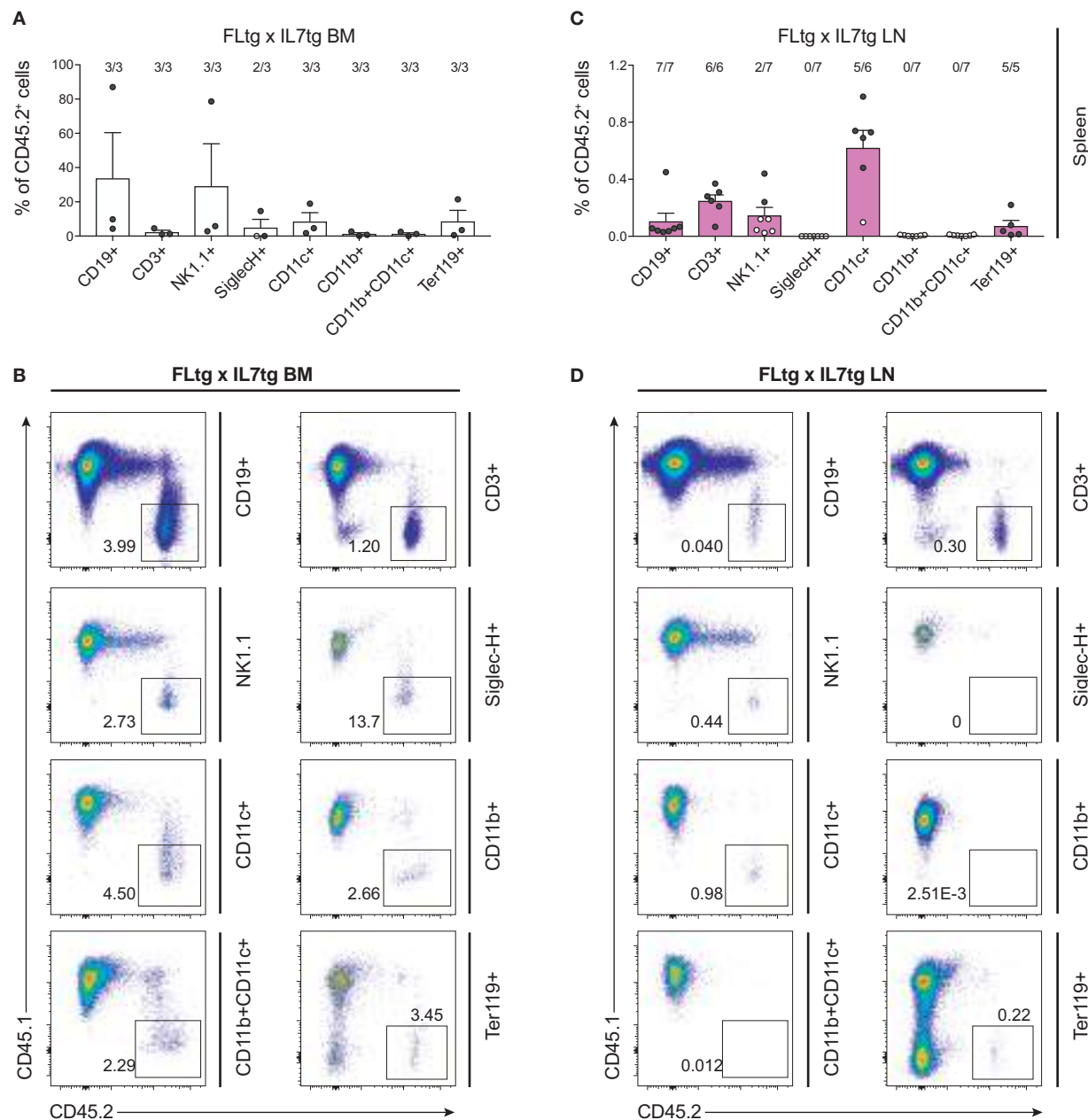


**FIGURE 8 |** Hematopoietic reconstitution potential of FLtgxIL7tg LN cells after secondary transplantation. **(A,C)** Percentage of CD45.2<sup>+</sup> donor cells within the indicated lineages in spleens of secondary CD45.1<sup>+</sup> recipients, which received BM or LN of CD45.1<sup>+</sup> mice reconstituted with FLtgxIL7tg BM (**A**) or FLtgxIL7tg LN (**C**). Results from three independently performed experiments are shown. Bars indicate mean  $\pm$  standard error of the mean. Black circles represent mice where the corresponding lineage was scored as positive for the presence of donor-derived cells (>50 cells in the CD45.2<sup>+</sup> gate) and white circles mice with no reconstitution (<50 cells in the CD45.2<sup>+</sup> gate). The ratio of positive-to-total mice analyzed for each lineage is indicated above the corresponding bar. Lineages were defined as follows: CD19<sup>+</sup>: CD11b<sup>-</sup>CD11c<sup>-</sup>CD3<sup>-</sup>CD19<sup>+</sup>; CD3<sup>+</sup>: CD11b<sup>-</sup>CD11c<sup>-</sup>CD19<sup>-</sup>CD3<sup>+</sup>; NK1.1<sup>+</sup>: CD3<sup>-</sup>CD11c<sup>-</sup>B220<sup>-</sup>SiglecH<sup>-</sup>NK1.1<sup>+</sup>; SiglecH<sup>+</sup>: CD11b<sup>-</sup>NK1.1<sup>-</sup>B220<sup>+</sup>SiglecH<sup>+</sup>; CD11c<sup>+</sup>: NK1.1<sup>-</sup>SiglecH<sup>-</sup>B220<sup>-</sup>CD11b<sup>-</sup>CD11c<sup>+</sup>; CD11b<sup>+</sup>: NK1.1<sup>-</sup>SiglecH<sup>-</sup>B220<sup>-</sup>CD11c<sup>-</sup>CD11b<sup>+</sup>; CD11b+CD11c<sup>+</sup>: NK1.1<sup>-</sup>SiglecH<sup>-</sup>B220<sup>-</sup>CD11b<sup>+</sup>CD11c<sup>+</sup>; Ter119<sup>+</sup>: Ter119<sup>+</sup>. **(B,D)** Representative FACS plots showing the CD45.2<sup>+</sup> donor population identified within the lineages shown in **(A,C)**. Left: FLtgxIL7tg BM as primary donor; right : FLtgxIL7tg LN as primary donor.

(53–55) or cytokine over-expression (56, 57) can lead to extra-medullary hematopoiesis. However, the main extra-medullary site where hematopoietic progenitors are detected in both patients and mice is the spleen, whereas no such precursors have

been reported in LN in these cases. Hematopoietic progenitors have been shown to circulate to the periphery through blood and lymph, but only very small numbers have been detected in lymph under normal conditions and they were practically undetected

in LN (58). A human NK precursor has been detected in LN (59), while it has been shown that at early time points after BM transplantation T cell lymphopoiesis can occur in extra-thymic sites, including LN (60). Interestingly, repeated administration of FL in mice has led to pronounced presence of immature hematopoietic progenitors in the spleen, as seen in our FLtg and FLtgxIL7tg mice, but not in LN (61). It appears that in FLtgxIL7tg mice, the expansion of both lymphoid and myeloid progenitors due to the combined action of both cytokines is sufficient to cause the accumulation of hematopoietic progenitors not only in the spleen but also in LN. This indicates that the environment in secondary lymphoid organs is able to support hematopoiesis in “emergency” situations, such as the one in FLtgxIL7tg mice, which manifest a pronounced myelo- and lympho-proliferative disease. However, it remains unknown whether this ability of the FLtgxIL7tg LN to support the accumulation of progenitors is due to alterations in the LN niche caused by high FL and IL-7 expression, e.g., up-regulated expression of other cytokines or adhesion molecules by LN stromal cells. Moreover, an interesting question is whether the FLtgxIL7tg LN is a site of on-going hematopoiesis, or if the progenitors only migrate there and accumulate without differentiating further. In support of the former hypothesis, FLtgxIL7tg LN-residing progenitors are functional in reconstituting hematopoietic cells after transfer to irradiated recipients (Figures 7, 8) and all hematopoietic developmental stages are represented in the LN in ratios similar to the ones found in WT BM. Further experiments would be needed to address this issue.

Collectively, our present analysis of FLtgxIL7tg mice demonstrates the *in vivo* synergistic action of FL and IL-7 in promoting lymphoid development and expansion. This is summarized in Supplementary Figure 9. Our data provide evidence that secondary lymphoid organs can support the maintenance of hematopoietic progenitors in conditions of abnormal hematopoiesis. Further studies of these mice might

elucidate the requirements for extra-medullary residence and hematopoietic activity of HSC; an issue of clinical importance for the treatment of lympho-proliferative disorders and blood malignancies.

## AUTHOR CONTRIBUTIONS

FK, LvM, GC, SH, LA-S, HR, CE, MR, MM, GCv, and PT performed experiments. FK, PT, and AR analyzed data. PT wrote the manuscript. JA and RC contributed experimental ideas and revised the manuscript. PT and AR designed the study.

## FUNDING

AR was holder of the chair in immunology endowed by L. Hoffmann – La Roche Ltd., Basel. This study was supported by the Swiss National Science Foundation (310030B\_160330/1) and by the People Program (Marie Curie Actions) of the European Union’s Seventh Framework Program FP7/2007-2013 under Research Executive Agency grant agreement number 315902. RC was supported by Science Foundation Ireland under grant numbers SFI09/SRC/B1794 and SFI07/SK/B1233b.

## ACKNOWLEDGMENTS

We thank Dr Geoffrey Brown for critical reading of the manuscript and helpful comments. We dedicate this paper to the memory of our colleague, friend, group leader and mentor AR.

## SUPPLEMENTARY MATERIAL

The Supplementary Material for this article can be found online at: <https://www.frontiersin.org/articles/10.3389/fimmu.2018.02258/full#supplementary-material>

## REFERENCES

1. Metcalf D. Hematopoietic cytokines. *Blood* (2008) 111:485–91. doi: 10.1182/blood-2007-03-079681
2. Brown G, Mooney CJ, Alberti-Servera L, Muenchow L, Toellner KM, Ceredig R, et al. Versatility of stem and progenitor cells and the instructive actions of cytokines on hematopoiesis. *Crit Rev Clin Lab Sci.* (2015) 52:168–79. doi: 10.3109/10408363.2015.1021412
3. Brown G, Tsapogas P, Ceredig R. The changing face of hematopoiesis: a spectrum of options is available to stem cells. *Immunol Cell Biol.* (2018). doi: 10.1111/imcb.12055. [Epub ahead of print].
4. Gilliland DG, Griffin JD. The roles of FLT3 in hematopoiesis and leukemia. *Blood* (2002) 100:1532–42. doi: 10.1182/blood-2002-02-0492
5. Stirewalt DL, Radich JP. The role of FLT3 in haematopoietic malignancies. *Nat Rev Cancer* (2003) 3:650–65. doi: 10.1038/nrc1169
6. Tsapogas P, Mooney CJ, Brown G, Rolink A. The Cytokine Flt3-Ligand in Normal and Malignant Hematopoiesis. *Int J Mol Sci.* (2017) 18:E1115. doi: 10.3390/ijms18061115
7. Adolfsson J, Borge OJ, Bryder D, Theilgaard-Monch K, Astrand-Grundstrom I, Sitnicka E, et al. Upregulation of Flt3 expression within the bone marrow Lin(-)Sca1(+)c-kit(+) stem cell compartment is accompanied by loss of self-renewal capacity. *Immunity* (2001) 15:659–69. doi: 10.1016/S1074-7613(01)00220-5
8. Mackarehtschian K, Hardin JD, Moore KA, Boast S, Goff SP, Lemischka IR. Targeted disruption of the flk2/flt3 gene leads to deficiencies in primitive hematopoietic progenitors. *Immunity* (1995) 3:147–61.
9. McKenna HJ, Stocking KL, Miller RE, Brasel K, De Smedt T, Maraskovsky E, et al. Mice lacking flt3 ligand have deficient hematopoiesis affecting hematopoietic progenitor cells, dendritic cells, and natural killer cells. *Blood* (2000) 95:3489–97.
10. Buza-Vidas N, Cheng M, Duarte S, Nozad H, Jacobsen SE, Sitnicka E. Crucial role of FLT3 ligand in immune reconstitution after bone marrow transplantation and high-dose chemotherapy. *Blood* (2007) 110:424–32. doi: 10.1182/blood-2006-09-047480
11. Holmes ML, Carotta S, Corcoran LM, Nutt SL. Repression of Flt3 by Pax5 is crucial for B-cell lineage commitment. *Genes Dev.* (2006) 20:933–8. doi: 10.1101/gad.1396206
12. Sitnicka E, Bryder D, Theilgaard-Monch K, Buza-Vidas N, Adolfsson J, Jacobsen SE. Key role of flt3 ligand in regulation of the common lymphoid progenitor but not in maintenance of the hematopoietic stem cell pool. *Immunity* (2002) 17:463–72. doi: 10.1016/S1074-7613(02)00419-3
13. von Muenchow L, Alberti-Servera L, Klein F, Capoferri G, Finke D, Ceredig R, et al. Permissive roles of cytokines interleukin-7 and Flt3 ligand in mouse

- B-cell lineage commitment. *Proc Natl Acad Sci USA*. (2016) 113:E8122–30. doi: 10.1073/pnas.1613316113
14. Kondo M, Weissman IL, Akashi K. (1997). Identification of clonogenic common lymphoid progenitors in mouse bone marrow. *Cell* 91:661–72.
  15. Namen AE, Schmierer AE, March CJ, Overell RW, Park LS, Urdal DL, et al. B cell precursor growth-promoting activity. Purification and characterization of a growth factor active on lymphocyte precursors. *J Exp Med*. (1988) 167:988–1002.
  16. Rolink A, Kudo A, Karasuyama H, Kikuchi Y, Melchers F. Long-term proliferating early pre B cell lines and clones with the potential to develop to surface Ig-positive, mitogen reactive B cells *in vitro* and *in vivo*. *EMBO J*. (1991) 10:327–36.
  17. Peschon JJ, Morrissey PJ, Grabstein KH, Ramsdell FJ, Maraskovsky E, Gliniak BC, et al. Early lymphocyte expansion is severely impaired in interleukin 7 receptor-deficient mice. *J Exp Med* (1994) 180:1955–60.
  18. von Freeden-Jeffry U, Vieira P, Lucian LA, McNeil T, Burdach SE, Murray R. Lymphopenia in interleukin (IL)-7 gene-deleted mice identifies IL-7 as a nonredundant cytokine. *J Exp Med* (1995) 181:1519–26.
  19. Akashi K, Kondo M, von Freeden-Jeffry U, Murray R, Weissman IL. Bcl-2 rescues T lymphopoiesis in interleukin-7 receptor-deficient mice. *Cell* (1997) 89:1033–41.
  20. Maraskovsky E, O'Reilly LA, Teepe M, Corcoran LM, Peschon JJ, Strasser A. Bcl-2 can rescue T lymphocyte development in interleukin-7 receptor-deficient mice but not in mutant rag-1–/– mice. *Cell* (1997) 89:1011–9.
  21. Carrette F, Surh CD. IL-7 signaling and CD127 receptor regulation in the control of T cell homeostasis. *Semin Immunol*. (2012) 24:209–17. doi: 10.1016/j.smim.2012.04.010
  22. Kondo M, Akashi K, Domen J, Sugamura K, Weissman IL. (1997). Bcl-2 rescues T lymphopoiesis, but not B or NK cell development, in common gamma chain-deficient mice. *Immunity* 7:155–62.
  23. Maraskovsky E, Peschon JJ, McKenna H, Teepe M, Strasser A. Overexpression of Bcl-2 does not rescue impaired B lymphopoiesis in IL-7 receptor-deficient mice but can enhance survival of mature B cells. *Int Immunol*. (1998) 10:1367–75.
  24. Dias S, Silva H Jr, Cumano A, Vieira P. Interleukin-7 is necessary to maintain the B cell potential in common lymphoid progenitors. *J Exp Med*. (2005) 201:971–9. doi: 10.1084/jem.20042393
  25. Tsapogas P, Zandi S, Ahlsberg J, Zetterblad J, Welinder E, Jonsson JI, et al. IL-7 mediates Ebf-1-dependent lineage restriction in early lymphoid progenitors. *Blood* (2011) 118:1283–90. doi: 10.1182/blood-2011-01-332189
  26. Malin S, McManus S, Cobaleda C, Novatchkova M, Delogu A, Bouillet P, et al. Role of STAT5 in controlling cell survival and immunoglobulin gene recombination during pro-B cell development. *Nat Immunol*. (2010) 11:171–9. doi: 10.1038/ni.1827
  27. Fisher AG, Burdet C, LeMeur M, Haasner D, Gerber P, Ceredig R. Lymphoproliferative disorders in an IL-7 transgenic mouse line. *Leukemia* (1993) 7(Suppl. 2):S66–8.
  28. Fisher AG, Burdet C, Bunce C, Merkenschlager M, Ceredig R. Lymphoproliferative disorders in IL-7 transgenic mice: expansion of immature B cells which retain macrophage potential. *Int Immunol*. (1995) 7:415–23.
  29. Mertsching E, Gräwunder U, Meyer V, Rolink T, Ceredig R. Phenotypic and functional analysis of B lymphopoiesis in interleukin-7-transgenic mice: expansion of pro/pre-B cell number and persistence of B lymphocyte development in lymph nodes and spleen. *Eur J Immunol*. (1996) 26:28–33. doi: 10.1002/eji.1830260105
  30. Sitnicka E, Brakebusch C, Martensson IL, Svensson M, Agace WW, Sigvardsson M, et al. Complementary signaling through flt3 and interleukin-7 receptor alpha is indispensable for fetal and adult B cell genesis. *J Exp Med*. (2003) 198:1495–506. doi: 10.1084/jem.20031152
  31. Ahlsberg J, Tsapogas P, Qian H, Zetterblad J, Zandi S, Mansson R, et al. Interleukin-7-induced Stat-5 acts in synergy with Flt-3 signaling to stimulate expansion of hematopoietic progenitor cells. *J Biol Chem*. (2010) 285:36275–84. doi: 10.1074/jbc.M110.155531
  32. Tsapogas P, Swee LK, Nusser A, Nuber N, Kreuzaler M, Capoferrini G, et al. *In vivo* evidence for an instructive role of fms-like tyrosine kinase-3 (FLT3) ligand in hematopoietic development. *Haematologica* (2014) 99:638–46. doi: 10.3324/haematol.2013.089482
  33. Mazzucchelli R, Durum SK. Interleukin-7 receptor expression: intelligent design. *Nat Rev Immunol*. (2007) 7:144–54. doi: 10.1038/nri2023
  34. Ceredig R, Rauch M, Balciunaite G, Rolink AG. Increasing Flt3L availability alters composition of a novel bone marrow lymphoid progenitor compartment. *Blood* (2006) 108:1216–22. doi: 10.1182/blood-2005-10-006643
  35. Mertsching E, Burdet C, Ceredig R. IL-7 transgenic mice: analysis of the role of IL-7 in the differentiation of thymocytes *in vivo* and *in vitro*. *Int Immunopharmacol*. (1995) 7:401–14.
  36. Swee LK, Bosco N, Malissen B, Ceredig R, Rolink A. Expansion of peripheral naturally occurring T regulatory cells by Fms-like tyrosine kinase 3 ligand treatment. *Blood* (2009) 113:6277–87. doi: 10.1182/blood-2008-06-161026
  37. Carvalho TL, Mota-Santos T, Cumano A, Demengeot J, Vieira P. Arrested B lymphopoiesis and persistence of activated B cells in adult interleukin 7(–/–) mice. *J Exp Med* (2001) 194:1141–50. doi: 10.1084/jem.194.8.1141
  38. Jensen CT, Kharazi S, Boiers C, Cheng M, Lubking A, Sitnicka E, et al. FLT3 ligand and not TSLP is the key regulator of IL-7-independent B-1 and B-2 B lymphopoiesis. *Blood* (2008) 112:2297–304. doi: 10.1182/blood-2008-04-150508
  39. Alberti-Silvera L, von Muenchow L, Tsapogas P, Capoferrini G, Eschbach K, Beisel C, et al. Single-cell RNA sequencing reveals developmental heterogeneity among early lymphoid progenitors. *EMBO J* (2017) 36:3619–33. doi: 10.15252/embj.201797105
  40. Balciunaite G, Ceredig R, Massa S, Rolink AG. A B220+ CD117+ CD19+ hematopoietic progenitor with potent lymphoid and myeloid developmental potential. *Eur J Immunol*. (2005) 35:2019–30. doi: 10.1002/eji.200526318
  41. Kiel MJ, Yilmaz OH, Iwashita T, Yilmaz OH, Terhorst C, Morrison SJ. SLAM family receptors distinguish hematopoietic stem and progenitor cells and reveal endothelial niches for stem cells. *Cell* (2005) 121:1109–21. doi: 10.1016/j.cell.2005.05.026
  42. Pronk CJ, Rossi DJ, Mansson R, Attema JL, Nordahl GL, Chan CK, et al. Elucidation of the phenotypic, functional, and molecular topography of a myeloerythroid progenitor cell hierarchy. *Cell Stem Cell* (2007) 1:428–42. doi: 10.1016/j.stem.2007.07.005
  43. Onai N, Obata-Onai A, Schmid MA, Ohteki T, Jarrossay D, Manz MG. Identification of clonogenic common Flt3+M-CSFR+ plasmacytoid and conventional dendritic cell progenitors in mouse bone marrow. *Nat Immunol*. (2007) 8:1207–16. doi: 10.1038/ni1518
  44. Liu K, Victora GD, Schwickert TA, Guermonprez P, Meredith MM, Yao K, et al. *In vivo* analysis of dendritic cell development and homeostasis. *Science* (2009) 324:392–7. doi: 10.1126/science.1170540
  45. Rodrigues PF, Alberti-Silvera L, Eremin A, Grajales-Reyes GE, Ivanek R, Tussiwand R. Distinct progenitor lineages contribute to the heterogeneity of plasmacytoid dendritic cells. *Nat Immunol*. (2018) 19:711–22. doi: 10.1038/s41590-018-0136-9
  46. Tan JT, Dudl E, LeRoy E, Murray R, Sprent J, Weinberg KI, et al. IL-7 is critical for homeostatic proliferation and survival of naive T cells. *Proc Natl Acad Sci USA*. (2001) 98:8732–7. doi: 10.1073/pnas.161126098
  47. Balciunaite G, Ceredig R, Rolink AG. The earliest subpopulation of mouse thymocytes contains potent T, significant macrophage, and natural killer cell but no B-lymphocyte potential. *Blood* (2005) 105:1930–6. doi: 10.1182/blood-2004-08-3087
  48. Luc S, Luis TC, Boukarabila H, Macaulay IC, Buza-Vidas N, Bouriez-Jones T, et al. The earliest thymic T cell progenitors sustain B cell and myeloid lineage potential. *Nat Immunol*. (2012) 13:412–9. doi: 10.1038/ni.2255
  49. Mooney CJ, Cunningham A, Tsapogas P, Toellner KM, Brown G. Selective expression of Flt3 within the mouse hematopoietic stem cell compartment. *Int J Mol Sci*. (2017) 18:E1037. doi: 10.3390/ijms18051037
  50. Johns JL, Christopher MM. Extramedullary hematopoiesis: a new look at the underlying stem cell niche, theories of development, and occurrence in animals. *Vet Pathol*. (2012) 49:508–23. doi: 10.1177/0300985811432344
  51. Chiu SC, Liu HH, Chen CL, Chen PR, Liu MC, Lin SZ, et al. Extramedullary hematopoiesis (EMH) in laboratory animals: offering an insight into stem cell research. *Cell Transplant* (2015) 24:349–66. doi: 10.3727/096368915X686850

52. Sefc L, Psenak O, Sykora V, Sulc K, Necas E. Response of hematopoiesis to cyclophosphamide follows highly specific patterns in bone marrow and spleen. *J Hematother Stem Cell Res.* (2003) 12:47–61. doi: 10.1089/152581603321210136
53. Hsieh PP, Olsen RJ, O’Malley DP, Konoplev SN, Hussong JW, Dunphy CH, et al. The role of Janus Kinase 2 V617F mutation in extramedullary hematopoiesis of the spleen in neoplastic myeloid disorders. *Mod Pathol.* (2007) 20:929–35. doi: 10.1038/modpathol.3800826
54. Sasaki M, Knobbe CB, Munger JC, Lind EF, Brenner D, Brustle A, et al. IDH1(R132H) mutation increases murine haematopoietic progenitors and alters epigenetics. *Nature* (2012) 488:656–9. doi: 10.1038/nature11323
55. Chang T, Krisman K, Theobald EH, Xu J, Akutagawa J, Lauchle JO, et al. Sustained MEK inhibition abrogates myeloproliferative disease in Nf1 mutant mice. *J Clin Invest.* (2013) 123:335–9. doi: 10.1172/JCI63193
56. Peters M, Schirmacher P, Goldschmitt J, Odenthal M, Peschel C, Fattori E, et al. Extramedullary expansion of hematopoietic progenitor cells in interleukin (IL)-6-sIL-6R double transgenic mice. *J Exp Med.* (1997) 185:755–66.
57. Khaldoyanidi S, Sikora L, Broide DH, Rothenberg ME, Sriramarao P. Constitutive overexpression of IL-5 induces extramedullary hematopoiesis in the spleen. *Blood* (2003) 101:863–8. doi: 10.1182/blood-2002-03-0735
58. Massberg S, Schaerli P, Knezevic-Maramica I, Kollnberger M, Tubo N, Moseman EA, et al. Immunosurveillance by hematopoietic progenitor cells trafficking through blood, lymph, and peripheral tissues. *Cell* (2007) 131:994–1008. doi: 10.1016/j.cell.2007.09.047
59. Freud AG, Becknell B, Roychowdhury S, Mao HC, Ferketich AK, Nuovo GJ, et al. A human CD34(+) subset resides in lymph nodes and differentiates into CD56bright natural killer cells. *Immunity* (2005) 22:295–304. doi: 10.1016/j.immuni.2005.01.013
60. Maillard I, Schwarz BA, Sambandam A, Fang T, Shestova O, Xu L, et al. Notch-dependent T-lineage commitment occurs at extrathymic sites following bone marrow transplantation. *Blood* (2006) 107:3511–19. doi: 10.1182/blood-2005-08-3454
61. Shurin MR, Pandharipande PP, Zorina TD, Haluszczak C, Subbotin VM, Hunter O, et al. FLT3 ligand induces the generation of functionally active dendritic cells in mice. *Cell Immunol.* (1997) 179:174–84. doi: 10.1006/cimm.1997.1152

**Conflict of Interest Statement:** The authors declare that the research was conducted in the absence of any commercial or financial relationships that could be construed as a potential conflict of interest.

Copyright © 2018 Klein, von Muenchow, Capoferro, Heiler, Alberti-Servera, Rolink, Engdahl, Rolink, Mitrovic, Cvijetic, Andersson, Ceredig, Tsapogas and Rolink. This is an open-access article distributed under the terms of the Creative Commons Attribution License (CC BY). The use, distribution or reproduction in other forums is permitted, provided the original author(s) and the copyright owner(s) are credited and that the original publication in this journal is cited, in accordance with accepted academic practice. No use, distribution or reproduction is permitted which does not comply with these terms.



# PU.1 Is Required for the Developmental Progression of Multipotent Progenitors to Common Lymphoid Progenitors

Swee Heng Milon Pang<sup>1,2</sup>, Carolyn A. de Graaf<sup>1,2</sup>, Douglas J. Hilton<sup>1,2</sup>,  
Nicholas D. Huntington<sup>1,2</sup>, Sebastian Carotta<sup>1,2,3†</sup>, Li Wu<sup>1,2,4#†</sup> and Stephen L. Nutt<sup>1,2#†</sup>

<sup>1</sup> The Walter and Eliza Hall Institute of Medical Research, Parkville, VIC, Australia, <sup>2</sup> Department of Medical Biology, University of Melbourne, Parkville, VIC, Australia, <sup>3</sup> Oncology Research, Boehringer Ingelheim, Vienna, Austria, <sup>4</sup> Institute for Immunology, Tsinghua University School of Medicine, Beijing, China

## OPEN ACCESS

### Edited by:

Rhodri Ceredig,  
National University of Ireland  
Galway, Ireland

### Reviewed by:

Paulo Vieira,  
Institut Pasteur, France  
Rodney P. DeKoter,  
University of Western Ontario,  
Canada

### \*Correspondence:

Li Wu  
wuli@tsinghua.edu.cn;  
Stephen L. Nutt  
nutt@wehi.edu.au

<sup>†</sup>These authors have contributed  
equally to this work.

### Specialty section:

This article was submitted  
to B Cell Biology,  
a section of the journal  
*Frontiers in Immunology*

Received: 12 April 2018

Accepted: 22 May 2018

Published: 11 June 2018

### Citation:

Pang SHM, de Graaf CA, Hilton DJ,  
Huntington ND, Carotta S, Wu L and  
Nutt SL (2018) PU.1 Is Required for  
the Developmental Progression  
of Multipotent Progenitors to  
Common Lymphoid Progenitors.  
*Front. Immunol.* 9:1264.  
doi: 10.3389/fimmu.2018.01264

The transcription factor PU.1 is required for the development of mature myeloid and lymphoid cells. Due to this essential role and the importance of PU.1 in regulating several signature markers of lymphoid progenitors, its precise function in early lymphopoiesis has been difficult to define. Here, we demonstrate that PU.1 was required for efficient generation of lymphoid-primed multipotent progenitors (LMPPs) from hematopoietic stem cells and was essential for the subsequent formation of common lymphoid progenitors (CLPs). By contrast, further differentiation into the B-cell lineage was independent of PU.1. Examination of the transcriptional changes in conditional progenitors revealed that PU.1 activates lymphoid genes in LMPPs, while repressing genes normally expressed in neutrophils. These data identify PU.1 as a critical regulator of lymphoid priming and the transition between LMPPs and CLPs.

**Keywords:** PU.1, transcription factor, multipotent progenitor, common lymphoid progenitor, Rag1

## INTRODUCTION

Hematopoietic stem cells (HSCs) are responsible for the development of all mature blood cell types. HSCs are found within the lineage (Lin)<sup>-</sup>Sca-1<sup>+</sup>c-Kit<sup>+</sup> (LSK) population of the bone marrow (BM) and are identified within the LSK population as CD150<sup>+</sup>CD48<sup>-</sup> cells [reviewed by Wilson et al. (1)]. The LSK population also includes lymphoid-primed multipotent progenitors (LMPPs) whose potential is skewed toward lymphocyte and myeloid differentiation (2). LMPPs are defined by a characteristically high cell surface concentration of Flt3 and express of a number of lymphoid transcripts, a process termed lymphoid priming. One of the genes subject to lineage priming is *Rag1*. Indeed the expression of a GFP reporter expressed from the *Rag1* locus can be used to identify a population termed the early lymphoid progenitor (ELP) that overlaps with the LMPP (3). The common lymphoid progenitor (CLP) is developmentally downstream of the LMPP and its potential appears largely restricted to the lymphoid lineages, *in vivo*, if not *in vitro* (4–6). CLPs upregulate expression of IL-7R $\alpha$ , while maintaining Flt3 and Rag1/GFP (7, 8). Signaling through both, Flt3 and IL-7R $\alpha$ , is required for development to the B cell progenitor stages (9). CLPs can be further divided through the expression of Ly6D into a true “all lymphocytic progenitor” (ALP, Ly6D<sup>-</sup>), which can give rise to all lymphocytic lineages, and a “B cell biased lymphocytic progenitor” (BLP, Ly6D<sup>+</sup>) (5, 7). BLPs differentiate directly into committed B cells through the concerted activity of E2A, EBF1, and Pax5 (10).

PU.1, encoded by the *Spi1* gene, has long been implicated as a key regulator of the cell fate decisions between the myeloid and lymphoid lineages (11–13). PU.1 concentration is highest in myeloid cells where it functions as a pioneer factor to broadly promote lineage-specific gene expression (14). PU.1 expression is reduced approximately 10-fold early during B-lymphopoiesis, and this low expression is maintained throughout the B cell differentiation process (15, 16). This change in PU.1 concentration is driven at least in part by a positive feedback loop that lengthens cell cycle duration, thus allowing accumulation of PU.1 protein in myeloid cells (17). The appropriate regulation of PU.1 expression is key to the lineage commitment process as deregulation of PU.1 leads in certain lineages to developmental blockade and can result in leukemia formation (18–22). The distinct concentrations of PU.1 in myeloid and lymphoid progenitors are thought to differentially activate a gene regulatory network involving PU.1, Ikaros, and secondary determinants such as Egr1 and Gfi1 (23–25). In this model, low PU.1 is achieved through the activity of Ikaros and Gfi1, resulting in the activation of EBF and the B cell program. This regulatory network is by no means complete, as other factors including E2A (26), Myb (27), and Mef2c (28) have also been implicated in the priming and differentiation of lymphoid progenitors in the BM.

PU.1-deficient embryos or adult mice conditionally deficient for PU.1 in HSCs lack mature lymphocytes (29). However, the determination as to when in lymphoid development PU.1 is required has been complicated by the regulation of several of the key diagnostic markers for LMPPs and CLPs (Flt3 and IL-7R $\alpha$ ) by PU.1 (12, 30, 31). Interestingly, conditional inactivation of PU.1 downstream of CLPs (by an *in vitro* retroviral transduction approach) (32) or B cells by CD19-Cre allows B cell development to proceed (33, 34), suggesting that the window of requirement for PU.1 is between the HSC and CLP stages. To address this issue directly, we have generated PU.1-deficient HSCs that also carry the Rag1/GFP reporter allele, thus enabling us to unambiguously identify LMPPs and CLPs without PU.1, while Rag1/Cre enabled the deletion of PU.1 in CLPs.

## MATERIALS AND METHODS

### Mice

The *Spi1*<sup>gfp</sup> (floxed exon 5 of *Spi1* and a GFP knockin into the 3' untranslated region) (16), *Spi1*<sup>fl/fl</sup>-*MxCre*<sup>+</sup> (35), *Rag1*<sup>gfp/+</sup> (36), *Rag1*<sup>cre/+</sup> (37), and *Rosa26-CreER*<sup>T2</sup> (38) mice have been previously described. For conditional inactivation of PU.1, *Spi1*<sup>fl/fl</sup> or *Spi1*<sup>fl/fl</sup>-*MxCre*<sup>+</sup> mice were injected intraperitoneal (i.p.) with 5  $\mu$ g/g body weight of polyIC (GE Healthcare) twice at 3-day intervals. Mice were analyzed 14, 28, and 42 days after the first polyIC injection. Experimental mice were used at 6–12 weeks of age and maintained on a C57Bl/6 background.

### Preparation of Hematopoietic Progenitors

Hematopoietic cells were flushed from the tibia and femur of both legs. To enrich for hematopoietic progenitor populations in the BM, antibodies to the following surface molecules were used immunomagnetic bead depletion of lineage (Lin) marker-positive BM cells: CD2 (RM2-1), CD3 (KT-3.1), CD8 (53-6.7), CD11b/

MAC-1 (M1-70), Gr-1 (RA6-8C5), B220 (RA3-6B2), and erythrocyte (TER119). Lin<sup>+</sup> cells were exposed to BioMag goat anti-rat IgG beads (Qiagen) and depleted with a Dynal MPC-L magnet (Invitrogen). Lin<sup>-</sup> BM cells were stained with labeled antibodies as described below.

### Flow Cytometry

The following anti-mouse mAbs were used: Sca-1 (E13161.7, produced in house), c-Kit (ACK2, produced in house), Flt3 (A2F10.1; BD Pharmingen), IL-7R $\alpha$  (B12-1; eBioscience, Bioof), Ly6C (5075-3.6), Ly6D (49-H4, BD Pharmingen), CD19 (ID3; BD Pharmingen, eBioscience), B220 (RA3-6B2; BD Pharmingen, eBioscience), IgM (331.12, BD Pharmingen), NK1.1 (PK136, BD Pharmingen), CD49b (HM $\alpha$ 2, BD Pharmingen), TCR $\beta$  (H57-597, BD Pharmingen), CD45.1 (A20, eBioscience), and CD34 (RAM34; BD Pharmingen). Anti-rat immunoglobulin phycoerythrin and PE Cy7-streptavidin (BD Pharmingen) were used as secondary detection reagents.

Single cell suspensions were prepared in balanced salt solution with 2% (v/v) fetal calf serum. Cell staining was on ice for 30 min with fluorescent or biotin conjugated antibodies and the samples were processed on an LSRII or LSRFortessa flow cytometer (BD Biosciences). Propidium iodide exclusion was used to determine cell viability. Data were analyzed using FlowJo software (Treestar Inc.).

### RNA Isolation, Amplification From LSK Cells, and Array Analysis

Total RNA was isolated from LSK cells of PU.1 conditional deleted and wild-type animals (three pools of 15–20 mice treated with 5  $\mu$ g/g of body weight polyIC 14 days previously) using RNeasy kits (Qiagen). RNA was amplified with the Illumina Total Prep RNA Amplification Kit (Ambion) and quantity and quality assessed using the Agilent Bioanalyzer 2100. Labeled cRNA was hybridized to Illumina MouseWG-6 V 2.0 Expression BeadChips at the Australian Genome Research Facility, Melbourne.

The resulting arrays were analyzed in R using the Bioconductor package *limma* (39). Raw intensities were normalized by using the *neqc* function, which performs background and quantile normalization using control probes (40). Probes not detected in any sample were removed (detection *p* value < 0.05). Pairwise comparisons used linear modeling and empirical Bayes moderated *t* statistics (41). The false discovery rate (FDR) was controlled by the Benjamini–Hochberg algorithm. Differentially expressed probes had an FDR of <0.05. Multi-dimensional scaling (MDS) plot was produced using expression data for wild-type progenitor and stem cell populations obtained from <http://haemosphere.org> (42) using *plotMDS* function in *limma* using the top 500 differentially expressed genes. Lineage-specific gene sets obtained from <http://haemosphere.org> (42) were used in gene set tests. *p* Values were obtained with rotation gene set testing (ROAST) using the *mroast* in *limma*, Benjamini–Hochberg correction for multiple testing and 9,999 rotations. Barcode plots were made using the *barcodeplot* function of the *limma* package.

Gene ontology analyses were obtained from PANTHER Classification System version 11.0 (43). Statistical overrepresentation test was performed on activated and repressed genes, using

PANTHER GO-Slim Biological Process. Only results with  $p$  value  $<0.05$  and positive fold enrichment  $>1$  are displayed.

## Quantitative Real-Time RT-PCR

Total RNA was isolated from purified cells using TRIzol (Invitrogen). cDNA synthesis used iScript Reverse Transcription Supermix (Bio-Rad). Quantification of gene expression was performed in triplicate with QuantiTect SYBR Green PCR kit (Qiagen) on a C1000 Thermal Cycler (Bio-Rad). The primers are listed in Table S1 in Supplementary Material.

## In Vitro Clonogenic Assays

To determine the progenitor frequencies, sorted populations were seeded in limiting dilution on OP9 stromal cells in media containing 2% IL-7 supernatant and 5 ng/ml Flt3L. 350 nM 4-hydroxytamoxifen (4OT) was added at day 0. The media was diluted 1:3 on day 1 to reduce any cytotoxic effect of the 4OT. Cells were scored after 7–10 days as described (44). The clonogenic frequency was calculated using the ELDA software (45).

## Statistical Analysis

Statistical analysis used the GraphPad Prism software. For the non-microarray data, sample size analysis indicates that the

power to detect a twofold change with a type error of  $<5\%$  and power of 90% confidence and an SD of 20% of the mean is 4 mice/genotype. We used between 5 and 14 mice/genotype over two to three independent experiments as outlined in the figure legends. Paired or unpaired, two-tailed, Student's  $t$ -test for two samples with equal variance was used as appropriate.

## RESULTS

### PU.1 Expression Peaks in LMPPs During Early Lymphopoiesis

Previous studies have reported that LSK cells and CLPs express relatively high amounts of PU.1 (15, 16, 46). However, fine mapping of PU.1 expression in the LMPPs and the ALP and BLP fractions of the CLP has not been reported. In order to quantify the expression of *Spi1* mRNA in these purified progenitor populations, we utilized mice homozygous for a PU.1/GFP reporter allele that does not impact on PU.1 function (16) and correlates extremely well with PU.1 protein (17). Flow cytometric analysis revealed robust PU.1/GFP expression in all multipotent progenitors (MPPs) with lymphoid potential, with expression peaking in LMPPs (Figures S1A–C in Supplementary Material). PU.1 expression reduced slightly in ALPs and BLPs, before dropping

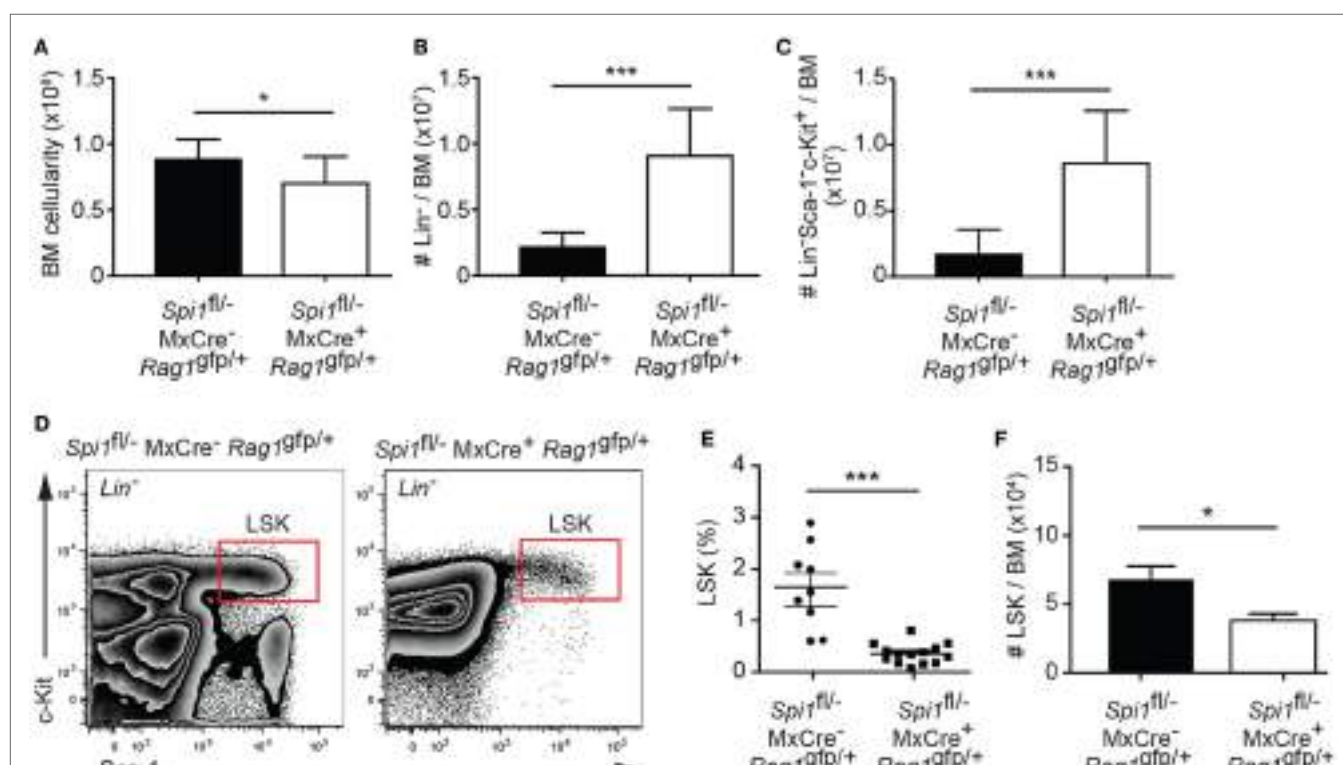


**FIGURE 1 |** Reduced numbers of hematopoietic progenitors from PU.1 conditionally deficient bone marrow (BM). *Spi1*<sup>fl/fl</sup>-MxCre<sup>-</sup>*Rag1*<sup>gfp/+</sup> and *Spi1*<sup>fl/fl</sup>-MxCre<sup>+</sup>*Rag1*<sup>gfp/+</sup> mice were injected with polyIC on days 0 and 3, and analyzed by flow cytometry on day 14. Graph shows (A) the absolute cell numbers in the BM (2x femur and tibia), (B) the number of Lin<sup>-</sup> cells, and (C) the number of Lin<sup>-</sup>Sca-1+c-Kit<sup>+</sup> cells in BM preparation. (D) Representative flow cytometry plot of Lin<sup>-</sup> BM preparations from the mice of indicated genotypes. Boxes indicate the position of the LSK populations. (E) Graph shows the proportion of LSK cells in Lin<sup>-</sup> BM preparation. Each dot represents an individual BM sample. Horizontal line shows the mean  $\pm$  SD. (F) Absolute LSK cell numbers in the BM. Data in the graphs are the mean cell number  $\pm$  SD from between 9 and 14 mice per genotype.  $p$  Values compare the indicated groups using an unpaired  $t$ -test. \* $p < 0.05$ , \*\*\* $p < 0.001$ .

to the characteristic low expression in pro-B-cells and absence in NK cells. The expression of PU.1/GFP matched closely the expression of *Spi1* mRNA in the corresponding populations in the ImmGen<sup>1</sup> (Figure S1D in Supplementary Material) and Gene Expression Commons<sup>2</sup> [Figure S1E in Supplementary Material (47)] databases. Thus within the lymphoid developmental pathway, PU.1 expression peaks at the LMPP stage.

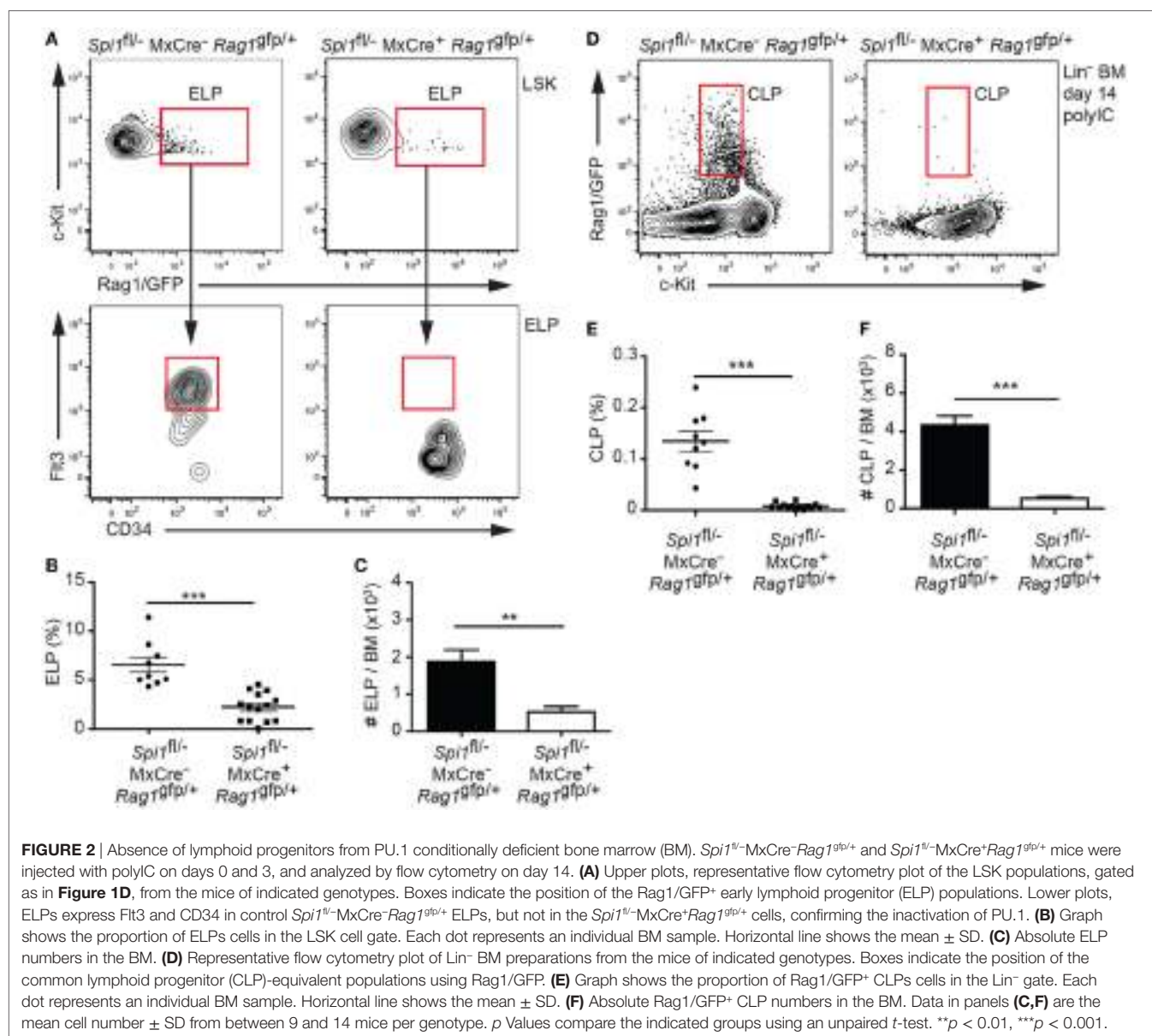
## Analysis of PU.1-Deficient Lymphopoiesis Using Rag1/GFP

Conventional fractionation of the lymphoid progenitor compartment relies heavily on cell surface markers Flt3 and IL-7R. We

have previously shown that the gene encoding Flt3, the defining marker of LMPPs within the LSK pool and expressed on all CLPs, is an obligate PU.1 target gene [(30) and confirmed in all BM progenitors in Figures S2A–D in Supplementary Material], while others have shown that PU.1 regulates the gene encoding the IL-7Rα chain (12), the defining marker of CLPs. To assess the impact of PU.1 inactivation for lymphoid progenitors independently of Flt3 and IL-7R, we have utilized an alternative strategy to identify these populations using Rag1/GFP (36). Rag1/GFP expressing cells within the LSK population define ELPs (3–6% within the LSK cells), which has been demonstrated to be the true lymphoid-primed subset of the LMPP (3). Despite being lymphoid-primed, virtually all ELPs co-express CD34 and Flt3 (Figure S3A in Supplementary Material) and only a low proportion (7.3 ± 1.2%) expressed cell surface IL-7R. Similarly, there is a high degree of surface marker expression overlap between conventionally

<sup>1</sup>www.immgen.org (Accessed: March 26, 2018).

<sup>2</sup>https://gexc.riken.jp/models/3/genes (Accessed: September 18, 2017).



defined CLPs ( $\text{Lin}^- \text{Sca-1}^+ \text{c-Kit}^{\text{int}} \text{Flt3}^+ \text{IL-7R}^\alpha$ ) and  $\text{Lin}^- \text{Sca-1}^+ \text{c-Kit}^{\text{int}} \text{Rag1/GFP}^+$  CLPs (Figure S3B in Supplementary Material) (7, 8). Importantly, our previous RNAseq analysis has shown that *Rag1* expression is independent of PU.1 in B cell progenitors (48). Thus *Rag1/GFP* can be used as a reliable surrogate for Flt3 and IL-7R in the identification of LMPPs and CLPs in the absence of PU.1.

To investigate the requirement of PU.1 in hematopoietic progenitors, we have administered polyIC into *Spi1<sup>fl/fl</sup>-MxCre-Rag1<sup>gfp/+</sup>* or *Spi1<sup>fl/fl</sup>-MxCre<sup>+</sup>Rag1<sup>gfp/+</sup>* mice, to generate heterozygous and null cells, respectively. PolyIC activates the MxCre transgene *via* the type I interferon pathway (49), a process that transiently perturbs BM hematopoiesis, although we have previously shown that control hematopoiesis returns to the steady state within 14 days of the treatment (35). The mouse *Spi1* and *Rag1* genes are closely linked on chromosome 2. Due to inefficient meiotic crossover, we were unable to any offspring of *Spi1<sup>fl/fl</sup>* x *Rag1<sup>gfp/+</sup>* crosses carrying the *Spi1<sup>fl</sup>* and *Rag1<sup>gfp</sup>* alleles on the same chromosome. We did, however, obtain a single recombination event from a *Spi1<sup>fl/fl</sup>* and *Rag1<sup>gfp/+</sup>* cross that resulted in linkage between the *Spi1<sup>fl</sup>* (null) allele and *Rag1<sup>gfp</sup>*. Thus for this technical reason, we compared *Spi1<sup>fl/fl</sup>-MxCre-Rag1<sup>gfp/+</sup>* (control) and *Spi1<sup>fl/fl</sup>-MxCre<sup>+</sup>Rag1<sup>gfp/+</sup>* (experimental) genotypes in each experiment. At this time point, PU.1 inactivation resulted in a modest reduction in overall BM cellularity, but a markedly increased proportion of these cells were  $\text{Lin}^-$  progenitors (Figures 1A,B). The increased  $\text{Lin}^-$  compartment in *Spi1<sup>fl/fl</sup>-MxCre<sup>+</sup>Rag1<sup>gfp/+</sup>* mice was due to an increase in the proportion of Sca-1 $^-$ c-Kit $^+$  myeloid progenitors as we have previously shown [Figures 1C,D (35)]. This analysis also revealed a highly significant reduction in the proportion of LSK cells without PU.1 (Figures 1D,E). However, when absolute cellularity was determined, it became apparent that loss of PU.1 resulted in a twofold reduction in LSK cells (Figure 1F). Thus the loss of PU.1 had a relatively mild impact on the frequency of LSK cells.

Analysis of the ELP fraction of the LSK revealed that PU.1 inactivation resulted in a significant decrease in the proportion and frequency of ELPs (Figures 2A–C). Importantly, the remaining ELPs lacked Flt3, suggesting that they were PU.1 deficient (Figure 2A). By contrast, analysis of the *Rag1/GFP* $^+$  CLP fraction showed an absence of CLPs in the BM, indicating that PU.1 was essential for the formation of these cells (Figures 2D–F). Although the experiments described in Figures 1 and 2 were conducted 14 days after the initial polyIC treatment, we believe that this represented the steady-state situation as analysis of the frequency of the LSK, ELP, and CLP populations at days 28 and 42 after polyIC exposure produced very similar results (Figures 3A–C). Taken together these data indicate that the requirement for PU.1 progressively increases as lymphoid progenitors transition between the LSK and CLP compartments.

## PU.1 Is Dispensable From the CLP Stage of Development

The data described above demonstrated that PU.1 was required for the development of *Rag1/GFP* $^+$  CLPs from LMPPs, although whether PU.1 has an essential function in CLPs was unclear. A previous study showed that removal of PU.1 in CLPs was

compatible with B cell development (32), however, as that study required the CLPs to be cultured for 2 days in B cell promoting conditions prior to Cre activation and PU.1 removal, it remained to be determined if PU.1 was required at the CLP stage of differentiation *in vivo*. To address this question, we crossed the *Spi1<sup>fl/fl</sup>* allele to *Rag1<sup>cre/+</sup>* knockin mice (note that *Rag1<sup>cre/gfp</sup>* mice lacked lymphocytes beyond the pro-B/T cell stage due to the absence of *Rag1* function but allowed the tracking of the *Rag1/GFP* $^+$  CLPs). In this case, we achieved the desired meiotic crossover, producing a copy of chromosome 2 carrying *Spi1<sup>fl</sup>* and *Rag1<sup>fl</sup>*. *Rag1/Cre* has been shown to initiate deletion of a floxed allele in the LSK compartment (37), has substantial but not complete activity at the CLP stage (50) and complete deletion in pro-B and pro-T cells (51). To check for the efficacy of *Rag1/Cre* in lymphoid progenitors, we assessed Flt3 expression in  $\text{Lin}^-$  BM from *Spi1<sup>fl/fl</sup>-Rag1<sup>cre/gfp</sup>* and control *Spi1<sup>fl/fl</sup>-Rag1<sup>gfp/+</sup>* mice as a surrogate

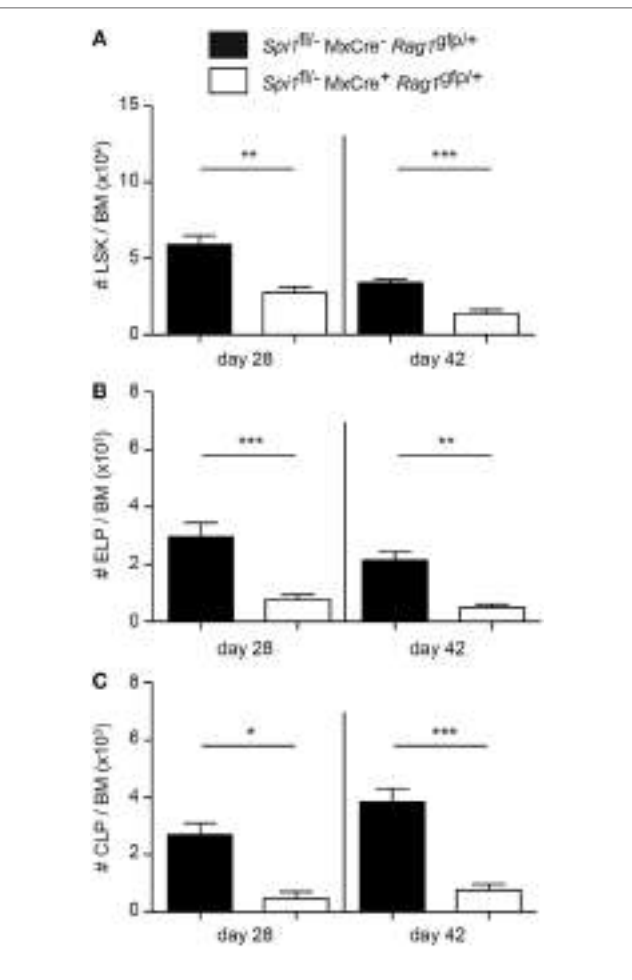


**FIGURE 3 |** Sustained reduction in lymphoid progenitors in PU.1 conditionally deficient bone marrow (BM). *Spi1<sup>fl/fl</sup>-MxCre-Rag1<sup>gfp/+</sup>* and *Spi1<sup>fl/fl</sup>-MxCre<sup>+</sup>Rag1<sup>gfp/+</sup>* mice were injected with polyIC on days 0 and 3, and analyzed by flow cytometry on days 28 and 42. Total numbers of (A) LSK cells, (B) *Rag1/GFP* $^+$  early lymphoid progenitors, and (C) *Rag1/GFP* $^+$  common lymphoid progenitors (CLPs) in the BM of indicated genotypes were calculated. The data are mean  $\pm$  SD from between 5 and 8 mice per genotype. *p* Values compare the indicated groups using an unpaired *t*-test. \**p* < 0.05, \*\**p* < 0.01, \*\*\**p* < 0.001.

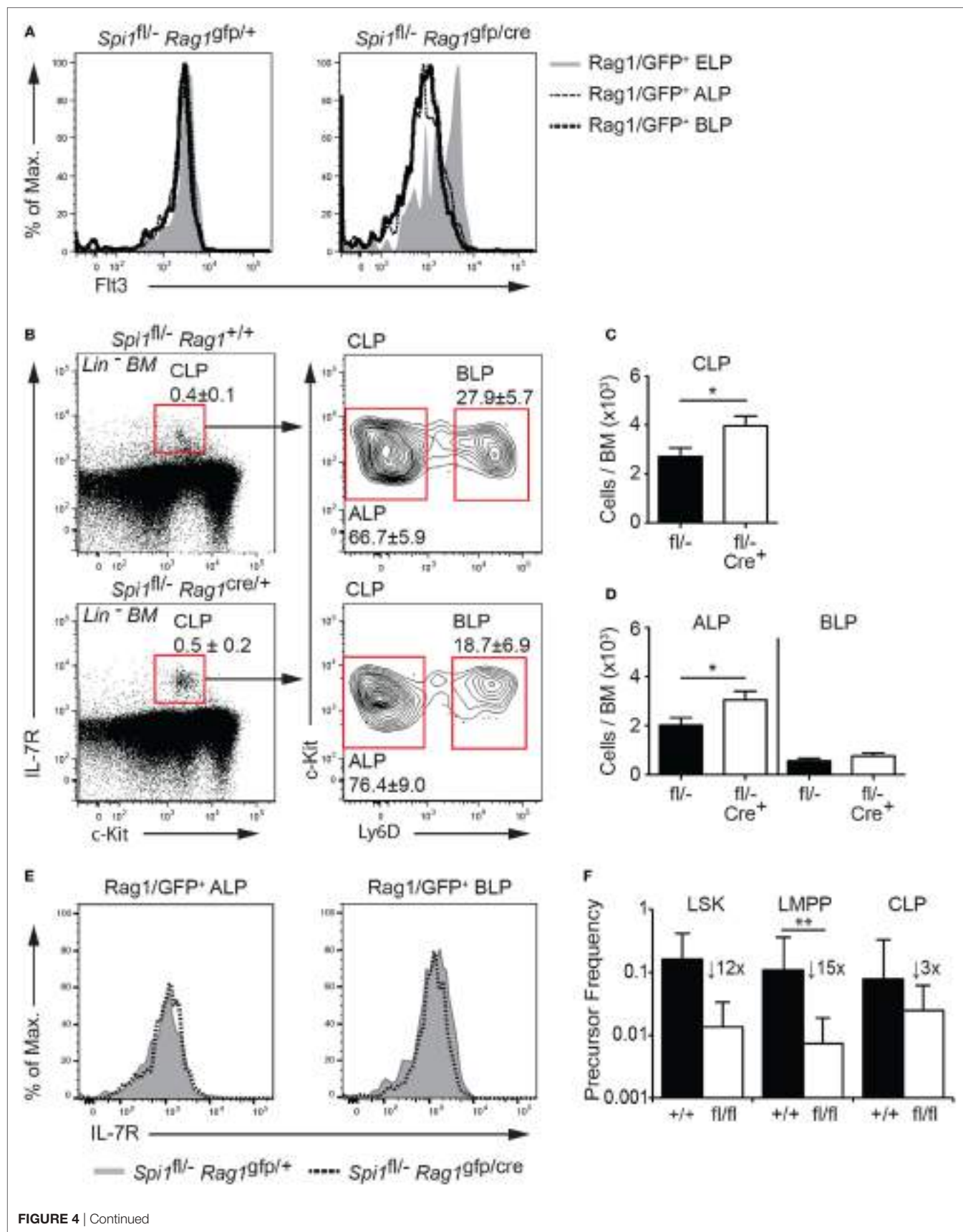


FIGURE 4 | Continued

**FIGURE 4 |** PU.1 is not required for the persistence of common lymphoid progenitors (CLPs). **(A)** Lineage-depleted ( $\text{Lin}^-$ ) bone marrow (BM) was isolated from  $\text{Spi}^{fl/fl}\text{-Rag}1^{+/gfp}$  and  $\text{Spi}^{fl/fl}\text{-Rag}1^{cre/gfp}$  mice and Rag1/GFP $^+$  early lymphoid progenitors (ELPs), all lymphocyte progenitors (ALPs), and biased lymphocyte progenitors (BLPs) of each indicated genotype were assessed for Flt3. **(B–D)**  $\text{Lin}^-$  BM from  $\text{Spi}^{fl/fl}\text{-Rag}1^{+/+}$  and  $\text{Spi}^{fl/fl}\text{-Rag}1^{cre/+}$  mice were analyzed for the **(B)** frequency and **(C)** number of CLPs and **(D)** number of ALPs and BLPs. Boxes show the position of gating for the cell type being analyzed. **(E)** Lineage-depleted ( $\text{Lin}^-$ ) BM was isolated from  $\text{Spi}^{fl/fl}\text{-Rag}1^{+/gfp}$  and  $\text{Spi}^{fl/fl}\text{-Rag}1^{cre/gfp}$  mice and Rag1/GFP $^+$  ALPs and BLPs of each indicated genotype were assessed for IL-7R. Data in panels **(A,E)** are representative of two experiments each consisting of two mice per genotype. Data in panels **(B–D)** are the mean  $\pm$  SD from between 9 and 13 mice per genotype. **(F)** Sorted LSK cells, lymphoid-primed multipotent progenitors (LMPPs), and CLPs from  $\text{Spi}^{fl/fl}\text{CreER}^{T2}$  and control  $\text{Spi}^{+/+}\text{CreER}^{T2}$  mice and cultured in limiting dilution with OP9 stromal cells in the presence of IL-7 and Flt3L for 7–10 days. 350 nM 4-hydroxytamoxifen was added to all cultures on day 1 and diluted threefold after 24 h. The mean clonogenic frequency  $\pm$  5% confidence interval of two experiments each with triplicate measurements is shown. *p* Values compare the indicated groups using an unpaired *t*-test. \**p* < 0.05, \*\**p* < 0.01.

marker for PU.1 deletion. We observed a marked reduction of Flt3 expression in ALPs and BLPs within the CLP compartment (**Figure 4A**), suggesting that *Spi1* deletion occurred efficiently in those cells, while as expected the majority of ELPs maintained Flt3 expression (**Figure 4A**). The fluorescence intensity of the IL-7R was similar between the genotypes suggesting that PU.1 was not required for *Il7r* expression at the ALP or BLP stages of development (**Figure 4E**).

In keeping with the onset of *Spi1* inactivation at the CLP stage, the proportion and absolute number of LSK cells and LMPPs in the BM of  $\text{Spi}^{fl/fl}\text{-Rag}1^{cre/+}$  and control  $\text{Spi}^{fl/fl}\text{-Rag}1^{+/+}$  mice was equivalent (Figures S4A–D in Supplementary Material). Closer examination of the CLP compartment revealed a statistically significant increase in total CLPs in the absence of PU.1, which resulted from a similarly increased proportion and frequency of ALPs (**Figures 4B–D**). The frequency of BLPs, the earliest B cell progenitor and lineage committed pro and pre-B cells were equivalent between the genotypes suggesting that PU.1 activity appears largely dispensable for the differentiation of CLPs into mature lymphoid lineages *in vivo* (**Figures 4B–D** and data not shown).

The conclusion that PU.1 was not required beyond the transition to the CLP stage was supported by *in vitro* clonogenic assays. These experiments utilized  $\text{Spi}^{fl/fl}$  mice crossed to the *Rosa26-CreER}^{T2}* ( $\text{Spi}^{fl/fl}\text{CreER}^{T2}$ ) allele that allows 4-hydroxytamoxifen (Tam) mediated induction of Cre activity *in vitro*. LSK cells, LMPPs and CLPs were isolated from the BM of  $\text{Spi}^{fl/fl}\text{CreER}^{T2}$  and control  $\text{Spi}^{+/+}\text{CreER}^{T2}$  mice and cultured in limiting dilution with OP9 stromal cells, plus Flt3L, and IL-7 for 7–10 days. All cultures were exposed to 350 nM Tam for the first day. As expected, all progenitor fractions from the control PU.1 $^{+/+}\text{CreER}^{T2}$  gave rise to B cell colonies at a cloning frequency of ~10% (**Figure 4F**). LSK cells and LMPPs from  $\text{Spi}^{fl/fl}\text{CreER}^{T2}$  mice showed marked reduction in B cell clonogenic potential (11.9-fold reduction for HSCs and 14.7-fold reduction for LMPPs) compared to controls. By contrast, CLPs from the same mice were much less sensitive to PU.1 loss (threefold reduction compared to controls) a finding in agreement with a previous study (32). Collectively, these results demonstrate that PU.1 is required for the LMPP to CLP transition and suggested no obligate role for this factor at subsequent points in early B cell development.

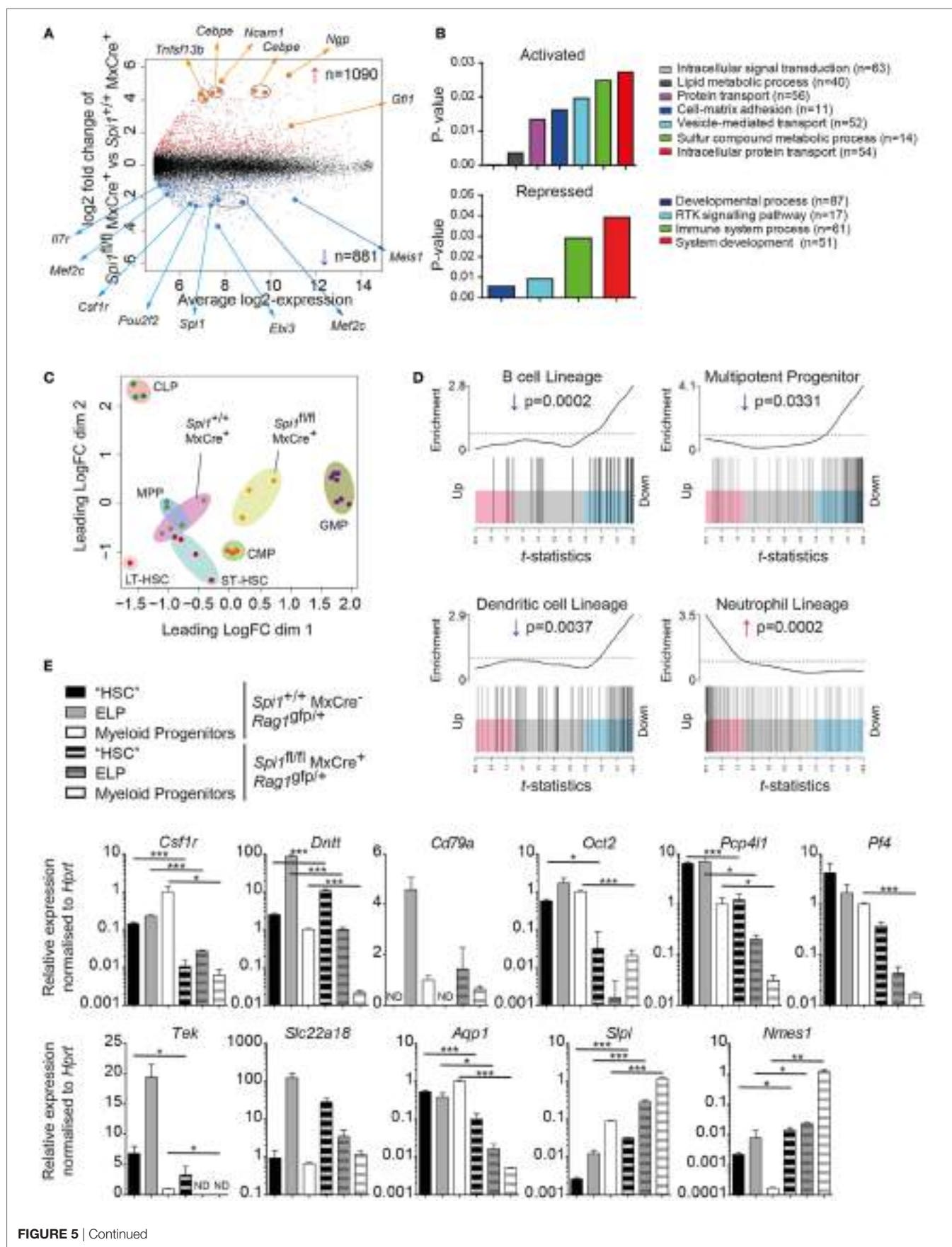
## PU.1 Activates Lymphoid Associated Genes in MPP Cells

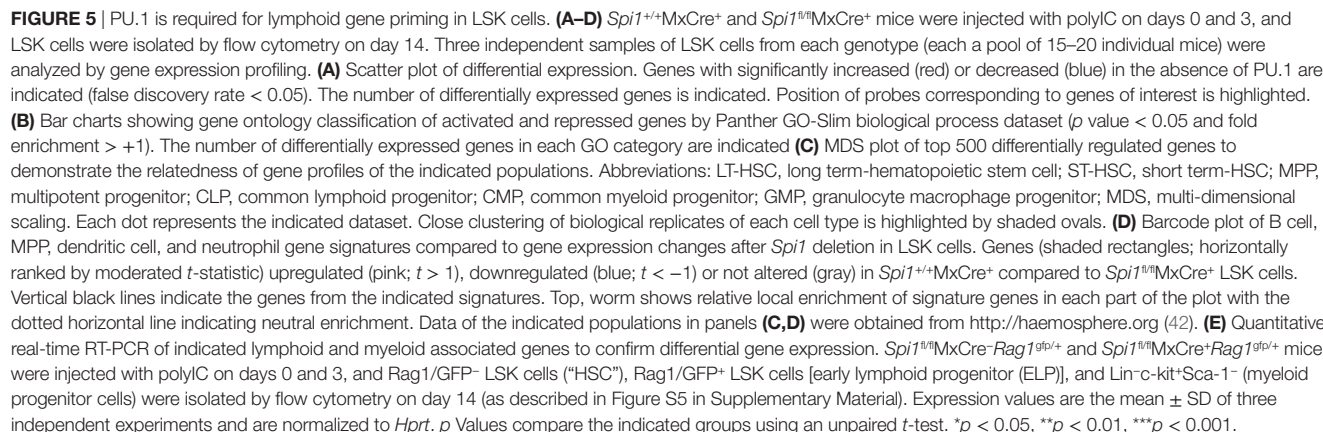
In order to examine the transcriptional roles of PU.1 in early progenitor populations, we purified wild type ( $\text{Spi}^{+/+}\text{MxCre}^+$

and PU.1-deficient ( $\text{Spi}^{fl/fl}\text{MxCre}^+$ ) LSK cells from mice treated 14 days previously with polyIC, and subjected the cells for gene expression profiling by oligonucleotide microarray. Analysis of this data revealed 1,971 differentially expressed transcripts, including 1,090 whose expression increased in the absence of PU.1, such as the transcription factors *Gfi1* and *Cebpe*, and 881 genes that required PU.1 for full expression including the known targets *Csf1r*, *Il7r*, and *Mef2c* (FDR < 0.05, **Figure 5A**). *Ebf1*, another target of PU.1 in pro-B cells (52), was not differentially expressed between the wild type and PU.1-deficient hematopoietic progenitors. We confirmed the efficient inactivation of *Spi1* as the signal detected from the oligonucleotide probe corresponding to the floxed *Spi1* exon 5 decreased >80% in each sample (**Figure 5A**). Pathway analysis revealed that the activated genes encoded proteins mostly involved in signaling, adhesion, and metabolic processes, while the repressed genes were associated with developmental and immune processes (**Figure 5B**).

To explore the relationships between the wild type and PU.1-deficient hematopoietic progenitors in an unbiased way, we measured the transcriptional distance between any pair of expression profiles. This analysis used the *leading fold change*, defined as the average fold change for the 500 genes most different between the samples. Data are shown on an MDS plot where the distances on the plot correspond to log2-leading fold change (**Figure 5C**). This analysis revealed that PU.1-deficient LSK cells clustered closely to the myeloid progenitors (common myeloid progenitor and granulocyte macrophage progenitor), in contrast to the control LSK cells that clustered adjacent to the defined HSC (LT- and ST-) and MPP populations (**Figure 5C**). This conclusion was further supported by cell lineage-specific gene set testing showing that repressed genes were enriched for the neutrophil lineage associated transcripts (**Figures 5A,D**), most likely representing the aberrant c-Kit $^{\text{int}}$  population observed in the PU.1-deficient LSK cells [Figures 1C,D and (35)]. Most importantly, signatures of MPPs, B cell, and DC lineages were lost in the absence of PU.1 (**Figure 5D**).

To confirm the role for PU.1 in promoting the transcriptional priming of lymphoid genes in the MPPs, we analyzed the expression of some of the cohort of neutrophil and B cell specific genes identified in **Figure 5D**, in purified Rag1/GFP $^+$  (ELP) and Rag1/GFP $^-$  (“HSC”) LSK cells, as well as Lin $^-$ Sca-1 $^-$ c-kit $^+$  myeloid progenitors from the BM of  $\text{Spi}^{fl/fl}\text{MxCre}^+\text{Rag}1^{gfp/+}$  (from a newly generated mouse line housing a meiotic recombination producing linked *Spi1* $^{\text{n}}$  and *Rag1* $^{gfp}$ ) and control  $\text{Spi}^{+/+}\text{MxCre}^-\text{Rag}1^{gfp/+}$  mice (**Figure 5E**; Figure S5 in Supplementary Material). The efficient deletion of *Spi1* was confirmed by the absence of Flt3 on the cell





surface (Figure S5 in Supplementary Material), and again by the reduced mRNA for *Csf1r* (encoded for MCSF-R) whose expression is regulated by PU.1 (53) (Figure 5E). In agreement with the gene expression studies, we confirmed eight downregulated genes for the B cell lineage (*Dntt*, *Cd79a*, *Oct2*, *Pcp4l1*, *Pf4*, *Tek*, *Slc22a18*, and *Aqp1*) and two upregulated genes (*Slpi*, *Nmes1*) for neutrophil lineage in PU.1-deficient ELPs (Figure 5E). Together, these data demonstrate that PU.1 is broadly required to prime the expression of lymphoid genes and suppress some neutrophil genes in ELPs for subsequent formation into CLPs.

## DISCUSSION

PU.1 is one of a small group of transcriptional regulators, including Ikaros, E2A, Mef2c, EBF1, Myb, and Pax5 that control the specification and commitment of lymphoid progenitors to the B cell pathway (54–56). Although, it has long been known that PU.1 is required for lymphocyte formation from either the fetal or adult HSCs, the function of PU.1 in lymphopoiesis and the exact point at which it is required has proven more elusive. Here, we demonstrate using conditional mutagenesis that PU.1 is required for efficient LMPP formation and for the subsequent differentiation to the CLP stage.

It has been proposed that the concentration of PU.1 in MPPs determines myeloid (high PU.1) or lymphoid (low PU.1) outcomes (13). Our analysis of *Spi1* transcription using a GFP reporter allele that did not impact on PU.1 function (16) suggests that *Spi1* was relatively uniformly expressed throughout early hematopoietic development, with expression peaking at the LMPP stage. These data mirrored closely the expression of *Spi1* mRNA in wild-type hematopoietic cells. Within the lymphoid developmental pathway PU.1 expression slowly declined but was not markedly downregulated until the pro-B cell (Fraction B) stage. By contrast, myeloid progenitors express an even higher concentration of PU.1 than that observed in LMPPs, which peaks in mature myeloid cells (13, 15–17, 19, 30, 57).

One of the limitations in mapping PU.1 function in early lymphopoiesis has been due to its role in the transcriptional regulation of the genes encoding Flt3 (30) and the  $\alpha$  chain of the IL-7R (12), markers critical for defining the LMPP and CLP. Expression of Rag1/GFP in the LSK compartment defined ELPs that are the most lymphoid-primed component of the LMPP, while GFP

expression in Lin<sup>-</sup>Sca-1<sup>+c-kit<sup>int</sup></sup> cells defined CLPs, independent of either Flt3 or IL-7R. Generation of PU.1-deficient hematopoietic progenitors expressing Rag1/GFP overcame this technical bottleneck, as the expression of *Rag1* is PU.1 independent in both pro-B cells and ALPs [(48) and data not shown]. This analysis revealed that PU.1 was required for the efficient production of LMPPs and was essential for CLP formation. The requirement was very stage specific as the removal of PU.1 using Rag1/Cre was compatible with CLP formation and B cell differentiation, in agreement with a previous study using a less direct approach (32). Thus, the critical role of PU.1 in lymphopoiesis occurs before the CLP stage of development by inducing lymphoid-specific genes and keeping myeloid genes in check at the LMPP stage. Although in the current study we have only addressed PU.1 function in adult BM lymphopoiesis, recent analysis of mice homozygous for a hypomorphic allele of *Spi1* [URE $\Delta/\Delta$  (20)] demonstrated a concentration dependent function for PU.1 in controlling distinct waves of fetal and adult B-lymphopoiesis, suggesting additional complexities in the process (58). It should also be noted that the importance of PU.1 in some aspects of later B cell differentiation, such as at the pre- and mature B cell stages is masked by functional redundancy with the closely related gene, SpiB (59–61).

The phenotype arising from PU.1 deficiency, is broadly similar to that observed in mice lacking E2A (26), Mef2c (28), Ikaros (31, 62), and Myb (27), factors also required for the priming of lymphoid lineage genes in LSK cells. The links between PU.1 and the other members of this gene regulatory network are only partially understood. PU.1 directly regulates *Mef2c*, a factor that also regulates the myeloid versus lymphoid fate decision in hematopoietic progenitors and is essential for the formation of CLPs (28). It has been proposed that PU.1 concentration is determined by a regulatory circuit whereby activation of the lymphocyte-promoting factor Ikaros, itself an essential for lymphopoiesis, represses PU.1 expression either directly or via the induction of the repressor Gfi1 (25). In keeping with this concept, B cell development is impaired in the absence of Gfi1 and can be partially restored by the removal of one allele of *Spi1* or by shRNA-mediated knockdown of *Spi1*. Interestingly, Gfi1 expression was increased in PU.1-deficient LSK cells, suggesting that PU.1 also functions at some level to repress Gfi1 (Figure 5A). Similar counteracting networks are also known to result in multi-lineage priming and contribute to myeloid cell

lineage determination (63). Together with the regulation of the two key cytokine receptors, Flt3 and IL-7R, it is likely that the regulation of these targets is sufficient to explain the important function of PU.1 in the transition from the LMPP to CLP stage of development.

## AVAILABILITY OF DATA AND MATERIAL

The microarray gene expression data are publicly available at the Gene Expression Omnibus ([www.ncbi.nlm.nih.gov/geo](http://www.ncbi.nlm.nih.gov/geo)), accession number GSE89642.

## ETHICS STATEMENT

This study was carried out in accordance with the recommendations of the Australian Code for the Care and Use of Animals for Scientific Purposes. The Walter and Eliza Hall Institute Animal Ethics Committee approved the protocols.

## AUTHOR CONTRIBUTIONS

SP performed all experiments; CG performed the bioinformatics; SP, CG, SC, LW, and SN designed and analyzed the data; DH, NH, SC, LW, and SN supervised the research; SP and SN wrote the manuscript.

## REFERENCES

1. Wilson A, Oser GM, Jaworski M, Blanco-Bose WE, Laurenti E, Adolphe C, et al. Dormant and self-renewing hematopoietic stem cells and their niches. *Ann N Y Acad Sci* (2007) 1106:64–75. doi:10.1196/annals.1392.021
2. Adolfsson J, Mansson R, Buza-Vidas N, Hultquist A, Liuba K, Jensen CT, et al. Identification of Flt3+ lympho-myeloid stem cells lacking erythromegakaryocytic potential: a revised road map for adult blood lineage commitment. *Cell* (2005) 121(2):295–306. doi:10.1016/j.cell.2005.02.013
3. Igarashi H, Gregory SC, Yokota T, Sakaguchi N, Kincade PW. Transcription from the RAG1 locus marks the earliest lymphocyte progenitors in bone marrow. *Immunity* (2002) 17(2):117–30. doi:10.1016/S1074-7613(02)00366-7
4. Akashi K, Kondo M, von Freeden-Jeffry U, Murray R, Weissman IL. Bcl-2 rescues T lymphopoiesis in interleukin-7 receptor-deficient mice. *Cell* (1997) 89(7):1033–41. doi:10.1016/S0092-8674(00)80291-3
5. Inlay MA, Bhattacharya D, Sahoo D, Serwold T, Seita J, Karsunky H, et al. Ly6d marks the earliest stage of B-cell specification and identifies the branchpoint between B-cell and T-cell development. *Genes Dev* (2009) 23(20):2376–81. doi:10.1101/gad.1836009
6. Karsunky H, Inlay MA, Serwold T, Bhattacharya D, Weissman IL. Flk2+ common lymphoid progenitors possess equivalent differentiation potential for the B and T lineages. *Blood* (2008) 111(12):5562–70. doi:10.1182/blood-2007-11-126219
7. Mansson R, Zandi S, Welinder E, Tsapogas P, Sakaguchi N, Bryder D, et al. Single-cell analysis of the common lymphoid progenitor compartment reveals functional and molecular heterogeneity. *Blood* (2010) 115(13):2601–9. doi:10.1182/blood-2009-08-236398
8. Zhang Q, Esplin BL, Iida R, Garrett KP, Huang ZL, Medina KL, et al. RAG-1 and Ly6D independently reflect progression in the B lymphoid lineage. *PLoS One* (2013) 8(8):e72397. doi:10.1371/journal.pone.0072397
9. Vossenrich CA, Cumano A, Muller W, Di Santo JP, Vieira P. Thymic stromal-derived lymphopoietin distinguishes fetal from adult B cell development. *Nat Immunol* (2003) 4(8):773–9. doi:10.1038/ni956
10. Boller S, Grosschedl R. The regulatory network of B-cell differentiation: a focused view of early B-cell factor 1 function. *Immunol Rev* (2014) 261(1):102–15. doi:10.1111/imr.12206
11. Dakic A, Wu L, Nutt SL. Is PU.1 a dosage-sensitive regulator of haemopoietic lineage commitment and leukaemogenesis? *Trends Immunol* (2007) 28(3):108–14. doi:10.1016/j.it.2007.01.006
12. DeKoter RP, Lee HJ, Singh H. PU.1 regulates expression of the interleukin-7 receptor in lymphoid progenitors. *Immunity* (2002) 16(2):297–309. doi:10.1016/S1074-7613(02)00269-8
13. DeKoter RP, Singh H. Regulation of B lymphocyte and macrophage development by graded expression of PU.1. *Science* (2000) 288(5470):1439–41. doi:10.1126/science.288.5470.1439
14. Heinz S, Benner C, Spann N, Bertolino E, Lin YC, Laslo P, et al. Simple combinations of lineage-determining transcription factors prime cis-regulatory elements required for macrophage and B cell identities. *Mol Cell* (2010) 38(4):576–89. doi:10.1016/j.molcel.2010.05.004
15. Back J, Allman D, Chan S, Kastner P. Visualizing PU.1 activity during hematopoiesis. *Exp Hematol* (2005) 33(4):395–402. doi:10.1016/j.exphem.2004.12.010
16. Nutt SL, Metcalf D, D'Amico A, Polli M, Wu L. Dynamic regulation of PU.1 expression in multipotent hematopoietic progenitors. *J Exp Med* (2005) 201(2):221–31. doi:10.1084/jem.20041535
17. Kueh HY, Champhekar A, Nutt SL, Elowitz MB, Rothenberg EV. Positive feedback between PU.1 and the cell cycle controls myeloid differentiation. *Science* (2013) 341(6146):670–3. doi:10.1126/science.1240831
18. Anderson MK, Weiss AH, Hernandez-Hoyos G, Dionne CJ, Rothenberg EV. Constitutive expression of PU.1 in fetal hematopoietic progenitors blocks T cell development at the pro-T cell stage. *Immunity* (2002) 16(2):285–96. doi:10.1016/S1074-7613(02)00277-7
19. Laiosa CV, Stadtfeld M, Xie H, de Andres-Aguayo L, Graf T. Reprogramming of committed T cell progenitors to macrophages and dendritic cells by C/EBP alpha and PU.1 transcription factors. *Immunity* (2006) 25(5):731–44. doi:10.1016/j.immuni.2006.09.011
20. Rosenbauer F, Owens BM, Yu L, Tumang JR, Steidl U, Kutok JL, et al. Lymphoid cell growth and transformation are suppressed by a key regulatory element of the gene encoding PU.1. *Nat Genet* (2006) 38(1):27–37. doi:10.1038/ng1679
21. Rosenbauer F, Wagner K, Kutok JL, Iwasaki H, Le Beau MM, Okuno Y, et al. Acute myeloid leukemia induced by graded reduction of a lineage-specific transcription factor, PU.1. *Nat Genet* (2004) 36(6):624–30. doi:10.1038/ng1361
22. Verbiest T, Bouffler S, Nutt SL, Badie C. PU.1 downregulation in murine radiation-induced acute myeloid leukaemia (AML): from molecular mechanism to human AML. *Carcinogenesis* (2015) 36(4):413–9. doi:10.1093/carcin/bgv016
23. Laslo P, Spooner CJ, Warmflash A, Lancki DW, Lee HJ, Sciammas R, et al. Multilineage transcriptional priming and determination of alternate hematopoietic cell fates. *Cell* (2006) 126(4):755–66. doi:10.1016/j.cell.2006.06.052

## ACKNOWLEDGMENTS

We thank N. Sakaguchi (Kumamoto University) for the *Rag1<sup>gfp</sup>* mice and J. Leahy, N. Iannarella, K. Elder, T. Camilleri, S. O'Connor, and the institute flow cytometry facility for technical assistance.

## FUNDING

This work was supported by grants from the National Health and Medical Research Council (NHMRC) of Australia (575500, 1054925, 1058238 to SN, 1048278 to SN and LW, and 637345 to SC). SP was supported by the Leukaemia Foundation of Australia, CG by an NHMRC Early Career Fellowship, and SC by an NHMRC Career Development Fellowship. This work was made possible through Victorian State Government Operational Infrastructure Support and Australian Government NHMRC IRIIS.

## SUPPLEMENTARY MATERIAL

The Supplementary Material for this article can be found online at <https://www.frontiersin.org/articles/10.3389/fimmu.2018.01264/full#supplementary-material>.

24. Reynaud D, Demarco IA, Reddy KL, Schjerven H, Bertolini E, Chen Z, et al. Regulation of B cell fate commitment and immunoglobulin heavy-chain gene rearrangements by Ikaros. *Nat Immunol* (2008) 9(8):927–36. doi:10.1038/ni.1626
25. Spooner CJ, Cheng JX, Pujadas E, Laslo P, Singh H. A recurrent network involving the transcription factors PU.1 and Gf1 orchestrates innate and adaptive immune cell fates. *Immunity* (2009) 31(4):576–86. doi:10.1016/j.immuni.2009.07.011
26. Dias S, Mansson R, Gurbuxani S, Sigvardsson M, Kee BL. E2A proteins promote development of lymphoid-primed multipotent progenitors. *Immunity* (2008) 29(2):217–27. doi:10.1016/j.immuni.2008.05.015
27. Greig KT, de Graaf CA, Murphy JM, Carpinelli MR, Pang SH, Frampton J, et al. Critical roles for c-Myb in lymphoid priming and early B-cell development. *Blood* (2010) 115(14):2796–805. doi:10.1182/blood-2009-08-239210
28. Stehling-Sun S, Dade J, Nutt SL, DeKoter RP, Camargo FD. Regulation of lymphoid versus myeloid fate ‘choice’ by the transcription factor Mef2c. *Nat Immunol* (2009) 10(3):289–96. doi:10.1038/ni.1694
29. Scott EW, Simon MC, Anastasi J, Singh H. Requirement of transcription factor PU.1 in the development of multiple hematopoietic lineages. *Science* (1994) 265(5178):1573–7. doi:10.1126/science.8079170
30. Carotta S, Dakic A, D’Amico A, Pang SH, Greig KT, Nutt SL, et al. The transcription factor PU.1 controls dendritic cell development and Flt3 cytokine receptor expression in a dose-dependent manner. *Immunity* (2010) 32(5):628–41. doi:10.1016/j.immuni.2010.05.005
31. Yoshida T, Ng SY, Yuniga-Pflucker JC, Georgopoulos K. Early hematopoietic lineage restrictions directed by Ikaros. *Nat Immunol* (2006) 7(4):382–91. doi:10.1038/ni1314
32. Iwasaki H, Somoza C, Shigematsu H, Duprez EA, Iwasaki-Arai J, Mizuno S, et al. Distinctive and indispensable roles of PU.1 in maintenance of hematopoietic stem cells and their differentiation. *Blood* (2005) 106(5):1590–600. doi:10.1182/blood-2005-03-0860
33. Polli M, Dakic A, Light A, Wu L, Tarlinton DM, Nutt SL. The development of functional B lymphocytes in conditional PU.1 knock-out mice. *Blood* (2005) 106(6):2083–90. doi:10.1182/blood-2005-01-0283
34. Ye M, Ermakova O, Graf T. PU.1 is not strictly required for B cell development and its absence induces a B-2 to B-1 cell switch. *J Exp Med* (2005) 202(10):1411–22. doi:10.1084/jem.20051089
35. Dakic A, Metcalf D, Di Rago L, Mifsud S, Wu L, Nutt SL. PU.1 regulates the commitment of adult hematopoietic progenitors and restricts granulopoiesis. *J Exp Med* (2005) 201(9):1487–502. doi:10.1084/jem.20050075
36. Kuwata N, Igarashi H, Ohmura T, Aizawa S, Sakaguchi N. Cutting edge: absence of expression of RAG1 in peritoneal B-1 cells detected by knocking into RAG1 locus with green fluorescent protein gene. *J Immunol* (1999) 163(12):6355–9.
37. McCormack MP, Forster A, Drynan L, Pannell R, Rabbitts TH. The LMO2 T-cell oncogene is activated via chromosomal translocations or retroviral insertion during gene therapy but has no mandatory role in normal T-cell development. *Mol Cell Biol* (2003) 23(24):9003–13. doi:10.1128/MCB.23.24.9003-9013.2003
38. Seibler J, Zevnik B, Kuter-Luks B, Andreas S, Kern H, Hennek T, et al. Rapid generation of inducible mouse mutants. *Nucleic Acids Res* (2003) 31(4):e12. doi:10.1093/nar/gng012
39. Ritchie ME, Phipson B, Wu D, Hu Y, Law CW, Shi W, et al. limma powers differential expression analyses for RNA-sequencing and microarray studies. *Nucleic Acids Res* (2015) 43(7):e47. doi:10.1093/nar/gkv007
40. Shi W, Oshlack A, Smyth GK. Optimizing the noise versus bias trade-off for Illumina whole genome expression BeadChips. *Nucleic Acids Res* (2010) 38(22):e204. doi:10.1093/nar/gkq871
41. Smyth GK. Linear models and empirical bayes methods for assessing differential expression in microarray experiments. *Stat Appl Genet Mol Biol* (2004) 3:Article3. doi:10.2202/1544-6115.1027
42. de Graaf CA, Choi J, Baldwin TM, Bolden JE, Fairfax KA, Robinson AJ, et al. Haemopedia: an expression atlas of murine hematopoietic cells. *Stem Cell Reports* (2016) 7(3):571–82. doi:10.1016/j.stemcr.2016.07.007
43. Mi H, Poudel S, Muruganujan A, Casagrande JT, Thomas PD. PANTHER version 10: expanded protein families and functions, and analysis tools. *Nucleic Acids Res* (2016) 44(D1):D336–42. doi:10.1093/nar/gkv1194
44. Carotta S, Brady J, Wu L, Nutt SL. Transient Notch signaling induces NK cell potential in Pax5-deficient pro-B cells. *Eur J Immunol* (2006) 36(12):3294–304. doi:10.1002/eji.200636325
45. Hu Y, Smyth GK. ELDA: extreme limiting dilution analysis for comparing depleted and enriched populations in stem cell and other assays. *J Immunol Methods* (2009) 347(1–2):70–8. doi:10.1016/j.jim.2009.06.008
46. Hoppe PS, Schwarzbacher M, Loeffler D, Kokkaliaris KD, Hilsenbeck O, Moritz N, et al. Early myeloid lineage choice is not initiated by random PU.1 to GATA1 protein ratios. *Nature* (2016) 535(7611):299–302. doi:10.1038/nature18320
47. Seita J, Sahoo D, Rossi DJ, Bhattacharya D, Serwold T, Inlay MA, et al. Gene expression commons: an open platform for absolute gene expression profiling. *PLoS One* (2012) 7(7):e40321. doi:10.1371/journal.pone.0040321
48. Pang SH, Minnich M, Gangatirkar P, Zheng Z, Ebert A, Song G, et al. PU.1 cooperates with IRF4 and IRF8 to suppress pre-B-cell leukemia. *Leukemia* (2016) 30(6):1375–87. doi:10.1038/leu.2016.27
49. Kuhn R, Schwenk F, Aguet M, Rajewsky K. Inducible gene targeting in mice. *Science* (1995) 269(5229):1427–9. doi:10.1126/science.7660125
50. Welner RS, Esplin BL, Garrett KP, Pelayo R, Luche H, Fehling HJ, et al. Asynchronous RAG-1 expression during B lymphopoiesis. *J Immunol* (2009) 183(12):7768–77. doi:10.4049/jimmunol.0902333
51. Malin S, McManus S, Cobaleda C, Novatchkova M, Delogu A, Bouillet P, et al. Role of STAT5 in controlling cell survival and immunoglobulin gene recombination during pro-B cell development. *Nat Immunol* (2010) 11(2):171–9. doi:10.1038/ni.1827
52. Medina KL, Pongubala JM, Reddy KL, Lancki DW, Dekoter R, Kieslinger M, et al. Assembling a gene regulatory network for specification of the B cell fate. *Dev Cell* (2004) 7(4):607–17. doi:10.1016/j.devcel.2004.08.006
53. Zhang DE, Hetherington CJ, Chen HM, Tenen DG. The macrophage transcription factor PU.1 directs tissue-specific expression of the macrophage colony-stimulating factor receptor. *Mol Cell Biol* (1994) 14(1):373–81. doi:10.1128/MCB.14.1.373
54. Cobaleda C, Schebesta A, Delogu A, Busslinger M. Pax5: the guardian of B cell identity and function. *Nat Immunol* (2007) 8(5):463–70. doi:10.1038/ni1454
55. Laslo P, Pongubala JM, Lancki DW, Singh H. Gene regulatory networks directing myeloid and lymphoid cell fates within the immune system. *Semin Immunol* (2008) 20(4):228–35. doi:10.1016/j.smim.2008.08.003
56. Nutt SL, Kee BL. The transcriptional regulation of B cell lineage commitment. *Immunity* (2007) 26(6):715–25. doi:10.1016/j.immuni.2007.05.010
57. Carotta S, Wu L, Nutt SL. Surprising new roles for PU.1 in the adaptive immune response. *Immunol Rev* (2010) 238(1):63–75. doi:10.1111/j.1600-065X.2010.00955.x
58. Montecino-Rodriguez E, Fice M, Casero D, Berent-Maoz B, Barber CL, Dorshkind K. Distinct genetic networks orchestrate the emergence of specific waves of fetal and adult B-1 and B-2 development. *Immunity* (2016) 45(3):527–39. doi:10.1016/j.immuni.2016.07.012
59. Batista CR, Li SK, Xu LS, Solomon LA, DeKoter RP. PU.1 regulates Ig light chain transcription and rearrangement in pre-B cells during B cell development. *J Immunol* (2017) 198(4):1565–74. doi:10.4049/jimmunol.1601709
60. Sokalski KM, Li SK, Welch I, Cadieux-Pitre HA, Gruda MR, DeKoter RP. Deletion of genes encoding PU.1 and Spi-B in B cells impairs differentiation and induces pre-B cell acute lymphoblastic leukemia. *Blood* (2011) 118(10):2801–8. doi:10.1182/blood-2011-02-335539
61. Willis SN, Tellier J, Liao Y, Trezise S, Light A, O’Donnell K, et al. Environmental sensing by mature B cells is controlled by the transcription factors PU.1 and Spi-B. *Nat Commun* (2017) 8(1):1426. doi:10.1038/s41467-017-01605-1
62. Ng SY, Yoshida T, Georgopoulos K. Ikaros and chromatin regulation in early hematopoiesis. *Curr Opin Immunol* (2007) 19(2):116–22. doi:10.1016/j.co.2007.02.014
63. Olsson A, Venkatasubramanian M, Chaudhri VK, Aronow BJ, Salomonis N, Singh H, et al. Single-cell analysis of mixed-lineage states leading to a binary cell fate choice. *Nature* (2016) 537(7622):698–702. doi:10.1038/nature19348

**Conflict of Interest Statement:** The authors declare that the research was conducted in the absence of any commercial or financial relationships that could be construed as a potential conflict of interest.

Copyright © 2018 Pang, de Graaf, Hilton, Huntington, Carotta, Wu and Nutt. This is an open-access article distributed under the terms of the Creative Commons Attribution License (CC BY). The use, distribution or reproduction in other forums is permitted, provided the original author(s) and the copyright owner are credited and that the original publication in this journal is cited, in accordance with accepted academic practice. No use, distribution or reproduction is permitted which does not comply with these terms.



# The Role of the Pre-B Cell Receptor in B Cell Development, Repertoire Selection, and Tolerance

Thomas H. Winkler<sup>1\*</sup> and Inga-Lill Mårtensson<sup>2</sup>

<sup>1</sup> Chair of Genetics, Department of Biology, Nikolaus-Fiebiger-Center for Molecular Medicine, Friedrich-Alexander-University Erlangen-Nuremberg, Erlangen, Germany, <sup>2</sup> Department of Rheumatology and Inflammation Research, Institute of Medicine, The Sahlgrenska Academy, University of Gothenburg, Gothenburg, Sweden

## OPEN ACCESS

### Edited by:

Harry W. Schroeder,  
University of Alabama at Birmingham,  
United States

### Reviewed by:

Bonnie B. Blomberg,  
University of Miami, United States  
Raul M. Torres,  
University of Colorado, United States

### \*Correspondence:

Thomas H. Winkler  
thomas.winkler@fau.de

### Specialty section:

This article was submitted to  
B Cell Biology,  
a section of the journal  
*Frontiers in Immunology*

Received: 10 July 2018

Accepted: 01 October 2018

Published: 15 November 2018

### Citation:

Winkler TH and Mårtensson I-L (2018)  
The Role of the Pre-B Cell Receptor in  
B Cell Development, Repertoire  
Selection, and Tolerance.  
*Front. Immunol.* 9:2423.  
doi: 10.3389/fimmu.2018.02423

Around four decades ago, it had been observed that there were cell lines as well as cells in the fetal liver that expressed antibody  $\mu$  heavy ( $\mu$ H) chains in the apparent absence of *bona fide* light chains. It was thus possible that these cells expressed another molecule(s), that assembled with  $\mu$ H chains. The ensuing studies led to the discovery of the pre-B cell receptor (pre-BCR), which is assembled from Ig  $\mu$ H and surrogate light (SL) chains, together with the signaling molecules Ig $\alpha$  and  $\beta$ . It is expressed on a fraction of pro-B (pre-BI) cells and most large pre-B(II) cells, and has been implicated in IgH chain allelic exclusion and down-regulation of the recombination machinery, assessment of the expressed  $\mu$ H chains and shaping the IgH repertoire, transition from the pro-B to pre-B stage, pre-B cell expansion, and cessation.

**Keywords:** surrogate light chain, pre-B cells, B-cell development, allelic exclusion, VpreB,  $\lambda$ -5

## THE GENES ENCODING SL CHAIN

In the late 70's, it was shown that certain cell lines and cells in the fetal liver expressed antibody  $\mu$  heavy ( $\mu$ H) chains in the absence of *bona fide* light chains (1, 2) which was surprising considering that  $\mu$ H chains by themselves might be toxic to the cell. A few years thereafter, a gene termed  $\lambda$ .5 was cloned in mice (3), which showed homology to the constant region of Ig  $\lambda$ L chains, C $\lambda$ 1–4, hence the fifth. However, by contrast to Ig  $\lambda$ L (and  $\kappa$ L) chains,  $\lambda$ .5 did not undergo recombination. Around that time a molecule termed omega was shown to associate with  $\mu$ H chains in pre-B but not B cell lines (4), and it was suggested that this might function as a "surrogate" for *bona fide* IgL chains, and "may well prove to be the product of the  $\lambda$ .5 gene." Subsequently it was indeed found to be the case. Anyhow, examining the  $\lambda$ .5 gene in more detail it was clear that exons 2 and 3 showed homology to J and C of bona fide  $\lambda$  light chains whereas exon 1 did not show homology to Ig or any other known protein (5). It was thus unclear whether a variable-like gene or gene segment was missing. Soon thereafter, the VpreB1 and VpreB2 genes were cloned (6). The two genes are 97% identical, and did indeed show homology to Ig V gene segments in exon 1 whereas exon 2 did not show homology to Ig or any other known protein. It was later on shown that both VpreB genes are transcribed, although VpreB2 is expressed at lower levels than VpreB1 (7). The human counterpart, VPREB1 was cloned soon thereafter of which there is only one in the genome (8), and it turned out that IGLL1 ( $\lambda$ .5) had already been cloned (14.1) (9, 10). There are two additional IGLL1, 16.1, and 16.2, which are pseudogenes though seemingly used as templates in a process termed gene conversion (11). The genes encoding surrogate light (SL) chain are located on the same chromosome as Ig  $\lambda$ L chains, on chromosome 16 and 22, in mice and humans, respectively. In mice, VpreB1 and  $\lambda$ .5 are located 4–5 kb apart, whereas VpreB2 is located approximately 1 Mb downstream of  $\lambda$ .5 and around

1 Mb upstream of the  $\lambda$ L locus. The organization of these genes in humans is quite different in that VPREB1 is located within the  $\lambda$ L V gene segments whereas IGLL1 (14.1, 16.1, and 16.2) is located downstream of C $\lambda$ 7. For simplicity, the genes in both mice and humans are hereafter termed VpreB1 and  $\lambda$ 5.

## THE pre-BCR COMPLEX

That the VpreB1 and  $\lambda$ 5 genes encode the SL chain and did indeed form a complex with  $\mu$ H chains was demonstrated by several groups, and it was also shown that the signaling molecules Ig $\alpha$  and  $\beta$  were part of the complex and necessary for pre-B cell receptor (pre-BCR)-mediated signaling (Figure 1) (12, 13). As mentioned, the VpreB and  $\lambda$ 5 genes show homology to IgL chains, V $\lambda$  and J-C $\lambda$ , respectively, and each gene also encodes a unique region (UR). The VpreB-UR is encoded by the second exon and results in a tail of around 20 amino acid (aa) residues, and the  $\lambda$ 5-UR is encoded by the first exon and results in a tail of  $\sim$  50 aa. Both URs are unusual in that they contain a high proportion of charged residues, the VpreB-UR contains several negatively charged and the  $\lambda$ 5-UR several positively charged aa residues of which most are arginine. Proper folding and stabilization of SL chain require the URs as well as the extra beta-strand in  $\lambda$ 5 (14). Structure analyses of a mouse pre-BCR using NMR suggested that the two URs meet and protrude where the CDR3 of L chains would be located in a BCR (15) (Figure 1). This as well as the importance of the extra beta-strand in IGLL1 was confirmed after crystallization of a human pre-BCR (16), although most of the two URs were removed in order to crystallize the complex. Nevertheless, this study also suggested that a pre-BCR resembles a BCR with the exception of the URs that appear to protrude from the complex. The latter has implications in that it indicates that the pre-BCR might bind one or more ligand(s). Additional NMR studies have shown that the human  $\lambda$ 5-UR displays a helical structure (15) and binds to galectin-1 (17).

## A LEAKY PHENOTYPE OF SL CHAIN DEFICIENT MICE

After the discovery of the SL proteins and genes, as discussed above, the question was, what the function of such a SL chain would be during B cell development. With the advent of gene targeting in embryonic stem cells (18) and the first germline transmission of the targeted cells to generate knockout mice (19) gene targeting was the first choice to illuminate the function of the SL chain in the mouse. Already in 1992, Kitamura et al. published the analysis of the  $\lambda$ 5 knockout ( $\lambda$ 5T) mouse (20). The  $\lambda$ 5T mouse was among the first 50 knockout mice ever created, illustrating the interest in the function of the SL chain at the time. The phenotype of the mice was surprising to the authors as B cell numbers and frequencies were reduced in the mutant mice but B lymphocytes were clearly present and serum immunoglobulin levels reached almost normal levels (20). Moreover, later on the genes of the other component of the SL chain were mutated, namely VpreB1 and VpreB2, where VpreB1/VpreB2

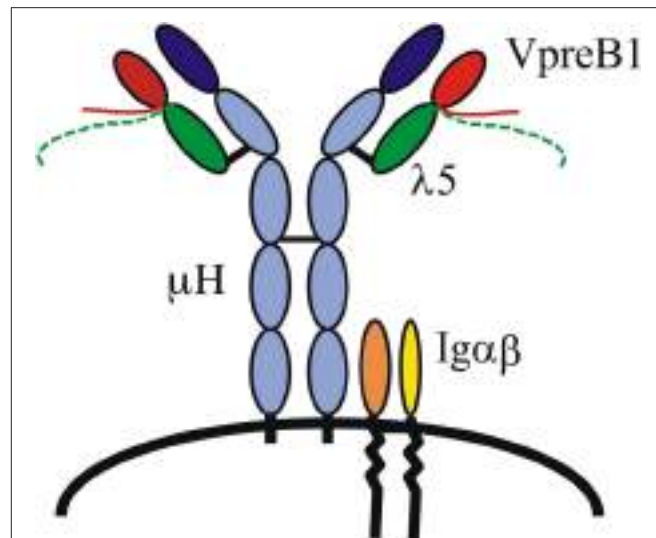


**FIGURE 1 |** The pre-B cell receptor (pre-BCR). A pre-BCR is assembled from antibody heavy ( $\mu$ H) and surrogate light chains together with the signaling molecules Ig $\alpha$  and Ig $\beta$ . The SL chain is composed of VpreB1/2 and  $\lambda$ 5. VpreB and  $\lambda$ 5 each contains a unique region, depicted as tails protruding from the respective molecule.

double-mutant mice displayed a phenotype very similar to  $\lambda$ 5T mice (21). Targeting the two separately demonstrated a slight reduction in pre-B cells in mice lacking VpreB1 but not in those lacking VpreB2, presumably due to the lower expression levels of the latter (22, 23). The complete deletion of  $\lambda$ 5, VpreB1, and VpreB2 resulted in no additional phenotype regarding B cell numbers (24).

In the year before, Kitamura et al. used a knockout mouse model in which the membrane part of  $\mu$ H chain was deleted to show that expression of a membrane bound  $\mu$ H chain is absolutely essential for the development of B lymphocytes (25). Likewise, mice with targeted mutations in the *Rag-1* or *Rag-2* genes, unable to perform VDJ recombination and therefore unable to express a  $\mu$ HC protein, had no detectable mature B cells in the lymphoid organs (26, 27). This had been published just 2 months before the publication of the  $\lambda$ 5T mouse. As the signaling capacity of the pre-BCR as well as the BCR was believed to be dependent on Ig $\alpha$  and Ig $\beta$  (28, 29), it was not surprising that *B29/Ig $\beta$*  mutant mice also lacked B cells in the peripheral lymphoid organs (30). In addition, it was later shown that Ig $\alpha$  and Ig $\beta$  are not redundant in their function, as also Ig $\alpha$  deficient mice lack detectable B cells (31). In light of the complete absence of B cells in these knockout mice with defects in the formation, the membrane deposition or signaling capacity of the preBCR, the incomplete phenotype of  $\lambda$ 5T mice was puzzling and the phenotype was called “leaky” (20), perhaps referring to the leaky phenotype of *scid* mice (32). Clearly, much had to be learned about B cell development at the time. Over the next 4–5 years, several laboratories, including that of Ton Rolink and Fritz Melchers at the Basel Institute of Immunology were involved in unraveling the cellular and molecular processes of

B cell development, and in particular the role of the SL chain. During this time, the phenotype of the pre-T $\alpha$  (part of the pre-T cell receptor) knockout mice was published with an astonishingly similar phenotype to that of the  $\lambda$ 5T mice in the development of  $\alpha/\beta$  T cells (33). T cell development is strongly impaired but mature  $\alpha/\beta$  T cells do develop.

## UNDERSTANDING THE FUNCTION OF THE PRE-B CELL RECEPTOR IN B CELL DEVELOPMENT

The earliest understanding of the coordinated development of B lymphocytes according to the rearrangement status of the immunoglobulin genes was derived from the analysis of Abelson virus-transformed pro- and pre-B cell lines. In a seminal paper published 1984 by Alt and colleagues the ordered rearrangement model of B cell development was proposed (34). The positive regulatory role of the  $\mu$ H chain on progression in differentiation was directly shown in transformed B cell lines that sequentially undergo Ig rearrangements in cell culture (35). The experiments with transformed cell lines suggested that D to J $_H$  precede V $_H$  to DJ rearrangements in the IgH locus and IgH rearrangement precedes that of IgL. In addition, the experiments by Reth et al. on transformed pre-B cell lines suggested that a successfully rearranged IgH, i.e., encoding a  $\mu$ H chain protein, directly mediates differentiation as well as recombination of the IgL loci (35). This apparently strict dependency on  $\mu$ HC expression for IgL recombination was later debated in the context of explaining the leaky phenotype of the  $\lambda$ 5T mouse. Ehlich et al. had shown that the IgH and IgL loci rearrange independently at early stages of B cell development (36). In the laboratory of Rolink and Melchers, IgkL recombination independent of  $\mu$ H chain expression was shown in IL-7-cultured pre-B cell lines and clones (37), but IgL rearrangement only occurred after differentiation into small pre-B cells.

Several different models for B cell development were proposed in 1991 and used by different laboratories over the coming years (38–40). The scheme proposed by Osmond (39) used the expression of the TdT and  $\mu$ H chain proteins in combination with B220-positivity to distinguish three  $\mu$ H chain negative pro-B cell stages, large cycling and small resting pre-B cells expressing intracellular  $\mu$ HC (ic $\mu$ HC) and resting B cells expressing surface  $\mu$ H chain (IgM) (39). Hardy et al. described several early pro-B cell subpopulations with the help of the cell surface markers B220, CD43, BP-1(CD249), and heat-stable antigen (HSA, CD24) (38), resulting in three fractions A, B, and C that were c $\mu$ HC negative. CD43-negative pre-B cells were termed fraction D and surface IgM positive cells fraction E and fraction F, the latter co-expressing IgD. The clear advantage of this characterization as opposed to the intracellular markers used by Osmond was the possibility to separate living cells by FACS was possible for further analysis, e.g., in *in vitro* culture systems and for RNA/DNA analyses. The scheme proposed by Rolink and Melchers (40), finally, focused entirely on the Ig rearrangement status of the B cell progenitors and precursors for their nomenclature. B cell progenitors without rearrangements in the Ig loci were named

pro-B cells, DJ $_H$ -rearranged cells were named pre-BI and those with a V $_H$ DJ $_H$ -rearrangement were named pre-BII cells. SL chain expression was found in pro-B, pre-BI and pre-BII cells but not in IgM surface positive B cells (40). Interestingly, none of the schemes at that time had a clear idea at which stages exactly the pre-BCR would be expressed, which was described on the cell surface of cell lines by Tsubata and Reth (13).

A break-through for further insights into the role of the SL chain in B cell development was when the Rolink and Melchers laboratory discovered two surface markers whose expression matched the  $\mu$ HC-negative and  $\mu$ HC-positive stages of pro-B and pre-B cells, respectively. The membrane tyrosine kinase c-kit (CD117) is expressed on  $\mu$ HC-negative pro-B cells in the BM (41) and CD25 on  $\mu$ H chain positive pre-B cells (42). The latter publication has 222 citations until today. With the help of monoclonal antibodies against the SL chain Karasuyama et al. showed that the SL chain is expressed on cycling cells which are  $\mu$ H chain negative and are also present in Rag-deficient mice, i.e., on pro-B cells (43). This correlated with RNA-expression data published before, showing that  $\lambda$ 5 and VpreB1 are expressed in fractions B and C according to the nomenclature of Hardy (44). Both publications agreed that SL chain expression is confined to cycling cells at early stages of B cell development in the mouse (43, 44). This was in contrast to findings by the group of Max Cooper analyzing human pre-B cell development and describing surface pre-BCR expression at late stages of pre-B cell development (45). Whereas it was still not possible to detect the pre-BCR on the surface in mice, in humans a weak surface expression was inevitably shown by Lassoued et al. (45), confirming the potential signaling function proposed by Tsubata and Reth (13). With yet another monoclonal antibody shown to specifically bind to an epitope formed by the  $\mu$ HC in complex with the SL chain it was finally possible to detect the pre-BCR on the cell surface of *ex vivo* isolated mouse bone marrow B lymphocytes (46). Two different complexes containing the SL chain were detected on pro- and pre-B cells isolated from the bone marrow. One complex present on all c-kit positive pro-B cells consisted of  $\lambda$ 5 and VpreB1 but not  $\mu$ HC. As these were pro-B cells, the complex was termed a pro-BCR, a receptor that in addition to SL chain consists of several molecules, of which only one has been characterized, BILL-Cadherin/cadherin-17 (47). Also, human pro-B cells express a pro-BCR (48). The other complex, as detected by the pre-BCR specific antibody SL156 was present on a small subpopulation of extremely large and cycling pre-B cells at the transition of pro-B and pre-B cells. These cells have downregulated c-kit almost entirely and express CD25 as a marker for pre-B cells (46). These finding not only reconciled the discrepancies between human and mouse SL chain expression but also placed the pre-BCR expression at a heavily cycling stage of B cell developmental at the transition from the pro-B to pre-B cell stage.

The heavily cycling status of pre-BCR positive cells and the detection of a significant population of c $\mu$ HC-positive CD25 $^{+}$  pre-B cells that apparently have downregulated SL chain expression [(42–44), (46)] before they become small pre-B cells led the group of Rolink and Melchers to propose the model of proliferative expansion of pre-B cells as a major function of

the SL chain (49). According to this model that is now widely accepted, the pre-BCR induces the proliferative expansion of pre-B cells that have undergone successful  $V_{H}DJ_{H}$  recombination and express a  $\mu$ HC (49) (**Figure 2**). This also explained the observation that Rag-deficient mice expressing a  $\mu$ H chain transgene fill up the pre-B cell compartment to normal numbers (42). In addition, this model explains the phenotype of the  $\lambda.5$  knockout mouse (**Figure 2**). In the absence of proliferative expansion pre-B cells could develop further albeit with very low efficiency to the small pre-B cell stage in which light chain recombination is activated. Interestingly, Decker et al. proposed already in 1991 that pre-B cells would undergo five to six divisions subsequent to  $V_{H}$  to  $DJ_{H}$  rearrangement (50). A publication by Rolink et al. showed that even in culture medium sorted pro-B become pre-B cells *in vitro* and divide spontaneously up to six times (51). This cell division was not observed, when pro-B cells from  $\lambda.5$  knockout mice were sorted and cultured. Finally, Hess et al. directly demonstrated induction of proliferation mediated by the pre-BCR using a tetracycline-system where  $\mu$ H chain expression could be switched on and off in Rag-deficient pro-B cells (52). Using five to six cell divisions as an assumption for cells at the pre-B stage,  $\lambda.5T$  mice would have a 32- to 64-fold reduced pre-B cell compartment and accordingly a similar decrease in immature B cells. This reflects almost exactly the reduction of the pre-B and immature B cell compartment originally suggested (20) and also obtained by the quantitative analysis of the  $\lambda.5$  knockout mice published by Rolink et al. (53). The SL chain is necessary to generate large enough numbers of B cells (**Figure 2**). Although the proliferative expansion of pre-B cells generates cells with identical IgH rearrangements this is not a problem for repertoire diversity, as each cell will randomly rearrange and express a different IgL chain (**Figure 2**). In addition, and discussed later, the pre-BCR considerably shapes the  $V_{H}$ -repertoire.

## THE ROLE OF THE PRE-B CELL RECEPTOR FOR ALLELIC EXCLUSION

The ordered rearrangement model of B cell development also supports a regulated mechanism of IgH allelic exclusion in which a  $V_{H}DJ_{H}$  rearrangement, if productive, prevents an additional  $V_{H}$ -to- $DJ_{H}$  rearrangement on the other allele (34). As this feedback inhibition model predicted, the targeted disruption of  $\mu$ HC membrane exon was shown to cause loss of IgH allelic exclusion (54). Surprisingly, in the  $\lambda.5T$  mouse allelic exclusion was found to be perfectly normal, when analyzing mature B cells (20). This was puzzling and suggested to the authors that *bona fide* IgL chains could substitute for SL chain. Whereas, it was consistently found that IgL recombination does not require expression of SL chain expression or  $\mu$ H chain (36, 37), it was vividly discussed at the International Titisee Conference in 1994<sup>1</sup>, whether IgL rearrangement is occurring at early stages of B cell development (36, 44, 55, 56), and hence could substitute for SL chain in the  $\lambda.5T$  mouse, including signaling of allelic exclusion.

<sup>1</sup>[https://www.bifonds.de/titisee-conferences/past-conferences/past-conference/items/titisee-conferences-pastic\\_19941005-70itc.html](https://www.bifonds.de/titisee-conferences/past-conferences/past-conference/items/titisee-conferences-pastic_19941005-70itc.html)

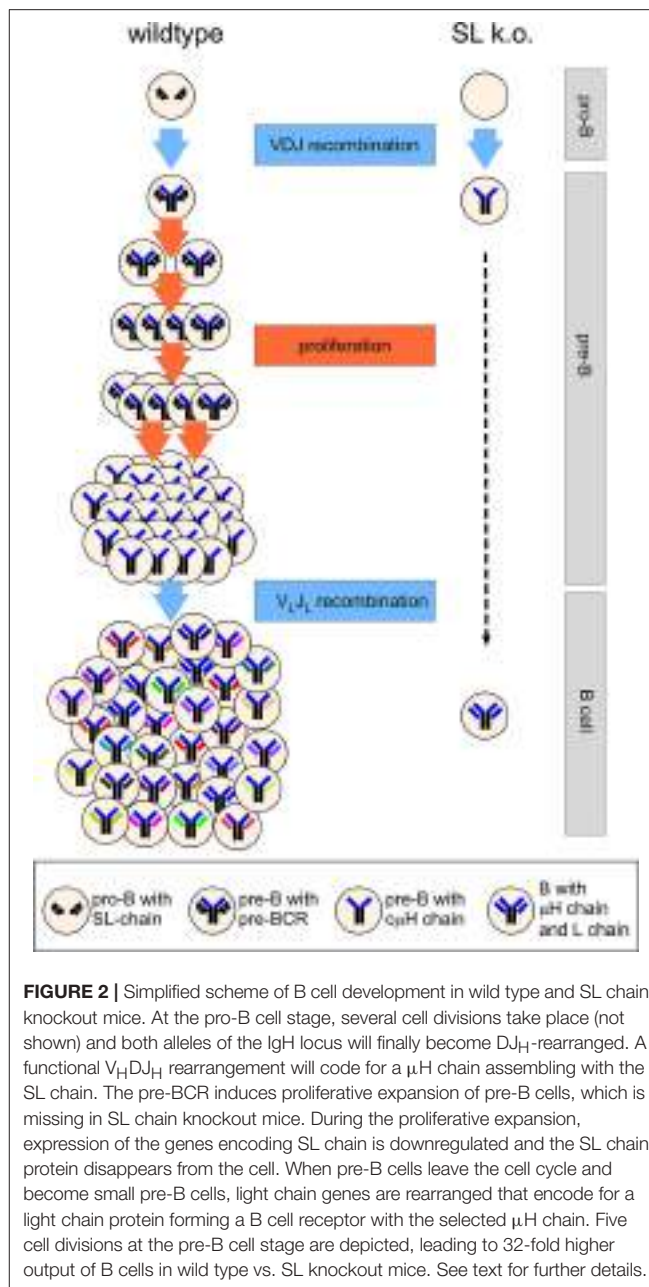


**FIGURE 2 |** Simplified scheme of B cell development in wild type and SL chain knockout mice. At the pro-B cell stage, several cell divisions take place (not shown) and both alleles of the IgH locus will finally become  $DJ_{H}$ -rearranged. A functional  $V_{H}DJ_{H}$  rearrangement will code for a  $\mu$ H chain assembling with the SL chain. The pre-BCR induces proliferative expansion of pre-B cells, which is missing in SL chain knockout mice. During the proliferative expansion, expression of the genes encoding SL chain is downregulated and the SL chain protein disappears from the cell. When pre-B cells leave the cell cycle and become small pre-B cells, light chain genes are rearranged that encode for a light chain protein forming a B cell receptor with the selected  $\mu$ H chain. Five cell divisions at the pre-B cell stage are depicted, leading to 32-fold higher output of B cells in wild type vs. SL knockout mice. See text for further details.

It was surprising when the new technology of single-cell rearrangement PCR revealed that  $\mu$ H chain double-producing B precursor cells are generated in  $\lambda.5T$  mice but apparently not in wild type mice (57). These  $\mu$ HC double-producing cells do not appear as surface  $\mu$ H chain double-positive cells, however (57). The most likely explanation for this conundrum was provided by the finding that pre-B cells showing allelic inclusion display allelic exclusion at the level of pre-BCR surface expression (58). This study found that double-producers were present also in wild type mice. In cells with both alleles functionally rearranged, i.e., allelic inclusion, only one of the  $\mu$ Hcs is able to be expressed on the cell surface. Similar findings were published for a  $\mu$ HC that was unable to pair with the SL but also with *bona fide* IgL chains (59).

It was therefore proposed that one important function of the SL chain is to test for pairing capabilities of newly formed  $\mu$ HCs for later stages of development when the *bona fide* LC is rearranged (60). In light of the apparently conflicting results regarding allelic inclusion at the level of VDJ-rearrangement, this concept offers an explanation that currently is generally agreed upon (61).

As a potential mechanism for an immediate signaling of feedback inhibition, the complete downregulation of Rag-1 and Rag-2 transcription in pre-BCR positive pre-B cells was described (62). In addition, the Rag-2 protein was found to be destabilized in the S phase of these rapidly dividing cells (62, 63). Additional mechanisms at the chromatin level have to be operating to assure allelic exclusion at later stages of development, when the Rag genes are re-expressed, at the small pre-B cell stage [reviewed in (64, 65)]. It is interesting, however, that  $\mu$ H chains can reach the cell surface and still have the capacity to signal in the absence of SL chain, including down-regulation of the V(D)J-recombinase machinery (21, 66, 67).

## HUMORAL IMMUNODEFICIENCY IN PATIENTS WITH MUTATED SL GENES

In humans, the SL chains and the pre-BCR are expressed at corresponding stages (48, 68, 69). In 1998, the detailed molecular analysis of 8 patients with sporadic agammaglobulinemia for mutations in candidate genes revealed one patient with mutations on both alleles of the gene for  $\lambda$ 5 (70). In this patient, B cell development shows a complete block of differentiation as B cells were undetectable up to an age of 5 years. Whereas, the maternal allele carried a stop codon in the first exon of  $\lambda$ 5 the paternal allele demonstrated a three-base pair substitution in exon 3. A similar, broader sequencing analysis of 33 patients with primary immunodeficiency discovered two sisters being homozygous for a deletion in the  $\lambda$ 5 gene in exon 2 (71). As no additional clinical details were provided, it remains unclear whether also in these two sisters B lymphopoiesis is completely blocked. It is still unknown, why the phenotype of mutations in the SL chain in humans have a much more complete phenotype regarding B cell development. Interestingly, mutations in Bruton's tyrosine kinase *btk* leads to an almost complete block in B cell development in humans but only a mild block in *btk*-deficient mice (72). This suggests different signaling requirements for mouse and human pre-B cell development, as illustrated by apparently different levels of redundancy of Tec kinase members in humans and mice (73).

## CELL AUTONOMOUS SIGNALING AND/OR LIGAND-MEDIATED SIGNALING BY THE PRE-BCR

Mouse pro-B cells that do not express a pre-BCR ( $\mu$ H<sup>-</sup>) require stromal cells and high levels of IL-7 in order to proliferate. This is in contrast to pre-B cells that do not require stromal cells but do require a pre-BCR and low concentrations of IL-7 (51, 66, 74–76). The latter was interpreted as ligand-independent cell autonomous signaling. Pre-BCR-mediated signaling in a

cell autonomous manner has been confirmed, and shown to rely on a particular aa residue in the  $\mu$ H chain (N46) (77), although whether this signal takes place between receptors on the one and same cell, on neighboring cells or both is unclear. Nevertheless, this does not exclude that the pre-BCR can also interact with a ligand. Indeed, at least two ligands have been described. Early work demonstrated the importance of Galectin-1, produced by stromal cells, as a pre-BCR ligand in humans, which requires the  $\lambda$ 5-UR (78). In mice, stromal cell associated heparan sulfate was shown to be important, which would engage with the  $\lambda$ 5-UR in the context of a pre-BCR (79). A potential explanation for different ligands could be that there are differences between mouse and human (79), that the stromal cells that produce IL7 are not the same as those that produce galectin-1, and are located in different BM niches (80). As the pre-BCR mediates several signals this may also account for different requirements. Nevertheless, whether the pre-BCR mediates signals in a ligand-dependent or -independent manner, cell surface levels depend on the respective UR. The  $\lambda$ 5-UR is required for rapid internalization and signaling; in its absence mutant receptors with reduced signalling capacity accumulate on the surface (81). By contrast, the absence of the VpreB1-UR increases internalisation and hence was concluded to balance the rate of internalization (47). Moreover, pre-BCR surface levels are important as they seemingly regulate both proliferation and survival (82).

## THE pre-BCR SHAPES THE IgH REPERTOIRE

In mice, there are 195 V<sub>H</sub> gene segments of which 110 are functional and can be divided into 16 families (83). Among the V<sub>H</sub> genes the V<sub>H</sub>1 (J558), V<sub>H</sub>2 (Q52), and V<sub>H</sub>5 (7183) are the most studied, for several reasons. For instance, usage of the DJ<sub>H</sub>-proximal V<sub>H</sub> genes, V<sub>H</sub>2 and V<sub>H</sub>5, and especially V<sub>H</sub>5-2 (81X), is especially high in the fetal and neonatal repertoire (84, 85). Differentiating B cells of adult bone marrow mimic fetal development and in adult BM V<sub>H</sub> usage changes at the pro-B to pre-B cell transition (86, 87) whereas it is not markedly changed at later stages. At the pre-B cell stage V<sub>H</sub>1 usage increases whilst that of V<sub>H</sub>5 decreases. The discovery of the pre-BCR and that it is expressed at a time during BM B cell development when the V<sub>H</sub> repertoire changes indicated its potential involvement. This was investigated early on in  $\lambda$ 5T mice. The results confirmed previous studies in wild type mice, which is quite remarkable considering that the studies were performed by single cell PCR analyzing 25–30 cells per population (88). The low numbers were due to low detection levels of both alleles in each cell, and the number of cellular fractions analyzed, hence a remarkable accomplishment almost 25 years ago. At that time, pre-B cells expressing intracellular  $\mu$ H chains and splenic follicular B cells from  $\lambda$ 5T mice were analyzed, which showed a more frequent usage of the V<sub>H</sub>5 and V<sub>H</sub>2 (Q52) genes and less frequent usage of V<sub>H</sub>1 genes among pre-B cells. Therefore, the preBCR contributes to repertoire selection at the preB cell stage. However, V<sub>H</sub> usage in the spleen of  $\lambda$ 5T mice was similar to the corresponding cells

from wild type control mice. The interpretation was that when there was no SL chain, the change in the repertoire observed in splenic B cells must be mediated by *bona fide* light chains, although at a later stage in development.

In light of the close interactions of the VpreB chain with the IgH chain complementarity region 3 (H-CDR3) in the crystal structure of the preBCR (16) an influence of the preBCR on the shaping of the antibody repertoire was postulated. Detailed analysis indeed revealed that a particular amino acid composition in the H-CDR3, in particular tyrosine at position 101 is positively selected by interactions with VpreB (89). Interestingly, in the mouse the combination of evolutionary selection of a preferred reading frame usage in the D-elements as well as somatic selection by the invariant SL chain together favour the presence of tyrosine at key positions in the antigen-binding site of antibodies (89). As this tyrosine residue is frequently found in contact with the antigen in antibody/antigen complexes, preBCR selection directly influences the antigen binding characteristics of the mature antibody repertoire (90).

## A ROLE FOR THE PRE-BCR IN B CELL TOLERANCE?

Immature B cells expressing poly- and/or autoreactive BCRs undergo negative selection in order to prevent their development into naïve B cells. It has been suggested, however, that at the pre-B stage poly-reactivity is a requirement for positive selection and expansion in mice (91). The poly-/autoreactivity relates to the  $\lambda$ 5-UR with its high number of positively charged aa residues. These are mainly arginine, an aa typically found in anti-DNA and polyreactive antibodies, e.g., in the (H-CDR3) (92). As mentioned above, pre-BCR signalling is reduced in the absence of the  $\lambda$ 5-UR. However, the  $\lambda$ 5-UR can be replaced by a polyreactive H-CDR3 (from human antibodies) resulting in a signalling competent receptor (91). This lead to the conclusion that the pre-BCR is “self-reactive,” and that the “autoreactivity” is driven by the  $\lambda$ 5-UR and is required for positive selection of pre-B cells.

The pre-BCR appears to also counter-selects particular  $\mu$ H chains, in fact those that express a H-CDR3 with basic aa residues, e.g., arginine (93, 94). In wild type control mice, this selection takes place in pro-B cells, i.e., at the transition into the pre-B cell stage and was based on the analyses of the  $V_H$ 5 family (94), a selection that is not as evident when analyzing all  $V_H$  genes by NGS (95). Nevertheless, the absence of the entire SL chain ( $SLC^{-/-}$ ) in mice results in pre-B cells expressing  $\mu$ H chains with a much higher proportion of basic aa residues in the H-CDR3 (95). Whether this is a result of positive selection and proliferative expansion, in line with the above-mentioned requirement for poly-/autoreactivity is currently unclear (91), as at least some of the expansion is likely due to signaling through the IL-7R (66, 76). Anyhow, negative selection at the immature B cell stage in  $SLC^{-/-}$  mice is more prominent than in controls, inferred from a higher proportion of cells prone to apoptosis (96), and interpreted as a result of the expansion of “autoreactive” pre-B cells (95). Central B-cell tolerance is despite of this incomplete.

In addition, also peripheral B-cell tolerance is incomplete, and results in a higher proportion of splenic FO B cells expressing  $\mu$ H chains with basic aa residues in their H-CDR3 (95). A subset of the FO B cells are activated and initiates autoimmune reactions. Whether this is due to SL chain being required for termination of signaling earlier in development is currently unclear (97). Nevertheless, the autoimmune reactions include spontaneous formation of T-cell dependent germinal centers, memory B cells and plasma cells that secrete autoantibodies, typical of those found in lupus (SLE), e.g., anti-DNA and anti-nuclear antibodies (ANAs) (94, 95). Whether this is unique to mice lacking the entire SL chain is unclear, although splenic B cells in  $\lambda$ 5T mice are also enriched for those expressing IgH chains with an arginine-rich H-CDR3 (98), and more recent work has shown that also  $\lambda$ 5T mice secrete autoantibodies (90). In  $SLC^{-/-}$  mice a subset of B cells resembles memory B cells expressing low levels of CD21 ( $CD21^{-/low}$ ) (99). Memory B cells with a  $CD21^{-/low}$  phenotype expand under conditions of chronic immune stimulation in humans, e.g., in patients with autoimmune disease, SLE and RA, or pathogenic infections, malaria, and HIV (100).  $CD21^{-/low}$  B cells have also been described in wild type control mice, termed age associated B cells (ABCs) as they accumulate with age (101). However, at least at a young age most of the ABCs in wild type control mice are not memory B cells whereas those in  $SLC^{-/-}$  mice are (99). Moreover, the ABCs in  $SLC^{-/-}$  mice are not polyreactive but rather autoreactive producing typical lupus autoantibodies, e.g., anti-Smith antigens. The ABCs are mainly IgM that show signs of somatic hypermutation, and strong selection of the H-CDR3, whereas the GC B cells are mainly IgG2c<sup>+</sup> and likely the source of the plasma cells that produce the serum anti-DNA and ANAs (94, 95). Perhaps surprisingly, the small number of ANA-reactive ABC hybridomas analyzed so far did not show any signs of somatic hypermutations in the  $V_H$ . However, whether they express IgL chains with mutations is currently unclear. In this context it was recently shown only that some of the ANA-reactive hybridomas from aged mice also express germ line encoded IgH chains, and that the autoreactivity was due to mutations in the IgL chain (102). In fact, substitution of one aa residue in the Igk CDR1 was sufficient to convert the antibody to being ANA-reactive. The similarities between the hybridomas from aged mice and the ABCs in  $SLC^{-/-}$  mice could be taken as an indication that aged mice are reminiscent of young  $SLC^{-/-}$  mice. However, whether this is the case requires additional studies.

## CONCLUSION

We conclude that pre-BCR mediated signaling has been implicated in:

- Proliferation
- Survival
- Downregulation of the RAG recombinases
- IgH allelic exclusion
- Silencing of the genes encoding SL chain
- Selection of the IgH repertoire

- Positive selection of pre-B cells
- Negative selection

It should be noted though that we still do not fully understand all these events, and especially not which signals are mediated at what stage. For instance, it has been proposed that the pre-BCR mediates early and late signals (103). The early signals might be those taking place in the pre-BCR<sup>+</sup> pro-B (pre-B1) cells (c-kit<sup>+</sup>CD25<sup>-</sup>) and the late signals in the pre-BCR<sup>+</sup> pre-B (large pre-BII) cells (c-kit<sup>-</sup>CD25<sup>+</sup>). In addition, the role of the SL chain in human pre-B cell development is only partially understood. New technologies as CRISPR/Cas9 gene editing and humanized mice would now allow the analysis of this question.

## REFERENCES

- Burrows P, LeJeune M, Kearney JF. Evidence that murine pre-B cells synthesize  $\mu$  heavy chains but no light chains. *Nature* (1979) 280:838–40. doi: 10.1038/280838a0
- Siden EJ, Baltimore D, Clark D, Rosenberg NE. Immunoglobulin synthesis by lymphoid cells transformed *in vitro* by Abelson murine leukemia virus. *Cell* (1979) 16:389–96. doi: 10.1016/0092-8674(79)90014-X
- Sakaguchi N, Melchers F. Lambda 5, a new light-chain-related locus selectively expressed in pre-B lymphocytes. *Nature* (1986) 324:579–82. doi: 10.1038/324579a0
- Pillai S, Baltimore D. Formation of disulphide-linked mu 2 omega 2 tetramers in pre-B cells by the 18K omega-immunoglobulin light chain. *Nature* (1987) 329:172–4. doi: 10.1038/329172a0
- Kudo A, Sakaguchi N, Melchers F. Organization of the murine Ig-related lambda 5 gene transcribed selectively in pre-B lymphocytes. *Embo J.* (1987) 6:103–7. doi: 10.1002/j.1460-2075.1987.tb04725.x
- Kudo A, Melchers F. A second gene, VpreB in the lambda 5 locus of the mouse, which appears to be selectively expressed in pre-B lymphocytes. *Embo J.* (1987) 6:2267–72. doi: 10.1002/j.1460-2075.1987.tb02500.x
- Dul JL, Argon Y, Winkler T, ten Boekel E, Melchers F, Mårtensson IL. The murine VpreB1 and VpreB2 genes both encode a protein of the surrogate light chain and are co-expressed during B cell development. *Eur J Immunol.* (1996) 26:906–13. doi: 10.1002/eji.1830260428
- Bauer SR, Kudo A, Melchers F. Structure and pre-B lymphocyte restricted expression of the VpreB in humans and conservation of its structure in other mammalian species. *EMBO J.* (1988) 7:111–6. doi: 10.1002/j.1460-2075.1988.tb02789.x
- Chang H, Dmitrovsky E, Hieter PA, Mitchell K, Leder P, Turoczi L, et al. Identification of three new Ig lambda-like genes in man. *J Exp Med.* (1986) 163:425–35. doi: 10.1084/jem.163.2.425
- Hollis GF, Evans RJ, Stafford-Hollis JM, Korsmeyer SJ, McKearn JP. Immunoglobulin lambda light-chain-related genes 14.1 and 16.1 are expressed in pre-B cells and may encode the human immunoglobulin omega light-chain protein. *Proc Natl Acad Sci USA.* (1989) 86:5552–6. doi: 10.1073/pnas.86.14.5552
- Conley ME, Rapalus L, Boylin EC, Rohrer J, Minegishi Y. Gene conversion events contribute to the polymorphic variation of the surrogate light chain gene lambda 5/14.1. *Clin Immunol.* (1999) 93:162–7. doi: 10.1006/clim.1999.4785
- Karasuyama H, Kudo A, Melchers F. The proteins encoded by the VpreB and lambda 5 pre-B cell-specific genes can associate with each other and with mu heavy chain. *J Exp Med.* (1990) 172:969–72. doi: 10.1084/jem.172.3.969
- Tsubata T, Reth M. The products of pre-B cell-specific genes (lambda 5 and VpreB) and the immunoglobulin mu chain form a complex that is transported onto the cell surface. *J Exp Med.* (1990) 172:973–6. doi: 10.1084/jem.172.3.973
- Minegishi Y, Hendershot LM, Conley ME. Novel mechanisms control the folding and assembly of lambda 5/14.1 and VpreB to produce an intact surrogate light chain. *Proc Natl Acad Sci USA.* (1999) 96:3041–6. doi: 10.1073/pnas.96.6.3041
- Lanig H, Bradl H, Jack HM. Three-dimensional modeling of a pre-B-cell receptor. *Mol Immunol.* (2004) 40:1263–72. doi: 10.1016/j.molimm.2003.11.030
- Bankovich AJ, Raunser S, Juo ZS, Walz T, Davis MM, Garcia KC. Structural insight into pre-B cell receptor function. *Science* (2007) 316:291–4. doi: 10.1126/science.1139412
- Elantak L, Espeli M, Boned A, Bornet O, Bonzi J, Gauthier L, et al. Structural basis for galectin-1-dependent pre-B cell receptor (pre-BCR) activation. *J Biol Chem.* (2012) 287:44703–13. doi: 10.1074/jbc.M112.395152
- Thomas KR, Capecchi MR. Site-directed mutagenesis by gene targeting in mouse embryo-derived stem cells. *Cell* (1987) 51:503–12. doi: 10.1016/0092-8674(87)90646-5
- Thompson S, Clarke AR, Pow AM, Hooper ML, Melton DW. Germ line transmission and expression of a corrected HPRT gene produced by gene targeting in embryonic stem cells. *Cell* (1989) 56:313–21. doi: 10.1016/0092-8674(89)90905-7
- Kitamura D, Kudo A, Schaal S, Müller W, Melchers F, Rajewsky K. A critical role of lambda 5 protein in B cell development. *Cell* (1992) 69:823–31. doi: 10.1016/0092-8674(92)90293-L
- Mundt C, Licence S, Shimizu T, Melchers F, Mårtensson IL. Loss of precursor B cell expansion but not allelic exclusion in VpreB1/VpreB2 double-deficient mice. *J Exp Med.* (2001) 193:435–45. doi: 10.1084/jem.193.4.435
- Mårtensson A, Argon Y, Melchers F, Dul JL, Mårtensson IL. Partial block in B lymphocyte development at the transition into the pre-B cell receptor stage in Vpre-B1-deficient mice. *Int Immunol.* (1999) 11:453–60. doi: 10.1093/intimm/11.3.453
- Mundt C, Licence S, Maxwell G, Melchers F, Mårtensson IL. Only VpreB1, but not VpreB2, is expressed at levels which allow normal development of B cells. *Int Immunol.* (2006) 18:163–72. doi: 10.1093/intimm/dxh359
- Shimizu T, Mundt C, Licence S, Melchers F, Mårtensson IL. VpreB1/VpreB2/lambda 5 triple-deficient mice show impaired B cell development but functional allelic exclusion of the IgH locus. *J Immunol.* (2002) 168:6286–93. doi: 10.4049/jimmunol.168.12.6286
- Kitamura D, Roes J, Kühn R, Rajewsky K. A B cell-deficient mouse by targeted disruption of the membrane exon of the immunoglobulin mu chain gene. *Nature* (1991) 350:423–6. doi: 10.1038/350423a0
- Mombaerts P, Iacomini J, Johnson RS, Herrup K, Tonegawa S, Papaioannou VE. RAG-1-deficient mice have no mature B and T lymphocytes. *Cell* (1992) 68:869–77. doi: 10.1016/0092-8674(92)90030-G
- Shinkai Y, Rathbun G, Lam KP, Olitz EM, Stewart V, Mendelsohn M, et al. RAG-2-deficient mice lack mature lymphocytes owing to inability to initiate V(D)J rearrangement. *Cell* (1992) 68:855–67. doi: 10.1016/0092-8674(92)90029-C

## AUTHOR CONTRIBUTIONS

All authors listed have made a substantial, direct and intellectual contribution to the work, and approved it for publication.

## FUNDING

This work was funded by the Deutsche Forschungsgemeinschaft (DFG) through the grant TRR130 (project P11) to TW and through grants from Reumatikerförbundet, King Gustav V fund, the Swedish Cancer Foundation and the Swedish Childhood Cancer Foundation to I-LM.

28. Reth M, Hombach J, Wienands J, Campbell KS, Chien N, Justement LB, et al. The B-cell antigen receptor complex. *Immunol Today* (1991) 12:196–201. doi: 10.1016/0167-5699(91)90053-V
29. Venkitaraman AR, Williams GT, Dariavach P, Neuberger MS. The B-cell antigen receptor of the five immunoglobulin classes. *Nature* (1991) 352:777–81. doi: 10.1038/35277a0
30. Gong S, Nussenzweig MC. Regulation of an early developmental checkpoint in the B cell pathway by Ig beta. *Science* (1996) 272:411–4. doi: 10.1126/science.272.5260.411
31. Pelanda R, Braun U, Hobeika E, Nussenzweig MC, Reth M. B cell progenitors are arrested in maturation but have intact VDJ recombination in the absence of Ig-a and Ig-b. *J Immunol.* (2002) 169:865–72. doi: 10.4049/jimmunol.169.2.865
32. Bosma GC, Fried M, Custer RP, Carroll A, Gibson DM, Bosma MJ. Evidence of functional lymphocytes in some (leaky) scid mice. *J Exp Med.* (1988) 167:1016–33. doi: 10.1084/jem.167.3.1016
33. Fehling HJ, Krotkova A, Saint-Ruf C, von Boehmer H. Crucial role of the pre-T-cell receptor alpha gene in development of alpha beta but not gamma delta T cells. *Nature* (1995) 375:795–8. doi: 10.1038/375795a0
34. Alt FW, Yancopoulos GD, Blackwell TK, Wood C, Thomas E, Boss M, et al. Ordered rearrangement of immunoglobulin heavy chain variable region segments. *EMBO J.* (1984) 3:1209–19. doi: 10.1002/j.1460-2075.1984.tb01955.x
35. Reth MG, Ammirati P, Jackson S, Alt FW. Regulated progression of a cultured pre-B-cell line to the B-cell stage. *Nature* (1985) 317:353–5. doi: 10.1038/317353a0
36. Ehlich A, Schaal S, Gu H, Kitamura D, Müller W, Rajewsky K. Immunoglobulin heavy and light chain genes rearrange independently at early stages of B cell development. *Cell* (1993) 72:695–704. doi: 10.1016/0092-8674(93)90398-A
37. Grawunder U, Haasner D, Melchers F, Rolink A. Rearrangement and expression of kappa light chain genes can occur without mu heavy chain expression during differentiation of pre-B cells. *Int Immunol.* (1993) 5:1609–18. doi: 10.1093/intimm/5.12.1609
38. Hardy RR, Carmack CE, Shinton SA, Kemp JD, Hayakawa K. Resolution and characterization of pro-B and pre-pro-B cell stages in normal mouse bone marrow. *J Exp Med.* (1991) 173:1213–25. doi: 10.1084/jem.173.5.1213
39. Osmond DG. Proliferation kinetics and the lifespan of B cells in central and peripheral lymphoid organs. *Curr Opin Immunol.* (1991) 3:179–85. doi: 10.1016/0952-7915(91)90047-5
40. Rolink A, Melchers F. Molecular and cellular origins of B lymphocyte diversity. *Cell* (1991) 66:1081–94. doi: 10.1016/0092-8674(91)90032-T
41. Rolink A, Streb M, Nishikawa S, Melchers F. The c-kit-encoded tyrosine kinase regulates the proliferation of early pre-B cells. *Eur J Immunol.* (1991b) 21:2609–12. doi: 10.1002/eji.1830211044
42. Rolink A, Grawunder U, Winkler TH, Karasuyama H, Melchers F. IL-2 receptor alpha chain (CD25, TAC) expression defines a crucial stage in pre-B cell development. *Int Immunol.* (1994) 6:1257–64. doi: 10.1093/intimm/6.8.1257
43. Karasuyama H, Rolink A, Shinkai Y, Young F, Alt FW, Melchers F. The expression of Vpre-B/lambda 5 surrogate light chain in early bone marrow precursor B cells of normal and B cell-deficient mutant mice. *Cell* (1994) 77:133–43. doi: 10.1016/0092-8674(94)90241-0
44. Li YS, Hayakawa K, Hardy RR. The regulated expression of B lineage associated genes during B cell differentiation in bone marrow and fetal liver. *J Exp Med.* (1993) 178:951–60. doi: 10.1084/jem.178.3.951
45. Lassoued K, Nuñez CA, Billips L, Kubagawa H, Monteiro RC, LeBlanc TW, et al. Expression of surrogate light chain receptors is restricted to a late stage in pre-B cell differentiation. *Cell* (1993) 73:73–86. doi: 10.1016/0092-8674(93)90161-1
46. Winkler TH, Rolink AG, Melchers F, Karasuyama H. Precursor B cells of mouse bone marrow express two different complexes with the surrogate light chain on the surface. *J Immunol.* (1995) 25:446–50.
47. Knoll M, Yanagisawa Y, Simmons S, Engels N, Wienands J, Melchers F, et al. The non-Ig parts of the VpreB and lambda5 proteins of the surrogate light chain play opposite roles in the surface representation of the precursor B cell receptor. *J Immunol.* (2012) 188:6010–7. doi: 10.4049/jimmunol.1200071
48. Meffre E, Fougeriou M, Argenson JN, Aubaniac JM, Schiff C. Cell surface expression of surrogate light chain (YL) in the absence of m on human pro-B cell lines and normal pro-B cells. *Eur J Immunol.* (1996) 26:2172–80. doi: 10.1002/eji.1830260932
49. Melchers F, Rolink A, Grawunder U, Winkler TH, Karasuyama H, Ghia P, et al. Positive and negative selection events during B lymphopoiesis. *Curr Opin Immunol.* (1995) 7:214–27. doi: 10.1016/0952-7915(95)80006-9
50. Decker DJ, Boyle NE, Koziol JA, Klinman NR. The expression of the Ig H chain repertoire in developing bone marrow B lineage cells. *J Immunol.* (1991) 146:350–61.
51. Rolink AG, Winkler T, Melchers F, Andersson J. Precursor B cell receptor-dependent B cell proliferation and differentiation does not require the bone marrow or fetal liver environment. *J Exp Med.* (2000) 191:23–32. doi: 10.1084/jem.191.1.23
52. Hess J, Werner A, Wirth T, Melchers F, Jäck HM, Winkler TH. Induction of pre-B cell proliferation after *de novo* synthesis of the pre-B cell receptor. *Proc Natl Acad Sci USA.* (2001) 98:1745–50. doi: 10.1073/pnas.98.4.1745
53. Rolink A, Karasuyama H, Grawunder U, Haasner D, Kudo A, Melchers F. B cell development in mice with a defective lambda 5 gene. *Eur J Immunol.* (1993) 23:1284–8. doi: 10.1002/eji.1830230614
54. Kitamura D, Rajewsky K. Targeted disruption of mu chain membrane exon causes loss of heavy-chain allelic exclusion. *Nature* (1992) 356:154–6. doi: 10.1038/356154a0
55. ten Boekel E, Melchers F, Rolink A. The status of Ig loci rearrangements in single cells from different stages of B cell development. *Int Immunol.* (1995) 7:1013–9. doi: 10.1093/intimm/7.6.1013
56. Pelanda R, Schaal S, Torres RM, Rajewsky K. A prematurely expressed Ig(kappa) transgene, but not V(kappa)J(kappa) gene segment targeted into the Ig(kappa) locus, can rescue B cell development in lambda5-deficient mice. *Immunity* (1996) 5:229–39. doi: 10.1016/S1074-7613(00)80318-0
57. Löfert D, Ehlich A, Müller W, Rajewsky K. Surrogate light chain expression is required to establish immunoglobulin heavy chain allelic exclusion during early B cell development. *Immunity* (1996) 4:133–44. doi: 10.1016/S1074-7613(00)80678-0
58. ten Boekel E, Melchers F, Rolink AG. Precursor B cells showing H chain allelic inclusion display allelic exclusion at the level of pre-B cell receptor surface expression. *Immunity* (1998) 8:199–207. doi: 10.1016/S1074-7613(00)80472-0
59. Kline GH, Hartwell L, Beck-Engeser GB, Keyna U, Zaharevitz S, Klinman NR, et al. Pre-B cell receptor-mediated selection of pre-B cells synthesizing functional mu heavy chains. *J Immunol.* (1998) 161:1608–18.
60. Vettermann C, Herrmann K, Jäck HM. Powered by pairing: the surrogate light chain amplifies immunoglobulin heavy chain signaling and pre-selects the antibody repertoire. *Semin Immunol.* (2006) 18:44–55. doi: 10.1016/j.smim.2006.01.001
61. Melchers F. The pre-B-cell receptor: selector of fitting immunoglobulin heavy chains for the B-cell repertoire. *Nat Rev Immunol.* (2005) 5:578–84. doi: 10.1038/nri1649
62. Grawunder U, Leu TM, Schatz DG, Werner A, Rolink AG, Melchers F, et al. Down-regulation of RAG1 and RAG2 gene expression in preB cells after functional immunoglobulin heavy chain rearrangement. *Immunity* (1995) 3:601–8. doi: 10.1016/1074-7613(95)90131-0
63. Lin WC, Desiderio S. Cell cycle regulation of V(D)J recombination-activating protein RAG-2. *Proc Natl Acad Sci USA.* (1994) 91:2733–7. doi: 10.1073/pnas.91.7.2733
64. Vettermann C, Schlissel MS. Allelic exclusion of immunoglobulin genes: models and mechanisms. *Immunol Rev.* (2010) 237:22–42. doi: 10.1111/j.1600-065X.2010.00935.x
65. Levin-Klein R, Bergman Y. Epigenetic regulation of monoallelic rearrangement (allelic exclusion) of antigen receptor genes. *Front Immunol.* (2014) 5:625. doi: 10.3389/fimmu.2014.00625
66. Schuh W, Meister S, Roth E, Jäck HM. Cutting edge: signaling and cell surface expression of a mu H chain in the absence of lambda 5: a paradigm

- revisited. *J Immunol.* (2003) 171:3343–7. doi: 10.4049/jimmunol.171.7.3343
67. Galler GR, Mundt C, Parker M, Pelanda R, Mårtensson IL, Winkler TH. Surface mu heavy chain signals down-regulation of the V(D)J-recombinase machinery in the absence of surrogate light chain components. *J Exp Med.* (2004) 199:1523–32. doi: 10.1084/jem.20031523
  68. Ghia P A, ten Boekel E, Sanz E, de la Hera A, Rolink A, Melchers F. Ordering of human bone marrow B lymphocyte precursors by single-cell polymerase chain reaction analyses of the rearrangement status of the immunoglobulin H and L chain gene loci. *J Exp Med.* (1996) 184:2217–29. doi: 10.1084/jem.184.6.2217
  69. Wang YH, Nomura J, Faye-Petersen OM, Cooper MD. Surrogate light chain production during B cell differentiation: differential intracellular versus cell surface expression. *J Immunol.* (1998) 161:1132–9.
  70. Minegishi Y, Coustan-Smith E, Wang YH, Cooper MD, Campana D, Conley ME. Mutations in the human lambda5/14.1 gene result in B cell deficiency and agammaglobulinemia. *J Exp Med.* (1998) 187:71–7. doi: 10.1084/jem.187.1.71
  71. Moens LN, Falk-Sorqvist E, Asplund AC, Bernatowska E, Smith CI, Nilsson M. Diagnostics of primary immunodeficiency diseases: a sequencing capture approach. *PLoS ONE* (2014) 9:e114901. doi: 10.1371/journal.pone.0114901
  72. Hendriks RW, de Brujin MF, Maas A, Dingjan GM, Karis A, Grosveld F. Inactivation of Btk by insertion of lacZ reveals defects in B cell development only past the pre-B cell stage. *EMBO J.* (1996) 15:4862–72. doi: 10.1002/j.1460-2075.1996.tb0867.x
  73. Ellmeier W, Jung S, Sunshine MJ, Hatam F, Xu Y, Baltimore D, et al. Severe B cell deficiency in mice lacking the tec kinase family members Tec and Btk. *J Exp Med.* (2000) 192:1611–24. doi: 10.1084/jem.192.11.1611
  74. Rolink A, Kudo A, Karasuyama H, Kikuchi Y, Melchers F. Long-term proliferating early pre B cell lines and clones with the potential to develop to surface Ig-positive, mitogen reactive B cells *in vitro* and *in vivo*. *Embo J.* (1991a) 10:327–36. doi: 10.1002/j.1460-2075.1991.tb07953.x
  75. Ray RJ, Stoddart A, Pennycook JL, Huner HO, Furlonger C, Wu GE, et al. Stromal cell-independent maturation of IL-7-responsive pro-B cells. *J Immunol.* (1998) 160:5886–97.
  76. Erlandsson L, Licence S, Gaspari F, Lane P, Corcoran AE, Martensson IL. Both the pre-BCR and the IL-7Ralpha are essential for expansion at the pre-BII cell stage *in vivo*. *Eur J Immunol.* (2005) 35:1969–76. doi: 10.1002/eji.200425821
  77. Ubelhart R, Bach MP, Eschbach C, Wossning T, Reth M, Jumaa H. N-linked glycosylation selectively regulates autonomous precursor BCR function. *Nat Immunol.* (2010) 11:759–65. doi: 10.1038/ni.1903
  78. Gauthier L, Rossi B, Roux F, Termine E, Schiff C. Galectin-1 is a stromal cell ligand of the pre-B cell receptor (BCR) implicated in synapse formation between pre-B and stromal cells and in pre-BCR triggering. *Proc Natl Acad Sci USA.* (2002) 99:13014–9. doi: 10.1073/pnas.20023999
  79. Bradl H, Wittmann J, Milius D, Vettermann C, Jack HM. Interaction of murine precursor B cell receptor with stroma cells is controlled by the unique tail of lambda 5 and stroma cell-associated heparan sulfate. *J Immunol.* (2003) 171:2338–48. doi: 10.4049/jimmunol.171.5.2338
  80. Mourcin F, Breton C, Tellier J, Narang P, Chasson L, Jorquera A, et al. Galectin-1-expressing stromal cells constitute a specific niche for pre-BII cell development in mouse bone marrow. *Blood* (2011) 117:6552–61. doi: 10.1182/blood-2010-12-323113
  81. Ohnishi K, Melchers F. The nonimmunoglobulin portion of lambda5 mediates cell-autonomous pre-B cell receptor signaling. *Nat Immunol.* (2003) 4:849–56. doi: 10.1038/ni959
  82. Kawano Y, Yoshikawa S, Minegishi Y, Karasuyama H. Pre-B cell receptor assesses the quality of IgH chains and tunes the pre-B cell repertoire by delivering differential signals. *J Immunol.* (2006) 177:2242–9. doi: 10.4049/jimmunol.177.4.2242
  83. Johnston CM, Wood AL, Bolland DJ, Corcoran AE. Complete sequence assembly and characterization of the C57BL/6 mouse Ig heavy chain V region. *J Immunol.* (2006) 176:4221–34. doi: 10.4049/jimmunol.176.7.4221
  84. Wu GE, Paige CJ. VH gene family utilization in colonies derived from B and pre-B cells detected by the RNA colony blot assay. *Embo J.* (1986) 5:3475–81. doi: 10.1002/j.1460-2075.1986.tb04672.x
  85. Yancopoulos GD, Malynn BA, Alt FW. Developmentally regulated and strain-specific expression of murine VH gene families. *J Exp Med.* (1988) 168:417–35. doi: 10.1084/jem.168.1.417
  86. Freitas AA, Andrade L, Lembezat MP, Coutinho A. Selection of VH gene repertoires: differentiating B cells of adult bone marrow mimic fetal development. *Int Immunol.* (1990) 2:15–23. doi: 10.1093/intimm/2.1.15
  87. Huetz F, Carlsson L, Tornberg UC, Holmberg D. V-region directed selection in differentiating B lymphocytes. *EMBO J.* (1993) 12:1819–26. doi: 10.1002/j.1460-2075.1993.tb05830.x
  88. ten Boekel E, Melchers F, Rolink AG. Changes in the V(H) gene repertoire of developing precursor B lymphocytes in mouse bone marrow mediated by the pre-B cell receptor. *Immunity* (1997) 7:357–68. doi: 10.1016/S1074-7613(00)80357-X
  89. Khass M, Blackburn T, Burrows PD, Walter MR, Capriotti E, Schroeder HW Jr. VpreB serves as an invariant surrogate antigen for selecting immunoglobulin antigen-binding sites. *Sci Immunol.* (2016) 1:aaf6628. doi: 10.1126/sciimmunol.aaf6628
  90. Khass M, Blackburn T, Elgavish A, Burrows PD, Schroeder HW Jr. In the absence of central pre-B cell receptor selection, peripheral selection attempts to optimize the antibody repertoire by enriching for CDR-H3 Y101. *Front Immunol.* (2018) 9:120. doi: 10.3389/fimmu.2018.00120
  91. Kohler F, Hug E, Eschbach C, Meixlperger S, Hobeika E, Kofer J, et al. Autoreactive B cell receptors mimic autonomous pre-B cell receptor signaling and induce proliferation of early B cells. *Immunity* (2008) 29:912–21. doi: 10.1016/j.immuni.2008.10.013
  92. Radic MZ, Weigert M. Genetic and structural evidence for antigen selection of anti-DNA antibodies. *Annu Rev Immunol.* (1994) 12:487–520. doi: 10.1146/annurev.ij.12.040194.002415
  93. Minegishi Y, Conley ME. Negative selection at the pre-BCR checkpoint elicited by human mu heavy chains with unusual CDR3 regions. *Immunity* (2001) 14:631–41. doi: 10.1016/S1074-7613(01)00131-5
  94. Keenan RA, De Riva A, Corleis B, Hepburn L, Licence S, Winkler TH, et al. Censoring of autoreactive B cell development by the pre-B cell receptor. *Science* (2008) 321:696–9. doi: 10.1126/science.1157533
  95. Grimsholm O, Ren W, Bernardi AI, Chen H, Park G, Camponeschi A, et al. Absence of surrogate light chain results in spontaneous autoreactive germinal centres expanding VH81X-expressing B cells. *Nat Commun.* (2015) 6:7077. doi: 10.1038/ncomms8077
  96. Ren W, Grimsholm O, Bernardi AI, Hook N, Stern A, Cavallini N, et al. Surrogate light chain is required for central and peripheral B-cell tolerance and inhibits anti-DNA antibody production by marginal zone B cells. *Eur J Immunol.* (2015) 45:1228–37. doi: 10.1002/eji.201444917
  97. van Loo PF, Dingjan GM, Maas A, Hendriks RW. Surrogate-light-chain silencing is not critical for the limitation of pre-B cell expansion but is for the termination of constitutive signaling. *Immunity* (2007) 27:468–80. doi: 10.1016/j.immuni.2007.07.018
  98. Sun L, Kono N, Shimizu T, Toh H, Xue H, Numata O, et al. Distorted antibody repertoire developed in the absence of pre-B cell receptor formation. *Biochem Biophys Res Commun.* (2018) 495:1411–7. doi: 10.1016/j.bbrc.2017.11.171
  99. Aranburu A, Hook N, Gerasimcik N, Corleis B, Ren W, Camponeschi A, et al. Age-associated B cells expanded in autoimmune mice are

- memory cells sharing H-CDR3-selected repertoires. *Eur J Immunol.* (2017). doi: 10.1002/eji.201747127. [Epub ahead of print].
100. Thorarinsdottir K, Camponeschi A, Gjertsson I, Martensson IL. CD21<sup>-/low</sup> B cells: a snapshot of a unique B cell subset in health and disease. *Scand J Immunol.* (2015) 82:254–61. doi: 10.1111/sji.12339
101. Rubtsova K, Rubtsov AV, Cancro MP, Marrack P. Age-associated B cells: a T-bet-dependent effector with roles in protective and pathogenic immunity. *J Immunol.* (2015) 195:1933–7. doi: 10.4049/jimmunol.1501209
102. Faderl M, Klein F, Wirz OF, Heiler S, Alberti-Servera L, Engdahl C, et al. Two distinct pathways in mice generate antinuclear antigen-reactive B cell repertoires. *Front Immunol.* (2018) 9:16. doi: 10.3389/fimmu.2018.00016
103. Reth M, Nielsen P. Signaling circuits in early B-cell development. *Adv Immunol.* (2014) 122:129–75. doi: 10.1016/B978-0-12-800267-4.00004-3

**Conflict of Interest Statement:** The authors declare that the research was conducted in the absence of any commercial or financial relationships that could be construed as a potential conflict of interest.

Copyright © 2018 Winkler and Mårtensson. This is an open-access article distributed under the terms of the Creative Commons Attribution License (CC BY). The use, distribution or reproduction in other forums is permitted, provided the original author(s) and the copyright owner(s) are credited and that the original publication in this journal is cited, in accordance with accepted academic practice. No use, distribution or reproduction is permitted which does not comply with these terms.



OPEN ACCESS

**Edited by:**

Hermann Eibel,  
Universitätsklinikum Freiburg,  
Germany

**Reviewed by:**

Thomas H. Winkler,  
Friedrich-Alexander-Universität  
Erlangen-Nürnberg, Germany

Kay L. Medina,  
Mayo Clinic, United States  
Rachel Maurie Gerstein,  
University of Massachusetts  
Medical School, United States

**\*Correspondence:**

Elias Hobeika  
elias.hobeika@uni-ulm.de;  
Michael Reth  
michael.reth@bioss.uni-freiburg.de

**†Present address:**

Elias Hobeika,  
Department of Tumor Immunology,  
Institute of Immunology, Ulm  
University Hospital, Ulm, Germany  
Ella Levit-Zerdoun,  
German Cancer Consortium (DKTK)  
Partner Site Freiburg, German  
Cancer Center (DKFZ), Heidelberg,  
Germany; Institute of Molecular  
Medicine and Cell Research,  
Freiburg, Germany  
Roberta Pelanda,  
Department of Immunology and  
Microbiology, University of Colorado  
School of Medicine, Aurora,  
CO, United States;  
Department of Biomedical  
Research, National Jewish  
Health, Denver, CO,  
United States

**Specialty section:**

This article was submitted  
to *B Cell Biology*,  
a section of the journal  
*Frontiers in Immunology*

**Received:** 28 March 2018

**Accepted:** 23 July 2018

**Published:** 06 August 2018

**Citation:**

Hobeika E, Dautzenberg M,  
Levit-Zerdoun E, Pelanda R and  
Reth M (2018) Conditional Selection  
of B Cells in Mice With an  
Inducible B Cell Development.  
*Front. Immunol.* 9:1806.  
doi: 10.3389/fimmu.2018.01806

# Conditional Selection of B Cells in Mice With an Inducible B Cell Development

Elias Hobeika<sup>1,2\*</sup>, Marcel Dautzenberg<sup>1,2</sup>, Ella Levit-Zerdoun<sup>2,3,4†</sup>, Roberta Pelanda<sup>5†</sup>  
and Michael Reth<sup>1,2\*</sup>

<sup>1</sup> Centre for Biological Signaling Studies (BIOSS), Biology III, Faculty of Biology, Albert-Ludwigs-University of Freiburg, Freiburg, Germany, <sup>2</sup> Max Planck Institute of Immunobiology and Epigenetics, Freiburg, Germany, <sup>3</sup> Department of Molecular Immunology, Biology III, Faculty of Biology, Albert-Ludwigs-University of Freiburg, Freiburg, Germany, <sup>4</sup> International Max Planck Research School for Molecular and Cellular Biology, Freiburg, Germany, <sup>5</sup> Department of Immunology and Microbiology, University of Colorado School of Medicine, Aurora, CO, United States

Developing B cells undergo defined maturation steps in the bone marrow and in the spleen. The timing and the factors that control these differentiation steps are not fully understood. By targeting the B cell-restricted *mb-1* locus to generate an *mb-1* allele that expresses a tamoxifen inducible Cre and another allele in which *mb-1* expression can be controlled by Cre, we have established a mouse model with an inducible B cell compartment. With these mice, we studied in detail the kinetics of B cell development and the consequence of BCR activation at a defined B cell maturation stage. Contrary to expectations, transitional 1-B cells exposed to anti-IgM reagents *in vivo* did not die but instead developed into transitional 2 (T2)-B cells with upregulated Bcl-2 expression. We show, however, that these T2-B cells had an increased dependency on the B cell survival factor B cell activating factor when compared to non-stimulated B cells. Overall, our findings indicate that the inducible *mb-1* mouse strain represents a useful model, which allows studying the signals that control the selection of B cells in greater detail.

**Keywords:** Cre/loxP, MerCreMer, *imb-1* mouse, transitional B cells, Ig- $\alpha$ , tamoxifen, B cell activating factor, B cell development

## INTRODUCTION

B cell lymphopoiesis is a highly regulated process that begins with B cell progenitors (pro-B cells) and progresses through distinct stages (1–3). Pro-B cells, like B cells at later stages, are distinguished by the expression of Ig $\alpha$  and Ig $\beta$ , the respective products of the B cell-specific genes *mb-1* and *B29* (2). These two proteins are crucial for B cell development. Indeed, the loss of Ig $\alpha$  or Ig $\beta$  expression in knockout mice (4–6), or in rare cases of human Ig $\alpha$  or Ig $\beta$  deficiency (7–9), results in a complete block of B cell development at the pro-B cell stage. This is because the developmental progression of pro-B cells requires the expression of the precursor B cell antigen receptor (pre-BCR) (10, 11) which comprises the  $\mu$  heavy (H) chain, a surrogate light chain (composed of VpreB and lambda 5 chains), and the Ig $\alpha$ /Ig $\beta$  (CD79a/CD79b) heterodimer (12). Upon the expression of a functional pre-BCR, the pre-B cells first proliferate, then rearrange their Ig light chain loci and differentiate into immature B cells carrying a B cell antigen receptor (BCR) of the IgM class on their surface (13, 14). The immature B cells leave the bone marrow (BM) to continue their differentiation in the spleen (15–19).

The IgM-expressing immature B cells in the spleen are divided into two major subgroups, namely the transitional 1 (T1) and transitional 2 (T2) B cells (20, 21). T1-B cells are negative for the surface markers

CD23 and CD21 whereas T2-B cells express both markers (21, 22). A third transitional population, T3-B cells have been described. They arise from T2-B cells and have a similar phenotype, with the exception of IgM expression, which is strongly down modulated (20). However, T3-B cells are believed to represent an unresponsive (anergic) state rather than an intermediate maturation stage (23, 24). All transitional B cells also express the CD93 (AA4.1) marker originally detected by a monoclonal antibody (clone 493) generated by the Rolink group (22). The T2-B cells then develop into CD93 (AA4.1)-mature follicular (M) and marginal zone (MZ) B cells defined as IgM<sup>low</sup>IgD<sup>high</sup>CD23<sup>high</sup>CD21<sup>+</sup> and IgM<sup>high</sup>IgD<sup>low</sup>CD23<sup>low</sup>CD21<sup>high</sup> cells, respectively (13, 20, 21, 25). Both cell fates are controlled by BCR-mediated signaling pathways (21, 26, 27).

The further development of T2-B cells requires the B cell activating factor (BAFF) (28–33), which is also known as Blys, and signaling through the classical and alternative NF-κB pathways (34–36). BAFF is a member of the TNF family and is implicated in peripheral B cell development. Mice lacking the BAFF-receptor (BAFF-R or BR3) have a block at the T1 stage (37, 38). On the other hand, mice overexpressing BAFF have a lenient peripheral B cell selection and develop autoimmune diseases (39, 40).

Cre is a site-directed DNA recombinase that specifically cuts DNA at *loxP* sites and can be employed for the activation or deletion of genes in the mouse (41–44). Previously, we and others have shown that chimeric Cre proteins with an appended mutated binding domain of the murine α-estrogen receptor (Mer) can be regulated by tamoxifen (45–48). In particular, MerCreMer, a fusion protein carrying a Mer domain at both the N- and C-terminus of Cre, demonstrates a very tight regulation of recombinase activity (49). This construct has been prominently used to study heart muscle development and hematopoietic stem cell fates (50–52). In the past, we have used a related inducible Cre system to study mature B cells lacking the expression of the spleen tyrosine kinase Syk or that of Igα and the BCR (53, 54). Here, we employ the MerCreMer/*loxP* system to generate mice in which the expression of the *mb-1* gene, and thus of Igα, is induced by tamoxifen treatment. With this system, we can generate a short wave of developing B cells in the adult mouse and monitor the kinetics of their development. At day 5 post induction (p.i.) most B cells in these mice are transitional T1-B cells, which are thought to be highly sensitive to negative selection upon BCR engagement (55, 56). Surprisingly, the *in vivo* stimulation of the T1-B cells with anti-IgM antibodies does not lead to their deletion but rather their survival and accelerated differentiation to the T2-B cell stage by upregulation of Bcl-2. The survival of stimulated T2-B cells requires, however, the presence of BAFF or the BAFF-R.

## RESULTS

### Generation of Mice With an Inducible B Cell Development

To study the kinetics of B cell development *in vivo*, we generated mice that are born without mature B cells but that can be induced to transiently produce B cells at any time in their life. In these mice the expression of the *mb-1* gene, which is essential for B cell development, can be regulated by our MerCreMer/*loxP* technique. The

*mb-1* gene has five exons (Figure 1A). Using BALB/c embryonic stem (ES) cells, this gene was altered by homologous recombination with two different targeting vectors to create two distinct mutant alleles. The first vector was used to replace *mb-1* exons 1, 2, and 3 with a cDNA sequence encoding MerCreMer (Figure 1B). The MerCreMer cDNA cassette is therefore transcribed under the control of the endogenous *mb-1* promoter, further enhanced through the insertion of the μ intronic enhancer inserted 5' of the *mb-1* promoter. In the second targeting experiment, which we have previously described (47), we inserted a “flip/flop” *mb-1*/EGFP cassette flanked by two *loxP* sites (“floxed”) pointing in opposite directions (Figure 1C). This cassette, which replaced *mb-1* exons 2 and 3, contained a cDNA coding for a membrane-bound form of the enhanced green fluorescent protein (mEGFP) and, in the opposite transcriptional orientation, a cDNA of the *mb-1* coding sequence from exon 2 through exon 5 (Figure 1C). The mEGFP/*mb-1*<sup>inv</sup> allele produces mEGFP in place of Igα, which, in the absence of another *mb-1* functional allele, leads to the arrest of B cell development at the pro-B cell stage. Cre-mediated recombination can invert the floxed DNA sequence, thus placing the *mb-1* exons 2–5 cDNA in the right orientation to allow the proper splicing from exon 1 (Figure 1D). This newly generated *mb-1*/mEGFP<sup>inv</sup> allele expresses Ig-α (but not EGFP) allowing for B cell generation. Thus, the *mb-1* “flip/flop” allele can mediate the alternative expression of either Ig-α or mEGFP. Germ line transmission of the two targeted *mb-1* alleles (*mb-1*MerCreMer and mEGFP/*mb-1*<sup>inv</sup>) were confirmed by Southern blot analysis of tail genomic DNA (Figure 1E). We then generated BALB/c mice that carry both differently targeted *mb-1* alleles and thus are defective in Ig-α expression. Here, we refer to these mice with a tamoxifen inducible (i) switch from EGFP to Ig-α expression as imb-1 mice. In the BM, these mice have B220<sup>+</sup> pro-B cells but no IgM<sup>+</sup> B cells (Figure 2A, d0). B cells are also absent from the blood (Figure 2B, d0). The fact that the imb-1 mice display a complete block of B cell development at the pro-B cell stage is also demonstrated by the absence of immunoglobulin isotypes in their sera (data not shown). These data show overall that MerCreMer activity is tightly regulated in the mouse.

### Kinetics of B Cell Development in the BM and Spleen of imb-1 Mice

To efficiently activate MerCreMer in pro-B cells, we treated the imb-1 mice orally with a single dose of 6 mg of tamoxifen citrate dissolved in lipids. Already 4 h after this treatment, the mice contained enough tamoxifen in the blood to activate MerCreMer in a cultured B cell line carrying an EGFP reporter cassette, and sufficient levels of tamoxifen were maintained until day 4 after administration (Figure S1 in Supplementary Material). In the BM and the blood of tamoxifen-treated imb-1 mice, IgM<sup>+</sup> B cells were first detected between days 5 and 6 p.i. and reached their highest levels at day 10 p.i. (Figures 2A–D). The late onset of IgM<sup>+</sup> B cell appearance in the treated imb-1 mice may be due to the fact that the mEGFP/*mb-1*<sup>inv</sup> allele only becomes stabilized once the tamoxifen concentration and MerCreMer activity has declined (days 5–6; Figure S1A in Supplementary Material), in addition to the need for productive rearrangements at both the Ig heavy

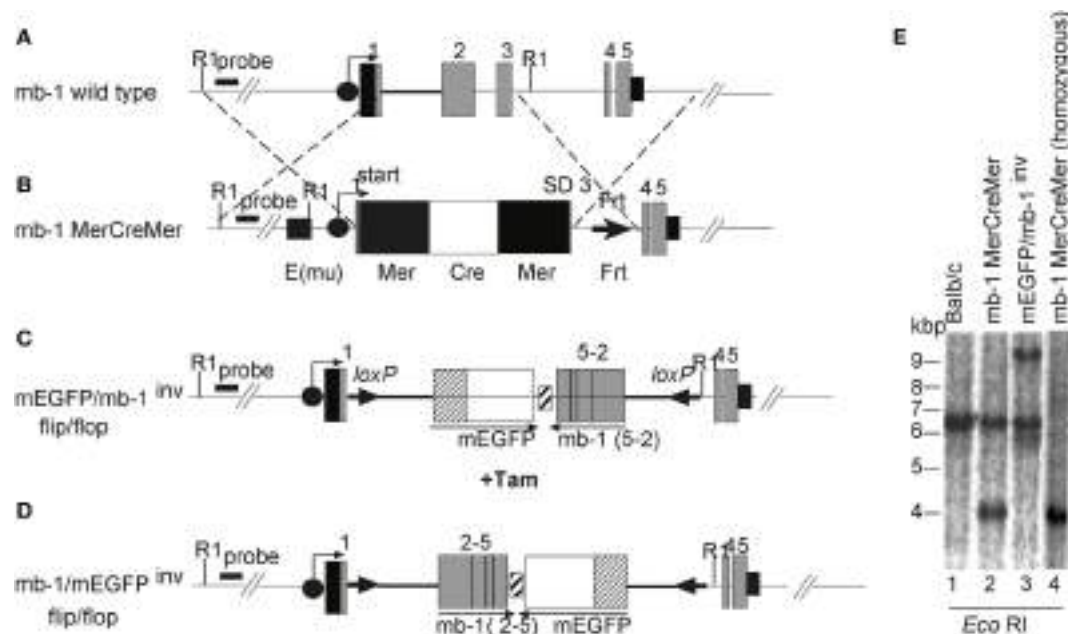


**FIGURE 1 |** Generation of mice carrying a modification at the *mb-1* locus. Schematic representations of (A) the *mb-1* wild-type allele and the knockin alleles, (B) *mb-1* MerCreMer, (C) membrane-bound form of the enhanced green fluorescent protein (*mEGFP*)/*mb-1*<sup>inv</sup>, and (D) *mb-1*/*mEGFP*<sup>inv</sup> (not drawn to scale). The *mb-1*MerCreMer strain was crossed to either *mEGFP*/*mb-1*<sup>inv</sup> or *mb-1*/*mEGFP*<sup>inv</sup> to generate the *imb-1* and the *cmb-1* strains, respectively. The black circles with an arrow represent the *mb-1* promoter. The gray boxes indicate the *mb-1* exons, and the small black box after exon 5 represents the 3' untranslated region and the *mb-1* polyA sequence. In (B), the black square 5' of the *mb-1* promoter represents the immunoglobulin heavy chain intron enhancer (Emu), the black and white boxes represent (Mer) and the humanized Cre (hCre), respectively. The black triangle indicates the Frt site left after deletion of the Neo' cassette by the transient transfection with the enhanced fip recombinase (fipe). Constructs (C,D) were previously described in Ref. (47). (E) Southern blot analysis of *mEGFP*/*mb-1*<sup>inv</sup> and *mb-1* MerCreMer heterozygous mice relative to wild-type control. Genomic DNA was prepared from tails of the designated mice, digested with EcoRI and hybridized with a radioactive labeled 5' external probe to identify the homologously recombined alleles. The analysis by Southern blot gives 4.1 and 9.6 kb fragments for the DNA targeted with MerCreMer and the “flip/flop” cassette (*mEGFP*/*mb-1*<sup>inv</sup> or *mb-1*/*mEGFP*<sup>inv</sup>), respectively (Figure 1E, lanes 2 and 3 and data not shown). Wild-type DNA generates a 6.4 kb fragment with the same enzyme (Figure 1E, lane 1). Lane 4 represents an *mb-1* MerCreMer homozygous mouse.

and light chain loci. After day 15, only very few IgM<sup>+</sup> B cells were observed in the BM and blood of treated mice (Figures 2A–D, d15). Apparently at this time point, all newly generated B cells have left the BM and, in the absence of (tamoxifen and) MerCreMer activity, new B cells cannot be generated. Thus, only a short wave of B cell development is induced in tamoxifen-treated *imb-1* mice. As a positive control for these experiments, we analyzed the BM and blood of untreated mice carrying in the germ line the *mb-1*/*mEGFP*<sup>inv</sup> and *mb-1*MerCreMer alleles (*cmb-1* mice) and that have, therefore, a continuous *mb-1* expression and unperturbed B cell development (Figures 2A–D).

To assess factors influencing the efficiency of B cell production, the *imb-1* and the *cmb-1* control mice were bred with B1-8H mice (57), which carry the productively rearranged V<sub>H</sub>D<sub>H</sub>J<sub>H</sub> exon coding for the B1-8 VH domain as a knockin at the *Igh* locus. All pro-B cells of *imb-1*/B1-8H and *cmb-1*/B1-8H mice express a  $\mu$ -chain in the cytoplasm (data not shown). In spite of the early H chain expression in all pro-B cells, no B cell development took place beyond this stage in untreated *imb-1*/B1-8H mice, again demonstrating the tight regulation of the MerCreMer enzyme *in vivo* (Figures 2E,F, d0). Upon treatment with tamoxifen, the *imb-1*/B1-8H mice produced threefold to fivefold more B cells in the BM and the blood than

*imb-1* mice, although with similar kinetics of B cell development (Figures 2C–H). These data suggest that the major factor responsible for delayed B cell development in *imb-1* mice is the rate of tamoxifen catabolism and the consequent stabilization of the inducible *mb-1* allele.

In the spleens of tamoxifen-treated *imb-1* mice, the first immigrant B cells were detected at days 5–6 p.i. (Figures 3A,B,E). These B cells expressed IgM and were mostly negative for CD21 and CD23, thus displaying the phenotype of T1-B cells (Figures 3A,B,E, d5–d6). Some B cells were detected within the CD23<sup>+</sup> gate at days 5–6, which had not yet acquired CD21 expression (Figure 3A). By day 10, roughly 56% of the B cells within the CD23<sup>+</sup> gate were IgM<sup>dim/+</sup>, but still negative for CD21 whereas the other 44% were IgM<sup>dim/+</sup> CD21<sup>+</sup>, thus displaying the phenotype of T2-B cells (Figures 3A,B, d10). Therefore, during their maturation in the spleen, B cells seem to first acquire CD23 and only later the CD21 surface marker. Small amounts of mature follicular B cells (CD23<sup>+</sup>CD21<sup>+</sup> and IgM<sup>low</sup>) appeared at day 10 and were the majority of splenic B cells by day 20 p.i. (Figure 3A, d10 and d20). Mature B cells persisted in the spleen of induced *imb-1* mice for 40 days (Figure 3, d40), although their numbers declined with time (data not shown).

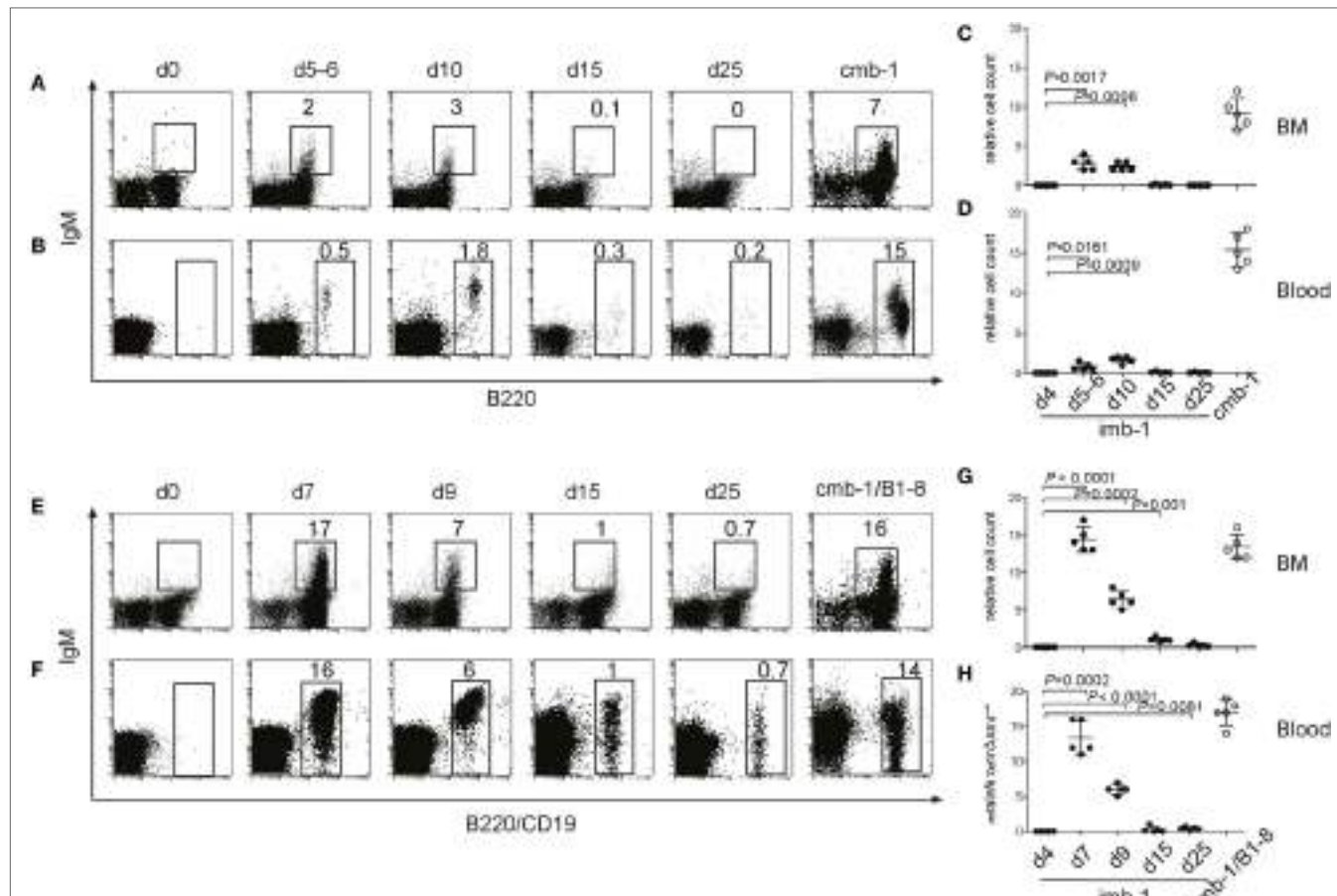


**FIGURE 2 |** B-cell migration from the bone marrow (BM) into the secondary lymphoid organs of imb-1 mice takes place in a wave. **(A,B)** B220 versus IgM staining of total lymphocytes derived from BM **(A)** or blood **(B)** of imb-1 mice analyzed at different time points after a single treatment with tamoxifen [days 5–6, 10, 15, and 25 post induction (p.i.)]. Uninduced mice (d0) as well as cmb-1 mice served as controls. Representative data from three independent experiments with two mice at each time point are shown. **(C,D)** Statistical analysis of the relative cell count (percentage) of B220<sup>+</sup>IgM<sup>+</sup> B cells (BM) or total B220<sup>+</sup> B cells (blood) in the total lymphocyte gate of tamoxifen-treated imb-1 mice at days 4, 5–6, 10, 15, and 25. Mean  $\pm$  SD of  $n = 5$  is indicated for each time point; each dot represents an individual mouse.  $P$  values are indicated and were obtained using the one-sample  $t$ -test. **(E,F)** IgM versus B220 (upper panel; BM), or IgM versus CD19 (lower panel; blood) staining of total lymphocytes derived from the BM **(E)** and blood **(F)**, respectively, of imb-1/B1-8H (designated imb-1/B1-8) mice at indicated time points p.i.. Uninduced mice (d0) as well as cmb-1/B1-8H mice served as controls. The percentages for B220<sup>+</sup>IgM<sup>+</sup> (BM) and total CD19<sup>+</sup> (blood) cells inside each box are indicated. Representative data from two independent experiments with two to three mice at each time point are shown. **(G,H)** Statistical analysis of the percentage of B220<sup>+</sup>IgM<sup>+</sup> B cells (BM) or CD19<sup>+</sup> B cells (blood) within the lymphocyte gate in tamoxifen-treated imb-1/B1-8H mice at days 4, 7, 9, 15, and 25. Mean  $\pm$  SD of  $n = 5$  is indicated for each time point; each dot represents an individual mouse.  $P$  values are indicated and were obtained using the one-sample  $t$ -test.

Marginal zone B cells ( $\text{IgM}^{\text{high}}\text{CD21}^+$  but  $\text{CD23}^-$ ) were first detected at day 20 p.i. and became more prominent by day 40 p.i. (Figures 3B,E; d20 and d40). This late development of MZ B cells is in accordance with their time of appearance in neonates and immune deficient mice after adoptive transfer (21, 58). The kinetics of B cell development in the spleen of imb-1/B1-8H mice was similar to that seen in imb-1 mice, although higher numbers of B cells were generated (Figures 3C,D,F,G). The improved cellular yields in imb-1/B1-8H mice show even more clearly that B cells acquire the CD23 marker prior to CD21 expression (Figure 3C, d7–d25; Figure S1B in Supplementary Material; d7).

## No Deletion of T1-B Cells Upon *In Vivo* Treatment With Anti-IgM

Immature T1-B cells in the spleen are characterized as CD93 (AA4.1<sup>+</sup>),  $\text{CD23}^-$ ,  $\text{CD21}^-$ ,  $\text{IgM}^{\text{high}}$ , and  $\text{IgD}^{\text{low}}$  (20, 21). Based on *in vitro* studies, the T1-B cells have been considered to be sensitive to negative selection and to undergo apoptosis upon engagement of their BCR (59). The imb-1/B1-8H mice provide an ideal system to test this hypothesis *in vivo*. Whereas in the spleens of wild-type mice T1-B cells are a minority, these cells are the majority of B cells in the spleen of imb-1/B1-8H mice at days 5–6 after their treatment with tamoxifen (Figure S2 in Supplementary Material). Furthermore, at days 5–6 p.i., imb-1/B1-8H

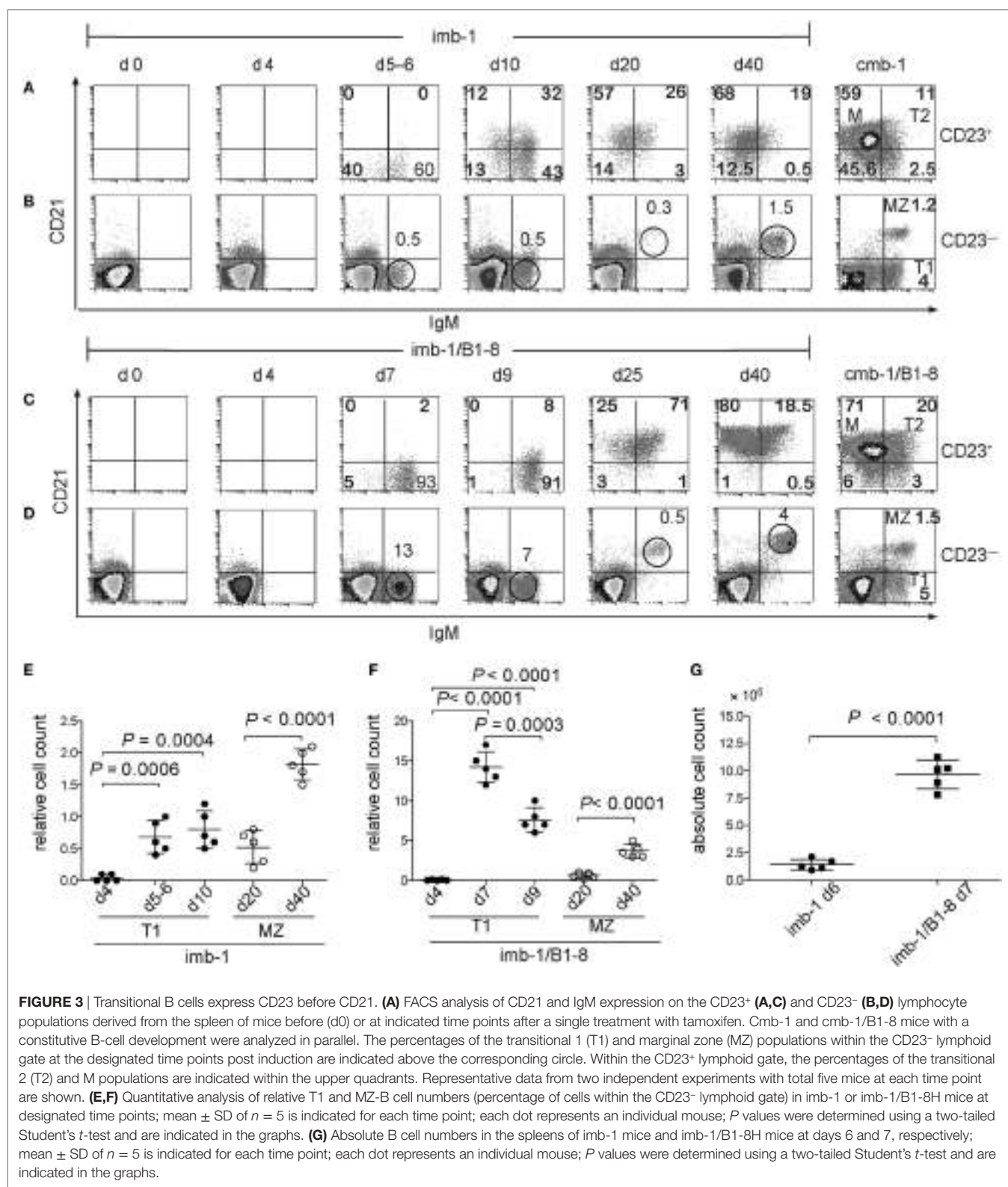


**FIGURE 3 |** Transitional B cells express CD23 before CD21. **(A)** FACS analysis of CD21 and IgM expression on the CD23<sup>+</sup> **(A,C)** and CD23<sup>-</sup> **(B,D)** lymphocyte populations derived from the spleen of mice before (d0) or at indicated time points after a single treatment with tamoxifen. Cmb-1 and cmb-1/B1-8 mice with a constitutive B-cell development were analyzed in parallel. The percentages of the transitional 1 (T1) and marginal zone (MZ) populations within the CD23<sup>-</sup> lymphoid gate at the designated time points post induction are indicated above the corresponding circle. Within the CD23<sup>+</sup> lymphoid gate, the percentages of the transitional 2 (T2) and M populations are indicated within the upper quadrants. Representative data from two independent experiments with total five mice at each time point are shown. **(E,F)** Quantitative analysis of relative T1 and MZ-B cell numbers (percentage of cells within the CD23<sup>-</sup> lymphoid gate) in imb-1 or imb-1/B1-8H mice at designated time points; mean  $\pm$  SD of  $n = 5$  is indicated for each time point; each dot represents an individual mouse;  $P$  values were determined using a two-tailed Student's *t*-test and are indicated in the graphs. **(G)** Absolute B cell numbers in the spleens of imb-1 mice and imb-1/B1-8H mice at days 6 and 7, respectively; mean  $\pm$  SD of  $n = 5$  is indicated for each time point; each dot represents an individual mouse;  $P$  values were determined using a two-tailed Student's *t*-test and are indicated in the graphs.

mice have not produced any soluble antibodies (data not shown) and, thus, injected anti-IgM reagents can bind to the BCR on the surface of T1-B cells without being quenched by soluble IgM in the serum.

To test for the behavior of T1-B cells upon engagement of their BCR *in vivo*, we treated imb-1/B1-8H mice at late day 5 p.i. (when the newly generated B cells first appeared in the blood of most mice) with 100  $\mu$ g of anti-IgM F(ab')<sub>2</sub> and analyzed their

spleens at day 7 p.i. by flow cytometry (**Figure 4A**). Compared to B cells in untreated mice, the T1-B cells in anti-IgM treated imb-1/B1-8H mice appeared activated and/or differentiated as indicated by higher MHC class II and IgD-BCR expression, but

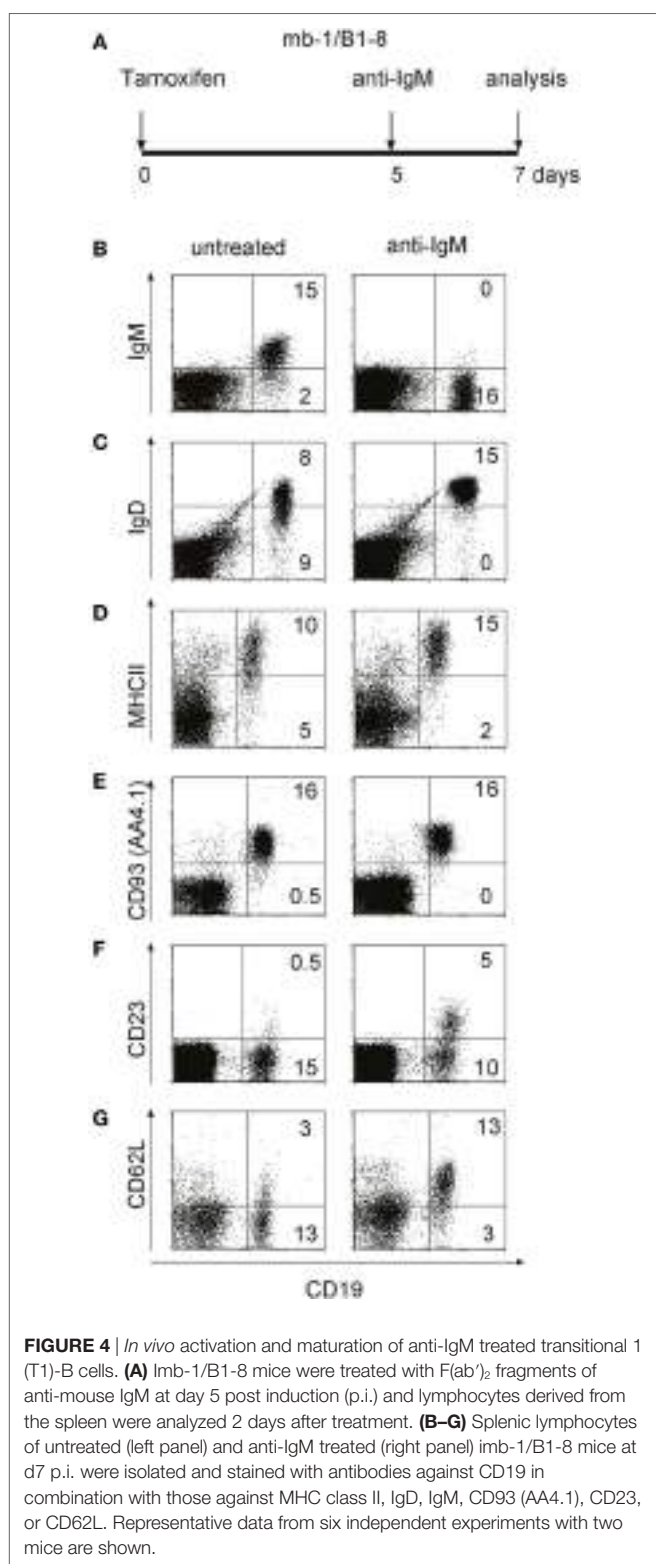


**FIGURE 4 |** *In vivo* activation and maturation of anti-IgM treated transitional 1 (T1)-B cells. **(A)** Imb-1/B1-8 mice were treated with F(ab')<sub>2</sub> fragments of anti-mouse IgM at day 5 post induction (p.i.) and lymphocytes derived from the spleen were analyzed 2 days after treatment. **(B–G)** Splenic lymphocytes of untreated (left panel) and anti-IgM treated (right panel) imb-1/B1-8 mice at d7 p.i. were isolated and stained with antibodies against CD19 in combination with those against MHC class II, IgD, IgM, CD93 (AA4.1), CD23, or CD62L. Representative data from six independent experiments with two mice are shown.

reduced IgM-BCR levels on their cell surface (**Figures 4A–D**). Since the anti-IgM treatment leads to IgM-BCR internalization (data not shown) and the increase of IgD may not be a good indicator of further maturation, we assessed B cells of imb-1/B1-8H mice for additional surface markers that identify the stage of B cell maturation. While the T1-B cells of tamoxifen-treated mice still expressed CD93 (AA4.1; **Figure 4E**), which identifies a transitional stage, they also displayed the CD23 and CD62L markers, suggesting that upon stimulation they undergo an enhanced differentiation toward the T2-B cell stage (**Figures 4F,G**) (21, 59). For these experiments, we chose mice, which at day 5 p.i. had similar amounts of B cells in their blood. As the B cell numbers in the spleens of treated imb-1 mice could vary from mouse to mouse, we repeated the experiment several times using imb-1/B1-8H and imb-1 mice. In all experiments, anti-IgM treatment led to an increased differentiation toward the (IgD<sup>high</sup>IgM<sup>low</sup>) T2-B cell stage, but not to a reduction of absolute B cell numbers in the spleen (Figure S3A in Supplementary Material). This was also confirmed by a transfer experiment where we isolated EGFP<sup>+</sup>CD23<sup>-</sup> T1-B cells from induced RERT/EGFP mice (described in Figures S4D,E in Supplementary Material) at day 5 p.i. and injected the same number of these B cells into Rag2<sup>-/-</sup>γc<sup>-/-</sup> mice. Three hours after transfer, the host mice were either left untreated or treated with 100 µg of anti-IgM F(ab')<sub>2</sub> and the B cells of these mice were analyzed 36 h later by flow cytometry (Figure S3B in Supplementary Material). Again, *in vivo* stimulated T1-B cells showed an increased differentiation to T2-B cells (IgD<sup>high</sup>IgM<sup>low</sup> and CD23<sup>+</sup>), but the B cell numbers were similar in the untreated and anti-IgM treated mice (Figure S3 in Supplementary Material and data not shown).

Overall, these data indicate that transitional B cells undergo activation and differentiation and not death upon their BCR engagement *in vivo*.

## Stimulated T2-B Cells Require a BAFF Signal for Survival

To elucidate the molecular mechanism behind the surprising survival of *in vivo* stimulated T1- and T2-B cells, we analyzed the expression of anti-apoptotic molecules in these cells. In particular, the pro-survival factor Bcl-2 plays an important role in the survival of B cells at different developmental stages. To test for Bcl-2 expression in T1- and T2-B cells, we used specific anti-Bcl-2 antibodies and an intracellular staining protocol. Interestingly, T2-B cells isolated at day 7 p.i. from an anti-IgM-treated imb-1/B1-8H mouse showed elevated Bcl-2 levels in comparison to B cells isolated from untreated mice (**Figure 5A**, right panel, and **Figure 5B**). To exclude that the observed differences in Bcl-2 levels were due to an increased cell size after anti-IgM treatment, we assessed the forward scatter (FSC), which is directly proportional to cell size, of the T2 B cells derived from either untreated or anti-IgM-treated mice. We found no increase in cell size in T2 B cells from anti-IgM-treated mice. In fact, the FSC of these cells was somewhat reduced compared to the untreated control cells (Figure S4A in Supplementary Material). Notably, no difference in Bcl-2 expression level was found in T1-B cells isolated from either untreated or anti-IgM-treated mice (**Figure 5A**, left panel,

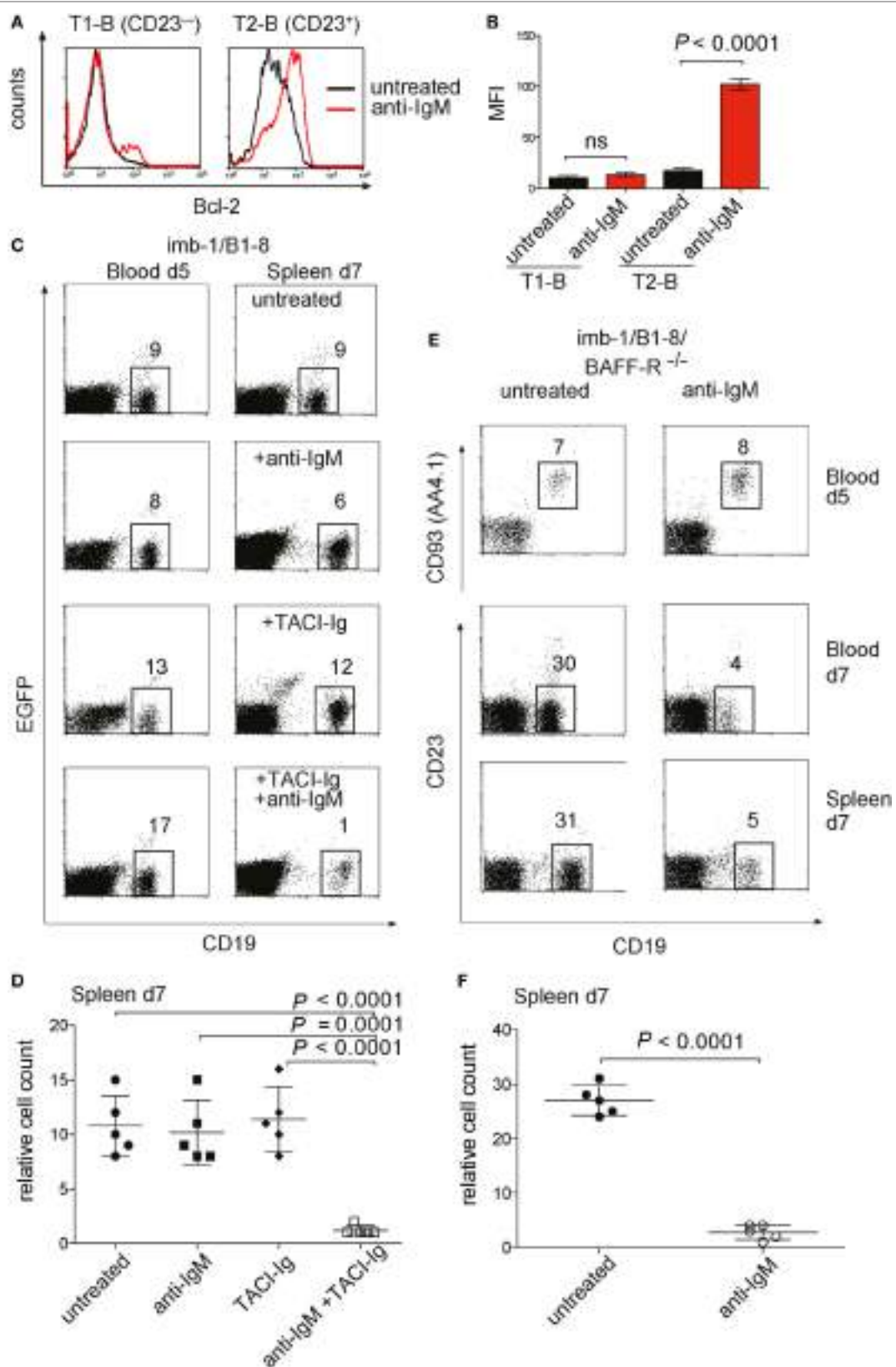


FIGURE 5 | Continued

**FIGURE 5 |** Bcl-2 expression and survival of transitional B cells from anti-IgM treated imb-1. **(A)** Histograms of intracellular expression level of Bcl-2 in splenic B cells derived from CD21-CD23<sup>IgM<sup>high</sup>IgD<sup>low</sup> transitional 1 (T1) (left panel) and CD21<sup>+CD23<sup>IgM<sup>high</sup>IgD<sup>high</sup> transitional 2 (T2) (right panel) B cells. B cells from untreated mice, black line; from anti-IgM treated mice, red line. The cells were analyzed at day 7 post induction (p.i.) (2 days after anti-IgM injection). Representative data from five independent experiments with two mice are shown. **(B)** Statistical analysis of median fluorescence intensity (MFI) values of Bcl-2 in the designated B cell population with or without anti-IgM treatment. Mean  $\pm$  SD of  $n = 5$  is indicated for each time point; The  $P$  value was obtained using a two-tailed Student's  $t$ -test. **(C)** Treatment of imb-1/B1-8H derived splenocytes with TACI-Ig and anti-IgM. Left panel: CD19 versus EGFP dot plots of lymphocytes from the blood of imb-1/B1-8 mice at day 5 p.i. Right panel: CD19 versus EGFP dot plot of lymphocytes from spleens at day 7 p.i. treated with anti-IgM (upper row), TACI-Ig (middle row), or a combination of anti-IgM and TACI-Ig (bottom row). The numbers in gates indicate percentages of B cells. Representative data from three independent experiments with two mice for each treatment are shown. **(D)** Quantitative analyses of imb-1/B1-8H-derived splenic CD19<sup>+</sup> B cells (within lymphoid gate) at day 7 p.i. Treatment is designated in the graph; mean  $\pm$  SD of  $n = 5$  is indicated for each time point; each dot represents an individual mouse;  $P$  values were obtained using a two-tailed Student's  $t$ -test and are indicated in the graphs. **(E)** Anti-IgM treatment of transitional B cells in the absence of BAFF-R. imb-1/B1-8/BAFF-R<sup>-/-</sup> mice at day 5 p.i. were either left untreated (left panel) or treated with anti-IgM (right panel). Upper row: CD19 versus CD93 (AA4.1) dot plot on blood derived B cells at day 5 p.i. before anti-IgM injection. The middle and lower rows depict dot plot analyses representing CD19 versus CD23 expression on B cells derived from either blood (middle row) or spleen (bottom row) at day 7 p.i., which were left untreated (left panel) or received anti-IgM at day 5 p.i. (right panel). Representative data from three independent experiments with two mice are shown. **(F)** Quantitative analyses of imb-1/B1-8H/BAFF-R<sup>-/-</sup>-derived splenic B cells (%CD19<sup>+</sup> in lymphoid gate) at day 7 p.i. Treatment is designated in the graph; mean  $\pm$  SD of  $n = 5$  is indicated for each time point; each dot represents an individual mouse;  $P$  value was obtained using a two-tailed Student's  $t$ -test and is indicated in the graphs.</sup></sup></sup>

and **Figure 5B**). A previous study has proposed that T1-B cells are lost whereas T2-B cells persist upon BCR engagement due to expression of the pro-survival factor Bcl-xL (60). We have assessed the expression of Bcl-xL in T1- and T2-B cells (separated based on CD23 expression) and found no induction of Bcl-xL upon anti-IgM treatment (Figure S4B in Supplementary Material). These data suggest that the engagement of the BCR on T1-B cells not only promotes differentiation to the T2-B cell stage but also initiates a survival program by upregulation of Bcl-2.

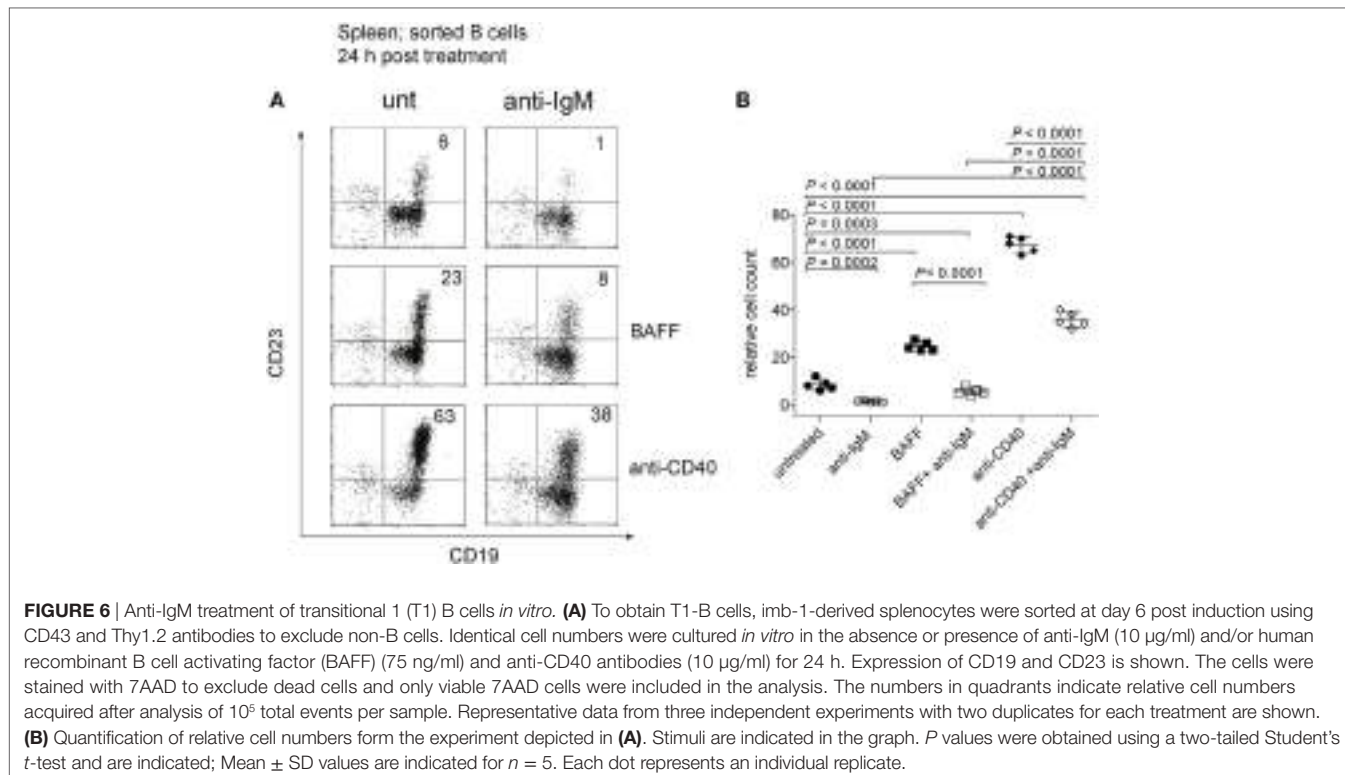
The transcription of the Bcl-2 gene is under the control of the NF- $\kappa$ B pathway (61), and it has been shown that signals from the BCR and the BAFF-R cooperate in NF- $\kappa$ B activation (62). The spleen of imb-1 and imb-1/B1-8H mice contains no B cells before tamoxifen treatment and only a few mature B cells are detected in the spleens at days 5–7 after induction (**Figure 3G**). Therefore, one can assume that there is little competition among these B cells for the abundant BAFF in the spleen of these mice. This notion is supported by previous publications reporting that soluble BAFF levels rise in the absence of B cells and excessive BAFF concentrations lead to increased survival of antigen-engaged B cells (63–67). To study the role of BAFF in the survival and differentiation of B cells in the imb-1 mouse, we interfered with BAFF signaling by either removing BAFF with the soluble decoy receptor TACI-Ig or by employing BAFF-R-deficient mice (38). We injected imb-1/B1-8H mice with anti-IgM, TACI-Ig (at days 0, 3, and 5 p.i.), or both reagents and monitored the number of CD19<sup>+</sup> B cells in the blood at day 5 after the final TACI-Ig and before anti-IgM injection, and at day 7 after treatment in the spleen (**Figures 5C,D**). Whereas each reagent alone had no effect on B cell numbers, the combination of both reagents resulted in a drastic reduction of B cells (from  $10.8 \pm 2.8\%$  in the untreated control to  $1.2 \pm 0.4\%$  after TACI-Ig + anti-IgM treatment at day 7, **Figures 5C,D**) in the spleen. These data indicate that the BCR-stimulated T1-B cells require BAFF signaling for their survival whereas naive T1-B cells can survive in the spleen for some time without BAFF.

A similar conclusion was drawn from the study of imb-1 mice lacking the BAFF-R. After the induction of B cell development, the imb-1/B1-8H/BAFF-R<sup>-/-</sup> mice were either left untreated or received anti-IgM F(ab')<sub>2</sub> at day 5 p.i. (**Figures 5E,F**). In the absence of BCR stimulation, the BAFF-R-deficient T1-B cells

developed normally and were first detected in the blood at day 5 p.i. However, the treatment with anti-IgM resulted in a drastic reduction of B cell numbers at day 7 p.i. in the blood (from 30 to 4%) and in the spleen (from  $27 \pm 2.7$  to  $2.8 \pm 1.3\%$ ) in these mice (**Figures 5E,F**). Furthermore, B-cell development in the imb-1/BAFF-R<sup>-/-</sup> mice is partially blocked at the T1-B cell to T2 transition, which is evident by the lack of CD23 marker characteristic for T2-B cells (**Figure 5E**, lower panel, relative to **Figure 4F**).

The imb-1 mice have only one functional but targeted *mb-1* allele (*mb-1/mEGFP<sup>inv</sup>*) and therefore their T1-B cells express Ig- $\alpha$  and the IgM-BCR at twofold to threefold lower amounts than T1-B cells from wild-type mice [Figure S4C in Supplementary Material and Ref. (68)]. To exclude that the lack of negative selection of T1-B cells in anti-IgM treated imb-1 mice is due to the lower IgM-BCR expression and thus signaling (68, 69) we developed another mouse model (RERT/EGFP) with an inducible B cell compartment. RERT mice express tamoxifen-regulated Cre-ER<sup>T2</sup> under the control of the RNA polymerase II promoter (70, 71). RERT mice were crossed to *mEGFP/mb-1<sup>inv</sup>* mice to generate RERT/EGFP animals that carry two floxed *mEGFP/mb-1<sup>inv</sup>* alleles (Figure S4D in Supplementary Material). A Cre-ER<sup>T2</sup>-mediated inversion of both *mb-1* alleles results in the loss of EGFP, allowing the expression of two copies of *mb-1*. This leads to higher IgM-BCR surface level in RERT/EGFP T1-B cells compared to imb-1-derived T1-B cells (Figures S4E,F in Supplementary Material). The kinetics of B cell development and the upregulation of Bcl-2 in anti-IgM treated T2-B cells were similar in RERT/EGFP and imb-1 mice (Figure S4G in Supplementary Material and data not shown). Therefore, the survival of transitional B cells in anti-IgM treated imb-1 mice is not the result of low IgM-BCR expression but rather a part of their normal developmental program in the presence of excess BAFF.

Previous studies have shown that immature B cells stimulated with anti-IgM *in vitro* die rapidly by apoptosis (55), whereas we found survival of these cells *in vivo*. To clarify this issue, we isolated T1-B cells from imb-1 mice at day 5 p.i. and cultured them *in vitro* for 24 and 48 h without or with 10  $\mu$ g/ml of anti-IgM F(ab')<sub>2</sub>. During the 24 h *in vitro* culture, approximately 6% of T1-B cells developed into CD23<sup>+</sup> B cells (**Figures 6A,B**). The anti-IgM treatment greatly reduced the numbers of these cells



(**Figures 6A,B**). We cultured the isolated T1-B cells either with BAFF (75 ng/ml) or anti-CD40 (10 µg/ml) antibody, two stimuli that activate the NF-κB pathway in B cells (72). In the presence of these reagents, 23 and 63% of the living B cells, respectively, displayed CD23 expression (**Figures 6A,B**). The increase of CD23<sup>+</sup> cells in the BAFF containing culture may be a result of CD23 gene activation *via* BAFF, which has been described before (73). Anti-CD40 treatment resulted in a very high expression of CD23 indicating that the cells indeed differentiated, possibly in T2 B cells (**Figures 6A,B**). It is feasible that longer stimulation with anti-CD40 might lead to differentiation of these cells into blasts as they become more mature (74). The addition of either BAFF or anti-CD40 only partially prevented the cultured T1-B and T2-B cells from anti-IgM-mediated apoptosis after 24 h (**Figures 6A,B**). However, only 1, 3, and 6% of viable cells were detected after 48 h of culture stimulated with anti-IgM alone or in combination with BAFF or anti-CD40, respectively (Figure S5 in Supplementary Material). These results suggest that upon BCR engagement, T1-B cells require additional factors apart from BAFF and CD40 for their survival and differentiation *in vivo*.

## DISCUSSION

In this study, we show that the tamoxifen-induced MerCreMer recombinase is tightly regulated *in vivo* and can be used to activate genes in the mouse. We took advantage of this feature to generate the imb-1 mouse with an inducible B cell compartment. Only upon tamoxifen-treatment do imb-1 mice produce mature B cells

and this allowed us to monitor the kinetics of B cell development and to test for factors that influence this process.

The Cre/LoxP technique is most often used for the conditional deletion of floxed genes. For these loss-of-function approaches, the efficiency of Cre activity is particularly important, as a low frequency of gene deletion may not result in a detectable phenotype. On the other hand, for the activation of a gene with a selective advantage (gain-of-function), the tightness of Cre regulation is more important than its efficiency, and here the MerCreMer recombinase can be employed successfully for developmental studies in the mouse. Indeed, the activity of MerCreMer is extremely well regulated as none of the many pro-B cells that are generated daily in the imb-1 mouse mature in the absence of tamoxifen. This is in line with an earlier study using our mb-1MerCreMer mouse model to induce a conditional RAG1 allele and subsequently a wave of B cell development including B-1 B cells (48). Thus, we argue that the double fusion Cre enzyme MerCreMer, is one of the most tightly regulated Cre enzymes available.

The oral administration of a single dose of 6 mg of tamoxifen to either imb-1 or imb-1/B1-8H mice induces a homogeneous and transient wave of developing B cells that allowed us to study the kinetics of B cell development. The first IgM<sup>+</sup> B cells appeared between days 5 and 6 p.i. in the BM. This took longer than the 2 days reported for B cell maturation in the BM of BALB/c mice measured by BrdU labeling (75). The reason for this delay may be due to the fact that in tamoxifen-treated mice, it takes 4 days before the tamoxifen concentration in the blood falls below the threshold of MerCreMer activation (Figure S1A in Supplementary

Material). Because the mb-1/EGFP cassette can be repeatedly recombined, pro-B cells with stable Ig- $\alpha$  expression are probably produced only after day 4 in these mice. As soon as immature B cells appeared in the BM and the blood of imb-1 mice, they were also found in the spleen, suggesting that the completion of V(D)J recombination and the export of B cells from the BM to the spleen is a rapid process. It is also possible, and we have no way to exclude, that a fraction of B cell development takes place directly in the spleen. Consistent with previous findings, the first immigrant B cells in the spleen are IgM<sup>high</sup> T1-B cells that are negative for both the CD23 and the CD21 markers (21). However, we also detect an intermediate CD23<sup>+</sup>CD21<sup>-</sup> B cell population that appears prior to the generation of the CD23<sup>+</sup>CD21<sup>+</sup> T2-B and follicular B cells (Figures 3A,C, d5–d6; Figure S1B in Supplementary Material, d5–d6) (20). Thus, our data suggest that splenic B cell maturation proceeds first *via* the upregulation of CD23 and than with that of CD21. Interestingly, a study by the Allman group has previously identified a population of newly formed immature B cells in the BM, which was CD93<sup>+</sup>CD23<sup>+</sup>CD21<sup>-</sup> and thus resembled later transitional stages in the spleen. However, the developmental kinetics and the renewal rate of this population resembled those of immature B cells in the BM. The authors of this study have thus concluded that newly immigrant populations from the BM are heterogeneous and comprise mature and semi-mature B cells (76). Since the imb-1 and imb-1/B1-8 mice are devoid of peripheral B cells prior to the tamoxifen-induced B cell development, it is possible that such semi-mature B cells are more prominently represented in the spleens of these mice compared to mice with an intact B cell development.

In imb-1 mice, the development of T1-B into T2-B cells is a rapid process that occurs in 3–4 days, whereas the development of T2-B cells into follicular or MZ B cells takes roughly 10–20 days. It is not clear why the final maturation of B cells in the spleen takes so long, but it is likely that T2 B-cells require additional signals for their maturation. This notion is supported by the fact that mutant mice lacking elements of the BCR signaling pathways are often arrested at the T2-B cell stage (77). BrdU-labeling experiments indicate that most of the newly emigrant B cells have a short life span (3–5 days) and that only a few of the transitional B cells enter the long-lived B cell pool (17, 78). This suggests that many immature and transitional B cells are primed for negative selection upon engagement of their BCR by self-antigens. Indeed, in mouse models of tolerance the transitional B cells show a rapid antigen-induced apoptosis (79–82). Furthermore, *in vitro* studies with different immature B cell lines or with purified transitional splenic B cells indicate that the main response upon exposure to anti-BCR antibodies is apoptosis (59, 83). It thus came as a surprise that T1-B cells exposed to anti-IgM reagents in imb-1 mice do not die but develop into T2-B cells upregulating the pro-survival factor Bcl-2 (Figures 4 and 5A). Moreover, *in vivo* treatment with anti-IgM resulted in a phenotype of IgM, IgD, and CD23 expression similar to that of mature B cells in wild-type mice (Figure S3 in Supplementary Material). This finding is reminiscent of that shown by the expression of Nur-77 in splenic B cells (84) and suggests that maturation of T1-B cells into T2 and follicular B cells require some level of BCR engagement.

However, one should keep in mind that anti-BCR antibodies are not stimulating the BCR in the same way as cognate antigen (85). Moreover, goat anti-IgM was used for these studies. Thus, we cannot exclude the possibility that after anti-IgM injection into mice, the T1 B cells presented goat Ig-derived peptides to T cells, which then promoted B cell survival and maturation *via* T cell help (86, 87). However, we find this unlikely given that we injected F(ab')<sub>2</sub> Ab fragments without adjuvant, and that the changes in B cell maturation were already visible two days after injection, not only in imb-1 but also in Rag2<sup>-/-</sup>γc<sup>-/-</sup> mice, injected with imb-1-derived B cells (Figure 4; Figure S3 in Supplementary Material). Furthermore, due to low expression of the BCR on the surface of imb-1 B cells, the BCR nanoislands might not be formed correctly, resulting in altered response to BCR engagement (88, 89). Furthermore, the survival of the BCR-stimulated T2-B cells in the imb-1 mice was strictly dependent on the BAFF signaling system whereas non-stimulated naïve T1-B and T2-B cells could survive in these mice for some time without BAFF. We are aware of the fact that imb-1 mice are lymphopenic where the few generated B cells do not compete for limiting growth factors as is probably the case for newly generated B cells in wild-type mice (39, 65, 90, 91). A survival of auto-reactive T cell clones in the thymus has also been observed in a lymphopenic mouse model (52). However, we think that the imb-1 model may help to better characterize the survival niches of B cells of defined developmental stages *in vivo*. Clearly, in the imb-1 mouse, the stimulated T1-B cells require more pro-survival signals such as BAFF than non-stimulated T2-B cells, similar to what has previously been observed for the anergic anti-hen egg lysozyme B cells (40, 63). Only the stimulated T2-B cells, however, displayed an upregulation of the pro-survival factor Bcl-2, indicating that the NF-κB signaling pathway was activated in these cells. Indeed, genetic and biochemical studies have shown that the canonical and non-canonical NF-κB signaling pathways play an essential role for the survival and further development of T2-B cells (36, 61, 92). It was recently suggested that the signals from the BCR and the BAFF-R cooperate to ensure a prolonged NF-κB activation and, thus, the survival of stimulated B cells (62). Furthermore, it has been shown that the overexpression of either Bcl-2 or Bcl-xL rehabilitates the survival of BAFF-R deficient B cells, suggesting that BAFF rescues B cells from apoptosis (31, 38, 93). However, our studies of *in vitro* cultured T1-B cells from imb-1 mice suggest that BAFF is not the only factor controlling the survival of transitional B cell *in vivo*. According to Sandel and Monroe (55), the site of antigen encounter is important for the decision whether immature B cells are rescued or undergo apoptosis. Therefore, the cellular BM microenvironment protects immature B cells from apoptosis by inducing RAG re-expression and subsequent receptor editing whereas splenic microenvironment does not prevent the rapid demise of stimulated transitional B cells resulting in their negative selection. In the BM, CD90<sup>lo</sup> cells, which have later been identified as basophils (94), seem to provide the rescuing signal to immature B cells. Interestingly, basophils (and also mast cells) have been attributed with the production of high levels of BAFF, IL-4, IL-6, IL-13, and other cytokines, thereby contributing to the survival niche of immature but also mature activated B cells *in vivo*. Basophils have even

been reported to home to sites of inflammation in the periphery thus supporting activated B cells and plasma cells [reviewed in Ref. (95)]. It is thus feasible that, due to lymphopenia in imb-1 mice at the start of the experiments, there is an altered splenic microenvironment, where basophils, mast cells, and their products contribute to the enhanced survival of anti-IgM-treated T1 B cells *in vivo*. Furthermore, not only *in vitro* but also in an *in vivo* situation, stimulation through CD40 certainly plays an important role in B cell activation. From the results shown in Figure S3 in Supplementary Material one could assume, however, that CD40 ligand (L) does not account for the survival of the T1 B cells after anti-IgM stimulation *in vivo* since T1 B cells stimulated with anti-IgM still survive in the transfer experiments into Rag $2^{-/-}$ -γc $^{-/-}$  mice, which lack T cells and therefore CD40L. However, other cell types, including basophils and mast cells, can express CD40L, thus mimicking “T-cell help” (95) and might therefore play an important role in the *in vivo* survival, in addition to BAFF. Clearly more remains to be learned about the signals that control the selection of B cells (*in vitro* and) *in vivo*, and the imb-1 mouse strain represents a useful model in which to study these events in more detail.

Finally, the imb-1 and RERT/EGFP models can be employed in studies of BCR signaling in lymphoma and leukemogenesis. Many B cell lymphomas are dependent on BCR signaling (96), such as, e.g., chronic lymphocytic leukemia (CLL). Combining the imb-1 or RERT/EGFP mouse lines with transgenic Tcl-1 lines, the latter serving as model for CLL (97), would result in generation of B cells either with low or with nearly physiological BCR surface expression and would thus allow studying the influence of BCR expression dosage on CLL development.

## MATERIALS AND METHODS

### Generation of Targeting Vector and Targeted ES Cell Clones

Two genomic clones containing the complete mouse *mb-1* locus from the BALB/c strain (98) were kindly provided by Dr. N. Sakaguchi (Kumamoto, Japan) and were used for the generation of the mb-1 MerCreMer targeting vector in order to replace exons 1 and 2 of the *mb-1* locus. The Cre cDNA was derived from the pBlueiCre plasmid kindly provided by R. Sprengel (Max Planck Institute for Medical Research, Heidelberg, Germany) (99). A 3-kb cDNA encoding for MerCreMer was recovered from the pAn MerCreMer vector, containing the cDNA of MerCreMer under the human β-actin promoter and subcloned in the pBSmb-1 backbone, which encodes the BALB/c genomic *mb-1* promoter and the short arm of homology of the *mb-1* locus. The ATG codon derived from MerCreMer is in-frame with the ATG from exon 1 of the *mb-1* gene. In addition, the splice donor site from the *mb-1* exon 3 was introduced by oligonucleotides after the stop codon of MerCreMer. The E-mu enhancer was introduced as a blunted 990 bp XbaI fragment 5' from the *mb-1* promoter. The 9.6 kb genomic long arm of homology beginning within intron 3, as well as a Neo<sup>r</sup> cassette flanked by two Frt sites in the same direction,

was cloned in a last step to give the targeting construct. The generation of the reporter mEGFP/*mb-1*<sup>inv</sup> vector was described before (47).

BALB/c ES cells ( $1 \times 10^7$ ) (100) were electroporated in 900 μl transfection buffer (20 mM HEPES, pH 7.0; 137 mM NaCl; 5 mM KCl; 0.7 mM Na<sub>2</sub>HPO<sub>4</sub>; 6 mM glucose; 0.1 mM 2-β-ME) with 20 μg linearized vector at 240 v and 475 μF. ES cells were cultured in DMEM selection medium containing 10% FCS, L-glutamine, sodium pyruvate, penicillin/streptomycin, and G418 (320 μg/ml). Three clones out of 480 gave the expected bands for the targeted allele by Southern blot analysis. Digestion with *Eco*RI results in a 4.1 kb fragment for mb-1 MerCreMer and a 7.6 kb fragment for both mEGFP/*mb-1*<sup>inv</sup> and *mb-1*/mEGFP<sup>inv</sup>, compared with a 6.4 kb fragment from BALB/c genomic DNA. The neo cassette was deleted by transient expression of the enhanced (Flpe) recombinase kindly provided by Dr. F. Stewart (Dresden, Germany) (101). Two independent clones were injected into C57BL/6J blastocysts at the transgene facility of the Max-Planck-Institute of Immunobiology (Freiburg, Germany). Five chimeric mice were obtained, and only one transmitted the mutation to the germ line.

### Mouse Experiments

The reporter mice mEGFP/*mb-1*<sup>inv</sup> and *mb-1*/mEGFP<sup>inv</sup> have been described (47). Intercrossing of mb-1MerCreMer mice to mEGFP/*mb-1*<sup>inv</sup> mice gave rise to the imb-1 strain, and crossing mb-1MerCreMer to *mb-1*/mEGFP<sup>inv</sup> resulted in the cmb-1 strain. The B1-8H mice (57) harboring a VDJ transgene derived from the (4-hydroxy-3-nitro-phenyl acetyl) (NP)-binding antibody B1-8 (102) at the VH locus, were crossed to imb-1 and cmb-1. The RERT mouse strain (70) was kindly provided by M. Baracid (Madrid, Spain) (71). The crossing of the RERT with the mEGFP/*mb-1*<sup>inv</sup> strain generated the RERT/EGFP mouse strain, schematically depicted in Figure S4B in Supplementary Material. The B1-8H and BAFF-R $^{-/-}$  mouse strain was obtained from K. Rajewsky (38, 57). Mating of the BAFF-R $^{-/-}$  mouse with the imb-1 mouse resulted in the imb-1/BAFF-R $^{-/-}$  mouse strain. Mice used throughout this study were 6–8 weeks old. All animal studies were carried out in accordance with the German Animal Welfare Act, having been reviewed by the regional council and approved under license #G-09/103. All mice were maintained in a barrier mouse facility, or under specific pathogen-free conditions at the animal facility of the MPI-IE.

### Southern Blot and PCR Analysis

A 170-bp genomic *mb-1* fragment located 2 kb 5' of the *mb-1* promoter (103) was used as an external probe to discriminate between wild-type (7.6 kb) and the MerCreMer targeted allele (4.1 kb) when hybridized to *Eco*RI-digested genomic DNA. Screening for the reporter mice has been described earlier (47). PCR screening of genomic DNA derived from tails of the different transgenic mice used in the experiments was done as follows: for MerCreMer detection, an hCre PCR was used with the following primers hCredir: CCCTGTGGATGCCACCTC and hCrerev: GTCCTGGCATCTGTCAGAG. Ta = 58°C; Tex = 1 min and 30 cycles give a 450-bp product. In addition, an

EGFP PCR was designed to detect the insertion of mEGFP/mb-1<sup>inv</sup> or mb-1/mEGFP<sup>inv</sup> in the reporter strains. Two primers were designed GFPdir; GGTGGTGCCCATCCTGGTCG and GFPrev; GTACAGCTCGTCCATGCCGAG. A 700-bp product is detected under the same conditions as in the above-mentioned PCR. Homozygous mice were identified by the lack of B lymphocytes in peripheral blood caused by the Ig-α deficiency.

### Tamoxifen Treatment of Mice

Tamoxifen citrate® tablets 30 mg (AstraZeneca) were emulsified in clinoleic® 20% (Baxter), a mixture of olive and soybean oil in a 5:1 ratio. In all experiments, mice were treated 1× orally with 6 mg the suspension, by gavage with the help of a curved needle. Mice were then analyzed at different times p.i.

### Analysis of Mice With Inducible B Cell Development

The absence of B cells in imb-1 and RERT/EGFP mice before induction with tamoxifen citrate was verified by FACS analysis of peripheral blood. The mice were bled again at day 5 p.i. and monitored for B cell development in the periphery. The mice with comparable relative B cell percentage in their peripheral blood were chosen for each experiment.

### Treatment of Mice

imb-1 or RERT/EGFP mice were injected i.p. at day 5 p.i., with 100 µg goat anti-mouse IgM heavy chain antibodies [polyclonal IgG F(ab')<sub>2</sub>; #115-006-075] (Jackson ImmunoResearch laboratories). Another goat anti-mouse IgM F(ab')<sub>2</sub> fragment (endotoxin low) was applied in the same studies to ensure for reproducibility (Southern biotechnology cat. #1022-14). Untreated mice received polyclonal goat IgG, F(ab')<sub>2</sub> fragment (cat# 005-000-006) (Jackson ImmunoResearch laboratories). TACI-Ig was purchased from (R&D). The mice were injected i.p. three times at days 0, 3, and 5 p.i. with 50 µg per mouse TACI-Ig (Atacicept, Merck) and were monitored at day 7 p.i.

### Generation of the J558 MerCreMer/loxP-Stop-loxP mEGFP Reporter Cell Line

The myeloma cell line J558L μm3-11 MerCreMer/loxP-Stop-loxP mEGFP (referred to as J558; MCM/loxEGFP) reporter cell line carries a Cre-reporter vector with a loxP-Stop-loxP EGFP cassette coding for an mEGFP, expressed under the control of the human β-actin promoter. In the 5' region of the vector a floxed DNA cassette bearing a Stop codon and a polyA sequence prevents the expression of EGFP. Cre-mediated deletion of the floxed Stop sequence results in EGFP expression and can be monitored by FACScan analysis. The cell line was generated as follows. Two MCM targeting vectors were linearized and transfected into the J558L/loxP-stop-loxP EGFP reporter cell line. For this the reporter cells growing at the exponential phase were harvested by centrifugation (Varifuge 3.0 F, 339 × g, at 4°C for 5 min) and washed twice with PBS and 1 × 10<sup>7</sup> cells were resuspended in 300 µl of RPMI medium and transferred into an electroporation cuvette (EquiBio ECU 104). Linearized plasmid DNA (10 µg) purified with the Qiagen Maxi Kit was added and the cells were

incubated on ice for 5 min. The cells were electroporated using a BioRad Gene pulser II at 260 V, 960 µF, after which the samples were maintained on ice for another 10 min. A “mock” control containing the same cell number was subjected to electroporation in the absence of DNA. The electroporated cells were resuspended in 48 ml RPMI medium, plated into two 24-well plates (Greiner) at 1 ml/well and incubated at 37°C and 5% CO<sub>2</sub>. The medium was replaced after 2 days with fresh medium containing the desired selection factor (G418 or hygromycin).

### Preparation of Cell Suspension From Lymphoid Organs

Single cell suspensions from BM, spleen, and blood were prepared as described (103).

### Antibodies for FACS Analysis

For each sample 1–2 × 10<sup>6</sup> cells were incubated with various combinations of antibodies as indicated. The antibodies for lymphocyte staining were against the following mouse antigens: B220 (clone RA3-6B2), CD19 (clone 1D3), CD21 (clone 7G6), CD23 (clone B3B4), IgD (clone 11-26), Bcl-2 (clone 3F11), purchased from BD (Becton Dickinson). Biotinylated Abs were detected by Streptavidin-PerCp (BD). Anti-mouse IgM was from Jackson ImmunoResearch Laboratories. Anti-mouse CD93 (C1qRp; clone AA4.1), MHC class II (I-A/I-E) (clone M5/114.15.2), CD62L (clone MEL-14), CD24 (clone M1/69), CD40 (clone 1C10) antibodies were from (eBioscience), and anti-CD40 antibodies (clone 3/23) were from (BD). In the mouse experiments, the dead cells were excluded based on FSC/SSC. In the *in vitro* experiments, 7-aminoantimycin D (7AAD) was used to exclude dead cells and was purchased from (SouthernBiotech). Four-color flow cytometry was performed on a FACSCalibur™ flow cytometer (BD). Flow cytometric profiles were analyzed using CELLQuest™ software (BD) and FlowJo (Tree Star). Prior to all the stainings, the cells were incubated with an anti-Fc receptor antibody (clone 2.4G2) to block unspecific binding.

### Intracellular Staining

For each sample 1–2 × 10<sup>6</sup> cells were washed in PBS and then fixed in a 2% formaldehyde solution for 15 min at room temperature. The cells were washed two times in PBS and then stained for 15 min at room temperature with anti-Bcl-2 (Clone 3F11; BD) or anti-Bcl-xL (Clone H-5, Santa Cruz Biotechnology) in 0.05% saponin in PBS.

### Cell Sorting, Transfer, and *In Vitro* Stimulation

Transitional 1-B cells from imb-1 mice were sorted by negative selection using CD43 and Thy1.2 antibodies to exclude non-B cells. T1-B cells from RERT/EGFP mice were sorted based on EGFP expression. These cells closely resemble imb-1-derived T1-B cells due to their expression of one copy of the mb-1 allele, whereas EGFP is expressed from the second mb-1 allele and thus serves as a reporter. To exclude CD23<sup>+</sup> population, the cells were further stained with an anti-CD23 antibody (clone B3B4;

BD). The sorted EGFP<sup>+</sup>CD23<sup>-</sup> T1-B cells (purity ≈ 98%; Figure S3B in Supplementary Material) were immediately transferred i.v. into Rag2<sup>-/-</sup>γc<sup>-/-</sup> mice and either left untreated or treated with F(ab')<sub>2</sub> fragment of anti-IgM 3 h after transfer of EGFP positive cells.

For *in vitro* stimulation experiments, soluble human recombinant BAFF (R&D) was applied at 75 ng/ml; anti-CD40 (FGK45) was a gift from the late Ton Rolink and was applied at 10 µg/ml; anti-IgM [polyclonal IgG F(ab')<sub>2</sub>; #115-006-075] was applied at 10 µg/ml.

## Statistical Analysis

Statistical testing was performed using one-sample *t*-test unpaired two-tailed Student's *t*-test (with *n* = five mice per group) was carried out using Prism 4 software (GraphPad Software Inc.).

## ETHICS STATEMENT

Mice used throughout this study were 6–8 weeks old. All animal studies were carried out in accordance with the German Animal Welfare Act, having been reviewed by the regional council and approved under license #G-09/103. All mice were maintained in a barrier mouse facility, or under specific pathogen-free conditions at the animal facility of the MPI-IE.

## AUTHOR CONTRIBUTIONS

EH, RP, and MR designed the study. EH, EL-Z, and MD conducted the experiments. MR, EH, RP, and EL-Z wrote the manuscript.

## REFERENCES

1. Rajewsky K. Clonal selection and learning in the antibody system. *Nature* (1996) 381:751–8. doi:10.1038/381751a0
2. Hardy RR, Hayakawa K. B cell development pathways. *Annu Rev Immunol* (2001) 19:595–621. doi:10.1146/annurev.immunol.19.1.595
3. Melchers F, Strasser A, Bauer SR, Kudo A, Thalmann P, Rolink A. B cell development in fetal liver. *Adv Exp Med Biol* (1991) 292:201–5. doi:10.1007/978-1-4684-5943-2\_22
4. Gong S, Nussenzweig MC. Regulation of an early developmental checkpoint in the B cell pathway by Ig beta. *Science* (1996) 272:411–4. doi:10.1126/science.272.5260.411
5. Pelanda R, Braun U, Hobeika E, Nussenzweig MC, Reth M. B cell progenitors are arrested in maturation but have intact VDJ recombination in the absence of Ig-alpha and Ig-beta. *J Immunol* (2002) 169:865–72. doi:10.4049/jimmunol.169.2.865
6. Meffre E, Nussenzweig MC. Deletion of immunoglobulin beta in developing B cells leads to cell death. *Proc Natl Acad Sci U S A* (2002) 99:11334–9. doi:10.1073/pnas.172369999
7. Wang Y, Kanegae H, Sanal O, Tezcan I, Ersoy F, Futatani T, et al. Novel Igalpha (CD79a) gene mutation in a Turkish patient with B cell-deficient agammaglobulinemia. *Am J Med Genet* (2002) 108:333–6. doi:10.1002/ajmg.10296
8. Minegishi Y, Coustan-Smith E, Rapalus L, Ersoy F, Campana D, Conley ME. Mutations in Igalpha (CD79a) result in a complete block in B-cell development. *J Clin Invest* (1999) 104:1115–21. doi:10.1172/JCI7696
9. Ferrari S, Lougaris V, Caraffi S, Zuntini R, Yang J, Soresina A, et al. Mutations of the Igbeta gene cause agammaglobulinemia in man. *J Exp Med* (2007) 204:2047–51. doi:10.1084/jem.20070264
10. Shimizu T, Mundt C, Licence S, Melchers F, Martensson IL. VpreB1/VpreB2/lambda 5 triple-deficient mice show impaired B cell development but functional allelic exclusion of the IgH locus. *J Immunol* (2002) 168:6286–93. doi:10.4049/jimmunol.168.12.6286
11. Kitamura D, Roes J, Kuhn R, Rajewsky K. A B cell-deficient mouse by targeted disruption of the membrane exon of the immunoglobulin mu chain gene. *Nature* (1991) 350:423–6. doi:10.1038/350423a0
12. Melchers F, Haasner D, Grawunder U, Kalberer C, Karasuyama H, Winkler T, et al. Roles of IgH and L chains and of surrogate H and L chains in the development of cells of the B lymphocyte lineage. *Annu Rev Immunol* (1994) 12:209–25. doi:10.1146/annurev.iy.12.040194.001233
13. Rolink AG, ten Boekel E, Yamagami T, Ceredig R, Andersson J, Melchers F. B cell development in the mouse from early progenitors to mature B cells. *Immunol Lett* (1999) 68:89–93. doi:10.1016/S0165-2478(99)00035-8
14. Reth M, Nielsen P. Signaling circuits in early B-cell development. *Adv Immunol* (2014) 122:129–75. doi:10.1016/B978-0-12-800267-4.00004-3
15. Chung JB, Silverman M, Monroe JG. Transitional B cells: step by step towards immune competence. *Trends Immunol* (2003) 24:343–9. doi:10.1016/S1471-4906(03)00119-4
16. Wang LD, Clark MR. B-cell antigen-receptor signalling in lymphocyte development. *Immunology* (2003) 110:411–20. doi:10.1111/j.1365-2567.2003.01756.x
17. Rolink AG, Andersson J, Melchers F. Molecular mechanisms guiding late stages of B-cell development. *Immunol Rev* (2004) 197:41–50. doi:10.1111/j.0105-2896.2004.0101.x
18. Thomas MD, Srivastava B, Allman D. Regulation of peripheral B cell maturation. *Cell Immunol* (2006) 239:92–102. doi:10.1016/j.cellimm.2006.04.007
19. Tussiwand R, Bosco N, Ceredig R, Rolink AG. Tolerance checkpoints in B-cell development: Johnny B good. *Eur J Immunol* (2009) 39:2317–24. doi:10.1002/eji.200939633
20. Allman D, Lindsley RC, DeMuth W, Rudd K, Shinton SA, Hardy RR. Resolution of three nonproliferative immature splenic B cell subsets reveals

## ACKNOWLEDGMENTS

We wish to dedicate this paper to the memory of the late Ton Rolink who greatly contributed to the better understanding of B cell development and to the fruitful interaction of the B cell community. Through fruitful discussions, Ton greatly contributed to this work and also provided us with a multitude of materials including the anti-CD40 antibody. We thank Benoit Kanzler for injecting the mb-1 targeted ES cell lines; Klaus Rajewsky for the B1-8 mice and, together with Marc Schmidt-Suprian for the BAFF-R<sup>-/-</sup> mice, and Mariano Barbacid for RERT mice. We thank N. Sakaguchi for the mb-1 genomic DNA and R. Sprengel for the iCre coding DNA. We thank Hassan Jumaa, Ingrid Mecklenbräuker, Peter Nielsen, and Marc Schmidt-Suprian for fruitful discussions and critical reading of the manuscript.

## FUNDING

This work was supported by the grants SFB1074, A9N (EH), SFB764, P07, and TRR130, P02 (MR) from the Deutsche Forschungsgemeinschaft (DFG), and the Excellence Initiative of the German Federal and State Governments (EXC294) (MR). EL-Z was supported by the International Max Planck Research School for Molecular and Cell Biology (IMPRS-MCB).

## SUPPLEMENTARY MATERIAL

The Supplementary Material for this article can be found online at <https://www.frontiersin.org/articles/10.3389/fimmu.2018.01806/full#supplementary-material>.

- multiple selection points during peripheral B cell maturation. *J Immunol* (2001) 167:6834–40. doi:10.4049/jimmunol.167.12.6834
21. Loder F, Mutschler B, Ray RJ, Paige CJ, Sideras P, Torres R, et al. B cell development in the spleen takes place in discrete steps and is determined by the quality of B cell receptor-derived signals. *J Exp Med* (1999) 190:75–89. doi:10.1084/jem.190.1.75
  22. Rolink AG, Andersson J, Melchers F. Characterization of immature B cells by a novel monoclonal antibody, by turnover and by mitogen reactivity. *Eur J Immunol* (1998) 28:3738–48. doi:10.1002/(SICI)1521-4141(199811)28:11<3738::AID-IMMU3738>3.0.CO;2-Q
  23. Merrell KT, Benschop RJ, Gauld SB, Aviszus K, Decote-Ricardo D, Wysocki LJ, et al. Identification of anergic B cells within a wild-type repertoire. *Immunity* (2006) 25:953–62. doi:10.1016/j.jimmuni.2006.10.017
  24. Teague BN, Pan Y, Mudd PA, Nakken B, Zhang Q, Szodoray P, et al. Cutting edge: transitional T3 B cells do not give rise to mature B cells, have undergone selection, and are reduced in murine lupus. *J Immunol* (2007) 178:7511–5. doi:10.4049/jimmunol.178.12.7511
  25. Martin F, Kearney JF. CD21high IgMhigh splenic B cells enriched in the marginal zone: distinct phenotypes and functions. *Curr Top Microbiol Immunol* (1999) 246:45–50; discussion 51–2.
  26. Casola S, Otipoby KL, Alimzhanov M, Humme S, Uyttersprot N, Kutok JL, et al. B cell receptor signal strength determines B cell fate. *Nat Immunol* (2004) 5:317–27. doi:10.1038/ni1036
  27. Wen L, Brill-Dashoff J, Shinton SA, Asano M, Hardy RR, Hayakawa K. Evidence of marginal-zone B cell-positive selection in spleen. *Immunity* (2005) 23:297–308. doi:10.1016/j.jimmuni.2005.08.007
  28. Schneider P, MacKay F, Steiner V, Hofmann K, Bodmer JL, Holler N, et al. BAFF, a novel ligand of the tumor necrosis factor family, stimulates B cell growth. *J Exp Med* (1999) 189:1747–56. doi:10.1084/jem.189.11.1747
  29. Crowley JE, Treml LS, Stadanlick JE, Carpenter E, Cancro MP. Homeostatic niche specification among naïve and activated B cells: a growing role for the BLyS family of receptors and ligands. *Semin Immunol* (2005) 17:193–9. doi:10.1016/j.smim.2005.02.001
  30. Batten M, Groom J, Cachero TG, Qian F, Schneider P, Tschopp J, et al. BAFF mediates survival of peripheral immature B lymphocytes. *J Exp Med* (2000) 192:1453–66. doi:10.1084/jem.192.10.1453
  31. Rolink AG, Tschopp J, Schneider P, Melchers F. BAFF is a survival and maturation factor for mouse B cells. *Eur J Immunol* (2002) 32:2004–10. doi:10.1002/1521-4141(200207)32:7<2004::AID-IMMU2004>3.0.CO;2-5
  32. Hsu BL, Harless SM, Lindsley RC, Hilbert DM, Cancro MP. Cutting edge: BLyS enables survival of transitional and mature B cells through distinct mediators. *J Immunol* (2002) 168:5993–6. doi:10.4049/jimmunol.168.12.5993
  33. Rowland SL, Leahy KF, Halverson R, Torres RM, Pelanda RA. BAFF receptor signaling aids the differentiation of immature B cells into transitional B cells following tonic BCR signaling. *J Immunol* (2010) 185:4570–81. doi:10.4049/jimmunol.1001708
  34. Cariappa A, Liou HC, Horwitz BH, Pillai S. Nuclear factor kappa B is required for the development of marginal zone B lymphocytes. *J Exp Med* (2000) 192:1175–82. doi:10.1084/jem.192.8.1175
  35. Sasaki Y, Derudder E, Hobeika E, Pelanda R, Reth M, Rajewsky K, et al. Canonical NF-κappaB activity, dispensable for B cell development, replaces BAFF-receptor signals and promotes B cell proliferation upon activation. *Immunity* (2006) 24:729–39. doi:10.1016/j.jimmuni.2006.04.005
  36. Sen R. Control of B lymphocyte apoptosis by the transcription factor NF-κappaB. *Immunity* (2006) 25:871–83. doi:10.1016/j.jimmuni.2006.12.003
  37. Thompson JS, Bixler SA, Qian F, Vora K, Scott ML, Cachero TG, et al. BAFF-R, a newly identified TNF receptor that specifically interacts with BAFF. *Science* (2001) 293:2108–11. doi:10.1126/science.1061965
  38. Sasaki Y, Casola S, Kutok JL, Rajewsky K, Schmidt-Suppli M. TNF family member B cell-activating factor (BAFF) receptor-dependent and -independent roles for BAFF in B cell physiology. *J Immunol* (2004) 173:2245–52. doi:10.4049/jimmunol.173.4.2245
  39. Mackay F, Woodcock SA, Lawton P, Ambrose C, Baetscher M, Schneider P, et al. Mice transgenic for BAFF develop lymphocytic disorders along with autoimmune manifestations. *J Exp Med* (1999) 190:1697–710. doi:10.1084/jem.190.11.1697
  40. Thien M, Phan TG, Gardam S, Amesbury M, Basten A, Mackay F, et al. Excess BAFF rescues self-reactive B cells from peripheral deletion and allows them to enter forbidden follicular and marginal zone niches. *Immunity* (2004) 20:785–98. doi:10.1016/j.jimmuni.2004.05.010
  41. Rajewsky K, Gu H, Kuhn R, Betz UA, Muller W, Roes J, et al. Conditional gene targeting. *J Clin Invest* (1996) 98:600–3. doi:10.1172/JCI118828
  42. Le Y, Sauer B. Conditional gene knockout using cre recombinase. *Methods Mol Biol* (2000) 136:477–85. doi:10.1385/1-59259-065-9:477
  43. Kuhn R, Torres RM. Cre/loxP recombination system and gene targeting. *Methods Mol Biol* (2002) 180:175–204. doi:10.1385/1-59259-178-7:175
  44. Gu H, Marth JD, Orban PC, Mossmann H, Rajewsky K. Deletion of a DNA polymerase beta gene segment in T cells using cell type-specific gene targeting. *Science* (1994) 265:103–6. doi:10.1126/science.8016642
  45. Zhang Y, Riesterer C, Ayrall AM, Sablitzky F, Littlewood TD, Reth M. Inducible site-directed recombination in mouse embryonic stem cells. *Nucleic Acids Res* (1996) 24:543–8. doi:10.1093/nar/24.4.543
  46. Feil R, Brocard J, Mascrez B, LeMeur M, Metzger D, Chambon P. Ligand-activated site-specific recombination in mice. *Proc Natl Acad Sci U S A* (1996) 93:10887–90. doi:10.1073/pnas.93.20.10887
  47. Pelanda R, Hobeika E, Kurokawa T, Zhang Y, Kuppig S, Reth M. Cre recombinase-controlled expression of the mb-1 allele. *Genesis* (2002) 32:154–7. doi:10.1002/gene.10070
  48. Duber S, Hafner M, Krey M, Lienenklaus S, Roy B, Hobeika E, et al. Induction of B-cell development in adult mice reveals the ability of bone marrow to produce B-1a cells. *Blood* (2009) 114:4960–7. doi:10.1182/blood-2009-04-218156
  49. Zhang Y, Wienands J, Zurn C, Reth M. Induction of the antigen receptor expression on B lymphocytes results in rapid competence for signaling of SLP-65 and Syk. *EMBO J* (1998) 17:7304–10. doi:10.1093/emboj/17.24.7304
  50. Pei W, Feyerabend TB, Rossler J, Wang X, Postrach D, Busch K, et al. Polyloxy barcoding reveals haematopoietic stem cell fates realized *in vivo*. *Nature* (2017) 548:456–60. doi:10.1038/nature23653
  51. van Berlo JH, Kanisicak O, Maillet M, Vagnozzi RJ, Karch J, Lin SC, et al. c-kit+ cells minimally contribute cardiomyocytes to the heart. *Nature* (2014) 509:337–41. doi:10.1038/nature13309
  52. Busch K, Klapproth K, Barile M, Flossdorf M, Holland-Letz T, Schlenner SM, et al. Fundamental properties of unperturbed haematopoiesis from stem cells *in vivo*. *Nature* (2015) 518:542–6. doi:10.1038/nature14242
  53. Hobeika E, Levit-Zerdoun E, Anastasopoulou V, Pohlmeyer R, Altmeier S, Alsadeq A, et al. CD19 and BAFF-R can signal to promote B-cell survival in the absence of Syk. *EMBO J* (2015) 34:925–39. doi:10.15252/embj.201489732
  54. Levit-Zerdoun E, Becker M, Pohlmeyer R, Wilhelm I, Maity PC, Rajewsky K, et al. Survival of Igalpha-deficient mature B CELLS REQUIRES BAFF-R function. *J Immunol* (2016) 196:2348–60. doi:10.1084/jimmunol.1501707
  55. Sandel PC, Monroe JG. Negative selection of immature B cells by receptor editing or deletion is determined by site of antigen encounter. *Immunity* (1999) 10:289–99. doi:10.1016/S1074-7613(00)80029-1
  56. Carsotti R, Kohler G, Lamers MC. Transitional B cells are the target of negative selection in the B cell compartment. *J Exp Med* (1995) 181:2129–40. doi:10.1084/jem.181.6.2129
  57. Sonoda E, Pewzner-Jung Y, Schwers S, Taki S, Jung S, Eilat D, et al. B cell development under the condition of allelic inclusion. *Immunity* (1997) 6:225–33. doi:10.1016/S1074-7613(00)80325-8
  58. Martin F, Kearney JF. Marginal-zone B cells. *Nat Rev Immunol* (2002) 2:323–35. doi:10.1038/nri799
  59. Sater RA, Sandel PC, Monroe JG. B cell receptor-induced apoptosis in primary transitional murine B cells: signaling requirements and modulation by T cell help. *Int Immunopharmacol* (1998) 10:1673–82. doi:10.1093/intimm/10.11.1673
  60. Petro JB, Gerstein RM, Lowe J, Carter RS, Shinners N, Khan WN. Transitional type 1 and 2 B lymphocyte subsets are differentially responsive to antigen receptor signaling. *J Biol Chem* (2002) 277:48009–19. doi:10.1074/jbc.M200305200
  61. Claudio E, Brown K, Park S, Wang H, Siebenlist U. BAFF-induced NEMO-independent processing of NF-κappa B2 in maturing B cells. *Nat Immunol* (2002) 3:958–65. doi:10.1038/ni842
  62. Stadanlick JE, Kaileh M, Karnell FG, Scholz JL, Miller JP, Quinn WJ III, et al. Tonic B cell antigen receptor signals supply an NF-κappaB substrate for pro-survival BLyS signaling. *Nat Immunol* (2008) 9:1379–87. doi:10.1038/ni.1666
  63. Lesley R, Xu Y, Kalled SL, Hess DM, Schwab SR, Shu HB, et al. Reduced competitiveness of autoantigen-engaged B cells due to increased dependence on BAFF. *Immunity* (2004) 20:441–53. doi:10.1016/S1074-7613(04)00079-2

64. Bossen C, Cachero TG, Tardivel A, Ingold K, Willen L, Dobles M, et al. TACI, unlike BAFF-R, is solely activated by oligomeric BAFF and APRIL to support survival of activated B cells and plasmablasts. *Blood* (2008) 111:1004–12. doi:10.1182/blood-2007-09-110874
65. Kreuzaler M, Rauch M, Salzer U, Birmelin J, Rizzi M, Grimbacher B, et al. Soluble BAFF levels inversely correlate with peripheral B cell numbers and the expression of BAFF receptors. *J Immunol* (2012) 188:497–503. doi:10.4049/jimmunol.1209010
66. Lavie F, Miceli-Richard C, Ittah M, Sellam J, Gottenberg JE, Mariette X. Increase of B cell-activating factor of the TNF family (BAFF) after rituximab treatment: insights into a new regulating system of BAFF production. *Ann Rheum Dis* (2007) 66:700–3. doi:10.1136/ard.2006.060772
67. Vigolo M, Chambers MG, Willen L, Chevalley D, Maskos K, Lammens A, et al. A loop region of BAFF controls B cell survival and regulates recognition by different inhibitors. *Nat Commun* (2018) 9:1199. doi:10.1038/s41467-018-03323-8
68. Rowland SL, DePersis CL, Torres RM, Pelanda R. Ras activation of Erk restores impaired tonic BCR signaling and rescues immature B cell differentiation. *J Exp Med* (2010) 207:607–21. doi:10.1084/jem.20091673
69. Roy V, Chang NH, Cai Y, Bonventi G, Wither J. Aberrant IgM signaling promotes survival of transitional T1 B cells and prevents tolerance induction in lupus-prone New Zealand black mice. *J Immunol* (2005) 175:7363–71. doi:10.4049/jimmunol.175.11.7363
70. Brocard J, Warot X, Wendling O, Messadeq N, Vonesch JL, Chambon P, et al. Spatio-temporally controlled site-specific somatic mutagenesis in the mouse. *Proc Natl Acad Sci U S A* (1997) 94:14559–63. doi:10.1073/pnas.94.26.14559
71. Mijimolla N, Velasco J, Dubus P, Guerra C, Weinbaum CA, Casey PJ, et al. Protein farnesyltransferase in embryogenesis, adult homeostasis, and tumor development. *Cancer Cell* (2005) 7:313–24. doi:10.1016/j.ccr.2005.03.004
72. Rickert RC, Jellusova J, Miletic AV. Signaling by the tumor necrosis factor receptor superfamily in B-cell biology and disease. *Immunol Rev* (2011) 244:115–33. doi:10.1111/j.1600-065X.2011.01067.x
73. Gorelik L, Cutler AH, Thill G, Miklasz SD, Shea DE, Ambrose C, et al. Cutting edge: BAFF regulates CD21/35 and CD23 expression independent of its B cell survival function. *J Immunol* (2004) 172:762–6. doi:10.4049/jimmunol.172.2.762
74. Rolink A, Melchers F, Andersson J. The SCID but not the RAG-2 gene product is required for S mu-S epsilon heavy chain class switching. *Immunity* (1996) 5:319–30. doi:10.1016/S1074-7613(00)80258-7
75. Levine MH, Haberman AM, Sant'Angelo DB, Hannum LG, Cancro MP, Janeway CA Jr, et al. A B-cell receptor-specific selection step governs immature to mature B cell differentiation. *Proc Natl Acad Sci U S A* (2000) 97:2743–8. doi:10.1073/pnas.050552997
76. Lindsley RC, Thomas M, Srivastava B, Allman D. Generation of peripheral B cells occurs via two spatially and temporally distinct pathways. *Blood* (2007) 109:2521–8. doi:10.1182/blood-2006-04-018085
77. Kurosaki T. Functional dissection of BCR signaling pathways. *Curr Opin Immunol* (2000) 12:276–81. doi:10.1016/S0952-7915(00)00087-X
78. Allman DM, Ferguson SE, Lentz VM, Cancro MP. Peripheral B cell maturation. II. Heat-stable antigen(hi) splenic B cells are an immature developmental intermediate in the production of long-lived marrow-derived B cells. *J Immunol* (1993) 151:4431–44.
79. Hartley SB, Crosbie J, Brink R, Kantor AB, Basten A, Goodnow CC. Elimination from peripheral lymphoid tissues of self-reactive B lymphocytes recognizing membrane-bound antigens. *Nature* (1991) 353:765–9. doi:10.1038/353765a0
80. Russell DM, Dembic Z, Morahan G, Miller JF, Burki K, Nemazee D. Peripheral deletion of self-reactive B cells. *Nature* (1991) 354:308–11. doi:10.1038/354308a0
81. Cyster JG, Hartley SB, Goodnow CC. Competition for follicular niches excludes self-reactive cells from the recirculating B-cell repertoire. *Nature* (1994) 371:389–95. doi:10.1038/371389a0
82. Fulcher DA, Basten A. Reduced life span of anergic self-reactive B cells in a double-transgenic model. *J Exp Med* (1994) 179:125–34. doi:10.1084/jem.179.1.125
83. Carey GB, Donjerkovic D, Mueller CM, Liu S, Hinshaw JA, Tonnetti L, et al. B-cell receptor and Fas-mediated signals for life and death. *Immunol Rev* (2000) 176:105–15. doi:10.1034/j.1600-065X.2000.00502.x
84. Zikherman J, Parameswaran R, Weiss A. Endogenous antigen tunes the responsiveness of naive B cells but not T cells. *Nature* (2012) 489:160–4. doi:10.1038/nature11311
85. Volkmann C, Brings N, Becker M, Hobeika E, Yang J, Reth M. Molecular requirements of the B-cell antigen receptor for sensing monovalent antigens. *EMBO J* (2016) 35:2371–81. doi:10.1525/embj.201694177
86. Heiser RA, Snyder CM, St Clair J, Wysocki LJ. Aborted germinal center reactions and B cell memory by follicular T cells specific for a B cell receptor V region peptide. *J Immunol* (2011) 187:212–21. doi:10.4049/jimmunol.1002328
87. Yan J, Wolff MJ, Unternaehrer J, Mellman I, Mamula MJ. Targeting antigen to CD19 on B cells efficiently activates T cells. *Int Immunopharmacol* (2005) 17:869–77. doi:10.1093/intimm/dxh266
88. Klasener K, Maity PC, Hobeika E, Yang J, Reth M. B cell activation involves nanoscale receptor reorganizations and inside-out signaling by Syk. *Elife* (2014) 3:e02069. doi:10.7554/elife.02069
89. Maity PC, Yang J, Klaesener K, Reth M. The nanoscale organization of the B lymphocyte membrane. *Biochim Biophys Acta* (2015) 1853:830–40. doi:10.1016/j.bbapmcr.2014.11.010
90. Thompson JS, Schneider P, Kalled SL, Wang L, Lefevre EA, Cachero TG, et al. BAFF binds to the tumor necrosis factor receptor-like molecule B cell maturation antigen and is important for maintaining the peripheral B cell population. *J Exp Med* (2000) 192:129–35. doi:10.1084/jem.192.1.129
91. Singh NJ, Schwartz RH. The lymphopenic mouse in immunology: from patron to pariah. *Immunity* (2006) 25:851–5. doi:10.1016/j.jimmuni.2006.12.002
92. Meyer-Bahlburg A, Andrews SF, Yu KO, Porcelli SA, Rawlings DJ. Characterization of a late transitional B cell population highly sensitive to BAFF-mediated homeostatic proliferation. *J Exp Med* (2008) 205:155–68. doi:10.1084/jem.20071088
93. Amanra IJ, Dingwall JP, Hayes CE. Enforced bcl-xL gene expression restored splenic B lymphocyte development in BAFF-R mutant mice. *J Immunol* (2003) 170:4593–600. doi:10.4049/jimmunol.170.9.4593
94. Moreau JM, Cen S, Berger A, Furlonger C, Paige CJ. Bone marrow basophils provide survival signals to immature B cells in vitro but are dispensable in vivo. *PLoS One* (2017) 12:e0185509. doi:10.1371/journal.pone.0185509
95. Merluzzi S, Betto E, Ceccaroni AA, Magris R, Giunta M, Mion F. Mast cells, basophils and B cell connection network. *Mol Immunol* (2015) 63:94–103. doi:10.1016/j.molimm.2014.02.016
96. Koehler S, Burger JA. B-cell receptor signaling in chronic lymphocytic leukemia and other B-cell malignancies. *Clin Adv Hematol Oncol* (2016) 14:55–65.
97. Bresin A, D'Abundo L, Narducci MG, Fiorenza MT, Croce CM, Negrini M, et al. TCL1 transgenic mouse model as a tool for the study of therapeutic targets and microenvironment in human B-cell chronic lymphocytic leukemia. *Cell Death Dis* (2016) 7:e2071. doi:10.1038/cddis.2015.419
98. Kashiwamura S, Koyama T, Matsuo T, Steinmetz M, Kimoto M, Sakaguchi N. Structure of the murine mb-1 gene encoding a putative slgM-associated molecule. *J Immunol* (1990) 145:337–43.
99. Shimshek DR, Kim J, Hubner MR, Spergel DJ, Buchholz F, Casanova E, et al. Codon-improved Cre recombinase (iCre) expression in the mouse. *Genesis* (2002) 32:19–26. doi:10.1002/gene.10023
100. Noben-Trauth N, Kohler G, Burki K, Ledermann B. Efficient targeting of the IL-4 gene in a BALB/c embryonic stem cell line. *Transgenic Res* (1996) 5:487–91. doi:10.1007/BF01980214
101. Buchholz F, Angrand PO, Stewart AF. Improved properties of FLP recombinase evolved by cycling mutagenesis. *Nat Biotechnol* (1998) 16:657–62. doi:10.1038/nbt0798-657
102. Reth M, Hammerling GJ, Rajewsky K. Analysis of the repertoire of anti-NP antibodies in C57BL/6 mice by cell fusion. I. Characterization of antibody families in the primary and hyperimmune response. *Eur J Immunol* (1978) 8:393–400. doi:10.1002/eji.1830080605
103. Hobeika E, Thiemann S, Storch B, Jumaa H, Nielsen PJ, Pelanda R, et al. Testing gene function early in the B cell lineage in mb1-cre mice. *Proc Natl Acad Sci U S A* (2006) 103:13789–94. doi:10.1073/pnas.0605944103

**Conflict of Interest Statement:** The authors declare that the research was conducted in the absence of any commercial or financial relationships that could be construed as a potential conflict of interest.

Copyright © 2018 Hobeika, Dautzenberg, Levitt-Zerdoun, Pelanda and Reth. This is an open-access article distributed under the terms of the Creative Commons Attribution License (CC BY). The use, distribution or reproduction in other forums is permitted, provided the original author(s) and the copyright owner(s) are credited and that the original publication in this journal is cited, in accordance with accepted academic practice. No use, distribution or reproduction is permitted which does not comply with these terms.



# Induced B Cell Development in Adult Mice

Anne-Margarete Brennecke<sup>1</sup>, Sandra Düber<sup>1</sup>, Bishnudeo Roy<sup>1</sup>, Irene Thomsen<sup>2</sup>, Annette I. Garbe<sup>1,3</sup>, Frank Klawonn<sup>4</sup>, Oliver Pabst<sup>2,5</sup>, Karsten Kretschmer<sup>1,6</sup> and Siegfried Weiss<sup>1,2\*</sup>

<sup>1</sup> Molecular Immunology, Helmholtz Centre for Infection Research, Braunschweig, Germany, <sup>2</sup> Medical School Hannover, Institute of Immunology, Hannover, Germany, <sup>3</sup> Osteoimmunology, DFG-Center for Regenerative Therapies Dresden, Center for Molecular and Cellular Bioengineering, Technische Universität Dresden, Dresden, Germany, <sup>4</sup> Biostatistics Group, Helmholtz Centre for Infection Research, Braunschweig, Germany, <sup>5</sup> Institute of Molecular Medicine, RWTH Aachen University, Aachen, Germany, <sup>6</sup> Molecular and Cellular Immunology/Immune Regulation, DFG-Center for Regenerative Therapies Dresden, Center for Molecular and Cellular Bioengineering, Technische Universität Dresden, Dresden, Germany

## OPEN ACCESS

### Edited by:

Rhodri Ceredig,  
National University of Ireland Galway,  
Ireland

### Reviewed by:

John Kearney,  
University of Alabama at Birmingham,  
United States  
Geoffrey Brown,  
University of Birmingham,  
United Kingdom

### \*Correspondence:

Siegfried Weiss  
siegfried.weiss@helmholtz-hzi.de

### Specialty section:

This article was submitted to  
B Cell Biology,  
a section of the journal  
*Frontiers in Immunology*

Received: 01 June 2018

Accepted: 08 October 2018

Published: 31 October 2018

### Citation:

Brennecke A-M, Düber S, Roy B, Thomsen I, Garbe AI, Klawonn F, Pabst O, Kretschmer K and Weiss S (2018) Induced B Cell Development in Adult Mice. *Front. Immunol.* 9:2483.  
doi: 10.3389/fimmu.2018.02483

We employed the B-Indu-Rag1 model in which the coding exon of recombination-activating gene 1 (Rag1) is inactivated by inversion. It is flanked by inverted loxP sites. Accordingly, B cell development is stopped at the pro/pre B-I cell precursor stage. A B cell-specific Cre recombinase fused to a mutated estrogen receptor allows the induction of RAG1 function and B cell development by application of Tamoxifen. Since Rag1 function is recovered in a non-self-renewing precursor cell, only single waves of development can be induced. Using this system, we could determine that B cells minimally require 5 days to undergo development from pro/preB-I cells to the large and 6 days to the small preB-II cell stage. First immature transitional (T) 1 and T2 B cells could be detected in the bone marrow at day 6 and day 7, respectively, while their appearance in the spleen took one additional day. We also tested a contribution of adult bone marrow to the pool of B-1 cells. Sublethally irradiated syngeneic WT mice were adoptively transferred with bone marrow of B-Indu-Rag1 mice and B cell development was induced after 6 weeks. A significant portion of donor derived B-1 cells could be detected in such adult mice. Finally, early VH gene usage was tested after induction of B cell development. During the earliest time points the VH genes proximal to D/J were found to be predominantly rearranged. At later time points, the large family of the most distal VH prevailed.

**Keywords:** bone marrow, RAG, B cell development, B-2/B-1a/B-1b, antibodies, CSR, T-dependent/-independent, VH usage

## INTRODUCTION

B cells are key players in adaptive immunity. However, they also play an important role as innate-like effector cells (1). Various subpopulations can be defined according to these functions. This is also reflected by specific sets of surface markers that are diagnostic for such particular B cell subpopulations. Thus, subpopulations like B-1a, B-2, and marginal zone (MZ) B cells in the spleen and B-1a, B-1b, and B-2 cells in the peritoneal cavity can be distinguished.

In adulthood, B cells continuously arise from hematopoietic stem cells (HSCs) that reside mainly in the bone marrow (BM). In contrast, in the fetus the liver is the major B cell generating organ (2).

In earlier studies, it was suggested that the B-1a cell population could only develop during the fetal stage and is maintained by self-renewal (3). This was based on findings where B-1a cells could not be detected after adoptive transfer of adult BM cells. However, more recently several groups have demonstrated the existence of BM-residing precursor cells that could give rise to B-1a cells even in adult mice (4, 5). Thus, adult BM sustains the potential to give rise to B-1a cells. Nevertheless, a contribution of such precursor cells to the pool of adult B-1a cells in unmanipulated adult mice has not been clearly shown yet.

Development of B-2 cells in the adult BM has been studied very extensively. Cellular markers and status of immunoglobulin rearrangement at the various stages have been established and correlated. In brief: the early committed B cell precursors known as proB/preB-I cells can be identified by the expression of c-kit and B220 and partial lack of CD19 (6). This stage is followed by the stage of large cycling pre-B-II cell ( $B220^+CD25^+$ ), then of the stage of small preB-II cell ( $B220^+CD25^+$ ) and finally the stage of the immature B cell ( $B200^+sIgM^+$ ). At such developmental stages, rearrangement and expression of the immunoglobulin gene segments takes place in an ordered fashion i.e., DJ and VDJ at the pro-B/preB-I, preB cell receptor expression at the large preB-II and rearrangement of gene segments of the light (L) chain loci at the small preB-II cell stage. Subsequently, immature B cells are the first B cells to express surface IgM. They emigrate from the BM and complete their development to mature B cells ( $CD19^+CD93^-IgM^+$ ) in the peripheral lymphoid organs in two clearly discernable transitional steps: T1,  $CD19^+CD93^+IgM^+CD23^-$ , and T2,  $CD19^+CD93^+IgM^+CD23^+$  (7).

To study B cell development, we have established a new recombinant mouse system—B-Indu-Rag1 (8). In such mice, B cell development is arrested in the pro-B cell stage due to an inversion of the coding exon 2 of the recombination-activating gene 1 (*Rag1*). In addition, the inversion is flanked by two loxP sites in opposite direction. These mice also express the recombinase Cre fused to a mutant estrogen receptor. It is driven by the B cell-specific *mb1* promoter. Hence, B cell development can be induced specifically. Upon application of Tamoxifen (TAM), the coding exon of the *Rag1* gene is inverted and expression of *Rag1* is activated. Thus, B cell development starts in a synchronized way. Since *Rag1* expression is initiated in a precursor cell that is not self-renewing, only a single wave of B cell development can be induced. Using such mice, it is possible to monitor several parameters of B cell development, like the minimal timing that developing B cell require for completion of particular stages, as well as the time that the majority of developing B cells remain in a particular stage. Only a rough estimate exists for the time that such processes require. Data from fetal liver exist on the timing required for B cell development from the c-kit<sup>+</sup> proB cell to the first IgM<sup>+</sup> B cell. It was estimated of roughly 6–7 days (9, 10).

The locus encoding the V regions of the murine heavy (IgH) chain contains 15 different VH families comprising more than 100 different individual gene segments (11, 12). It was claimed that during fetal development of B cells, the V gene segments most proximal to the constant (C) region are used

first (13). The explanation given suggested that activation of particular V gene families for rearrangement might require different signals. Proximal V gene segments should become accessible first because V genes more distal to Cμ would require the presence of IL-7 for accessibility (14). Similar suggestions were made for early progenitors during adulthood (15, 16). We wanted to confirm these findings in the B-Indu-Rag1 mice, since early after induction of B cell development in such mice, the rearrangement process should be in synchrony (8). Rare rearrangements during the early phase might be diluted out under steady-state conditions or might be lost due to selection processes. Here, they should become detectable shortly after application of the inducer TAM in such mice.

In the present work, we used the B-Indu-Rag1 model to estimate the length of time that a B cell precursor requires to pass the various stages of B cell development in the adult. We could further show that, indeed, at the earliest time points after induction, preferentially the V gene segments most proximal to Cμ are rearranged. Finally, by adoptive transfer experiments into sublethally irradiated recipient mice, we show that B-1 cells arising from adult progenitors are able to contribute to the B-1 cell pool of adult mice.

## MATERIALS AND METHODS

### Mice

B-Indu-Rag1 mice were described in Duber et al. (8). CB20, Igα<sup>-/-</sup> (17) and RAG1<sup>-/-</sup> (18) mice were obtained from the Basel Institute for Immunology and kept under specific pathogen free conditions (SPF) in the animal facility of the Helmholtz Centre of Infection Research. BALB/c mice were purchased from Janvier (Le Genest-Saint-Isle, France). Mice, aged between 8 and 14 weeks were used for the experiments. For induction of B cell development or as control, 400 μl of a 20 mg/ml solution of TAM (Ratiopharm) in ClinOleic (Baxter) was administered orally. All animal studies were performed in strict accordance with German Animal Welfare legislation. All protocols were approved by the Institutional Animal Welfare Officer (Tierschutzbeauftragter), and necessary licenses were obtained from the regional license granting body (LAVES, permission number 33.9-42502-04-11/0390).

### Flow Cytometry and Adoptive Cell Transfer

Single cells were obtained by flushing lymphoid organs or the peritoneum of mice with ice-cold IMDM (Iscove's modified Dulbecco's medium, GibcoBRL/Invitrogen). Erythrocytes were lysed by incubation with ACK buffer (0.15 M NH<sub>4</sub>Cl, 10 mM KHCO<sub>3</sub>, 0.1 mM Na<sub>2</sub>EDTA, pH 7.2) for 2–3 min on ice. For the isolation of cells originating from blood, cardiac-blood was collected into 500 μl of PBS including 50 μl 1:100 diluted heparin 25,000 (Ratiopharm). Erythrocytes were lysed by adding Erythrocyte-lysis buffer (2.06 g Tris-base, 7.49 g NH<sub>4</sub>Cl in a total volume of 11 H<sub>2</sub>O, pH 7.2) for 5 min at RT. Cells were centrifuged for 5 min at 1,000 rpm 4°C. The supernatant was discarded and the steps were repeated until the cell pellet was white. For T cell transfer, 3 × 10<sup>6</sup> splenocytes, isolated from B cell-free Igα<sup>-/-</sup> mice (10–14 weeks old) were injected i.v. in a volume of 100–200

$\mu$ l sterile PBS into CB20 or RAG1 $^{-/-}$  mice and were analyzed by flow cytometry to confirm the composition (40–50% of T cells). For flow cytometric analysis, cells were resuspended in 1x PBS containing 2% FCS and 0.5 mM EDTA. Cells were stained with the following antibodies conjugated with fluorophors or biotin directed against: CD11b, CD3, CD4, CD5, CD8, CD25, CD40, CD23, CD93 (all eBioscience), B220, CD19, CD43, CD21, IgMa, IgMb (all BDPharmingen), IgD (clone 1.19, prepared in our lab). Biotinylated antibodies were revealed using various streptavidin conjugates (BD Biosciences or Southern Biotech). BrdU labeling at day 9 after TAM application and staining were performed exactly according to manufacturer's protocol (FITC BrdU Flow Kit, BDPharmingen). Flow cytometric analysis always included gating on lymphocytes, exclusion of doublets as well as exclusion of dead cells by DAPI staining. Analysis was carried out using an LSRII or Fortessa (Becton Dickinson). Data were analyzed using DIVA software (Becton Dickinson) or FlowJo. Cell sorting was carried out on a FACSAria (Becton Dickinson).

## Ig Concentration Measurements and ELISPOT

IgA concentration from intestinal wash out was determined by ELISA according to standard protocol (8) using goat anti-mouse IgA (Sigma) as coating antibody and peroxidase coupled goat anti-mouse IgA (Sigma) as detection antibody. Immunoglobulin concentrations from sera were measured using a kit according to the manufacturer's protocol (Mouse Immunoglobulin Isotyping Panel 6plex FlowCytomix Multiplex, eBioscience). Flow cytometry was carried out using analyser LSRII (Becton Dickinson). ELISPOPs were performed according to standard protocols (8). ELISPOPs detecting IgA and IgG secreting cells were performed according to the same protocol, using anti-IgA (clone C10-3, BD Pharmingen) or goat anti-mouse IgG (Sigma) as capturing antibodies and biotinylated anti-IgA (clone 11-44-2, eBioscience) or biotinylated goat anti-mouse IgG (MABTECH) as secondary antibodies.

## BM Transfer

For adoptive transfer, 8–12 weeks old B-Indu-Rag1 mice were used as donors. BM cells of both femurs were prepared and  $3 \times 10^6$  cells were injected i.v. into sublethally irradiated (5 Gy) 8-week-old Rag1 $^{-/-}$  or CB20 mice. B cell development in the recipients was induced by TAM application 6 weeks after irradiation and cell transfer and analyzed after 3 weeks.

## Nucleotide Sequence Analysis of V<sub>H</sub> Genes

Total RNA from BM cells from induced mice after 1–7 days and sorted BM cells from wild-type (Wt) mice was isolated using RNeasy MiniKit (Qiagen). cDNA synthesis was performed using RevertAid Reverse Transcriptase (Fermentas) using IgM-specific primers: 5'-ATGGCCACCAAGATTCTTATCAGA-3' and 5'-GAGGTGCAGCT GCAGGA GTCTGG-3'. For template library generation of IgM sequences, PCR with a primer binding in the constant  $\mu$  region (5'-CTATGCGCCTTG CCAGC CCGCTCAGA(MID)ATTGGGAAGGACTGA-3') in combination with a primer binding in the V<sub>H</sub> region of all

V<sub>H</sub> genes 5'-CGTATGCCCTCCCTCGCGCCATCAGGA GGT GCAGCTGCAGGAGTCTGG-3' was performed. MID (multiple identifier) consists of 4 nucleotides in 9 different variations for identification of single samples in a single lane. PCR conditions were as follows: 95°C, 1 min; 35x (95°C, 30 s, 55°C, 40 s, 72°C, 40 s); 72°C, 10 s. Amplicons were purified by gel extraction (QIAquick Gel Extraction kit; Qiagen). Sequencing by the 454 method and data analysis was done exactly as described (19).

## Curve Fitting

To model the development of the frequency of B cell subsets over time, three parametric functions were considered: The constant function  $f(t) = a$  with the only parameter  $a$ , representing no (significant) change over time the linear function  $f(t) = a \cdot t + b$  with two parameters for a linear increase or decrease over time and the bell-shaped parametric curve  $f(t) = a + b \cdot \exp((t - c)^2/d)$ . Parameters  $a$  and  $c$  can shift the curve in y- or x-direction, respectively; parameters  $b$  and  $d$  can stretch the curve in y- or x-direction, respectively. The bell shaped curve models an increasing behavior followed by a decrease or vice versa. A least squares approach was used to fit the curves to the data. In the case of the bell-shaped function being nonlinear in its parameters, the fitting was carried out with the function optim within the statistics software R (20). It would not be meaningful to base the choice of the best of the three models on the error, i.e., the mean squared error because the most complex model—here the bell-shaped function—would always yield the smallest error. The corrected Akaike information criterion (AIC) (21) is a method used for choosing the most suitable model among—usually linear—parametric functions of different complexity in terms of the numbers of parameters. The corrected AIC evaluates the different parametric functions based on the variance of the residuals, the number of parameters and the sample size. Especially for small sample sizes as considered here, using the residuals directly would favor parametric functions with a tendency to overfitting. Therefore, the variance of the residuals was estimated based on leave-one-out cross-validation. With leave-one-out cross-validation the residual at each point for a parametric function is computed by removing the point from the data set, computing the corresponding parameters of the function based on the remaining data points and then taking the residual of the point that was not involved in the parameter estimation. This is repeated for each data point and each of the three parametric functions. The bell-shaped parametric curve is not only a nonlinear function but also nonlinear in its parameters, making it much more flexible than the constant and the linear model. To account for this extreme flexibility and not favor the bell-shaped curve, each of the four parameters of the bell-shaped function was counted twice for the corrected AIC.

## Statistical Analysis

Statistical analysis was done using a *Mann-Whitney-U-test* or a two-tailed Student *t-test*. A *p* value < 0.05 was considered statistically significant.

## RESULTS

### Development of B Cell Progenitors in the BM of Adult Mice

We intended to use the power of the B-Indu-Rag1 mice to establish or to confirm parameters of B cell development in the adult mouse. First, we estimated the timing that proB/preB-I cells need for their developmental progression to the subsequent stages of the B cell lineage. B-Indu-Rag1 mice were induced once with TAM and at different time points cells were isolated from different tissues and analyzed by flow cytometry (**Supplementary Figure S1**). A first increase in percentage of progenitor cell could be detected from day 5 on for the large preB-II cells ( $B220^+AA4.1^+CD25^+CD40^-IgM^-$ ; **Figure 1A** and **Supplementary Figure S2**). Similarly, a first increase could be observed for small preB-II cells ( $B220^+AA4.1^+CD25^+CD40^+IgM^-$ ; **Supplementary Figure S2A**) at day 6 (**Figure 1A** and **Supplementary Figure S2A**). At days 7 and 11 the respective subset reached maximum (**Figure 1A** and **Supplementary Figure S2A**). By applying least square analysis, a time span of day 8 to day 13 could be defined, in which the majority of small preB-II cells were found. Since B cell development was induced only once (i.e., by a single-dose administration of TAM), the percentages of the preB cell subsets declined after reaching the peak. No further differentiation from proB/preB-I cell is expected to replenish the preB-II cell compartment.

Immature B cells (T1 and T2) migrate out of the BM via the blood stream into the spleen where they further mature (22). Both subsets are  $CD19^+AA4.1^+$  (**Supplementary Figure S1B**). Due to expression of CD23 and IgM it is possible to distinguish these two populations (23). After TAM application, the first T1 cells could be detected at day 6 in the BM, while T2 cells required one day more (**Figure 1B** and **Supplementary Figure S2B**). In blood, such cells appeared roughly at the same time: in contrast, appearance in spleen was detected with a delay of one-day for both subsets. Highest percentage of transitional B cells was found between day 10 and 12 in all locations analyzed. The peak at day 11 for blood and day 12 for spleen (**Figure 1B**) was confirmed by least square analysis (**Supplementary Figure S2B**). In addition, in all particular locations specific cells were detected first in the T1 and then in the T2 compartment. This confirms the notion of a stepwise maturation of transitional B cells from T1 to T2 (23, 24).

The sequential maturation also became clear, when comparing the relative cellularity in the T1 and T2 compartments. Due to continuous generation and maturation in adult WT mice, the ratio between the two different transitional B cell subsets remained equal over time. Since B cell maturation in B-Indu-Rag1 mice starts with the time of induction, the ratio changes over time (**Figure 1C**). Interestingly, in BM the ratio declined nearly to zero at day 15. This verified that transitional B cells first develop in the BM and later on migrate into the periphery (**Figure 1C**).

Proliferation of T1 and T2 cells without exogenous B cell receptor (BCR) stimulation has been described before (25). Proliferation of such cells suggested expansion of both B cell

populations during this stage. To confirm population expansion by proliferation of transitional B cells in the B-Indu-Rag1 model, we used BrdU incorporation. We expected that proliferative expansion would take place before the population reaches peak levels. Thus, we analyzed the cells at day 9 after induction. In blood, no proliferating transitional B cells were detected. In contrast, strong proliferation of T1 B cells could be found in BM and minor proliferation in spleen (2 and 0.1%, respectively; **Figure 1D**). No BrdU incorporation in T2 cells could be observed under these conditions (data not shown).

### First Detection of Mature B Cells as Early as 11 Days Post-induction

Immature B cells migrate from BM to the spleen to continue further maturation (22, 26). To determine the time frame for these events, the first appearance of mature B cells was analyzed. Mice were treated once with TAM and the presence of B cell populations in different locations was monitored in kinetics studies (day 5, 6, 7, 11, 15, and 21 after induction). In spleen, all mature B cells are  $CD19^+$ , and due to their differential expression of CD21, CD23 and CD5, they can be divided into the different subsets (**Supplementary Figure S3**). All B cell subsets could be found in significant numbers at day 15 after TAM administration (**Figure 2A** and **Supplementary Figure S4**). While with time percentages of B-1a and MZ cells approached the percentages found in WT mice, the percentage of B-2 cells remained relatively low compared to WT mice. This might be due to the self-renewing capacity of B-1a and MZ B cells. By analyzing BrdU incorporation 15 days post induction in spleen and PeC, hardly any proliferating  $CD19^+$  B cells could be detected at these locations (**Figure 2B**). In general, the percentages of B-1a and MZ cells in spleen (induced mice: 0.3 and 3%, respectively) were much lower, as compared to the B-2 cell population (induced mice: up to 10%; **Figure 2A**; **Supplementary Figure S4**).

Some mature B cells, after maturation in the spleen, migrate back to the BM (24). Consequently, we analyzed the minimal time mature B cells require to develop and to migrate back to the BM. To this end, we divided B cells into two populations: both express CD19, but one population, mainly B-2 cells, are  $IgM^+IgD^+$  and the other, consisting of B-1 cells, is  $IgM^{hi}IgD^{lo}$ . It is thought that especially  $IgM^+IgD^+$  B cells in the BM are the major population that matures in the spleen and recirculates back to the BM (27). Indeed, we could show that this population increased over time (**Figure 2A**). The first mature  $IgM^+IgD^+$  cells can be detected 15 days post induction in the BM (**Figure 2A** and **Supplementary Figure S2**). In general, and similar to WT mice, only very low percentages of  $IgM^{hi}IgD^{lo}$  B cells could be detected in the BM (max. 0.6% in WT mice; data not shown). The major mature B cell population in the BM consists of  $IgM^+IgD^+$  B cells. In induced mice, the  $IgM^+IgD^+$  population rose only up to 0.6%, whereas it is roughly 7% in Wt mice (**Figure 2A**).

The main producers of natural IgM are B-1a cells. They can react to T cell-independent stimulation and act as innate-like cells (28). Their task in the immune system is to quickly produce antibodies upon infection. In contrast to B-2 cells, B-1a cells are self-renewing and their progenitors are mainly found in fetal

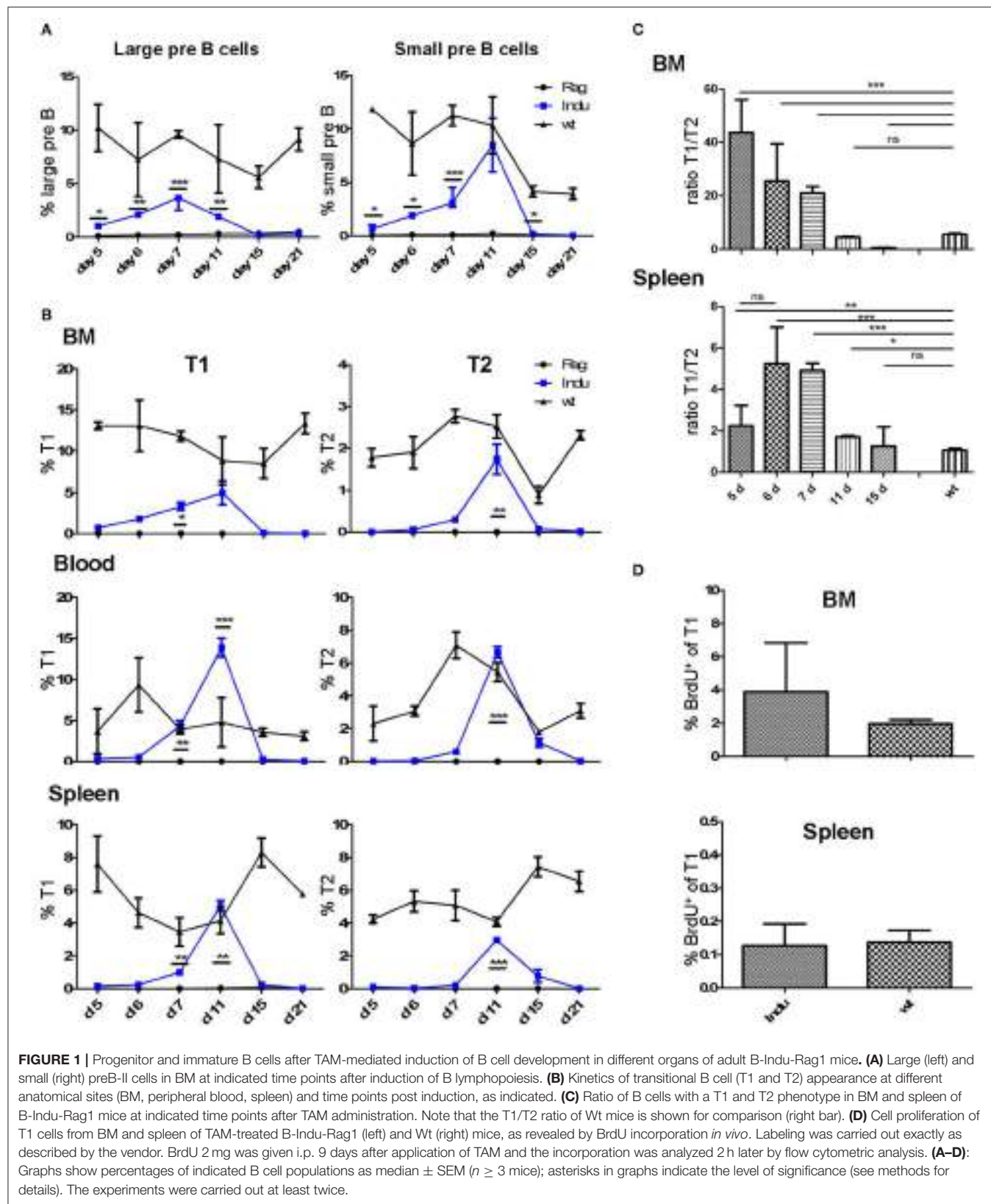


**FIGURE 1 |** Progenitor and immature B cells after TAM-mediated induction of B cell development in different organs of adult B-Indu-Rag1 mice. **(A)** Large (left) and small (right) preB-II cells in BM at indicated time points after induction of B lymphopoiesis. **(B)** Kinetics of transitional B cell (T1 and T2) appearance at different anatomical sites (BM, peripheral blood, spleen) and time points post induction, as indicated. **(C)** Ratio of B cells with a T1 and T2 phenotype in BM and spleen of B-Indu-Rag1 mice at indicated time points after TAM administration. Note that the T1/T2 ratio of Wt mice is shown for comparison (right bar). **(D)** Cell proliferation of T1 cells from BM and spleen of TAM-treated B-Indu-Rag1 (left) and Wt (right) mice, as revealed by BrdU incorporation *in vivo*. Labeling was carried out exactly as described by the vendor. BrdU 2 mg was given i.p. 9 days after application of TAM and the incorporation was analyzed 2 h later by flow cytometric analysis. **(A–D):** Graphs show percentages of indicated B cell populations as median  $\pm$  SEM ( $n \geq 3$  mice); asterisks in graphs indicate the level of significance (see methods for details). The experiments were carried out at least twice.

liver. Nevertheless, also in adult BM some B-1a progenitors are present (5, 8, 29). Therefore, we expected to find newly developed B-1a cells in the periphery after induction (8). Similarly, we also expected to find B-2 and B-1b cells after induction. The latter is normally enriched in the peritoneal cavity. At this anatomical site, we could detect B-2 cells ( $CD19^+CD43^-CD11b^-CD5^-$ ) first around 11 days after TAM induction, whereas the B-1 cell subsets were found roughly from day 15 onwards (Figure 2A and Supplementary Figures S4, S5). While the percentages of B-1a ( $CD19^+CD43^+CD11b^+CD5^+$ ) and B-2 cells were not reaching the level of Wt mice, the percentage of B-1b cells ( $CD19^+CD43^+CD11b^+CD5^-$ ) in the peritoneal cavity was rising above Wt-level as seen before (17% compared to 6% after 8 weeks, Figure 2A and Supplementary Figure S5) (8). Eight weeks after induction, also the absolute number of B-1b cells in induced mice was reaching the level of Wt mice. In contrast, the absolute numbers of the other subsets never reached WT-level.

Importantly, at this time point the increase of mature B cell populations cannot be attributed to cell proliferation, as we detected no increased BrdU incorporation (Figure 2B). Therefore, the question remained where the higher percentages, especially of B-1b cell population arise from over time. No progenitors can be detected after day 11 and the transitional B cell subsets also vanished at day 21 (Figure 2B).

## Ig's Increase Over Time in Serum and Gut

To analyse the functionality of the B cell populations after TAM induction, we investigated their ability to produce Ig's. Thus, the Ig concentration in serum of the different mouse groups was determined. Similar to the increase of the B cell subsets in the different organs, Ig's became first detectable at day 15 after induction (Figure 3A). However, this was found only for IgM, IgG2a, and IgG3. The IgA and IgG2b subclasses could first be detected in significant amounts after 21 days of TAM induction. IgG1 was not increasing significantly at all. At the same time, the highest concentration could be detected for IgM with a tendency to reach WT levels. This is the only Ig that rises to a concentration of 50  $\mu$ g/ml. All other Ig subclasses did not rise above 1  $\mu$ g/ml within the observation time (Figure 3A). Obviously, efficient switching of B cells to other Ig subclasses was not supported in B-Indu-Rag1 mice, most likely due to the lack of T cell help.

Intestinal IgA might be mainly derived from B2 cells that were triggered in the Peyer's Patches or mesenteric lymph nodes and, after differentiation, migrated into the lamina propria (LP). In addition, B-1 cells are claimed to be able to migrate to intestinal LP (24). For some time, it was believed that B-1 might be key players in intestinal immune responses by switching to IgA-secreting cells in a T cell-independent manner (24). However, recently it was shown that LP-derived IgA<sup>+</sup> cells might not be derived from peritoneal B-1a, but rather from B-1b cells (30). To analyse the functionality of B cells in the induced mice in more detail and to investigate the kinetics of IgA accumulation in the gut, intestinal washout was analyzed at 11, 15, and 21 days after induction. In such mice, nearly no IgA in the intestinal wash out became detectable (Figure 3B). Only 230 ng/ml at day 21 after

induction could be determined, as compared to 500  $\mu$ g/ml in Wt mice during steady state.

IgM in serum of the induced mice was most likely due to an overall increase in the numbers of B cells actively secreting IgM. In contrast, a few B cells could be present that secrete high amounts of IgM, which then accumulate over time. Therefore, we performed ELISPOTs of B cells at different time points from spleen and BM, in the absence of any deliberate stimulation *in vitro*. The number of IgM secreting cells was increasing over time in the spleen (Figure 3C). While only 15 IgM-secreting cells/ $10^5$  cells were detectable in spleen 11 days after TAM induction, this number increased to 125 IgM-secreting cells/ $10^5$  cells at day 21. In the BM, at day 11, only very low numbers of IgM-secreting cells could be detected in the induced mice. This suggested that IgM-secreting cells in spleen might be short-lived plasma cells. Long lived plasma cells are expected to migrate to BM (Figure 3C). However, plasma blasts derived from B-1a cells might behave differently.

## T Cells Help to Increase B Cell Numbers Mainly in Spleen

To differentiate into an antibody secreting plasma cell or a memory B cell, B-2 cells require help from T cells. This takes place in secondary lymphoid organs, like spleen or lymph nodes. In addition, the cytokine-milieu that is available during the activation of a B cell is decisive for the class and subclass of Ig expressed after differentiation (31, 32). To analyse the T cell requirement for efficient development of such B cells, T cells were adoptively transferred into B-Indu-Rag1 mice 1 day before TAM administration. The presence of various B cell subsets was analyzed by flow cytometry 3 and 8 weeks after induction. In BM, nearly no mature B cells could be detected, independent of whether T cells were transferred or not (Figure 4). In spleen, B-1a cells were found in significantly higher numbers, when T cells were available (Indu+T) than without T cell transfer (Indu; Figure 4). For MZ B cells, this was only true for the later (8 weeks) time point, while B-2 cells were found to be increased at both time points (3 and 8 weeks). In peritoneal cavity, only a slight influence of the T cells on the numbers of B cells was observed (Figure 4).

As T cells obviously influence the development and differentiation of B cells, their effect on Ig secretion was investigated. Serum from mice taken at different time points after induction was analyzed. No differences in IgM concentrations between Indu and Indu+T could be observed (Figure 5A). In contrast, for all other Ig's (IgA, IgG1, IgG2a, IgG2b, and IgG3), marked differences were found. For each class or subclass, the concentration was significantly higher at day 21 post induction, when T cells were available. Analyzing later time points, no significant differences could be observed any more, except for IgA. Here, a significant higher concentration in T cell-reconstituted mice became apparent at 8 weeks post induction (Figure 5A).

Similarly, in intestinal wash outs, the IgA concentration was altered: at 3 or 8 weeks after TAM induction, mice that received adoptively transferred T cells consistently showed higher IgA concentrations, as compared to mice without T cells (Figure 5B).

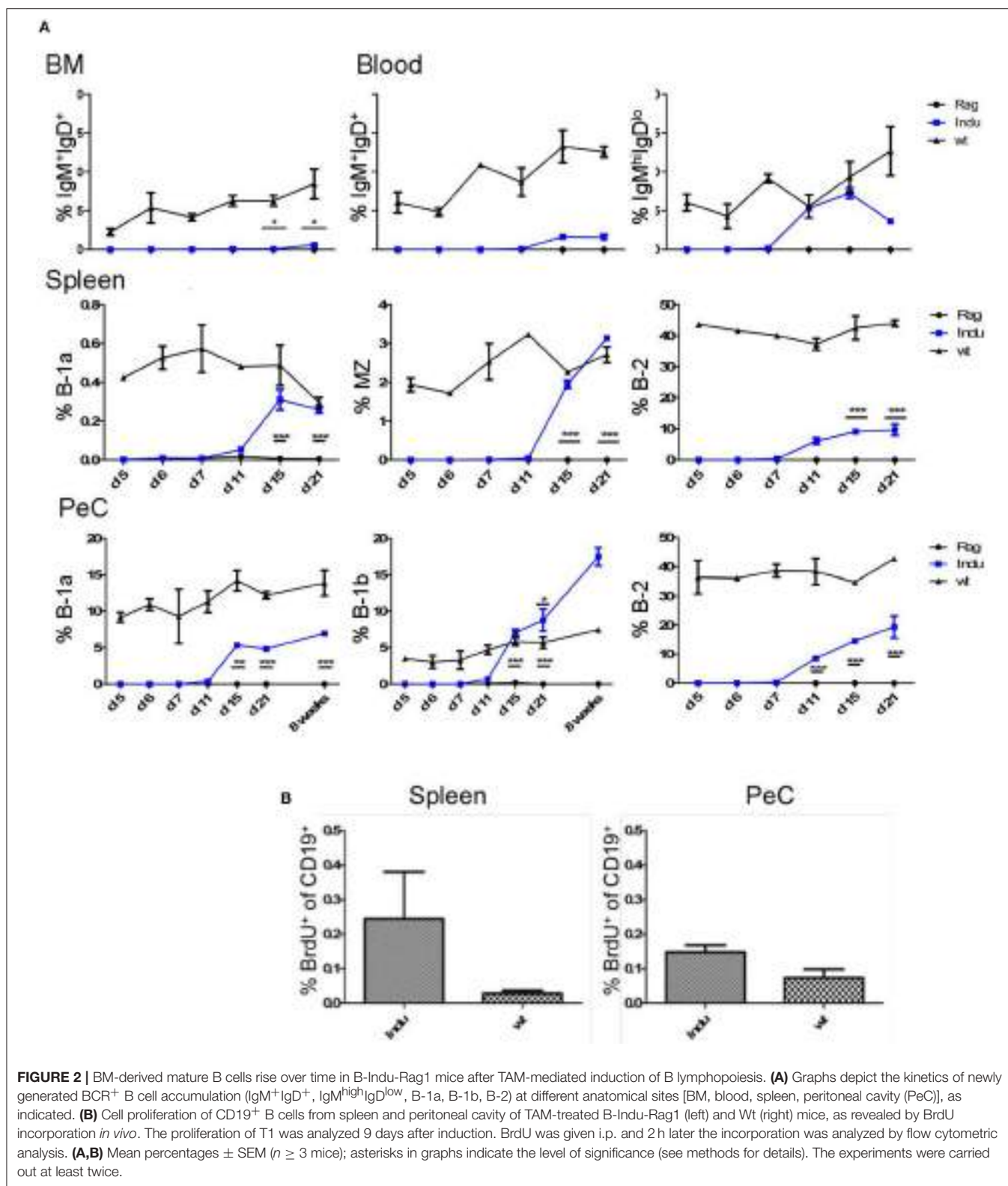


**FIGURE 2 |** BM-derived mature B cells rise over time in B-Indu-Rag1 mice after TAM-mediated induction of B lymphopoiesis. **(A)** Graphs depict the kinetics of newly generated BCR<sup>+</sup> B cell accumulation ( $\text{IgM}^+\text{IgD}^+$ ,  $\text{IgM}^{\text{high}}\text{IgD}^{\text{low}}$ , B-1a, B-1b, B-2) at different anatomical sites [BM, blood, spleen, peritoneal cavity (PeC)], as indicated. **(B)** Cell proliferation of CD19<sup>+</sup> B cells from spleen and peritoneal cavity of TAM-treated B-Indu-Rag1 (left) and Wt (right) mice, as revealed by BrdU incorporation *in vivo*. The proliferation of T1 was analyzed 9 days after induction. BrdU was given i.p. and 2 h later the incorporation was analyzed by flow cytometric analysis. **(A,B)** Mean percentages  $\pm$  SEM ( $n \geq 3$  mice); asterisks in graphs indicate the level of significance (see methods for details). The experiments were carried out at least twice.

In addition to higher serum concentration, the number of Ig-secreting cells was increased when T cells were available (Figure 5C). This held true for IgA and IgG, while numbers

of IgM-secreting cells appeared largely similar, irrespective of whether or not TAM-induced mice were adoptively transferred with T cells (Figure 5C).

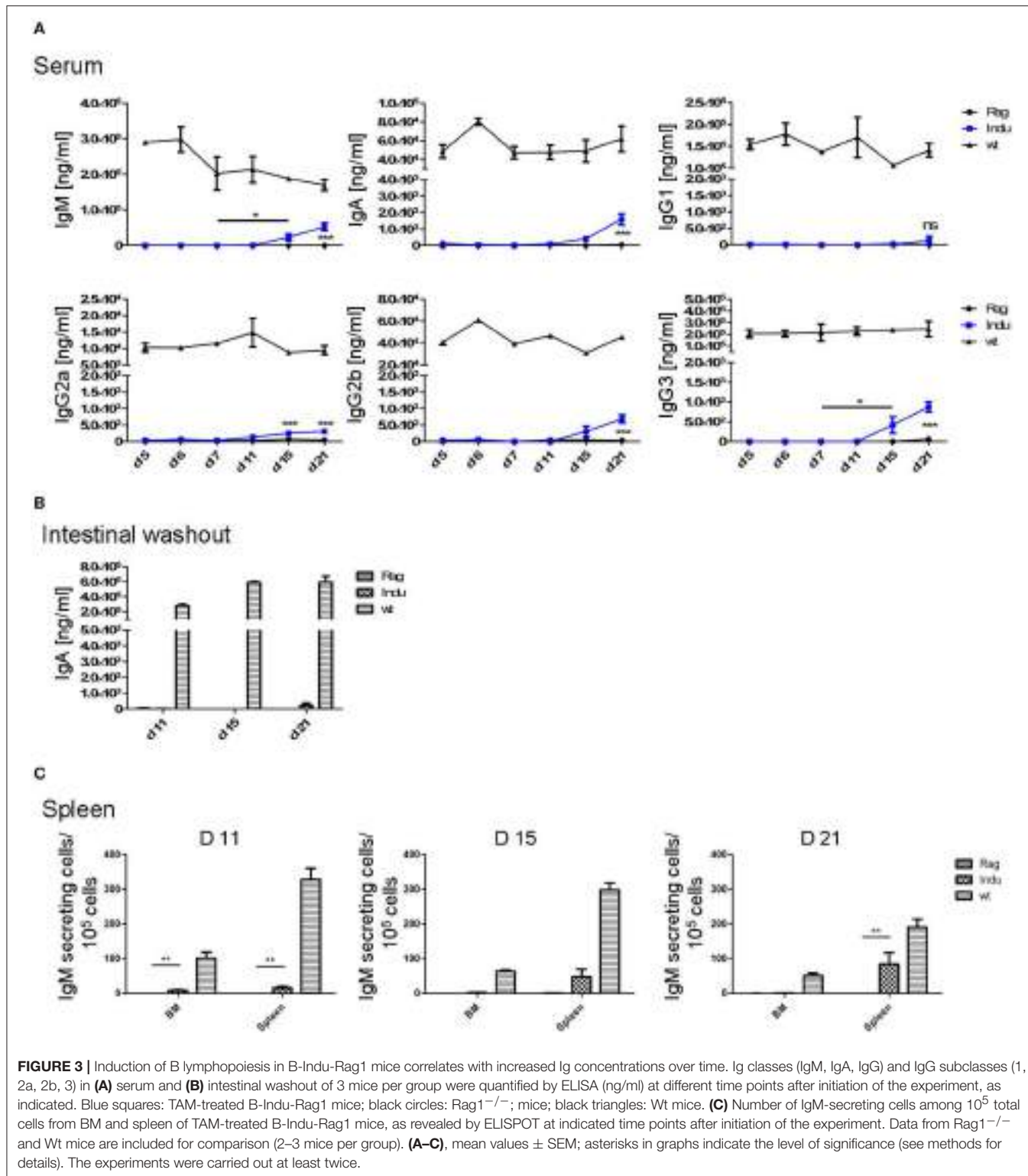
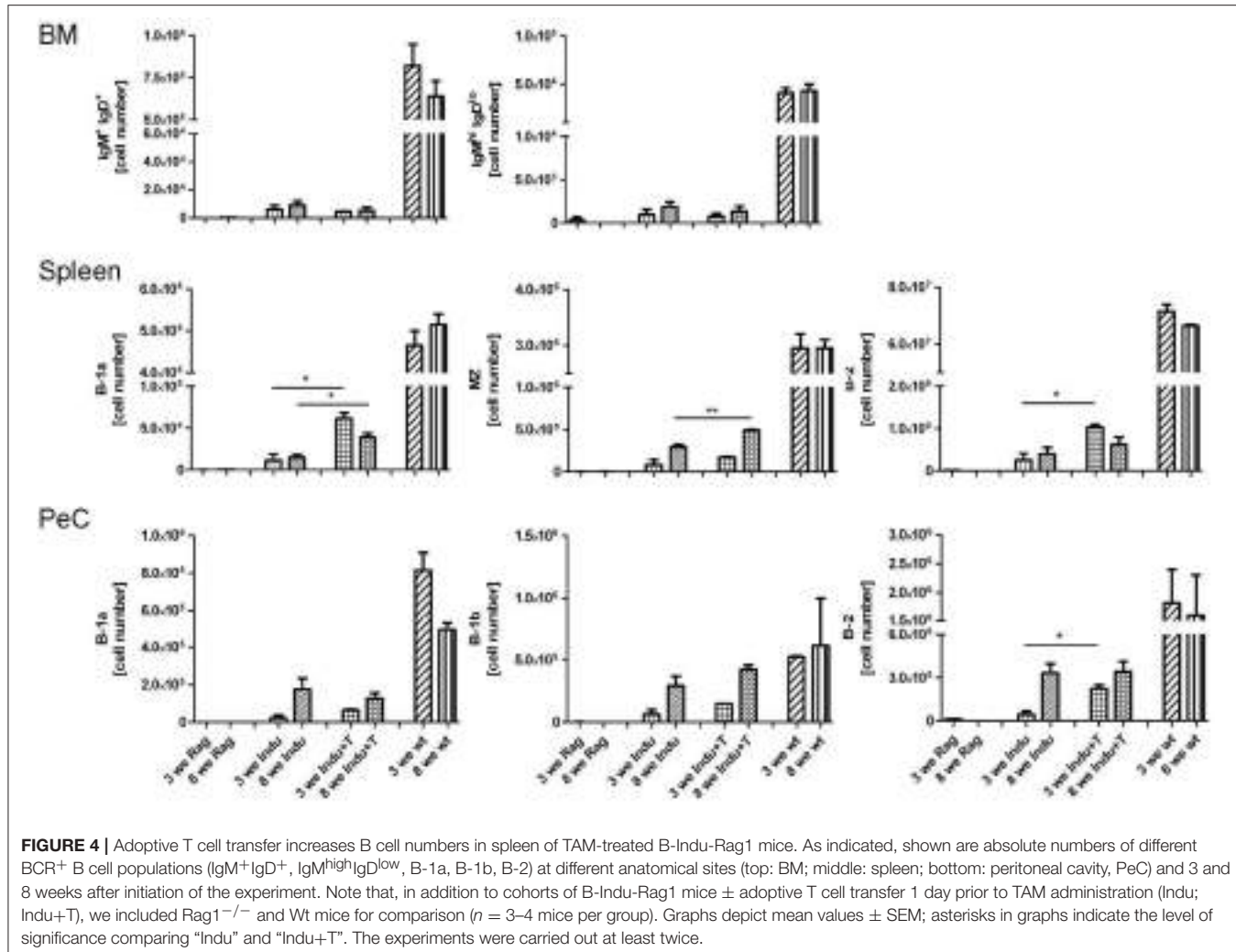


**FIGURE 3 |** Induction of B lymphopoiesis in B-Indu-Rag1 mice correlates with increased Ig concentrations over time. Ig classes (IgM, IgA, IgG) and IgG subclasses (1, 2a, 2b, 3) in (A) serum and (B) intestinal washout of 3 mice per group were quantified by ELISA (ng/ml) at different time points after initiation of the experiment, as indicated. Blue squares: TAM-treated B-Indu-Rag1 mice; black circles: Rag1<sup>-/-</sup>; mice; black triangles: Wt mice. (C) Number of IgM-secreting cells among  $10^5$  total cells from BM and spleen of TAM-treated B-Indu-Rag1 mice, as revealed by ELISPOT at indicated time points after initiation of the experiment. Data from Rag1<sup>-/-</sup> and Wt mice are included for comparison (2–3 mice per group). (A–C), mean values  $\pm$  SEM; asterisks in graphs indicate the level of significance (see methods for details). The experiments were carried out at least twice.

## B Lymphopoiesis in Adult BM can Contribute to the Peripheral B-1a Cell Pool

B-1a cells can arise from adult BM (5, 29), as was also shown using the B-Indu-Rag1 model (8). Similarly, in the present study

we could show that readily detectable numbers of B-1a cells can arise from adult murine BM, in which only B cell development is possible and T cells are completely absent. Such adult BM-derived B-1a cells were functional, as they spontaneously



secrete IgM, show PtC specificity and can survive for extended time periods in Rag1<sup>-/-</sup> recipients after adoptive transfer (8). Thus far, the question whether B-1a cells still arise in adult mice was mainly approached in lymphopenic mice. Whether they also arise in a normal immunocompetent environment, is still not completely answered. In an effort to experimentally recapitulate physiological conditions as closely as possible, Rag1<sup>-/-</sup> or CB20 mice (IgM<sup>b</sup>) were sublethally irradiated and subsequently reconstituted with total BM cells isolated from B-Indu-Rag1 mice (IgM<sup>a</sup>). Mice were kept for 6 weeks to allow recovery and re-establishment of a functional BM environment. Then, mice were induced once with TAM, followed by flow cytometric analysis of B cell subsets in peritoneal cavity after 21 days.

As expected, the majority of B cells in the peritoneal cavity of CB20 recipients was derived from endogenous IgM<sup>b</sup> progenitors (Figure 6A). However, we could also detect IgM<sup>a</sup>+ B cells derived from the donor BM (Figure 6A). In immune-compromised Rag1<sup>-/-</sup> mice, in which the endogenous BM does not contribute to B cell development, B-1 cells dominated over

B-2 cells (Figure 6B). Similar results had been obtained in TAM-treated B-Indu-Rag1 mice without T cell transfer (Figure 2). In contrast, in CB20 mice with a functional endogenous B cell compartment, nearly all newly developed donor-derived B cells could be assigned to the B-2 cell subset (77%). Nevertheless, donor-derived B-1a cells as well as B-1b cells could be found in the peritoneal cavity of such mice. The percentage of B-1a and B-1b cells was much lower, when B cell development was induced in mice with endogenous B cell development (B-1a: 27 to 6%; B-1b: 18 to 5%, Figure 6B). A similar situation was observed in the spleen: nearly all B cells were IgM<sup>b</sup>+ as they arose from recipient progenitors and only a minor population was donor-derived (data not shown). Taken together, precursors in the adult BM most likely continued to contribute to the mature peripheral pool of B-1a cells. Thus, our data indicated that the development of B-1 cells is supported in the adult, even when a complete immune environment exists. However, and as expected, B-1 cell development was severely downscaled under these conditions (Figure 6B), perhaps due to competition with developing B-2 cells.

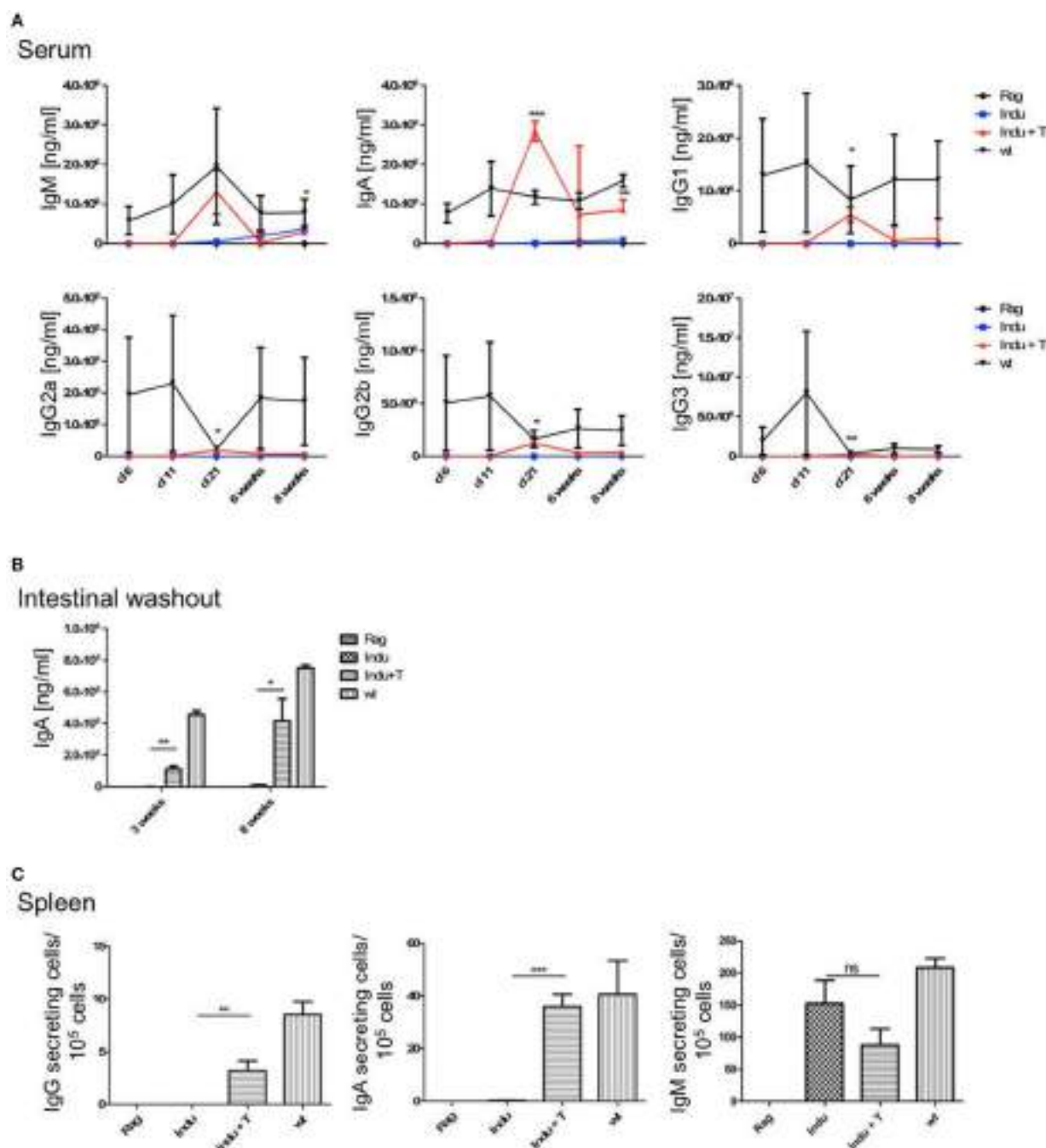
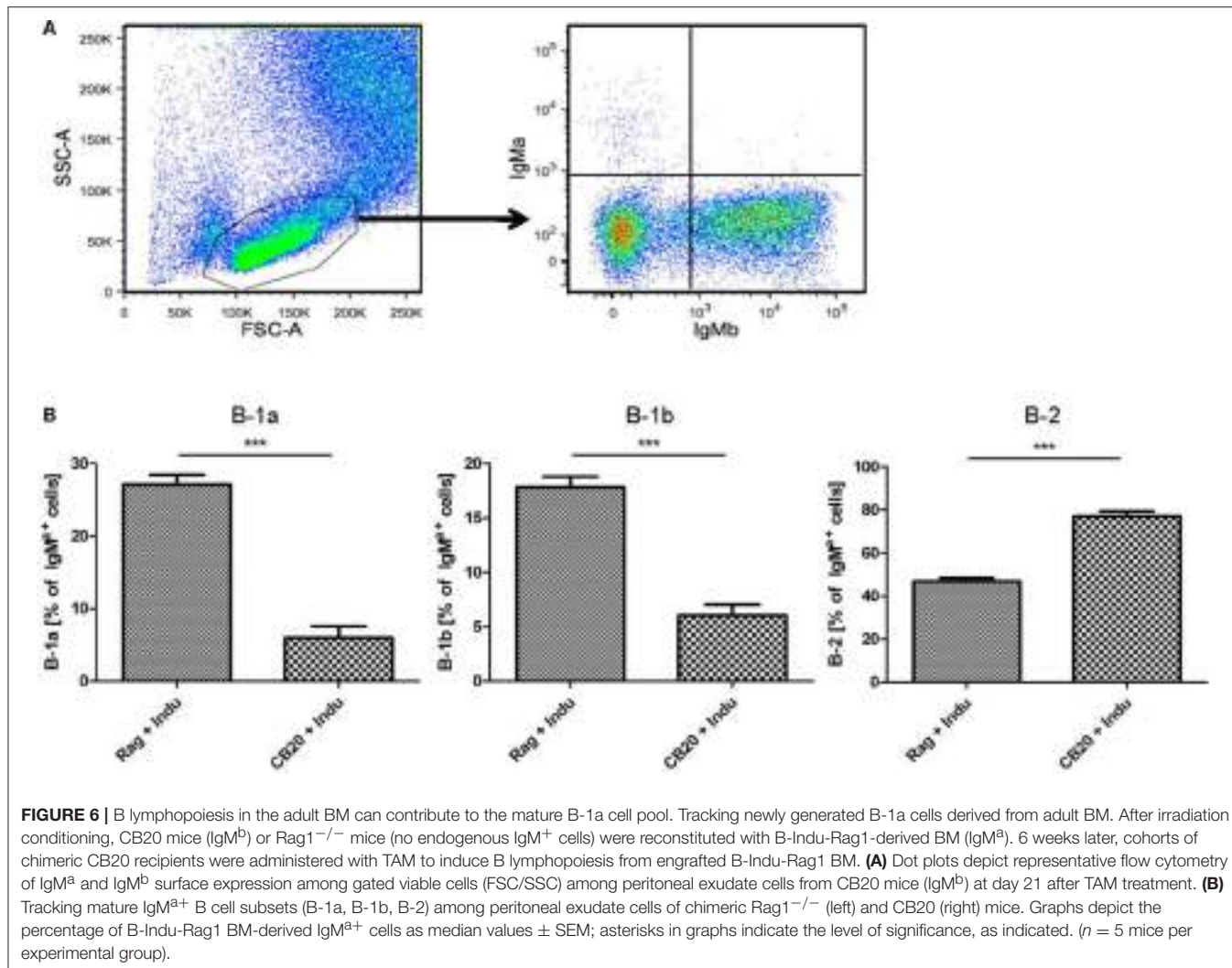


**FIGURE 5 |** T cell transfer enhances Ig secretion by newly generated B cells. See legends to **Figures 3, 4** for experimental details. In brief, at indicated time points after initiation of the experiment, mouse cohorts described in **Figure 4** were subjected to ELISA-based Ig quantification in **(A)** serum ( $n = 2\text{--}4$  mice per group) and **(B)** intestinal washout ( $n = 3$ ). **(C)** Number of Ig-secreting B cells determined by ELISpot. Graphs depict Ig concentrations (ng/ml) or number of Ig-producing cells as median values  $\pm$  SEM; asterisks in graphs indicate the level of significance comparing “Indu” and “Indu+T”.

## Preferential Usage of Proximal V<sub>H</sub> Genes in the Adult BM

In B-Indu-Rag1 mice, shortly after TAM-mediated induction of B cell development, the process of IgH chain rearrangement to generate functional pre-BCRs should be in synchrony (8).

Such initial VDJ recombination processes might be obscured under steady-state conditions in WT mice. Therefore, we next analyzed the rearrangement kinetics during TAM-induced B lymphopoiesis in the BM of B-Indu-Rag1 mice. Total BM cells were harvested daily from day 1 after TAM administration up



to day 7. Gene-specific RT-PCR to assess  $V_H$  gene expression after rearrangement was carried out. For analysis, sequences of the PCR products were established. In addition, sorted large and small preB cells (**Supplementary Figure S2A**), isolated from control WT (BALB/c) BM cells were included for comparison. Interestingly, the experiment revealed that the preference of  $V_H$  usage varies over time (**Figure 7A**). At early time points, relatively few rearrangements involved the IgHV<sub>1</sub> (former J558) family. This is the largest family that is found 5' and most distal from the D and J gene cluster. In contrast, the proximal  $V_H$  families were found to be predominantly rearranged. At later time points, however, almost half of the detected VDJ rearrangements involved the IgHV<sub>1</sub> family. Similar data had been described for B cells derived from fetal liver (13). When large and small preB-2 cells subsets from WT mice were analyzed for comparison (i.e., developing B cells in steady state), the data were comparable to those obtained at late time points from BM cells of TAM-induced B-Indu-Rag1 mice (**Figure 7B**). Thus, our experiments using the B-Indu-Rag1 model confirmed the notion that B cells at their initial developmental phase preferentially

engage proximal  $V_H$  gene segments for rearrangement. Only when rearrangement is not taking place at this initial stage they also deviate usage to the distal  $V_H$  families.

## DISCUSSION

The Indu-Rag1 mouse represents a highly versatile system to study various aspects of T and B cell development. For instance, when the Indu-Rag1 mouse is crossed to a mouse expressing a fusion of the Cre recombinase with a mutated estradiol receptor driven by the ubiquitously active Rosa26 promoter, induction of Cre activates Rag1 expression in HSCs. Since such cells are self-renewing, continuous T and B lymphopoiesis can be initiated. This approach has been recently used to characterize IL-17-producing  $\gamma\delta$  T cells (33) and early developmental stages of thymus-derived FoxP3<sup>+</sup> T cells (34). In the present work, the Cre recombinase is driven by the B cell-specific mb-1 promoter. Cre is flanked on both sites with a mutated estradiol receptor, which renders its expression tightly controlled and inducible by TAM.

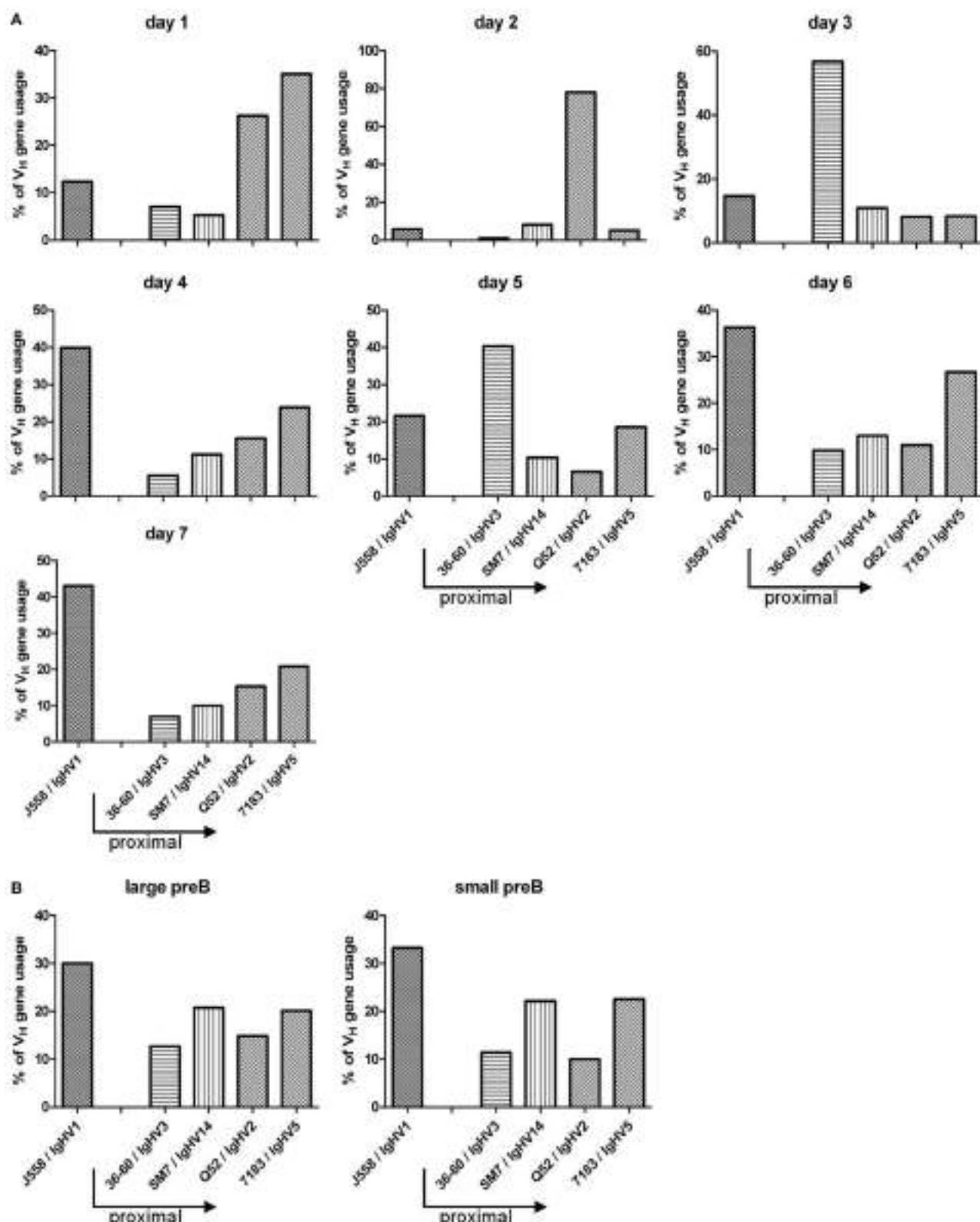


**FIGURE 7 |** TAM-induced early B cell development in the adult BM is strongly biased toward VDJ rearrangements that involve proximal VH gene segments. **(A)** Kinetics of VH gene usage in the BM of B-Indu-Rag1 mice after induction of B lymphopoiesis, as revealed by analysis of sequenced RT-PCR products at indicated time points after TAM administration. Mean number of analyzed sequences: 407. **(B)** Quantification of VH gene usage in FACS-purified populations of large and small preB-II cells from BM of Wt mice (BALB/c) with continuous B cell development. Mean number of analyzed sequences: 472. Arrows in graphs indicate the position of individual VH gene families relative to the D/J clusters of the murine IgH gene locus (proximal to D/J: 36-60, SM7, Q52, 7183; distal: J558).

By and large, no B cell development can be observed under non-inducing conditions, consistent with the severe developmental block at the pro/preB cell stage. TAM application leads to a single wave of development because pro-B cell precursors with activated *Rag1* gene expression are not self-renewing. Thus, they will be quickly exhausted. This B-Indu-Rag1 model has previously been successfully used to further corroborate the hypothesis that functional B-1a cells can develop from progenitors residing in the adult BM (8).

These previous experiments on B cell development in B-Indu-Rag1 mice involved several rounds of TAM administration (8). In contrast, in the present work, TAM was administered as a single dose, resulting in a single wave of B cell development. This allowed us to show that pro/preB cells differentiate into large and small preB-2 cell subsets within 5 and 6 days, respectively. The peak of these two BM subsets was detected 7 and 11 days after TAM induction, respectively. A clear order of differentiation could be observed. First, the large preB cells develop and later on the small preB cells. Small preB-II cells are known to differentiate from the proliferating large preB cell population. Nevertheless, differentiation from large to small preB-II cells appears to occur almost at the same time. Apparently, some of the large preB-II cells had quickly and functionally rearranged their IgH chain locus. This would predict that such large preB-II cells use mainly the proximal V<sub>H</sub> gene segments. This hypothesis could be tested in future studies by establishing the V<sub>H</sub> usage of isolated cell subsets. Additionally, some cells might be able to quickly proceed to generate a functional IgL chain. Again, one would predict that mainly the IgLk locus is rearranged under these conditions (35).

A similar order of first appearance could be observed for transitional B cells: BM, T1: day 6, T2: day 7; spleen, T1: day 7, T2: day 8. Both T1 and T2 subsets peak at day 11 or 12 post induction. However, in contrast to the T1 subset, T2 cells remain detectable up to day 15 in blood and spleen. The fact that T1 cells disappear first is consistent with the notion of stepwise maturation of transitional B cells and their precursor-product relationship (23, 24). Clearly, only one wave of development takes place, as beyond 21 days post induction, no progenitor subsets can be detected anymore. This is also reflected by the T1/T2 ratio. By that time all progenitors have differentiated into mature B cells.

The first immature IgM<sup>+</sup> B cells (T1) can be detected 6–7 days post induction. This is consistent with previous data obtained for B cell development in fetal liver. Here, the first c-kit<sup>+</sup> progenitors can be detected at day 11 after fertilization (9). Six days later, the first IgM<sup>+</sup> B cells can be detected in the fetus (10). This kinetics is very similar to the data obtained in the present work: Cells expressing c-kit<sup>+</sup> can be found at day 0 of induction and the first IgM<sup>+</sup> immature B cells became detectable 6 days later.

After TAM administration, the mature B cell compartment in peripheral organs increased starting with day 11, indicating that mature B cells (especially B-2 cells) need a minimum of 11 days for full maturation.

We could clearly show that the observed increase in cell appearance is not due to cell proliferation, as neither transitional B cells nor mature B cells show higher proliferation, as compared to fully immunocompetent WT mice in steady state. For

transitional B cells, it was shown before that the T2 subset proliferates to a higher extend, when the BCR is stimulated (25). This was not the case in the present study, as no proliferation of T2 cells could be observed (data not shown).

Interestingly, B-1 and MZ B cells appear later than B-2 cells. This could indicate that the differentiation of such B cells requires more time. However, there is no indication for such scenario. More likely is that the precursor frequency for such cells is lower than for B-2 cells. Therefore, it requires more time for these cells to accumulate in significant numbers for detection.

Eight weeks after induction, B-1a and B-1b cells can still be found in elevated percentages in peritoneal cavity. In contrast, the B-2 cell population was found to be reduced. This is consistent with the notion that B-1 cells are self-renewing, whereas homeostasis of the B-2 compartment critically depends on the continuous replenishment from precursor cells.

The higher percentage of B-1b cells accumulating in TAM-induced mice compared to WT mice is consistent with data shown before (8). None of the other B cell populations in the peritoneal cavity increased to the same extend. The reason for the selective increase in the B-1b subset is still unclear. A possible explanation could be that the recently described B-1 precursor in BM leads mainly to B-1b cells (5).

By ELISPOT assays the first IgM secreting cells could be detected by day 11. Apparently, this does not lead to a significant increase in secretory IgM. At present, it is unclear whether these IgM-producing cells are of B-1a or B-2 origin. Under the given experimental conditions, both B cell subsets are likely to have the potential to give rise to short-lived plasma cells (36). No IgM-secreting cells could be found in BM at that time point.

Despite the presence of serum IgG and IgA, no Ig's could be detected in the intestinal wash out. This finding appears surprising, considering that the gut-associated lymphoid tissue is well-known to support T-independent Ig class switch recombination (37, 38). It might well be that, at the time point selected for our analysis, IgA-secreting cells have not colonized the intestinal LP yet.

A recent publication employing humanized mice indicated that human T cells are strictly required for the terminal differentiation of mature B cells. The absence of T cells resulted in a developmental arrest at the transitional stage (39). Based on the present work, it appears that the findings for human cells in mice does not extend to the development of murine B cells in their natural environment. Indeed, our experiments in TAM-treated B-Indu-Rag1 mice provided no evidence for a developmental block at the transitional B cell stage.

Interestingly, a T cell-effect on splenic B-1a cells could be observed. The B-1a numbers were significantly increased in B-Indu-Rag1 mice that received adoptively transferred T cells prior to TAM administration, as compared to TAM-treated mice without T cell transfer. In contrast, the population size of peritoneal B-1a cells appears to be completely independent of T cells. The reason underlying this T cell-effect in the spleen is at present unclear. It is known that B-1a cells react to their specific antigen in a T-independent manner (40). In addition, the differences between B-1a cell populations from spleen and peritoneal cavity are still ill-defined. Possibly, migration of B1a

cells to the spleen is supported by T cells, a scenario that we have observed before (Roy, unpublished).

It is known that the cytokine milieu, which critically determines the outcome of Ig class switch recombination in activated B cells (31, 32) is at least in part dependent on T cells. Thus, the appearance of some of the Ig classes is highly dependent on the presence of T cells (41). Therefore, the serum Ig concentrations of TAM-induced mice that received adoptively transferred T cells, were additionally compared to sera of TAM-induced mice without T cell transfer. After 21 days, at which time point the first significant amounts of Ig's could be detected after TAM-mediated induction of B cell development, the Ig serum concentration was higher, when T cells were present. This correlated with increased numbers of Ig-secreting B cells in such mice. Even for intestinal wash out, it could be shown that the IgA secretion is highly dependent on T cells (37). Thus, still a high number of B cells do require T cells for the switching to IgA-secretion, and possibly also for migration and homing to the gut.

Nevertheless, while these experiments underscore the requirement for T cell help in Ig secretion, it appears that only short-lived plasma cells develop under these circumstances. Except for IgA, the increase in serum Ig was transient and lost at later time points of our kinetics analysis. Continuously high IgA concentration in the presence of T cells could potentially be attributed to the continuous immune stimulation provided by commensal bacteria located in the gut of SPF mice. These stimuli are supposed to activate B cells in a T cell-independent manner (38). This is obviously not sufficient for an increase in IgA, neither in the intestinal washout, nor in serum. The requirement of T cells for B cell maturation was again be confirmed by ELISPOT.

Under our experimental conditions, most Ig levels never reach normal levels. This is in contrast to mice in which B cell development had been stopped or was shown to be defective after birth. Such mice show a large portion of activated B cells and serum levels and plasma cell numbers are normal or even enhanced (42, 43). Why the B cell compartment is not filled up after induction and does not behave as in such lymphopenic mice, is unclear. A longer observation period might be required. Alternatively, the receptor repertoire under our conditions might be to restricted for a efficient expansion although previously we could show that the expected specificities are found in B-Indu-Rag1 mice (8).

The present study and previous publications (5, 8, 29, 44) indicate that B-1a cells can develop also from adult BM. As these B-1a cells are developing in an immunodeficient environment, it could be still argued that the adult BM might not give rise to these B-1a cells in a complete and functional immune environment. Therefore, we established BM chimeras in sublethally irradiated mice. We argued that such mice recover normal homeostasis within 6 weeks. Thus, Tam-induced B cell development occurs in a "quasi-normal" environment. Indeed, B-1a cells were observed that were derived from newly induced B cell progenitors under these conditions. However, when other competing B cells are available, it appears that such progenitors are more likely to develop into B-2 than into B-1 cells. This confirms data obtained by other groups on the presence of N-nucleotide additions of

V-D-J junctions of B cell receptors from B1a cells of aged mice. This was taken as evidence for a contribution of newly formed adult B cells to the B-1a pool (44, 45). The exact mechanisms that govern the B-2/B-1a lineage fate decision in the adult BM under fully physiological conditions remains to be determined. Recently, Lin28b has been suggested to represent a B-1a cell-supporting transcription factor that drives such lineage decisions in fetal vs. adult mice (46, 47). In fact, some previous transfer experiments failed to provide evidence for the development of B-1a cells from the BM of adult mice (48), perhaps owing to the fact that the population size of newly developed B-1a cells in the adult is exceedingly small. This could also explain why in more recent experiments, no newly formed B1a cells derived from unmanipulated adult HSCs could be observed (49). In any case, in the present work, it could be clearly shown that also in immunocompetent mice B-1a cells do develop from adult BM-residing progenitors and that such newly generated cells contribute to the adult B-1a cell pool.

Previous studies showed that, in developing B cells in the young adult BM, the proximal V<sub>H</sub> genes are used more often (15). This could be confirmed by using the B-Indu-Rag1 mouse. In the first days of B cell development after TAM induction, the proximal genes, close to the D and J clusters were preferentially found to be rearranged, whereas at later days the distal (J558; VH1) gene segments predominated. A clear shift from proximal to distal gene usage can be seen in our kinetics studies, as there are by day 7 post induction around 40% of gene segments used from the VH1 (J558) family, whereas it is only 10% by day 1–3. The normal sorted large and small preB cells that were included as controls gave the expected results. We therefore feel that we can exclude a bias due to the use of RNA and RT-PCR for analysis. Although higher numbers of sequences might provide a clearer picture, it appears that an individual B cell precursor has the chance to rearrange a proximal V<sub>H</sub> gene segment first. As the process is slow, only some cells will be able to successfully assemble such V<sub>H</sub> genes and express a functional heavy chain. Such cells will have a head start for further differentiation. They are most likely identical with the pre-B1 cells that reach the next differentiation stage within the shortest time observed in the present work. Cells that require more time for IgH chain rearrangement have then the complete repertoire available, since the locus is now completely open due to cytokine activity or other not yet defined signals. As in normal WT mice B cell development is not synchronized, this could not be clearly defined in earlier experiments. Along this line, it was also shown before that in B cell precursors isolated from Rag2<sup>-/-</sup> mice the histone assembly of distal VH genes allowing their active recombination was highly dependent on IL-7 (14). In the present mouse model, it would be possible to investigate this phenomenon in more molecular details *in vivo*.

## AUTHOR CONTRIBUTIONS

A-MB, SD, BR, and IT designed, performed and analyzed the experiments. FK analyzed experiments and performed statistical analyses. AG, OP, KK, and SW conceived the research. SW guided

its design, analysis, and interpretation. A-MB, AG, KK, and SW wrote the manuscript.

## SUPPLEMENTARY MATERIAL

The Supplementary Material for this article can be found online at: <https://www.frontiersin.org/articles/10.3389/fimmu.2018.02483/full#supplementary-material>

**Supplementary Figure S1 |** Flow cytometric gating for large and small preB cells as well as for T1 and T2 transitional cells. **(A)** Shown is an example of staining of BM cells from a B-Indu-Rag1 mouse analyzed 6 days after induction. Cells were gated for lymphocytes using forward and sideward scatter. Doublets were excluded by applying FSC area and heights against each other. Dead cells were excluded by gating for DAPI-negative cells. Those cells were then gated for B220<sup>+</sup>AA4.1<sup>+</sup> cells for immature B cell population as shown and finally for CD25 and CD40. IgM bearing cells were excluded. **(B)** Shown is a representative staining for BM cells of an induced Indu-BRag1 mouse. Gating was done as in A. Transitional B cells amongst B cell progenitors could be differentiated into T1 and T2 as CD23<sup>-</sup>IgM<sup>+</sup> (T1) and CD23<sup>+</sup>IgM<sup>+</sup> (T2). Similar gating was performed for all tissues analyzed.

**Supplementary Figure S2 |** Results of least squares fitting. In each case, a constant, a linear and a bell-shaped model were fitted. The lines shown

correspond to the best model according to Akaike's information criterion.

**(A).** Frequencies of indicated B cell developmental stages based on data from **Figure 1A** were used and fitted by least square statistics. **(B).** Data from **Figure 1B** were used and fitted by least square statistics.

**Supplementary Figure S3 |** Gating strategy for mature B cells. Shown is a representative staining for cells isolated from spleen of an induced B-Indu-Rag1 mouse. Cells were gated for lymphocytes first using forward and sideward scatter. Doublets were excluded by applying FSC area and heights against each other. Dead cells were excluded by gating for DAPI-negative cells. Those cells were then gated for CD19 and furthermore classified according to the figure and CD23, CD21, CD5 expression.

**Supplementary Figure S4 |** Gating strategy for peritoneal mature B cell populations. Shown is a representative staining for cells isolated from peritoneal cavity of an induced B-Indu-Rag1 mouse. Cells were gated for lymphocytes first using forward and sideward scatter. Doublets were excluded by applying FSC area and heights against each other. Dead cells were excluded by gating for DAPI-negative cells. Cells were further subdivided based on their expression of CD19, CD43, Mac-1 (CD11b), and CD5.

**Supplementary Figure S5 |** Results of least squares fitting for mature B cells. Analysis was carried out like for **Figure S2**. Frequencies of indicated BCR<sup>+</sup> B cell subsets based on data from **Figure 2** were used and fitted by least square statistics.

## REFERENCES

- Baumgarth N. Innate-like B cells and their rules of engagement. *Adv Exp Med Biol.* (2013) 785:57–66. doi: 10.1007/978-1-4614-6217-0\_7
- Hardy RR, Hayakawa K. B cell development pathways. *Annu Rev Immunol.* (2001) 19:595–621. doi: 10.1146/annurev.immunol.19.1.595
- Hayakawa K, Hardy RR. Development and function of B-1 cells. *Curr Opin Immunol.* (2000) 12:346–53. doi: 10.1016/S0952-7915(00)00098-4
- Esplin BL, Welner RS, Zhang Q, Borghesi LA, Kincade PW. A differentiation pathway for B1 cells in adult bone marrow. *Proc Natl Acad Sci USA.* (2009) 106:5773–8. doi: 10.1073/pnas.0811632106
- Montecino-Rodriguez E, Leathers H, Dorshkind K. Identification of a B-1 B cell-specified progenitor. *Nat Immunol.* (2006) 7:293–301. doi: 10.1038/ni1301
- Rolink A, Melchers F. Molecular and cellular origins of B lymphocyte diversity. *Cell* (1991) 66:1081–94. doi: 10.1016/0092-8674(91)90032-T
- Pieper K, Grimbacher B, Eibel H. B-cell biology and development. *J Allergy Clin Immunol.* (2013) 131:959–71. doi: 10.1016/j.jaci.2013.01.046
- Duber S, Hafner M, Krey M, Lienenklaus S, Roy B, Hobeika E, et al. Induction of B-cell development in adult mice reveals the ability of bone marrow to produce B-1a cells. *Blood* (2009) 114:4960–7. doi: 10.1182/blood-2009-04-218156
- de Andres B, Gonzalo P, Minguez S, Martinez-Marin JA, Soro PG, Marcos MA, et al. The first 3 days of B-cell development in the mouse embryo. *Blood* (2002) 100:4074–81. doi: 10.1182/blood-2002-03-0809
- Raff MC, Megson M, Owen JJ, Cooper MD. Early production of intracellular IgM by B-lymphocyte precursors in mouse. *Nature* (1976) 259:224–6. doi: 10.1038/259224a0
- Chevillard C, Ozaki J, Herring CD, Riblet R. A three-megabase yeast artificial chromosome contig spanning the C57BL mouse Ig locus. *J Immunol.* (2002) 168:5659–66. doi: 10.4049/jimmunol.168.11.5659
- Chowdhury D, Sen R. Regulation of immunoglobulin heavy-chain gene rearrangements. *Immunol Rev.* (2004) 200:182–96. doi: 10.1111/j.0105-2896.2004.00177.x
- Wasserman R, Li YS, Shinton SA, Carmack CE, Manser T, Wiest DL, et al. A novel mechanism for B cell repertoire maturation based on response by B cell precursors to pre-B receptor assembly. *J Exp Med.* (1998) 187:259–64. doi: 10.1084/jem.187.2.259
- Chowdhury D, Sen R. Stepwise activation of the immunoglobulin mu heavy chain gene locus. *EMBO J.* (2001) 20:6394–403. doi: 10.1093/emboj/20.22.6394
- Malynn BA, Yancopoulos GD, Barth JE, Bona CA, Alt FW. Biased expression of JH-proximal VH genes occurs in the newly generated repertoire of neonatal and adult mice. *J Exp Med.* (1990) 171:843–59. doi: 10.1084/jem.171.3.843
- ten Boekel E, Melchers F, Rolink AG. Changes in the V(H) gene repertoire of developing precursor B lymphocytes in mouse bone marrow mediated by the pre-B cell receptor. *Immunity* (1997) 7:357–68. doi: 10.1016/S1074-7613(00)80357-X
- Torres RM, Flaswinkel H, Reth M, Rajewsky K. Aberrant B cell development and immune response in mice with a compromised BCR complex. *Science* (1996) 272:1804–8. doi: 10.1126/science.272.5269.1804
- Mombaerts P, Iacomini J, Johnson RS, Herrup K, Tonegawa S, Papaioannou VE. RAG-1-deficient mice have no mature B and T lymphocytes. *Cell* (1992) 68:869–77. doi: 10.1016/0092-8674(92)90030-G
- Lindner C, Thomsen I, Wahl B, Ugur M, Sethi MK, Friedrichsen M, et al. Diversification of memory B cells drives the continuous adaptation of secretory antibodies to gut microbiota. *Nat Immunol.* (2015) 16:880–8. doi: 10.1038/ni.3213
- Nash JC. On best practice optimization methods in R. *J Stat Softw.* (2014) 60:1–14. doi: 10.18637/jss.v060.i02
- Akaike H. A new look at the statistical model identification. *IEEE Trans Automatic Control* (1974) 19:716–23. doi: 10.1109/TAC.1974.1100705
- Ichii M, Oritani K, Kanakura Y. Early B lymphocyte development: Similarities and differences in human and mouse. *World J Stem Cells* (2014) 6:421–31. doi: 10.4252/wjsc.v6.i4.421
- Allman D, Lindsley RC, DeMuth W, Rudd K, Shinton SA, Hardy RR. Resolution of three nonproliferative immature splenic B cell subsets reveals multiple selection points during peripheral B cell maturation. *J Immunol.* (2001) 167:6834–40. doi: 10.4049/jimmunol.167.12.6834
- Allman D, Pillai S. Peripheral B cell subsets. *Curr Opin Immunol.* (2008) 20:149–57. doi: 10.1016/j.coim.2008.03.014
- Petro JB, Gerstein RM, Lowe J, Carter RS, Shinnars N, Khan WN. Transitional type 1 and 2 B lymphocyte subsets are differentially responsive to antigen receptor signaling. *J Biol Chem.* (2002) 277:48009–19. doi: 10.1074/jbc.M200305200
- Chung JB, Silverman M, Monroe JG. Transitional B cells: step by step towards immune competence. *Trends Immunol.* (2003) 24:343–9. doi: 10.1016/S1471-4906(03)00119-4
- Loder F, Mutschler B, Ray RJ, Paige CJ, Sideras P, Torres R, et al. B cell development in the spleen takes place in discrete steps and is determined by the quality of B cell receptor-derived signals. *J Exp Med.* (1999) 190:75–89. doi: 10.1084/jem.190.1.75

28. Baumgarth N. B-1 cell heterogeneity and the regulation of natural and antigen-induced IgM production. *Front Immunol.* (2016) 7:324. doi: 10.3389/fimmu.2016.00324
29. Yoshimoto M, Montecino-Rodriguez E, Ferkowicz MJ, Porayette P, Shelley WC, Conway SJ, et al. Embryonic day 9 yolk sac and intra-embryonic hemogenic endothelium independently generate a B-1 and marginal zone progenitor lacking B-2 potential. *Proc Natl Acad Sci USA.* (2011) 108:1468–73. doi: 10.1073/pnas.1015841108
30. Roy B, Agarwal S, Brennecke AM, Krey M, Pabst O, Duber S, et al. B-1-cell subpopulations contribute differently to gut immunity. *Eur J Immunol.* (2013) 43:2023–32. doi: 10.1002/eji.201243070
31. Manis JP, Tian M, Alt FW. Mechanism and control of class-switch recombination. *Trends Immunol.* (2002) 23:31–9. doi: 10.1016/S1471-4906(01)02111-1
32. Stavnezer J, Guikema JE, Schrader CE. Mechanism and regulation of class switch recombination. *Annu Rev Immunol.* (2008) 26:261–92. doi: 10.1146/annurev.immunol.26.021607.090248
33. Haas JD, Ravens S, Duber S, Sandrock I, Oberdorfer L, Kashani E, et al. Development of interleukin-17-producing gammadelta T cells is restricted to a functional embryonic wave. *Immunity* (2012) 37:48–59. doi: 10.1016/j.jimmuni.2012.06.003
34. Toker A, Engelbert D, Garg G, Polansky JK, Floess S, Miyao T, et al. Active demethylation of the Foxp3 locus leads to the generation of stable regulatory T cells within the thymus. *J Immunol.* (2013) 190:3180–8. doi: 10.4049/jimmunol.1203473
35. Engel H, Rolink A, Weiss S. B cells are programmed to activate kappa and lambda for rearrangement at consecutive developmental stages. *Eur J Immunol.* (1999) 29:2167–76. doi: 10.1002/(SICI)1521-4141(199907)29:07<2167::AID-IMMU2167>3.0.CO;2-H
36. Shapiro-Shelef M, Calame K. Regulation of plasma-cell development. *Nat Rev Immunol.* (2005) 5:230–42. doi: 10.1038/nri1572
37. Barone F, Patel P, Sanderson JD, Spencer J. Gut-associated lymphoid tissue contains the molecular machinery to support T-cell-dependent and T-cell-independent class switch recombination. *Mucosal Immunol.* (2009) 2:495–503. doi: 10.1038/mi.2009.106
38. Macpherson AJ, Gatto D, Sainsbury E, Harriman GR, Hengartner H, Zinkernagel RM. A primitive T cell-independent mechanism of intestinal mucosal IgA responses to commensal bacteria. *Science* (2000) 288:2222–6. doi: 10.1126/science.288.5474.2222
39. Lang J, Kelly M, Freed BM, McCarter MD, Kedl RM, Torres RM, et al. Studies of lymphocyte reconstitution in a humanized mouse model reveal a requirement of T cells for human B cell maturation. *J Immunol.* (2013) 190:2090–101. doi: 10.4049/jimmunol.1202810
40. Yang Y, Ghosn EE, Cole LE, Obukhanych TV, Sadate-Ngatchou P, Vogel SN, et al. Antigen-specific antibody responses in B-1a and their relationship to natural immunity. *Proc Natl Acad Sci USA.* (2012) 109:5382–7. doi: 10.1073/pnas.1121631109
41. Lenz VM, Manser T. Self-limiting systemic autoimmune disease during reconstitution of T cell-deficient mice with syngeneic T cells: support for a multifaceted role of T cells in the maintenance of peripheral B cell tolerance. *Int Immunol.* (2000) 12:1483–97. doi: 10.1093/intimm/12.11.1483
42. Carvalho TL, Mota-Santos T, Cumano A, Demengeot J, Vieira P. Arrested B lymphopoiesis and persistence of activated B cells in adult interleukin 7(-/-) mice. *J Exp Med.* (2001) 194:1141–50. doi: 10.1084/jem.194.8.1141
43. Hao Z, Rajewsky K. Homeostasis of peripheral B cells in the absence of B cell influx from the bone marrow. *J Exp Med.* (2001) 194:1151–64. doi: 10.1084/jem.194.8.1151
44. Holodick NE, Repetly K, Zhong X, Rothstein TL. Adult BM generates CD5+ B1 cells containing abundant N-region additions. *Eur J Immunol.* (2009) 39:2383–94. doi: 10.1002/eji.200838920
45. Holodick NE, Vizconde T, Hopkins TJ, Rothstein TL. Age-related decline in natural IgM function: diversification and selection of the B-1a cell pool with age. *J Immunol.* (2016) 196:4348–57. doi: 10.4049/jimmunol.1600073
46. Yuan J, Nguyen CK, Liu X, Kanelloupolou C, Muljo SA. Lin28b reprograms adult bone marrow hematopoietic progenitors to mediate fetal-like lymphopoiesis. *Science* (2012) 335:1195–200. doi: 10.1126/science.1216557
47. Zhou Y, Li YS, Bandi SR, Tang L, Shinton SA, Hayakawa K, et al. Lin28b promotes fetal B lymphopoiesis through the transcription factor Arid3a. *J Exp Med.* (2015) 212:569–80. doi: 10.1084/jem.20141510
48. Kantor AB, Herzenberg LA. Origin of murine B cell lineages. *Annu Rev Immunol.* (1993) 11:501–38. doi: 10.1146/annurev.iy.11.040193.002441
49. Pei W, Feyerabend TB, Rossler J, Wang X, Postrach D, Busch K, et al. Polyloxy barcoding reveals hematopoietic stem cell fates realized *in vivo*. *Nature* (2017) 548:456–60. doi: 10.1038/nature23653

**Conflict of Interest Statement:** The authors declare that the research was conducted in the absence of any commercial or financial relationships that could be construed as a potential conflict of interest.

Copyright © 2018 Brennecke, Düber, Roy, Thomsen, Garbe, Klawonn, Pabst, Kretschmer and Weiss. This is an open-access article distributed under the terms of the Creative Commons Attribution License (CC BY). The use, distribution or reproduction in other forums is permitted, provided the original author(s) and the copyright owner(s) are credited and that the original publication in this journal is cited, in accordance with accepted academic practice. No use, distribution or reproduction is permitted which does not comply with these terms.



# BAFF and BAFF-Receptor in B Cell Selection and Survival

Cristian R. Smulski and Hermann Eibel\*

Faculty of Medicine, Center for Chronic Immunodeficiency, Medical Center – University of Freiburg, Freiburg, Germany

The BAFF-receptor (BAFFR) is encoded by the TNFRSF13C gene and is one of the main pro-survival receptors in B cells. Its function is impressively documented in humans by a homozygous deletion within exon 2, which leads to an almost complete block of B cell development at the stage of immature/transitional B cells. The resulting immunodeficiency is characterized by B-lymphopenia, agammaglobulinemia, and impaired humoral immune responses. However, different from mutations affecting pathway components coupled to B cell antigen receptor (BCR) signaling, BAFFR-deficient B cells can still develop into IgA-secreting plasma cells. Therefore, BAFFR deficiency in humans is characterized by very few circulating B cells, very low IgM and IgG serum concentrations but normal or high IgA levels.

## OPEN ACCESS

### Edited by:

Harry W. Schroeder,  
University of Alabama at Birmingham,  
United States

### Reviewed by:

Yi Hao,  
Tongji Medical College, Huazhong  
University of Science and Technology,  
China

Mike Cancro,  
University of Pennsylvania,  
United States

### \*Correspondence:

Hermann Eibel  
[hermann.eibel@uniklinik-freiburg.de](mailto:hermann.eibel@uniklinik-freiburg.de)

### Specialty section:

This article was submitted to  
B Cell Biology,  
a section of the journal  
*Frontiers in Immunology*

Received: 12 June 2018

Accepted: 14 September 2018

Published: 08 October 2018

### Citation:

Smulski CR and Eibel H (2018) BAFF and BAFF-Receptor in B Cell Selection and Survival. *Front. Immunol.* 9:2285.  
doi: 10.3389/fimmu.2018.02285

## BAFFR STRUCTURE AND EXPRESSION

Structurally, BAFFR is an atypical representative of the TNF-receptor super-family. Members of this family are typically characterized by several extracellular cysteine-rich domains (CRDs), which serve for ligand binding as well as for ligand-independent assembly of receptor monomers into dimers, trimers or multimers (1–6). Unlike most other TNF-R family members, BAFFR contains only a partial CRD which serves for ligand binding as well as for self-assembly (7).

B lymphocyte development in human bone marrow proceeds through successive stages that are defined by the immunoglobulin gene rearrangement process. After the assembly and cell surface expression of functional IgM molecules, immature IgM<sup>+</sup> B cells are tested for their reactivity with self-antigens, which eventually can be corrected by receptor editing. Then, transitional B cells with low avidity to self-antigens can leave the bone marrow, enter the circulation, and migrate to the spleen where they complete these early steps of B cell development [reviewed in (8)]. BAFFR [BAFFR = *B* cell activating factor of the TNF-family receptor (9); a.k.a. BR3, Bcnd (10–12)] expression starts when the immature B cells develop to transitional B cells (13, 14), which then receive BAFFR-dependent pro-survival signals to rescue them from premature cell death (15–17). At protein level, the BAFFR is expressed on the surface of all human peripheral B cell subsets except for plasma cells and for centroblasts located in the dark zone of germinal centers. Its expression is upregulated after the expression of functional B cell antigen receptors (BCR) in response to tonic BCR signaling, which enhances BAFFR expression by immature and transitional B cells (15, 18). Although the induction of BAFFR expression seems to depend on the expression of functional B cell receptors, it can be maintained in mice after the ablation of SYK, a key element of BCR signaling (19), as well as in cells which were depleted from Ig- $\alpha$  (CD79A), an essential BCR component (20), supporting in both cases the survival of B cells with impaired BCR-signaling. Figure 1 summarizes the development of immature/transitional B cells and the expression of receptors for BAFF in the different subsets.

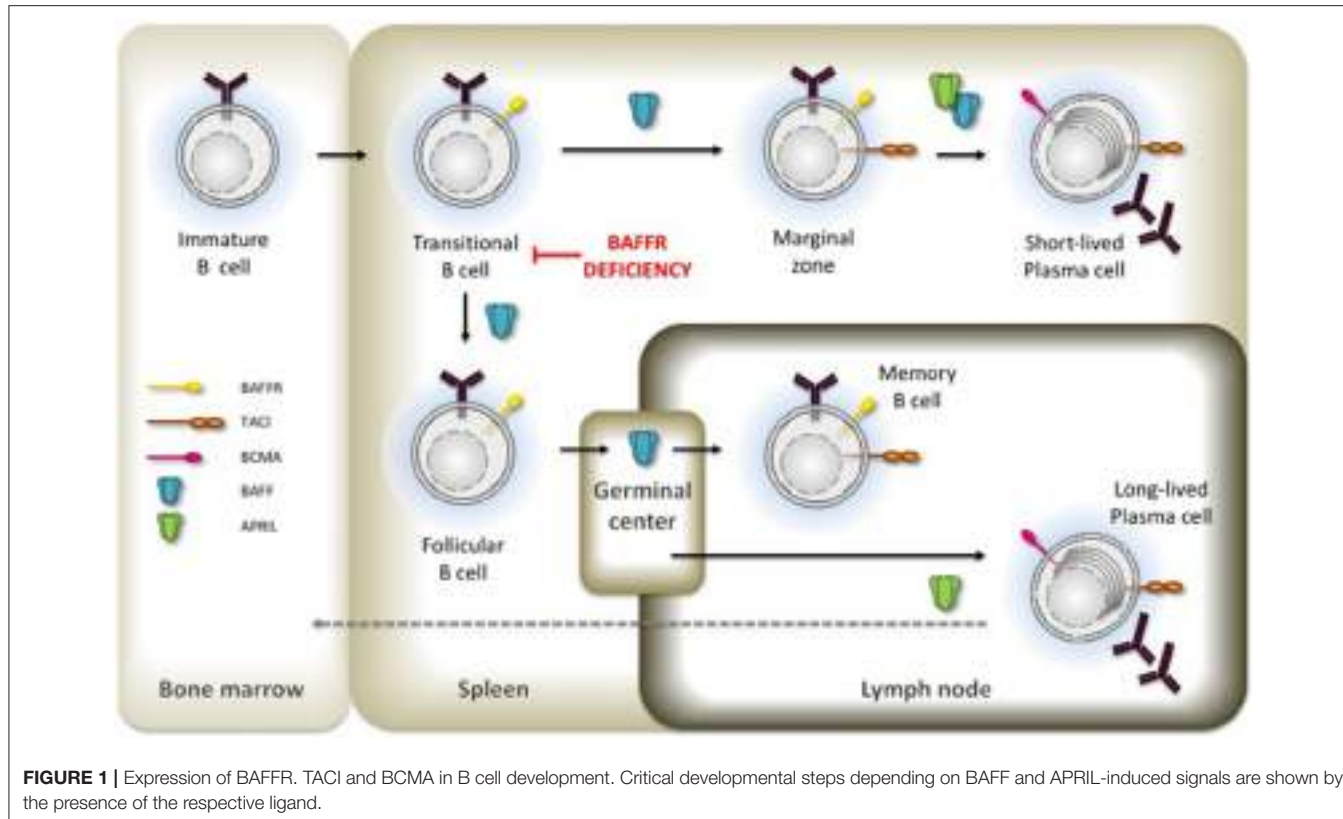


**FIGURE 1 |** Expression of BAFFR, TACI and BCMA in B cell development. Critical developmental steps depending on BAFF and APRIL-induced signals are shown by the presence of the respective ligand.

## LIGAND BINDING

BAFFR binds the TNF-like molecule BAFF [BAFF = *B* cell activating factor of the TNF-family (21); a.k.a. BLYS (22), TALL-1 (23), zTNF4(24)] as single ligand (9, 12, 25). In contrast, the two other closely related, BAFF-binding receptors TACI (*T* cell activator and calcium modulating ligand interactor) and BCMA (*B* cell maturation antigen) (24) can additionally bind to APRIL [*a* proliferation-inducing ligand, (26)], another member of the TNF- $\alpha$  family, which supports the survival of plasma cells (27). TACI is expressed by activated B cells, marginal zone B cells, switched memory B cells and by plasma cells (24, 28–30). Compared to BAFFR, TACI has different functions by serving on the one hand as decoy receptor (31) while triggering, on the other hand, immunoglobulin class-switch recombination (32). Different from BAFFR and TACI, BCMA is upregulated in activated B cells and expressed constitutively by long-lived plasma cells supporting their survival (33). Both ligands, BAFF (21, 22) and APRIL (26) are type II transmembrane proteins forming homo- as well as heterotrimers (22, 34–36). BAFF is expressed as membrane-bound ligand (see also contribution of Kowalczyk-Quintas et al. to this Research Topic), which is then processed by the membrane-bound protease furin resulting in a soluble form. Soluble BAFF exists as trimer and can associate into a virus-like capsid called 60-mer, composed of 20 trimeric units (35, 37, 38). The assembly of 60-mers depends on trimer-trimer interactions mediated by a small loop called the “flap” (34, 35). Without the flap region BAFF can still assemble into trimers,

which can bind to BAFFR but this form of BAFF does neither initiate downstream signaling cascades nor does it support B cell survival. Therefore, crosslinking of multiple BAFF-BAFFR complexes via the flap-region is essential for BAFFR-dependent B cell responses (39).

BAFF and APRIL are expressed by monocytes, macrophages, dendritic cells, bone marrow stroma cells (21, 23, 40), and by T cells (21, 41). The expression of both ligands increases under pro-inflammatory conditions (42) and correlates inversely with the expression of BAFFR and TACI (43).

## BAFFR SIGNALING AND TARGET GENES

BAFF binding to BAFFR activates several downstream pathways that regulate basic survival functions including protein synthesis and energy metabolism required to extend the half-life of immature, transitional, and mature B cells.

Like the TNF-receptor family members CD40, LT $\beta$ R, and RANK, BAFFR triggers the non-canonical NF- $\kappa$ B2-dependent pathway (44, 45). NF- $\kappa$ B2 belongs together with NF- $\kappa$ B1, RelA, RelB, and c-Rel to the group of NF- $\kappa$ B/Rel transcription factors [reviewed in (46)]. Activation of NF- $\kappa$ B1 is a very rapid process (47). Upon MAP3K7 (TAK1)-dependent phosphorylation, IKK $\alpha$ , IKK $\beta$ , IKK $\gamma$  assemble into the inhibitor of kappa-B kinase (IKK) complex and phosphorylate I $\kappa$ B $\alpha$ , the inhibitor of NF- $\kappa$ B1. This

allows its proteasomal degradation and nuclear translocation of NF- $\kappa$ B p50/relA and p50-c-rel heterodimers, which are constantly generated by the association between the processed form of NF- $\kappa$ B1/p105 and relA or c-Rel. In the nucleus, the NF- $\kappa$ B heterodimers mainly act as transcriptional activators regulating a plethora of target genes including the gene for NF- $\kappa$ B2 (48).

Different from NF- $\kappa$ B1, the activation of the non-canonical NF- $\kappa$ B2 pathway by BAFF is a slow and complex process (44) which relies on the activation of the NF- $\kappa$ B inducing kinase NIK (MAP3K14) (49, 50). In the absence of BAFF (or of other NF- $\kappa$ B2-inducing factors), NIK binds TRAF3, which promotes the proteasomal degradation of the kinase after its ubiquitinylation by a complex with ubiquitin-E3 ligase activity composed of the cellular inhibitors of apoptosis cIAP1 and cIAP2, TRAF2 and TRAF3 (51). NIK degradation prevents the accumulation of the kinase and the phosphorylation of NF- $\kappa$ B2 by IKK $\alpha$  (IKK1), which itself is activated through phosphorylation by NIK (52). When BAFF binds to BAFFR, it leads to the aggregation of BAFF receptors which recruit TRAF3 to their intracellular part. This allows the dissociation of the NIK-TRAF2/3-cIAP1/2 complex (53–55), exposes the TRAF3 lysine residue K46 to ubiquitin ligases and allows proteasomal degradation of TRAF3 (56). By reducing the number of available TRAF3 molecules, newly synthesized NIK can accumulate (53) and phosphorylate IKK1 (52). The active form of IKK1 then phosphorylates NF- $\kappa$ B2 p100 at the C-terminal serine residues 866 and 870 (50), which now becomes a target of the E3 ubiquitin ligase  $\beta$ TrCP, which adds ubiquitin to lysine residue K856. Ubiquitylated NF- $\kappa$ B2 then binds to the regulatory subunit of the proteasome (56) promoting the cleavage of the p100 precursor into the active p52 form which forms an heterodimer with relB and translocates into the nucleus to regulate the transcription of NF- $\kappa$ B2 target genes. The complexity of this multi-step reaction, which is dependent on the relative concentration of TRAF and its association with BAFFR (57) explains why BAFF-induced activation of NF- $\kappa$ B2 target genes is a slow process.

Downstream of NF- $\kappa$ B2 several target genes have been identified. These include ICOSL, a co-stimulatory ligand for ICOS, which is expressed by activated T cells, provides co-stimulatory signals, and promotes the development of follicular T-helper cells (58). Analysis of B cells from NIK-deficient patients underlines the role of NIK and NF- $\kappa$ B2 in activating ICOSL expression as NIK-deficient cells do not upregulate ICOSL in response to CD40L (59).

As pointed out above, BAFF binding to BAFFR recruits TRAF3 to the receptor reducing the concentrations of available TRAF3. This allows—similar to the accumulation of NIK—the accumulation of the transcriptional regulator “cAMP response element binding protein” CREB, which in resting cells is initially complexed to TRAF3 inducing its ubiquitinylation and degradation. Accumulation of CREB increases the expression of its target gene Mcl-1 (60), a Bcl-family member with powerful anti-apoptotic activity, which acts by stabilizing the mitochondrial outer membrane (61). The deubiquitinating enzyme OTUD7B represents another NF- $\kappa$ B2 target gene (62). Activation of BAFFR increases OTUD7B expression and the

newly synthesized deubiquitinase then binds to TRAF3 resulting in the formation of a high molecular weight complex including OTUD7B, TRAF3, TRAF2, and cIAP1/2. This leads to the deubiquitylation and stabilization of TRAF3, which now can bind and inactivate NIK again resulting in the downregulation of BAFFR signaling. Thus, OTUB7 acts as negative regulator of the NF- $\kappa$ B2 and limits BAFFR-dependent cellular activation (62).

In addition to NF- $\kappa$ B2 signaling, binding of BAFF to BAFFR activates the phosphoinositide-3-kinase-dependent signaling cascade. An elegant series of experiments carried out in mice demonstrated that activation PI3K pathway by BAFFR makes use of components belonging to the B cell antigen receptor pathway (63, 64). Similar to the B cell receptor (65), BAFFR-induced signals remodel the cytoskeleton by interacting with a network which includes the tetraspanin CD81, the co-receptor CD19 and the Wiscott-Aldrich syndrome interacting protein WIP (66). This suggests that BAFFR seems to be part of a large complex of transmembrane and membrane-associated proteins using common signaling components that are activated in a context-dependent manner. Downstream of PI3K, the AKT/mTOR axis initiates the metabolic reprogramming of B cells resulting in an increased cellular fitness and lifespan [reviewed in (67)]. In mice, BAFF induces the PI3K-dependent phosphorylation of AKT at both Ser437 and T308 (68, 69) allowing the phosphorylation of downstream substrates including GSK3 $\beta$ , the transcription factor FOXO, the small ribosomal subunit protein S6 and the translation inhibitor 4EBP1. Since phosphorylated S6 activates while non-phosphorylated 4EBP1 inhibits translation, BAFFR is an important regulator of protein synthesis. In addition to protein synthesis, BAFFR-dependent activation of the PI3K pathway stabilizes MCL-1 by phosphorylating GSK3 $\beta$  and PIM2 (61, 68, 69), leading to enhanced mitochondrial function and an increase in ATP production. **Figure 2** summarizes essential features of BAFFR signaling.

## BAFFR PROCESSING

Besides the activation of several downstream signaling pathways BAFF binding to BAFFR causes the shedding of the extracellular part of BAFFR (70). The proteolytic cleavage of BAFFR is catalyzed by the metalloprotease ADAM10 and requires the co-expression of TACI. Since TACI is expressed by marginal zone and by switched memory B cells, BAFFR shedding by ADAM10 in response to BAFF binding affects mainly these B cell subsets. After the extracellular part of BAFFR has been released, its transmembrane part and the cytoplasmic domain are internalized and translocated to lysosomes where they are most likely degraded. Thus, BAFFR processing differs from the shedding of TACI, which is cleaved constitutively by ADAM10 in the absence of ligand. Processing of TACI removes its extracellular domain, which can act as decoy receptor for both BAFF and APRIL (31). Similar to TACI, BCMA is also processed constitutively, not by ADAM proteases but by  $\gamma$ -secretase (71). As it has been described for Notch,  $\gamma$ -secretase also cleaves the part of TACI which remains in the plasma membrane after the extracellular part has been shed by ADAM10 (31), but it remains

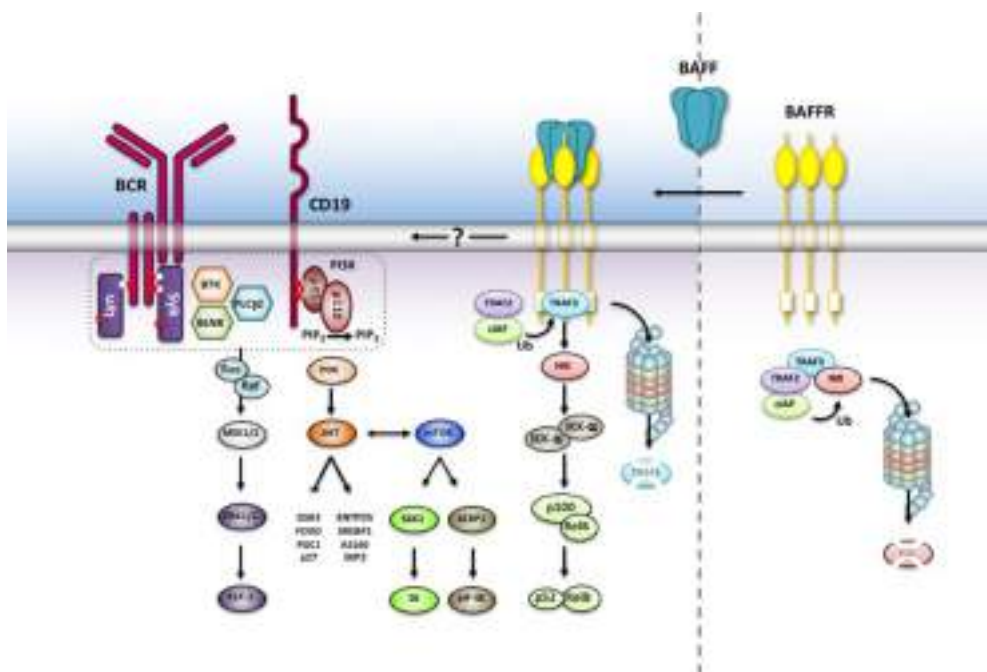


**FIGURE 2 |** BAFFR-induced intracellular signaling. Without BAFF, NIK is complexed to TRAF3 and degraded in the proteasome. BAFF binding to BAFFR recruits TRAF3 to BAFFR and stabilizes NIK while TRAF3 is degraded by the proteasome. NIK activates the non-canonical NF- $\kappa$ B2 signaling pathway and allows nuclear translocation of NF- $\kappa$ B2 p52/relB heterodimers. BAFF binding also activates the PI3K pathway, which shares common components with BCR signaling. The exact mechanisms leading to PI3K activation are still not understood.

to be shown if the released intracellular form of TACI has a biological function analogous to the intracellular part of Notch, which participates directly in the transcriptional regulation of target genes (72).

Since BAFFR shedding is induced by ligand binding to BAFFR, the released extracellular domain of BAFFR is most likely still complexed with BAFF preventing its function as soluble decoy receptor like soluble TACI or BCMA. If BAFF dissociates from soluble BAFFR, the soluble form of BAFFR most likely also loses its ligand binding activity, which also argues against its decoy receptor function. As a result of the constitutive shedding of TACI and BCMA, the surface expression levels of both receptors are rather low (31, 71), and differs from BAFFR expression levels, which are high on all B cell subsets except for germinal center B cells (70).

Germinal center B cells undergo proliferation, somatic hypermutation and immunoglobulin class-switch recombination in the dark zone, from where they migrate to the light zone, where they are selected by their affinity to their cognate antigen into the switched memory B cell and long-lived plasma cell pool (73). While light zone B cells express close to normal levels of BAFFRs which are not bound to BAFF, BAFFRs expressed by dark zone B cells are heavily loaded with BAFF inducing BAFFR-dependent survival signals as well as BAFFR processing by ADAM17. Thus, while BAFF-induced BAFFR processing limits initial survival signals for dark zone cells (70), the survival of light zone B cells is regulated by the affinity of their surface

immunoglobulins, which has to be above the thresholds set by interacting T-follicular helper cells and by the competing IgG and IgA antibodies secreted by plasma cells surrounding the B cell follicle (74).

## BAFFR AND B CELL SURVIVAL

From the analysis of the BAFFR encoding *Bcnd* mutation discovered in the A/WySnJ mouse strain (10, 11) and after the identification of BAFF as pro-survival cytokine for B cells (21, 75) it became clear that both proteins form a ligand-receptor pair which is essential for B cell survival (9, 12). Of interest, the different mouse models revealed that not all B cell subsets are equally dependent on BAFFR-induced survival signals. While *Baffr*-deficient A/WySnJ or Baff- and Baffr-KO mice had much less follicular and marginal zone B cells (B2 B cells) than the corresponding controls, the inactivation of the *Baff* or *Baffr* genes did not affect the population of peritoneal B1 B cells (11, 25, 76). In the mouse, B1 cells form a distinct, innate-like B cell subset, which develops before and shortly after birth and is maintained by self-renewal through limited proliferation but not, as follicular and marginal zone B cells, by *de novo* generation from hematopoietic precursor cells [reviewed in (77, 78)]. Apart from differences in CD5 expression, B1 cells can be separated into two subsets by the expression of plasma cell alloantigen (PC1; a.k.a ectonucleotide pyrophosphatase phosphodiesterase 1;

ENPP1). PC1<sup>low</sup> B1 cells develop from early B1 precursor cells during fetal life and differentiate in the gut into IgA secreting plasma cells (79). Interestingly, *Baff*- and *Baffr*-deficient mice as well as BAFFR-deficient humans have decreased titers of serum IgG and IgM but not of IgA (11, 25, 76, 80), which may be due to the differentiation of BAFF-independent PC1<sup>low</sup> B1 cells developing in the gut into IgA secreting plasma cells. Similar to genetic ablation of BAFF and BAFFR expression, injection of anti-BAFF (81) or anti-BAFFR antibodies (82) or of TACI-Ig (83, 84) resulted in the depletion of transitional-2, follicular and of marginal zone B cells but spared pro- and pre-B cells, immature, and transitional-1 B cells. In addition, these depletion experiments showed that switched memory B cells and plasma cells can survive after depleting BAFF or blocking BAFF-BAFFR interactions. Thus, the development and maintenance of the follicular and marginal zone B cell pool strongly depends on BAFF and BAFFR, whereas B1 B cells and switched memory B cells can survive without BAFF, although they express similar levels of BAFFR as the BAFF-dependent subsets. Future studies have to reveal, why BAFFR is expressed on these cells and if it has any function.

## THE ROLE OF BAFFR IN B CELL SELECTION AND AUTOIMMUNITY

BAFFR expression starts in the bone marrow when B cells become IgM<sup>+</sup> immature B cells, which undergo negative selection for autoreactive B cells. Since BAFFR-dependent signals prolong the survival of B cells, it was of interest to analyze if BAFF binding to BAFFR plays a role in the selection of B cells into the pool of mature B lymphocytes. Using a rearranged immunoglobulin V-gene knock-in mouse model (18), R. Pelanda and her group demonstrated that IgM<sup>+</sup> IgD<sup>-</sup> autoreactive B cells with low IgM surface expression express low levels of BAFFR and do not respond to BAFF-induced survival signals. In contrast, non-autoreactive IgM<sup>+</sup> IgD<sup>-</sup> B cells expressing more IgM on the cell surface also expressed, proportional to IgM, more BAFFR and developed into IgM<sup>+</sup> IgD<sup>+</sup> CD21<sup>+</sup> CD23<sup>-</sup> transitional-1 B cells. These cells respond to BAFFR by developing into IgM<sup>+</sup> IgD<sup>+</sup> CD21<sup>+</sup> CD23<sup>+</sup> transitional-2 cells and later into mature B lymphocytes as it had been shown before in other mouse models (76, 81). A similar conclusion was reached by the group of Rolink (85) by carefully analyzing RAG-2 expression and B cell receptor editing by mouse and human IgM<sup>+</sup> immature B cells from bone marrow. They found that BAFFR surface levels correlate directly with IgM but inversely with RAG-2 expression and receptor editing. Interestingly, anti-IgM treatment downregulates BAFFR on the surface of immature and transitional B cells while it enhances its expression on the surface of mature B cells (85). Since the inactivation of two Rho-GTPase encoding genes *Rac1* and *Rac2* does not only abolish BCR-induced intracellular calcium flux and the activation of the PI3K pathway but also BAFFR expression (86), BCR-dependent activation of Rac GTPases seems to induce the transcription of the *Baffr* gene in immature B cells.

B cells undergo a second phase of selection in germinal centers. Since excess of BAFF promotes the development of autoreactive B cells (75), BAFF-induces signals which interfere with mechanisms regulating the selection of B cells in the germinal center and with the equilibrium between BAFF-induced survival of dark zone B cells and affinity-based selection of centrocytes in the light zone. Genome-wide genetic association studies carried out with samples from multiple sclerosis (MS) and systemic lupus erythematosus (SLE) patients now provide evidence that genetically encoded changes of BAFF levels result in increased concentrations and correlate with the increased risk of developing autoimmunity (87). The genetic change results from a small deletion within the 3'UTR of BAFF mRNA. The deletion creates a new polyadenylation site allowing the premature termination of BAFF transcription. This shorter version of BAFF mRNA lacks an important regulatory sequence containing the binding site for miRNA-15a. This prevents micro-RNA directed control of excessive BAFF mRNA resulting in 1.5 to 2-fold increase in BAFF levels in a gene-dosage dependent manner. Like in the BAFF-transgenic mice, higher BAFF levels in humans increase the numbers of circulating B cells, promote the development of plasma cells, and result in higher serum IgG and IgM concentrations in homozygous carriers of this *TNFSF13B* variant (87).

Ablation of TACI expression or function not only cause immunodeficiency but also increases the risk of developing autoimmunity (88–90). The autoimmunity is now best explained by the decoy receptor function of TACI. In humans, the TACI variants C104R or C104Y, which reside in the second CRD abolish ligand-binding activity of TACI without preventing cell surface expression of the receptor. ADAM10-induced processing therefore sheds soluble forms of TACI, which cannot serve as decoy receptors to neutralize excessive BAFF levels. Therefore BAFF levels are increased in TACI-deficient patients (43) enhancing the risk of developing autoimmunity and lymphoproliferation, two characteristic features described in TACI deficiency in humans (89, 90) and mice (12, 88, 91).

However, point mutations or ablation of TACI expression also causes immunodeficiency. This can be best explained by the role of TACI in supporting T-independent immune responses (32, 92–95) and the survival of plasma cells (28, 30).

## BAFFR DEFICIENCY IN HUMANS

In humans, only two cases of BAFFR-deficiency resulting from complete inactivation of the BAFFR encoding gene *TNFRSF13C* have been described so far. In both cases, the autosomal-recessive, homozygous 24bp in-frame deletion (80) removes the codons of highly conserved eight amino acids (LVLALVLV) from the transmembrane region of BAFFR, which extends from residues (76–98). The truncated BAFFR protein is highly unstable although *in silico* modeling predicts that the mutant BAFFR protein would be able to form a new transmembrane region between the resulting residues (70–92), which partially overlaps the TM region of the *wild type* protein. The lack of BAFFR expression causes an arrest of B cell differentiation at

the transition from CD10<sup>+</sup> immature/transitional 1 B cells to transitional 2 / naïve and marginal zone B cells. The homozygous mutation has full penetrance whereas the heterozygous deletion is phenotypically indistinguishable from healthy donors. Many of the immunological characteristics of human BAFFR deficiency have been described in Baffr<sup>-/-</sup> mice. The common features include very low numbers of circulating B cells, low IgM and IgG antibody titers but increased levels of serum IgA. Nevertheless, there are some clear differences between BAFFR-deficient humans and mice. First of all, inactivation of the BAFFR encoding *Tnfsf13c* gene in mice still allows normal development of B1 B cells, whereas in BAFFR-deficient humans have neither B1 B cells nor any other B cell subset, which would resemble B1 B cells. However, if B1 B cells would develop in humans as in mice from precursor cells during embryonic life and persist by homeostatic proliferation (78, 96, 97), they might have been disappeared in the BAFFR deficient patients like they also can disappear in old mice. On the other hand, the severe block in the development of follicular and marginal zone B cells might have created more space for the expansion of B1 B cells which then also would have had the chance to compensate the lack of these B2 B cell populations and to develop into IgA secreting plasma cells in the gut as it has been observed in mice (79). Interestingly, both BAFFR deficient patients have an effective output of immature B cells from bone marrow resulting in high numbers of transitional B cells, which are comparable to much younger adults. Different from Baffr<sup>-/-</sup> mice, both BAFFR-deficient humans suffered from severe lymphopenia. This difference might also be age-related or it might depend on differences regulating the size of the B cell pool, which are not well understood but known to vary between different individuals (98–100). Since IgM<sup>+</sup> CD27<sup>+</sup> marginal zone B cells control infections with encapsulated bacteria (101), the absence of marginal zone B cells resulted in defective T-independent vaccination responses against Pneumovax, which consists of a mixture of 23 different *S.pneumoniae* cell wall polysaccharides. Notably, the low but detectable IgG response against the T-dependent antigen tetanus toxoid, the high IgA serum concentrations and the presence of IgA<sup>+</sup> plasma cells in the lamina propria of the small intestine showed that BAFFR-deficiency does not completely exclude the development of B cells into plasma cells. Similar results were observed in Baffr<sup>-/-</sup> mice in which BAFFR-deficient B cells were found to complete the germinal center reaction (102) and to develop into switched memory B cells and plasma cells which survive without BAFFR (103). Upon depletion of BAFF by BAFF-neutralizing treatment with anti-BAFF monoclonal antibodies (Belimumab, Benlysta) or with soluble TACI-Ig (Atacicept), BAFFR-independent long-term survival of memory B cells has also been detected in SLE patients. These clinical studies show the strong (>75%) decline of naive B cell numbers that is followed by an increase in switched memory B cells (104, 105). Similar to the numbers of switched memory B cells, IgG antibody concentrations, which were build-up before starting the BAFF-neutralizing therapy, remained constant whereas the increase of antibody titers against neoantigens from influenza virus was significantly lower in belimumab-treated patients than in controls (106). In a similar study, the population of switched memory B cells did also not

decrease within a half year treatment of rheumatoid arthritis patients with TACI-Ig fusion protein atacicept (107).

In addition to the BAFFR deletion, different missense mutations have been described for BAFFR. The mutants were found in patients suffering from common variable immunodeficiency (CVID), the most frequent form of primary immunodeficiency which is characterized by low or absent IgM, IgG, and IgA serum titers, low numbers or absent circulating switched memory B cells and the absence of circulating plasma cells (108, 109). The BAFFR missense mutations change amino acid residues in the extra- or intracellular part of BAFFR (110–112) but they do interfere with B cell development or survival in a way which would be comparable to the BAFFR deletion mutant. Therefore, their contribution to the development of CVID and antibody deficiency remains to be shown. In this context, the P21R BAFFR variant, which is encoded by a frequent single nucleotide polymorphism (rs77874543), represents one exception. The proline 21 is located in a small loop directly preceding the BAFF binding domain. Functional and biochemical studies showed that this small loop region is essential for ligand-independent association of BAFFR polypeptide chains into multimers. It therefore represents the pre-ligand assembly domain of BAFFR (7). Although the P21R-related defect in BAFFR clustering reduces the number of BAFF molecules able to bind BAFFR on the surface of B cells by at least 50%, it does not interfere with the development of transitional B cells to naive mature B cells. Since BAFFR multimerization strongly enhances BAFF binding, B cells carrying the P21R mutation develop less efficiently into IgM secreting plasmablasts. Moreover, the homozygous P21R variant is completely resistant

**TABLE 1 |** Comparison between human and mouse BAFFR.

BAFFR	Human	Mouse
Expression starts in immature IgM <sup>+</sup> D <sup>-</sup> bone marrow B cells	+	+
Low expression during receptor editing	+	+
Expression induced by BCR signaling	+	+
Supports survival of transitional, follicular and marginal zone B cell	+	+
BAFFR-independent survival of switched memory and plasma cells	+	+
BAFFR-independent survival of B1 B cells	B1 B cells not found	+
High IgA levels in BAFFR deficiency	+	+
BAFF-induced BAFFR processing by ADAM10	+	Not analyzed
ADAM17-dependent BAFFR processing in dark zone GC B cells	+	Not analyzed
BAFFR-induced NIK-dependent activation of NF- $\kappa$ B2	+	+
BAFFR-induced activation of PI3K	+ (B lymphoma cells)	+
BAFFR-induced activation of ERK	+ (B lymphoma cells)	+
Autoimmunity induced by high BAFF concentrations	Genetic association with SLE and MS	+

against BAFF-induced processing of BAFFR by ADAM10 (70). The mutation seems to compensate its reduced ability to bind BAFF. This feature may mask in part the impaired differentiation of P21R<sup>+</sup> B cells into IgM secreting plasmablasts and prevent the development of overt immunodeficiency. **Table 1** summarizes the main differences in the studies of BAFF and BAFFR in humans and mouse models.

## PERSPECTIVES AND CONCLUSIONS

Studying the roles of BAFF and BAFF-receptors in experimental systems allowed the development of drugs which are now used to treat autoimmunity. So far, the BAFF-neutralizing monoclonal antibody belimumab is the only FDA- and EMA-approved biological drug for the treatment of patients with active refractory SLE. Application of the anti-BAFF antibody leads to a persistent, 50% improvement in about half of the SLE patients as reflected by lower anti-dsDNA titers, less corticosteroids, less cutaneous manifestations and less flares, while its adverse effects are similar as but less severe than the defects observed in BAFFR-deficiency and include respiratory, digestive and urinary tract infections [reviewed in (113)]. However, because of the lack of matched control groups, the efficacy of belimumab is still not completely clear. A second anti-BAFF antibody (tabalumab or LY2127399) has been tested in phase III studies and had similar effects like belimumab with an increase in complement activity and a decrease of anti-dsDNA IgG titers and B cell numbers leading to a mild clinical improvement in about 35% of patients treated in response to high dose treatment (114). The combination of tabalumab and bortezomib in a phase II study with multiple myeloma patients did not improve progression-free survival of the patients indicating that BAFF plays little or no role in disease progression (115). Similar to SLE, hyperactivated B cells are also discussed to play an important pathological role in the Sjögren's syndrome (116). Although in a trial study the treatment with the B cell-depleting anti-CD20 antibody did not lead to any improvement (117), new clinical trials with a novel BAFFR-specific monoclonal

(ianalumab/VAY736/NOV-5) just have started. Since increased BAFF levels correlate with the risk of developing multiple sclerosis (87), new clinical trials with MS patients with tabalumab are now being performed (118). However, it should be kept in mind that treatment of MS patients with atacicept resulted in severe adverse effects, suggesting that in MS the blockade of BAFF and APRIL removes B cells with regulatory and immunosuppressive function and spares the pathological cells (119, 120).

In summary, switched memory B cells can perfectly survive without receiving BAFFR- or TACI-dependent pro-survival signals and develop into IgA secreting plasma cells. Different from B1 B cells and from switched memory B cells, the survival of transitional, follicular and marginal zone B cells as well as the differentiation of transitional B cells into follicular and marginal zone B cells depends essentially on BAFFR-induced survival signals, which increase the life span of these cells by stabilizing mitochondria and by enhancing protein synthesis. Since IgA-secreting plasma cells can develop even in the absence of BAFFR, BAFFR-deficiency does not become manifest as dramatically as NIK or NF-κB2 deficiency, which both strongly impair B and T cell responses. Since BAFFR, TACI and BCMA play different but critical roles in regulating B cell development and survival, analysis of coupled signaling pathways, of processing reactions affecting the half-life of surface BAFFR, TACI and BCMA and of their protein interaction partners will provide deep insights into the mechanisms regulating B cell selection, autoimmunity and aging.

## AUTHOR CONTRIBUTIONS

All authors listed have made a substantial, direct and intellectual contribution to the work, and approved it for publication.

## FUNDING

This work was funded by the DFG through the TRR130 (P06) and through Ei235/9-1.

## REFERENCES

- Naismith JH, Sprang SR. Modularity in the TNF-receptor family. Elsevier Science, (1998).
- Siegel RM, Frederiksen JK, Zacharias DA, Chan FK, Johnson M, Lynch D, Tsien RY, et al. Fas preassociation required for apoptosis signaling and dominant inhibition by pathogenic mutations. *Science* (2000) 288:2354–7. doi: 10.1126/science.288.5475.2354
- Chan FK, Chun HJ, Zheng L, Siegel RM, Bui KL, Lenardo MJ. A domain in TNF receptors that mediates ligand-independent receptor assembly and signaling. *Science* (2000) 288:2351–4. doi: 10.1126/science.288.5475.2351
- Clancy L, Mruk K, Archer K, Woelfel M, Mongkolsapaya J, Scream G, et al. Preligand assembly domain-mediated ligand-independent association between TRAIL receptor 4 (TR4) and TR2 regulates TRAIL-induced apoptosis. *Proc Natl Acad Sci USA*. (2005) 102:18099–104. doi: 10.1073/pnas.0507329102
- Smulski CR, Beyrath J, Decossas M, Chekkat N, Wolff P, Estieu-Gionnet K, et al. Cysteine-rich domain 1 of CD40 mediates receptor self-assembly. *J Biol Chem*, (2013) 288:10914–22.
- Smulski CR, Decossas M, Chekkat N, Beyrath J, Willen L, Guichard G, et al. Hetero-oligomerization between the TNF receptor superfamily members CD40, Fas and TRAILR2 modulate CD40 signalling. *Cell Death Dis*. (2017) 8:e2601. doi: 10.1038/cddis.2017.22
- Pieper K, Rizzi M, Speletas M, Smulski CR, Sic H, Kraus H, et al. A common single nucleotide polymorphism impairs B-cell activating factor receptor's multimerization, contributing to common variable immunodeficiency. *J Allergy Clin Immunol*. (2014) 133:1222–5. doi: 10.1016/j.jaci.2013.11.021
- Pieper K, Grimbacher B, Eibel H. B-cell biology and development. *J Allergy Clin Immunol*, (2013) 131:959–71. doi: 10.1016/j.jaci.2013.01.046
- Thompson JS, Bixler SA, Qian F, Vora K, Scott ML, Cachero TG, et al. BAFF-R, a newly identified TNF receptor that specifically interacts with BAF. *Science* (2001) 293:2108–11. doi: 10.1126/science.1061965
- Lentz VM, Cancro MP, Nashold FE, Hayes CE. Bcnd governs recruitment of new B cells into the stable peripheral B cell pool in the A/WySnJ mouse. *J Immunol*. (1996) 157:598–606.
- Lentz VM, Hayes CE, Cancro MP. Bcnd decreases the life span of B-2 but not B-1 cells in A/WySnJ mice. *J Immunol*. (1998) 160:3743–7.

12. Yan M, Brady JR, Chan B, Lee WP, Hsu B, Harless S, et al. Identification of a novel receptor for B lymphocyte stimulator that is mutated in a mouse strain with severe B cell deficiency. *Curr Biol.* (2001) 11:1547–52. doi: 10.1016/S0960-9822(01)00481-X
13. Hsu BL, Harless SM, Lindsley RC, Hilbert DM, Cancro MP. Cutting edge: BLyS enables survival of transitional and mature B cells through distinct mediators. *J Immunol.* (2002) 168:5993–6. doi: 10.4049/jimmunol.168.12.5993
14. Mihalcik SA, Huddleston PM, III, Wu X, Jelinek DF. The structure of the TNFRSF13C promoter enables differential expression of BAFF-R during B cell ontogeny and terminal differentiation. *J Immunol.* (2010) 185:1045–54. doi: 10.4049/jimmunol.1001120
15. Smith SH, Cancro MP. Cutting edge: B cell receptor signals regulate BLyS receptor levels in mature B cells and their immediate progenitors. *J Immunol.* (2003) 170:5820–3. doi: 10.4049/jimmunol.170.12.5820
16. Ng LG, Sutherland AP, Newton R, Qian F, Cachero TG, Scott ML, et al. B cell-activating factor belonging to the TNF family (BAFF)-R is the principal BAFF receptor facilitating BAFF costimulation of circulating T and B cells. *J Immunol.* (2004) 173:807–17. doi: 10.4049/jimmunol.173.2.807
17. Rodig SJ, Shahsafaei A, Li B, Mackay CR, Dorfman DM. BAFF-R, the major B cell-activating factor receptor, is expressed on most mature B cells and B-cell lymphoproliferative disorders. *Hum Pathol.* (2005) 36:1113–9. doi: 10.1016/j.humpath.2005.08.005
18. Rowland SL, Leahy KF, Halverson R, Torres RM, Pelanda R. BAFF receptor signaling aids the differentiation of immature B cells into transitional B cells following tonic BCR signaling. *J Immunol.* (2010) 185:4570–81. doi: 10.4049/jimmunol.1001708
19. Hobeika E, Levitt-Zerdoun E, Anastasopoulou V, Pohlmeyer R, Altmeier S, Alsadeq A, et al. CD19 and BAFF-R can signal to promote B-cell survival in the absence of Syk. *EMBO J.* (2015) 34:925–39. doi: 10.1525/embj.201489732
20. Levitt-Zerdoun E, Becker M, Pohlmeyer R, Wilhelm I, Maity PC, Rajewsky K, et al. Survival of igalpha-deficient mature B cells requires BAFF-R function. *J Immunol.* (2016) 196:2348–60. doi: 10.4049/jimmunol.1501707
21. Schneider P, Mackay CR, Steiner V, Hofmann K, Bodmer JL, Holler N, et al. BAFF, a Novel Ligand of the Tumor Necrosis Factor Family, Stimulates B Cell Growth. *J. Exp. Med.* (1999) 189:1747–56.
22. Moore PA, Belvedere O, Orr A, Pieri K, LaFleur DW, Feng P, et al. BLyS: Member of the Tumor Necrosis Factor Family and B Lymphocyte Stimulator. *Science* (1999) 285:260–3.
23. Shu HB, Hu WH, Johnson H. TALL-1 is a novel member of the TNF family that is down-regulated by mitogens. *J Leukocyte Biol.* (1999) 65:680–3.
24. Gross JA, Johnston J, Mudri S, Enselman R, Dillon SR, Madden K, et al. TACI and BCMA are receptors for a TNF homologue implicated in B-cell autoimmune disease. *Nature*, (2000) 404:995–9. doi: 10.1038/35010115
25. Schiemann B, Gommerman JL, Vora K, Cachero TG, Shulga-Morskaya S, Dobles M, et al. An Essential Role for BAFF in the Normal Development of B Cells Through a BCMA-Independent Pathway. *Science* (2001) 293:2111–4. doi: 10.1126/science.1061964
26. Hahne M, Kataoka T, Schröter M, Hofmann K, Irmler M, Bodmer JL, et al. APRIL, a New Ligand of the Tumor Necrosis Factor Family Stimulates Tumor Cell Growth. *J Exp Med.* (1998) 188:1185–90.
27. Belnoue E, Pihlgren M, McGaha TL, Tougne C, Rochat AF, Bossen C, et al. APRIL is critical for plasmablast survival in the bone marrow and poorly expressed by early-life bone marrow stromal cells. *Blood* (2008) 111:2755–64. doi: 10.1182/blood-2007-09-110858
28. Mantchev GT, Cortesao CS, Rebrovich M, Cascalho M, Bram RJ. TACI is required for efficient plasma cell differentiation in response to T-independent type 2 Antigens. *J Immunol.* (2007) 179:2282–8. doi: 10.4049/jimmunol.179.4.2282
29. Ozcan E, Garibyan L, Lee JJ, Bram RJ, Lam KP, Geha RS. Transmembrane activator, calcium modulator, and cyclophilin ligand interactor drives plasma cell differentiation in LPS-activated B cells. *J Allergy Clin Immunol.* (2009) 123:1277–86 e5. doi: 10.1016/j.jaci.2009.03.019
30. Tsuji S, Cortesao C, Bram RJ, Platt JL, Cascalho M. TACI deficiency impairs sustained Blimp-1 expression in B cells decreasing long-lived plasma cells in the bone marrow. *Blood* (2011) 118:5832–9. doi: 10.1182/blood-2011-05-353961
31. Hoffmann FS, Kuhn PH, Laurent SA, Hauck SM, Berer K, Wendlinger SA, et al. The immunoregulator soluble TACI is released by ADAM10 and reflects B cell activation in autoimmunity. *J Immunol.* (2015) 194:542–52. doi: 10.4049/jimmunol.1402070
32. He B, Santamaria R, Xu W, Cols M, Chen K, Puga I, et al. The transmembrane activator TACI triggers immunoglobulin class switching by activating B cells through the adaptor MyD88. *Nat Immunol.* (2010) 11:836–45. doi: 10.1038/ni.1914
33. O'Connor BP, Raman VS, Erickson LD, Cook WJ, Weaver LK, Ahonen C, et al. BCMA is essential for the survival of long-lived bone marrow plasma cells. *J Exp Med.* (2004) 199:91–8. doi: 10.1084/jem.20031330
34. Karpusas M, Cachero TG, Qian F, Sjodin AB, Mullen C, Strauch K, et al. Crystal structure of extracellular human BAFF, a TNF family member that stimulates B lymphocytes. *J. Mol. Biol.* (2002) 315:1145–54. doi: 10.1006/jmbi.2001.5296
35. Liu Y, Xu L, Opalka N, Kappler J, Shu HB, Zhang B. Crystal structure of sTALL-1 reveals a virus-like assembly of TNF family ligands. *Cell Press* (2002) 108:383–394. doi: 10.1016/S0092-8674(02)00631-1
36. Schuepbach-Mallepell S, Das D, Willen L, Vigolo M, Tardivel A, Lebon L, et al. Stoichiometry of heteromeric BAFF and APRIL cytokines dictates their receptor binding and signaling properties. *J Biol Chem.* (2015) 290:16330–42. doi: 10.1074/jbc.M115.661405
37. Liu Y, Hong X, Kappler J, Jiang L, Zhang R, Xu L, et al. Ligand-receptor binding revealed by the TNF family member TALL-1. *Nature* (2003) 423:49–56. doi: 10.1038/nature01543
38. Cachero TG, Schwartz IM, Qian F, Day ES, Bossen C, Ingold K, et al. Formation of virus-like clusters is an intrinsic property of the tumor necrosis factor family member BAFF (B Cell Activating Factor). *Biochemistry* (2005) 45:2006–2013. doi: 10.1021/bi051685o
39. Vigolo M, Chambers MG, Willen L, Chevally D, Maskos K, Lammens A, et al. A loop region of BAFF controls B cell survival and regulates recognition by different inhibitors. *Nat Commun.* (2018) 9: 1199. doi: 10.1038/s41467-018-03323-8
40. Nardelli B, Belvedere O, Roschke V, Moore PA, Olsen HS, Migone TS, et al. Synthesis and release of B-lymphocyte stimulator from myeloid cells. *Blood J.* (2001) 97:198–204. doi: 10.1182/blood.V97.1.198
41. Thangaraj M, Masterman T, Helgeland L, Rot U, Jonsson MV, Eide GE, et al. The thymus is a source of B-cell-survival factors-APRIL and BAFF-in myasthenia gravis. *J Neuroimmunol.* (2006) 178:161–6. doi: 10.1016/j.jneuroim.2006.05.023
42. Litinskii MB, Nardelli B, Hilbert DM, He B, Schaffer A, Casali P, Cerutti A. DCs induce CD40-independent immunoglobulin class switching through BLyS and APRIL. *Nat Immunol.* (2002) 3:822–9. doi: 10.1038/ni829
43. Kreuzaler M, Rauch M, Salzer U, Birmelin J, Rizzi M, Grimbacher B, et al. Soluble BAFF levels inversely correlate with peripheral B cell numbers and the expression of BAFF receptors. *J Immunol.* (2012) 188:497–503. doi: 10.4049/jimmunol.1102321
44. Claudio E, Brown K, Park S, Wang H, Siebenlist U. BAFF-induced NEMO-independent processing of NF- $\kappa$ B2 in maturing B cells. *Nat Immunol.* (2002) 3:958–65. doi: 10.1038/ni842
45. Kayagaki N, Yan M, Seshasayee D, Wang H, Lee W, French DM, et al. BAFF/BLyS receptor 3 binds the B cell survival factor BAFF ligand through a discrete surface loop and promotes processing of NF- $\kappa$ B2. *Immunity* (2002) 17:515–24. doi: 10.1016/S1074-7613(02)00425-9
46. Zhang Q, Lenardo MJ, Baltimore D. 30 Years of NF- $\kappa$ B: a blossoming of relevance to human pathobiology. *Cell* (2017) 168:37–57. doi: 10.1016/j.cell.2016.12.012
47. Vallabhapurapu S, Karin M. Regulation and function of NF- $\kappa$ B transcription factors in the immune system. *Annu Rev Immunol.* (2009) 27:693–733. doi: 10.1146/annurev.immunol.021908
48. Gilmore TD. Introduction to NF- $\kappa$ B players, pathways, perspectives. *Oncogene* (2006) 25:6680–4. doi: 10.1038/sj.onc.1209954
49. Heusch M, Lin L, Gelezinunas R, Greene WC. The generation of nfkb2 p52: mechanism and efficiency. *Oncogene* (1999) 18:6201–8.
50. Xiao G, Harhaj EW, Sun SC. NF- $\kappa$ B-inducing kinase regulates the processing of NF- $\kappa$ B2 p100. *Mol Cell.* (2001) 7:401–9. doi: 10.1016/S1097-2765(01)00187-3

51. Liao G, Zhang M, Harhaj EW, Sun SC. Regulation of the NF-kappaB-inducing kinase by tumor necrosis factor receptor-associated factor 3-induced degradation. *J Biol Chem.* (2004) 279:26243–50. doi: 10.1074/jbc.M403286200
52. Ling L, Cao Z, Goeddel DV. NF-kappaB-inducing kinase activates IKK-alpha by phosphorylation of Ser-176. *Proc Natl Acad Sci USA.* (1998) 95:3792–7.
53. Gardam S, Sierra F, Basten A, Mackay F, Brink R. TRAF2 and TRAF3 signal adapters act cooperatively to control the maturation and survival signals delivered to B cells by the BAFF receptor. *Immunity* (2008) 28:391–401. doi: 10.1016/j.jimmuni.2008.01.009
54. Ni CZ, Oganesyan G, Welsh K, Zhu X, Reed JC, Satterthwait AC, et al. Key molecular contacts promote recognition of the BAFF receptor by TNF receptor-associated factor 3: implications for intracellular signaling regulation. *J Immunol.* (2004) 173:7394–400. doi: 10.4049/jimmunol.173.12.7394
55. Xu LG, Shu HB. TNFR-associated factor-3 is associated with BAFF-R and negatively regulates BAFF-R-mediated NF-kappa B activation and IL-10 production. *J Immunol.* (2002) 169:6883–9. doi: 10.4049/jimmunol.169.12.6883
56. Amir RE, Haecker H, Karin M, Ciechanover A. Mechanism of processing of the NF-kappa B2 p100 precursor: identification of the specific polyubiquitin chain-anchoring lysine residue and analysis of the role of NEDD8-modification on the SCF(beta-TrCP) ubiquitin ligase. *Oncogene*, (2004) 23:2540–7. doi: 10.1038/sj.onc.1207366
57. Lin WW, Hildebrand JM, Bishop GA. A complex relationship between TRAF3 and non-canonical NF-kappaB2 Activation in B Lymphocytes. *Front Immunol.* (2013) 4:477. doi: 10.3389/fimmu.2013.00477
58. Hu H, Wu X, Jin W, Chang M, Cheng X, Sun SC. Noncanonical NF-kappaB regulates inducible costimulator (ICOS) ligand expression and T follicular helper cell development. *Proc Natl Acad Sci USA.* (2011) 108:12827–32. doi: 10.1073/pnas.1105774108
59. Willmann KL, Klaver S, Dogu F, Santos-Valente E, Garncarz W, Bilic I, et al. Biallelic loss-of-function mutation in NIK causes a primary immunodeficiency with multifaceted aberrant lymphoid immunity. *Nat Commun.* (2014) 5:5360. doi: 10.1038/ncomms6360
60. Mambetsariev N, Lin WW, Stunz LL, Hanson BM, Hildebrand JM, Bishop GA. Nuclear TRAF3 is a negative regulator of CREB in B cells. *Proc Natl Acad Sci USA.* (2016) 113:1032–7. doi: 10.1073/pnas.1514586113
61. Maurer U, Charvet C, Wagman AS, Dejardin E, Green DR. Glycogen synthase kinase-3 regulates mitochondrial outer membrane permeabilization and apoptosis by destabilization of MCL-1. *Mol Cell.* (2006) 21:749–60. doi: 10.1016/j.molcel.2006.02.009
62. Hu H, Brittain GC, Chang JH, Puebla-Osorio N, Jin J, Zal A, et al. OTUD7B controls non-canonical NF-kappaB activation through deubiquitination of TRAF3. *Nature* (2013) 494:371–4. doi: 10.1038/nature11831
63. Schweighoffer E, Vanex L, Nys J, Cantrell D, McCleary S, Smithers N, et al. The BAFF receptor transduces survival signals by co-opting the B cell receptor signaling pathway. *Immunity* (2013) 38:475–88. doi: 10.1016/j.jimmuni.2012.11.015
64. Jellusova J, Miletic AV, Cato MH, Lin WW, Hu Y, Bishop GA, et al. Context-specific BAFF-R signaling by the NF-kappaB and PI3K pathways. *Cell Rep* (2013) 5:1022–35. doi: 10.1016/j.celrep.2013.10.022
65. Mattila PK, Feest C, Depoil D, Treanor B, Montaner B, Otipoby KL, et al. The actin and tetraspanin networks organize receptor nanoclusters to regulate B cell receptor-mediated signaling. *Immunity*, (2013) 38:461–74. doi: 10.1016/j.jimmuni.2012.11.019
66. Keppler SJ, Gasparri F, Burbage M, Aggarwal S, Frederico B, Geha RS, et al. Wiskott-aldrich syndrome interacting protein deficiency uncovers the role of the co-receptor CD19 as a generic hub for PI3 kinase signaling in B cells. *Immunity* (2015) 43:660–73. doi: 10.1016/j.jimmuni.2015.09.004
67. Jellusova J, Rickert RC. The PI3K pathway in B cell metabolism. *Crit Rev Biochem Mol Biol.* (2016) 51:359–78. doi: 10.1080/10409238.2016.1215288
68. Patke A, Mecklenbrauker I, Erdjument-Bromage H, Tempst P, Tarakhovsky A. BAFF controls B cell metabolic fitness through a PKC beta- and Akt-dependent mechanism. *J Exp Med.* (2006) 203:2551–62. doi: 10.1084/jem.20060990
69. Woodland RT, Fox CJ, Schmidt MR, Hammerman PS, Opferman JT, Korsmeyer SJ, et al. Multiple signaling pathways promote B lymphocyte stimulator dependent B-cell growth and survival. *Blood* (2008) 111:750–60. doi: 10.1182/blood-2007-03-077222
70. Smulski CR, Kury P, Seidel LM, Staiger HS, Edinger AK, Willen L, et al. BAFF- and TACI-dependent processing of BAFFR by adam proteases regulates the survival of B cells. *Cell Rep.* (2017) 18:2189–202. doi: 10.1016/j.celrep.2017.02.005
71. Laurent SA, Hoffmann FS, Kuhn PH, Cheng Q, Chu Y, Schmidt-Suprian M, et al. Gamma-Secretase directly sheds the survival receptor BCMA from plasma cells. *Nat Commun.* (2015) 6:7333. doi: 10.1038/ncomms8333
72. Kopan R, Ilagan MX. The canonical Notch signaling pathway: unfolding the activation mechanism. *Cell* (2009) 137:216–33. doi: 10.1016/j.cell.2009.03.045
73. Mesin L, Ersching J, Victoria GD. Germinal center B cell dynamics. *Immunity* (2016) 45:471–82. doi: 10.1016/j.jimmuni.2016.09.001
74. Kräutler NJ, Suan D, Butt D, Bourne K, Hermes JR, Chan TD, et al. Differentiation of germinal center B cells into plasma cells is initiated by high-affinity antigen and completed by Tfh cells. *J Exp Med.* (2017) 214:1259–67. doi: 10.1084/jem.20161533
75. Mackay F, Woodcock SA, Lawton P, Ambrose C, Baetscher M, Schneider P, et al. Mice transgenic for BAFF develop lymphocytic disorders along with autoimmune manifestations. *J Exp Med.* (1999) 190:1697–710.
76. Sasaki Y, Casola S, Kutok JL, Rajewsky K, Schmidt-Suprian M. TNF family member B cell-activating factor (BAFF) receptor-dependent and -independent roles for BAFF in B cell physiology. *J Immunol.* (2004) 173:2245–52. doi: 10.4049/jimmunol.173.4.2245
77. Baumgarth N. The double life of a B-1 cell: self-reactivity selects for protective effector functions. *Nat Rev Immunol.* (2010) 11:34. doi: 10.1038/nri2901
78. Hardy RR, Hayakawa K. Perspectives on fetal derived CD5+ B1 B cells. *Eur J Immunol.* (2015) 45:2978–84. doi: 10.1002/eji.201445146
79. Wang H, Shin DM, Abbasi S, Jain S, Kovalchuk AL, Beatty N, et al. Expression of plasma cell alloantigen 1 defines layered development of B-1a B-cell subsets with distinct innate-like functions. *Proc Natl Acad Sci USA.* (2012) 109:20077–82. doi: 10.1073/pnas.1212482109
80. Warnatz K, Salzer U, Rizzi M, Fischer B, Guttenberger S, Bohm J, et al. B-cell activating factor receptor deficiency is associated with an adult-onset antibody deficiency syndrome in humans. *Proc Natl Acad Sci USA.* (2009) 106:13945–50. doi: 10.1073/pnas.0903543106
81. Scholz JL, Crowley JE, Tomayko MM, Steinle N, O'Neill PJ, Quinn WJ, 3rd, et al. BLyS inhibition eliminates primary B cells but leaves natural and acquired humoral immunity intact. *Proc Natl Acad Sci USA.* (2008) 105:15517–22. doi: 10.1073/pnas.0807841105
82. Rauch M, Tussiwand R, Bosco N, Rolink AG. Crucial role for BAFF-BAFF-R signaling in the survival and maintenance of mature B cells. *PLoS ONE* (2009) 4:e5456. doi: 10.1371/journal.pone.0005456
83. Schneider P, Takatsuka H, Wilson A, Mackay F, Tardivel A, Lens S, et al. Maturation of marginal zone and follicular B cells requires B cell activating factor of the tumor necrosis factor family and is independent of B cell maturation antigen. *J Exp Med.* (2001) 194:1691–7. doi: 10.1084/jem.194.11.1691
84. Gross JA, Dillon SR, Mudri S, Johnston J, Littau A, Roque R, et al. TACI-Ig neutralizes molecules critical for B cell development and autoimmune disease: impaired B cell maturation in mice lacking BLyS. *Immunity* (2001) 15:289–302. doi: 10.1016/S1074-7613(01)00183-2
85. Tussiwand R, Rauch M, Fluck LA, Rolink AG. BAFF-R expression correlates with positive selection of immature B cells. *Eur J Immunol.* (2012) 42:206–16. doi: 10.1002/eji.201141957
86. Walmsley MJ, Ooi SK, Reynolds LF, Smith SH, Ruf S, Mathiot A, et al. Critical roles for Rac1 and Rac2 GTPases in B cell development and signaling. *Science* (2003) 302:459–62. doi: 10.1126/science.1089709
87. Steri M, Orru V, Iddha ML, Pitzalis M, Pala M, Zara I, et al. Overexpression of the cytokine BAFF and autoimmunity risk. *N Engl J Med.* (2017) 376:1615–26. doi: 10.1056/NEJMoa1610528
88. Yan M, Wang H, Chan B, Roose-Girma M, Erickson S, Baker T, et al. Activation and accumulation of B cells in TACI-deficient mice. *Nat Immunol.* (2001) 2:638–43. doi: 10.1038/89790

89. Salzer U, Chapel HM, Webster AD, Pan-Hammarstrom Q, Schmitt-Graeff A, Schlesier M, et al. Mutations in TNFRSF13B encoding TACI are associated with common variable immunodeficiency in humans. *Nat Genet.* (2005) 37:820–8. doi: 10.1038/ng1600
90. Castiglione E, Wilson SA, Garibyan L, Rachid R, Bonilla F, Schneider L, et al. TACI is mutant in common variable immunodeficiency and IgA deficiency. *Nat Genet.* (2005) 37:829–34. doi: 10.1038/ng1601
91. Seshasayee D, Valdez P, Yan M, Dixit VM, Tumas D, Grewal IS. Loss of TACI causes fatal lymphoproliferation and autoimmunity, establishing TACI as an inhibitory BLyS receptor. *Immunity* (2003) 18:279–88. doi: 10.1016/S1074-7613(03)00025-6
92. von Bülow G, van Deursen JM, Bram RJ. Regulation of the T-independent humoral response by TACI. *Immunity* (2001) 14:573–82. doi: 10.1016/S1074-7613(01)00130-3
93. Puga I, Cols M, Barra CM, He B, Cassis L, Gentile M, et al. B cell-helper neutrophils stimulate the diversification and production of immunoglobulin in the marginal zone of the spleen. *Nat Immunol.* (2011) 13:170–80. doi: 10.1038/ni.2194
94. Magri G, Miyajima M, Bascones S, Mortha A, Puga I, Cassis L, et al. Innate lymphoid cells integrate stromal and immunological signals to enhance antibody production by splenic marginal zone B cells. *Nat Immunol.* (2014) 15:354–64. doi: 10.1038/ni.2830
95. Sintes J, Gentile M, Zhang S, Garcia-Carmona Y, Magri G, Cassis L, et al. mTOR intersects antibody-inducing signals from TACI in marginal zone B cells. *Nat Commun.* (2017) 8:1462. doi: 10.1038/s41467-017-01602-4
96. Martin F, Kearney JF, B1 cells: similarities and differences with other B cell subsets. *Curr Opin Immunol.* (2001) 13:195–201. doi: 10.1016/S0952-7915(00)00204-1
97. Pillai S, Cariappa A, Moran ST. Positive selection and lineage commitment during peripheral B-lymphocyte development. *Immunol Rev.* (2004) 197:206–18. doi: 10.1111/j.0105-2896.2003.007.x
98. Morbach H, Eichhorn EM, Liese JG, Girschick HJ. Reference values for B cell subpopulations from infancy to adulthood. *Clin Exp Immunol.* (2010) 162:271–9. doi: 10.1111/j.1365-2249.2010.04206.x
99. Perez-Andres M, Paiva B, Nieto WG, Caraux A, Schmitz A, Almeida J, et al. Human peripheral blood B-cell compartments: a crossroad in B-cell traffic. *Cytometry B Clin Cytom.* (2010) 78(Suppl. 1):S47–60. doi: 10.1002/cyto.b.20547
100. Aranburu A, Piano Mortari E, Baban A, Giorda E, Cascioli S, Marcellini V, et al. Human B-cell memory is shaped by age- and tissue-specific T-independent and GC-dependent events. *Eur J Immunol.* (2016) 47:327–344. doi: 10.1002/eji.201646642
101. Kruetzmann S, Rosado MM, Weber H, Germing U, Tournilhac O, Peter HH, et al. Human immunoglobulin M memory B cells controlling *Streptococcus pneumoniae* infections are generated in the spleen. *J Exp Med.* (2003) 197:939–45. doi: 10.1084/jem.20022020
102. Rahman ZS, Rao SP, Kalled SL, Manser T. Normal induction but attenuated progression of germinal center responses in BAFF and BAFF-R signaling-deficient mice. *J Exp Med.* (2003) 198:1157–69. doi: 10.1084/jem.20020495
103. Benson MJ, Dillon SR, Castiglione E, Geha RS, Xu S, Lam KP, et al. Cutting edge: the dependence of plasma cells and independence of memory B cells on BAFF and APRIL. *J Immunol.* (2008) 180:3655–9. doi: 10.4049/jimmunol.180.6.3655
104. Furie R, Petri M, Zamani O, Cervera R, Wallace DJ, Tegzova D, et al. A phase III, randomized, placebo-controlled study of belimumab, a monoclonal antibody that inhibits B lymphocyte stimulator, in patients with systemic lupus erythematosus. *Arthritis Rheum.* (2011) 63:3918–30. doi: 10.1002/art.30613
105. Chatham WW, Wallace DJ, Stohl W, Latinis KM, Manzi S, McCune WJ, et al. Effect of belimumab on vaccine antigen antibodies to influenza, pneumococcal, and tetanus vaccines in patients with systemic lupus erythematosus in the BLISS-76 trial. *J Rheumatol.* (2012) 39:1632–40. doi: 10.3899/jrheum.111587
106. Stohl W, Hiepe F, Latinis KM, Thomas M, Scheinberg MA, Clarke A, et al. Belimumab reduces autoantibodies, normalizes low complement levels, and reduces select B cell populations in patients with systemic lupus erythematosus. *Arthritis Rheum.* (2012) 64:2328–37. doi: 10.1002/art.34400
107. van Vollenhoven RF, Kinnman N, Vincent E, Wax S, Bathon J. Atacicept in patients with rheumatoid arthritis and an inadequate response to methotrexate: results of a phase II, randomized, placebo-controlled trial. *Arthritis Rheum.* (2011) 63:1782–92. doi: 10.1002/art.30372
108. Abbott JK, Gelfand EW. Common variable immunodeficiency: diagnosis, management, and treatment. *Immunol Allergy Clin North Am.* (2015) 35:637–58. doi: 10.1016/j.iac.2015.07.009
109. Ameratunga R, Lehnert K, Woon ST, Gillis D, Bryant VL, Slade CA, et al. Review: diagnosing common variable immunodeficiency disorder in the era of genome sequencing. *Clin Rev Allergy Immunol.* (2018) 54:261–8. doi: 10.1007/s12016-017-8645-0
110. Losi CG, Silini A, Fiorini C, Soresina A, Meini A, Ferrari S, et al. Mutational analysis of human BAFF receptor TNFRSF13C (BAFF-R) in patients with common variable immunodeficiency. *J Clin Immunol.* (2005) 25:496–502. doi: 10.1007/s10875-005-5637-2
111. Hildebrand JM, Luo Z, Manske MK, Price-Troska T, Ziesmer SC, Lin W, et al. A BAFF-R mutation associated with non-Hodgkin lymphoma alters TRAF recruitment and reveals new insights into BAFF-R signaling. *J Exp Med.* (2010) 207:2569–79. doi: 10.1084/jem.20100857
112. Kutukculer N, Gulez N, Karaca NE, Aksu G, Berdeli A. Three different classifications, B lymphocyte subpopulations, TNFRSF13B (TACI), TNFRSF13C (BAFF-R), TNFSF13 (APRIL) gene mutations, CTLA-4 and ICOS gene polymorphisms in Turkish patients with common variable immunodeficiency. *J Clin Immunol.* (2012) 32:1165–79. doi: 10.1007/s10875-012-9717-9
113. Trentin F, Gatto M, Zen M, Maddalena L, Nalotto L, Saccon F, et al. Effectiveness, tolerability, and safety of belimumab in patients with refractory SLE: a review of observational clinical-practice-based studies. *Clin Rev Allergy Immunol.* (2018) 54:331–43. doi: 10.1007/s12016-018-8675-2
114. Isenberg DA, Petri M, Kalunian K, Tanaka Y, Urowitz MB, Hoffman RW, et al. Efficacy and safety of subcutaneous tabalumab in patients with systemic lupus erythematosus: results from ILLUMINATE-1, a 52-week, phase III, multicentre, randomised, double-blind, placebo-controlled study. *Ann Rheum Dis.* (2016) 75:323–31. doi: 10.1136/annrheumdis-2015-20765
115. Raje NS, Moreau P, Terpos E, Benboubker L, Grzasko N, Holstein SA, et al. Phase 2 study of tabalumab, a human anti-B-cell activating factor antibody, with bortezomib and dexamethasone in patients with previously treated multiple myeloma. *Br J Haematol.* (2017) 176:783–795. doi: 10.1111/bjh.14483
116. Nocturne G, Mariette X. B cells in the pathogenesis of primary Sjögren syndrome. *Nat Rev Rheumatol.* (2018) 14:133–145. doi: 10.1038/nrrheum.2018.1
117. Devauchelle-Pensec V, Mariette X, Jousse-Joulin S, Berthelot JM, Perdriger A, Puechal X, et al. Treatment of primary Sjögren syndrome with rituximab: a randomized trial. *Ann Intern Med.* (2014) 160:233–42. doi: 10.7326/M13-1085
118. Rahmazadeh R, Weber MS, Bruck W, Navardi S, Sahraian MA. B cells in multiple sclerosis therapy-A comprehensive review. *Acta Neurol Scand.* (2018) 137:544–556. doi: 10.1111/ane.12915
119. Kappos L, Hartung HP, Freedman MS, Boyko A, Radü EW, Mikol DD, et al. Atacicept in multiple sclerosis (ATAMS): a randomised, placebo-controlled, double-blind, phase 2 trial. *Lancet Neurol.* (2014) 13:353–63. doi: 10.1016/S1474-4422(14)70028-6
120. Sergott RC, Bennett JL, Rieckmann P, Montalban X, Mikol D, Freudensprung U, et al. ATON: results from a phase II randomized trial of the B-cell-targeting agent atacicept in patients with optic neuritis. *J Neurol Sci.* (2015) 351:174–8. doi: 10.1016/j.jns.2015.02.019

**Conflict of Interest Statement:** The authors declare that the research was conducted in the absence of any commercial or financial relationships that could be construed as a potential conflict of interest.

Copyright © 2018 Smulski and Eibel. This is an open-access article distributed under the terms of the Creative Commons Attribution License (CC BY). The use, distribution or reproduction in other forums is permitted, provided the original author(s) and the copyright owner(s) are credited and that the original publication in this journal is cited, in accordance with accepted academic practice. No use, distribution or reproduction is permitted which does not comply with these terms.



# Inhibition of Membrane-Bound BAFF by the Anti-BAFF Antibody Belimumab

Christine Kowalczyk-Quintas<sup>1</sup>, Dehlia Chevalley<sup>1</sup>, Laure Willen<sup>1</sup>, Camilla Jandus<sup>2</sup>, Michele Vigolo<sup>1</sup> and Pascal Schneider<sup>1\*</sup>

<sup>1</sup> Department of Biochemistry, University of Lausanne, Lausanne, Switzerland, <sup>2</sup> Department of Oncology UNIL CHUV, University of Lausanne, Lausanne, Switzerland

## OPEN ACCESS

### Edited by:

Hermann Eibel,  
Universitätsklinikum Freiburg,  
Germany

### Reviewed by:

Kang Chen,  
Wayne State University, United States  
Kathrin De La Rosa,  
Helmholtz-Gemeinschaft Deutscher  
Forschungszentren (HZ), Germany

### \*Correspondence:

Pascal Schneider  
pascal.schneider@unil.ch

### Specialty section:

This article was submitted to  
B Cell Biology,  
a section of the journal  
*Frontiers in Immunology*

Received: 01 May 2018

Accepted: 01 November 2018

Published: 20 November 2018

### Citation:

Kowalczyk-Quintas C, Chevalley D, Willen L, Jandus C, Vigolo M and Schneider P (2018) Inhibition of Membrane-Bound BAFF by the Anti-BAFF Antibody Belimumab. *Front. Immunol.* 9:2698.  
doi: 10.3389/fimmu.2018.02698

B cell activating factor of the TNF family (BAFF, also known as BLyS), a cytokine that regulates homeostasis of peripheral B cells, is elevated in the circulation of patients with autoimmune diseases such as systemic lupus erythematosus (SLE). BAFF is synthetized as a membrane-bound protein that can be processed to a soluble form after cleavage at a furin consensus sequence, a site that in principle can be recognized by any of the several proteases of the pro-protein convertase family. Belimumab is a human antibody approved for the treatment of SLE, often cited as specific for the soluble form of BAFF. Here we show in different experimental systems, including in a monocytic cell line (U937) that naturally expresses BAFF, that belimumab binds to membrane-bound BAFF with similar EC50 as the positive control atacicept, which is a decoy receptor for both BAFF and the related cytokine APRIL (a proliferation inducing ligand). In U937 cells, binding of both reagents was only detectable in furin-deficient U937 cells, showing that furin is the main BAFF processing protease in these cells. In CHO cells expressing membrane-bound BAFF lacking the stalk region, belimumab inhibited the activity of membrane-bound BAFF less efficiently than atacicept, while in furin-deficient U937 cells, belimumab inhibited membrane-bound BAFF and residual soluble BAFF as efficiently as atacicept. These reagents did not activate complement or antibody-dependent cell cytotoxicity upon binding to membrane-bound BAFF *in vitro*. In conclusion, our data show that belimumab can inhibit membrane-bound BAFF, and that BAFF in U937 cells is processed by furin.

**Keywords:** BAFF, BLyS, furin, protein shedding, complement, antibody-dependent cell death

## INTRODUCTION

BAFF and APRIL are important fitness and survival factors for B cells and plasma cells in the periphery. They exert their function through different receptors: BAFFR (BAFF receptor, TNFRSF13A) that binds to BAFF only, TACI (transmembrane activator and calcium modulator and cyclophilin ligand interactor, TNFRSF13B) that binds to BAFF and APRIL, and BCMA (B cell maturation antigen, TNFRSF17) that also binds to BAFF and APRIL [reviewed in (1)]. BAFFR transduces BAFF survival signals in transitional and naïve B cells, both of which are greatly decreased in BAFF-ko and BAFFR-ko mice (2–5). TACI and BCMA are expressed either upon B cell activation and/or at later stages of B cell differentiation. For example, BCMA is expressed in plasma cells that can use APRIL and/or BAFF for survival (6). Although BAFF is synthetized as a membrane-bound protein, it can be processed to a soluble form by cleavage at a furin consensus-processing site (7, 8). Furin belongs to the subtilisin/kexin-like pro-protein convertase

(PCSK) family of proteases, seven of which (PCSK1-2, furin and PCSK4-7) have arginines in their recognition sequences, and most of which are ubiquitously expressed. They are often redundant for substrate cleavage and they process a vast panel of targets, among others hormones, enzymes, receptors, cytokines and extracellular matrix components [reviewed in (9)]. With regard to BAFF, circulating levels are found elevated in diseases with involvement of auto-reactive B cells, including systemic lupus erythematosus (SLE) [reviewed in (10, 11)]. Belimumab, a human monoclonal IgG1 $\lambda$  anti-BAFF antibody approved by the FDA, can improve the condition of SLE patients (12, 13). Belimumab is specific for BAFF, and is more precisely described as an inhibitor of soluble BAFF (14, 15). Atacicept is another BAFF inhibitor consisting of the ligand-binding portion of the receptor TACI fused to a modified Fc portion of human IgG1 to remove binding to Fc receptors and to complement. Atacicept is characterized by a broader specificity of inhibition that includes APRIL and heteromers of BAFF and APRIL (16). Atacicept is under clinical development, also for the treatment of SLE (17). Here, we genetically inactivated furin in U937 histiocytic lymphoma cells that naturally express BAFF (18) to convert these cells from BAFF shedding into membrane-bound BAFF-expressing cells, indicating that furin itself is the main BAFF-processing protease in these cells. Membrane-bound BAFF on furin-deficient U937 was bound and inhibited by belimumab, suggesting that belimumab targets membrane-bound in addition to soluble BAFF.

## MATERIALS AND METHODS

### Proteins and Antibodies

Belimumab (registered trade name Benlysta), denosumab (registered trade name Xgeva), adalimumab (registered trade name Humira), and human IgG (intravenous immunoglobulins; registered trade name Kiovig) were purchased from the Pharmacy of Lausanne University Hospital (CHUV). Atacicept was kindly provided by Henry Hess (Merck KGaA). BCMA-Fc and Fc-BAFF were produced in CHO cells and affinity purified on Protein A-Sepharose, essentially as described (19). When indicated, dimeric BCMA-Fc was used. Dimeric BCMA-Fc was obtained as a defined peak after size fractionation by gel filtration on a Superdex 200 Increase 10/30 column (GE Healthcare) equilibrated in PBS. BCMA-COMP-Flag (20) was produced by transient transfection of HEK 293T cells with the polyethyleneimide method (21). 7-day-old conditioned cell supernatants in serum-free OptiMEM medium were collected and used directly.

### Cell Lines

HEK 293T and histiocytic lymphoma U937 cells were obtained from late Jürg Tschopp (University of Lausanne). CHO-S cells were from Thermoscientific (A1155701). CHO-3296 clone 7 expressing uncleavable BAFF (hBAFF  $\Delta$ 85-136) was

**Abbreviations:** BAFF, B cell activating factor of the TNF family; APRIL, A proliferation-inducing ligand; BAFFR, BAFF receptor; TACI, Transmembrane activator and CAML interactor; BCMA, B cell maturation antigen; SLE, systemic lupus erythematosus.

obtained by transfection with polyethyleneimide, selection for 3 passages in 500  $\mu$ g/ml of G418 sulfate (Calbiochem, 345812) and cloning by limiting dilution. Clones were screened for BAFF expression by staining with atacicept by flow cytometry (see “Flow cytometry”). U937 cell deficient for BAFF (U937-3515 clone B9) and U937 cells deficient for furin (U937-3511 clone D3) were generated by lentiviral transduction of CRISPR/Cas9-expression vectors with hBAFF gRNA, respectively hFurin gRNA (**Supplementary Table 1**). Annealed oligonucleotides 5'- CACCGACTGATAAGACCT ACGCCAT-3' and 5'- AAACATGGCCGTAGGTCTTATCAGT-3' (for hBAFF) or 5'- CACCGAAGTGCACGGAGTCTCACA C-3' and 5'- AACAGTGTGAGACTCCGTGCACTTC-3' (for hFurin) were cloned in the BsmBI restriction site of lentrcrispr v2 plasmid (Addgene #52961) (22). These plasmids were co-transfected with co-vectors pCMV-VSV-g (Addgene #8454) and psPAX2 (Addgene #12260) (**Supplementary Table 1**) into 293T cells with polyethyleneimide. The next day, cells were washed with PBS and cultured for an additional day in RPMI 10% FCS. Cell supernatants filtered at 0.45  $\mu$ m were supplemented with 8  $\mu$ g/ml polybrene (Sigma, H9268) and 2.5 ml were added to 2  $\times$  10 $^6$  pelleted U937 cells that were subsequently cultured overnight in a 12-well plate, then washed and expanded for 3 days in a 6-well plate in RPMI 10% FCS. Cells were then selected for 3 days in RPMI 10% FCS, 1  $\mu$ g/ml puromycin (EnzoLifeSciences ALX 380-028). Surviving cells were cloned in RPMI 10% FCS, in culture plates pre-coated for 5 min at 37°C with 1  $\mu$ g/ml of poly-lysine (Sigma P6407) in water. Furin-deficient clones and BAFF-deficient clones were identified by their impairment to release active soluble BAFF in their supernatants (see “Cytotoxic assays”). Jurkat JOM2 BAFFR:Fas-2308 cl21 reporter cells were as described (16, 23, 24). Jurkat cells expressing Fc $\gamma$ RIIIa and NFAT-driven luciferase were provided in the ADCC reporter bioassay core kit (Promega, G7010) and used as recommended by the manufacturer.

### Biotinylation

One milligram of belimumab or 1 mg of atacicept in 1 ml of 0.1 M Na-borate pH 8.8 were biotinylated for 2 h at room temperature with 10  $\mu$ l of EZ-Link<sup>TM</sup> sulfo-N-hydroxysuccinimide-LC-biotin (Pierce, #21335) at 30  $\mu$ g/ml in DMSO. Reaction was terminated by addition of 30  $\mu$ l of 1 M NH<sub>4</sub>Cl, and buffer was exchanged to PBS using a 30 kDa cutoff centrifugal device.

### CFSE Labeling

Carboxyfluorescein-succinimidyl ester (CFSE, Sigma 21888) at 10 mM in dimethylsulfoxide was stored at -70°C until use. BAFFR:Fas reporter cells ( $\sim$ 10 $^7$ ) were labeled by incubation for 8 min at 37°C in a freshly prepared mixture of PBS, 1% FCS and 2  $\mu$ M CFSE, or in PBS, 0.1  $\mu$ M CFSE. Reactions were quenched by the addition of RPMI 10% FCS, cells were harvested, washed twice with RPMI 10% FCS and used to assay membrane-bound BAFF (see “Cytotoxic assays with BAFFR:Fas reporter cells”).

## Cytotoxic Assays With BAFFR:Fas Reporter Cells

Recombinant Fc-hBAFF was used at the indicated concentrations, and BAFF in conditioned medium of CHO or U937 cells (parental or stable clones) was used at the indicated dilutions of supernatants. Inhibitors, when present, were used at the indicated concentrations and pre-incubated for at least 3 min with effectors in 50  $\mu$ l of RPMI 10% FCS. Unlabeled Jurkat JOM2 BAFFR:Fas-2308 clone 21 reporter cells (20,000–50,000/well) were added in 50  $\mu$ l of RPMI 10% FCS and incubated overnight ( $\sim$ 16 h) at 37°C, 5% CO<sub>2</sub>. Cell viability was then recorded by addition of 20  $\mu$ l of PMS/MTS (phenazine methosulfate at 45  $\mu$ g/ml and 3-(4,5-dimethylthiazol-2-yl)-5-(3-carboxymethoxyphenyl)-2-(4-sulfophenyl)-2H-tetrazolium at 2 mg/ml in PBS) and by monitoring absorbance at 492 nm after adequate color development ( $\sim$ 2–8 h) (24).

The measure of membrane-bound BAFF activity on U937 cells was performed in 96 well plates, in a final volume of 100  $\mu$ l of RPMI 10% FCS, at 37°C and with 5% CO<sub>2</sub>. 50  $\mu$ l of effector cells (U937-3515 clone B9 or U937-3511 clone D3, 10<sup>5</sup> cells), or 50  $\mu$ l of soluble effectors (Fc-hBAFF at 100 ng/ml) were mixed with 20  $\mu$ l of 5-fold concentrated inhibitors for 6 h, then 30  $\mu$ l of CFSE-labeled BAFFR:Fas reporter cells ( $\sim$ 5  $\times$  10<sup>4</sup>) were added

for an additional 11 h. Cells were transferred on ice in 1 ml tubes containing 10  $\mu$ l of 10  $\mu$ g/ml propidium iodide, and analyzed by flow cytometry (See “Flow cytometry”).

For the measure of membrane-bound BAFF on CHO-3296 cl7 cells, experiments were performed in 48 well plates. Untransfected CHO cells, or CHO-3296 cl7 cells (1.5  $\times$  10<sup>5</sup>/well) were left to adhere for 2 h, after which time medium was removed and replaced by 200  $\mu$ l of fresh medium. Wells without CHO cells contained medium only. Hundred  $\mu$ l of inhibitors (at 5-fold the final desired concentration), 50  $\mu$ l of Fc-BAFF at 1  $\mu$ g/ml (or 50  $\mu$ l of medium in conditions without Fc-BAFF) and 150  $\mu$ l of CFSE-labeled BAFFR:Fas reporter cells ( $\sim$ 2.5  $\times$  10<sup>5</sup> cells) were added and incubated for 11 h. Non adherent cells were transferred into 4 ml tubes, and then pooled with adherent cells detached with trypsin-EDTA. Cells were spun for 1 min at 5,000 rpm (2,400  $\times$  g), pellets were suspended in 100  $\mu$ l of PBS, 5% FCS and supplemented with 10  $\mu$ l of 10  $\mu$ g/ml propidium iodide before analysis (See “Flow cytometry”).

## Flow Cytometry

293T cells were co-transfected with hBAFF expression vectors and an EGFP expression vector as a tracer. Cells were stained 3 days later with the indicated amounts of atacicept

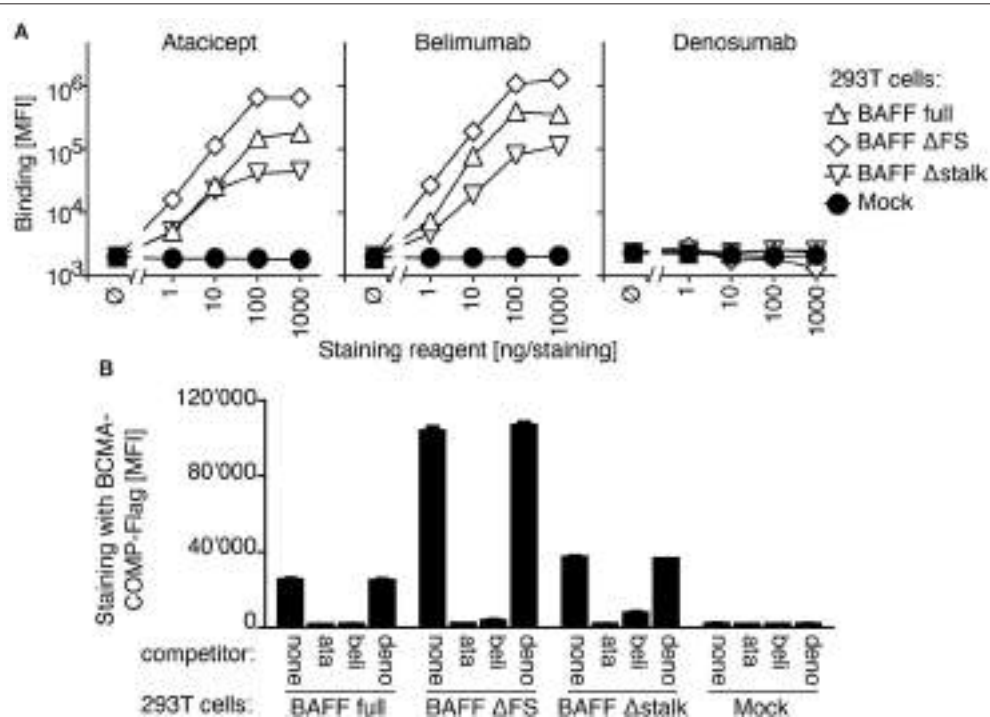


**FIGURE 1 |** Belimumab binding to BAFF on transfected 293T cells prevents concomitant binding of BCMA. **(A)** 293T cells transiently transfected with plasmids coding for full length BAFF wild type (BAFF full), full length BAFF with mutated furin site (BAFF ΔFS), full length BAFF deleted for the stalk region and furin site (BAFF Δstalk) or with empty plasmid (Mock) were stained with the indicated amounts of belimumab or atacicept, or denosumab as control. Mean fluorescence intensity (MFI) of staining (in the phycoerythrin channel) was monitored for cells expressing medium levels of co-transfected EGFP ( $2 \times 10^5$  to  $6 \times 10^5$  fluorescence units). Mean  $\pm$  SEM of triplicate measures (note that error bars are smaller than symbols). Experiment performed 5 times (twice in monoplicates, without BAFF Δstalk and denosumab controls). **(B)** 293T cells transfected as indicated (transfection distinct from that of panel **A**) were pre-incubated with buffer (none), atacicept (ata), belimumab (beli) or denosumab (deno) and then stained with BCMA-COMP-Flag and anti-Flag secondary reagents. Mean fluorescence intensity (MFI) was measured as in panel **A**. Mean  $\pm$  SEM of triplicate measures. Experiment performed 3 times (once in monoplicate, without denosumab control).

or belimumab in 50  $\mu$ l of PBS, 5% FCS for 20 min on ice, followed by phycoerythrin-coupled rat anti-human IgG (Southern Biotech Associate, 2040-09, 1/500). Alternatively, transfected cells were pre-incubated with 5  $\mu$ g of atacicept or belimumab in 25  $\mu$ l of PBS 5% FCS for 20 min on ice, then stained for 20 min, without wash, by addition of 25  $\mu$ l of BCMA-COMP-Flag in conditioned OptiMEM supernatants, followed by biotinylated anti-FLAG (Sigma, F9291, 1/500) and phycoerythrin-coupled streptavidin (eBioSciences, 12-4317-87, 1/500). Data was acquired with an AccuriC6 flow cytometer (BD Bioscience) and analyzed with the FlowJo software (TreeStar, Ashland, OR). Mean fluorescence intensity of atacicept, belimumab or BCMA-COMP-Flag staining was measured for cells expressing medium levels ( $2 \times 10^4$  to  $2 \times 10^5$  fluorescence units) of EGFP.

CHO-3296 clone 7 cells were stained with atacicept, belimumab or denosumab as described for transfected 293T cells, except that MFI was reported for all live cells. U937 cells (wild type, furin-deficient or BAFF-deficient) were pre-incubated with human IVIGs (50  $\mu$ g in 50  $\mu$ l of PBS, 5% FCS) for 20 min on ice, washed and stained for 20 min on ice with the indicated amount of biotinylated atacicept or biotinylated belimumab in 50  $\mu$ l of PBS 5% FCS followed by phycoerythrin-coupled streptavidin (1/500).

CFSE-labeled reporter cells (co-cultured with membrane-bound BAFF-expressing cells, recombinant Fc-BAFF or controls) were stained with propidium iodide as described (see “Cytotoxic assays with BAFFR:Fas reporter cells”) and analyzed by flow cytometry. The proportion of live reporter cells was calculated as follows: [number of live reporter cells / (number of live reporter cells + number of dead reporter cells)], where live cells were CFSE<sup>+</sup> PI<sup>-</sup> cells in the live FCS/SSC gate, and dead cells were all CFSE<sup>+</sup> cells in the dead FCS/SSC gate. This number was divided by the proportion of live cells in untreated controls to correct for spontaneous death, and multiplied by 100 to get the percentage of specific target cell viability.

## BAFF ELISA

BAFF in conditioned supernatant of U937 cells was quantified using the hypersensitive hBAFF ELISA kit (Adipogen, AG-45B-0001-KI01) according to the manufacturer's protocol. Supernatants of BAFF-deficient and furin-deficient cells were measured in duplicate at a dilution of 1/2, and those of wild type cells at dilutions of 1/4, 1/40, and 1/400.

## Complement Activation Assay

CHO-3296 clone 7 cells or CHO cells ( $2 \times 10^4$ /well in 80  $\mu$ l of DMEM/F12 (1/1) 2% FCS) were left to adhere overnight in

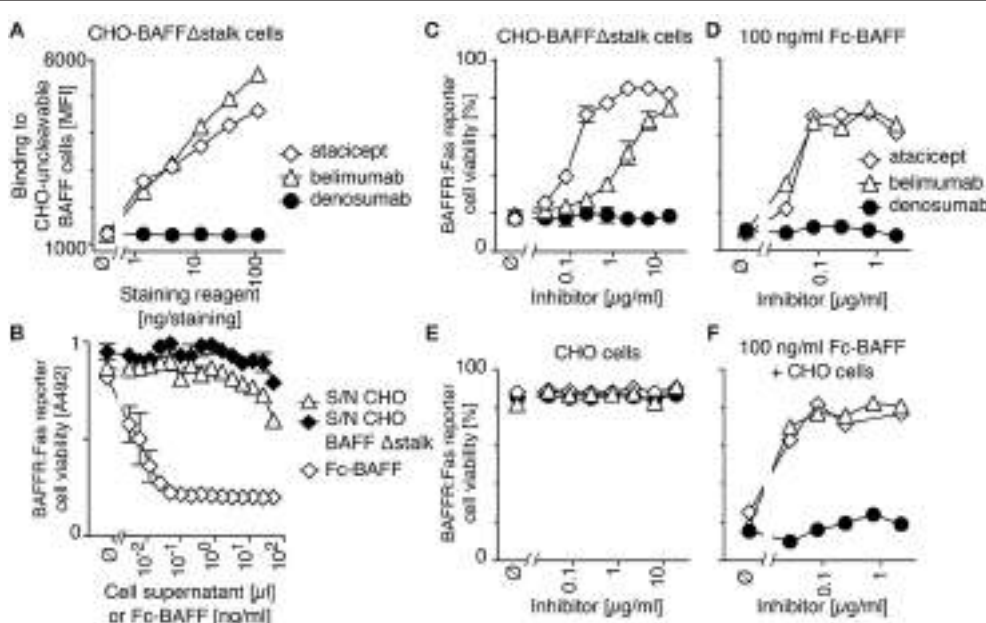


**FIGURE 2 |** Belimumab binds and partially inhibits membrane-bound BAFF lacking the stalk region expressed in CHO cells. **(A)** CHO cells stably expressing uncleavable BAFF  $\Delta$ stalk were stained with the indicated amounts of atacicept, belimumab or denosumab. Mean fluorescence intensity (MFI) of staining was monitored. Single measures were performed. Experiment performed 3 times. **(B)** BAFFr:Fas reporter cells were exposed to titrated amounts of conditioned supernatants of CHO cells with or without expression of uncleavable BAFF  $\Delta$ stalk, or to recombinant soluble BAFF (Fc-BAFF) added as a positive control. After overnight incubation, cell viability was monitored with the PMS/MTS test. Mean  $\pm$  SEM of triplicates. Experiment performed twice. **(C)** CFSE-labeled BAFFr:Fas reporter cells were co-cultured with CHO cells expressing uncleavable BAFF in the presence of increasing concentrations of atacicept, belimumab or denosumab. Cell viability after overnight incubation was measured by flow cytometry. Measures are duplicates (mean  $\pm$  SEM). Experiment performed twice. **(D)** Same as panel **C**, except that uncleavable BAFF  $\Delta$ stalk cells were replaced by a lethal dose of Fc-BAFF (100 ng/ml). Single measures were performed. Experiment performed twice. **(E)** Same as panel **C**, except that uncleavable BAFF  $\Delta$ stalk cells were replaced by control CHO cells. Single measures were performed. Experiment performed twice. **(F)** CFSE-labeled BAFFr:Fas reporter cells were co-cultured overnight with CHO cells and 100 ng/ml of Fc-BAFF, in the presence of inhibitors at the indicated concentrations. Single measures were performed. Experiment performed twice.

96-wells culture plates. Fc-containing reagents were then added in 10  $\mu$ l of medium, incubated for 10 min at room temperature before addition of 10  $\mu$ l of untreated or heat-inactivated (30 min at 56°C) normal human serum (from P.S.) for 2 h at 37°C. Cell viability was monitored with PMS/MTS (see “Cytotoxic assays with BAFFR:Fas reporter cells”).

## Antibody-Dependent Cell-Mediated Cytotoxicity Assay

Antibody-dependent cell-mediated cytotoxicity was measured using the ADCC core kit (Promega, G7010), according to the manufacturer's protocol. CHO-3296 clone 7 cells were used as targets, adalimumab, atacicept, BCMA-Fc and belimumab at the indicated concentrations were used as mediators, and Jurkat cells expressing both human Fc $\gamma$ RIIIa V158 and NFAT-induced luciferase were used as effectors. 25,000 target cells per well were seeded in 96 wells white plates in 100  $\mu$ l of DMEM:F12 2% FCS and left to adhere overnight. Ninety-five microliter of medium was removed and replaced by 25  $\mu$ l of RPMI supplemented with 4% of low Ig FCS, 25  $\mu$ l of the test reagent and 25  $\mu$ l of freshly defrosted effector cells. After 6 h of incubation, 75  $\mu$ l of luciferase substrate was added and luminescence was monitored 15 min later.

## Statistics

Replicate measurements are shown as mean  $\pm$  SEM. EC<sub>50</sub> of titration curves were determined after normalization of cell viability using the “non linear regression (curve fit)” followed by the “log(agonist) vs. normalized response–variable slope” function of Prism 7 (GraphPad Software).

## RESULTS

### Belimumab and Atacicept Bind to and Inhibit BAFF at the Surface of Transfected 293T or CHO Cells

In a FACS-based assay, both atacicept and belimumab stained 293T cells transfected with full length BAFF, but not mock-transfected cells. BAFF with a mutated furin consensus sequence (SRNKRAVGP → SRNKLQGP) (BAFF ΔFS) or BAFF lacking the stalk region linking the transmembrane domain to the extracellular receptor-binding domain, a deletion that included the furin consensus sequence (BAFF Δstalk) were also recognized by atacicept and belimumab, while the unrelated antibody denosumab stained none of these cells (Figure 1A). Binding of atacicept or belimumab to membrane-bound BAFF prevented subsequent binding of recombinant BCMA, one of the

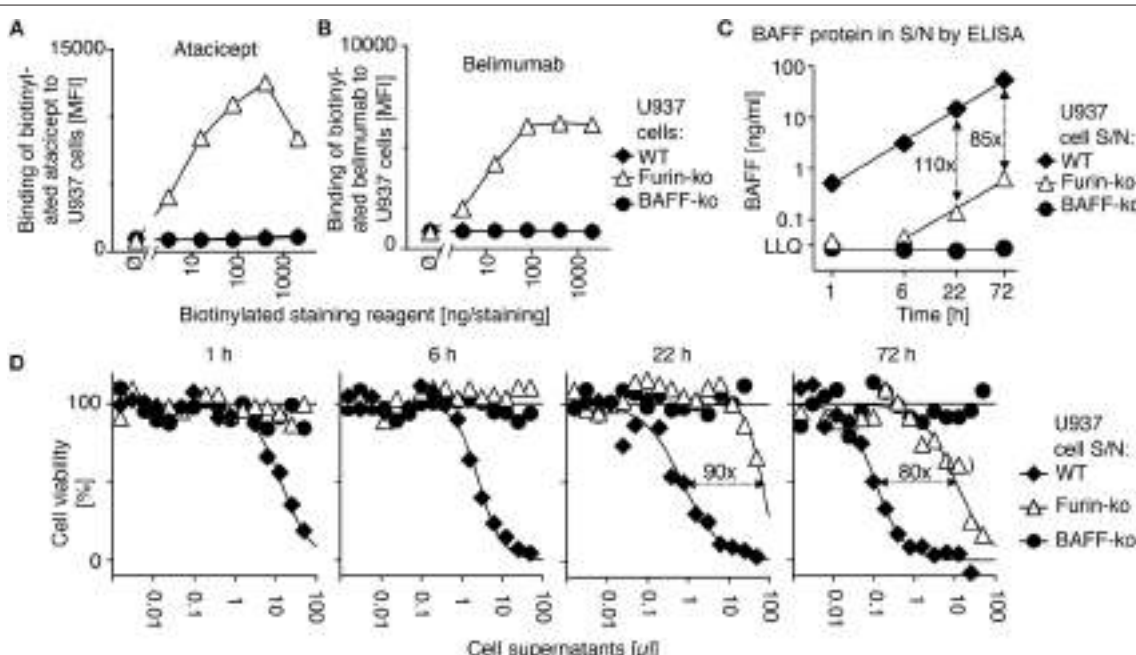


**FIGURE 3 |** Belimumab binds to membrane-bound BAFF in furin-deficient U937 cells. **(A)** Wild-type (WT), furin-deficient (furin-ko) and BAFF-deficient (BAFF-ko) U937 cells were stained with the indicated amounts of biotinylated atacicept after saturation of Fc receptors with human IgGs. Mean fluorescence intensity (MFI) of staining was monitored. Single measures were performed. Experiment performed four times. **(B)** Same as panel A, except that staining was performed with biotinylated belimumab. Experiment performed four times. **(C)** The indicated U937 cells were washed and then put in culture. Human BAFF was quantified by ELISA in conditioned cell supernatants collected at the indicated time points. LLQ: lower limit of quantification. Double-sided arrows indicate the fold difference between concentrations of BAFF in supernatants of wild type and furin-deficient U937 cells. Error bars of measures performed in duplicate ( $\text{mean} \pm \text{SEM}$ ) are smaller than symbol size. Experiment performed twice. **(D)** BAFFR:Fas reporter cells were exposed to titrated amounts of the same conditioned supernatants used in panel C. After an overnight incubation, cell viability was monitored with the PMS/MTS assay. Single measures were performed. Double sided arrows indicate the fold difference between EC<sub>50</sub> of wild type and furin-deficient supernatants. One measure indicated in brackets was excluded for the determination of EC<sub>50</sub>. Experiment performed twice in this format, and two more times with a single time point.

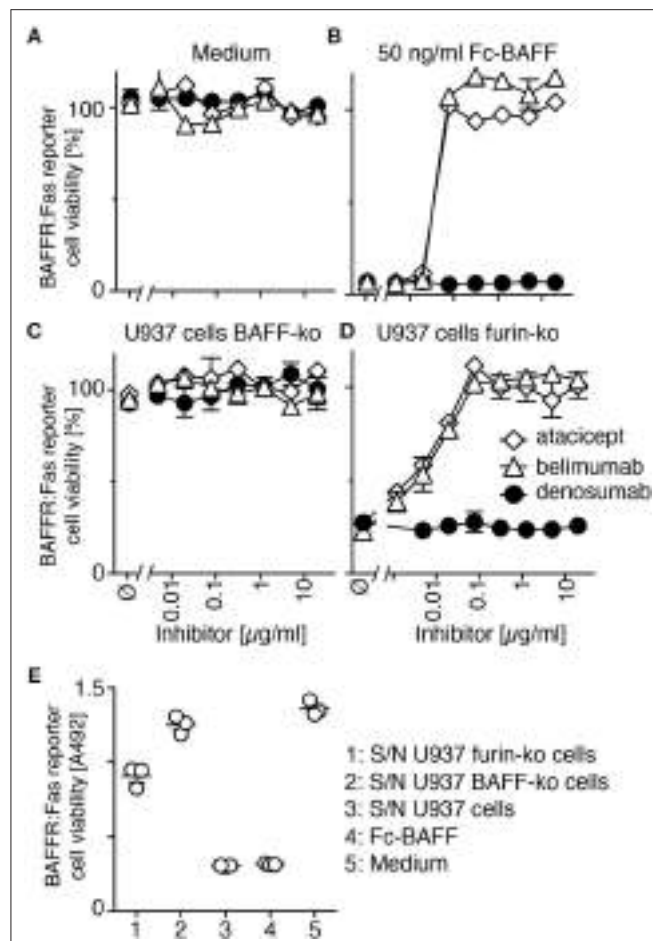


**FIGURE 4 |** Belimumab inhibits membrane-bound and residual soluble BAFF in furin-deficient U937 cells. **(A,B)** CFSE-labeled BAFFR:Fas reporter cells were exposed to **(A)** medium or to **(B)** a lethal dose of Fc-BAFF (50 ng/ml) in the presence of increasing concentrations of atacicept, belimumab or denosumab. Cell viability after overnight incubation was measured by flow cytometry. Mean of triplicates  $\pm$  SEM. Experiment performed twice. **(C,D)** CFSE-labeled BAFFR:Fas reporter cells were co-cultured overnight with **(C)** BAFF-deficient (BAFF-ko) or **(D)** furin-deficient (furin-ko) U937 cells in the presence of atacicept, belimumab or denosumab at the indicated concentrations. Mean of triplicates  $\pm$  SEM. Experiment performed twice. **(E)** BAFFR:Fas reporter cells were exposed to undiluted conditioned medium of the indicated U937 cells that were grown alone, but for the same time (17 h) and otherwise identical conditions to those of U937 cells used in panels **C** and **D**. Medium and Fc-BAFF at 50 ng/ml in medium pre-incubated alone for 17 h in the same conditions were used as controls. Viability of reporter cells was monitored with the PMS/MTS assay. Mean of triplicates  $\pm$  SEM. Experiment performed twice.

receptors for BAFF, suggesting that the binding of either atacicept or belimumab inhibits membrane-bound BAFF (**Figure 1B**).

In order to measure the activity of membrane-bound BAFF, we generated a stable clone of CHO cells expressing BAFF  $\Delta$ stalk, i.e., uncleavable membrane-bound BAFF. These cells stained with both atacicept and belimumab, but not with the control antibody denosumab (anti-RANKL) (**Figure 2A**) and did not release detectable levels of soluble BAFF activity in their supernatants (**Figure 2B**). Unlabeled CHO cells expressing uncleavable BAFF

were co-cultured with CFSE-labeled BAFFR:Fas reporter cells. In reporter cells, the extracellular domain of BAFFR is fused to the transmembrane and intracellular domains of the death receptor Fas, so that they are killed upon engagement of BAFFR, and so that BAFF inhibitors can protect them from BAFF-mediated killing. CHO cells expressing uncleavable BAFF readily killed BAFFR:Fas reporter cells, a killing that could be inhibited in a dose-dependent manner by both atacicept and belimumab, although atacicept was about 10 times more efficient than belimumab in this respect (**Figure 2C**). Reporter cells also died in response to soluble recombinant BAFF, but in this case inhibition by atacicept or belimumab was equally good (**Figure 2D**). Controls showed that atacicept, belimumab or untransfected CHO cells had no deleterious effect on reporter cells (**Figure 2E**), and that untransfected CHO cells did not prevent atacicept and belimumab from inhibiting soluble BAFF (**Figure 2F**). Taken together, these results show that binding of atacicept and belimumab to membrane-bound BAFF is inhibitory.

## Processing of Membrane-Bound BAFF to Active Soluble BAFF Is Mediated by Furin in U937 Cells

In order to determine the action of atacicept and belimumab on endogenous BAFF, we used monocytic U937 cells that naturally produce soluble BAFF (18, 25). Atacicept and belimumab did not stain wild type and BAFF-deficient U937 cells by flow cytometry (**Figures 3A,B**). However, CRISPR/Cas9-mediated deletion of furin with a construct targeting the active site of the protease abrogated  $>98\%$  of the release of both BAFF protein (**Figure 3C**) and BAFF activity (**Figure 3D**) in supernatants of U937 cells, while increasing cell surface levels of BAFF that became detectable by staining with both atacicept and belimumab (**Figures 3A,B**).

## Inhibition of Membrane-Bound BAFF in U937 Cells by Atacicept and Belimumab

Inhibition of non-mutated membrane-bound BAFF was tested in furin-deleted U937 cells. Atacicept and belimumab on their own were not toxic for reporter cells (**Figure 4A**). On the contrary, they both protected reporter cells from a lethal dose of soluble recombinant BAFF at roughly stoichiometric ratio (**Figure 4B**). BAFF-deficient U937 cells were harmless to BAFFR:Fas reporter cells (**Figure 4C**), but furin-deficient U937 cells, which express membrane-bound BAFF, efficiently killed them (**Figure 4D**). This killing was inhibited in a dose-dependent manner and with similar efficacy by both atacicept and belimumab, while the control antibody denosumab did not protect against membrane-bound BAFF (**Figure 4D**). An additional control showed that BAFF released into supernatant of furin-deficient U937 cells during the 17 h co-culture period could only kill about 30% of reporter cells (**Figure 4E**), indicating that the remaining toxicity of furin-deficient U937 cells on BAFFR:Fas reporter cells was due to membrane-bound BAFF (**Figure 4D**). Taken together, these results indicate that both endogenous membrane-bound BAFF and residual soluble BAFF

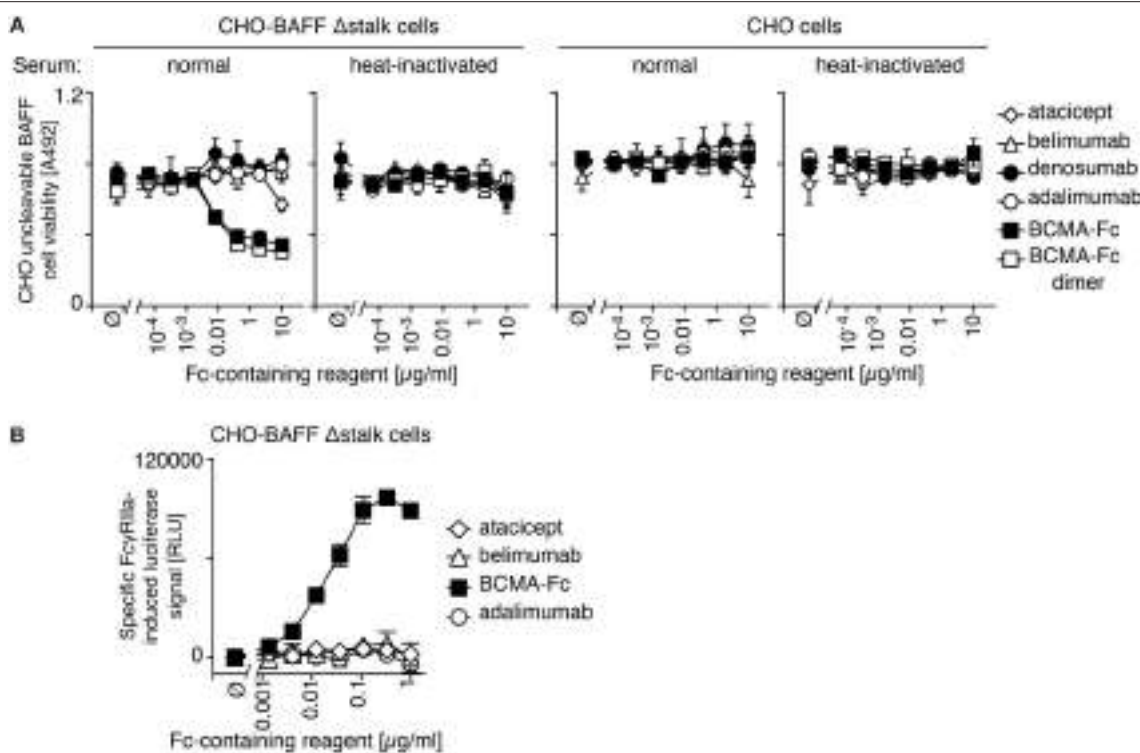


**FIGURE 5 |** No detectable effector function of belimumab bound to membrane-bound BAFF. **(A)** CHO BAFF Δstalk cells or CHO cells were pre-incubated for 30 min with atacicept, belimumab, denosumab, adalimumab, BCMA-Fc or size-fractionated (dimeric) BCMA-Fc at the indicated concentrations, and subsequently exposed for 2 h to normal human serum that had been heat-inactivated or not. Cells viability was monitored with the PMS/MTS assay. Mean ± SEM of duplicates. Experiment performed twice (but only once for the condition of dimeric BCMA-Fc). **(B)** CHO BAFF Δstalk cells were pre-incubated with atacicept, belimumab, BCMA-Fc, or adalimumab at the indicated concentrations, after which time surrogate effector cells of antibody-dependent cellular-mediated cytotoxicity were added. NFAT-driven luciferase expression is induced when opsonized IgG-containing molecules engage Fc<sub>γ</sub>RIIIa expressed in these reporter cells. Specific signal in relative luminescence units (RLU) was obtained after subtraction of background of unstimulated cells ( $\sim 10^5$  RLU). Mean ± SEM of triplicate measures. Experiment performed twice.

in U937 cells are bound and inhibited by atacicept and belimumab.

### Opsonized Atacicept and Belimumab Do Not Induce Complement or Cell-Mediated Toxicity

IgGs that are opsonized on a cell surface activate complement or antibody-dependent cell-mediated cytotoxicity via their fragment crystallizable (Fc) regions. Atacicept was used as a negative control because its mutated Fc region activates neither of these pathways. Neither atacicept nor belimumab activated complement when bound to CHO cells expressing uncleavable BAFF (Figure 5A). In contrast, BCMA-Fc, a BAFF-binding decoy receptor with a wild type human IgG1 Fc portion, decreased viability of target cells in the presence of normal human serum, but not in de-complemented serum and not in CHO cells expressing no BAFF (Figure 5A). Adalimumab, an anti-TNF antibody with reported ability to activate complement (26) had no activity in the absence of its target (Figure 5A). It is noteworthy that a purely dimeric preparation of BCMA-Fc, obtained after gel filtration, displayed the same activity as “crude” BCMA-Fc (Figure 5A).

Antibody-dependent cell-mediated cytotoxicity was monitored in a surrogate assay in which the activation of Fc<sub>γ</sub> receptor IIIa over-expressed in Jurkat T cells drives NFAT (nuclear factor of activated T cells)-dependent expression of luciferase. Neither atacicept nor belimumab activated reporter cells when bound to membrane-bound BAFF on CHO cells, while the positive control BCMA-Fc did (Figure 5B). We conclude from these data that atacicept and belimumab inhibit their target cytokine(s) in soluble or membrane-bound forms, but do not kill BAFF-expressing cells, at least *in vitro*.

### DISCUSSION

It was previously reported that belimumab inhibits BAFF, but not APRIL. In addition, belimumab does not inhibit any of the BAFF-APRIL heteromers, while atacicept inhibits BAFF, APRIL and heteromers thereof (16). Another difference is that soluble BAFF can exist as 3-mers, or can assemble as 60-mers (27). Belimumab cannot inhibit BAFF 60-mers unless they first dissociate into 3-mers, whereas atacicept and another anti-BAFF antibody, tabalumab, can inhibit BAFF 60-mers (28–30). Belimumab is often described in the literature as an inhibitor

of soluble BAFF. This conclusion probably finds its origin into the original description of the antibody, where belimumab could not stain IFN $\gamma$ -stimulated human monocytes by flow cytometry, while another antibody called 12D6 could (14). This was later interpreted as “ [...] , belimumab specifically recognizes the soluble, biologically active form of BLyS” (31). Our present results question this conclusion and re-enforce previous results obtained with over-expressed BAFF in CHO cells showing that belimumab can inhibit membrane-bound BAFF (28). The monoclonal antibodies 12D6, 2E5, and 9B6 can all stain human monocytes (7, 14, 18). It would be interesting to monitor their binding to wild type, furin-deficient and BAFF-deficient U937 cells side by side with belimumab to determine if they are really better binders of membrane-bound BAFF, or whether there might be other causes for their binding to monocytes.

It has long been recognized that BAFF is processed at a furin consensus site (7, 8). Here we provide the first indication that in U937 cells, BAFF is cleaved by furin, with no or little contribution of other members of the pro-protein convertase subtilisin/kexin family. However, we did not investigate whether this is also true for other cell lines or primary cells. Like *Baff*<sup>-ko</sup> mice, mice with non-cleavable BAFF have few mature B cells, indicating that membrane-bound BAFF, unlike soluble BAFF, does not support naïve B cells (32). But when follicular B cells were restored by administration of recombinant soluble BAFF 3-mer, full maturation of B cells, measured by CD23 expression, required membrane-bound BAFF (32). In mice with non-cleavable BAFF, membrane-bound BAFF co-localized with medullary fibroblastic reticular cells in lymph nodes. These cells make more direct contacts with plasma cells than any other cell type, and they can support survival of plasma cells *in vitro*, alone or together with macrophages, while other lymph node cell types cannot (33). This suggests that membrane-bound BAFF may be more important for plasma cells than for naïve B cells, possibly through activation of the receptors TACI and BCMA, and that inhibition of membrane-bound BAFF might be relevant to the mechanism of action of belimumab in SLE patients.

In this study, we have observed that belimumab binds normally to BAFF  $\Delta$ stalk overexpressed in CHO cells but was less efficient than atacicept to inhibit it. This was however not the case in furin-deficient U937 cells in which both atacicept and belimumab similarly inhibited full-length membrane-bound BAFF (and residual soluble BAFF). Thus, BAFF binding and BAFF inhibitory activities did not correlate well only for the pair of belimumab - BAFF  $\Delta$ stalk, but not for the pairs belimumab—full length BAFF, atacicept—BAFF  $\Delta$ stalk or atacicept—full-length BAFF. How can these results be reconciled in a molecular model? We have previously observed that atacicept binds and inhibits BAFF even when it is densely packed as 60-mers (30). It is therefore not surprising that atacicept can bind and inhibit membrane-bound BAFF irrespective of the length of the stalk region, as observed experimentally. We have also observed that, in contrast to intact belimumab, Fab fragments of belimumab did not or only very poorly inhibit the activity of BAFF 3-mers, probably because monovalent Fab can be displaced from BAFF by BAFFR (30). This would support a hypothetical model in which the first monovalent binding of belimumab to membrane-bound BAFF would allow cell staining by flow cytometry but would

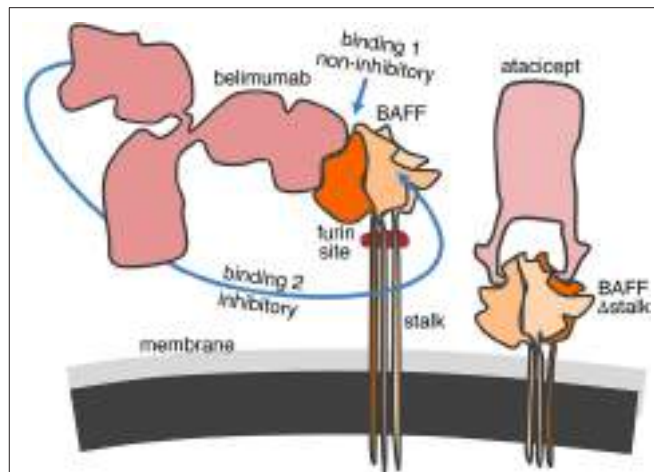


**FIGURE 6 |** Hypothetical model for the binding of belimumab and atacicept to membrane-bound BAFF. The 66 amino acids-long stalk of BAFF contains the furin cleavage site and, if linear and extended, could have three times the height of the globular TNF homology domain. In contrast, the engineered stalk-less BAFF is much closer to the membrane. Atacicept binds BAFF from the side opposite to the membrane and has free access regardless of the length of the stalk. Belimumab is not only bulkier but also binds more on the side of BAFF along the entire height of the TNF homology domain. The first binding of belimumab to membrane-bound BAFF is probably always easy, but insufficient to inhibit the biological activity of BAFF. Inhibition only takes place upon binding of the second arm of the antibody to membrane-bound BAFF. Movements of the antibody to reach its second binding site might be compromised for steric hindrance reasons if BAFF is located too close to the cell membrane in BAFF  $\Delta$ stalk.

be poorly inhibitory. Membrane-bound BAFF would only be inhibited upon binding of the second arm of the antibody that increases binding avidity, preventing efficient displacement by BAFFR. The molecular “gymnastic” that belimumab must accomplish to reach its second binding site on membrane-bound BAFF might be partially impaired for steric hindrance reasons in the specific case of BAFF  $\Delta$ stalk that is positioned very close to the cell membrane (**Figure 6**).

Interestingly, we find that belimumab does not activate complement and Fc receptors *in vitro*. If this holds true *in vivo*, belimumab should not act by depleting cells expressing membrane-BAFF, in line with the current view of the mechanism of action of belimumab.

Belimumab was the first targeted treatment, approved in 2011, for the treatment of SLE, but its clinical efficacy is limited and not all patients benefit from treatment; this also holds true for other BAFF-blocking agents that have been tested in clinical trials (34). Loss of tolerance and development of auto-immunity is multifactorial, and SLE likely encompasses a spectrum of conditions with distinct etiologies that may be more or less dependent on BAFF (35, 36). This diversity is also reflected in the various spontaneous or induced mouse models of the disease (37). Different forms of BAFF and APRIL may trigger BAFFR, TACI, and BCMA in distinct manners with effects that could both promote (e.g., stimulation of auto-reactive B cells) or counteract (e.g., stimulation of regulatory B cells) development of symptoms. Indeed, in a mouse model of lupus, intricate positive or negative actions of the different receptors on disease

severity have been described (38). In this context, it might not be superfluous to know the fine specificity of belimumab and other BAFF inhibitors.

## DATA AVAILABILITY

The authors declare that the data supporting the finding of this study are available within the article, in its **Supplementary Information File** and as a dataset doi: 10.5281/zenodo.1481232.

## AUTHOR CONTRIBUTIONS

PS and MV conceived experiments. CK-Q, DC, LW, and PS performed experiments with help of MV and CJ. PS wrote the

paper. All authors reviewed the results and approved the final version of the manuscript.

## ACKNOWLEDGMENTS

We thank Henry Hess (Merck, Darmstadt, Germany) for the gift of atacicept. This work was supported by grants (310030\_156961; 310030A\_176256) from the Swiss National Science Foundation (to PS).

## SUPPLEMENTARY MATERIAL

The Supplementary Material for this article can be found online at: <https://www.frontiersin.org/articles/10.3389/fimmu.2018.02698/full#supplementary-material>

## REFERENCES

- Bossen C, Schneider P. BAFF, APRIL and their receptors: structure, function and signaling. *Semin Immunol.* (2006) 18:263–75. doi: 10.1016/j.smim.2006.04.006
- Gross JA, Dillon SR, Mudri S, Johnston J, Littau A, Roque R, et al. TACI-Ig neutralizes molecules critical for B cell development and autoimmune disease impaired B cell maturation in mice lacking BlyS. *Immunity* (2001) 15:289–302. doi: 10.1016/S1074-7613(01)00183-2
- Schiemann B, Gommerman JL, Vora K, Cachero TG, Shulga-Morskaya S, Dobles M, et al. An essential role for BAFF in the normal development of B cells through a BCMA-independent pathway. *Science* (2001) 293:2111–4. doi: 10.1126/science.1061964
- Sasaki Y, Casola S, Kutok JL, Rajewsky K, Schmidt-Supplian M. TNF family member B cell-activating factor (BAFF) receptor-dependent and -independent roles for BAFF in B cell physiology. *J Immunol.* (2004) 173:2245–52. doi: 10.4049/jimmunol.173.4.2245
- Shulga-Morskaya S, Dobles M, Walsh ME, Ng LG, MacKay F, Rao SP, et al. B cell-activating factor belonging to the TNF family acts through separate receptors to support B cell survival and T cell-independent antibody formation. *J Immunol.* (2004) 173:2331–41. doi: 10.4049/jimmunol.173.4.2331
- Benson MJ, Dillon SR, Castigli E, Geha RS, Xu S, Lam KP, et al. Cutting edge: the dependence of plasma cells and independence of memory B cells on BAFF and APRIL. *J Immunol.* (2008) 180:3655–9. doi: 10.4049/jimmunol.180.6.3655
- Moore PA, Belvedere O, Orr A, Pieri K, LaFleur DW, Feng P, et al. BlyS: member of the tumor necrosis factor family and B lymphocyte stimulator. *Science* (1999) 285:260–3. doi: 10.1126/science.285.5425.260
- Schneider P, MacKay F, Steiner V, Hofmann K, Bodmer JL, Holler N, et al. BAFF, a novel ligand of the tumor necrosis factor family, stimulates B cell growth. *J Exp Med.* (1999) 189:1747–56. doi: 10.1084/jem.189.11.1747
- Turpeinen H, Ortutay Z, Pesu M. Genetics of the first seven proprotein convertase enzymes in health and disease. *Curr Genomics* (2013) 14:453–67. doi: 10.2174/1389202911314050010
- Stohl W. Therapeutic targeting of the BAFF/APRIL axis in systemic lupus erythematosus. *Expert Opin Ther Targets* (2014) 18:473–89. doi: 10.1517/14728222.2014.888415
- Samy E, Wax S, Huard B, Hess H, Schneider P. Targeting BAFF and APRIL in systemic lupus erythematosus and other antibody-associated diseases. *Int Rev Immunol.* (2017) 36:3–19. doi: 10.1080/08830185.2016.1276903
- Furie R, Petri M, Zamani O, Cervera R, Wallace DJ, Tegzova D, et al. A phase III, randomized, placebo-controlled study of belimumab, a monoclonal antibody that inhibits B lymphocyte stimulator, in patients with systemic lupus erythematosus. *Arthritis Rheum.* (2011) 63:3918–30. doi: 10.1002/art.30613
- Navarra SV, Guzman RM, Gallacher AE, Hall S, Levy RA, Jimenez RE, et al. Efficacy and safety of belimumab in patients with active systemic lupus erythematosus: a randomised, placebo-controlled, phase 3 trial. *Lancet* (2011) 377:721–31. doi: 10.1016/S0140-6736(10)61354-2
- Baker KP, Edwards BM, Main SH, Choi GH, Wager RE, Halpern WG, et al. Generation and characterization of LymphoStat-B, a human monoclonal antibody that antagonizes the bioactivities of B lymphocyte stimulator. *Arthritis Rheum.* (2003) 48:3253–65. doi: 10.1002/art.11299
- FDA (2017). "Benlysta (belimumab)." Benlysta Package Insert.
- Schuepbach-Mallepell S, Das D, Willen L, Vigolo M, Tardivel A, Lebon L, et al. Stoichiometry of heteromeric BAFF and APRIL cytokines dictates their receptor-binding and signaling properties. *J Biol Chem.* (2015) 290:16330–42. doi: 10.1074/jbc.M115.661405
- Merrill JT, Wallace DJ, Wax S, Kao A, Fraser PA, Chang P, et al. Efficacy and safety of atacicept in patients with systemic Lupus Erythematosus: results of a twenty-four-week, multicenter, randomized, double-blind, placebo-controlled, parallel-Arm, Phase IIb study. *Arthritis Rheumatol.* (2018) 70:266–76. doi: 10.1002/art.40360
- Nardelli B, Belvedere O, Roschke V, Moore PA, Olsen HS, Migone TS, et al. Synthesis and release of B-lymphocyte stimulator from myeloid cells. *Blood* (2001) 97:198–204. doi: 10.1182/blood.V97.1.198
- Schneider P. Production of recombinant TRAIL and TRAIL receptor:Fc chimeric proteins. *Meth Enzymol.* (2000) 322:322–45. doi: 10.1016/S0076-6879(00)22031-4
- Holler N, Kataoka T, Bodmer JL, Romero P, Romero J, Depertthes D, et al. Development of improved soluble inhibitors of FasL and CD40L based on oligomerized receptors. *J Immunol Methods* (2000) 237:159–73. doi: 10.1016/S0022-1759(99)00239-2
- Tom R, Bisson L, Durocher Y. Transfection of HEK293-EBNA1 cells in suspension with linear PEI for production of recombinant proteins. *CSH Protoc.* 3:1–4. (2008). doi: 10.1101/pdb.prot4977
- Shalem O, Sanjana NE, Hartenian E, Shi X, Scott DA, Mikkelsen T, et al. Genome-scale CRISPR-Cas9 knockout screening in human cells. *Science* (2014) 343:84–7. doi: 10.1126/science.1247005
- Nys J, Smulski CR, Tardivel A, Willen L, Kowalczyk C, Donze O, et al. No evidence that soluble TACI induces signalling via membrane-expressed BAFF and APRIL in myeloid cells. *PLoS ONE* (2013) 8:e61350. doi: 10.1371/journal.pone.0061350
- Schneider P, Willen L, Smulski CR. Tools and techniques to study ligand-receptor interactions and receptor activation by TNF superfamily members. *Methods Enzymol.* (2014) 545:103–25. doi: 10.1016/B978-0-12-801430-1.00005-6
- Cachero TG, Schwartz IM, Qian F, Day E. S., Bossen, C., Ingold, K., et al. Formation of virus-like clusters is an intrinsic property of the tumor necrosis factor family member BAFF (B cell activating factor). *Biochemistry* (2006) 45:2006–13. doi: 10.1021/bi0516850
- Yan L, Hu R, Tu S, Cheng WJ, Zheng Q, Wang JW, et al. Establishment of a cell model for screening antibody drugs against rheumatoid arthritis with ADCC and CDC. *Int J Clin Exp Med.* (2015) 8:20065–71.

27. Liu Y, Xu L, Opalka N, Kappler J, Shu HB, Zhang G. Crystal structure of sTALL-1 reveals a virus-like assembly of TNF family ligands. *Cell* (2002) 108:383–94. doi: 10.1016/S0092-8674(02)00631-1
28. Nicoletti AM, Kenny CH, Khalil AM, Pan Q, Ralph KL, Ritchie J, et al. Unexpected potency differences between B-Cell-Activating Factor (BAFF) antagonist antibodies against various forms of BAFF: Trimer, 60-Mer, and membrane-bound. *J Pharmacol Exp Ther.* (2016) 359:37–44. doi: 10.1124/jpet.116.236075
29. Shin W, Lee HT, Lim H, Lee SH, Son JY, Lee JU, et al. BAFF-neutralizing interaction of belimumab related to its therapeutic efficacy for treating systemic lupus erythematosus. *Nat Commun.* (2018) 9:1200. doi: 10.1038/s41467-018-03620-2
30. Vigolo M, Chambers MG, Willen L, Chevalley D, Maskos K, Lammens A, et al. A loop region of BAFF controls B cell survival and regulates recognition by different inhibitors. *Nat Commun.* (2018) 9:1199. doi: 10.1038/s41467-018-03323-8
31. Halpern WG, Lappin P, Zanardi T, Cai W, Corcoran M, Zhong J, et al. Chronic administration of belimumab, a BLyS antagonist, decreases tissue and peripheral blood B-lymphocyte populations in cynomolgus monkeys: pharmacokinetic, pharmacodynamic, and toxicologic effects. *Toxicol Sci.* (2006) 91:586–99. doi: 10.1093/toxsci/kfj148
32. Bossen C, Tardivel A, Willen L, Fletcher CA, Perroud M, Beermann F, et al. Mutation of the BAFF Furin cleavage site impairs B cell homeostasis and anitibody responses. *Eur J Immunol.* (2011) 41:787–97. doi: 10.1002/eji.201040591
33. Huang HY, Rivas-Caicedo A, Renevey F, Cannelle H, Peranzoni E, Scarpellino L, et al. Identification of a new subset of lymph node stromal cells involved in regulating plasma cell homeostasis. *Proc Natl Acad Sci USA.* (2018) 115:E6826–E6835. doi: 10.1073/pnas.1712628115
34. Stohl W. Inhibition of B cell activating factor (BAFF) in the management of systemic lupus erythematosus (SLE). *Expert Rev Clin Immunol.* (2017) 13:623–33. doi: 10.1080/1744666X.2017.1291343
35. Vincent FB, Morand EF, Schneider P, Mackay F. The BAFF/APRIL system in SLE pathogenesis. *Nat Rev Rheumatol.* (2014) 10:365–73. doi: 10.1038/nrrheum.2014.33
36. Tsokos GC, Lo MS, Costa Reis P, Sullivan KE. New insights into the immunopathogenesis of systemic lupus erythematosus. *Nat Rev Rheumatol.* (2016) 12:716–30. doi: 10.1038/nrrheum.2016.186
37. Li W, Titov AA, Morel L. An update on lupus animal models. *Curr Opin Rheumatol.* (2017) 29:434–41. doi: 10.1097/BOR.0000000000000412
38. Jacob CO, Yu N, Sindhava V, Cancro MP, Pawar RD, Puterman C, et al. Differential development of systemic lupus erythematosus in NZM 2328 mice deficient in discrete pairs of BAFF receptors. *Arthritis Rheumatol* (2015) 67:2523–35. doi: 10.1002/art.39210

**Conflict of Interest Statement:** PS receives research funds from Merck, KGaA for related research.

The remaining authors declare that the research was conducted in the absence of any commercial or financial relationships that could be construed as a potential conflict of interest.

Copyright © 2018 Kowalczyk-Quintas, Chevalley, Willen, Jandus, Vigolo and Schneider. This is an open-access article distributed under the terms of the Creative Commons Attribution License (CC BY). The use, distribution or reproduction in other forums is permitted, provided the original author(s) and the copyright owner(s) are credited and that the original publication in this journal is cited, in accordance with accepted academic practice. No use, distribution or reproduction is permitted which does not comply with these terms.



# Proapoptotic BIM Impacts B Lymphoid Homeostasis by Limiting the Survival of Mature B Cells in a Cell-Autonomous Manner

Rui Liu<sup>1</sup>, Ashleigh King<sup>1,2</sup>, Philippe Bouillet<sup>3,4</sup>, David M. Tarlinton<sup>5</sup>, Andreas Strasser<sup>3,4</sup> and Jörg Heierhorst<sup>1,2\*</sup>

<sup>1</sup>Molecular Genetics Unit, St. Vincent's Institute of Medical Research, Fitzroy, VIC, Australia, <sup>2</sup>Department of Medicine, St. Vincent's Health, The University of Melbourne, Fitzroy, VIC, Australia, <sup>3</sup>Molecular Genetics of Cancer Division, Walter and Eliza Hall Institute of Medical Research, Parkville, VIC, Australia, <sup>4</sup>Department of Medical Biology, The University of Melbourne, Parkville, VIC, Australia, <sup>5</sup>Department of Immunology and Pathology, Monash University, Melbourne, VIC, Australia

## OPEN ACCESS

### Edited by:

Rhodi Ceredig,  
National University of Ireland Galway,  
Ireland

### Reviewed by:

Raul M. Torres,  
University of Colorado Denver School  
of Medicine, United States  
David Nemazee,  
The Scripps Research Institute,  
United States

### \*Correspondence:

Jörg Heierhorst  
jheierhorst@svi.edu.au

### Specialty section:

This article was submitted to  
B Cell Biology,  
a section of the journal  
*Frontiers in Immunology*

Received: 25 January 2018

Accepted: 09 March 2018

Published: 22 March 2018

### Citation:

Liu R, King A, Bouillet P, Tarlinton DM,  
Strasser A and Heierhorst J (2018)  
Proapoptotic BIM Impacts  
B Lymphoid Homeostasis by Limiting  
the Survival of Mature B Cells in a  
Cell-Autonomous Manner.  
*Front. Immunol.* 9:592.  
doi: 10.3389/fimmu.2018.00592

The proapoptotic BH3-only protein BIM (*Bcl2l11*) plays key roles in the maintenance of multiple hematopoietic cell types. In mice, germline knockout or conditional pan-hematopoietic deletion of *Bim* results in marked splenomegaly and significantly increased numbers of B cells. However, it has remained unclear whether these abnormalities reflect the loss of cell-intrinsic functions of BIM within the B lymphoid lineage and, if so, which stages in the lifecycle of B cells are most impacted by the loss of BIM. Here, we show that B lymphoid-specific conditional deletion of *Bim* during early development (i.e., in pro-B cells using *Mb1-Cre*) or during the final differentiation steps (i.e., in transitional B cells using *Cd23-Cre*) led to a similar >2-fold expansion of the mature follicular B cell pool. Notably, while the expansion of mature B cells was quantitatively similar in conditional and germline *Bim*-deficient mice, the splenomegaly was significantly attenuated after B lymphoid-specific compared to global *Bim* deletion. *In vitro*, conditional loss of *Bim* substantially increased the survival of mature B cells that were refractory to activation by lipopolysaccharide. Finally, we also found that conditional deletion of just one *Bim* allele by *Mb1-Cre* dramatically accelerated the development of Myc-driven B cell lymphoma, in a manner that was comparable to the effect of germline *Bim* heterozygosity. These data indicate that, under physiological conditions, BIM regulates B cell homeostasis predominantly by limiting the life span of non-activated mature B cells, and that it can have additional effects on developing B cells under pathological conditions.

**Keywords:** apoptosis, cell death, BCL-2 family, BIM, BH3-only protein, B lymphocytes, B cell lymphoma

## INTRODUCTION

Members of the BCL-2 family of proteins play crucial roles in the regulation of the mitochondrial apoptotic cell death pathway (1). The BH3-only protein BIM, a proapoptotic member of this family, is particularly critical for regulating cell death/survival in the hematopoietic system. Germline knockout (KO) of *Bim* causes an increase in the number of cells in several hematopoietic subsets, including B cells, T cells, monocytes, and granulocytes, with a marked splenomegaly (2). In these mice, mature B cells are approximately doubled in number compared to wild-type (WT) controls. Upon *in vivo* antigen stimulation, B cells can differentiate into antibody-secreting plasma cells, which are also

greatly increased in number in *Bim* KO mice (2). This increase in plasma cells combined with defects in negative selection of autoreactive B cells (3) is thought to lead to the development of a severe auto-antibody-driven systemic lupus erythematosus-like autoimmune pathology with immune-complex glomerulonephritis on a mixed 129SV/JxC57BL/6 genetic background (2). These symptoms of autoimmunity, however, are significantly moderated on a C57BL/6 background (4). *Bim* KO mice on an inbred C57BL/6 background show an abnormally increased proportion of low-affinity B cell receptor (BCR)/surface-IgM expressing B cells in the germinal center, and they accumulate low-affinity memory B cells (5). Both of these cell populations would normally be eliminated by apoptotic cell death during selection for B cells with improved affinity for antigen arising from somatic mutation of their IgV genes (5). Conversely, loss of BIM specifically increases the survival of autoreactive immature B cells in the bone marrow, which demonstrated that BIM plays a key role in apoptosis activation by autoreactive BCRs during this developmental stage (3).

BIM expression levels increase progressively during B cell development (pre-pro-B < pro-B/pre-B < immature B < mature B) (6, 7), which may explain why loss of *Bim* has such profound effects on immature and mature B cell populations. However, loss of *Bim* can also increase cell numbers at earlier stages of B cell development under pathological conditions, for example, by supporting the survival (but not proliferation and differentiation) of developing B cells in the absence of IL-7 or the IL-7 receptor *in vivo* and *in vitro* (6, 8). In addition to BIM, other BH3-only proteins such as BMF and PUMA are expressed in B lymphoid cells, and their loss can also lead to increased B cell numbers (7) or synergistically increase B cell numbers in combination with the *Bim* KO (9), highlighting functional redundancies among the proapoptotic proteins.

The B lymphoid expansion resulting from the germline *Bim* KO is transplantable and affects both the follicular and marginal zone compartment (8). In addition, a floxed *Bim* allele has recently been generated, and its conditional deletion throughout the hematopoietic system using *Vav-Cre* recapitulates key features of the germline *Bim* KO phenotype, including increased white blood cell numbers and splenomegaly (10). Collectively, these findings indicate that the B cell-related features of the *Bim* KO phenotype emanate from an impact that is intrinsic to the hematopoietic cell lineage. However, whether these effects on B cell homeostasis are solely due to the loss of a function of BIM specifically within the B lymphoid cell lineage, or whether they may be in part due to an indirect, reactive consequence of losing BIM-dependent apoptosis in another hematopoietic cell type remains unresolved. In addition, if the alterations observed are due to the loss of B cell-intrinsic functions of BIM, it remains to be resolved to what extent they are caused by increased B cell production during their development in the bone marrow, or prolonged survival of mature B cells in the periphery. The relevance of these issues has recently been highlighted by the finding that conditional deletion of *Bim* in myeloid cells (using *LysM-Cre*) can in fact lead to increased splenic B cell numbers and immune-complex glomerulonephritis similar to that observed in germline *Bim* KO mice (11).

Thus, to investigate whether BIM regulates B cell homeostasis in a cell-intrinsic manner and to resolve the stage(s) of B cell development at which BIM may exert its most critical functions, we have here employed two different B lymphoid-specific CRE recombinase mouse strains for the conditional deletion of *Bim*: *Mb1-Cre* for deletion during the early developmental pro-B cell stage in the bone marrow (12), and *Cd23-Cre* for deletion at the nearly fully matured transitional B cell stages in peripheral lymphoid tissues (13).

## MATERIALS AND METHODS

### Mice

Animal experiments were performed according to the Australian Code for the Care and Use of Animals for Scientific Purposes, 8th Edition (2013), and approved by the St. Vincent's Hospital Melbourne Animal Ethics Committee, approval numbers 019/13 and 002/17.

*Mb1-Cre* (12), *Cd23-Cre* (13), *Eμ-Myc* (14), and *Bim-floxed* (10) mice had been generated, or backcrossed for at least 10 generations, on a C57BL6 background, and were housed in specific pathogen-free micro-isolators. All mice for bone marrow and splenic cell analyses were used at 8 weeks ± 3 days of age, and not selected on gender. Ethical endpoints for tumor-prone mice in survival analyses were determined by trained animal technicians who were blinded to the genotypes of individual mice.

### Immunoblots and Genotyping

Western blotting was performed as described (15) using antibodies against BIM (Cell Signaling Technology, C34C5) and β-actin (EMD Millipore/Merck, MAB1501) as a loading control. DNA from toe biopsies was genotyped using primers 5'-AAGAACCTAGGTTGACTCTAG-3' and 5'-AACCAACTGTACCTTGGCTATA-3' resulting in PCR products of ~1 kbp for the *Bim* floxed, ~0.8 kbp for the WT, and ~0.3 kbp for the *Bim*-deleted alleles. In addition, biopsies were genotyped with *Bim* KO primers (5'-AAGAACCTAGGTTGACTCTAG-3', 5'-CATTGCACTGAGATAGTGGTTGA-3', and 5'-CCCGTTGCACCACAGATGAA-3'; WT ~0.5 kbp, KO ~0.6 kbp) to exclude mice containing germline *Bim* null alleles as a result of ectopic CRE recombinase activity.

### Cell Preparations

Hind limbs were dissected and skin, muscle, and soft tissues were removed carefully. Both ends of the femur and tibia were cut and the bone marrow was flushed out with 1 mL of ice-cold MACS buffer (1× PBS, pH 7.2, 0.5% BSA, and 2 mM EDTA) using a 21 G needle. Bone marrow cell suspensions from femur and tibia were combined and mixed thoroughly.

Freshly dissected mouse spleens were weighed and gently homogenized in 2 mL cold MACS buffer on ice. Cell suspensions were passed sequentially through 70 and 40-μm cell strainers to remove debris, followed by washes of tubes and strainers with 4 mL MACS buffer to recover remaining cells.

B-1a cells were isolated by peritoneal lavage using 26 and 23 G needles with PBS containing 2% fetal bovine serum (FBS).

Total bone marrow, spleen, and peritoneal cavity leukocyte counts were determined using an automated KX-21N cell counter (Sysmex). Bone marrow cellularities indicated in the figures include tibias and femurs of two legs.

## Flow Cytometry

The following reagents were used for cell staining: B220-APC (eBioscience™, 17-0452-83), B220-FITC (Biolegend, 103206), BP1-PE (BD, 553735), CD11b-Pacific blue (eBioscience™, 48-0112-82), CD8-APC (eBioscience™, 17-0081-82), CD4-PE (eBioscience™, 12-0041-83), CD5-FITC (BD, 553021), CD11b-APC-Cy7 (BD, 557657), CD19-APC eFluor780 (eBioscience™, 47-0193-82), CD19-PerCP-Cy5.5 (eBioscience™, 45-0193-82), CD21-PE (Biolegend, 123410), CD23-biotin (BD, 553137), CD24-FITC (BD, 561777), CD43-biotin (BD, 553269), CD43-PE (BD, 553271), GR1-biotin (eBioscience, 13-5931-85), IgD-eFluor450 (eBioscience™, 48-5993-82), IgM-PE-Cy7 (BD, 552867), Brilliant Violet 605™ Streptavidin (Biolegend, 405229), and propidium iodide (Sigma, P4864-10ML). Our gating strategies for staining of bone marrow B lymphoid fractions according to Hardy et al. (16), total and mature splenic B cell numbers, and peritoneal cavity B-1a cell analyses were recently described (15, 17). Hardy fractions were gated as follows: A, B220<sup>+</sup> CD43<sup>+</sup> CD24<sup>low</sup> BP1<sup>-</sup>; B, B220<sup>+</sup> CD43<sup>+</sup> CD24<sup>high</sup> BP1<sup>-</sup>; C, B220<sup>+</sup> CD43<sup>+</sup> CD24<sup>low</sup> BP1<sup>+</sup>; C, B220<sup>+</sup> CD43<sup>+</sup> CD24<sup>high</sup> BP1<sup>+</sup>; D, B220<sup>+</sup> CD43<sup>-</sup> IgM<sup>+</sup> IgD<sup>-</sup>; E (immature B cells), B220<sup>+</sup>, CD43<sup>-</sup>, IgM<sup>+</sup>, IgD<sup>-</sup>; F (recirculating B cells), B220<sup>+</sup>, CD43<sup>-</sup>, IgD<sup>+</sup>. T1 transitional B cells were gated as B220<sup>+</sup>, IgM<sup>high</sup>, IgD<sup>low</sup>; T2 transitional B cells as B220<sup>+</sup>, IgM<sup>high</sup>, IgD<sup>high</sup>; and mature B cells as B220<sup>+</sup>, IgM<sup>low</sup>, IgD<sup>high</sup>. Hardy fractions A–D correspond to the Basel classification (18–20) as follows: Hardy A is equivalent to pre-pro-B cells (B220<sup>+</sup> CD43<sup>+</sup> CD19<sup>-</sup>); Hardy B/C represent pro-B/pre-B I cells (B220<sup>+</sup> CD43<sup>+</sup> CD19<sup>+</sup> c-kit<sup>+</sup> CD25<sup>-</sup> SL<sup>-</sup>); Hardy C corresponds to large pre-B II cells (B220<sup>+</sup> CD43<sup>-</sup> CD19<sup>+</sup> c-kit<sup>-</sup> CD25<sup>+</sup> SL<sup>+</sup>); and Hardy D corresponds to small pre-B II cells (B220<sup>+</sup> CD43<sup>-</sup> CD19<sup>+</sup> c-kit<sup>-</sup> CD25<sup>+</sup> SL<sup>-</sup>). For follicular and marginal zone B cell proportions, splenic cells were first gated on live B220<sup>+</sup> CD19<sup>+</sup> lymphocytes, followed by gating on CD21/35 and CD23 (follicular B cells: CD21/35<sup>lo</sup> CD23<sup>+</sup>; marginal zone B cells: CD21/35<sup>hi</sup> CD23<sup>-</sup>). FACS data were analyzed using FlowJo 10.3 software (Tree Star).

## B Cell Cultures and CellTrace Violet Staining

B cells were isolated from single-cell splenocyte suspensions using B cell isolation kits (Miltenyi Biotec, 130090862) and MACS Separation LS columns (Miltenyi Biotec, 130042401) following the manufacturer's instructions. 10 million isolated B cells were incubated with CellTrace™ Violet (CTV; Thermo Fisher Scientific, C34557) at 1:1,000 dilution at 37°C in the dark for 20 min, centrifuged at 300 × g for 10 min, and the cell pellet was washed once with 10 mL of MACS buffer. CTV-stained B cells were cultured in the B cell culture media (RPMI 1640 supplemented with 5% (v/v) FBS, 50 μM β-mercaptoethanol, 100 U/mL Penicillin G and 100 μg/mL streptomycin sulfate) at a seeding density of 1 million cells/mL. Cells were stimulated with 15 μg/mL lipopolysaccharide (LPS; Jomar Life Research,

tlrl-3pelps) or with 1/1,000 recombinant CD40L plus 1/100 conditioned mouse IL4 supernatant for 96 h, and applied to flow cytometry analysis (BD LSRLFortessa). Division and proliferation indices were determined using the cell proliferation module of FlowJo 10.3.

## Statistical Analysis

Data from independent experimental replicates were analyzed using GraphPad Prism software. The numbers of independent samples are indicated in the figures and tables. Error bars indicate the mean ± SEM. *p* Values were calculated using the two-tailed unpaired Student's *t*-test. The Mantel–Cox test was used for survival analyses.

## RESULTS

### Conditional Loss of BIM During Early Stages of B Lymphopoiesis Leads to Increased B Cell Numbers

To analyze cell-intrinsic effects of the loss of BIM on the B cell lineage, we crossed mice containing floxed *Bim* alleles (10) with mice containing the *Mb1-Cre* knock-in allele (12). Within the B lymphoid lineage, *Mb1-Cre* is active from the early pro-B cell stage (12), coinciding with the initiation of *Igh* gene locus rearrangement by V(D)J recombination. However, *Mb1-Cre* can have spurious ectopic activity in the germline (21), especially when transmitted via male breeders. During genotyping, we noticed unusually high frequencies (compared to our experience with other floxed loci, such as *Asciz*, *Dynll1*, *tp53*) of ectopic recombination of the floxed *Bim* allele, even in the female germline. Germline heterozygosity for *Bim* can result in some haplo-insufficiency phenotypes, such as reduced life span (2), pronounced acceleration of B cell lymphoma development in *Eμ-Myc* mice (22), and protection from polycystic kidney disease in the absence of *Bcl2* (23). We therefore only used *bona fide* *Mb1-Cre*<sup>ki/+</sup>*Bim*<sup>fl/fl</sup> mice for the analyses described here and excluded mice containing inadvertently rearranged germline *Bim*-deleted alleles to avoid any indirect effects from *Bim* heterozygosity in other cell types on the B lymphoid lineage.

*Mb1-Cre* *Bim*-deleted mice contained ~2-fold more total B cells in the spleen than matched *Mb1-Cre* *Bim*<sup>+/+</sup> control mice (*p* < 0.0001), and this was particularly pronounced among mature B cells, with a much smaller effect on transitional B cells (Figure 1A). In contrast, the numbers of innate-like B-1a cells in the peritoneal cavity [which emanate from distinctive fetal stem cells, as opposed to ongoing hematopoiesis for conventional B cells (24)] were not increased in *Mb1-Cre* *Bim*-deleted mice (Figure 1B). Efficient B cell-specific *Bim* deletion and loss of all the three BIM protein isoforms [which result from alternative splicing of the *Bim* pre-mRNA (25)] was confirmed by PCR genotyping and immunoblot analyses (Figures 1C,D).

This expansion of the mature B cell pool was also reflected in an ~4-fold increase in recirculating B cells in the bone marrow of *Mb1-Cre* *Bim*-deleted mice (Hardy fraction F; Figures 1E,F).

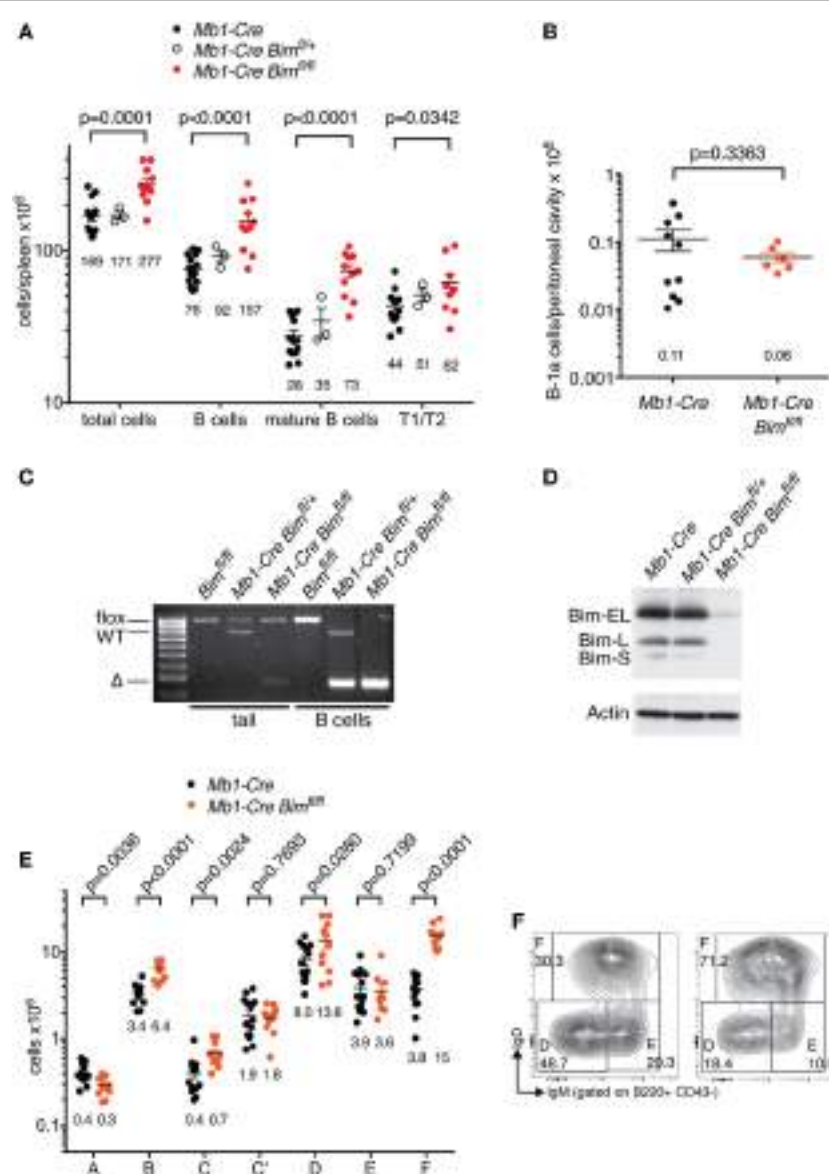


**FIGURE 1 |** B cell numbers in *Mb1-Cre Bim*-deleted mice. **(A)** Splenic cell numbers. Genotypes of groups are indicated above. Numbers below each group indicate the mean. Numbers for T1 and T2 transitional B cell stages are combined. **(B)** Numbers of B-1a cells in the peritoneal cavity. **(C)** PCR genotyping of genomic DNA isolated from tails or purified B cells of mice of the indicated genotypes. **(D)** Western blot analysis of purified B cells from mice of the indicated genotypes probed with an anti-BIM antibody and actin as a loading control. **(E)** Cell numbers for different developmental stages using the Hardy nomenclature (16). **(F)** Representative FACS plots for bone marrow B cell fractions D (small pre-B), E (immature B cells), and F (recirculating mature B cells).

Conditional *Bim* deletion also led to other significant changes in cellularity during distinct stages of B cell development in the bone marrow. This included a near-doubling of cells in the pro-B cell stage (when *Mb1-Cre* first becomes active; Hardy fraction B) that was carried over into the subsequent early pre-B cell stage (fraction C, when *Igh V(D)J* recombination is completed), and a <2-fold expansion of small pre-B cells (Hardy fraction D, during which *Igl* loci undergo VJ recombination) (Figure 1E). However, *Mb1-Cre Bim*-deleted mice contained normal numbers of cycling pre-B cells (Hardy fraction C'), the

stage when cells expressing a successfully rearranged pre-BCR undergo ~5 cycles of clonal expansion. Surprisingly, *Mb1-Cre Bim*-deleted mice also contained normal numbers of immature B cells (Hardy fraction E), the stage when cells expressing self-reactive BCRs are eliminated by a mechanism that involves BIM-dependent apoptosis (3).

Collectively, these data indicate that loss of BIM can affect several stages of B cell development in a lineage-intrinsic manner, and that this is balanced by compensatory changes at other developmental stages.

## Conditional *Bim* Deletion During the Transitional Stages of B Cell Development Leads to Cell-Intrinsic Expansion of the Mature Follicular B Cell Pool

The finding that the numbers of immature B cells (Hardy fraction E), which represent the final stage of B lymphoid development in the bone marrow, were not abnormally increased in *Mb1-Cre Bim*-deleted mice (Figure 1E) suggested that the expansion of the peripheral B cell pools in these mice may be due to an increased life span of mature B cells, rather than increased cell production during development. To test this hypothesis, we intercrossed mice containing floxed *Bim* alleles with mice containing a *Cd23-Cre* transgene. *Cd23-Cre* becomes active in transitional B cells after they have left the bone marrow, and recombination of floxed genes is only complete at the mature B cell stage in peripheral lymphoid organs (13). *Cd23-Cre* did not display ectopic germline activity toward the floxed *Bim* allele.

Consistent with our hypothesis, *Cd23-Cre*-mediated deletion of *Bim* led to a significant expansion of total and mature B cell numbers in the spleen and in the circulation compared to *Cd23-Cre Bim*<sup>+/+</sup> control mice (Figure 2A; Table 1). The increase in the numbers of mature B cells in *Cd23-Cre Bim*-deleted mice was comparable to the splenic B cell expansion in *Mb1-Cre Bim*-deleted mice (Figure 2A; note that the differences between *Mb1-Cre Bim*<sup>fl/fl</sup> and *Cd23 Bim*<sup>fl/fl</sup> mice were statistically not significant). Further analyses indicated that the expansion of the mature splenic B cell pool was restricted to the CD23-positive follicular B cell compartment, with no increase in the marginal zone B cells (Figure 2C, middle panel). To determine if this specificity for follicular cells was simply due to lower *Cd23-Cre* activity in the marginal zone B cells (which express only very low levels of CD23), we repeated similar analyses using *Mb1-Cre Bim*-deleted mice. Interestingly, loss of *Bim* during early B cell development, before the divergence of follicular and marginal zone cells, again led to a specific expansion of the follicular B cell compartment but not of marginal zone B cells (Figure 2C, right panel). These results indicate that marginal zone B cells are largely indifferent to the loss of *Bim*, which is consistent with the notion that they have a much longer life span than follicular B cells (26).

We also enumerated B lymphoid cells in the bone marrow of *Cd23-Cre Bim*-deleted mice. In line with the expansion of the mature B cell pool in the spleen (Figure 2A) and circulation (Table 1), the numbers of recirculating mature B cells (Hardy fraction F) were significantly increased in *Cd23-Cre Bim*<sup>fl/fl</sup> mice compared to control animals, similar to the *Mb1-Cre Bim*<sup>fl/fl</sup> mice. Surprisingly, we also found a significant increase of pro-B cells (Hardy fraction B) in *Cd23-Cre Bim*-deleted mice (Figure 2B). As *Cd23-Cre* is not active at this early developmental stage, this finding indicates that this pro-B cell expansion may be a secondary consequence of the increased mature B cell pool, possibly due to altered cytokine profiles. This indirect expansion of pro-B cells in *Cd23-Cre Bim*-deleted mice, therefore, implies that the quantitatively similar increase of pro-B cells in *Mb1-Cre Bim*-deleted mice may also be due

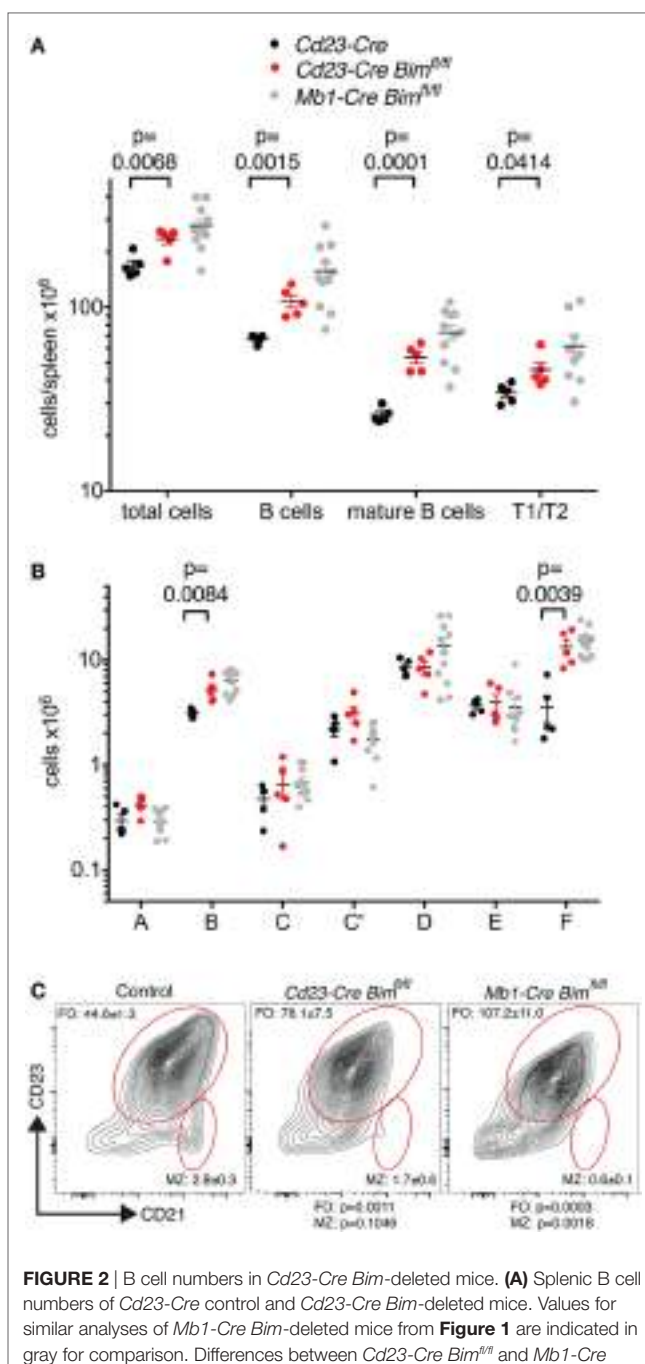


**FIGURE 2 |** B cell numbers in *Cd23-Cre Bim*-deleted mice. **(A)** Splenic B cell numbers of *Cd23-Cre* control and *Cd23-Cre Bim*-deleted mice. Values for similar analyses of *Mb1-Cre Bim*-deleted mice from Figure 1 are indicated in gray for comparison. Differences between *Cd23-Cre Bim*<sup>fl/fl</sup> and *Mb1-Cre Bim*<sup>fl/fl</sup> mice are not statistically significant. **(B)** Cell numbers for different bone marrow B cell developmental stages. **(C)** Representative FACS plots of B220<sup>+</sup> IgM<sup>+</sup>-gated spleen cells stained for follicular B cells and marginal zone B cells are indicated. Numbers in the plots indicate the mean  $\pm$  SE ( $n = 5$ ; *Cd23-Cre Bim*<sup>fl/fl</sup>,  $n = 3$ ; *Mb1-Cre Bim*<sup>fl/fl</sup>,  $n = 3$ ), and  $p$  values compared to control mice are indicated below.

to cell-extrinsic effects. In addition to the effects on the B lymphoid compartment, *Cd23 Bim*-deleted mice also exhibited a modest ~50% increase of splenic CD8<sup>+</sup> T cells, but other cell types in the circulation and spleen were not significantly changed compared to controls (Tables 1 and 2).

Collectively, these results from the analysis of the *Cd23-Cre*-mediated *Bim* deletion mice indicate that loss of *Bim* within mature B cells is sufficient to increase peripheral B cell numbers in a cell-intrinsic manner, and that this can cause a secondary increase in pro-B cells and CD8<sup>+</sup> T cells.

**TABLE 1 |** Blood cell numbers.

	Control (cells × 10 <sup>6</sup> /mL)	<i>Cd23-Cre Bim<sup>fl/fl</sup></i> (cells × 10 <sup>6</sup> /mL)	Significance
<b>Blood</b>			
White blood cells	12.53 ± 0.93	20.43 ± 3.05	<i>p</i> = 0.0477
B cells	5.270 ± 0.32	12.28 ± 2.51	<i>p</i> = 0.0324
CD4 <sup>+</sup> CD8 <sup>-</sup> T cells	1.628 ± 0.403	2.336 ± 0.306	
CD8 <sup>+</sup> CD4 <sup>-</sup> T cells	1.592 ± 0.292	2.049 ± 0.181	
CD4 <sup>+</sup> CD8 <sup>+</sup> T cells	0.069 ± 0.042	0.166 ± 0.147	
Granulocytes	1.868 ± 0.505	1.414 ± 0.537	
Monocytes	1.425 ± 0.227	1.496 ± 0.183	
Red blood cells	8,400 ± 120	8,977 ± 305	
Platelets	950 ± 193	1,157 ± 79	

*n* = 4.

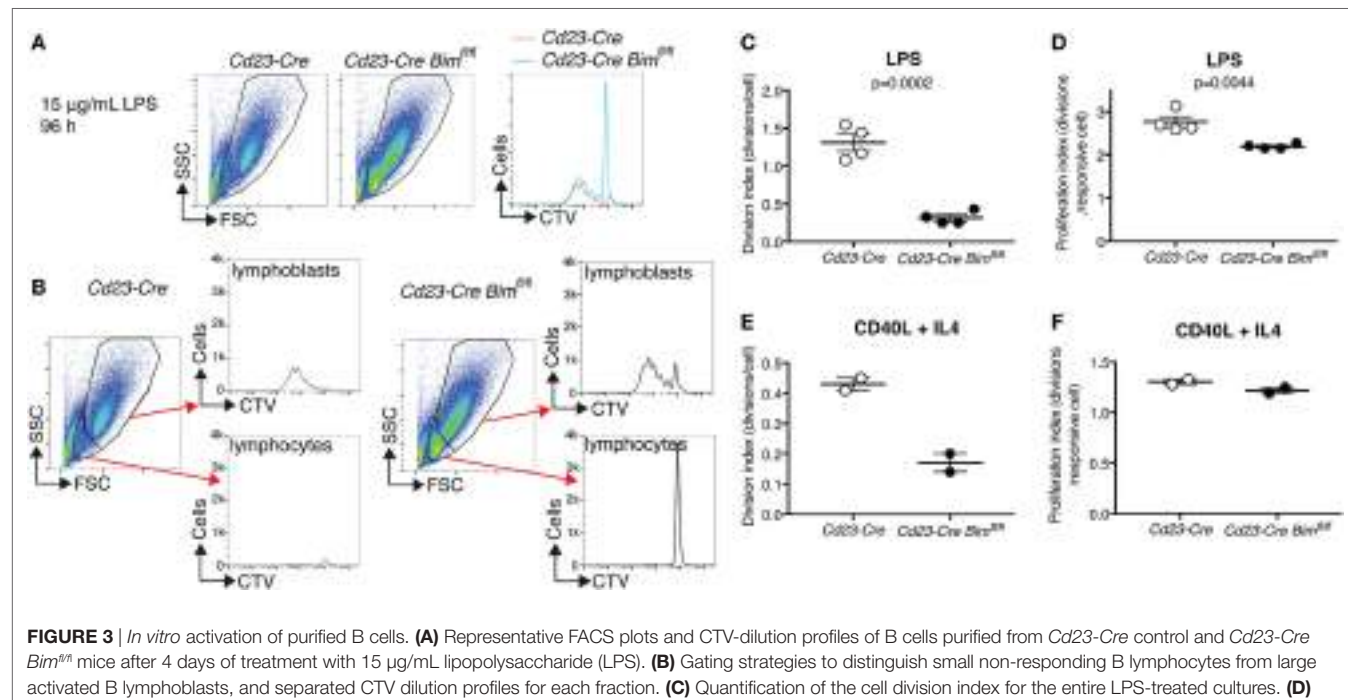
**TABLE 2 |** Splenic cell numbers.

	Control (cells × 10 <sup>6</sup> )	<i>Cd23-Cre Bim<sup>fl/fl</sup></i> (cells × 10 <sup>6</sup> )	Significance
<b>Spleen</b>			
B cells	82.21 ± 3.3546	117.17 ± 14.28	<i>p</i> = 0.0327
CD4 <sup>+</sup> CD8 <sup>-</sup> T cells	31.17 ± 2.20	35.93 ± 3.34	
CD8 <sup>+</sup> CD4 <sup>-</sup> T cells	16.50 ± 1.06	23.45 ± 2.01	<i>p</i> = 0.0141
CD4 <sup>+</sup> CD8 <sup>+</sup> T cells	0.655 ± 0.207	1.206 ± 0.205	
Granulocytes	6.885 ± 0.846	4.625 ± 1.075	
Monocytes	6.473 ± 0.42	5.140 ± 0.514	

Controls are *Cd23-Cre<sup>Tg/+</sup>* *Bim<sup>+/-</sup>* mice; *n* = 4.

## Loss of *Bim* Prevents the Elimination of Activation-Resistant Mature B Cells In Vitro

To assess how loss of *Bim* may lead to increased numbers of mature B cells, we performed *in vitro* B cell activation experiments using LPS and measured proliferation by dilution of CellTrace Violet (CTV). LPS induces a bi-phasic response in mature resting B cells. During the first phase, small B lymphocytes are activated to escape from their G<sub>0</sub> state by increasing their cell mass, and in the second phase these much larger lymphoblasts enter multiple rounds of cell division (27). It has previously been proposed that LPS activation of B cells leads to the inactivation of BIM as a result of multisite phosphorylation by ERK and subsequent ubiquitin-dependent proteasomal degradation (28). Interestingly, LPS-treated *Cd23-Cre Bim*-deleted B cells produced a similar number of dividing cells and a similar CTV dilution profile compared to *Cd23-Cre* control B cells (Figure 3A). However, whereas the small, non-blasting and undivided lymphocytes were almost completely lost from the cultures of control B cells after 4 days of LPS treatment, a substantial number of these resting cells survived in the cultures of *Cd23-Cre Bim*-deleted B cells (Figure 3B). Analysis of the CTV dilution assays, using the proliferation platform of the FlowJo software package, indicated that relative to the numbers of remaining undivided cells, there was a ~4-fold reduction in the average number of divisions per cell in the cultures of *Bim*-deleted B cells compared to the *Cd23-Cre* control B cells (Division index, Figure 3C). This difference was reduced to ~0.2-fold fewer divisions when only the activated cells that had divided at least once were taken into consideration (Proliferation index, Figure 3D). Qualitatively



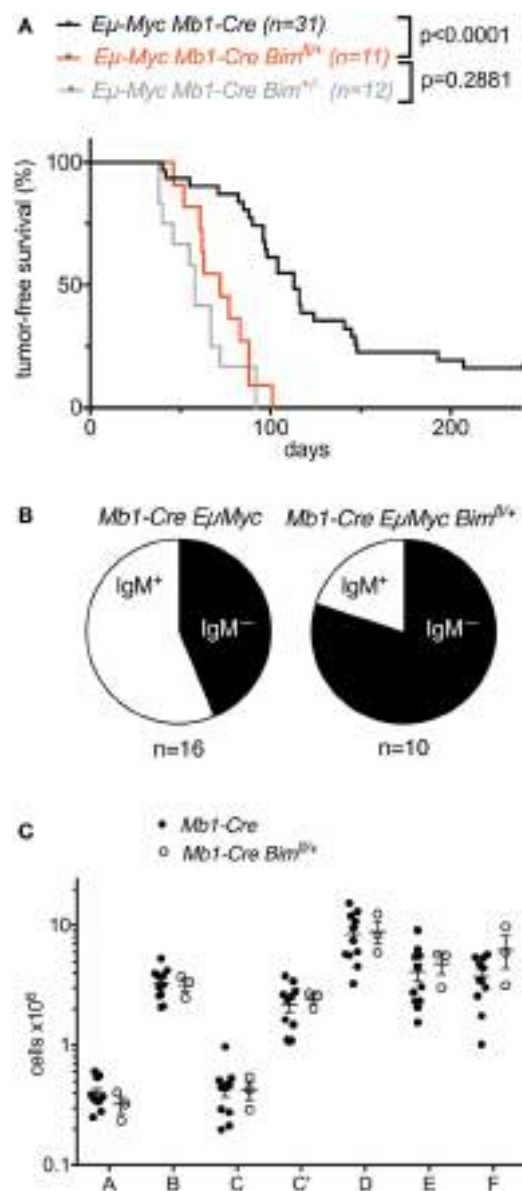


**FIGURE 4 |** Effect of conditional heterozygous *Bim* deletion on B cell lymphoma development in *Eμ-Myc* transgenic mice. **(A)** Survival analysis of *Eμ-Myc Mb1-Cre Bim<sup>fl/fl</sup>* mice compared to *Eμ-Myc Mb1-Cre* control mice and *Eμ-Myc Mb1-Cre Bim<sup>+/−</sup>* mice. Numbers for *Eμ-Myc Mb1-Cre Bim<sup>+/−</sup>* mice are from the study by Wong et al. (15). **(B)** Proportions of surface IgM-positive or surface IgM-negative lymphomas in the control and conditional *Bim*-heterozygous cohorts. **(C)** Comparison of bone marrow B cell developmental cell fractions in control and conditional *Bim*-heterozygous groups.

similar results were also obtained in response to treatment with CD40L (Figures 3E,F). Taken together, these results indicate that loss of BIM primarily increases the survival of activation-resistant resting B lymphocytes that do not exit the G<sub>0</sub> state, with a relatively minor effect on the survival of actively proliferating B lymphoblasts.

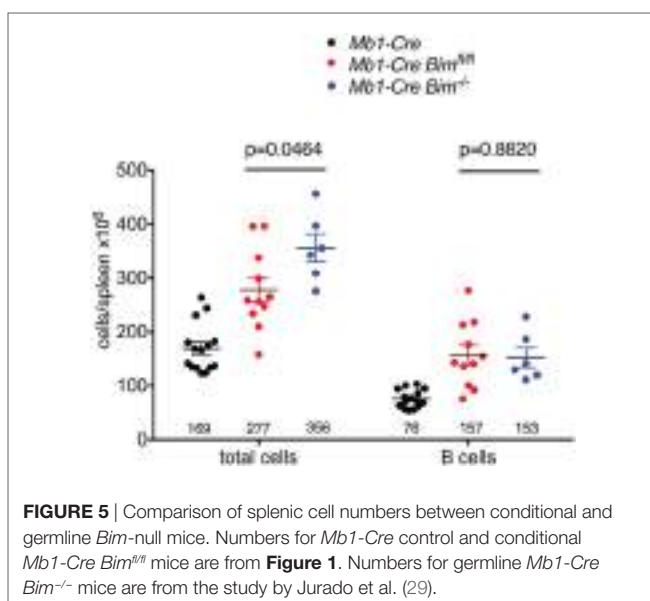


**FIGURE 5 |** Comparison of splenic cell numbers between conditional and germline *Bim*-null mice. Numbers for *Mb1-Cre* control and conditional *Mb1-Cre Bim<sup>fl/fl</sup>* mice are from Figure 1. Numbers for germline *Mb1-Cre Bim<sup>−/−</sup>* mice are from the study by Jurado et al. (29).

## Heterozygous Conditional *Bim* Deletion in Developing B Cells Accelerates MYC-Driven B Cell Lymphomagenesis

While the above experiments indicate that under normal physiological conditions B cell-intrinsic loss of *Bim* exerts its main effect on the mature B cell pool, there are several instances where germline loss of *Bim* can have profound effects on murine B cell development under pathological conditions (6, 8, 29). For example, in the context of MYC-driven B cell lymphomagenesis, it has been shown that the loss of even a single copy of *Bim* leads to dramatically accelerated lymphoma development emanating from the pre-B and immature B cell stages in the bone marrow of *Eμ-Myc* transgenic mice (22). We therefore also compared the effects of heterozygous germline versus heterozygous B lymphoid-intrinsic conditional *Bim* deletion on the time course of lymphoma development in *Eμ-Myc* mice.

Compared to *Mb1-Cre Eμ-Myc* control mice (that also contained an *Mb1-Cre* knock-in allele; median survival 113 days), conditional *Mb1-Cre Bim<sup>fl/fl</sup>* *Eμ-Myc* mice (median survival 72 days) exhibited significantly accelerated lymphoma development (Figure 4A). The survival curve for these B lymphoid-specific conditional *Bim* heterozygous mice was not significantly different from the survival curve for otherwise isogenic germline *Bim* heterozygous mice [that also contained an *Mb1-Cre* knock-in allele (15)] (Figure 4A). Among the tumors that formed in the *Mb1-Cre Bim*-deleted *Eμ-Myc* mice, there were higher proportions of surface IgM-negative precursor B cell lymphomas compared to the *Mb1-Cre Eμ-Myc* control mice (Figure 4B), although this difference was statistically not significant. It should be noted that heterozygous conditional *Bim* deletion did not affect normal B cell development compared to *Mb1-Cre* control mice (Figure 4C). Overall, these data indicate that the effect of *Bim* heterozygosity on the lymphoma development of *Eμ-Myc* transgenic mice is largely B lymphoid-intrinsic, without quantifiably significant compounding effects of *Bim* deficiency in other tissues, including their developmental niche in the bone marrow.

## DISCUSSION

One of the most prominent phenotypes of germline *Bim* KO mice is a profound increase in the number of peripheral B cells, and an associated splenomegaly, but it was unclear to what extent this was due to B lymphoid-specific functions of BIM or influenced by the absence of BIM in other tissues and hematopoietic cell types. Notably, the numbers of splenic B cells in the conditional *Mb1-Cre Bim*-deleted mice reported here are strikingly similar to those of germline *Bim* KO mice (on the same genetic background, at the same age and under the same housing conditions, albeit at different times) that also contained a *Mb1-Cre* knock-in allele (29) (**Figure 5**). In contrast, the total spleen cell numbers were significantly more increased in the germline *Bim*-null mice compared to the B lymphoid-specific *Bim*-deleted mice (**Figure 5**). These data therefore indicate that the B cell expansion in the *Bim* KO is largely due to cell-intrinsic changes within the B-lymphoid cell lineage, but the loss of *Bim* in other cell types is also an important contributor to the severity of the splenomegaly.

The pool of mature B cells is constantly regenerated in mice in unison with the elimination of non-reactive or dormant B cells that are not encountering antigens specific to their unique BCRs (30, 31). This raises the question whether loss of BIM affects B cell numbers by regulating the generation of new B cells or by regulating the survival of existing B cells. In addition to having increased numbers of mature B cells, the conditional *Mb1-Cre Bim*-deleted mice also contained more pro-B and pre-B cells than control animals (fractions B, C, and D; **Figure 1E**). However, this expansion of B lymphoid cells from earlier developmental stages was reversed to normal cellularity at the immature B cell stage (fraction F; **Figure 1E**), which represents the final stage before developing B cells emigrate from the bone marrow to peripheral lymphoid tissues including the spleen. This may be due to BIM-deleted cells undergoing fewer divisions at the large pre-B cell stage, perhaps due to limited availability of growth factors that drive this cell proliferation, or the elimination of excess cells by BH3-only proteins other than BIM. For example, the *Bmf* KO leads to more pronounced elevation of pre-B cells and immature/transitional B cells in the bone marrow than the *Bim* germline KO (7). Regardless, the observation that *Mb1-Cre Bim*-deleted mice have increased numbers of mature B cells but normal numbers of immature B cells suggests that the expansion of mature B cells caused by the absence of BIM may largely be due to their increased life span rather than increased survival of cells at earlier stages of B lymphopoiesis. This notion is supported by our analysis of conditional *Cd23-Cre Bim* mice, which delete *Bim* only during the final differentiation stages after B lymphoid cells have left the bone marrow, yet exhibit a quantitatively comparable peripheral mature B cell expansion to the *Mb1-Cre Bim* mice.

The conclusion of our *in vivo* analyses, that BIM regulates B cell homeostasis primarily through the stochastic elimination of superfluous mature B cells, is also corroborated by our *in vitro* data, which show that loss of BIM had a much more pronounced effect on the survival of activation-resistant mature B lymphocytes than on the proliferation of activated B lymphoblasts (**Figure 3**). It should be noted that these findings

for *in vitro*-cultured, conditionally *Bim*-deleted cells are consistent with earlier *in vitro* findings for purified B cells from germline *Bim* KO mice (28), where loss of BIM had a much more pronounced effect on apoptotic cell death of untreated resting cells than on the survival of LPS-stimulated cells after 24–48 h in culture. The latter suggests that other proapoptotic BH3-only proteins, possibly PUMA (5), or other cell death mechanisms, such as death receptor-mediated apoptosis (32), may be more important than BIM in the killing of activated B lymphoblasts.

While the considerations above relate to how BIM regulates B cell homeostasis under physiological conditions in otherwise normal mice, it has previously been shown that germline loss of *Bim* can also impact B cell development, for example, in the context of other mutations or under pathological conditions. A prominent example of this is the accelerated development of B cell lymphomas emanating from pre-B cells or immature B cells in *Eμ-Myc* transgenic mice (22). Our data indicate that the conditional and germline loss of *Bim* have quantitatively comparable effects in this context. Other examples of the effect of BIM on B cell development include the partial or complete rescue of B cell development defects of IL-7-deficient or IL-7 receptor-deficient mice (6, 8), *dicer*-deficient mice (33), or *Asciz*-deficient mice (29) by germline *Bim* KO. Indeed, we recently found that conditional *Bim* deletion can fully rescue the B cell developmental defects of *Mb1-Cre Dynll1*-deleted mice (17), which are mechanistically and quantitatively similar to those observed in the *Mb1-Cre Asciz*-deleted mice. This indicates that BIM exerts its effects on B cell development under pathological conditions, at least during B lymphomagenesis, also in a cell-intrinsic manner in the B lymphoid lineage.

Finally, while our data indicate that the expansion of mature B cells in *Bim* KO mice is largely driven in a cell-intrinsic manner, it has been reported that substantial B cell expansions can also be triggered by the conditional deletion of *Bim* within only the myeloid cell compartment (11). However, it should be noted that these analyses of *LysM-Cre Bim*-deleted mice were performed in much older mice (8 months versus 8 weeks of age for our mice) and after they had developed a multi-organ autoimmune syndrome. Nevertheless, these findings highlight that it would be worthwhile to monitor the *Cd23-Cre Bim*-deleted mice for longer periods to determine if B cell-specific loss of BIM eventually leads to age-dependent deposition of immune complexes in susceptible tissues, such as the glomeruli in the kidney, and the development of any autoimmune syndrome-like pathologies, although these would be expected to be relatively mild on a C57BL/6 background (see above).

## ETHICS STATEMENT

Animal experiments were performed according to the Australian Code for the Care and Use of Animals for Scientific Purposes, 8th Edition (2013), and approved by the St. Vincent's Hospital Melbourne Animal Ethics Committee, approval numbers 019/13 and 002/17.

## AUTHOR CONTRIBUTIONS

RL was involved in design, performing and analysis of experiments, and contributed to drafting of the manuscript. AK was involved in design, performing, and analysis of experiments. PB, DT, and AS provided resources and were involved in discussing experiments and editing the manuscript. JH was involved in the conception of the study, the design, analysis, and supervision of experiments, and drafting and editing of the manuscript.

## ACKNOWLEDGMENTS

We thank Nora Tenis for mouse genotyping and assistance with mouse colony maintenance, Dijana Miljkovic for FACS facility support, and the St. Vincent's Hospital Bioresources Centre for animal care.

## REFERENCES

- Strasser A. The role of BH3-only proteins in the immune system. *Nat Rev Immunol* (2005) 5(3):189–200. doi:10.1038/nri1568
- Bouillet P, Metcalf D, Huang DC, Tarlinton DM, Kay TW, Kontgen F, et al. Proapoptotic Bcl-2 relative Bim required for certain apoptotic responses, leukocyte homeostasis, and to preclude autoimmunity. *Science* (1999) 286(5445):1735–8. doi:10.1126/science.286.5445.1735
- Enders A, Bouillet P, Puthalakath H, Xu Y, Tarlinton DM, Strasser A. Loss of the pro-apoptotic BH3-only Bcl-2 family member Bim inhibits BCR stimulation-induced apoptosis and deletion of autoreactive B cells. *J Exp Med* (2003) 198(7):1119–26. doi:10.1084/jem.20030411
- Hughes PD, Belz GT, Fortner KA, Budd RC, Strasser A, Bouillet P. Apoptosis regulators Fas and Bim cooperate in shutdown of chronic immune responses and prevention of autoimmunity. *Immunity* (2008) 28(2):197–205. doi:10.1016/j.jimmuni.2007.12.017
- Fischer SF, Bouillet P, O'Donnell K, Light A, Tarlinton DM, Strasser A. Proapoptotic BH3-only protein Bim is essential for developmentally programmed death of germinal center-derived memory B cells and antibody-forming cells. *Blood* (2007) 110(12):3978–84. doi:10.1182/blood-2007-05-091306
- Oliver PM, Wang M, Zhu Y, White J, Kappler J, Marrack P. Loss of Bim allows precursor B cell survival but not precursor B cell differentiation in the absence of interleukin 7. *J Exp Med* (2004) 200(9):1179–87. doi:10.1084/jem.20041129
- Labi V, Erlacher M, Kiessling S, Manzl C, Frenzel A, O'Reilly L, et al. Loss of the BH3-only protein Bmf impairs B cell homeostasis and accelerates gamma irradiation-induced thymic lymphoma development. *J Exp Med* (2008) 205(3):641–55. doi:10.1084/jem.20071658
- Huntington ND, Labi V, Cumano A, Vieira P, Strasser A, Villunger A, et al. Loss of the pro-apoptotic BH3-only Bcl-2 family member Bim sustains B lymphopoiesis in the absence of IL-7. *Int Immunol* (2009) 21(6):715–25. doi:10.1093/intimm/dxp043
- Erlacher M, Labi V, Manzl C, Bock G, Tzankov A, Hacker G, et al. Puma cooperates with Bim, the rate-limiting BH3-only protein in cell death during lymphocyte development, in apoptosis induction. *J Exp Med* (2006) 203(13):2939–51. doi:10.1084/jem.20061552
- Herold MJ, Stuchbery R, Merino D, Willson T, Strasser A, Hildeman D, et al. Impact of conditional deletion of the pro-apoptotic BCL-2 family member BIM in mice. *Cell Death Dis* (2014) 5:e1446. doi:10.1038/cddis.2014.409
- Tsai F, Homan PJ, Agrawal H, Misharin AV, Abdala-Valencia H, Haines GK III, et al. Bim suppresses the development of SLE by limiting myeloid inflammatory responses. *J Exp Med* (2017) 214(12):3753–73. doi:10.1084/jem.20170479
- Hobeika E, Thiemann S, Storch B, Jumaa H, Nielsen PJ, Pelanda R, et al. Testing gene function early in the B cell lineage in mb1-cre mice. *Proc Natl Acad Sci U S A* (2006) 103(37):13789–94. doi:10.1073/pnas.0605944103
- Kwon K, Hutter C, Sun Q, Bilic I, Cobaleda C, Malin S, et al. Instructive role of the transcription factor E2A in early B lymphopoiesis and germinal center B cell development. *Immunity* (2008) 28(6):751–62. doi:10.1016/j.jimmuni.2008.04.014
- Adams JM, Harris AW, Pinkert CA, Corcoran LM, Alexander WS, Cory S, et al. The c-myc oncogene driven by immunoglobulin enhancers induces lymphoid malignancy in transgenic mice. *Nature* (1985) 318(6046):533–8. doi:10.1038/31853a0
- Wong DM, Li L, Jurado S, King A, Bamford R, Wall M, et al. The transcription factor ASCIZ and its target DYNLL1 are essential for the development and expansion of MYC-driven B cell lymphoma. *Cell Rep* (2016) 14:1488–99. doi:10.1016/j.celrep.2016.01.012
- Hardy RR, Carmack CE, Shinton SA, Kemp JD, Hayakawa K. Resolution and characterization of pro-B and pre-pro-B cell stages in normal mouse bone marrow. *J Exp Med* (1991) 173(5):1213–25. doi:10.1084/jem.173.5.1213
- King A, Li L, Wong DM, Liu R, Bamford R, Strasser A, et al. Dynein light chain regulates adaptive and innate B cell development by distinctive genetic mechanisms. *PLoS Genet* (2017) 13(9):e1007010. doi:10.1371/journal.pgen.1007010
- Rolink A, Grawunder U, Winkler TH, Karasuyama H, Melchers F. IL-2 receptor alpha chain (CD25, TAC) expression defines a crucial stage in pre-B cell development. *Int Immunol* (1994) 6(8):1257–64. doi:10.1093/intimm/6.8.1257
- ten Boekel E, Melchers F, Rolink A. The status of Ig loci rearrangements in single cells from different stages of B cell development. *Int Immunol* (1995) 7(6):1013–9. doi:10.1093/intimm/7.6.1013
- Rolink A, Melchers F. B-cell development in the mouse. *Immunol Lett* (1996) 54(2–3):157–61. doi:10.1016/S0165-2478(96)02666-1
- Rowth MA, DeMicco A, Horowitz JE, Yin B, Yang-Iott KS, Fusello AM, et al. Tp53 deletion in B lineage cells predisposes mice to lymphomas with oncogenic translocations. *Oncogene* (2011) 30(47):4757–64. doi:10.1038/onc.2011.191
- Egle A, Harris AW, Bouillet P, Cory S. Bim is a suppressor of Myc-induced mouse B cell leukemia. *Proc Natl Acad Sci U S A* (2004) 101(16):6164–9. doi:10.1073/pnas.0401471101
- Bouillet P, Cory S, Zhang LC, Strasser A, Adams JM. Degenerative disorders caused by Bcl-2 deficiency prevented by loss of its BH3-only antagonist Bim. *Dev Cell* (2001) 1(5):645–53. doi:10.1016/S1534-5807(01)00083-1
- Hardy RR. B-1 B cell development. *J Immunol* (2006) 177(5):2749–54. doi:10.4049/jimmunol.177.5.2749
- O'Connor L, Strasser A, O'Reilly LA, Hausmann G, Adams JM, Cory S, et al. Bim: a novel member of the Bcl-2 family that promotes apoptosis. *EMBO J* (1998) 17(2):384–95. doi:10.1093/emboj/17.2.384
- Hao Z, Rajewsky K. Homeostasis of peripheral B cells in the absence of B cell influx from the bone marrow. *J Exp Med* (2001) 194(8):1151–64. doi:10.1084/jem.194.8.1151
- Gerondakis S, Grumont RJ, Banerjee A. Regulating B-cell activation and survival in response to TLR signals. *Immunol Cell Biol* (2007) 85(6):471–5. doi:10.1038/sj.icb.7100097
- Banerjee A, Grumont R, Gugasyan R, White C, Strasser A, Gerondakis S. NF-kappaB1 and c-Rel cooperate to promote the survival of TLR4-activated B cells by neutralizing Bim via distinct mechanisms. *Blood* (2008) 112(13):5063–73. doi:10.1182/blood-2007-10-120832
- Jurado S, Gleeson K, O'Donnell K, Izon DJ, Walkley CR, Strasser A, et al. The Zinc-finger protein ASCIZ regulates B cell development via DYNLL1 and Bim. *J Exp Med* (2012) 209(9):1629–39. doi:10.1084/jem.20120785

## FUNDING

This work was supported by a NHMRC Senior Research Fellowship (1022469), a Worldwide Cancer Research grant (16-0156), grants-in-aid from the 5-point Foundation and the Margaret Walkom Bequest to JH; an Australian Postgraduate Award to AK; NHMRC Senior Principal Research Fellowship (1020363), NHMRC program grant (1016701), Cancer Council Victoria grant (1052309), Leukemia and Lymphoma Society (LLS) SCOR grant (7001-13) to AS; NHMRC program grant (1054925) and NHMRC Principal Research Fellowship (1060675) to DT; and NHMRC Independent Research Institutes Infrastructure Support, and Victorian State Government Operational Infrastructure Support grants.

30. LeBien TW, Tedder TF. B lymphocytes: how they develop and function. *Blood* (2008) 112(5):1570–80. doi:10.1182/blood-2008-02-078071
31. Melchers F. Checkpoints that control B cell development. *J Clin Invest* (2015) 125(6):2203–10. doi:10.1172/JCI78083
32. Strasser A, Jost PJ, Nagata S. The many roles of FAS receptor signaling in the immune system. *Immunity* (2009) 30(2):180–92. doi:10.1016/j.jimmuni.2009.01.001
33. Koralov SB, Muljo SA, Galler GR, Krek A, Chakraborty T, Kanellopoulou C, et al. Dicer ablation affects antibody diversity and cell survival in the B lymphocyte lineage. *Cell* (2008) 132(5):860–74. doi:10.1016/j.cell.2008.02.020

**Conflict of Interest Statement:** The authors declare that the research was conducted in the absence of any commercial or financial relationships that could be construed as a potential conflict of interest.

Copyright © 2018 Liu, King, Bouillet, Tarlinton, Strasser and Heierhorst. This is an open-access article distributed under the terms of the Creative Commons Attribution License (CC BY). The use, distribution or reproduction in other forums is permitted, provided the original author(s) and the copyright owner are credited and that the original publication in this journal is cited, in accordance with accepted academic practice. No use, distribution or reproduction is permitted which does not comply with these terms.



# Activation of the MEK-ERK Pathway Is Necessary but Not Sufficient for Breaking Central B Cell Tolerance

Sarah A. Greaves<sup>1</sup>, Jacob N. Peterson<sup>1</sup>, Raul M. Torres<sup>1,2</sup> and Roberta Pelanda<sup>1,2\*</sup>

<sup>1</sup> Department of Immunology and Microbiology, University of Colorado School of Medicine, Aurora, CO, United States,

<sup>2</sup> Department of Biomedical Research, National Jewish Health, Denver, CO, United States

## OPEN ACCESS

### Edited by:

Hermann Eibel,  
Universitätsklinikum Freiburg,  
Albert Ludwigs Universität  
Freiburg, Germany

### Reviewed by:

David Nemazee,  
The Scripps Research Institute,  
United States  
Juergen Konrad Wienands,  
Georg-August-Universität  
Göttingen, Germany

### \*Correspondence:

Roberta Pelanda  
roberta.pelanda@ucdenver.edu

### Specialty section:

This article was submitted  
to B Cell Biology,  
a section of the journal  
Frontiers in Immunology

Received: 23 January 2018

Accepted: 22 March 2018

Published: 09 April 2018

### Citation:

Greaves SA, Peterson JN, Torres RM  
and Pelanda R (2018) Activation  
of the MEK-ERK Pathway Is  
Necessary but Not Sufficient for  
Breaking Central B Cell Tolerance.  
*Front. Immunol.* 9:707.  
doi: 10.3389/fimmu.2018.00707

Newly generated bone marrow B cells are positively selected into the peripheral lymphoid tissue only when they express a B cell receptor (BCR) that is nonautoreactive or one that binds self-antigen with only minimal avidity. This positive selection process, moreover, is critically contingent on the ligand-independent tonic signals transduced by the BCR. We have previously shown that when autoreactive B cells express an active form of the rat sarcoma (RAS) oncogene, they upregulate the receptor for the B cell activating factor (BAFFR) and undergo differentiation *in vitro* and positive selection into the spleen *in vivo*, overcoming central tolerance. Based on the *in vitro* use of pharmacologic inhibitors, we further showed that this cell differentiation process is critically dependent on the activation of the mitogen-activated protein kinase kinase pathway MEK (MAPKK)-extracellular signal-regulated kinase (ERK), which is downstream of RAS. Here, we next investigated if activation of ERK is not only necessary but also sufficient to break central B cell tolerance and induce differentiation of autoreactive B cells *in vitro* and *in vivo*. Our results demonstrate that activation of ERK is critical for upregulating BAFFR and overcoming suboptimal levels of tonic BCR signals or low amounts of antigen-induced BCR signals during *in vitro* B cell differentiation. However, direct activation of ERK does not lead high avidity autoreactive B cells to increase BAFFR levels and undergo positive selection and differentiation *in vivo*. B cell-specific MEK-ERK activation in mice is also unable to lead to autoantibody secretion, and this in spite of a general increase of serum immunoglobulin levels. These findings indicate that additional pathways downstream of RAS are required for high avidity autoreactive B cells to break central and/or peripheral tolerance.

**Keywords:** B cells, B cell tolerance, BCR signaling, MAP kinase, ERK, B cell development, autoreactive B cells, mouse models

## INTRODUCTION

B cells developing in the bone marrow rearrange their immunoglobulin heavy (IgH) and immunoglobulin light (IgL) chain genes in order to form B cell receptors (BCRs) specific for a wide array of pathogens. Due to its random nature, this process also produces B cells that are reactive with self-antigens (i.e., autoreactive B cells). In fact, a large majority (~55–75%) of immature B cells that are newly generated in the bone marrow of mice and people are autoreactive (1, 2). In a healthy immunological system, these autoreactive immature B cells are eliminated or controlled by

mechanisms of negative selection known as B cell tolerance (1, 3–5). About half of these cells, those with BCRs with low avidity for self-antigen, enter the circulation and undergo further differentiation but are rendered anergic in the periphery and die shortly thereafter [reviewed in Ref. (6, 7)]. The other half, those with medium/high avidity BCRs for self-antigens, continue rearranging their IgL chain genes to form a new BCR, a central tolerance mechanism known as receptor editing (1, 3–5). Once these editing B cells produce a nonautoreactive (NA) BCR, a “tonic” ligand-independent signal is generated (8, 9). Our lab and others have shown that this tonic signal is crucial for the positive selection of B cells into the spleen, their differentiation into transitional and mature cell stages, and their long-term survival in the periphery (5, 10–12).

B cell repertoire studies have shown that in patients affected by some autoimmune diseases (including systemic lupus erythematosus), an increased number of autoreactive B cells escape from the bone marrow into the periphery to play a role in disease (13–15). In addition, many B cells participating in disease flares in lupus patients carry germline encoded Ig variable region sequences, suggesting they are direct descendants of B cells that escaped central tolerance (16). This has also been demonstrated in mice in which B cells expressing germline encoded Ig genes contribute to anti-nuclear antibody production (17). Determining the molecular mechanisms of how autoreactive and NA immature B cells undergo positive selection into the periphery is, therefore, of great importance in order to establish who is at risk for autoimmune diseases. This knowledge may also lead to the development of new therapies that restrict the bone marrow output of autoreactive B cells, thus decreasing the risk for the onset of these diseases. However, the molecular mechanisms that lead autoreactive B cells to break central tolerance are still largely unknown.

Rat sarcoma (RAS) is a small GTPase involved in many fundamental cellular processes, including cell differentiation and survival (18). RAS is thought to be the main activator of the extracellular signal-regulated kinase (ERK) pathway, *via* the intermediate MAP kinases RAF and MEK, all of which are also essential cell signaling components (19). In previous studies we have shown that basal activation of both RAS and ERK is higher in NA than autoreactive immature B cells of mouse models of central tolerance (20, 21). In addition, NA immature B cells bearing hypomorphic BCR levels with reduced tonic signaling (BCR-low cells) exhibit low levels of active RAS and ERK that are similar to those of autoreactive cells (20, 21). We have further shown that inhibition of the MAPK MEK-ERK pathway in NA immature B cell cultures prohibits cell differentiation into the transitional stage (20, 21). Taken together, these data have revealed a positive correlation between surface BCR levels and intracellular activity of the RAS-ERK pathway in immature B cells and have also indicated that basal activation of the ERK pathway is necessary for propagation of tonic BCR signaling and the differentiation of immature B cells into transitional B cells.

Heightened levels of phospho-ERK (pERK) have been observed in B cells from both lupus patients and some lupus mouse models (22–24) suggesting that this pathway contributes

to the generation and/or the survival and activation of autoreactive B cells. In support of this idea, we have shown that expression of a constitutively active form of NRAS (caNRAS) in NA BCR-low and in autoreactive immature B cells increases their basal pERK levels, inhibits receptor editing *in vitro* and *in vivo*, promotes *in vitro* cell differentiation, and, in some instances, induces the *in vivo* production of IgG autoantibodies (20, 21). Because activation of the MEK-ERK pathway is downstream of RAS, this has led us to hypothesize that activation of the ERK pathway is not only necessary but may also be sufficient to overcome defects in BCR tonic signaling or the presence of self-antigen-induced BCR signaling and, consequently, to promote the differentiation of NA BCR-low and autoreactive B cells. To our knowledge, whether activation of the ERK pathway overcomes B cell tolerance has never been tested.

To test this hypothesis, in this study, we used a gene cassette encoding a constitutively active form of MEK (caMEK) either as a retroviral-driven transgene in bone marrow cultures or as a Cre-regulated Rosa-26 targeted locus *in vivo*. This latter approach has been successfully employed to investigate the signaling pathways that ensure the BCR-dependent survival of mature B cells (25). Using these approaches we found that in bone marrow B cell cultures, ERK activation can overcome suboptimal levels of tonic BCR signals or low amounts of antigen-induced BCR signals to promote the differentiation of BCR-low or autoreactive immature B cells into transitional B cells. However, direct activation of the MEK-ERK pathway is unable to break B cell tolerance *in vivo*, neither preventing receptor editing nor allowing cell differentiation of high avidity autoreactive B cells. These findings indicate that activation of ERK is not sufficient to break central B cell tolerance and that additional pathways downstream of RAS are required for this outcome.

## MATERIALS AND METHODS

### Mice

Ig knock-in mice 3-83Igi,H-2<sup>d</sup> (NA), 3-83Igi,H-2<sup>d</sup>-low (NA with low BCR), and 3-83Igi,H-2<sup>b</sup> (autoreactive) have been previously described (20, 26–29) and were all on a BALB/c genetic background. BALB/c mb1-Cre mice described in Ref. (30) were kindly donated by Michael Reth (Max Planck Institute of Immunobiology and Epigenetics) and were bred to 3-83Igi,H-2<sup>b</sup> mice to generate 3-83Igi,H-2<sup>b</sup>-mb1-Cre mice. CB17 mice, bred in house, were used as wild-type controls. BALB/c mice (Stock No. 000651) were purchased from The Jackson Laboratory. The Rosa26-Lox-stop-Lox (LSL)-caMEK-GFP mice previously described in Ref. (25) were purchased from The Jackson Laboratory (Stock No. 012352) and were backcrossed to CB17,H-2<sup>b</sup> mice (4 generations) and then bred to 3-83Igi,H-2<sup>b</sup> mice (eight generations) to generate 3-83Igi,H-2<sup>b</sup>-R26-LSL-caMEK-GFP mb1-cre mice. Mice were analyzed at 7–9 weeks of age. Mice were bred and maintained in a specific pathogen-free facility at the University of Colorado Anschutz Medical Campus Vivarium (Aurora, CO, USA). Both male and female mice were used for experiments, and all animal procedures were approved by the UCD Institutional Animal Care and Use Committee.

## Retroviral Constructs and Production of Retroviral Particles

The following retroviral vectors encoding replication-deficient retroviruses were used: pMSCV-IRES-GFP (MIG) and pMSCV-GFP-IRES-hN-RasG12D(NRAS) were previously described (20). We obtained a shuttle vector containing constitutively active form of MEK [caMEK, MEK1-S218E/S222D (31)] from Addgene (plasmid #40809). The caMEK gene cassette was amplified from this plasmid using the primers caMEK-NotI (5'-AAAGCGGC CGCGTTACCCGGGTCCAAA-3') and caMEK-SalII (5'-AATG TCGACTTAGACGCCAGCAGCATG-3') and AccuTaq polymerase (Sigma). The PCR product was cloned between NotI and SalII in the retroviral pMSCV-IRES-GFP vector (20) to generate the pMSCV-caMEK-IRES-GFP plasmid. These vectors are based on the Murine Stem Cell Virus (MSCV) retroviral expression system and contain an internal ribosome entry site (IRES) for bicistronic gene expression. We obtained the ERK2 shRNA and luciferase shRNA sequences in shuttle vectors from Open Biosystems. The shRNA sequences were isolated from these vectors as XhoI-EcoRI fragments that were then cloned into the MCV-LTRmiR30-PIG (LMP) vector (Open Biosystems), kindly donated by John Cambier (University of Colorado), to create the MCV-LMP-ERK2-shRNA and MCV-LMP-luc-shRNA plasmids. Retroviral particles were produced as described previously (20).

## In Vitro Immature B-Cell Differentiation and Transduction

Bone marrow immature B cells were generated and differentiated *in vitro* as previously described (20, 21) based on a B cell culture system originally described in Ref. (32). Briefly, bone marrow cells were cultured in complete Iscove's Modified Dulbecco's Medium in the presence of IL-7 (made in house) for 4 days at which time IL-7 was removed by washing twice with PBS. Then, cells were plated at  $6-8 \times 10^6$  cells/mL with 10 ng/mL recombinant mouse BAFF (R&D Systems) for an additional 2–3 days to achieve cell differentiation (e.g., CD21 and IgD expression). Where indicated, cells were treated with either DMSO, 30  $\mu$ M of ERK1/2 inhibitor (FR180204; EMD Chemicals), or indicated concentrations of anti-3-83Ig idiotypic antibody S23 (33), during culture with BAFF. S23 was added to the culture each day in order to maintain BCR engagement. Retroviral transduction of immature B cells was performed as previously described (20).

## ELISAs

The 3-83IgM and total IgM serum titers were measured by ELISA as previously described (29). The 3-83IgG2a serum titer was measured by ELISA as previously described (29) and with the following modifications. Briefly, 96-well Nunc-Immuno MaxiSorp plates (Thermo Fisher Scientific) were coated with 10  $\mu$ g/mL of rat anti-mouse IgG2a (RMG2a-62) (purchased from BD Pharmingen). The 3-83IgG was detected using biotinylated anti-3-83Ig antibody (54.1) (34), followed by alkaline phosphatase (AP)-conjugated streptavidin (SouthernBiotech), and developed by the addition of AP substrate (*p*-nitro-phenyl phosphate; Sigma). For total IgG ELISA, 96-well Nunc-Immuno

MaxiSorp plates were coated with 10  $\mu$ g/mL of goat anti-mouse IgG (H+L) antibody, human ads-unlabeled (SouthernBiotech). Plates were detected with goat anti-mouse IgG, human ads-AP (SouthernBiotech). The standard used to measure total IgG concentration was a mixture of the following mouse unlabeled antibodies starting at 1  $\mu$ g/mL: IgG1 (15H6), IgG2a (HOPC-1), IgG2b (A-1), IgG3 (B10), all purchased from Southern Biotech. For the total IgE ELISA, plates were coated with 10  $\mu$ g/mL unlabeled goat anti-mouse IgA antibody (SouthernBiotech) and detected with goat anti-mouse IgA-AP antibody (SouthernBiotech). For the total IgE ELISA, plates were coated with 10  $\mu$ g/mL rat anti-mouse IgE antibody (23G3, SouthernBiotech), and detected with rat anti-mouse IgE-AP antibody (23G3, SouthernBiotech). The standards used to measure sera concentrations are as follows: mouse IgA-unlabeled (S107, SouthernBiotech, starting at 1  $\mu$ g/mL), mouse IgE-unlabeled (15.3, SouthernBiotech, starting at 0.2  $\mu$ g/mL). All ELISA plates were developed by the addition of AP substrate (Sigma) solubilized in 0.1 M diethanolamine and 0.02% NaN<sub>3</sub>. Plates were read as previously described (35).

## Generation of Retrovirus-Transduced Mixed Bone Marrow Chimeras

Bone marrow chimeras with transduced hematopoietic stem cells (i.e., retrogenic) were generated as previously described (36) with the following modifications. Briefly, donor 3-83Ig<sub>H-2<sup>d</sup></sub>-low bone marrow cells were transduced with two cycles of spin infection as previously described (36). Recipient BALB/c mice were lethally irradiated with two doses of 450 rad, 3 h apart. They then received a total of  $5 \times 10^5$  donor cells mixed at the indicated ratios in PBS *via* tail vein injection. Mice were analyzed 8–9 weeks later.

## Quantitative Real-Time PCR

*Ex vivo* bone marrow B cells (either B220<sup>+</sup> or B220<sup>+GFP+</sup>) were isolated using a FACSaria (BD Biosciences) cell sorter with a purity of >97%. Total RNA was purified using TRIzol (Invitrogen) and cDNA was synthesized using the SuperScript III First-Strand Synthesis system (Invitrogen). Murine *Rag1* (Mm01270936\_m1) and *Rag2* (Mm00501300\_m1) cDNAs were amplified using Applied Biosystems TaqMan primer and probe sets purchased from Thermo Fisher Scientific. Differences in specific mRNA levels were determined as previously described (21), and each sample was normalized to murine 18 s (Mm03928990\_g1, AB TaqMan). All samples were run in triplicate using the LightCycler 480 instrument (Roche).

## Flow Cytometry

Bone marrow and spleen single-cell suspensions were stained with fluorochrome or biotin-conjugated antibodies against mouse B220 (RA3-6B2), IgD (11-26c-2a), IgM<sup>a</sup> (MA-69), IgM<sup>b</sup> (AF6-78), pan-IgM (11/41), CD21 (7E9), CD23 (B3B4), CD24 (M1/69), Igλ (RML-42), CD19 (1D3), CD138 (281-2), CD86 (B7-2), CD69 (H1.2F3), CD1d (1B1), and CD44 (1M7) purchased from eBioscience, BD Pharmingen, or Biolegend. Anti-3-83Ig (H + κ) antibodies [54.1 (34)] were produced in house. Biotin-labeled antibodies were visualized with fluorochrome-conjugated streptavidin (BD Biosciences). The fluorescent chemical

compound 7-aminoactinomycin D (7AAD; eBioscience) was used to discriminate unfixed dead cells. Phospho-ERK and total ERK staining were performed on cells treated with the phosphatase inhibitor pervanadate for 5 min as previously described (20, 21). Zombie UV Fixable Viability kit from BioLegend was used to discriminate dead cells in fixed and permeabilized samples. Data acquisition was done on the CyAn cytometer (Beckman Coulter) or the BD LSRFortessa cytometer (BD Biosciences) and analyzed with FlowJo software (Tree Star). Analyses were performed on live B cells based on the incorporation of either 7AAD or Zombie UV and the pan B-cell marker B220 expression. Cell doublets were excluded based on the side scatter and pulse width for data analyzed on the CyAn cytometer or the forward scatter area and forward scatter height for data analyzed on the BD LSRFortessa.

## Statistical Data Analysis

Data were analyzed using GraphPad Prism software. Statistical significance was assessed using an unpaired, one-tail, Student's *t*-test. *P*-values of  $\leq 0.05$  were considered significant. Data are represented as mean  $\pm$  SEM.

## RESULTS

### ERK Contributes to Establishing Appropriate Expression of the BCR and BAFFR on Immature B Cells

Our previous studies have indicated that basal activation of the ERK pathway is necessary for the differentiation of immature B cells into transitional B cells. These studies, however, were performed with pharmacologic inhibitors of the ERK pathway that, due to potential off target effects, may lead to erroneous conclusions [e.g., (37)]. In order to confirm the requirement for ERK in the differentiation of transitional B cells, we expressed an shRNA specific for ERK2 [the ERK isoform more highly expressed in immature B cells (21)] in NA bone marrow B cells from the Ig knock-in mouse model 3-83IgI,H-2<sup>d</sup> (26, 28), and then measured their differentiation into CD21<sup>+</sup> transitional B cells (Figure S1A in Supplementary Material). Expression of ERK2-shRNA led to lower levels of total ERK and of pERK in immature B cells, levels that were particularly reduced in a fraction of transduced cells (Figures S1B,C in Supplementary Material). In agreement with previous observations obtained with the use of MEK and ERK inhibitors (20, 21), knock-down of ERK2 was accompanied by a decreased frequency of CD21<sup>+</sup> transitional B cells and, again, with a noticeable fraction expressing lower levels of CD21 (Figure S1D in Supplementary Material).

Results from our previous studies (20, 21) have led us to suggest that basal ERK activation is under the control of tonic BCR signaling in immature B cells and that a level of pERK above a set threshold is required for the differentiation of immature B cells into transitional B cells. In order to test this idea, we treated NA bone marrow B cell cultures with an ERK inhibitor, and measured surface IgM on cells that differentiated into IgD<sup>+</sup> transitional B cells. Pharmacologic inhibition of ERK led to the differentiation of fewer IgD<sup>+</sup> transitional B cells (data not shown), and the cells that were able to differentiate displayed higher surface IgM

levels when compared to control treated cells (Figure 1A). These data support the idea that a threshold of pERK under the control of surface IgM is required to promote ongoing immature B cell differentiation.

BAFFR expression and signaling contributes to the differentiation of immature into transitional B cells and of transitional into mature B cells (36, 38–40). Moreover, BAFFR is expressed at higher RNA and protein levels by NA immature B cells relative to BCR-low and autoreactive B cells (36). Therefore, we next asked if the activity of ERK is necessary for BAFFR expression by immature B cells. Upon treating cultures of NA bone marrow immature B cells with an ERK inhibitor we found significantly reduced expression of BAFFR relative to control (Figure 1B), suggesting that ERK activity contributes to the expression of BAFFR and the response of immature B cells to BAFF. Our previous studies have shown that the expression of caNRAS restores BAFFR levels on the surface of BCR-low immature B cells in culture (20, 36). Given that RAS is a potent activator of the ERK

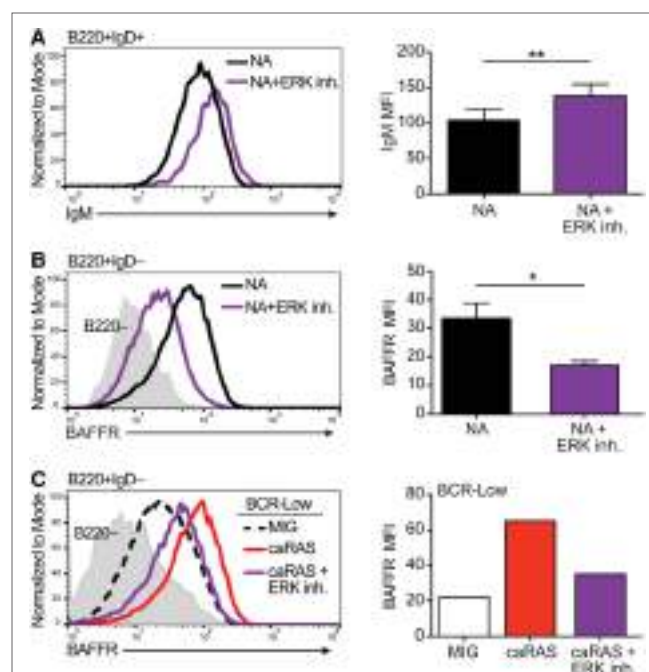


**FIGURE 1 |** Extracellular signal-regulated kinase (ERK) contributes to establishing appropriate expression of the BCR and BAFFR on immature B cells. **(A)** Representative histograms and quantification of IgM levels on nonautoreactive (NA) (3-83IgI,H-2<sup>d</sup>) bone marrow cells that were cultured in IL-7 for 4 days and then incubated with either BAFF + DMSO (black) or BAFF + 30  $\mu$ M ERK1/2 inhibitor (FR180204, purple) for 3 days. Shown are B220<sup>+</sup>IgD<sup>+</sup> transitional B cells. *N* = 4 total, from four independent experiments. **(B)** Representative histograms and quantification of BAFFR levels on NA bone marrow cells that were cultured in IL-7 for 4 days along with either DMSO (black) or 30  $\mu$ M ERK1/2 inhibitor (purple). Shown are B220<sup>+</sup>IgD<sup>-</sup> immature B cells. *N* = 3 total, from three independent experiments. **(C)** Representative histograms and quantification of BAFFR levels on BCR-low bone marrow cells that were cultured in IL-7 for 4 days and transduced with either MIG control or caRAS and then incubated with either DMSO (MIG, black dashed line or white bar and caRAS, red) or 30  $\mu$ M ERK1/2 inhibitor (caRAS, purple). Data are representative of two independent experiments. \**P*  $\leq$  0.05, \*\**P*  $\leq$  0.01.

pathway (41), we questioned whether the upregulation of BAFFR mediated by caNRAS (36) also requires ERK activity. To test this, we transduced BCR-low immature B cell cultures with caNRAS and then treated the cells with an ERK inhibitor. Inhibition of ERK almost completely prevented the induction of BAFFR expression mediated by caNRAS (**Figure 1C**).

Taken together, these data reinforce the conclusion that under the control of surface IgM and tonic BCR signaling, the ERK pathway plays a crucial role in the differentiation of immature B cells into transitional B cells and, thus, for the establishment of central B cell tolerance. They also indicate a critical role of ERK downstream of RAS in the upregulation of BAFFR, an event that contributes to the generation of transitional B cells in mice. We next asked whether direct activation of the ERK pathway is also sufficient to overcome defective tonic signals and to break central B cell tolerance.

### **ERK Activation Overcomes Suboptimal Levels of Tonic BCR Signals or Low Amounts of Antigen-Induced BCR Signals During the *In Vitro* Differentiation of Immature B Cells Into Transitional B Cells**

To determine if ERK activation alone could facilitate BAFFR expression to levels similarly driven by caNRAS and could also promote the differentiation of BCR-low B cells, we conducted *in vitro* experiments with a constitutively active form of MEK (caMEK), the kinase that directly activates ERK. A gene encoding caMEK [MEK1-S218E/S222D (31)] was cloned into a retroviral vector that includes an IRES-GFP cassette, and caMEK-IRES-GFP retroviral particles were transduced into BCR-low immature B cells in an IL-7 culture.

To ensure the function of caMEK, we compared pERK levels in B cells transduced with caMEK or control retrovirus. In order to measure pERK in “naïve” immature B cells, we previously demonstrated the need to amplify this signal with a pervanadate treatment, and we have shown that the pERK signal in pervanadate-treated cells is proportional to the basal level in untreated cells (21). Expression of caMEK in pervanadate-treated BCR-low immature B cells increased pERK levels to those present in BCR-normal NA cells. These levels were also similar to those achieved with the expression of caNRAS (**Figure 2A**). However, in spite of its ability to increase ERK activity, caMEK failed to increase the expression of BAFFR (**Figure 2B**). Despite low BAFFR levels, BCR-low immature B cells expressing caMEK differentiated into CD21<sup>+</sup> transitional B cells similarly to BCR-normal NA B cells, although to a lesser extent relative to BCR-low cells expressing caNRAS (**Figure 2C**). The ability of caMEK to promote B cell differentiation was dose-dependent because higher levels of caMEK, as indicated by GFP intensity, resulted in higher amounts of pERK and frequency of CD21<sup>+</sup> cells (**Figures 2D,E**). Thus, these data confirm our previous findings (20) that immature B cells expressing low levels of BCR display low levels of pERK and BAFFR and do not differentiate into transitional B cells. Furthermore, these data extend these findings to indicate that activation of the ERK pathway restores normal differentiation of immature BCR-low B cells into transitional B cells in culture,

but to a lower extent than what was achieved by activation of the RAS pathway.

We have previously shown that expression of caNRAS promotes the *in vitro* differentiation of high avidity autoreactive immature B cells into transitional B cells and *via* a process requiring the activity of ERK (21). To explore whether direct activation of ERK is sufficient to induce the differentiation of autoreactive B cells, we transduced autoreactive immature B cells (from the 3-83Ig,H-2<sup>b</sup> mouse model) with caMEK and analyzed their differentiation *in vitro*. Similar to that observed with NA BCR-low B cells, the expression of caMEK in autoreactive B cells led to significantly increased levels of basal pERK, comparable to the levels expressed by NA B cells (**Figure 3A**). But again, caMEK was unable to increase BAFFR expression (**Figure 3B**). However, while caMEK corrected the impaired differentiation of BCR-low cells (**Figures 2C,E**), it did not overcome the developmental block in autoreactive immature B cells (**Figure 3C**). Indeed, the frequency of CD21<sup>+</sup> B cells in caMEK-expressing 3-83Ig,H-2<sup>b</sup> cells was equivalent to that of the control MIG-transduced cells (**Figure 3C**). These data, therefore, indicate that activation of the MEK-ERK pathway is not sufficient to rescue the differentiation of autoreactive B cells *in vitro*, at least not when the autoreactive cells exhibit high avidity for self-antigen, as is the case for B cells from 3-83Ig,H-2<sup>b</sup> mice (42).

Autoreactive immature B cells with low avidity for self-antigen experience low levels of self-antigen-induced BCR signaling (43) but also retain a discernable amount of surface IgM and resulting tonic BCR signals (21). In order to test whether constitutive activation of the MEK-ERK pathway could overcome tolerance set by low avidity BCR-induced signals, we used decreasing amounts of the agonistic anti-3-83Ig idiotypic antibody S23 (33) to mimic decreasing availability of self-antigen. Specifically, NA 3-83Ig,H-2<sup>d</sup> immature B cells were transduced with caMEK or MIG and then incubated with varying concentrations of anti-3-83Ig S23 mAb until analysis of cell differentiation (**Figure 3D**). Consistent with the previous results (**Figure 3C**), expression of caMEK did not promote the differentiation of 3-83Ig<sup>+</sup> B cells incubated with high concentrations of S23 (**Figure 3E**). However, a measurable and significant increase in cell differentiation was observed in cells expressing caMEK relative to control (MIG) with diminishing doses of S23 (**Figure 3E**). This suggests that ERK activation may be able to overcome low levels of self-antigen-mediated signals to induce positive selection and differentiation of low-avidity autoreactive immature B cells.

The above findings indicate that activation of the MEK-ERK pathway is able to overcome defective tonic BCR signaling and low level of antigen-induced BCR signaling during the *in vitro* differentiation of immature B cells into transitional B cells and *via* a process independent on the expression of BAFFR.

### **Constitutive Activation of the MEK-ERK Pathway Does not Overcome B Cell Tolerance *In Vivo***

The bone marrow culture system only partially reflects the processes of central B cell selection and B cell differentiation and

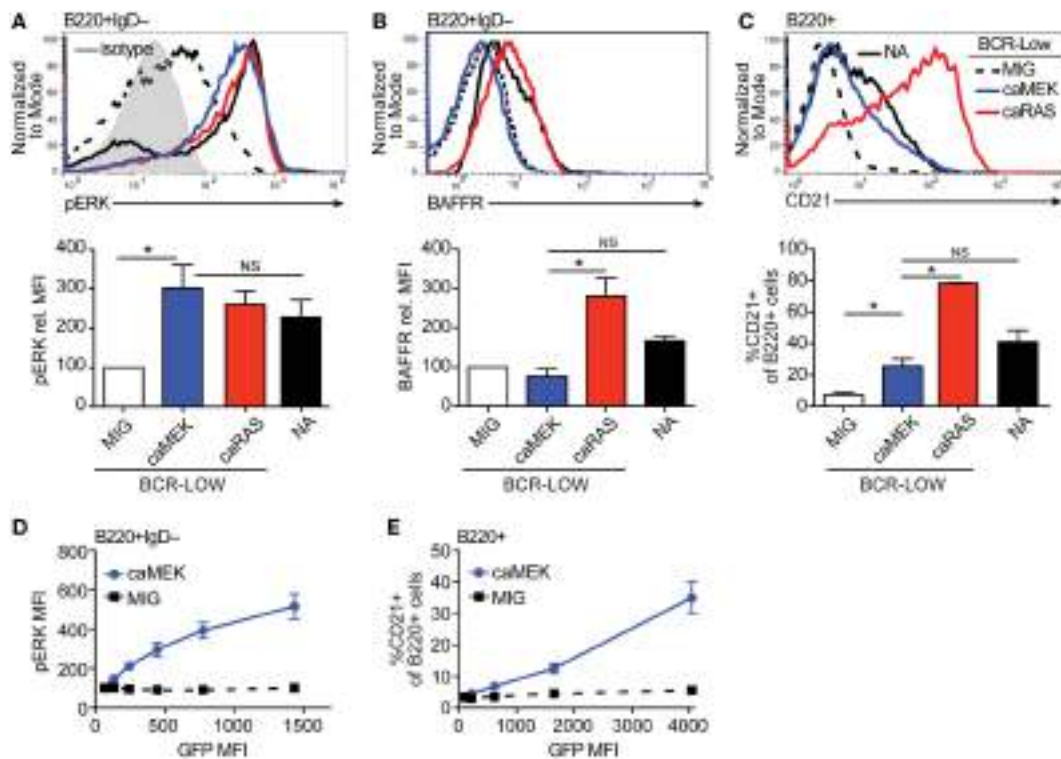


**FIGURE 2 |** Extracellular signal-regulated kinase (ERK) activation drives differentiation of BCR-low immature B cells *in vitro*. **(A,B)** Representative histograms and bar graph quantification of pERK (**A**) and BAFFR (**B**) in bone marrow immature (B220<sup>+</sup>IgD<sup>-</sup>) B cells cultured for 4 days with IL-7. The cells analyzed were either nonautoreactive (NA) (3-83IgI, H-2<sup>b</sup>) BCR normal cells (NA, black solid line) or BCR-low cells transduced with MIG (black dashed line), caMEK (blue line), or caNRas (red line). The analysis of transduced cells was performed on GFP<sup>+</sup> cells in all experiments. Staining of pERK was done on cells treated with pervanadate to allow for pERK signal detection. The gray shaded histogram in **(A)** represents isotype control antibody. **(C)** Representative histograms and bar graph quantification of the frequency of CD21<sup>+</sup> cells in the B220<sup>+</sup> B cell population after 3 days of culture with BAFF. **(D,E)** BCR-low B cells transduced with either caMEK (blue) or MIG control (black) were gated based on increasing GFP expression, which correlates with caMEK expression in caMEK transduced cells. The pERK MFI (**D**) or the frequency of CD21<sup>+</sup> cells (**E**) were plotted against the GFP MFI of the individual segments. In all panels,  $N = 3$  total, from three independent experiments. \* $P \leq 0.05$ ; NS, not significant.

cannot be used to investigate the generation of mature B cells or the implementation of peripheral tolerance. To test whether activation of the ERK pathway can overcome, at least partially, central and peripheral B cell tolerance *in vivo*, we crossed 3-83IgI, H-2<sup>b</sup> mice to mb1-Cre mice (30) and Rosa26-lox-stop-lox-caMEK-GFP mice (25) to generate 3-83IgI, H-2<sup>b</sup> LSL-caMEK-mb1Cre animals in which caMEK is only expressed in 3-83 autoreactive B cells (Figure 4A).

Expression of caMEK, which was marked by the presence of GFP, was exclusively observed in B220<sup>+</sup> B cells in the bone marrow and spleen of LSL-caMEK-mb1Cre mice (Figure S2 in Supplementary Material). To confirm the functionality of the Rosa26 caMEK allele in the B cell lineage, we measured pERK levels in bone marrow immature B cells in which the pERK signal was amplified with pervanadate treatment. Bone marrow immature B cells are normally identified as B220<sup>+</sup>IgM<sup>+</sup>IgD<sup>-</sup>, but we analyzed pERK in B220<sup>+</sup>IgD<sup>-</sup> cells because IgM is largely internalized in 3-83Ig<sup>+</sup> autoreactive B cells, and about 90% of B220<sup>+</sup>IgD<sup>-</sup> cells are nevertheless immature B cells in (3-83) Ig knock-in mice due to the absence of pre-B cells (26). The expression of caMEK in autoreactive immature B cells increased their

pERK levels to those observed in NA B cells (Figure 4B), and this was not a consequence of differences in surface IgM (Figure 4E) in the presence of pervanadate treatment, as could be argued based on previous studies (44). Thus, these data indicate that caMEK expression in developing B cells leads to meaningful activation of the ERK pathway.

Central B cell tolerance was investigated *in vivo* by first analyzing the phenotype of bone marrow B cells. As shown in Figures 4C,D, activation of the ERK pathway did not alter the total number of B220<sup>+</sup> cells, nor the numbers of immature (CD21<sup>-</sup>CD23<sup>-</sup>), T1-like (CD21<sup>+</sup>CD23<sup>-</sup>), and T2-like (CD21<sup>+</sup>CD23<sup>+</sup>) B cell populations in the bone marrow of 3-83IgI, H-2<sup>b</sup> mice. Surface levels of IgM were also equivalent (Figure 4E). However, we did find a slight but significant reduction in numbers of recirculating mature (CD24<sup>low</sup>CD21<sup>+</sup>) B cells (Figure 4D).

It was previously indicated that the ERK pathway plays a role in receptor editing (45), although our previous *in vitro* studies suggest it does not (21). In accordance with our previous findings, we did not see changes in parameters associated with receptor editing such as the number of surface IgM<sup>-</sup> (editing) and IgM<sup>+</sup> (edited) cells, frequency of  $\lambda^+$  cells, and expression of *Rag1/2*

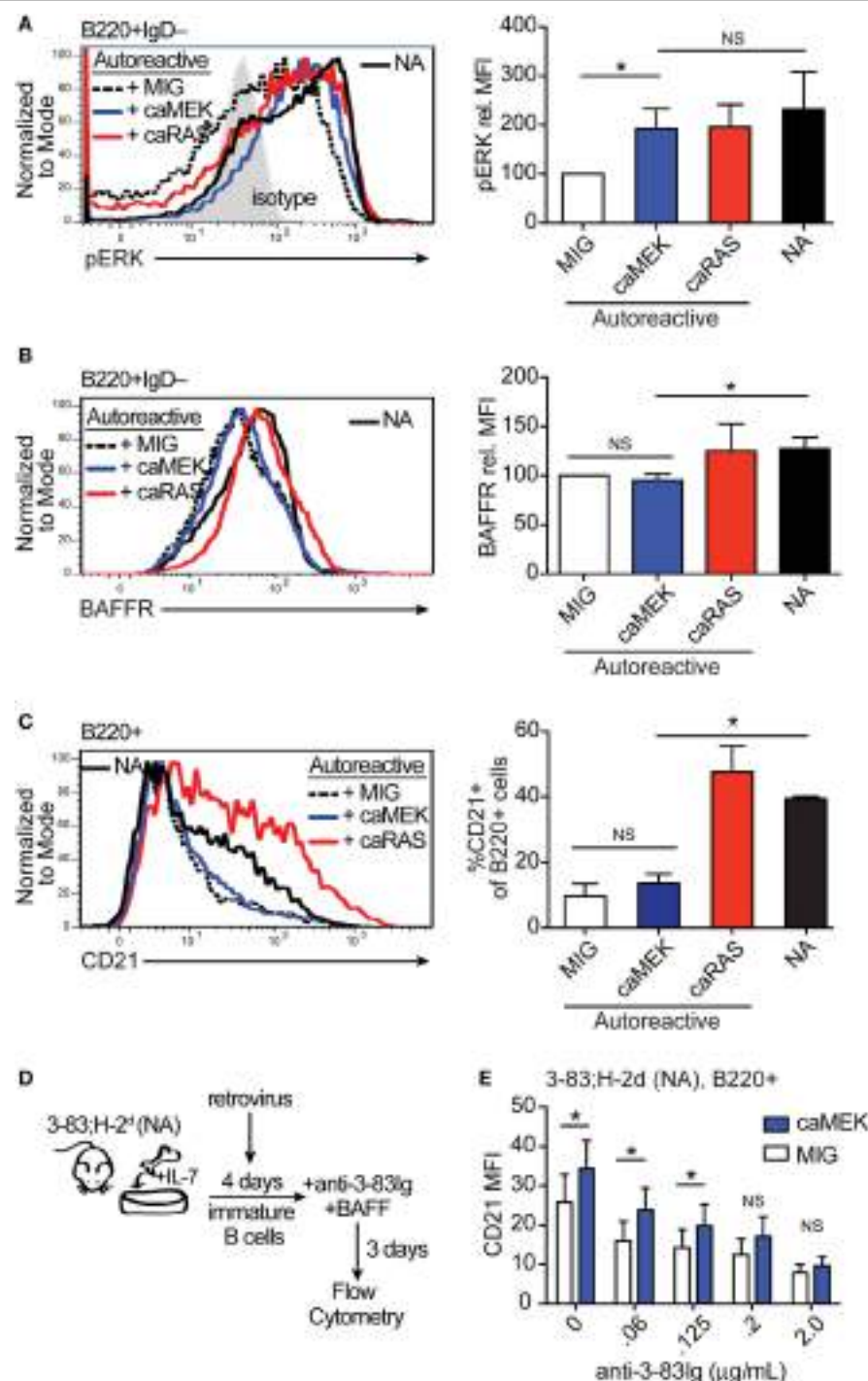


**FIGURE 3 |** Extracellular signal-regulated kinase (ERK) activation drives the differentiation of low-avidity, but not high-avidity autoreactive B cells *in vitro*. **(A,B)** Representative histograms and bar graph quantification of phospho-ERK (pERK) **(A)** and BAFFR **(B)** in bone marrow immature B cells (B220+IgD<sup>-</sup>) cultured for 4 days with IL-7. The B cells analyzed were either non-transduced nonautoreactive (NA) (3-83Ig,H-2<sup>d</sup>) cells (black solid line) or autoreactive (3-83Ig,H-2<sup>d</sup>) cells transduced with MIG control (black dashed line), caMEK (blue line), or caRas (red line) retroviral vectors. Transduced cells were gated on GFP<sup>+</sup> for analyses. Staining of pERK (in A) was done on cells treated with pervanadate. The gray shaded histogram in **(A)** represents isotype control antibody. **(C)** Representative histograms and bar graph quantification of the frequency of CD21<sup>+</sup> cells in the B220<sup>+</sup> B cell population after 3 days of culture with BAFF. **(D)** Schematic of the system utilized to investigate the effect of caMEK on the *in vitro* differentiation of immature B cells cultured with increasing amounts of BCR stimulation. 3-83Ig,H-2<sup>d</sup> bone marrow cells were cultured with IL-7 for 4 days and transduced with retrovirus carrying either caMEK or MIG on the second day of culture. Cells were then incubated with BAFF and increasing amounts of an agonistic anti-3-83 Ig idiotypic mAb (S23), this latter added each day during a 3 days culture. **(E)** CD21 expression (MFI) on B cells treated as described in **(D)**: caMEK-GFP, blue bars and MIG, white bars. In all panels,  $N = 3$  total, from three independent experiments. \* $P \leq 0.05$ ; NS, not significant.

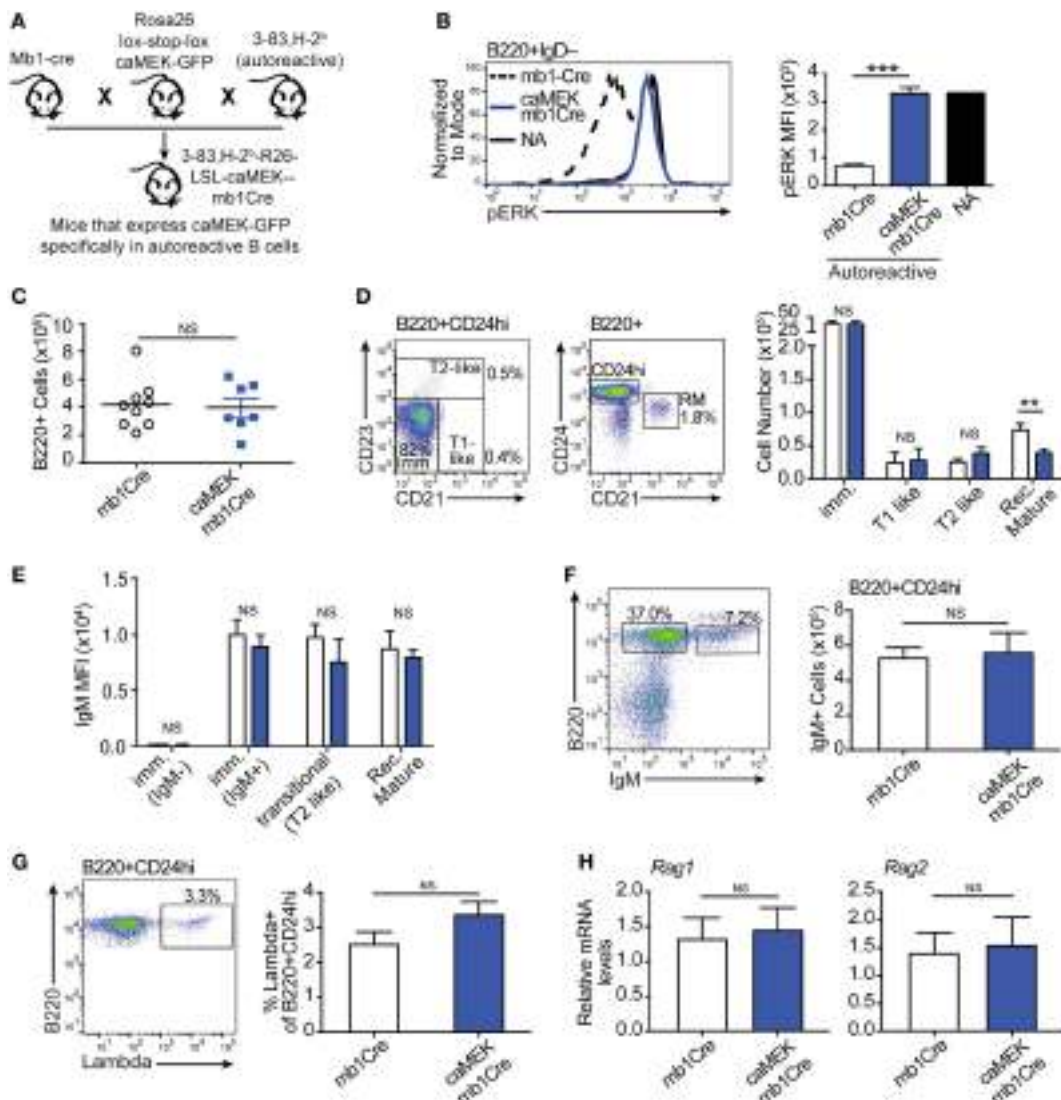


**FIGURE 4 |** Constitutive extracellular signal-regulated kinase (ERK) activation does not rescue the *in vivo* development of autoreactive bone marrow B cells. **(A)** Schematic of the *in vivo* model for caMEK expression in autoreactive B cells. **(B)** Representative histograms and bar graph quantification of pERK levels in ex vivo immature B cells (B220+IgD-) from the bone marrow of NA (3-83Igi,H-2<sup>b</sup>) mice and autoreactive (3-83Igi,H-2<sup>b</sup>) mb1Cre or R26-LSL-caMEK-GFP-mb1Cre (caMEK-mb1Cre) mice. Cells were treated with pervanadate before pERK staining. **(C)** Absolute numbers of B220+ cells in the bone marrow of 3-83Igi,H-2<sup>b</sup> mb1Cre and R26-LSL-caMEK-GFP-mb1Cre mice. **(D)** Gating strategy and bar graph quantification of cell numbers in bone marrow B cell populations from 3-83Igi,H-2<sup>b</sup> mb1Cre and R26-LSL-caMEK-GFP-mb1Cre mice. B cell subsets were discriminated as: immature B cells (B220+CD24<sup>hi</sup>CD21-CD23<sup>+</sup>), T1-like B cells (B220+CD24<sup>hi</sup>CD21+CD23<sup>+</sup>), T2-like B cells (B220+CD24<sup>hi</sup>CD21+CD23<sup>+</sup>), and recirculating mature B cells (B220+CD24<sup>lo</sup>CD21<sup>hi</sup>). **(E)** Mean fluorescence intensity of IgM surface expression on B cells belonging to the B cell subsets gated as in **(D)**. **(F)** Gating strategy and quantification of the number of IgM<sup>+</sup> (edited) and IgM<sup>-</sup> (editing) cells within the bone marrow immature (B220+CD24<sup>hi</sup>) B cell population from 3-83Igi,H-2<sup>b</sup> mb1Cre and R26-LSL-caMEK-GFP-mb1Cre mice. **(G)** Gating strategy and quantification of the percentage of  $\lambda$ + cells within immature (B220+CD24<sup>hi</sup>) bone marrow B cells from 3-83Igi,H-2<sup>b</sup> mb1Cre and R26-LSL-caMEK-GFP-mb1Cre mice. For panels **(A–F)**,  $N = 9$  total 3-83Igi,H-2<sup>b</sup>-mb1Cre mice and  $N = 7$  total 3-83Igi,H-2<sup>b</sup>-R26-LSL-caMEK-GFP-mb1Cre mice, analyzed in four independent experiments. **(H)** Relative Rag1 and Rag2 mRNA levels in B220+ or B220+GFP<sup>+</sup> cells sorted from the bone marrow of 3-83Igi,H-2<sup>b</sup>-mb1Cre or 3-83Igi,H-2<sup>b</sup>-R26-LSL-caMEK-GFP-mb1Cre mice, respectively. Data were normalized to 18 s mRNA levels and are expressed as fold change over the average mRNA levels in 3-83Igi,H-2<sup>b</sup>-mb1Cre cells.  $N = 3$  mice from one experiment. In all panels, B cells from 3-83Igi,H-2<sup>b</sup> R26-LSL-caMEK-GFP-mb1Cre mice were additionally gated on GFP<sup>+</sup> to analyze only the cells expressing caMEK. \*\* $P \leq 0.01$ , \*\*\* $P \leq 0.001$ , NS, not significant.

genes, within the bone marrow immature B cell population (Figures 4F–H).

We next evaluated the extent to which activation of the ERK pathway affects B cell tolerance by analyzing the phenotype of

peripheral B cells. In the spleen of 3-83Igi,H-2<sup>b</sup> caMEK-mb1Cre mice, we noticed a slight, although not significant, increase in pERK expression (Figure 5A). We also observed a minor, but significant reduction in total B220<sup>+</sup> cell numbers (Figure 5B), but

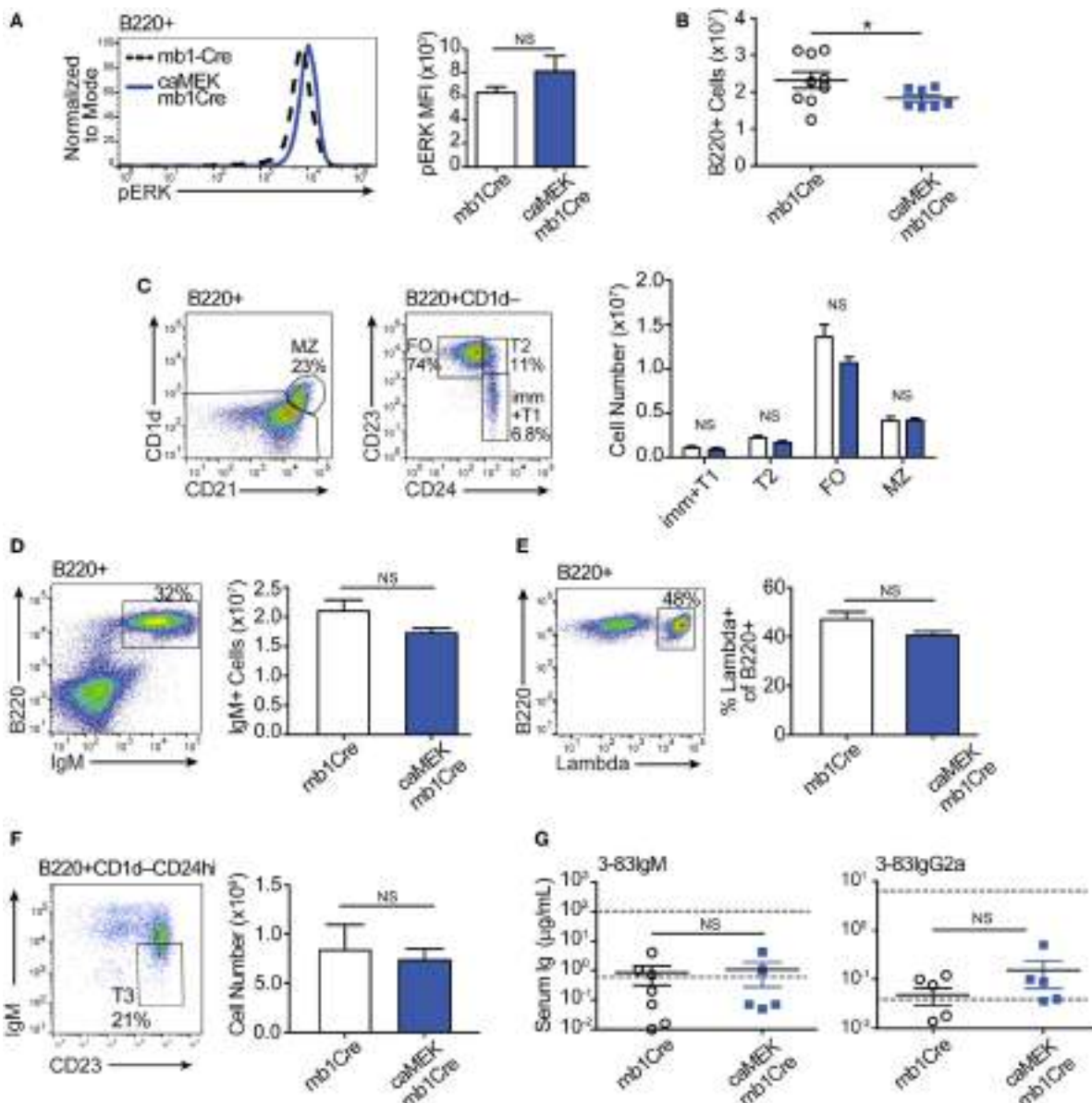


**FIGURE 5 |** Constitutive extracellular signal-regulated kinase (ERK) activation does not break the central or peripheral tolerance of autoreactive 3-83Ig<sup>+</sup> B cells *in vivo*. **(A)** Representative histograms and bar graph quantification of phospho-ERK (pERK) levels in ex vivo B220<sup>+</sup> B cells from the spleen of autoreactive 3-83Ig<sub>H-2<sup>b</sup></sub> mb1Cre and R26-LSL-caMEK-GFP-mb1Cre mice. Cells were treated with pervanadate before pERK staining. **(B)** Absolute number of B220<sup>+</sup> cells in the spleens of 3-83Ig<sub>H-2<sup>b</sup></sub> mb1Cre and R26-LSL-caMEK-GFP-mb1Cre mice. **(C)** Gating strategy and bar graph quantification of splenic B cell populations from 3-83Ig<sub>H-2<sup>b</sup></sub> mb1Cre and R26-LSL-caMEK-GFP-mb1Cre mice. B cell subsets were discriminated as: immature/transitional 1 B cells (B220<sup>+</sup>CD1d<sup>+</sup>CD24<sup>hi</sup>CD23<sup>-</sup>), transitional 2 B cells (B220<sup>+</sup>CD1d<sup>+</sup>CD24<sup>hi</sup>CD23<sup>+</sup>), follicular B cells (B220<sup>+</sup>CD1d<sup>+</sup>CD24<sup>lo</sup>CD23<sup>+</sup>), and marginal zone B cells (B220<sup>+</sup>CD1d<sup>+</sup>CD21<sup>hi</sup>). **(D)** Gating strategy and quantification of IgM<sup>+</sup> B cell numbers from the spleens of 3-83Ig<sub>H-2<sup>b</sup></sub> mb1Cre and R26-LSL-caMEK-GFP-mb1Cre mice. **(E)** Gating strategy and quantification of the percentage of  $\lambda^+$  cells within B220<sup>+</sup> B cells from the spleen of 3-83Ig<sub>H-2<sup>b</sup></sub> mb1Cre and R26-LSL-caMEK-GFP-mb1Cre mice. For panels **(A–E)**,  $N = 9$  total 3-83Ig<sub>H-2<sup>b</sup></sub> mb1Cre mice, and  $N = 7$  total 3-83Ig<sub>H-2<sup>b</sup></sub>-R26-LSL-caMEK-GFP-mb1Cre mice, analyzed in four independent experiments. **(F)** Gating strategy and quantification of T3 B cell numbers (CD23<sup>+</sup>IgM<sup>+</sup>) within the transitional B cell population (B220<sup>+</sup>CD1d<sup>+</sup>CD24<sup>hi</sup>) from the spleen of 3-83Ig<sub>H-2<sup>b</sup></sub> mb1Cre and R26-LSL-caMEK-GFP-mb1Cre mice. In panels **(A–F)**, B cells from 3-83Ig<sub>H-2<sup>b</sup></sub> R26-LSL-caMEK-GFP-mb1Cre mice were additionally gated on GFP<sup>+</sup> to analyze only the cells expressing caMEK. **(G)** Concentration ( $\mu\text{g/mL}$ ) of 3-83IgM and 3-83IgG2a in the sera of 3-83Ig<sub>H-2<sup>b</sup></sub>-mb1Cre controls ( $N = 7$ ) and 3-83Ig<sub>H-2<sup>b</sup></sub>-R26-LSL-caMEK-GFP-mb1Cre mice ( $N = 5$ ). The bottom dotted lines represent background detection levels from a wild-type control and the top dotted lines represent Ig levels present in 3-83Ig<sub>H-2<sup>d</sup></sub> nonautoreactive (NA) positive control mice. \* $P \leq 0.05$ ; NS, not significant.

there were no other significant differences in individual splenic B cell subsets compared to mb1Cre only littermate controls (Figure 5C). There were also no differences in IgM<sup>+</sup> cell numbers

or in the percent of  $\lambda^+$  B cells between caMEK and control mice (Figures 5D,E), confirming our conclusions that central B cell tolerance was equivalent in its extent or mechanism. Because

ERK signaling has been thought to maintain anergy in a subset of autoreactive B cells (43), we analyzed the T3 B cell subset to investigate whether expression of caMEK leads to increased numbers of anergic B cells (6). However, we found no difference in the T3 population of caMEK mice compared to controls (**Figure 5F**). In the past, we have shown that about 20% of splenic B cells in 3-83Igi,H-2<sup>b</sup> mice retains expression of the 3-83 autoreactive BCR, although this is generally intracellular and the antibody is minimally secreted (29). Thus, we questioned next whether caMEK would relax peripheral tolerance and increase secretion of the 3-83 autoantibody. Again, we observed no significant differences in the concentrations of 3-83IgM and 3-83IgG2a secreted antibodies in serum of caMEK and control mice, antibodies that were detected only at background (wild-type) levels (**Figure 5G**). In summary, these data indicate that caMEK expression by high avidity autoreactive B cells does not lead to a break in either central or peripheral tolerance *in vivo*.

To establish whether the inability of caMEK to correct defects in B cell differentiation *in vivo* was restricted to autoreactive B cells, we also investigated the effect of caMEK on the *in vivo* development of NA BCR-low B cells. For these studies, we generated bone marrow chimeras of Ig<sup>h<sup>a</sup></sup> BCR-low cells transduced with either caMEK-GFP or GFP only, mixed with non-transduced Ig<sup>h<sup>b</sup></sup> wild-type competitor cells (Figure S3A in Supplementary Material) using a method previously described (20). We found that although ERK activation was increased, BCR-low B cells expressing caMEK were unable to differentiate *in vivo* (Figures S3B–E in Supplementary Material), similar to that observed for autoreactive B cells.

Taken together, these data indicate that when assessed *in vivo*, direct activation of the ERK pathway is unable to compensate for defective tonic BCR signaling or self-antigen-induced BCR signals during B cell development and tolerance.

## Constitutive Activation of the ERK Pathway in B Cells Leads to Higher Levels of Serum Antibodies but Not to Higher Numbers of Activated B Cells

Published studies indicate that ERK is necessary for the expression of BLIMP-1 and the generation of plasma cells in response to foreign antigen (46). However, continuous BCR signaling through the ERK pathway, as present in self-reactive B cells, leads to inhibition of BLIMP-1 and plasma cell generation *via* a mechanism that has been suggested to be necessary for the maintenance of B cell anergy (43, 47). We were therefore interested in whether constitutive activation of the MEK-ERK pathway has either a positive or negative impact on B cell activation and antibody production.

To address this, we evaluated naïve 3-83Igi,H-2<sup>b</sup> caMEK and control mice for the expression of activation markers on B cells and the levels of total serum IgS, taking into consideration that the peripheral B cell population of 3-83Igi,H-2<sup>b</sup> mice is mainly composed of edited polyclonal NA B cells (28, 29). Our analyses did not detect any significant differences in the expression of CD86 and CD69 activation markers and in that of CD44 and CD138 plasmablast markers on caMEK splenic B cells, relative

to control (**Figures 6A–D**). We did, however, find a significant increase of CD23 surface levels in caMEK B cells (**Figure 6E**). CD23 is known to be a receptor for IgE, and previous studies have reported that IgE is able to regulate the expression of CD23 *in vivo* (48). Based on this and the known contribution of ERK to plasma cell development (46), we hypothesized that constitutive activation of the MEK-ERK pathway could alter antibody production, and we tested this possibility by measuring total Ig isotypes in the sera of caMEK and control mice. These analyses detected significantly higher levels of total IgM, IgG, and IgE, but not IgA, in caMEK mice compared to littermate controls (**Figure 6F**).

Thus, by showing that B cell-specific constitutive activation of the MEK-ERK pathway increases basal antibody production, these data support a B cell-intrinsic role of ERK in plasma cell generation and antibody secretion.

## DISCUSSION

The present study extends our understanding of how central B cell tolerance is intrinsically regulated and how autoreactive B cells are selected out of the bone marrow and into the circulation, this latter a phenomenon that occurs more frequently in many autoimmune patients. We have previously established that activation of the RAS cascade can break central B cell tolerance in mice, leading to inhibition of receptor editing and development of autoreactive B cells, a process requiring ERK. In this study, we tested whether intrinsic activation of the ERK pathway in immature B cells is not only necessary, but also sufficient to mediate BCR-derived signaling events that promote cell differentiation and positive selection into the mature population. Our data demonstrate that constitutive activation of the MEK-ERK pathway can intrinsically overcome suboptimal levels of tonic BCR signaling and low amounts of antigen-induced BCR signaling to promote the differentiation of immature B cells into transitional B cells, but only *in vitro*. *In vivo*, however, activation of the MEK-ERK pathway is unable to break either central or peripheral B cell tolerance, despite its ability to generally enhance serum antibody levels.

The RAS-ERK pathway has been positively linked to a variety of processes during B cell development. Starting at the very early B cell subsets, it has been shown that ERK activity is essential for the pro-B cell to pre-B cell transition (49, 50). Furthermore, the ERK kinase signals downstream of the pre-BCR to upregulate genes associated with cell proliferation and survival (50). In contrast to these positive effects exercised during early B cell development, ERK can have quite a negative effect during the transitional B cells stage. In fact, it has been shown that B cells can activate the ERK pathway both dependently and independently of Ca<sup>2+</sup> signaling, and that Ca<sup>2+</sup>-dependent activation of the ERK pathway is responsible for inducing apoptosis (i.e., clonal deletion) of autoreactive B cells at the transitional stage (51).

In this study we show that, differing from what was previously achieved with constitutive activation of RAS (20, 21), direct ERK activation is not sufficient to induce positive selection and bone marrow export of either NA BCR-low or autoreactive B cells. We additionally show that basal activation of the ERK pathway, such as achieved in the 3-83Igi,H-2<sup>b</sup>,caMEK,mb1-cre mice, does not

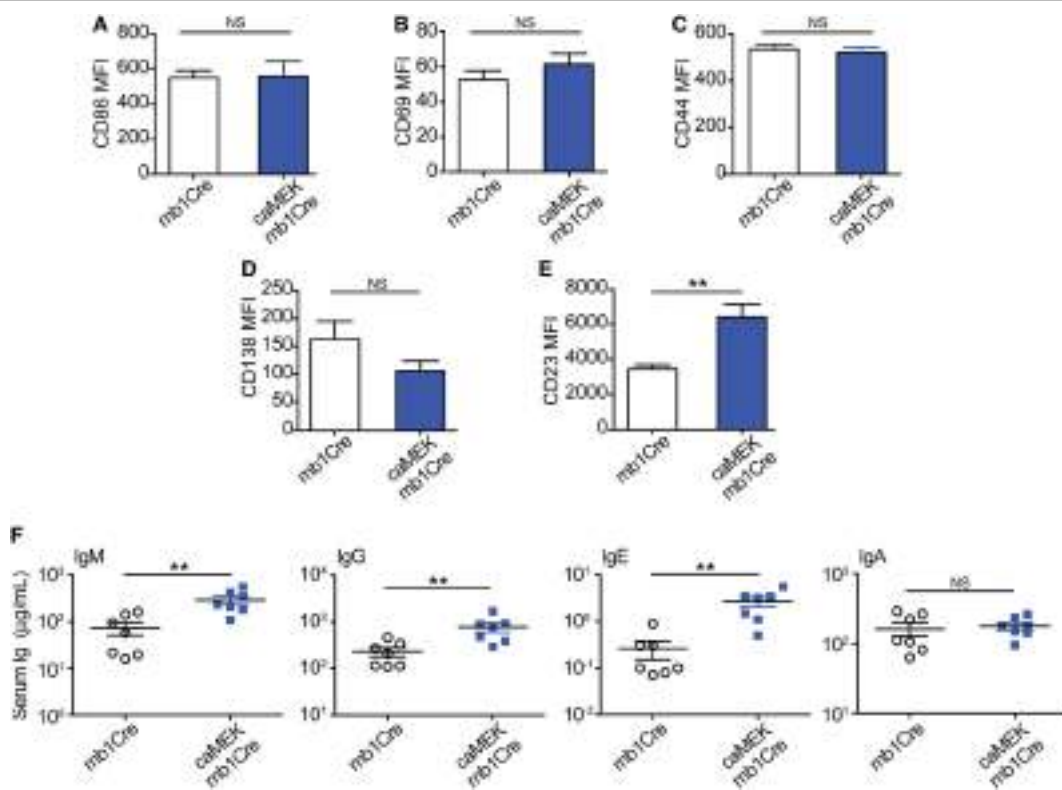


**FIGURE 6 |** B cell-specific expression of caMEK does not induce B cell activation, but increases serum Ig levels. **(A–E)** MFI levels of **(A)** CD86, **(B)** CD69, **(C)** CD44, **(D)** CD138, and **(E)** CD23 on splenic B220<sup>+</sup> B cells from 3-83IgI, H-2<sup>b</sup> mb1Cre and B220<sup>+</sup>GFP<sup>+</sup> B cells R26-LSL-caMEK-GFP-mb1Cre mice.  $N = 9$  total 3-83IgI, H-2<sup>b</sup>-mb1Cre mice and  $N = 7$  total 3-83IgI, H-2<sup>b</sup>-R26-LSL-caMEK-GFP-mb1Cre mice, analyzed in four independent experiments. **(F)** Concentrations ( $\mu\text{g}/\text{mL}$ ) of total IgM, IgG, IgE, and IgA in the sera of 3-83IgI, H-2<sup>b</sup>-mb1Cre littermate controls ( $N = 7$ , open circles) and 3-83IgI, H-2<sup>b</sup>-R26-LSL-caMEK-GFP-mb1Cre ( $N = 7$ , filled squares) mice. \*\* $P \leq 0.01$ ; NS, not significant.

induce general apoptosis of transitional B cells. This is evident by the overall normal B cell maturation observed in 3-83IgI, H-2<sup>b</sup>, caMEK, mb1-cre mice. Thus, our data disagree with a general pro-apoptotic role of ERK in transitional B cells (51). We did notice, however, a slight reduction in recirculating mature B cells in the bone marrow and of total B cells in the spleen of the caMEK mice (Figures 4D and 5B). Therefore, it is possible that these changes are caused by mechanisms of negative selection resulting from a small subset of caMEK-positive B cells acquiring greater than basal levels of ERK activation and subsequently undergoing clonal deletion. Clearly, other possibilities exist such as ERK mediated alteration of cell trafficking.

This study, as well as our previous study (21), convincingly shows that the ERK pathway does not regulate *Rag1/2* expression and, thus, receptor editing, in autoreactive immature B cells. These findings contrast with published studies from other groups suggesting that ERK is able to inhibit receptor editing (45, 52). Although the basis for this discrepancy is not clear, we note that in our experiments caMEK increased pERK in (pervanadate-treated) autoreactive cells to levels similarly expressed by NA immature B cells and, thus, reflecting normal physiology. The other studies either used a B cell lymphoma (52) which, as a transformed cell, possibly displays aberrant signaling properties,

or employed ERK activated by a constitutively active form of RAF (45). Because in this latter study pERK levels were not reported, we cannot exclude the possibility they were higher than those promoted by caMEK in our studies, leading to distinct B cell fates.

Throughout our studies, we observed some discrepancies between the results we obtained from the *in vitro* B cell cultures and the *in vivo* mouse models. Namely, we saw that activation of the MEK-ERK pathway was able to promote differentiation of BCR-low cells in bone marrow cell cultures but not in mixed retrogenic bone marrow chimeras. There could be several reasons for this discrepancy. One of these is based on the knowledge that autoreactive B cells are better able to thrive in *in vitro* B cell culture systems than in *in vivo* mouse models (53), and this could also be true for BCR-low NA immature B cells. We also noticed that, although necessary, ERK activation is not sufficient to induce BAFFR expression on immature B cells. It may be argued that the generation of transitional B cells is more dependent on BAFFR expression and signaling *in vivo* than *in vitro*. BAFF has been shown to mediate B cell survival via ERK but also via PI3K-AKT (54, 55). Thus, expression of caMEK may relieve the requirement for BAFF-induced ERK activation *in vitro*, but not *in vivo* where activation of the PI3K-AKT pathway may be needed because of heightened cell competition. Overall, our data suggest that ERK

activation can overcome the requirement for tonic BCR and BAFFR signaling in the differentiation of immature B cells into transitional B cells *in vitro*, but not *in vivo*.

Because phospho-ERK levels are elevated in anergic B cells, it has been proposed that ERK activation may be responsible for the induction or maintenance of anergy (6, 43). However, whether ERK activation alone is able to induce a state of B cell anergy has never been directly tested. Our data show that there was no difference in the size of the T3 B cell population in caMEK and control mice, suggesting that B cell-intrinsic ERK activation alone may not be sufficient to induce an anergic phenotype. It must however be noted that in these previous studies (6, 43, 46, 47, 49) pERK levels were measured by Western Blot and were typically not quantified. Therefore, we cannot exclude that quantitative differences in ERK activation between these and our studies are responsible for the differences observed in B cell anergy. Additional studies have suggested that constitutive activation of the ERK pathway is responsible for inhibiting antibody responses to TLR agonists in autoreactive B cells (47, 49). However, seemingly conflicting findings based on the use of conditional ERK deficient mice have shown that ERK activity is indispensable for BLIMP expression, generation of plasma cells, and T cell-dependent antibody responses (46). Although these data initially seem to be contradictory, it is possible that ERK activation in B cells produces different outcomes at distinct stages of differentiation (i.e., transitional versus follicular B cells), during T cell-independent vs. T cell-dependent antibody responses, or whether the B cells are autoreactive or not. Indeed, our data seem to support this idea by demonstrating that continuous activation of the ERK pathway in B cells of naïve mice enhances basal antibody production but does not promote autoantibody secretion.

It was surprising to find that constitutive activation of MEK-ERK did not lead to general B cell activation, or to changes in numbers of marginal zone B cells whose development is regulated by BCR signaling (56). Despite a lack of general B cell activation, CD23 expression on B cells and levels of IgE in serum of caMEK mice were both elevated. It has previously been reported that IgE and CD23 regulate each other. Specifically, CD23 transgenic mice produce lower IgE (57), while B cells of IgE transgenic mice show CD23 upregulation (58). Given we observed increase of both CD23 and IgE as well as higher levels of other Ig isotypes (IgM, IgG), we conclude that B cell-intrinsic expression of caMEK leads first to higher IgE production which in turn positively regulates CD23 expression on B cells. As mentioned above, mice with conditional deletion of ERK in B cells indicate ERK's requirement for plasma cell generation (46). Our data showing enhanced serum Ig levels in caMEK mice support this conclusion.

Overall, our data indicate there are significant differences in the individual abilities of the RAS and ERK pathways in mediating B cell selection and maturation both *in vitro* and *in vivo*. ERK is often thought of as the main signaling mediator downstream of RAS. However, our findings clearly show that while basal activation of the MEK-ERK pathway in immature

B cells is necessary for the upregulation of BAFFR and the generation of transitional B cells, at least *in vitro*, activation of this pathway *in vivo* is not sufficient for overcoming defects in tonic BCR signaling and for breaking B cell tolerance, both in the bone marrow and in the periphery. Thus, these results argue that there are parallel pathways downstream of RAS and distinct from MEK-ERK signaling that converge to induce BAFFR expression, inhibition of receptor editing, and positive selection of developing B cells and that may additionally regulate autoreactive B cell generation in autoimmunity. We have previously shown that inhibition of PI3K also diminishes, to some extent, the cell differentiation induced by RAS activation in immature B cells. In addition, PI3K is required for the RAS-mediated inhibition of receptor editing (21). This suggests that PI3K may be the pathway through which RAS mediates crucial signals in immature B cell selection and maturation and we are currently exploring this possibility.

## ETHICS STATEMENT

All animal procedures were approved by the UCD Institutional Animal Care and Use Committee.

## AUTHOR CONTRIBUTIONS

SG, RP, and RT contributed conception and design of the study; SG performed all experiments with the technical assistance of JP. SG analyzed data and drew conclusions together with RP. SG wrote the first draft of the manuscript. SG, RP, and RT contributed to manuscript revision, read and approved the submitted version.

## ACKNOWLEDGMENTS

We thank Dr. Sarah Rowland for cloning and testing the ERK shRNA sequences. We thank the HIMSR and ImmunoMicro Flow Facility at the University of Colorado AMC for assistance with cell sorting and analysis, and the Vivarium at the University of Colorado AMC for assistance with mouse husbandry. We are very grateful to all members of our labs, and particularly to Dr. Chiara Babolin, for the numerous useful discussions.

## FUNDING

This work was supported by the National Institute of Health grants AI052310 (to RP) and AI052157 (to RT). It was also supported in part by the Cancer Center Support Grant P30CA046934 for shared resource.

## SUPPLEMENTARY MATERIAL

The Supplementary Material for this article can be found online at <https://www.frontiersin.org/articles/10.3389/fimmu.2018.00707/full#supplementary-material>.

## REFERENCES

- Grandien A, Fuchs R, Nobrega A, Andersson J, Coutinho A. Negative selection of multireactive B cell clones in normal adult mice. *Eur J Immunol* (1994) 24(6):1345–52. doi:10.1002/eji.1830240616
- Wardemann H, Yurasov S, Schaefer A, Young JW, Meffre E, Nussenzweig MC. Predominant autoantibody production by early human B cell precursors. *Science* (2003) 301(5638):1374–7. doi:10.1126/science.1086907
- Nemazee D. Receptor editing in lymphocyte development and central tolerance. *Nat Rev Immunol* (2006) 6(10):728–40. doi:10.1038/nri1939
- Pelanda R, Torres RM. Receptor editing for better or for worse. *Curr Opin Immunol* (2006) 18(2):184–90. doi:10.1016/j.co.2006.01.005
- Pelanda R, Torres RM. Central B-cell tolerance: where selection begins. *Cold Spring Harb Perspect Biol* (2012) 4(4):a007146. doi:10.1101/cshperspect.a007146
- Cambier JC, Gauld SB, Merrell KT, Vilen BJ. B-cell anergy: from transgenic models to naturally occurring anergic B cells? *Nat Rev Immunol* (2007) 7(8):633–43. doi:10.1038/nri2133
- Goodnow CC, Vinuesa CG, Randall KL, Mackay F, Brink R. Control systems and decision making for antibody production. *Nat Immunol* (2010) 11(8):681–8. doi:10.1038/ni.1900
- Bannish G, Fuentes-Panana EM, Cambier JC, Pear WS, Monroe JG. Ligand-independent signaling functions for the B lymphocyte antigen receptor and their role in positive selection during B lymphopoiesis. *J Exp Med* (2001) 194(11):1583–96. doi:10.1084/jem.194.11.1583
- Tze LE, Schram BR, Lam KP, Hogquist KA, Hippchen KL, Liu J, et al. Basal immunoglobulin signaling actively maintains developmental stage in immature B cells. *PLoS Biol* (2005) 3(3):e82. doi:10.1371/journal.pbio.0030082
- Lam KP, Kuhn R, Rajewsky K. In vivo ablation of surface immunoglobulin on mature B cells by inducible gene targeting results in rapid cell death. *Cell* (1997) 90(6):1073–83. doi:10.1016/S0092-8674(00)80373-6
- Kouskoff V, Lacaud G, Pape K, Retter M, Nemazee D. B cell receptor expression level determines the fate of developing B lymphocytes: receptor editing versus selection. *Proc Natl Acad Sci U S A* (2000) 97(13):7435–9. doi:10.1073/pnas.130182597
- Kraus M, Alimzhanov MB, Rajewsky N, Rajewsky K. Survival of resting mature B lymphocytes depends on BCR signaling via the Igalpha/beta heterodimer. *Cell* (2004) 117(6):787–800. doi:10.1016/j.cell.2004.05.014
- Wardemann H, Nussenzweig MC. B-cell self-tolerance in humans. *Adv Immunol* (2007) 95:83–110. doi:10.1016/S0065-2776(07)95003-8
- Meffre E, Wardemann H. B-cell tolerance checkpoints in health and autoimmunity. *Curr Opin Immunol* (2008) 20(6):632–8. doi:10.1016/j.co.2008.09.001
- Meffre E. The establishment of early B cell tolerance in humans: lessons from primary immunodeficiency diseases. *Ann N Y Acad Sci* (2011) 1246:1–10. doi:10.1111/j.1749-6632.2011.06347.x
- Tipton CM, Fucile CF, Darce J, Chida A, Ichikawa T, Gregoretti I, et al. Diversity, cellular origin and autoreactivity of antibody-secreting cell population expansions in acute systemic lupus erythematosus. *Nat Immunol* (2015) 16(7):755–65. doi:10.1038/ni.3175
- Faderl M, Klein F, Wirz OF, Heiler S, Alberti-Servera L, Engdahl C, et al. Two distinct pathways in mice generate antinuclear antigen-reactive B cell repertoires. *Front Immunol* (2018) 9:16. doi:10.3389/fimmu.2018.00016
- Rajalingam K, Schreck R, Rapp UR, Albert S. Ras oncogenes and their downstream targets. *Biochim Biophys Acta* (2007) 1773(8):1177–95. doi:10.1016/j.bbamcr.2007.01.012
- Roskoski R Jr. ERK1/2 MAP kinases: structure, function, and regulation. *Pharmacol Res* (2012) 66(2):105–43. doi:10.1016/j.phrs.2012.04.005
- Rowland SL, DePersis CL, Torres RM, Pelanda R. Ras activation of Erk restores impaired tonic BCR signaling and rescues immature B cell differentiation. *J Exp Med* (2010) 207(3):607–21. doi:10.1084/jem.20091673
- Teodorovic LS, Babolin C, Rowland SL, Greaves SA, Baldwin DP, Torres RM, et al. Activation of Ras overcomes B-cell tolerance to promote differentiation of autoreactive B cells and production of autoantibodies. *Proc Natl Acad Sci U S A* (2014) 111(27):E2797–806. doi:10.1073/pnas.1402159111
- Grammer AC, Fischer R, Lee O, Zhang X, Lipsky PE. Flow cytometric assessment of the signaling status of human B lymphocytes from normal and autoimmune individuals. *Arthritis Res Ther* (2004) 6(1):28–38. doi:10.1186/ar1155
- Wu T, Qin X, Kurepa Z, Kumar KR, Liu K, Kanta H, et al. Shared signaling networks active in B cells isolated from genetically distinct mouse models of lupus. *J Clin Invest* (2007) 117(8):2186–96. doi:10.1172/JCI30398
- Wong CK, Wong PT, Tam LS, Li EK, Chen DP, Lam CW. Activation profile of intracellular mitogen-activated protein kinases in peripheral lymphocytes of patients with systemic lupus erythematosus. *J Clin Immunol* (2009) 29(6):738–46. doi:10.1007/s10875-009-9318-4
- Srinivasan L, Sasaki Y, Calado DP, Zhang B, Paik JH, DePinho RA, et al. PI3 kinase signals BCR-dependent mature B cell survival. *Cell* (2009) 139(3):573–86. doi:10.1016/j.cell.2009.08.041
- Pelanda R, Schwers S, Sonoda E, Torres RM, Nemazee D, Rajewsky K. Receptor editing in a transgenic mouse model: site, efficiency, and role in B cell tolerance and antibody diversification. *Immunity* (1997) 7(6):765–75. doi:10.1016/S1074-7613(00)80395-7
- Braun U, Rajewsky K, Pelanda R. Different sensitivity to receptor editing of B cells from mice hemizygous or homozygous for targeted Ig transgenes. *Proc Natl Acad Sci U S A* (2000) 97(13):7429–34. doi:10.1073/pnas.050578497
- Halverson R, Torres RM, Pelanda R. Receptor editing is the main mechanism of B cell tolerance toward membrane antigens. *Nat Immunol* (2004) 5(6):645–50. doi:10.1038/ni1076
- Liu S, Velez MG, Humann J, Rowland S, Conrad FJ, Halverson R, et al. Receptor editing can lead to allelic inclusion and development of B cells that retain antibodies reacting with high avidity autoantigens. *J Immunol* (2005) 175(8):5067–76. doi:10.4049/jimmunol.175.8.5067
- Hobeika E, Thiemann S, Storch B, Jumaa H, Nielsen PJ, Pelanda R, et al. Testing gene function early in the B cell lineage in mb1-cre mice. *Proc Natl Acad Sci U S A* (2006) 103(37):13789–94. doi:10.1073/pnas.0605944103
- Mansour SJ, Candia JM, Gloor KK, Ahn NG. Constitutively active mitogen-activated protein kinase kinase 1 (MAPKK1) and MAPKK2 mediate similar transcriptional and morphological responses. *Cell Growth Differ* (1996) 7(2):243–50.
- Rolink A, Ghia P, Grawunder U, Haasner D, Karasuyama H, Kalberer C, et al. In-vitro analyses of mechanisms of B-cell development. *Semin Immunol* (1995) 7(3):155–67. doi:10.1016/1044-5323(95)90043-8
- Verkoczy L, Ait-Azzouzene D, Skog P, Martensson A, Lang J, Duong B, et al. A role for nuclear factor kappa B/rel transcription factors in the regulation of the recombinase activator genes. *Immunity* (2005) 22(4):519–31. doi:10.1016/j.immuni.2005.03.006
- Nemazee DA, Burki K. Clonal deletion of B lymphocytes in a transgenic mouse bearing anti-MHC class I antibody genes. *Nature* (1989) 337(6207):562–6. doi:10.1038/337562a0
- Teodorovic LS, Riccardi C, Torres RM, Pelanda R. Murine B cell development and antibody responses to model antigens are not impaired in the absence of the TNF receptor GITR. *PLoS One* (2012) 7(2):e31632. doi:10.1371/journal.pone.0031632
- Rowland SL, Leahy KF, Halverson R, Torres RM, Pelanda R. BAFF receptor signaling aids the differentiation of immature B cells into transitional B cells following tonic BCR signaling. *J Immunol* (2010) 185(8):4570–81. doi:10.4049/jimmunol.1001708
- Jacque E, Schweighoffer E, Tybulewicz VL, Ley SC. BAFF activation of the ERK5 MAP kinase pathway regulates B cell survival. *J Exp Med* (2015) 212(6):883–92. doi:10.1084/jem.20142127
- Yan M, Brady JR, Chan B, Lee WP, Hsu B, Harless S, et al. Identification of a novel receptor for B lymphocyte stimulator that is mutated in a mouse strain with severe B cell deficiency. *Curr Biol* (2001) 11(19):1547–52. doi:10.1016/S0960-9822(01)00481-X
- Sasaki Y, Casola S, Kutok JL, Rajewsky K, Schmidt-Suppli M. TNF family member B cell-activating factor (BAFF) receptor-dependent and -independent roles for BAFF in B cell physiology. *J Immunol* (2004) 173(4):2245–52. doi:10.4049/jimmunol.173.4.2245
- Tussiwand R, Rauch M, Fluck LA, Rolink AG. BAFF-R expression correlates with positive selection of immature B cells. *Eur J Immunol* (2012) 42(1):206–16. doi:10.1002/eji.201141957
- Jacob A, Cooney D, Pradhan M, Coggeshall KM. Convergence of signaling pathways on the activation of ERK in B cells. *J Biol Chem* (2002) 277(26):23420–6. doi:10.1074/jbc.M202485200
- Lang J, Jackson M, Teyton L, Brunmark A, Kane K, Nemazee D. B cells are exquisitely sensitive to central tolerance and receptor editing induced by

- ultralow affinity, membrane-bound antigen. *J Exp Med* (1996) 184(5):1685–97. doi:10.1084/jem.184.5.1685
43. Healy JI, Dolmetsch RE, Timmerman LA, Cyster JG, Thomas ML, Crabtree GR, et al. Different nuclear signals are activated by the B cell receptor during positive versus negative signaling. *Immunity* (1997) 6(4):419–28. doi:10.1016/S1074-7613(00)80285-X
44. Wienands J, Larbolette O, Reth M. Evidence for a preformed transducer complex organized by the B cell antigen receptor. *Proc Natl Acad Sci U S A* (1996) 93(15):7865–70. doi:10.1073/pnas.93.15.7865
45. Ramsey LB, Vegoe AL, Miller AT, Cooke MP, Farrar MA. Tonic BCR signaling represses receptor editing via Raf- and calcium-dependent signaling pathways. *Immunol Lett* (2011) 135(1–2):74–7. doi:10.1016/j.imlet.2010.09.018
46. Yasuda T, Kometani K, Takahashi N, Imai Y, Aiba Y, Kurosaki T. ERKs induce expression of the transcriptional repressor Blimp-1 and subsequent plasma cell differentiation. *Sci Signal* (2011) 4(169):ra25. doi:10.1126/scisignal.2001592
47. Rui L, Healy JI, Blasioli J, Goodnow CC. ERK signaling is a molecular switch integrating opposing inputs from B cell receptor and T cell cytokines to control TLR4-driven plasma cell differentiation. *J Immunol* (2006) 177(8):5337–46. doi:10.4049/jimmunol.177.8.5337
48. Kisselgof AB, Oettgen HC. The expression of murine B cell CD23, in vivo, is regulated by its ligand, IgE. *Int Immunol* (1998) 10(9):1377–84. doi:10.1093/intimm/10.9.1377
49. Rui L, Vinuela CG, Blasioli J, Goodnow CC. Resistance to CpG DNA-induced autoimmunity through tolerogenic B cell antigen receptor ERK signaling. *Nat Immunol* (2003) 4(6):594–600. doi:10.1038/ni924
50. Yasuda T, Sanjo H, Pages G, Kawano Y, Karasuyama H, Pouyssegur J, et al. Erk kinases link pre-B cell receptor signaling to transcriptional events required for early B cell expansion. *Immunity* (2008) 28(4):499–508. doi:10.1016/j.immuni.2008.02.015
51. Limnander A, Depeille P, Freedman TS, Liou J, Leitges M, Kurosaki T, et al. STIM1, PKC-delta and RasGRP set a threshold for proapoptotic Erk signaling during B cell development. *Nat Immunol* (2011) 12(5):425–33. doi:10.1038/ni.2016
52. Novak R, Jacob E, Haimovich J, Avni O, Melamed D. The MAPK/ERK and PI3K pathways additively coordinate the transcription of recombination-activating genes in B lineage cells. *J Immunol* (2010) 185(6):3239–47. doi:10.4049/jimmunol.1001430
53. Holl TM, Haynes BF, Kelsoe G. Stromal cell independent B cell development in vitro: generation and recovery of autoreactive clones. *J Immunol Methods* (2010) 354(1–2):53–67. doi:10.1016/j.jim.2010.01.007
54. Craxton A, Draves KE, Gruppi A, Clark EA. BAFF regulates B cell survival by downregulating the BH3-only family member Bim via the ERK pathway. *J Exp Med* (2005) 202(10):1363–74. doi:10.1084/jem.20051283
55. Otipoby KL, Sasaki Y, Schmidt-Supplien M, Patke A, Gareus R, Pasparakis M, et al. BAFF activates Akt and Erk through BAFF-R in an IKK1-dependent manner in primary mouse B cells. *Proc Natl Acad Sci U S A* (2008) 105(34):12435–8. doi:10.1073/pnas.0805460105
56. Pillai S, Cariappa A. The follicular versus marginal zone B lymphocyte cell fate decision. *Nat Rev Immunol* (2009) 9(11):767–77. doi:10.1038/nri2656
57. Payet ME, Woodward EC, Conrad DH. Humoral response suppression observed with CD23 transgenics. *J Immunol* (1999) 163(1):217–23.
58. Matsuo K, Taya C, Kubo S, Toyama-Sorimachi N, Kitamura F, Ra C, et al. Establishment of antigen-specific IgE transgenic mice to study pathological and immunobiological roles of IgE in vivo. *Int Immunol* (1999) 11(6):987–94. doi:10.1093/intimm/11.6.987

**Conflict of Interest Statement:** The authors declare that the research was conducted in the absence of any commercial or financial relationships that could be construed as a potential conflict of interest.

Copyright © 2018 Greaves, Peterson, Torres and Pelanda. This is an open-access article distributed under the terms of the Creative Commons Attribution License (CC BY). The use, distribution or reproduction in other forums is permitted, provided the original author(s) and the copyright owner are credited and that the original publication in this journal is cited, in accordance with accepted academic practice. No use, distribution or reproduction is permitted which does not comply with these terms.



# Corrigendum: Activation of the MEK-ERK Pathway Is Necessary but Not Sufficient for Breaking Central B Cell Tolerance

Sarah A. Greaves<sup>1</sup>, Jacob N. Peterson<sup>1</sup>, Raul M. Torres<sup>1,2</sup> and Roberta Pelanda<sup>1,2\*</sup>

<sup>1</sup> Department of Immunology and Microbiology, University of Colorado School of Medicine, Aurora, CO, United States,

<sup>2</sup> Department of Biomedical Research, National Jewish Health, Denver, CO, United States

**Keywords:** B cells, B cell tolerance, BCR signaling, MAP kinase, ERK, B cell development, autoreactive B cells, mouse models

## OPEN ACCESS

### Approved by:

Frontiers in Immunology Editorial Office,  
Frontiers Media SA, Switzerland

### \*Correspondence:

Roberta Pelanda  
roberta.pelanda@ucdenver.edu

### Specialty section:

This article was submitted to  
B Cell Biology,  
a section of the journal  
*Frontiers in Immunology*

**Received:** 15 August 2018

**Accepted:** 06 September 2018

**Published:** 27 September 2018

### Citation:

Greaves SA, Peterson JN, Torres RM and Pelanda R (2018) Corrigendum:  
Activation of the MEK-ERK Pathway Is  
Necessary but Not Sufficient for  
Breaking Central B Cell Tolerance.  
*Front. Immunol.* 9:2218.  
doi: 10.3389/fimmu.2018.02218

## A Corrigendum on

### Activation of the MEK-ERK Pathway Is Necessary but Not Sufficient for Breaking Central B Cell Tolerance

by Greaves SA, Peterson JN, Torres RM, Pelanda R. *Front. Immunol.* (2018) 9:707.  
doi: 10.3389/fimmu.2018.00707

In the original article, a mistake was found in affiliation 1. The state should be CO (Colorado) instead of IL (Illinois). The authors apologize for this error and state that this does not change the scientific conclusions of the article in any way.

The original article has been updated.

**Conflict of Interest Statement:** The authors declare that the research was conducted in the absence of any commercial or financial relationships that could be construed as a potential conflict of interest.

Copyright © 2018 Greaves, Peterson, Torres and Pelanda. This is an open-access article distributed under the terms of the Creative Commons Attribution License (CC BY). The use, distribution or reproduction in other forums is permitted, provided the original author(s) and the copyright owner(s) are credited and that the original publication in this journal is cited, in accordance with accepted academic practice. No use, distribution or reproduction is permitted which does not comply with these terms.



# The Transcriptional Regulation of Germinal Center Formation

Shuang Song<sup>1,2</sup> and Patrick D. Matthias<sup>1,2\*</sup>

<sup>1</sup> Friedrich Miescher Institute for Biomedical Research, Basel, Switzerland, <sup>2</sup> Faculty of Sciences, University of Basel, Basel, Switzerland

Germinal centers (GCs) are essential structures of the humoral immune response, which form in the periphery in response to T cell dependent antigens. During the GC reaction, B cells undergo critical differentiation steps, which ultimately lead to the generation of antibodies with altered effector function and higher affinity for the selected antigen. Remarkably, many of the B cell tumors have their origin in the GCs; thus, understanding how the formation of these structures is regulated or deregulated is of high medical importance. This review gives an overview of the transcription factors that have been linked to the generation of GCs, and of their roles in the process.

**Keywords:** hematopoiesis, transcription factors, B cell development, germinal center (GCs), transcriptional regulation, germinal center development, germinal center maintenance, plasma cell and memory B cell differentiation

## OPEN ACCESS

### Edited by:

Rhodri Ceredig,  
National University of Ireland Galway,  
Ireland

### Reviewed by:

Antony Basten,  
Garvan Institute of Medical Research,  
Australia

Kai-Michael Toellner,  
University of Birmingham,  
United Kingdom

### \*Correspondence:

Patrick D. Matthias  
patrick.matthias@fmi.ch

### Specialty section:

This article was submitted to  
B Cell Biology,  
a section of the journal  
*Frontiers in Immunology*

**Received:** 30 June 2018

**Accepted:** 16 August 2018

**Published:** 05 September 2018

### Citation:

Song S and Matthias PD (2018) The  
Transcriptional Regulation of Germinal  
Center Formation.  
*Front. Immunol.* 9:2026.  
doi: 10.3389/fimmu.2018.02026

## BACKGROUND TO B CELL DEVELOPMENT

B (and T) cells represent a unique model of cellular development, in which cells of multiple differentiation stages can be identified based on surface markers and readily isolated. Owing to these advantages, the lymphoid system has been used widely, beyond immunology, as a developmental paradigm in which the role of transcription factors (TFs) or signaling molecules can be tested experimentally. Several excellent reviews exist that describe in detail how B lymphocytes develop, what regulatory circuits are critical, or the details of GC development (1–11). We will therefore not discuss these aspects in detail, but will only give a high-level overview, and then focus this review on the transcriptional control of GCs formation.

B cells originate and develop in the bone marrow from hematopoietic stem cells (HSCs) that differentiate into progenitor stages of increasingly restricted potential. Once committed to the B lineage, B cell progenitors go through several successive stages, at which key events of their developmental fate take place. In particular, the PreB stage represents the phase during which immunoglobulin (Ig) genes, which code for the antibody molecules, rearrange their DNA segments in order to produce functional genes. The heavy chain rearranges first at the ProB stage, followed by the light chain at the small PreB-II stage. Immature B cells then express IgM at their surface and exit the bone marrow to enter the circulation and move to peripheral lymphoid organs such as the spleen or the lymph nodes. There, marginal zone (MZ) B cells play vital functions in T cell-independent humoral immune responses against blood-borne pathogens, follicular B cells can capture antigen presented by Follicular Dendritic Cells (FDCs) and present it to CD4<sup>+</sup> follicular T helper cells (T<sub>FH</sub>) that are located around the B cell zone of the developing GC. This is the time during which critical signals, sent by the T<sub>FH</sub> cells, induce isotype switching (so-called class switching, which exchanges IgM for IgG) and expansion of B cell clones starts. These B cells are called centroblasts and form the dark zone (DZ) of the GC. After several rounds of proliferation, somatic hypermutation begins, a process by which the Ig DNA becomes mutated under the

action of activation-induced cytidine deaminase (AID), leading to the generation of diverse clones expressing antibodies with different, potentially higher, affinity for antigen. From there, the B cells (centroblasts) move to the adjacent region called the light zone (LZ), where they express their antibody on the cell surface. GC B cells in the light zone are called centrocytes and are in a near apoptotic state. It is there that selection for the quality (affinity) of the antibody takes place: based on the affinity of the antibody for the antigen, the B cell can be eliminated or rescued and sent back to the dark zone as centroblast for an additional round of mutations, followed by renewed entry into the light zone and further antibody affinity testing. At some point in this dark zone–light zone selection cycle, the B cell expresses a high affinity antibody and can now exit the GC as a plasma cell that secretes high amounts of the antibody, or as a memory B cell that is ready to be reactivated upon future encounter with the antigen.

The rest of this review will put the emphasis on the transcriptional control of the formation and function of GCs, and highlight in particular TFs that are essential.

## TRANSCRIPTION FACTORS REGULATING GC FORMATION

### GC Initiation

Initiation of the GC reaction involves activation of the B cell receptor (BCR) by antigen engagement, followed by interaction of these B cells with antigen presenting cells and T<sub>FH</sub> cells, which provide further activation signals (2, 3). **Figure 1** summarizes the molecular networks regulating initiation and function of the germinal centers reaction.

Transcription factors that are downstream of the BCR, such as the transcription coactivator OBF1 (a.k.a. OCA-B, or Bob1), a B cell-specific coactivator for the octamer transcription factors OCT1 and OCT2, are critical for GC formation (15–18). Mice deficient in *Pou2f2* (encoding OCT2), *Pou2af1* (encoding OBF1) or both showed complete lack of GCs (19). The underlying molecular mechanism is not clear yet, and the target genes of OBF1/OCT2 in the context of the germinal center reaction are largely unknown, although Spi-B which itself is required for GCs (20, 21) has been identified as a downstream target of OBF1 (22). Moreover, in CD4<sup>+</sup> T cells OBF1 and OCT1/OCT2 directly bind to the promoter region of *Bcl6* and activate its transcription, thereby promoting the development of T<sub>FH</sub> cells (23). The putative role of these factors in regulating *Bcl6* expression in early GC B cells remains to be investigated.

BCL6 is a zinc finger TF that is essential for germinal center formation, as *Bcl6*-null mice completely lack GCs and affinity maturation (3, 24). During the early phase of the GC response, antigen stimulated B cells rely on T<sub>FH</sub> cells for differentiation into GC B cells, and interaction between T<sub>FH</sub> and B cells leads to the upregulation of BCL6 (25). Moreover, the upregulation of BCL6 leads to stabilized conjugation between B and T<sub>FH</sub> cells, creating a positive feedback loop that enhances the GC formation program (3, 25). Failure in BCL6 upregulation prevents B cells from entering GC clusters and impairs the upregulation of CXCR4, a

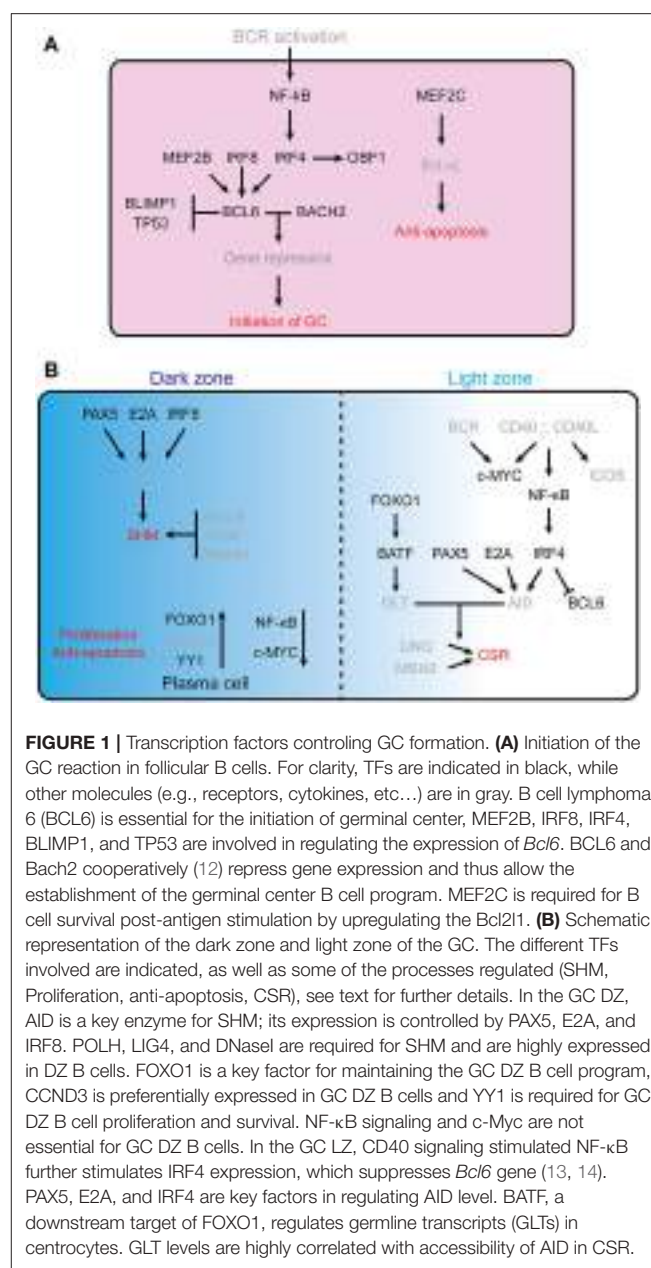


**FIGURE 1 |** Transcription factors controlling GC formation. **(A)** Initiation of the GC reaction in follicular B cells. For clarity, TFs are indicated in black, while other molecules (e.g., receptors, cytokines, etc...) are in gray. B cell lymphoma 6 (BCL6) is essential for the initiation of germinal center, MEF2B, IRF8, IRF4, BLIMP1, and TP53 are involved in regulating the expression of *Bcl6*. BCL6 and Bach2 cooperatively (12) repress gene expression and thus allow the establishment of the germinal center B cell program. MEF2C is required for B cell survival post-antigen stimulation by upregulating the *Bcl211*. **(B)** Schematic representation of the dark zone and light zone of the GC. The different TFs involved are indicated, as well as some of the processes regulated (SHM, Proliferation, anti-apoptosis, CSR), see text for further details. In the GC DZ, AID is a key enzyme for SHM; its expression is controlled by PAX5, E2A, and IRF8. POLH, LIG4, and DNasel are required for SHM and are highly expressed in DZ B cells. FOXO1 is a key factor for maintaining the GC DZ B cell program, CCND3 is preferentially expressed in GC DZ B cells and YY1 is required for GC DZ B cell proliferation and survival. NF-κB signaling and c-Myc are not essential for GC DZ B cells. In the GC LZ, CD40 signaling stimulated NF-κB further stimulates IRF4 expression, which suppresses *Bcl6* gene (13, 14). PAX5, E2A, and IRF4 are key factors in regulating AID level. BATF, a downstream target of FOXO1, regulates germline transcripts (GLTs) in centrocytes. GLT levels are highly correlated with accessibility of AID in CSR.

chemokine receptor expressed on germinal center DZ B cells that is critical for the maintenance of GC structural integrity (25).

IRF4 is required at the early stage of GC formation. In transplantation experiments, *Irf4*<sup>−/−</sup> B cells fail to differentiate into GC B cells (26). Conditional knockout of *Irf4* by CD19cre which deletes from early B cells onwards leads to impaired GC formation (26). In contrast, once GCs have formed or initiated, IRF4 is no longer needed, as conditional knockout by Cγ1cre which deletes in already formed GC cells has minimal effects on GC differentiation (27). These results suggest that IRF4 is required for the very early phase upon T-cell-dependent antigen stimulation. Additional evidence supporting this idea is the rapid upregulation of IRF4 following BCR stimulation (28). Moreover, IRF4 is involved in modulating the expression of BCL6 and

OBF1, which both are key factors for GC initiation (3, 26). Taken together, IRF4 plays an important role in the early initiation phase of GC formation, possibly by regulating the induction of *Bcl6* and *Pou2af1*.

IRF8 was reported to upregulate BCL6 and AID levels in GC B cells (29, 30), and it was shown to promote GC B cells survival by regulating the expression level of MDM2 (31). However, deletion of IRF8 in B cells did not affect GC formation (32). Moreover, IRF8 is involved in the regulation of the BCL6-related transcriptional program in GC cells by directly interacting with BCOR (B cell lymphoma 6 corepressor) and BCL6. In transactivation assays, IRF8 augments the transcription repressive activity of BCL6 (33).

MEF2C is required for the proliferation and survival of B cells upon antigen receptor stimulation by upregulating the expression level of *Bcl2l1* (encoding the Bcl-xL protein) and several cell cycle related genes (34). Specific deletion of *Mef2c* in B cells leads to reduced proliferation and increased cell apoptosis upon anti-IgM stimulation. However, the responses are normal in the case of LPS, CD40, IL4, BAFF and RP105 stimulations. By histological examination, reduced number of GC follicles are observed in the spleens of *Mef2C<sup>f/f</sup>*-CD19cre mice immunized with sheep red blood cells (SRBC) (34). MEF2B, another member of the MEF2 family, has been found to be mutated in ca. 11% of diffuse large B cell lymphoma (DLBCL), which are GC-derived tumors (35). MEF2B directly activates *Bcl6* transcription by binding to the regulatory region 1 kb upstream of the *Bcl6* gene transcription start site (35). Mutation of the MEF2B binding motif in the *Bcl6* gene promoter abrogates *Bcl6* transcription activity in cotransfection assays in 293T cells. Furthermore, knockdown of MEF2B protein by shRNAs leads to downregulation of BCL6 and upregulation of BCL6 target genes. These data suggest that MEF2B plays an important role in early GC formation by modulating *Bcl6* expression (35, 36).

BATF is a transcription factor of the AP-1 family, which is involved in GC structure establishment and class switch recombination. *Batf<sup>-/-</sup>* mice failed to develop normal GC structures when immunized with SRBC, as characterized by a lack of CD95 or GL7 positive B cells (37). *Batf*-null T<sub>FH</sub> cells lack expression of the chemokine receptor CXCR5, which is essential for GC structure integrity. Additionally, the expression of *Bcl6* and *c-Maf*, both of which are important factors for T<sub>FH</sub> cells development, is downregulated in absence of BATF (37).

c-MYC is another TF indispensable during the early phase of germinal center formation. Its expression is induced already 1–2 days after immunization (38) and it is required for GC maintenance, as conditional deletion of *c-Myc* by Cγ1cre leads to impaired GCs (39).

## GC Development

The dark zone and the light zone of the GC are organized by the expression of the chemokine receptors CXCR4 and CXCR5, respectively (40). Thus, one can expect that TFs critical for CXCR4 and CXCR5 expression will be important for GCs.

## GC Dark Zone

The germinal center DZ is characterized by an interconnected network of CXCL12 expressing reticular cells and compactly filled with rapidly proliferating centroblasts (41).

FOXO1 is highly expressed in human and mouse GC B cells, and its expression is largely specific to DZ B cells (with also some expression in naïve B cells) (42). Like in *Cxcr4<sup>-/-</sup>* mice, GCs from *Foxo1<sup>f/f</sup>*-Cγ1cre mice completely lack a DZ structure, while the differentiation of plasma cells is normal (42, 43). *Foxo1*-null GCs lack proper structural polarization and show an even distribution of the FDC network (42). FOXO1, together with BCL6, represses the expression of B lymphocyte induced maturation protein 1 (BLIMP1), a key factor promoting differentiation of GC B cells into plasma cells, which is encoded by the *Prdm1* gene. By binding to the *Prdm1* promoter region, FOXO1 and BCL6 maintain the germinal center DZ program (42).

*Bcl6*-null GC precursor B cells fail to upregulate the expression of CXCR4 (25), which is a crucial chemokine receptor for GC DZ B cells. c-MYC is required throughout the early and late initiation phases of GC formation, but is not expressed in the proliferating DZ B cells (3), where it is repressed by BCL6 (38).

YY1 is required for GC B cell proliferation and GC development at least partly by modulating cell apoptosis (44). Deletion of *Yy1* specifically in GC B cells leads to a significant decrease in the number of DZ B cells, and elevated cell apoptosis (44).

## Somatic hypermutation (SHM)

SHM generates a wide repertoire of affinities toward specific antigens, and mainly takes place in the DZ (45), although some extrafollicular SHM has been reported in transgenic mice deficient in the ability to establish GCs (46). AID, encoded by the *Aicda* gene, is the enzyme responsible for SHM and class switch recombination (47, 48). AID deaminates cytidines in DNA (49–54), followed by error-prone repair involving different DNA repair factors and ultimately leading to the introduction of somatic mutations (55). Thus, transcription factors which affect the expression of *Aicda* and DNA-damage tolerance related genes should be important for SHM. E proteins (56), PAX5 (57) and IRF8 (29) have been associated with positive regulation of *Aicda* transcription.

FOXO1 is involved in SHM by affecting the protein level of AID: *Foxo1*-null GC B cells show reduced level of AID enzyme, while mRNA level of *Aicda* is unchanged. Therefore, *Foxo1*-null GC B cells carry lower level of mutations in Ig locus than control cells (58).

*Irf8* mRNA level peaks in centroblasts, and IRF8 regulates SHM by modulating the expression of *Aicda* and *Bcl6*: knockdown of IRF8 by siRNA leads to decreased transcription of *Aicda* and *Bcl6* (29). By ChIP, IRF8 binds to the promoter regions of *Aicda* and *Bcl6* in both human and mouse B cells. Furthermore, luciferase assays showed that IRF8 directly regulates the transcription of *Aicda* and *Bcl6* in HeLa cells cotransfected with an IRF8 expression vector and a reporter containing promoter regions of *Aicda* or *Bcl6* (29). Moreover,

IRF8 promotes GC B cells survival by regulating the expression level of MDM2 in the case of DNA damage (31).

*Aicda* expression is significantly reduced in activated B cells in which the helix-loop-helix factor ID3 is ectopically expressed. The possible mechanism is that ID3 inhibits the DNA-binding activity of E-proteins which activate the expression of *Aicda* (56, 59).

### Light Zone

Three crucial B-cell developmental processes take place in the GC light zone: (i) selection of B cells that produce high-affinity antibodies, (ii) CSR, and (iii) initiation of centrocytes differentiation into plasma cells or memory B cells (9).

After rapid expansion in the DZ, B cells migrate to the LZ where those carrying high affinity B cell receptor genes are selected. The BCR pathway plays a fundamental role in this process: BCR signaling leads to phosphorylated AKT, and activated AKT further phosphorylates FOXO1 which then relocates from the nucleus to the cytoplasm (60). CD40 stimulation leads to NF-κB-mediated upregulation of IRF4 (13), which in turn represses *Bcl6* transcription (61). Together, these coordinated actions terminate the dark zone-associated transcriptional programme and allow establishment of the LZ transcriptome (13).

c-MYC is absent in most GC B cells, however, its expression is induced in high affinity BCR presenting GC B cells when receiving help from T<sub>FH</sub> cells, in a process that requires both BCR and CD40 signaling (60). In addition to the requirement of c-MYC activity during the initial stage of GC formation, c-MYC is needed for GC maintenance in the late GC response (38). With the help from T<sub>FH</sub> cells, c-MYC is transiently induced and upregulated in a small fraction of high affinity BCR expressing GC B cells within the LZ compartment. The Omomyc protein inhibits c-MYC function by antagonizing its DNA binding activity (62). Specific inhibition of c-MYC function by Doxycyclin-induced Omomyc expression in late GC B cells (10 days post-immunization by SRBC) leads to reduced GC size, indicating that c-MYC is required for GC maintenance once GCs are established (38).

### Affinity maturation

FOXO1 is necessary for effective antibody affinity maturation: SHM frequency is comparable between WT and *Foxo1*-null GC B cells, but a severely decreased number of GC B cells harboring high affinity antibodies is observed in *Foxo1*-null GCs (42). Furthermore, *Foxo1*-null GC B cells have a lower level of cell surface BCR and are ineffective in activating T<sub>FH</sub> cells in the LZ; this leads to lower stimulation of T<sub>FH</sub> cells in the GC microenvironment and reduced production of IL-21, a cytokine that is vital for antibody affinity maturation (58). Thus, FOXO1 regulates antibody affinity maturation through both antigen presentation and T<sub>FH</sub> cell activation (42, 58).

c-MYC is transiently induced in LZ B cells after receiving help from T<sub>FH</sub> cells (38); selected GC B cells with induced c-MYC present high affinity BCR on the cell surface, and subsequently migrate into the DZ for the next iteration of proliferation and SHM (38, 39). However, in *Foxo1*-null GC B cells, the expression

level of c-MYC is downregulated even under the help from T<sub>FH</sub> cells. BATF, which controls the expression of *Aicda*, is another TF downregulated in the absence of *Foxo1* (58).

### Class Switch Recombination

Like SHM, CSR also requires the expression of *Aicda* (47, 48). However, CSR depends on a different domain of the AID protein (63, 64). It is worthwhile mentioning that CSR already takes place before the GCs are formed, following B cell activation (65, 66). Much of the knowledge about CSR and the required factors originates from *in vitro* B cell activation experiments.

IRF4 was shown to regulate CSR in CD40 and IL4 stimulated B cells (27, 67). In the absence of IRF4, the *Aicda* expression level is decreased (67), and CSR is impaired (67). However, the expression of other genes important for CSR, such as Ung or Msh2 remains normal in *Irf4*<sup>-/-</sup> B cells. Therefore, the CSR defects in *Irf4*-null B cells seem to mainly reflect the impaired *Aicda* expression (67).

FOXO1 deficiency results in impaired class-switching: the compartment of *Igg1*-switched B cells in *Foxo1*-null GCs is heavily reduced, with accumulation of IgM<sup>+</sup> GC B cells. Yet, the expression level of *Aicda* is similar between WT and *Foxo1*<sup>fl/fl</sup>-Cylcre GC B cells (42). In addition, *Foxo1*-null GC B cells display significantly lower expression of germline transcripts (GLTs) across the Ig locus. GLTs coincide with open chromatin and allow the exposure of switch regions to AID, which in turn induces single-strand DNA breaks through which class switch recombination is accomplished (68, 69). Thus, lower levels of GLTs correlate with reduced accessibility of AID toward the class switch regions. At the molecular level, FOXO1 possibly modulates GLT and post-switch transcripts by binding to I-mu, the 3' IgH enhancer and a super-enhancer (70) in the Ig locus. Moreover, the transcription factor BATF, which is necessary for the expression of Ig GLTs and subsequent CSR (37), is downregulated upon FOXO1 depletion (42).

PAX5 binds to the promoter region of *Aicda* and activates its expression. Overexpression of PAX5 in a ProB cell line induces the expression *Aicda*, while ID2 has an antagonizing effect on this induction. Moreover, PAX5, E2A, and AID directly interact with each other and form a complex, which contributes to directing AID to the *Igh* locus for CSR (71). In addition, ID2 and ID3 negatively regulate CSR by repressing *Aicda* expression (56, 57).

BATF directly controls the expression of *Aicda*. By ChIP-seq and EMSA, BATF was shown to bind to the regulatory region of *Aicda*. In line with this, the expression level of *Aicda* is downregulated in *Batf*<sup>-/-</sup> mice (37). Consequently, production of isotype switched antibodies is almost completely missing, although IgM production upon T-cell-dependent or -independent antigen stimulation is still normal in *Batf*<sup>-/-</sup> mice (37). Moreover, *Batf*<sup>-/-</sup> mice display a reduction in GLTs from different isotypes, except those from μ-chain. Germline transcription initiated by switch region (I) region promoters, located upstream of the different constant heavy chain exons, is required for AID targeting and successful CSR (8, 54). Taken together, BATF regulates CSR by modulating the expression of *Aicda* and GLTs from the Ig locus.

## TFs Controlling the Migration of Cells Between Dark and Light Zone

The LZ-to-DZ transition is mainly driven by high affinity antibody presentation on the surface of GC B cells and the subsequent help from T<sub>FH</sub> cells toward high affinity antibody LZ cells (58, 72–74).

*Foxo1*-null GC B cells showed reduced level of surface BCR and Igβ when compared to WT cells (58). Therefore, reduced antigen presentation on *Foxo1*<sup>−/−</sup> GC LZ B cells fails to effectively activate T<sub>FH</sub> cells, resulting in lower number of T<sub>FH</sub> cells and decreased production of IL-21, an important cytokine for GC B cell differentiation and affinity maturation promoted by T<sub>FH</sub> cells (75, 76). Moreover, *Foxo1*-null GC LZ B cells express less IL21R, further abrogating the ability to receive help from T<sub>FH</sub> cells (BCR and CD40 signal). Therefore, the LZ-to-DZ migration of selected cells is impaired in the absence of *Foxo1* (58) and *Foxo1*-null GC B cells are trapped in the LZ compartment. Furthermore, *Foxo1*-null GC B cells showed lower proliferation rate in the LZ compartment, in spite of harboring a high affinity BCR, indicating defects in cyclic reentry mediated by help from T<sub>FH</sub> cells which is coupled with the LZ-to-DZ migration (58).

Interaction between high affinity BCR expressing LZ B cells and T<sub>FH</sub> cells leads to activation of c-MYC expression (60), which promotes cyclic reentry and LZ-to-DZ migration (58).

## Differentiation: Memory/Plasma Cell Fate Decision

**Figure 2** summarizes the molecular networks involved in plasma cell and memory B cell differentiation.

Transient and low expression of *Irf4* leads to the expression of *Bcl6* and *Pou2af1* during the early phase of GC formation, while sustained and high level expression of *Irf4* is required for plasma cell differentiation (26). *Irf4* expression is induced to a high level in the fraction of LZ B cells which present high affinity antibodies (26, 28). BLIMP1 is a transcriptional repressor that is essential for plasma cell development: *Prdm1*-deficient mice cannot produce plasma cells and overexpression of BLIMP1 is sufficient to induce plasmablast differentiation (77, 78). *Prdm1* is a downstream target of IRF4, and BLIMP1 can further increase the level of IRF4, thus reinforcing the plasma cell differentiation program in a feed forward loop (26, 79). Moreover, BLIMP1 represses the expression of *Aicda* (79) and *Abf1* (80).

BLIMP1, together with IRF4, acts upstream of X-box binding protein 1 (XBPI), a transcription factor that is essential for upregulation of the secretory apparatus required for antibody production in plasma cells (27, 81, 82). PAX5 represses XBPI and thus prevents plasma cell differentiation (83). Conversely, downregulation of *Pax5* by BLIMP1 is a necessary step for induction of *Xbp-1* and activation of the plasma cell program (81, 84). However, in the absence of IRF4, BLIMP1 alone is not sufficient for plasma cell differentiation. Moreover, BLIMP1 is required for post-transcriptional regulation of XBPI mRNA, by which the active form XBPI protein is generated (85). XBPI directly regulates *Pou2af1* expression in plasma cells (86), which might be important for IgG production, since OBF1 and OCT2 are required for normal IgG expression (87). *Irf4*-deficient

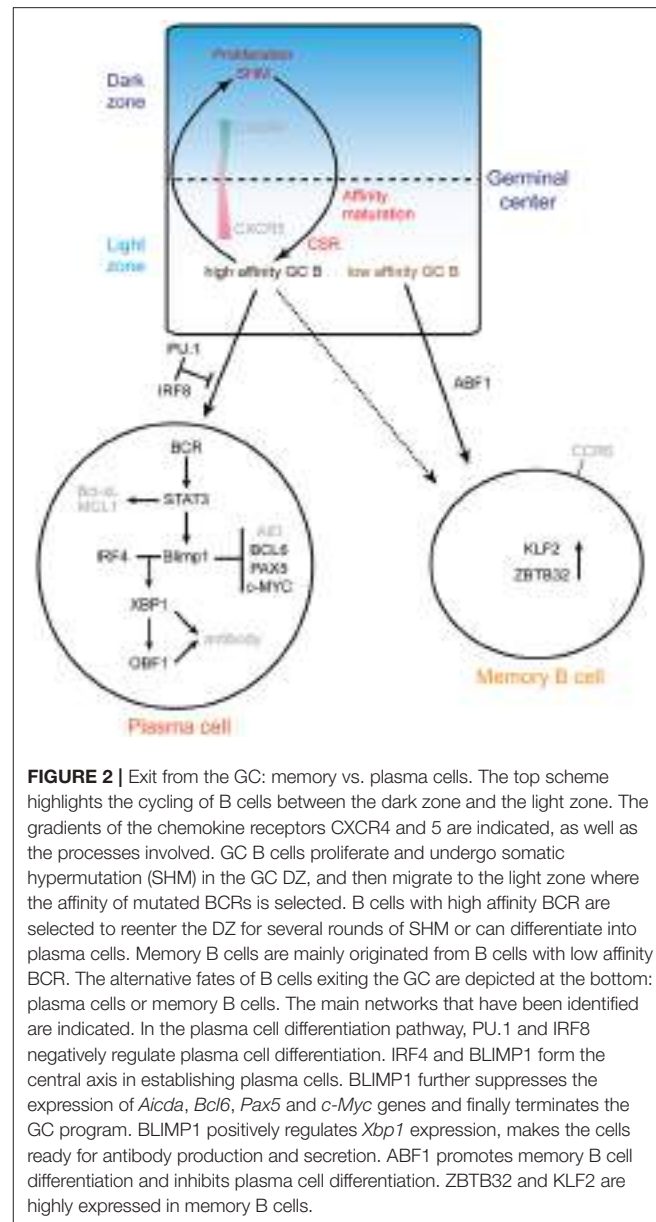


**FIGURE 2 |** Exit from the GC: memory vs. plasma cells. The top scheme highlights the cycling of B cells between the dark zone and the light zone. The gradients of the chemokine receptors CXCR4 and 5 are indicated, as well as the processes involved. GC B cells proliferate and undergo somatic hypermutation (SHM) in the GC DZ, and then migrate to the light zone where the affinity of mutated BCRs is selected. B cells with high affinity BCR are selected to reenter the DZ for several rounds of SHM or can differentiate into plasma cells. Memory B cells are mainly originated from B cells with low affinity BCR. The alternative fates of B cells exiting the GC are depicted at the bottom: plasma cells or memory B cells. The main networks that have been identified are indicated. In the plasma cell differentiation pathway, PU.1 and IRF8 negatively regulate plasma cell differentiation. IRF4 and BLIMP1 form the central axis in establishing plasma cells. BLIMP1 further suppresses the expression of *Aicda*, *Bcl6*, *Pax5* and *c-Myc* genes and finally terminates the GC program. BLIMP1 positively regulates *Xbp1* expression, makes the cells ready for antibody production and secretion. ABF1 promotes memory B cell differentiation and inhibits plasma cell differentiation. ZBTB32 and KLF2 are highly expressed in memory B cells.

(Cγ1cre) mice completely lack CD138<sup>+</sup> (aka Syndecan1<sup>hi</sup>) plasma cells in spleen, peripheral blood and bone marrow (27). In addition to the important yet mechanistically unclear role of OBF1 in the early development of GC formation, this factor is required for antibody production (both unswitched and switched isotypes) in T-dependent antigen stimulation and normal antibody secreting cell differentiation, as the number of antibody-secreting Syndecan1<sup>hi</sup> cells is dramatically reduced in absence of OBF1 (88). Moreover, OBF1 is required for the induction of *Prdm1* (88). Taken together, IRF4 and BLIMP1 function together to drive the transition from GC B cells to plasma cells by repressing the GC program and enhancing the plasma cell differentiation program.

In contrast, IRF8 together with PU.1 inhibit the GC B cell differentiation toward plasma cells, suggesting that the balance

between IRF4 and IRF8 may be critical for the fate of B cells at this developmental transition (89). In addition, STAT3 regulates the differentiation of plasma cells possibly by promoting cell survival through activating the expression of pro-survival genes such as *Bcl2l1* and *Mcl1* (90, 91).

It is not resolved yet which transcription factor(s) play a major role in regulating the differentiation of memory B cells (92); however, recent evidence suggests that memory B cells originate from the low affinity compartment of the LZ (92, 93). Comparison of the transcriptome profiles from high- and low-affinity BCR expressing GC B cells in the LZ compartment showed that genes involved in DZ maintenance and cyclic reentry are downregulated in low-affinity fractions (with switched isotype), where *Bach2* and *Pax5* are upregulated (93). As indicated above, upregulation of these transcription factors blocks plasma cell differentiation (94–96).

*BACH2* regulates LZ B cells to commit to the memory B cell differentiation path in a dosage dependent manner, as complete knockout or haploinsufficiency of *Bach2* lead to lower memory B cell differentiation (93). Furthermore, T<sub>FH</sub> cell interaction and affinity maturation in LZ compartment are negatively correlated with *Bach2* expression, thus confirming that memory B cells are generated from low affinity fraction in the LZ compartment (92, 93).

Activated B cell Factor 1 (ABF-1), a helix-loop-helix TF predominantly expressed in memory B cells, blocks the plasma cell differentiation program (80). An inducible ABF-1-ER mouse model demonstrated that induction of ABF-1 promotes GC formation and memory B cell differentiation (80, 97). ZBTB32 and KLF2 are two factors expressed in memory B cells and which inhibit the GC response (98). They have been associated with memory B cells (99), but further mechanistic studies are needed to understand their specific role. BCL6 is a known inhibitor of plasma cell differentiation which directly represses the expression of *Prdm1* (100, 101). STAT5 directly modulates the expression

level of *Bcl6*, which in turn directly represses *Prdm1* expression, and thus promotes memory B cell differentiation.

## OUTLOOK AND OPEN QUESTIONS

A central theme is that often multiple distinct TFs act in concert to promote, or repress, specific steps of GC development. Some factors, such as BCL6 or BLIMP1, are considered to be master regulators for GC or plasma cell development, respectively. Yet, many other factors have been shown to be important (FOXO1, IRF4) or sometimes essential (OBF1, OCT2). In most cases, however, additional mechanistic studies are required to precisely understand how these factors fit in the overall regulatory circuitry. Moreover, it is often not clear how the TFs perform their function in this biological paradigm: which co-activators or co-repressors are involved and what epigenetic regulators are required?

Finally, intensive investigations have been conducted to understand the interaction between high affinity BCR expressing GC B cells and T<sub>FH</sub> cells, yet little is known about how GC B cells are determined by transcriptional regulators to proceed with the LZ-to-DZ migration, or commit to the plasma cell differentiation cascade.

## AUTHOR CONTRIBUTIONS

SS wrote the manuscript and PM corrected the manuscript.

## ACKNOWLEDGMENTS

This work was supported by the Novartis Research Foundation. We thank all lab members and colleagues for useful discussions. This review is dedicated to our friend and colleague Antonius (Ton) Rolink, with whom we have had a very long-standing collaboration; it was always fun.

## REFERENCES

- Matthias P, Rolink AG. Transcriptional networks in developing and mature B cells. *Nat Rev Immunol.* (2005) 5:497–508. doi: 10.1038/nri1633
- Victora GD, Nussenzweig MC. Germinal centers. *Annu Rev Immunol.* (2012) 30:429–57. doi: 10.1146/annurev-immunol-020711-075032
- De Silva NS, Klein U. Dynamics of B cells in germinal centres. *Nat Rev Immunol.* (2015) 15:137–48. doi: 10.1038/nri3804
- Mesin L, Ersching J, Victora GD. Germinal center B Cell Dynamics. *Immunity* (2016) 45:471–82. doi: 10.1016/j.immuni.2016.09.001
- Shapiro-Shelef M, Calame K. Regulation of plasma-cell development. *Nat Rev Immunol.* (2005) 5:230–42. doi: 10.1038/nri1572
- Wagner SD, Neuberger MS. Somatic hypermutation of immunoglobulin genes. *Annu Rev Immunol.* (1996) 14:441–57. doi: 10.1146/annurev.immunol.14.1.441
- Allen CD, Okada T, Cyster JG. Germinal-center organization and cellular dynamics. *Immunity* (2007) 27:190–202. doi: 10.1016/j.immuni.2007.07.009
- Stavnezer J, Guikema JE, Schrader CE. Mechanism and regulation of class switch recombination. *Annu Rev Immunol.* (2008) 26:261–92. doi: 10.1146/annurev.immunol.26.021607.090248
- Klein U, Dalla-Favera R. Germinal centres: role in B-cell physiology and malignancy. *Nat Rev Immunol.* (2008) 8:22–33. doi: 10.1038/nri2217
- Pillai S, Cariappa A. The follicular versus marginal zone B lymphocyte cell fate decision. *Nat Rev Immunol.* (2009) 9:767–77. doi: 10.1038/nri2656
- Hardy RR, Hayakawa K. B cell development pathways. *Annu Rev Immunol.* (2001) 19:595–621. doi: 10.1146/annurev.immunol.19.1.595
- Huang C, Geng H, Boss I, Wang L, Melnick A. Cooperative transcriptional repression by BCL6 and BACH2 in germinal center B-cell differentiation. *Blood* (2014) 123:1012–20. doi: 10.1182/blood-2013-07-518605
- Saito M, Gao J, Basso K, Kitagawa Y, Smith PM, Bhagat G, et al. A signaling pathway mediating downregulation of BCL6 in germinal center B cells is blocked by BCL6 gene alterations in B cell lymphoma. *Cancer Cell.* (2007) 12:280–92. doi: 10.1016/j.ccr.2007.08.011
- Heise N, De Silva NS, Silva K, Carette A, Simonetti G, Pasparakis M, et al. Germinal center B cell maintenance and differentiation are controlled by distinct NF-κappaB transcription factor subunits. *J Exp Med.* (2014) 211:2103–18. doi: 10.1084/jem.20132613
- Kim U, Qin XF, Gong S, Stevens S, Luo Y, Nussenzweig MC, et al. The B-cell-specific transcription coactivator OCA-B-OBF-1-Bob-1 is essential for normal production of immunoglobulin isotypes. *Nature* (1996) 383:542–7.
- Schubart DB, Rolink A, Kosco-Vilbois MH, Botteri F, Matthias P. B-cell-specific coactivator OBF-1/OCA-B/Bob1 required for immune response and germinal centre formation. *Nature* (1996) 383:538–42. doi: 10.1038/383538a0

17. Luo Y, Roeder RG. Cloning, functional characterization, and mechanism of action of the B-cell-specific transcriptional coactivator OCA-B. *Mol Cell Biol.* (1995) 15:4115–24. doi: 10.1128/MCB.15.8.4115
18. Strubin M, Newell JW, Matthias P. OBF-1, a novel B cell-specific coactivator that stimulates immunoglobulin promoter activity through association with octamer-binding proteins. *Cell* (1995) 80:497–506. doi: 10.1016/0092-8674(95)90500-6
19. Schubart K, Massa S, Schubart D, Corcoran LM, Rolink AG, Matthias P. B cell development and immunoglobulin gene transcription in the absence of Oct-2 and OBF-1. *Nat Immunol.* (2001) 2:69–74. doi: 10.1038/83190
20. Garrett-Sinha LA, Su GH, Rao S, Kabak S, Hao Z, Clark MR, et al. PU.1 and Spi-B are required for normal B cell receptor-mediated signal transduction. *Immunity* (1999) 10:399–408. doi: 10.1016/S1074-7613(00)80040-0
21. Su GH, Chen HM, Muthusamy N, Garrett-Sinha LA, Baunoch D, Tenen DG, et al. Defective B cell receptor-mediated responses in mice lacking the Ets protein, Spi-B. *EMBO J.* (1997) 16:7118–29. doi: 10.1093/emboj/16.23.7118
22. Bartholdy B, Du Rourre C, Bordon A, Emslie D, Corcoran LM, Matthias P. The Ets factor Spi-B is a direct critical target of the coactivator OBF-1. *Proc Natl Acad Sci USA.* (2006) 103:11665–70. doi: 10.1073/pnas.0509430103
23. Stauss D, Brunner C, Berberich-Siebelt F, Hopken UE, Lipp M, Muller G. The transcriptional coactivator Bob1 promotes the development of follicular T helper cells via Bcl6. *EMBO J.* (2016) 35:881–98. doi: 10.1525/embj.201591459
24. Crotty S, Johnston RJ, Schoenberger SP. Effectors and memories: Bcl-6 and Blimp-1 in T and B lymphocyte differentiation. *Nat Immunol.* (2010) 11:114–20. doi: 10.1038/ni.1837
25. Kitano M, Moriyama S, Ando Y, Hikida M, Mori Y, Kurosaki T, et al. Bcl6 protein expression shapes pre-germinal center B cell dynamics and follicular helper T cell heterogeneity. *Immunity* (2011) 34:961–72. doi: 10.1016/j.jimmuni.2011.03.025
26. Ochiai K, Maienschein-Cline M, Simonetti G, Chen J, Rosenthal R, Brink R, et al. Transcriptional regulation of germinal center B and plasma cell fates by dynamical control of IRF4. *Immunity* (2013) 38:918–29. doi: 10.1016/j.jimmuni.2013.04.009
27. Klein U, Casola S, Cattoretti G, Shen Q, Lia M, Mo T, et al. Transcription factor IRF4 controls plasma cell differentiation and class-switch recombination. *Nat Immunol.* (2006) 7:773–82. doi: 10.1038/ni1357
28. Sciammas R, Li Y, Warmflash A, Song Y, Dinner AR, Singh H. An incoherent regulatory network architecture that orchestrates B cell diversification in response to antigen signaling. *Mol Syst Biol.* (2011) 7:495. doi: 10.1038/msb.2011.25
29. Lee CH, Melchers M, Wang H, Torrey TA, Slota R, Qi CF, et al. Regulation of the germinal center gene program by interferon (IFN) regulatory factor 8/IFN consensus sequence-binding protein. *J Exp Med.* (2006) 203:63–72. doi: 10.1084/jem.20051450
30. Qi CF, Li ZY, Raffeld M, Wang HS, Kovalchuk AL, Morse HC. Differential expression of IRF8 in subsets of macrophages and dendritic cells and effects of IRF8 deficiency on splenic B cell and macrophage compartments. *Immunol Res.* (2009) 45:62–74. doi: 10.1007/s12026-008-8032-2
31. Zhou JX, Lee CH, Qi CF, Wang H, Naghashfar Z, Abbasi S, et al. IFN regulatory factor 8 regulates MDM2 in germinal center B cells. *J Immunol.* (2009) 183:3188–94. doi: 10.4049/jimmunol.0803693
32. Feng J, Wang H, Shin DM, Masiuk M, Qi CF, Morse HC III. IFN regulatory factor 8 restricts the size of the marginal zone and follicular B cell pools. *J Immunol.* (2011) 186:1458–66. doi: 10.4049/jimmunol.1001950
33. Yoon J, Feng X, Kim YS, Shin DM, Hatzik K, Wang H, et al. Interferon regulatory factor 8 (IRF8) interacts with the B cell lymphoma 6 (BCL6) corepressor BCOR. *J Biol Chem.* (2014) 289:34250–7. doi: 10.1074/jbc.M114.571182
34. Wilker PR, Kohyama M, Sandau MM, Albring JC, Nakagawa O, Schwarz JJ, et al. Transcription factor Mef2c is required for B cell proliferation and survival after antigen receptor stimulation. *Nat Immunol.* (2008) 9:603–12. doi: 10.1038/ni.1609
35. Ying CY, Dominguez-Sola D, Fabi M, Lorenz IC, Hussein S, Bansal M, et al. MEF2B mutations lead to deregulated expression of the oncogene BCL6 in diffuse large B cell lymphoma. *Nat Immunol.* (2013) 14:1084–92. doi: 10.1038/ni.2688
36. Pon JR, Marra MA. MEF2 transcription factors: developmental regulators and emerging cancer genes. *Oncotarget* (2016) 7:2297–312. doi: 10.18632/oncotarget.6223
37. Ise W, Kohyama M, Schraml BU, Zhang T, Schwer B, Basu U, et al. The transcription factor BATF controls the global regulators of class-switch recombination in both B cells and T cells. *Nat Immunol.* (2011) 12:536–43. doi: 10.1038/ni.2037
38. Dominguez-Sola D, Victora GD, Ying CY, Phan RT, Saito M, Nussenzweig MC, et al. The proto-oncogene MYC is required for selection in the germinal center and cyclic reentry. *Nat Immunol.* (2012) 13:1083–91. doi: 10.1038/ni.2428
39. Calado DP, Sasaki Y, Godinho SA, Pellerin A, Kochert K, Sleckman BP, et al. The cell-cycle regulator c-Myc is essential for the formation and maintenance of germinal centers. *Nat Immunol.* (2012) 13:1092–100. doi: 10.1038/ni.2418
40. Allen CD, Ansel KM, Low C, Lesley R, Tamamura H, Fujii N, et al. Germinal center dark and light zone organization is mediated by CXCR4 and CXCR5. *Nat Immunol.* (2004) 5:943–52. doi: 10.1038/ni1100
41. Bannard O, Horton RM, Allen CD, An J, Nagasawa T, Cyster JG. Germinal center centroblasts transition to a centrocyte phenotype according to a timed program and depend on the dark zone for effective selection. *Immunity* (2013) 39:912–24. doi: 10.1016/j.jimmuni.2013.08.038
42. Dominguez-Sola D, Kung J, Holmes AB, Wells VA, Mo T, Basso K, et al. The FOXO1 transcription factor instructs the germinal center dark zone program. *Immunity* (2015) 43:1064–74. doi: 10.1016/j.jimmuni.2015.10.015
43. Sander S, Chu VT, Yasuda T, Franklin A, Graf R, Calado DP, et al. PI3 Kinase and FOXO1 transcription factor activity differentially control b cells in the germinal center light and dark zones. *Immunity* (2015) 43:1075–86. doi: 10.1016/j.jimmuni.2015.10.021
44. Trabucco SE, Gerstein RM, Zhang H. YY1 Regulates the germinal center reaction by inhibiting apoptosis. *J Immunol.* (2016) 197:1699–707. doi: 10.4049/jimmunol.1600721
45. Oropallo MA, Cerutti A. Germinal center reaction: antigen affinity and presentation explain it all. *Trends Immunol.* (2014) 35:287–9. doi: 10.1016/j.it.2014.06.001
46. Toyama H, Okada S, Hatano M, Takahashi Y, Takeda N, Ichii H, et al. Memory B cells without somatic hypermutation are generated from Bcl6-deficient B cells. *Immunity* (2002) 17:329–39. doi: 10.1016/S1074-7613(02)00387-4
47. Muramatsu M, Kinoshita K, Fagarasan S, Yamada S, Shinkai Y, Honjo T. Class switch recombination and hypermutation require activation-induced cytidine deaminase (AID), a potential RNA editing enzyme. *Cell* (2000) 102:553–63. doi: 10.1016/S0092-8674(00)00078-7
48. Revy P, Muto T, Levy Y, Geissmann F, Plebani A, Sanal O, et al. Activation-induced cytidine deaminase (AID) deficiency causes the autosomal recessive form of the Hyper-IgM syndrome (HIGM2). *Cell* (2000) 102:565–75. doi: 10.1016/S0092-8674(00)00079-9
49. Petersen-Mahrt SK, Harris RS, Neuberger MS. AID mutates E. coli suggesting a DNA deamination mechanism for antibody diversification. *Nature* (2002) 418:99–103. doi: 10.1038/nature00862
50. Bransteitter R, Pham P, Scharff MD, Goodman MF. Activation-induced cytidine deaminase deaminates deoxycytidine on single-stranded DNA but requires the action of RNase. *Proc Natl Acad Sci USA.* (2003) 100:4102–7. doi: 10.1073/pnas.0730835100
51. Chaudhuri J, Tian M, Khuong C, Chua K, Pinaud E, Alt FW. Transcription-targeted DNA deamination by the AID antibody diversification enzyme. *Nature* (2003) 422:726–30. doi: 10.1038/nature01574
52. Di Noia J, Neuberger MS. Altering the pathway of immunoglobulin hypermutation by inhibiting uracil-DNA glycosylase. *Nature* (2002) 419:43–8. doi: 10.1038/nature00981
53. Dickerson SK, Market E, Besmer E, Papavasiliou FN. AID mediates hypermutation by deaminating single stranded DNA. *J Exp Med.* (2003) 197:1291–6. doi: 10.1084/jem.20030481
54. Ramiro AR, Stavropoulos P, Jankovic M, Nussenzweig MC. Transcription enhances AID-mediated cytidine deamination by exposing single-stranded DNA on the nontemplate strand. *Nat Immunol.* (2003) 4:452–6. doi: 10.1038/ni920

55. Chahwan R, Edelmann W, Scharff MD, Roa S. AIDing antibody diversity by error-prone mismatch repair. *Semin Immunol.* (2012) 24:293–300. doi: 10.1016/j.smim.2012.05.005
56. Sayegh CE, Quong MW, Agata Y, Murre C. E-proteins directly regulate expression of activation-induced deaminase in mature B cells. *Nat Immunol.* (2003) 4:586–93. doi: 10.1038/ni923
57. Gonda H, Sugai M, Nambu Y, Katakai T, Agata Y, Mori KJ, et al. The balance between Pax5 and Id2 activities is the key to AID gene expression. *J Exp Med.* (2003) 198:1427–37. doi: 10.1084/jem.20030802
58. Inoue T, Shinnakasu R, Ise W, Kawai C, Egawa T, Kurosaki T. The transcription factor Foxo1 controls germinal center B cell proliferation in response to T cell help. *J Exp Med.* (2017) 214:1181–98. doi: 10.1084/jem.20161263
59. Quong MW, Harris DP, Swain SL, Murre C. E2A activity is induced during B-cell activation to promote immunoglobulin class switch recombination. *EMBO J.* (1999) 18:6307–18. doi: 10.1093/emboj/18.22.6307
60. Luo W, Weisel F, Shlomchik MJ. B cell receptor and CD40 signaling are rewired for synergistic induction of the c-Myc transcription factor in germinal center B cells. *Immunity* (2018) 48:313–26 e5. doi: 10.1016/j.jimmuni.2018.01.008
61. Allman D, Jain A, Dent A, Maile RR, Selvaggi T, Kehry MR, et al. BCL-6 expression during B-cell activation. *Blood* (1996) 87:5257–68.
62. Soucek L, Jucker R, Panacchia L, Ricordy R, Tato F, Nasi S. Omomyc, a potential Myc dominant negative, enhances Myc-induced apoptosis. *Cancer Res.* (2002) 62:3507–10.
63. Barreto V, Reina-San-Martin B, Ramiro AR, McBride KM, Nussenzweig MC. C-terminal deletion of AID uncouples class switch recombination from somatic hypermutation and gene conversion. *Molecular Cell* (2003) 12:501–8. doi: 10.1016/S1097-2765(03)00309-5
64. Ta VT, Nagaoka H, Catalan N, Durandy A, Fischer A, Imai K, et al. AID mutant analyses indicate requirement for class-switch-specific cofactors. *Nat Immunol.* (2003) 4:843–8. doi: 10.1038/ni964
65. Chan TD, Gatto D, Wood K, Camidge T, Basten A, Brink R. Antigen affinity controls rapid T-dependent antibody production by driving the expansion rather than the differentiation or extrafollicular migration of early plasmablasts. *J Immunol.* (2009) 183:3139–49. doi: 10.4049/jimmunol.0901690
66. Zhang Y, Garcia-Ibanez L, Toellner KM. Regulation of germinal center B-cell differentiation. *Immunol Rev.* (2016) 270:8–19. doi: 10.1111/imr.12396
67. Sciammas R, Shaffer AL, Schatz JH, Zhao H, Staudt LM, Singh H. Graded expression of interferon regulatory factor-4 coordinates isotype switching with plasma cell differentiation. *Immunity* (2006) 25:225–36. doi: 10.1016/j.jimmuni.2006.07.009
68. Chaudhuri J, Basu U, Zarrin A, Yan C, Franco S, Perlot T, et al. Evolution of the immunoglobulin heavy chain class switch recombination mechanism. *Adv Immunol.* (2007) 157–214. doi: 10.1016/S0065-2776(06)94006-1
69. Pavri R, Nussenzweig MC. AID targeting in antibody diversity. *Adv Immunol.* (2011) 110:1–26. doi: 10.1016/B978-0-12-387663-8.00005-3
70. Qian J, Wang Q, Dose M, Pruitt N, Kieffer-Kwon KR, Resch W, et al. B cell super-enhancers and regulatory clusters recruit AID tumorigenic activity. *Cell* (2014) 159:1524–37. doi: 10.1016/j.cell.2014.11.013
71. Hauser J, Grundstrom C, Kumar R, Grundstrom T. Regulated localization of an AID complex with E2A, PAX5 and IRF4 at the IgH locus. *Mol Immunol.* (2016) 80:78–90. doi: 10.1016/j.molimm.2016.10.014
72. Allen CD, Okada T, Tang HL, Cyster JG. Imaging of germinal center selection events during affinity maturation. *Science* (2007) 315:528–31. doi: 10.1126/science.1136736
73. Victora GD, Schwickert TA, Fooksman DR, Kamphorst AO, Meyer-Hermann M, Dustin ML, et al. Germinal center dynamics revealed by multiphoton microscopy with a photoactivatable fluorescent reporter. *Cell* (2010) 143:592–605. doi: 10.1016/j.cell.2010.10.032
74. Liu D, Xu H, Shih C, Wan Z, Ma X, Ma W, et al. T-B-cell entanglement and ICOSL-driven feed-forward regulation of germinal centre reaction. *Nature* (2015) 517:214–8. doi: 10.1038/nature13803
75. Linterman MA, Beaton L, Yu D, Ramiscal RR, Srivastava M, Hogan JJ, et al. IL-21 acts directly on B cells to regulate Bcl-6 expression and germinal center responses. *J Exp Med.* (2010) 207:353–63. doi: 10.1084/jem.20091738
76. Zotos D, Coquet JM, Zhang Y, Light A, D'Costa K, Kallies A, et al. IL-21 regulates germinal center B cell differentiation and proliferation through a B cell-intrinsic mechanism. *J Exp Med.* (2010) 207:365–78. doi: 10.1084/jem.20091777
77. Turner CA Jr, Mack DH, Davis MM. Blimp-1, a novel zinc finger-containing protein that can drive the maturation of B lymphocytes into immunoglobulin-secreting cells. *Cell* (1994) 77:297–306. doi: 10.1016/0092-8674(94)90321-2
78. Shapiro-Shelef M, Lin KI, McHeyzer-Williams LJ, Liao J, McHeyzer-Williams MG, Calame K. Blimp-1 is required for the formation of immunoglobulin secreting plasma cells and pre-plasma memory B cells. *Immunity* (2003) 19:607–20. doi: 10.1016/S1074-7613(03)00267-X
79. Minnich M, Tagoh H, Bonelt P, Axelsson E, Fischer M, Cebolla B, et al. Multifunctional role of the transcription factor Blimp-1 in coordinating plasma cell differentiation. *Nat Immunol.* (2016) 17:331–43. doi: 10.1038/ni.3349
80. Chiu YK, Lin IY, Su ST, Wang KH, Yang SY, Tsai DY, et al. Transcription factor ABF-1 suppresses plasma cell differentiation but facilitates memory B cell formation. *J Immunol.* (2014) 193:2207–17. doi: 10.4049/jimmunol.1400411
81. Reimold AM, Iwakoshi NN, Manis J, Vallabhajosyula P, Szomolanyi-Tsuda E, Gravallese EM, et al. Plasma cell differentiation requires the transcription factor XBP-1. *Nature* (2001) 412:300–7. doi: 10.1038/35085509
82. Shaffer AL, Shapiro-Shelef M, Iwakoshi NN, Lee AH, Qian SB, Zhao H, et al. XBP1, downstream of Blimp-1, expands the secretory apparatus and other organelles, and increases protein synthesis in plasma cell differentiation. *Immunity* (2004) 21:81–93. doi: 10.1016/j.jimmuni.2004.06.010
83. Recaldin T, Fear DJ. Transcription factors regulating B cell fate in the germinal centre. *Clin Exp Immunol.* (2016) 183:65–75. doi: 10.1111/cei.12702
84. Lin KI, Angelin-Duclos C, Kuo TC, Calame K. Blimp-1-dependent repression of Pax-5 is required for differentiation of B cells to immunoglobulin M-secreting plasma cells. *Mol Cell Biol.* (2002) 22:4771–80. doi: 10.1128/MCB.22.13.4771-4780.2002
85. Tellier J, Shi W, Minnich M, Liao Y, Crawford S, Smyth GK, et al. Blimp-1 controls plasma cell function through the regulation of immunoglobulin secretion and the unfolded protein response. *Nat Immunol.* (2016) 17:323–30. doi: 10.1038/ni.3348
86. Shen Y, Hendershot LM. Identification of ERdj3 and OBF-1/BOB-1/OCA-B as direct targets of XBP-1 during plasma cell differentiation. *J Immunol.* (2007) 179:2969–78. doi: 10.4049/jimmunol.179.5.2969
87. Ren X, Siegel R, Kim U, Roeder RG. Direct interactions of OCA-B and TFII-I regulate immunoglobulin heavy-chain gene transcription by facilitating enhancer-promoter communication. *Mol Cell* (2011) 42:342–55. doi: 10.1016/j.molcel.2011.04.011
88. Corcoran LM, Hasbold J, Dietrich W, Hawkins E, Kallies A, Nutt SL, et al. Differential requirement for OBF-1 during antibody-secreting cell differentiation. *J Exp Med.* (2005) 201:1385–96. doi: 10.1084/jem.20042325
89. Carotta S, Willis SN, Hasbold J, Inouye M, Pang SH, Emslie D, et al. The transcription factors IRF8 and PU.1 negatively regulate plasma cell differentiation. *J Exp Med.* (2014) 211:2169–81. doi: 10.1084/jem.20140425
90. Fornek JL, Tygrett LT, Waldschmidt TJ, Poli V, Ricker RC, Kansas GS. Critical role for Stat3 in T-dependent terminal differentiation of IgG B cells. *Blood* (2006) 107:1085–91. doi: 10.1182/blood-2005-07-2871
91. Ding C, Chen X, Dascani P, Hu X, Bolli R, Zhang HG, et al. STAT3 signaling in B cells is critical for germinal center maintenance and contributes to the pathogenesis of murine models of lupus. *J Immunol.* (2016) 196:4477–86. doi: 10.4049/jimmunol.1502043
92. Suan D, Krautler NJ, Maag JLV, Butt D, Bourne K, Hermes JR, et al. CCR6 Defines memory B cell precursors in mouse and human germinal centers, revealing light-zone location and predominant low antigen affinity. *Immunity* (2017) 47:1142–53.e4. doi: 10.1016/j.jimmuni.2017.11.022
93. Shinnakasu R, Inoue T, Kometani K, Moriyama S, Adachi Y, Nakayama M, et al. Regulated selection of germinal-center cells into the memory B cell compartment. *Nat Immunol.* (2016) 17:861–9. doi: 10.1038/ni.3460
94. Basso K, Dalla-Favera R. Roles of BCL6 in normal and transformed germinal center B cells. *Immunol Rev.* (2012) 247:172–83. doi: 10.1111/j.1600-065X.2012.01112.x

95. Igarashi K, Ochiai K, Muto A. Architecture and dynamics of the transcription factor network that regulates B-to-plasma cell differentiation. *J Biochem.* (2007) 141:783–9. doi: 10.1093/jb/mvm106
96. Cobaleda C, Schebesta A, Delogu A, Busslinger M. Pax5: the guardian of B cell identity and function. *Nat Immunol.* (2007) 8:463–70. doi: 10.1038/ni1454
97. Zuccarino-Catania GV, Sadanand S, Weisel FJ, Tomayko MM, Meng H, Kleinstein SH, et al. CD80 and PD-L2 define functionally distinct memory B cell subsets that are independent of antibody isotype. *Nat Immunol.* (2014) 15:631–7. doi: 10.1038/ni.2914
98. Wang Y, Shi J, Yan J, Xiao Z, Hou X, Lu P, et al. Germinal-center development of memory B cells driven by IL-9 from follicular helper T cells. *Nat Immunol.* (2017) 18:921–30. doi: 10.1038/ni.3788
99. Bhattacharya D, Cheah MT, Franco CB, Hosen N, Pin CL, Sha WC, et al. Transcriptional profiling of antigen-dependent murine B cell differentiation and memory formation. *J Immunol.* (2007) 179:6808–19. doi: 10.4049/jimmunol.179.10.6808
100. Scheeren FA, Naspetti M, Diehl S, Schotte R, Nagasawa M, Wijnands E, et al. STAT5 regulates the self-renewal capacity and differentiation of human memory B cells and controls Bcl-6 expression. *Nat Immunol.* (2005) 6:303–13. doi: 10.1038/ni1172
101. Tunyaplin C, Shaffer AL, Angelin-Duclos CD, Yu X, Staudt LM, Calame KL. Direct repression of prdm1 by Bcl-6 inhibits plasmacytic differentiation. *J Immunol.* (2004) 173:1158–65. doi: 10.4049/jimmunol.173.2.1158

**Conflict of Interest Statement:** The authors declare that the research was conducted in the absence of any commercial or financial relationships that could be construed as a potential conflict of interest.

Copyright © 2018 Song and Matthias. This is an open-access article distributed under the terms of the Creative Commons Attribution License (CC BY). The use, distribution or reproduction in other forums is permitted, provided the original author(s) and the copyright owner(s) are credited and that the original publication in this journal is cited, in accordance with accepted academic practice. No use, distribution or reproduction is permitted which does not comply with these terms.



# From Mice to Men: How B Cell Immunology Helped the Understanding of Leukemia Development

**Paolo Ghia\***

IRCCS Ospedale San Raffaele, Università Vita-Salute San Raffaele, Milan, Italy

**Keywords:** B cells, immunoglobulins, B cell development, B cell receptor (BCR), chronic lymphocytic leukemia

The work on normal B lymphocytes, immunoglobulins, and antigenic stimulation performed at the Basel institute in the early '90s, also by Anton G. Rolink, shaped and molded the way B cell lymphomas and in particular Chronic Lymphocytic Leukemia (CLL) are interpreted today.

Words like *Immunoglobulin rearrangements*, *somatic mutations*, and *B Cell Receptors*, which 25 years ago were of interest only to basic immunologists like Ton, became common and trivial (if ever possible) terms also in hematological and clinical gatherings. Nowadays immunologists are in fact regularly invited to such meetings as key-note speakers to explain the basic functionality of the immune system, which has direct implications on the daily clinical practice.

## OPEN ACCESS

### Edited by:

Thomas H. Winkler,  
Friedrich-Alexander-Universität  
Erlangen-Nürnberg, Germany

### Reviewed by:

Michael Zemlin,  
Universitätsklinikum des Saarlandes,  
Germany

Gregory C. Ippolito,  
University of Texas at Austin,  
United States

### \*Correspondence:

Paolo Ghia  
ghia.paolo@hsr.it

### Specialty section:

This article was submitted to  
B Cell Biology,  
a section of the journal  
*Frontiers in Immunology*

**Received:** 24 May 2018

**Accepted:** 27 September 2018

**Published:** 24 October 2018

### Citation:

Ghia P (2018) From Mice to Men:  
How B Cell Immunology Helped the  
Understanding of Leukemia  
Development.  
*Front. Immunol.* 9:2402.  
doi: 10.3389/fimmu.2018.02402

During that pioneering period we also learnt that animal models were not merely a surrogate tool for human organisms, necessary only for obvious reasons of simplicity and convenience, but on the contrary that they may provide precise insights that could be directly applied to the human system. This turned out to be true in the case of the maturation process of B lymphocyte progenitors and precursors in the bone marrow, as we demonstrated that the developmental ordering of the different stages of differentiation in human bone marrow were superimposable to those described by Ton years earlier in mice, with only few small but potentially interesting differences in phenotypic markers (1, 2). In light of such evidence, additional observations on B cell aging in mice and men have also been made, pointing to a progressive decrease of B cell production with age in both organisms (3) and to a restriction of the diversity of the repertoire, as underscored by the appearance of clonal B cell populations consisting of plasma cells or mature (mainly CD5<sup>+</sup>) B cells in the spleens of aged mice (4). Monoclonal Gammopathy of Undetermined Significance (MGUS) a premalignant phase for Multiple Myeloma (5) typical and common in the elderly, can be considered the human counterpart of murine monoclonal plasma cell expansions. At that time, no expansions of CD5<sup>+</sup> mature B cells were known in aging individuals. In a subsequent publication (3), we initially suggested that CD5<sup>+</sup> B cell clonal populations present in old mice might be considered analogous to precursors of Chronic Lymphocytic Leukemia (CLL), the most frequent B cell neoplasm in the elderly (6), which is characterized by clonal expansion of CD5<sup>+</sup> B cells and for which no pre-leukemic phase was defined.

Few years later, such reasoning justified a large observational study involving hundreds of healthy elderly individuals in a quest for clonal expansions of mature B cells using high-sensitive flow cytometric techniques, not in spleens or lymphoid tissues as in mice but in the best surrogate available in humans i.e., the peripheral blood (7). This led to the discovery of either CD5<sup>-</sup> or CD5<sup>+</sup> monoclonal B lymphocytes in almost 10% of individuals above 40 years of age with an increasing frequency associated with age, peaking at an impressive 50% in healthy individuals aged more than 90 years (8). Similar observations became at the same time available from the UK (9), Spain (10), and the US (11, 12), suggesting the universality of the phenomenon that has been later defined by an international consortium as Monoclonal B cell Lymphocytosis (MBL) (13), potentially involving

either CD5<sup>-</sup> or CD5<sup>+</sup> B lymphocytes. CD5<sup>+</sup> MBL is the most frequent, accounting for two thirds of all MBL, and is characterized by the presence of monoclonal B cells with a phenotype identical to CLL (CD20<sup>dim</sup>, CD5<sup>+</sup>, IG<sup>dim</sup>) in the peripheral blood, at concentrations lower than those required for the diagnosis of CLL ( $5 \times 10^9/l$ ) (13). Later on, we reported that MBL can be further distinguished into “low-count” MBL (LC-MBL) and “high-count” MBL (HC-MBL), based on the number of circulating CLL-like cells (more or less than  $0.5 \times 10^9/l$ , respectively) (14). The former does not virtually progress into a clinically relevant disease and may be considered an interesting model to study B cell aging (15), while the latter may evolve into a clinically relevant CLL at a rate of 1% per year (9, 16) and may be considered a real pre-leukemic phase of CLL (12), with all the obvious clinical and pathogenetic implications. All these findings recently provided ground for the inclusion of MBL as a new disease entity within the classification of lymphoid neoplasms by the World Health Organization (WHO), similarly to MGUS (17). Nowadays, there are patients around the world diagnosed and followed-up because of the presence of MBL.

While MBL showed us, thanks to cross-fertilization between mouse and human immunology, how discoveries can sometimes be predictable, the progress of science remains unpredictable in other instances. This is best exemplified by Immunoglobulin genes, a unique exception to the gene-protein dogma in genetics because of the rearrangement process and the introduction of mutations, making them probably one of the most enlightening models of nature adaptation but also the least digestible concept to medical students and alike. The first study to show the developmental order of B progenitor and precursors of the B lymphocytes in the human bone marrow, performed at the Basel Institute under Ton's supervision, was entirely based on the description of the rearrangement status of the Immunoglobulin Heavy and Light chain gene loci, assessed at single cell level (2). In a pre-internet era, the gene sequences for all IG loci could only be collected one by one from printed text books and volumes and needed to be manually curated and aligned, a work that nowadays can be done online in a click. At that time, all that work appeared frustratingly far from the possibility of a concrete application in medicine. A few years later, that knowledge unexpectedly became crucial to better understand the pathogenesis of CLL, following the seminal observation that the presence of somatic mutations within the rearranged clonotypic IGHV genes associated with a better clinical outcome and prognosis in CLL patients (18, 19). This originated from the analysis of somatic hypermutation in neoplastic B cells to track back the cell of origin of mature and immature B cell neoplasms. Strangely enough, CLL, the easiest leukemia to diagnose with a typical and unique phenotype, was indeed a mixture of cases with and without somatic mutations within the IGHV genes, which puzzled all hematologists (and immunologists alike) (20). This observation fueled endless discussions and experiments aiming at clarifying the distinct origin of these 2 subsets of CLL while trying to explain the remarkable uniqueness of the surface phenotypic appearance (21). Only more recently several studies demonstrated that indeed the presence of somatic hypermutations was associated with deeper

and more prolonged responses to immunochemotherapy, in particular to the combination of fludarabine, cyclophosphamide, and rituximab (FCR), the gold standard for the treatment of young, fit CLL patients. IG-mutated patients experience long term remissions reaching a plateau on the PFS curve, with no relapses beyond 10 years, an unprecedented finding in a disease that is still considered incurable (22–24). This transformed the IGHV gene mutational status from a prognostic marker in CLL into a predictive factor, allowing for a better upfront selection of the patients who are more likely to benefit from the use of immunochemotherapy. Testing for IGHV gene mutations is now recommended in the recent update of the guidelines by the International Workshop on CLL (iwCLL) (25), where it is stated that the determination of the somatic hypermutation status of the IGHV genes should always be performed before deciding the treatment of a patient with CLL, as it has relevant implications on the choice of the most effective treatment. This is now probably one of the most prominent examples of personalized medicine approaches that is envisioned in many types of cancer but that in CLL has become reality. A validated consensus methodology for reliable clinical-grade analysis of IGHV genes has been established by the European research Initiative on CLL (ERIC) and moved out of research laboratories into diagnostic facilities (26).

From a scientific point of view, IG gene analysis also became central in the study of CLL pathogenesis and culminated with the creation, as part of an international consortium (IgCLL, [www.igcll.com](http://www.igcll.com)), of a world-wide database collecting to date over 30.000 IG sequences from CLL patients. This remarkable collection helped identify and consolidate the unexpected finding that different unrelated CLL patients share very similar if not identical sequence motifs within the variable heavy chain complementarity determining region 3 (VH CDR3), thus defining “stereotyped” B-cell receptor (BcR) (27). This made it possible to group at least 30% of CLL patients into subsets with similar BcR that, besides similar immunogenetic features, also share similar molecular and functional features and clinical prognosis beyond the simplistic dichotomy of mutational status (28). From an immunological point of view, the presence of stereotypy suggests the recognition of common structures, thus implying that CLL ontogeny is not stochastic but rather driven by interactions between the clonogenic cells and a restricted set of antigenic elements (27).

Thanks to all these molecular findings, it became evident that immunoglobulins and in particular the entire B cell receptor are central players in CLL pathogenesis, even overshadowing in some occasions the role of genetic aberrations. At variance with many other B cell neoplasias characterized by a single distinct genetic abnormality, a number of gross genomic abnormalities including deletion 11q, 13q, 17p, and trisomy 12, are found in different proportions of CLL cases (29). Moreover, high-throughput studies have revealed a further remarkable genetic heterogeneity, with certain genes (*NOTCH1*, *SF3B1*, *TP53*) mutated in only 10–15% of patients (30–32) and others mutated at even lower frequencies (e.g., *NFKBIE*, *RSP15*, *EGR2*) (33). No unifying genetic mechanisms or lesions have thus been identified insofar.

On the contrary it has been demonstrated that the signaling pathway downstream of the BcR is active in all cases of CLL, regardless of the mutational status and immunogenetic features of the patient (34). This is particularly true in the leukemic cells obtained from lymph nodes, where CLL cells are believed to encounter the relevant antigenic elements in the context of the so-called *proliferation centers*, considered the reservoir of the disease: there, leukemic cells get to proliferate and expand also thanks to additional signals originating from T cells, stromal cells and monocytic-derived cells, or through other immune receptors such as the TLRs.

In a proportion of cases, a number of foreign or auto-antigens (35, 36) have been identified as able to interact and stimulate the leukemic BcR, in particular neoantigens, newly exposed in the context of apoptotic bodies produced during physiological cell turnover. However, the notion that classic auto-antigen recognition and binding is important for CLL ontogeny has been challenged by the recent demonstration of cell-autonomous signaling, a novel type of signal generation, occurring specifically in CLL amongst B cell lymphomas, through self recognition as a result of the interaction of the leukemic BcR IG with a conserved epitope of the same or adjacent BcR IGs (37). Autonomous signaling has first been demonstrated in B cell precursors where the pre-BCR has evolved to ensure self-recognition, allowing for positive selection at the pre-B cell stage (38). Interestingly, different portions of the Immunoglobulin are recognized by different stereotyped receptors, each with affinities that appear to associate with distinct clinical outcomes and/or biological responses (39). This heterogeneity resembles the long-known evidence that antigen-dependent stimulation in CLL may also be pleiotropic and may associate with clinical outcome, ranging from full activation and proliferation to anergy and survival (40). The former appears to be typical of more aggressive CLL, particularly with unmutated IGs, while the latter associates with more indolent cases, usually with mutated IGs, thus providing a functional basis for the clinical heterogeneity of the disease. It still remains to be elucidated how antigen-dependent and autonomous signaling cooperate in the onset and maintenance of CLL.

Despite the molecular evidence of the centrality of the BcR in CLL, the final proof that the BCR stimulation is crucial in

all cases of CLL, regardless of the differences in mutational status, antigenic affinities or strength of autonomous signaling, has come from the impressive and virtually universal efficacy of the therapeutic inhibition of the BcR signaling pathway in CLL patients.

The accumulating knowledge of the biology and immunology behind CLL has been applied to the research for innovative therapies, leading to the design and approval of novel mechanism-based drugs such as ibrutinib (41) and Idelalisib (in association with the anti-CD20 antibody Rituximab) (42), targeting molecules downstream the BcR, namely BTK and PI3Kδ. Both drugs have shown greater efficacy and better tolerability than chemoimmunotherapy and have even dramatically changed the prognosis of high-risk CLL patients, including those with TP53 aberrations.

Thanks to the immunological knowledge (and human wisdom) that has developed at the Basel Institute also thanks to Ton Rolink, all physicians may find themselves less at loss in a changing world of hematology where immunology has become central for understanding neoplastic diseases to the benefit of the patients. As unexpected as this was, it has become reality and it should encourage us all to be in part immunologists if we want to better understand the pathogenesis of leukemias and lymphomas. And we should all teach future generations to do so with fun every day!

## AUTHOR CONTRIBUTIONS

The author confirms being the sole contributor of this work and has approved it for publication.

## FUNDING

This work was supported in part by the Associazione Italiana per la Ricerca sul Cancro, AIRC (Investigator Grant #20246 and 5x1000 Research Program #21198).

## ACKNOWLEDGMENTS

I am personally indebted to Ton, a mentor, a colleague, a friend: I have been lucky to call him all three.

## REFERENCES

- ten Boekel E, Melchers F, Rolink, A. The status of Ig loci rearrangements in single cells from different stages of B cell development. *Int Immunol.* (1995) 7:1013–9. doi: 10.1093/intimm/7.6.1013
- Ghia P, ten Boekel E, Sanz E, de la Hera A, Rolink A, Melchers F. Ordering of human bone marrow B lymphocyte precursors by single-cell polymerase chain reaction analyses of the rearrangement status of the immunoglobulin H and L chain gene loci. *J Exp Med.* (1996) 184:2217–29. doi: 10.1084/jem.184.6.2217
- Ghia P, Melchers F, Rolink AG. Age-dependent changes in B lymphocyte development in man and mouse. *Exp Gerontol.* (2000) 35:159–65. doi: 10.1016/S0531-5565(99)00095-9
- LeMaoult J, Manavalan JS, Dyall R, Szabo P, Nikolic-Zugic J, Weksler ME. Cellular basis of B cell clonal populations in old mice. *J Immunol.* (1999) 162:6384–91.
- Kumar SK, Rajkumar V, Kyle RA, van Duin M, Sonneveld P, Mateos MV, et al. Multiple myeloma. *Nat Rev Dis Primers* 3:17046. doi: 10.1038/nrdp.2017.46
- Scarfo L, Ferreri AJ, Ghia P. Chronic lymphocytic leukaemia. *Crit Rev Oncol Hematol.* (2016) 104:169–82. doi: 10.1016/j.critrevonc.2016.06.003
- Ghia P, Prato G, Scielzo C, Stella S, Geuna M, Guida G, et al. Monoclonal CD5+ and CD5- B-lymphocyte expansions are frequent in the peripheral blood of the elderly. *Blood* (2004) 103:2337–42. doi: 10.1182/blood-2003-09-3277
- Scarfo L, Dagklis A, Scielzo C, Fazi C, Ghia P. CLL-like monoclonal B-cell lymphocytosis: are we all bound to have it? *Semin Cancer Biol.* (2010) 20:384–90. doi: 10.1016/j.semancer.2010.08.005
- Rawstron AC, Bennett FL, O'Connor SJ, Kwok M, Fenton JA, Plummer M, et al. Monoclonal B-cell lymphocytosis and chronic lymphocytic leukemia. *N Engl J Med.* (2008) 359:575–83. doi: 10.1056/NEJMoa075290

10. Nieto WG, Almeida J, Romero A, Teodosio C, Lopez A, Henriques AF, et al. Increased frequency (12%) of circulating chronic lymphocytic leukemia-like B-cell clones in healthy subjects using a highly sensitive multicolor flow cytometry approach. *Blood* (2009) 114:33–7. doi: 10.1182/blood-2009-01-197368
11. Shanafelt TD, Kay NE, Call TG, Zent CS, Jelinek DF, LaPlant B, et al. MBL or CLL: which classification best categorizes the clinical course of patients with an absolute lymphocyte count > or = 5 x 10(9) L(-1) but a B-cell lymphocyte count < 5 x 10(9) L(-1)? *Leuk Res.* (2008) 32:1458–61. doi: 10.1016/j.leukres.2007.11.030
12. Landgren O, Albajar M, Ma W, Abbas F, Hayes RB, Ghia P, et al. B-cell clones as early markers for chronic lymphocytic leukemia. *N Engl J Med.* (2009) 360:659–67. doi: 10.1056/NEJMoa0806122
13. Marti GE, Rawstron AC, Ghia P, Hillmen P, Houlston RS, Kay N, et al. Diagnostic criteria for monoclonal B-cell lymphocytosis. *Br J Haematol.* (2005) 130:325–32. doi: 10.1111/j.1365-2141.2005.05550.x
14. Rawstron AC, Shanafelt T, Lanasa MC, Landgren O, Hanson C, Orfao A, et al. Different biology and clinical outcome according to the absolute numbers of clonal B-cells in monoclonal B-cell lymphocytosis (MBL). *Cytometry B Clin Cytom.* (2010) 78(Suppl. 1):S19–23. doi: 10.1002/cyto.b.20533
15. Fazi C, Scarfo L, Pecciarini L, Cottini F, Dagklis A, Janus A, et al. General population low-count CLL-like MBL persists over time without clinical progression, although carrying the same cytogenetic abnormalities of CLL. *Blood* (2011) 118:6618–25. doi: 10.1182/blood-2011-05-357251
16. Shanafelt TD, Kay NE, Jenkins G, Call TG, Zent CS, Jelinek DF, et al. B-cell count and survival: differentiating chronic lymphocytic leukemia from monoclonal B-cell lymphocytosis based on clinical outcome. *Blood* (2009) 113:4188–96. doi: 10.1182/blood-2008-09-176149
17. Swerdlow SH, Campo E, Pileri SA, Harris NL, Stein H, Siebert R, et al. The 2016 revision of the World Health Organization classification of lymphoid neoplasms. *Blood* (2016) 127:2375–90. doi: 10.1182/blood-2016-01-643569
18. Damle RN, Wasil T, Fais F, Ghiotto F, Valetto A, Allen SL, et al. Ig V gene mutation status and CD38 expression as novel prognostic indicators in chronic lymphocytic leukemia. *Blood* (1999) 94:1840–7.
19. Hamblin TJ, Davis Z, Gardiner A, Oscier DG, Stevenson FK. Unmutated Ig V(H) genes are associated with a more aggressive form of chronic lymphocytic leukemia. *Blood* (1999) 94:1848–54.
20. Schroeder HW Jr, Dighiero G. The pathogenesis of chronic lymphocytic leukemia: analysis of the antibody repertoire. *Immunol Today* (1994) 15:288–94. doi: 10.1016/0167-5699(94)90009-4
21. Chiorazzi N, Rai KR, Ferrarini M. Chronic lymphocytic leukemia. *N Engl J Med.* (2005) 352:804–15. doi: 10.1056/NEJMra041720
22. Rossi D, Terzi-di-Bergamo L, De Paoli L, Cerri M, Ghilardi G, Chiarenza A, et al. Molecular prediction of durable remission after first-line fludarabine-cyclophosphamide-rituximab in chronic lymphocytic leukemia. *Blood* (2015) 126:1921–4. doi: 10.1182/blood-2015-05-647925
23. Fischer K, Bahlo J, Fink AM, Goede V, Herling CD, Cramer P, et al. Long-term remissions after FCR chemoimmunotherapy in previously untreated patients with CLL: updated results of the CLL8 trial. *Blood* (2016) 127:208–15. doi: 10.1182/blood-2015-06-651125
24. Thompson PA, Tam CS, O'Brien SM, Wierda WG, Stingo F, Keating MJ, et al. Fludarabine, cyclophosphamide, and rituximab treatment achieves long-term disease-free survival in IGHV-mutated chronic lymphocytic leukemia. *Blood* (2016) 127:303–9. doi: 10.1182/blood-2015-09-667675
25. Hallek M, Cheson BD, Catovsky D, Caligaris-Cappio F, Dighiero G, Dohner H, et al. Guidelines for diagnosis, indications for treatment, response assessment and supportive management of chronic lymphocytic leukemia. *Blood* (2018) 131:2745–60. doi: 10.1182/blood-2017-09-806398
26. Rosenquist R, Ghia P, Hadzidimitriou A, Sutton LA, Agathangelidis A, Bialiakas P, et al. Immunoglobulin gene sequence analysis in chronic lymphocytic leukemia: updated ERIC recommendations. *Leukemia* (2017) 31:1477–81. doi: 10.1038/leu.2017.125
27. Stamatopoulos K, Agathangelidis A, Rosenquist R, Ghia P. Antigen receptor stereotypy in chronic lymphocytic leukemia. *Leukemia* (2017) 31:282–91. doi: 10.1038/leu.2016.322
28. Agathangelidis A, Darzentas N, Hadzidimitriou A, Brochet X, Murray F, Yan XJ, et al. Stereotyped B-cell receptors in one-third of chronic lymphocytic leukemia: a molecular classification with implications for targeted therapies. *Blood* (2012) 119:4467–75. doi: 10.1182/blood-2011-11-393694
29. Dohner H, Stilgenbauer S, Benner A, Leupolt E, Krober A, Bullinger L, et al. Genomic aberrations and survival in chronic lymphocytic leukemia. *N Engl J Med.* (2000) 343:1910–6. doi: 10.1056/NEJM200012283432602
30. Puente XS, Pinyol M, Quesada V, Conde L, Ordonez GR, Villamor N, et al. Whole-genome sequencing identifies recurrent mutations in chronic lymphocytic leukaemia. *Nature* (2011) 475:101–5. doi: 10.1038/nature10113
31. Wang L, Lawrence MS, Wan Y, Stojanov P, Sougnez C, Stevenson K, et al. SF3B1 and other novel cancer genes in chronic lymphocytic leukemia. *N Engl J Med.* (2011) 365:2497–506. doi: 10.1056/NEJMoa1109016
32. Rossi D, Fangazio M, Rasi S, Vaisitti T, Monti S, Cresta S, et al. Disruption of BIRC3 associates with fludarabine chemoresistance in TP53 wild-type chronic lymphocytic leukemia. *Blood* (2012) 119:2854–62. doi: 10.1182/blood-2011-12-395673
33. Rosenquist R, Rosenwald A, Du MQ, Gaidano G, Groenen P, Wotherspoon A, et al. Clinical impact of recurrently mutated genes on lymphoma diagnostics: state-of-the-art and beyond. *Haematologica* (2016) 101:1002–9. doi: 10.3324/haematol.2015.134510
34. Herishanu Y, Perez-Galan P, Liu D, Biancotto A, Pittaluga S, Vire B, et al. The lymph node microenvironment promotes B-cell receptor signaling, NF- $\kappa$ B activation, and tumor proliferation in chronic lymphocytic leukemia. *Blood* (2011) 117:563–74. doi: 10.1182/blood-2010-05-284984
35. Herve M, Xu K, Ng YS, Wardemann H, Albesiano E, Messmer BT, et al. Unmutated and mutated chronic lymphocytic leukemias derive from self-reactive B cell precursors despite expressing different antibody reactivity. *J Clin Invest.* (2005) 115:1636–43. doi: 10.1172/JCI24387
36. Lanemo Myhrinder A, Hellqvist E, Sidorova E, Soderberg A, Baxendale H, Dahle C, et al. A new perspective: molecular motifs on oxidized LDL, apoptotic cells, and bacteria are targets for chronic lymphocytic leukemia antibodies. *Blood* (2008) 111:3838–48. doi: 10.1182/blood-2007-11-125450
37. Duhren-von Minden M, Ubelhart R, Schneider D, Wossning T, Bach MP, Buchner M, et al. Chronic lymphocytic leukaemia is driven by antigen-independent cell-autonomous signalling. *Nature* (2012) 489:309–12. doi: 10.1038/nature11309
38. Kohler F, Hug E, Eschbach C, Meixlsperger S, Hobeika E, Kofer J, et al. Autoreactive B cell receptors mimic autonomous pre-B cell receptor signaling and induce proliferation of early B cells. *Immunity* (2008) 29:912–21. doi: 10.1016/j.jimmuni.2008.10.013
39. Minici C, Gounari M, Ubelhart R, Scarfo L, Duhren-von Minden M, Schneider D, et al. Distinct homotypic B-cell receptor interactions shape the outcome of chronic lymphocytic leukaemia. *Nat Commun.* (2017) 8:15746. doi: 10.1038/ncomms15746
40. Muzio M, Apollonio B, Scielzo C, Frenquelli M, Vandoni I, Boussiotis V, et al. Constitutive activation of distinct BCR-signaling pathways in a subset of CLL patients: a molecular signature of anergy. *Blood* (2008) 112:188–95. doi: 10.1182/blood-2007-09-111344
41. Byrd JC, Brown JR, O'Brien S, Barrientos JC, Kay NE, Reddy NM, et al. Ibrutinib versus ofatumumab in previously treated chronic lymphoid leukemia. *N Engl J Med.* (2014) 371:213–23. doi: 10.1056/NEJMoa1400376
42. Furman RR, Sharman JP, Coutre SE, Cheson BD, Pagel JM, Hillmen P, et al. Idelalisib and rituximab in relapsed chronic lymphocytic leukemia. *N Engl J Med.* (2014) 370:997–1007. doi: 10.1056/NEJMoa1315226

**Conflict of Interest Statement:** The author declares that the research was conducted in the absence of any commercial or financial relationships that could be construed as a potential conflict of interest.

Copyright © 2018 Ghia. This is an open-access article distributed under the terms of the Creative Commons Attribution License (CC BY). The use, distribution or reproduction in other forums is permitted, provided the original author(s) and the copyright owner(s) are credited and that the original publication in this journal is cited, in accordance with accepted academic practice. No use, distribution or reproduction is permitted which does not comply with these terms.



# Modeling Hematological Diseases and Cancer With Patient-Specific Induced Pluripotent Stem Cells

Huensuk Kim<sup>1,2,3</sup> and Christoph Schaniel<sup>1,2,3,4,5\*</sup>

<sup>1</sup> Black Family Stem Cell Institute, Icahn School of Medicine at Mount Sinai, New York, NY, United States, <sup>2</sup> Department of Cell, Developmental and Regenerative Biology, Icahn School of Medicine at Mount Sinai, New York, NY, United States,

<sup>3</sup> Graduate School of Biomedical Sciences, Icahn School of Medicine at Mount Sinai, New York, NY, United States,

<sup>4</sup> Department of Pharmacological Sciences, Icahn School of Medicine at Mount Sinai, New York, NY, United States, <sup>5</sup> Mount Sinai Institute for Systems Biomedicine, Icahn School of Medicine at Mount Sinai, New York, NY, United States

## OPEN ACCESS

### Edited by:

Rhodri Ceredig,  
National University of Ireland Galway,  
Ireland

### Reviewed by:

Kay L. Medina,  
Mayo Clinic, United States

Encarnacion Montecino-Rodriguez,  
University of California, Los Angeles,  
United States

Geoffrey Brown,  
University of Birmingham,  
United Kingdom

### \*Correspondence:

Christoph Schaniel  
christoph.schaniel@mssm.edu

### Specialty section:

This article was submitted to  
B Cell Biology,  
a section of the journal  
*Frontiers in Immunology*

Received: 29 June 2018

Accepted: 10 September 2018

Published: 28 September 2018

### Citation:

Kim H and Schaniel C (2018)  
Modeling Hematological Diseases and  
Cancer With Patient-Specific Induced  
Pluripotent Stem Cells.  
*Front. Immunol.* 9:2243.  
doi: 10.3389/fimmu.2018.02243

The advent of induced pluripotent stem cells (iPSCs) together with recent advances in genome editing, microphysiological systems, tissue engineering and xenograft models present new opportunities for the investigation of hematological diseases and cancer in a patient-specific context. Here we review the progress in the field and discuss the advantages, limitations, and challenges of iPSC-based malignancy modeling. We will also discuss the use of iPSCs and its derivatives as cellular sources for drug target identification, drug development and evaluation of pharmacological responses.

**Keywords:** cancer, blood disorders, hematopoietic malignancies, induced pluripotent stem cells, model systems

## INTRODUCTION

Hematological diseases and cancers are devastating diseases with a high economic and social burden. Generally basic and preclinical cancer research relies on model systems in order to understand the cellular and molecular mechanisms of the malignant state at the cellular, organ and organism level. The hope is that the information gained from such model systems will be helpful in devising precise, effective, and personalized therapeutic strategies. Prototypically, these model systems include immortalized cell lines and genetically engineered, mutant mice. More recently, advanced patient-derived models such as conditionally reprogrammed cells (CRs) (1–3), patient-derived tumor xenografts (PDXs) (4), CRs combined with PDXs (5), and three-dimensional patient derived organoid cell cultures (6–9), engineered tissues (10–12), and microphysiological systems (MPSs) (13–20) have attracted the interest of the biomedical research community. One particular (r)evolution in modern era biomedical research arose with the breakthrough, Noble-prize awarded discovery of induced pluripotent stem cell (iPSC) generation from somatic cells (21–24). These iPSCs are akin embryonic stem cells, and can be maintained indefinitely in a self-renewing, undifferentiated pluripotent state in culture and be directed to differentiate to any cell type in the body, provided the right cues. Thus, the derivation of iPSCs from patient cells provides a new tool in the arsenal for investigation of disease and cancer pathogenesis, drug development and precision medicine (Figure 1).

## INDUCED PLURIPOTENT STEM CELL MODELS OF HEMATOLOGICAL DISEASES, BLOOD CELL CANCERS AND NON-HEMATOPOIETIC CANCERS

The use of iPSCs in the study of hematological diseases, cancer, and tumorigenicity is gaining momentum. It started with the generation of iPSCs from a human melanoma and a human prostate cancer cell line in 2008 (25). Since then numerous malignant cell lines have been reprogrammed that represent among other organs the brain, intestine, liver, lung, pancreas, prostate, and skin, as well as the blood (26–37) (**Table 1**).

The reprogramming of cancer cell lines was soon followed by the generation of iPSCs representing various hematological diseases, blood cell cancers, and non-hematopoietic cancers (38–77) (**Table 2**). These iPSCs were derived from primary patient cells, cancerous tissues or patient cells harboring known oncogenic lesions. In **Table 2** we summarize whether functional assays were performed in attempt to phenocopy the disease/malignancy, describe the phenotypes observed and whether the studies used genome editing to either create or correct disease/cancer-associated mutations.

### ADVANTAGES OF iPSCs

One of the main advantages of the iPSC technology is that hematological disease-associated and malignant lesions can be studied with human cells and in the genomic context of the patient. This is of considerable importance given that certain non-human models are not reflective of the human condition. An example is familial platelet disorder with a tendency to develop acute myeloid leukemia (FDP/AML) that is caused by inherited monoallelic mutations in *RUNX1* (80). FDP/AML presents with mild to moderate thrombocytopenia and bleeding due to impaired proplatelet formation, platelet activation defects, abnormal megakaryocyte differentiation and polyploidization, and a predisposition to develop AML (81). Neither, mouse nor zebrafish models of *RUNX1* mutations do develop a bleeding disorder or leukemia. In contrast, FDP/AML-iPSC derived “early wave” and “second wave” hematopoietic stem/progenitor cells showed aberrant hematopoiesis as occurs in FDP/AML patients (38, 42, 52, 64). Additionally, a person’s genomic background greatly influences disease/cancer severity and progression as well as therapeutic response. Second, iPSCs provide a self-renewable, cryopreservable source of cells that are scalable to fulfill any need in cell numbers for cellular, biochemical, molecular, and other downstream applications. Third, with the appropriate cues and protocols iPSCs can be differentiated *in vitro* to many, in the future hopefully all cell types present in the body, enabling the study of multi-cell type affected diseases/cancers with one patient iPSC source. As an example, Tulpule et al. were able to show that Shwachman-Diamond syndrome (SDS)-iPSCs were impaired in both exocrine pancreatic and hematopoietic differentiation with reduced myeloid cell generation *in vitro*, increased apoptosis, and elevated protease activity recapitulating SDS patient phenotypes (70). Forth when the somatic cells

used to generate iPSCs are isolated from primary hematological diseases/cancers or metastatic tumor specimens of non-germ line malignancies through biopsy, a bone marrow aspirate or blood sampling, normal cells will be inadvertently co-isolated along the malignant cells. Thus, the same reprogramming event can simultaneously generate paired malignant and normal iPSCs that share the same genetic background with exception of the disease-associated/cancerous lesion(s) in the malignant iPSCs. Distinguishing the normal iPSCs from the disease/cancer iPSCs has to be done retrospectively through genetic analysis (33, 55, 73). Alternatively, isogenic normal iPSCs can be established independently through a separate reprogramming experiment with somatic cells obtained from a non-malignant area adjacent to the tumor, a biopsy from an unaffected tissue such as the skin or from blood in the case of non-hematological disorders or cancers (33, 82). Another advantage of the iPSC technology is that reprogramming of malignant cells might establish iPSCs that represent various stages of disease progression, as cancers are often associated with serial accumulation of specific malignant mutations/lesions. Papapetrou et al. elegantly demonstrated this by using bone marrow or peripheral blood from four patients in different risk categories of myelodysplastic syndrome (MDS) or MDS/AML (56). They were successful in generating a library of iPSC lines that represents various disease stages including normal/healthy, preleukemia, low-risk MDS, high-risk MDS, and MDS/AML. The derived iPSC lines carried the respective gene mutations and chromosomal abnormalities found in the patients’ bone marrow or peripheral blood cells used for reprogramming. Moreover, hematopoietic differentiation of these iPSC lines representing the various disease stages captured corresponding cellular phenotypes of graded severity and disease specificity.

### LIMITATIONS AND CHALLENGES OF iPSC MODELING OF HUMAN MALIGNANCIES

Modeling hematological diseases and cancers with patient-specific iPSCs could face various hurdles due to technical, genomic stability and epigenome resetting challenges. It has been reported that some cancer cells are refractory to reprogramming (83, 84). This can have several reasons. For one, certain cancer cells and cells representing diverse stages may be difficult or even impossible to obtain and maintain for reprogramming purposes. Second, hematological diseases and cancers are often heterogeneous in nature, and reprogramming may preferentially select for cells with certain mutations and chromosomal aberrations and not others. Thus, the possibility exists that the panel of iPSC lines generated might not represent the entire heterogeneous composition of the patients’ malignancy. Third, some cancer-associated mutations or genetic lesions might interfere with the reprogramming process itself or prevent maintenance of the pluripotent state. Fourth, even if iPSCs from patients with certain genetic lesions could be established, the specific lesions may render the cell genetically unstable. This will lead to acquisition of additional mutations and genomic abnormalities, which no longer reflect the cancer’s genomic footprint and make the cells useless for proper disease

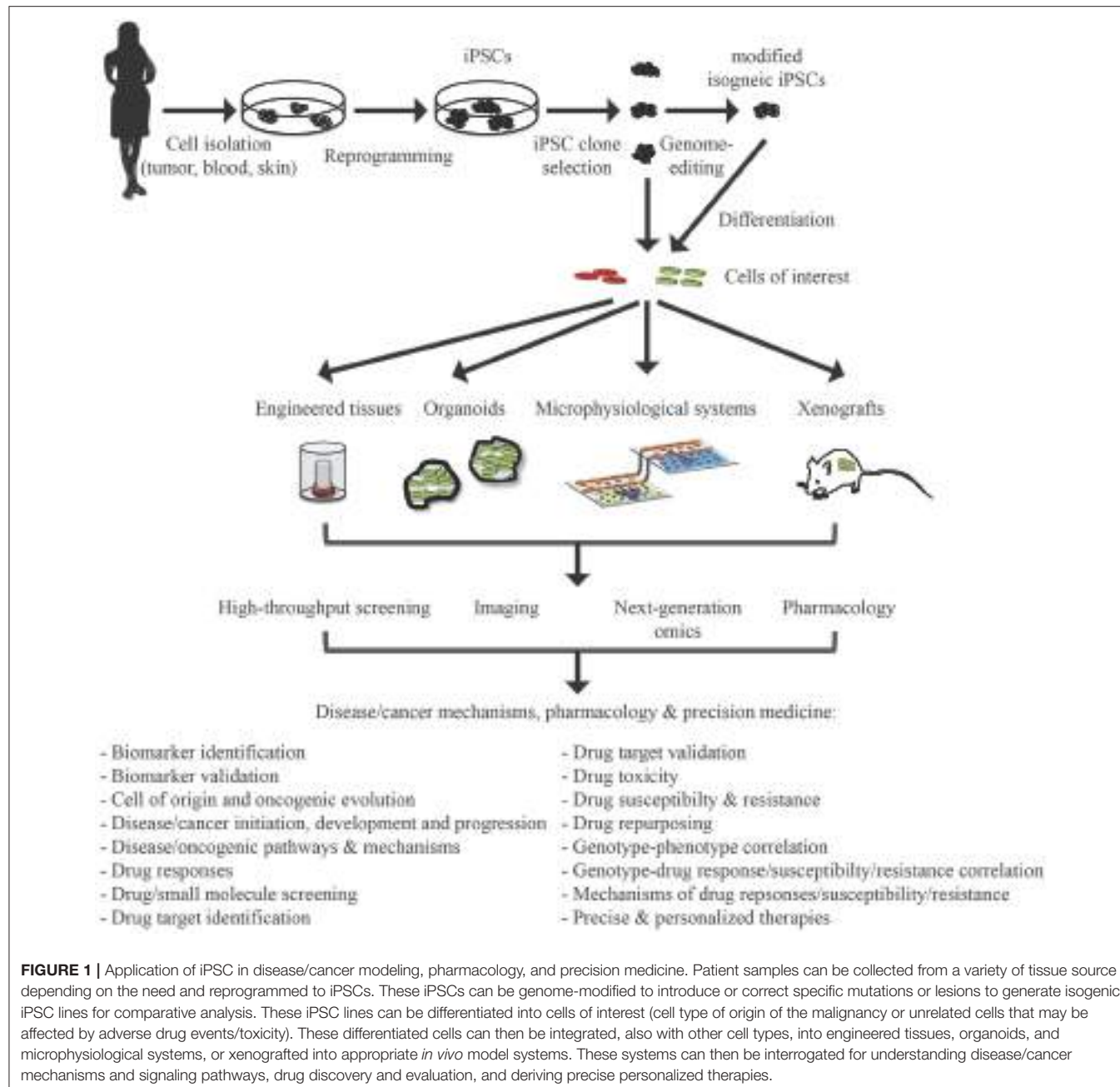


**FIGURE 1 |** Application of iPSC in disease/cancer modeling, pharmacology, and precision medicine. Patient samples can be collected from a variety of tissue source depending on the need and reprogrammed to iPSCs. These iPSCs can be genome-modified to introduce or correct specific mutations or lesions to generate isogenic iPSC lines for comparative analysis. These iPSC lines can be differentiated into cells of interest (cell type of origin of the malignancy or unrelated cells that may be affected by adverse drug events/toxicity). These differentiated cells can then be integrated, also with other cell types, into engineered tissues, organoids, and microphysiological systems, or xenografted into appropriate *in vivo* model systems. These systems can then be interrogated for understanding disease/cancer mechanisms and signaling pathways, drug discovery and evaluation, and deriving precise personalized therapies.

modeling. Examples of unsuccessful reprogramming include the inability to establish iPSC lines from highly purified leukemic blast cells from patients with cytogenetically different subtypes of B cell-ALL (B-ALL) (84), and from Fanconi anemia (FA)-fibroblasts in one case (83). It is noteworthy to mention that FA-iPSC lines have been successfully generated (62, 68, 75). However, the FA pathway facilitates efficient reprogramming (62) and FA cells are genetically unstable and predisposed to apoptosis (85). The latter is reflected by the observation of Yung et al. who showed that their FA-iPSC lines acquired significant additional abnormalities (hyperploidy) (75). The success in generating FA-iPSC likely

might be dependent on the reprogramming condition—hypoxia appears better than normoxia (62) -, which FA-associated gene (fifteen genes constitute the FA complementation group) is mutated or even the kind of mutation. The derivation of AML-iPSCs, although successful for three AML patients with rearrangements in *KMT2A/MLL* (41, 59), has failed for AMLs with different mutations or lesions as well as *KMT2A/MLL* leukemic aberrations (41, 59). Stanford et al. also reported that TSC2-deficiency represents a barrier to reprogramming (53), while TSC2-haploinsufficient allowed iPSC generation with TSC2<sup>+-</sup>-iPSC-derived smooth muscle cells recapitulating Lymphangioleiomyomatosis (LAM) features including increased

**TABLE 1 |** Human cancer cell line-derived iPSCs.

Cancer type	Cell line reprogrammed	References
Breast cancer	MCF-7	(34)
Cholangiocellular cancer	HuCC-T1	(27)
Chronic myeloid leukemia	KBM-7	(28)
Colorectal cancer	DLD-1, HCT116, HT-29	(27)
Esophageal cancer	TE-10	(27)
Ewing's sarcoma	SK-NEP1, CHLA-10	(30, 36)
Gastric cancer	MKN45	(27)
Glioblastoma multiforme	Glioblastoma multiforme neural stem cell lines G7 & G26	(32)
Hepatocellular cancer	PLC	(27)
Liposarcoma	SW872	(30)
Lung cancer	A549, H358, H460	(29, 31)
Melanoma	Colo, R545	(25, 26)
Oral squamous cell carcinoma	H103, H376	(37)
Osteosarcoma	Saos-2, HOS, MG-63, G-292, U2OS	(30, 35)
Pancreatic cancer	MIAPaCa-2, PANC-1	(27)
Prostate cancer	PC-3	(25)

mTORC1 activation, abnormal autophagy and LAM-associate biomarker expression (53).

Another possible limitation is the inability to derive cells of a defined cell type and developmental stage characteristic of the malignancy from iPSCs. Although protocols for generation of many general cell types have been established, the signaling cues and *in vitro* differentiation protocols for certain specialized cells, and developmental and maturation staged are still not fully understood. This is further complicated by the fact that differentiation and maturation efficiency is never 100% and, in most cases, the differentiation and maturation stage of a given cell within a population cannot easily be discriminated, thus, potentially hampering the correlation of disease phenotypes with the cellular phenotypes present in the culture. This issue could be resolved by introduction of stage-specific reporter genes via genome editing or by detailed stepwise characterization of the stages of differentiation and maturation in order to identify the exact stage at which the disease phenotype manifests. Additionally, the constant technological advances in single cell analyses at the cellular and molecular level will greatly improve disease modeling and mechanistic studies.

Cell reprogramming is associated with resetting of the starting cell's epigenetic landscape to that of a pluripotent stem cell. This resetting might eliminate characteristic features of the disease/cancer cell phenotype that might not be recreated upon differentiation, thus producing a significant difference between the disease/cancer iPSC model and the original disease/cancer cell. Here, it is worth bringing forth the theory that the initial oncogenic insult to the cancer-initiating cell might (re)program the epigenome toward a specific cancer cell fate (86). This potentially important aspect of malignancy could well be lost in iPSCs as reprogramming to iPSCs is accompanied by genome-wide epigenetic resetting (see *Epigenome, Cancer, and iPSCs*).

Additionally, if one agrees with Sánchez-García's tumor stem cell reprogramming viewpoint that cancer cell properties can reemerge upon differentiation and that this property is to a fixed, uni-differentiated cell fate then this may not reemerge in an iPSC model due to the fact that iPSCs by definition possess pluripotent differentiation ability. On the other hand, such a resetting might be looked at favorably in certain diseases/cancers of "pure" epigenetic origin for which one could envision of using cells differentiated from these epigenetically reset iPSCs as a regenerative therapy.

Last but not least, modeling systemic processes *in vitro* is a challenge, as generally iPSC are maintained isolated as functionally autonomous entities in two-dimensional culture systems and not physiological integrated within the disease/tumor microenvironment. Recent progress and use of tissue engineering, three-dimensional organoids, MPS and *in vivo* xenografts offers a window to more sophisticated modeling that enables incorporation of malignant cells with cellular and extracellular components of the disease/tumor microenvironment, nutrient supply, and mimicking of blood/lymph flow thus attempting to recapitulate the *in vivo* architecture and physiological condition in which the malignant cells reside and grow.

## EPIGENOME, CANCER, AND iPSCs

Hematological diseases and cancers are profoundly influenced by changes in the epigenome and associated with a specific epigenetic profile. Since reprogramming to pluripotency is achieved through a stepwise resetting of the epigenetic landscape of the starting cell to that of a self-renewing, pluripotent iPSC (87), it is foreseeable that under certain circumstances this could have a negative impact on specific disease/cancer iPSC-based models. For example, iPSCs derived from non-small cell lung cancer (NSCLC) cell lines reset the NSCLC-associated transcriptional and methylation pattern of associated oncogenes and tumor suppressors (31). Similarly, Zhang et al. showed that reprogramming of sarcoma cell lines with complex, abnormal karyotypes to iPSCs resets the sarcoma transcriptional and epigenetic pattern and that the derived iPSCs gained self-renewal and multi-lineage differentiation potential (30). Neither of these studies examined whether the cancer-associated epigenetic profile reminiscent of the original cancer cell could be reestablished upon differentiation. Comparably, iPSCs generated from patients with AML carrying *MLL* rearrangements retained the leukemic mutations but also reset leukemic DNA methylation and gene expression patterns (41). However, leukemic DNA methylation and gene expression profiles reemerged in AML-iPSC-derived hematopoietic cells. Similarly, human glioblastoma-derived iPSCs remain highly malignant after differentiation into neural progenitors and pancreatic ductal adenocarcinoma (PDAC)-iPSCs establish secondary pancreatic-cancer in patient-derived xenografts (see also below) (32, 33). These examples suggest that cancer cell properties, albeit reset in iPSCs, can reemerge upon differentiation to the appropriate cancer cell type.

**TABLE 2 |** Current patient-specific iPSC models of hematological diseases and cancer.

Hematological disease or cancer type	Functional assay(s)	Disease/Cancer Recapitulation	Genome editing	References
8p11 myeloproliferative syndrome (EMS)	<i>In vitro</i>	Yes—increased output in granulocyte-erythrocyte-macrophage-megakaryocyte, erythrocyte and macrophage colonies	No	(72)
AML	<i>In vitro &amp; in vivo</i>	Yes—preferential <i>in vitro</i> generation of granulocyte-macrophage, granulocyte and macrophage colonies and aggressive myeloid leukemia <i>in vivo</i>	No	(41)
	<i>In vitro</i>	Yes—reduction in blood cell specification and block in generation of granulocyte-macrophage and erythroid colonies	No	(59)
Aplastic anemia	<i>In vitro</i>	Yes—impaired proliferation of hematopoietic progenitors and reduced erythrocyte and myeloid cell output -	No	(60)
$\beta$ -thalassemia	No	N/A	No	(45)
	<i>In vitro</i>	Yes—reduced hematopoietic potential and absence of erythrocyte colonies	No	(71)
	<i>In vitro</i>	Yes—impaired erythrocyte colony formation	Yes—gene correction (generation of isogenic control)	(78)
Colorectal cancer (CRC)	<i>In vitro</i>	Yes—increased WNT signaling and enhanced proliferation of colonic epithelial cells	No	(43)
Diamond-Blackfan anemia (DBA)	<i>In vitro</i>	Yes—defective erythropoiesis	No	(44, 47)
Familial platelet disorder with acute myeloid leukemia (FDP/AML)	<i>In vitro</i>	Yes—defective hematopoiesis and impaired erythrocyte and megakaryocyte differentiation	No	(38, 42, 52, 64)
Fanconi anemia (FA)	<i>In vitro</i>	No—robust multilineage hematopoietic differentiation potential with a non-significant reduction in erythroid and myeloid cell colonies	No (but viral gene complementation before reprogramming)	(62)
	<i>In vitro</i>	Yes—reduced clonogenic potential and increased apoptosis of hematopoietic progenitors	No	(75)
	<i>In vitro</i>	Yes—defective hemangiogenic progenitors resulting in inefficient differentiation to hematopoietic and endothelial lineages	No	(68)
Glanzmann thrombasthenia (GT)	<i>In vitro</i>	Yes—absence of membrane expression of integrin $\alpha IIb\beta 3$ , reduction of platelet activation marker binding, impaired adherence to fibrinogen and defective platelet aggregation		(51, 63)
Juvenile myelomonocytic leukemia (JMML)	<i>In vitro</i>	Yes—enhanced production of myeloid cells with increased proliferative capacity and GM-CSF hypersensitivity	No	(46)
Juvenile myelomonocytic leukemia/Noonan Syndrome (JMML/NS)	<i>In vitro</i>	Yes—enhanced production of myeloid cells with increased proliferative capacity and GM-CSF hypersensitivity	No	(61)
Li-Fraumeni Syndrome (LFS)	<i>In vitro, in ovo &amp; in vivo</i>	Yes—osteosarcoma features including aberrant osteoblast differentiation and tumorigenicity, and involvement of <i>H19</i>	No	(58)
	<i>In vitro, in ovo &amp; in vivo</i>	Yes—osteosarcoma features including aberrant osteoblast differentiation and tumorigenicity, and paracrine and autocrine role of <i>SFRP2</i> in osteosarcomagenesis	yes—introduction of P53 mutations	(54)
Lymphangioleiomyomatosis (LAM)	<i>In vitro</i>	Yes—increased mTORC1 activation, abnormal autophagy and LAM-associate biomarker expression in smooth muscle cells	No	(53)
Multiple endocrine neoplasia type 2A (MEN2A)	No	N/A	Yes—mutation correction (generation of isogenic control)	(48, 79)
Myelodysplastic syndrome (MDS)	<i>In vitro</i>	Yes—drastically reduced hematopoietic differentiation potential and myeloid clonogenicity; increased cell death during <i>in vitro</i> differentiation	Yes—introduction of disease associated chr7q deletion	(55)

(Continued)

**TABLE 2 |** Continued

Hematological disease or cancer type	Functional assay(s)	Disease/Cancer Recapitulation	Genome editing	References
	<i>In vitro</i>	Yes—mild perturbation of hematopoietic differentiation with morphologic dysplasia	Yes—introduction and correction of disease associated <i>SRSF2 P95L</i> mutation	(40)
	<i>In vitro</i>	Yes—reduced ability to generate granulocyte-erythrocyte-macrophage-megakaryocyte and erythrocyte colonies <i>in vitro</i>	Yes—introduction of disease associated mutations	(56)
Myelodysplastic syndrome with acute myeloid leukemia (MDS/AML)	<i>In vitro &amp; in vivo</i>	Yes—reduced ability to generate granulocyte-erythrocyte-macrophage-megakaryocyte and erythrocyte colonies <i>in vitro</i> , and robust leukemia development <i>in vivo</i>	Yes—introduction of disease associated mutations	(56)
Myeloproliferative neoplasm (MPN)—Chronic myeloid leukemia (CML)	<i>In vitro</i>	Yes—reduced hematopoietic differentiation	No	(39)
	<i>In vitro &amp; in vivo</i>	Yes—CML-iPSC-derived hematopoietic cells were sensitive to imatinib	No	(57)
	No	N/A	No	(50)
Myeloproliferative neoplasm (MPN)—Essential thrombocythemia (ET)	<i>In vitro</i>	Yes—increased megakaryopoiesis	No	(69)
Myeloproliferative neoplasm (MPN)—Primary and secondary myelofibrosis (PMF/SMF)	<i>In vitro</i>	Yes—increased expression of MF-associated IL-8 in megakaryocytes	No	(49)
Myeloproliferative neoplasm (MPN)—Polycythemia vera (PV)	<i>In vitro</i>	Yes—increased erythropoiesis & PV patient similar gene expression	No	(74)
	<i>In vitro</i>	Yes—increased megakaryopoiesis and erythropoiesis; increased sensitivity to EPO and TPO	No	(65)
	<i>In vitro</i>	Yes—EPO-independent erythropoiesis	No	(73)
Pancreatic ductal adenocarcinoma (PDAC)	<i>In vivo</i>	Yes—development of pancreatic intraepithelial neoplasm (PanIN) precursors to PDAC, which subsequently progressed further to the invasive stage	No	(33)
Shwachman-Diamond syndrome (SDS)	<i>In vitro</i>	Yes—impaired exocrine pancreatic and hematopoietic differentiation with reduced myeloid cell generation <i>in vitro</i> , increased apoptosis, and elevated protease activity	No	(70)
Sickle cell disease (SCD)	No	N/A	Yes—mutation correction	(76)
	No	N/A	Yes—mutation correction	(66)
	No	N/A	Yes—mutation correction	(67)
Trisomy 21	<i>In vitro</i>	Yes—increased numbers of CD43 <sup>+</sup> CD235 <sup>+</sup> erythroid-megakaryocyte progenitors, and erythrocyte, granulocyte, macrophage, and megakaryocyte colonies	No	(77)

Remarkably, a recent report showed that the cellular context could significantly impact on the genetic information and behavior of malignant cells (88). Hashimoto et al. reprogrammed mouse colon tumor cells with loss of *Apc*. The reprogrammed tumor cells, *Apc*-iPSCs, displayed iPSC-like morphology and gene expression but lacked pluripotency and showed a trophectoderm-differentiation bias. Surprisingly, the majority of genes affected by the *Apc* mutation in *Apc*-iPSCs were different than those affected in the colon. Genetic *Apc*-rescue coupled with a subsequent deletion strategy revealed neoplastic growth specific to intestinal cells but not other cell types *in vivo*.

*vivo*. It is noteworthy though that the majority of *Apc*-iPSC-derived colonic legions remained in a pretumoral microadenoma stage and did not develop into full blown macroscopic colon tumors. These findings imply that disease cell properties and biological consequences of tumor-causing mutations are strongly depending on the cellular context and underscore that epigenetic regulation, which is critical for cell fate determination and fixing the malignant cell state in cancer (see also our discussion of this issue in *Limitations and challenges of iPSC modeling of human malignancies*), exerts great influence on disease development and progression.

## GENOME EDITING

Genetic modification of human pluripotent stem cells through conventional homologous recombination is hampered by extremely rare recombination events (89). Recent advances in genome editing technologies (zinc finger nucleases (ZFN), transcription activator-like effector nucleases (TALEN) and Clustered Regularly Interspaced Short Palindromic Repeats (CRISPR) with the Cas9 nuclease) that enable precise genetic modifications at the single nucleotide level efficiently are gaining wide use in iPSC disease modeling, including the investigation of hematological diseases and cancers (90–92). Genome editing can be used to correct or introduce disease-associated mutations, individually or in combinations, into patient-specific iPSCs or normal iPSCs, respectively, thus enabling systemic interrogation of gene function and disease development (89, 93). In both correction or introduction of mutation cases, iPSCs will be generated that bear the same genomic background and only differ in the specific genetic alteration, thus, providing ideal, isogenic iPSC pairs for comparative analysis. Genome editing through non-homologous end-joining will generate frame-shift mutations through introduction of small, random nucleotide insertions or deletions (indels) and, hence, is well suited for monoallelic or biallelic inactivation of haploinsufficient or classical tumor-suppressor genes. On the other hand, homology-directed repair (HDR) utilizing co-delivery of homologous donor DNA template to guide the homologous recombination-mediated repair process, will generate precise modifications and, thus, can be used to study point mutations in disease/cancer-associate genes or associated regulatory regions. For example, using ZFN or TALEN-based HDR, several groups succeeded in correcting of the causative, single-nucleotide mutations in *HBB* in sickle cell disease (SCD) and  $\beta$ -thalassemia iPSC lines (66, 67, 76, 78). Ma et al. showed that two distinct  $\beta$ -thalassemia major patient-corrected iPSC lines showed increased erythrocyte colony formation of hematopoietic progenitors compared to their isogenic, mutant iPSCs (78). Papapetrou et al. have conducted some of the most elegant gene editing for hematological malignancy modeling (56). Using correction or introduction of mutations via CRISPR/Cas9 in combination with patient-specific diseased or normal iPSCs, they modeled various disease progression stages ranging from normal/healthy, preleukemic, low-risk MDS, high-risk MDS to MDS/AML (56) as well as the contribution of the splicing factor SRSF2p.P95L mutant to MDS alone or in the context of MDS with del(7q) (40).

Genome editing systems can also be used to introduce or revert large-scale genetic lesions often associated with specific malignancies, including chromosomal deletions, inversions and translocations (55, 94–97). Brunet et al. used ZFNs and TALENs in human cells, including embryonic stem cell-derived mesenchymal precursors to generate  $t_{(11;22)}(q24;q12)$  *EWSR1-FLI1* fusion and  $t_{(2;5)}(p23;q35)$  *NMP1-ALK* fusion genomic translocations associated with Ewing sarcoma and anaplastic large cell lymphoma, respectively, or to revert the  $t_{(2;5)}(p23;q35)$  *NMP1-ALK* translocation (95). Torres-Ruiz et al. using CRISPR/Cas9 successfully recreated the  $t_{(11;22)}(q24;q12)$  *EWSR1-FLI1* fusion translocation in iPSCs (97). Using the

adeno-associated vector-mediated gene targeting of an HSV-tk transgene approach, Papapetrou et al. generated various deletions of chromosome 7q that let them to identify an approximately 20 Mb region spanning 7q32.3-7q36.1 as the critical region in del(7q)-associated MDS (55). We together with our colleagues and the late Ihor R. Lemischka previously generated iPSCs from a Li-Fraumeni syndrome (LFS) family to investigate the oncogenic role of mutant TP53 in the development of LFS-osteosarcoma (58). In a follow up-study we identified SFRP2 as an autocrine and paracrine factor involved in P53 mutation-mediated osteosarcomagenesis. Using genome-editing we confirmed a correlation between various P53 mutations and increased SFRP2 expression in iPSC and embryonic stem cell derived osteoblasts (54) and Kim et al. (under review).

## INTEGRATION OF iPSCs WITH TISSUE ENGINEERING, THREE-DIMENSIONAL ORGANOID AND MICROPHYSIOLOGICAL SYSTEMS

Diseases and cancers do not occur in a two-dimensional vacuum of malignant cells in culture but rather involve complex interactions and communication with neighboring cells and the microenvironment. Cells in the niche and the extracellular matrix provide anchor, biomechanical support and spatiotemporally regulated biochemical signals and nutrients needed for disease initiation, progression and survival. The use of tissue engineering, three-dimensional organoids and MPS attempts to more faithfully mimic the *in vivo* cellular milieu, architectural structure, spatial organization and physiological parameters than two-dimensional culture systems ever could. Integration of directed differentiation of iPSCs with tissue engineering, organoid cultures MPS are being developed for many complex tissues such as the heart, liver, kidney, intestine, eye, and brain (98, 99).

Organoids derived from primary resected tumors or biopsies are hailed to create opportunities to build large biobanks with relevant patient material for cancer research, drug evaluation and therapy development (100–109). With the goal of modeling human diseases of the large intestine, Chen et al. developed an efficient colonic organoid (CO) strategy using embryonic stem cells and iPSCs (43). Through a stepwise differentiation protocol following progressive normal development of definitive endoderm to hindgut endoderm to subsequently COs, using patient-specific colorectal cancer familial adenomatous polyposis (FAP)-iPSCs that carry a germline nonsense mutation in *APC* causing early termination of translation, they were able to demonstrate enhanced WNT signaling and increased epithelial cell proliferation. Additionally, they used these FAP-iPSC COs as a platform for testing drugs (see *iPSCs in drug development & pharmacology*).

As discussed in *iPSCs in xenograft models*, Zaret et al. modeled PDAC development using PDAC-iPSCs in combination with *in vivo* transplantation (33). In order to establish an *in vitro* model of early stage human pancreatic cancer, they harvest the PanIN structures from the developing PDAC-iPSC-derived teratomas

and set up organoid cultures. The formed organoids retained PDAC-associated marker expression and served as a platform for biomarker identification.

MPS, also known as microfluidic organ-on-a-chip, offer a precise means to integrate cells, including iPSC-derived cell types and 3-dimensional constructs or organoids, into an *in vitro* dynamic system that further incorporates vascular flow and micro-biofabrication that mimics the systematic architectural and spatial compositions and interactions among different cell-types, tissues and organs in the body. Use of MPS in cancer research is gaining traction to investigate complex cancer, growth, tumor-niche interactions, metastatic invasion, and drug delivery, efficacy and toxicity (13–20). However, the incorporation of iPSCs or derived progenies into MPS is just beginning (110–113). Advances in generating higher-order MPS that are able to link individual systems into a physiome- or body-on-a-chip (114, 115) coupled with inline detectors and fluorescent reporters (116–119) will enable dynamic, real-time interrogation of cellular, molecular, and biomechanical parameters of disease pathogenesis (initiation and progression) and drug responses.

## iPSCs IN XENOGRAFT MODELS

Patient-derived xenografts (PDXs) have become a prominent model system as they are presumed to more faithfully capture the cellular, molecular and physiological characteristics of primary and metastatic malignancies (120, 121). Additionally, PDX-models are gaining attraction in such field as biomarker identification, drug development and assessment of drug responses (122).

Transplantation of iPSCs or derived cells into appropriate animal models can provide a more physiological, three-dimensional *in vivo* environment and, hence, expand their experimental utility. PDAC has a very poor prognosis and until the elegant study by Zaret et al. lacked a human cell model of early disease progression (33). Subcutaneous, injection of iPSCs into immunocompromised mice is a process used to assess the pluripotency of iPSCs through the formation of teratomas. When Zaret et al. injected PDAC-iPSCs, ductal structures formed within the developing teratomas that had a more prominent architectural organization compared to controls. Detailed cellular and molecular characterization of these structures led to the conclusion that they resembled PanIN-stage like structures that eventually further progressed to an invasive PDAC stage.

Majeti et al. established an AML model based on iPSCs generated from patients with rearrangements of the KMT2A/MLL locus (41). Using intravenous or orthotopic transplantation into immunocompromised mice to evaluate leukemia formation *in vivo* they found that the ability to give rise to leukemia *in vivo* is dependent on transplantation of AML-iPSC-derived hematopoietic cells as AML-iPSCs lacked leukemic potential. Additionally, despite retaining the leukemic-driver mutations, AML-iPSCs reset the leukemic DNA methylation and gene expression patterns. Surprisingly, hematopoietic differentiation of these AML-iPSCs and leukemia

formation was sufficient to reestablish the leukemic DNA methylation and gene expression profile strongly suggesting that the genetic mutations/rearrangements of the KMT2A/MLL locus in AML-iPSCs reactivate a leukemic program in the context of hematopoietic cells (41).

It was recently reported that copy number alterations recurrently observed in primary human tumors gradually disappeared in PDXs, suggesting that events undergoing positive selection in humans can become dispensable during propagation in mice (123). In light of this observation and its critical implications for PDX-based disease/cancer modeling, cytogenetic analyses of PDX-donor cells after *in vivo* transplantation and propagation appears important in order to know whether the attempted PDX-model accurately retains the genetic lesions present in the original malignant cells or if they evolve, and if they evolve whether the evolution is specific to the patient or the host.

## iPSCs IN DRUG DEVELOPMENT AND PHARMACOLOGY

The cost of drug development from discovery, through clinical trials to approval and marketing is in excess of \$2.6 billion (124). As costly as clinical trials are, drug failures are key contributors to development costs. Induced PSCs and derived cells are gaining attraction and are being more widely used in translational-research settings, including discovery and validation of biomarkers and therapeutic targets, compound screening for drug discovery and drug repurposing, and preclinical drug susceptibility, efficacy and toxicity studies (33, 39, 41, 43, 57, 65, 72, 73, 110, 125–131). Of particular usefulness is that many different cell type, including cardiomyocytes, hepatocytes, neurons, and hematopoietic cells, can readily be generated from a diverse set (age, gender, race/ethnicity) of iPSCs from healthy individuals or patients with a given disease/cancer. This has been exemplified in the use of iPSCs in drug toxicity screening. Therapeutically effective drugs can cause serious unintended adverse events that limit or even prohibit their use. Several groups have used iPSC-derived cardiomyocytes to model and investigate anticancer drug-induced cardiotoxicity (132–137). In one case, cardiomyocytes generated from iPSCs from breast cancer patients were able to recapitulate patient-specific doxorubicin-induced cardiotoxicity at the cellular level (134). Another application is the evaluation of drug susceptibility and variable responses of phenotypic distinct cell populations, cancer subclones or patients (39, 41, 57, 65, 72, 73). Primary or acquired-drug resistance is a serious clinical problem. Induced PSCs derived either from drug-sensitive and drug-resistance patients or from cells of the same patients at the drug-sensitive and drug-resistant stage and iPSC derived cells might help decipher the mechanisms underlying drug-resistance. Examples along this line are from Bedel et al. (39) and Kumano et al. (57). They derived iPSC lines from CML patients that carry the abnormal Philadelphia chromosome that resulted from a translocation between chromosome 22 and 9 leading to the fused, oncogenic BCR-ABL tyrosine kinase. While both groups reported

that the generated CML-iPSC lines were resistant to the tyrosine kinase inhibitor imatinib, which is used to treat CML patients, Bedel *et al.* (39) found that CD34<sup>+</sup> hematopoietic progenitors obtained from their patient's CML-iPSCs were partially sensitive to imatinib and Kumano *et al.* (57) found imatinib-sensitivity in CML-iPSC derived CD34<sup>-</sup> hematopoietic cells but not CD34<sup>+</sup> hematopoietic progenitors, which recapitulated the pathophysiological feature of initial CML of that patient. In depth molecular characterization at the epigenome, transcriptome and proteome level will be necessary to discover the signaling networks responsible for the observed behavior. Induced PSCs and derived cells also present an opportunity for phenotypic drug testing and screening. This can be especially attractive for diseases with no previously characterized targets or drug treatment strategies. However, such phenotypic drug testing and screening requires the ability to identify cellular phenotypes or functional properties, such as proliferation, apoptosis, activation of a specific signaling pathway, a distinct metabolic profile that correlate with patient phenotypes and responses and thus can serve as surrogate readouts of therapeutic effectiveness (43, 110, 117, 130, 138). Undoubtedly, the next stage in drug discovery and pharmacological testing will expand on the integration of iPSC-based model systems with three-dimensional organoids and MPS (43, 110).

## CONCLUDING REMARKS

iPSC technology started a new, exciting era in biomedicine. The ease by which patient-specific iPSCs from various primary

or metastatic somatic tissues and blood of patients with hematological diseases and cancers can be derived provides a self-renewable, scalable and cryopreservable source of cells with the patient's genetic background. iPSCs are readily enable to genome-editing in order to either correct or introduce known or suspected disease-associated mutations. This novel tool enables attempts to successfully recapitulate various pathological disease states and features associated with malignancies in a patient-specific context. Integration of iPSC-based disease and cancer models with advanced, bioengineered physiological systems, *in vivo* PDX models, automated high-throughput-screening tools and next-generation omics approaches will lead to a greater mechanistic understanding of disease/cancer, the relationship between malignant cells and their microenvironment, and drug responses. Undoubtedly, iPSC technology is revolutionizing the way we approach disease modeling, preclinical cancer research, drug development and precision medicine.

## AUTHOR CONTRIBUTIONS

All authors listed have made a substantial, direct and intellectual contribution to the work, and approved it for publication.

## ACKNOWLEDGMENTS

The authors wish to acknowledge the late Ihor R. Lemischka for his support and mentorship over the years. HK is the recipient of an NCI Pre- to Post-doctoral Transition Award (1F99CA212489).

## REFERENCES

1. Liu X, Ory V, Chapman S, Yuan H, Albanese C, Kallakury B, et al. ROCK inhibitor and feeder cells induce the conditional reprogramming of epithelial cells. *Am J Pathol.* (2012) 180:599–607. doi: 10.1016/j.ajpath.2011.10.036
2. Suprynowicz FA, Upadhyay G, Krawczyk E, Kramer SC, Hebert JD, Liu X, et al. Conditionally reprogrammed cells represent a stem-like state of adult epithelial cells. *Proc Natl Acad Sci USA.* (2012) 109:20035–40. doi: 10.1073/pnas.1213241109
3. Liu X, Krawczyk E, Suprynowicz FA, Palechor-Ceron N, Yuan H, Dakic A, et al. Conditional reprogramming and long-term expansion of normal and tumor cells from human biospecimens. *Nat Protoc.* (2017) 12:439–51. doi: 10.1038/nprot.2016.174
4. Lai Y, Wei X, Lin S, Qin L, Cheng LLi P. Current status and perspectives of patient-derived xenograft models in cancer research. *J Hematol Oncol.* (2017) 10:106. doi: 10.1186/s13045-017-0470-7
5. Borodovsky A, McQuiston TJ, Stetson D, Ahmed A, Whitston D, Zhang J, et al. Generation of stable PDX derived cell lines using conditional reprogramming. *Mol Cancer.* (2017) 16:177. doi: 10.1186/s12943-017-0745-1
6. Sachs NC, Clevers H. Organoid cultures for the analysis of cancer phenotypes. *Curr Opin Genet Dev.* (2014) 24:68–73. doi: 10.1016/j.gde.2013.11.012
7. Fatehullah A, Tan SH, Barker N. Organoids as an *in vitro* model of human development and disease. *Nat Cell Biol.* (2016) 18:246–54. doi: 10.1038/ncb3312
8. Kretzschmar K, Clevers H. Organoids: modeling development and the stem cell niche in a dish. *Dev Cell.* (2016) 38:590–600. doi: 10.1016/j.devcel.2016.08.014
9. Weeber F, Ooft SN, Dijkstra KK, Voest EE. Tumor organoids as a pre-clinical cancer model for drug discovery. *Cell Chem Biol.* (2017) 24:1092–100. doi: 10.1016/j.chembiol.2017.06.012
10. Hutmacher DW, Horch RE, Loessner D, Rizzi S, Sieh S, Reichert JC, et al. Translating tissue engineering technology platforms into cancer research. *J Cell Mol Med.* (2009) 13:1417–27. doi: 10.1111/j.1582-4934.2009.00853.x
11. Hutmacher DW, Loessner D, Rizzi S, Kaplan DL, Mooney DJ, Clements JA. Can tissue engineering concepts advance tumor biology research? *Trends Biotechnol.* (2010) 28:125–33. doi: 10.1016/j.tibtech.2009.12.001
12. Holzapfel BM, Wagner F, Thibaudeau L, Levesque JP, Hutmacher DW. Concise review: humanized models of tumor immunology in the 21st century: convergence of cancer research and tissue engineering. *Stem Cells* (2015) 33:1696–704. doi: 10.1002/stem.1978
13. Hu S, Liu G, Chen W, Li X, Lu W, Lam RH, et al. Multiparametric biomechanical and biochemical phenotypic profiling of single cancer cells using an elasticity microcytometer. *Small* (2016) 12:2300–11. doi: 10.1002/smll.201503620
14. Portillo-Lara RA, Annabi N. Microengineered cancer-on-a-chip platforms to study the metastatic microenvironment. *Lab Chip.* (2016) 16:4063–81. doi: 10.1039/c6lc00718j
15. Fan Q, Liu R, Jiao Y, Tian C, Farrell JD, Diao W, et al. A novel 3-D bio-microfluidic system mimicking *in vivo* heterogeneous tumour microstructures reveals complex tumour-stroma interactions. *Lab Chip* (2017) 17:2852–60. doi: 10.1039/c7lc00191f
16. Armbrecht L, Gabernet G, Kurth F, Hiss JA, Schneider GD, Trichler PS. Characterisation of anticancer peptides at the single-cell level. *Lab Chip* (2017) 17:2933–40. doi: 10.1039/c7lc00505a
17. Low LAT, Tagle DA. Tissue chips - innovative tools for drug development and disease modeling. *Lab Chip* (2017) 17:3026–36. doi: 10.1039/c7lc00462a
18. Huang YL, Segall JE, Wu M. Microfluidic modeling of the biophysical microenvironment in tumor cell invasion. *Lab Chip* (2017) 17:3221–33. doi: 10.1039/c7lc00623c

19. Caballero D, Blackburn SM, de Pablo M, Samitier J, Albertazzi L. Tumour-vessel-on-a-chip models for drug delivery. *Lab Chip* (2017) 17:3760–71. doi: 10.1039/c7lc00574a
20. Hassell BA, Goyal G, Lee E, Sontheimer-Phelps A, Levy O, Chen CS, et al. Human organ chip models recapitulate orthotopic lung cancer growth, therapeutic responses, and tumor dormancy *in vitro*. *Cell Rep.* (2017) 21:508–16. doi: 10.1016/j.celrep.2017.09.043
21. Takahashi KY, Yamana S. Induction of pluripotent stem cells from mouse embryonic and adult fibroblast cultures by defined factors. *Cell* (2006) 126:663–76. doi: 10.1016/j.cell.2006.07.024
22. Yu J, Vodyanik MA, Smuga-Otto K, Antosiewicz-Bourget J, Frane JL, Tian S, et al. Induced pluripotent stem cell lines derived from human somatic cells. *Science* (2007) 318:1917–20. doi: 10.1126/science.1151526
23. Takahashi K, Tanabe K, Ohnuki M, Narita M, Ichisaka T, Tomoda K, et al. Induction of pluripotent stem cells from adult human fibroblasts by defined factors. *Cell* (2007) 131:861–72. doi: 10.1016/j.cell.2007.11.019
24. Park IH, Zhao R, West JA, Yabuuchi A, Huo H, Ince TA, et al. Reprogramming of human somatic cells to pluripotency with defined factors. *Nature* (2008) 451:141–6. doi: 10.1038/nature06534
25. Lin SL, Chang DC, Chang-Lin S, Lin CH, Wu DT, Chen DT, et al. Mir-302 reprograms human skin cancer cells into a pluripotent ES-cell-like state. *RNA* (2008) 14:2115–24. doi: 10.1261/rna.1162708
26. Utikal J, Maherli N, Kulalert W, Hochedlinger K. Sox2 is dispensable for the reprogramming of melanocytes and melanoma cells into induced pluripotent stem cells. *J Cell Sci.* (2009) 122(Pt 19):3502–10. doi: 10.1242/jcs.054783
27. Miyoshi N, Ishii H, Nagai K, Hoshino H, Mimori K, Tanaka F, et al. Defined factors induce reprogramming of gastrointestinal cancer cells. *Proc Natl Acad Sci USA.* (2010) 107:40–5. doi: 10.1073/pnas.0912407107
28. Carette JE, Pruszak J, Varadarajan M, Blomen VA, Gokhale S, Camargo FD, et al. Generation of iPSCs from cultured human malignant cells. *Blood* (2010) 115:4039–42. doi: 10.1182/blood-2009-07-231845
29. Mathieu J, Zhang Z, Zhou W, Wang AJ, Heddleston JM, Pinna CM, et al. HIF induces human embryonic stem cell markers in cancer cells. *Cancer Res.* (2011) 71:4640–52. doi: 10.1158/0008-5472.CAN-10-3320
30. Zhang X, Cruz FD, Terry M, Remotti FM,atushansky I. Terminal differentiation and loss of tumorigenicity of human cancers via pluripotency-based reprogramming. *Oncogene* (2013) 32:2249–60, 60 e1–21. doi: 10.1038/onc.2012.237
31. Mahalingam D, Kong CM, Lai J, Tay LL, Yang HW, Wang X. Reversal of aberrant cancer methylome and transcriptome upon direct reprogramming of lung cancer cells. *Sci Rep.* (2012) 2:592. doi: 10.1038/srep00592
32. Stricker SH, Feber A, Engstrom PG, Caren H, Kurian KM, Takashima Y, et al. Widespread resetting of DNA methylation in glioblastoma-initiating cells suppresses malignant cellular behavior in a lineage-dependent manner. *Genes Dev.* (2013) 27:654–69. doi: 10.1101/gad.212662.112
33. Kim J, Hoffman JP, Alpaugh RK, Rhim AD, Reichert M, Stanger BZ, et al. An iPSC line from human pancreatic ductal adenocarcinoma undergoes early to invasive stages of pancreatic cancer progression. *Cell Rep.* (2013) 3:2088–99. doi: 10.1016/j.celrep.2013.05.036
34. Corominas-Faja B, Cufi S, Oliveras-Ferraro C, Cuyas E, Lopez-Bonet E, Lupu R, et al. Nuclear reprogramming of luminal-like breast cancer cells generates Sox2-overexpressing cancer stem-like cellular states harboring transcriptional activation of the mTOR pathway. *Cell Cycle* (2013) 12:3109–24. doi: 10.4161/cc.26173
35. Choong PF, Teh HX, Teoh HK, Ong HK, Choo KB, Sugii S, et al. Heterogeneity of osteosarcoma cell lines led to variable responses in reprogramming. *Int J Med Sci.* (2014) 11:1154–60. doi: 10.7150/ijms.8281
36. Moore JB, Loeb DM, Hong KU, Sorensen PH, Triche TJ, Lee DW, et al. Epigenetic reprogramming and re-differentiation of a Ewing sarcoma cell line. *Front Cell Dev Biol.* (2015) 3:15. doi: 10.3389/fcell.2015.00015
37. Verusgam ND, Yeap SK, Ky H, Paterson IC, Khoo SP, Cheong SK, et al. Susceptibility of Human Oral Squamous Cell Carcinoma (OSCC) H103 and H376 cell lines to Retroviral OSKM mediated reprogramming. *PeerJ.* (2017) 5:e3174. doi: 10.7717/peerj.3174
38. Antony-Debre I, Manchev VT, Balayev N, Bluteau D, Tomowiak C, Legrand C, et al. Level of RUNX1 activity is critical for leukemic predisposition but not for thrombocytopenia. *Blood* (2015) 125:930–40. doi: 10.1182/blood-2014-06-585513
39. Bedel A, Pasquet JM, Lippert E, Taillepierre M, Lagarde V, Dabernat S, et al. Variable behavior of iPSCs derived from CML patients for response to TKI and hematopoietic differentiation. *PLoS ONE* (2013) 8:e71596. doi: 10.1371/journal.pone.0071596
40. Chang CJ, Kotini AG, Olszewska M, Georgomanoli M, Teruya-Feldstein J, Sperber H, et al. Dissecting the contributions of cooperating gene mutations to cancer phenotypes and drug responses with patient-derived iPSCs. *Stem Cell Reports* (2018) 10:1610–24. doi: 10.1016/j.stemcr.2018.03.020
41. Chao MP, Gentles AJ, Chatterjee S, Lan F, Reinisch A, Corces MR, et al. Human AML-iPSCs reacquire leukemic properties after differentiation and model clonal variation of disease. *Cell Stem Cell* (2017) 20:329–44 e7. doi: 10.1016/j.stem.2016.11.018
42. Connelly JP, Kwon EM, Gao Y, Trivedi NS, Elkahloun AG, Horwitz MS, et al. Targeted correction of RUNX1 mutation in FPD patient-specific induced pluripotent stem cells rescues megakaryopoietic defects. *Blood* (2014) 124:1926–30. doi: 10.1182/blood-2014-01-550525
43. Crespo M, Vilar E, Tsai SY, Chang K, Amin S, Srinivasan T, et al. Colonic organoids derived from human induced pluripotent stem cells for modeling colorectal cancer and drug testing. *Nat Med.* (2017) 23:878–84. doi: 10.1038/nm.4355
44. Doulatov S, Vo LT, Macari ER, Wahlster L, Kinney MA, Taylor AM, et al. Drug discovery for Diamond-Blackfan anemia using reprogrammed hematopoietic progenitors. *Sci Transl Med.* (2017) 9:eaah5645. doi: 10.1126/scitranslmed.aah5645
45. Espinoza JL, Elbadry MI, Chonabayashi K, Yoshida Y, Katagiri T, Harada K, et al. Hematopoiesis by iPSC-derived hematopoietic stem cells of aplastic anemia that escape cytotoxic T-cell attack. *Blood Adv.* (2018) 2:390–400. doi: 10.1182/bloodadvances.2017013342
46. Gandre-Babbe S, Paluru P, Aribanea C, Chou ST, Bresolin S, Lu L, et al. Patient-derived induced pluripotent stem cells recapitulate hematopoietic abnormalities of juvenile myelomonocytic leukemia. *Blood* (2013) 121:4925–9. doi: 10.1182/blood-2013-01-478412
47. Garcon L, Ge J, Manjunath SH, Mills JA, Apicella M, Parikh S, et al. Ribosomal and hematopoietic defects in induced pluripotent stem cells derived from Diamond Blackfan anemia patients. *Blood* (2013) 122:912–21. doi: 10.1182/blood-2013-01-478321
48. Hadoux J, Feraud O, Griscelli F, Opolon P, Divers D, Gobbo E, et al. Generation of an induced pluripotent stem cell line from a patient with hereditary multiple endocrine neoplasia 2A (MEN2A) syndrome with RET mutation. *Stem Cell Res.* (2016) 17:154–57. doi: 10.1016/j.scr.2016.06.008
49. Hosoi M, Kumano K, Taoka K, Arai S, Kataoka K, Ueda K, et al. Generation of induced pluripotent stem cells derived from primary and secondary myelofibrosis patient samples. *Exp Hematol.* (2014) 42:816–25. doi: 10.1016/j.exphem.2014.03.010
50. Hu K, Yu J, Sukuntha K, Tian S, Montgomery K, Choi KD, et al. Efficient generation of transgene-free induced pluripotent stem cells from normal and neoplastic bone marrow and cord blood mononuclear cells. *Blood* (2011) 117:e109–19. doi: 10.1182/blood-2010-07-298331
51. Hu L, Du L, Zhao Y, Li W, Ouyang Q, Zhou D, et al. Modeling Glanzmann thrombasthenia using patient specific iPSCs and restoring platelet aggregation function by CD41 overexpression. *Stem Cell Res.* (2017) 20:14–20. doi: 10.1016/j.scr.2017.02.003
52. Iizuka H, Kagoya Y, Kataoka K, Yoshimi A, Miyauchi M, Taoka K, et al. Targeted gene correction of RUNX1 in induced pluripotent stem cells derived from familial platelet disorder with propensity to myeloid malignancy restores normal megakaryopoiesis. *Exp Hematol.* (2015) 43:849–57. doi: 10.1016/j.exphem.2015.05.004
53. Julian LM, Delaney SP, Wang Y, Goldberg AA, Dore C, Yockell-Lelievre J, et al. Human pluripotent stem cell-derived TSC2-haploinsufficient smooth muscle cells recapitulate features of lymphangiomyomatosis. *Cancer Res.* (2017) 77:5491–502. doi: 10.1158/0008-5472.CAN-17-0925
54. Kim HS, Yoo S, Bernitz JM, Yuan Y, Gomes AM, Daniel MG, et al. Oncogenic role of sFRP2 in P53-mutant osteosarcoma development via autocrine and paracrine mechanism. *bioRxiv* (2018). doi: 10.1101/246454. [Epub ahead of print].
55. Kotini AG, Chang CJ, Boussaad I, Delrow JJ, Dolezal EK, Nagulapally AB, et al. Functional analysis of a chromosomal deletion associated with

- myelodysplastic syndromes using isogenic human induced pluripotent stem cells. *Nat Biotechnol.* (2015) 33:646–55. doi: 10.1038/nbt.3178
56. Kotini AG, Chang CJ, Chow A, Yuan H, Ho TC, Wang T, et al. Stage-specific human induced pluripotent stem cells map the progression of myeloid transformation to transplantable leukemia. *Cell Stem Cell* (2017) 20:315–28 e7. doi: 10.1016/j.stem.2017.01.009
  57. Kumano K, Arai S, Hosoi M, Taoka K, Takayama N, Otsu M, et al. Generation of induced pluripotent stem cells from primary chronic myelogenous leukemia patient samples. *Blood* (2012) 119:6234–42. doi: 10.1182/blood-2011-07-367441
  58. Lee DF, Su J, Kim HS, Chang B, Papatsenko D, Zhao R, et al. Modeling familial cancer with induced pluripotent stem cells. *Cell* (2015) 161:240–54. doi: 10.1016/j.cell.2015.02.045
  59. Lee JH, Salci KR, Reid JC, Orlando L, Tanasijevic B, Shapovalova Z, et al. Brief report: human acute myeloid leukemia reprogramming to pluripotency is a rare event and selects for patient hematopoietic cells devoid of leukemic mutations. *Stem Cells* (2017) 35:2095–102. doi: 10.1002/stem.2655
  60. Melguizo-Sanchis D, Xu Y, Taheem D, Yu M, Tilgner K, Barta T, et al. iPSC modeling of severe aplastic anemia reveals impaired differentiation and telomere shortening in blood progenitors. *Cell Death Dis.* (2018) 9:128. doi: 10.1038/s41419-017-0141-1
  61. Mulero-Navarro S, Sevilla A, Roman AC, Lee DF, D’Souza SL, Pardo S, et al. Myeloid dysregulation in a human induced pluripotent stem cell model of PTPN11-associated juvenile myelomonocytic leukemia. *Cell Rep.* (2015) 13:504–15. doi: 10.1016/j.celrep.2015.09.019
  62. Muller LU, Milsom MD, Harris CE, Vyas R, Brumme KM, Parmar K, et al. Overcoming reprogramming resistance of Fanconi anemia cells. *Blood* (2012) 119:5449–57. doi: 10.1182/blood-2012-02-408674
  63. Orban M, Goedel A, Haas J, Sandrock-Lang K, Gartner F, Jung CB, et al. Functional comparison of induced pluripotent stem cell- and blood-derived GPIIbIIa deficient platelets. *PLoS ONE* (2015) 10:e0115978. doi: 10.1371/journal.pone.0115978
  64. Sakurai M, Kunimoto H, Watanabe N, Fukuchi Y, Yuasa S, Yamazaki S, et al. Impaired hematopoietic differentiation of RUNX1-mutated induced pluripotent stem cells derived from FPD/AML patients. *Leukemia* (2014) 28:2344–54. doi: 10.1038/leu.2014.136
  65. Saliba J, Hamidi S, Lenglet G, Langlois T, Yin J, Cabagnols X, et al. Heterozygous and homozygous JAK2(V617F) states modeled by induced pluripotent stem cells from myeloproliferative neoplasm patients. *PLoS ONE* (2013) 8:e74257. doi: 10.1371/journal.pone.0074257
  66. Sebastian V, Maeder ML, Angstman JE, Haddad B, Khayter C, Yeo DT, et al. In situ genetic correction of the sickle cell anemia mutation in human induced pluripotent stem cells using engineered zinc finger nucleases. *Stem Cells* (2011) 29:1717–26. doi: 10.1002/stem.718
  67. Sun NZhao H. Seamless correction of the sickle cell disease mutation of the HBB gene in human induced pluripotent stem cells using TALENs. *Biotechnol Bioeng* (2014) 111:1048–53. doi: 10.1002/bit.25018
  68. Suzuki NM, Niwa A, Yabe M, Hira A, Okada C, Amano N, et al. Pluripotent cell models of fanconi anemia identify the early pathological defect in human hemoangiogenic progenitors. *Stem Cells Transl Med.* (2015) 4:333–8. doi: 10.5966/scbm.2013-0172
  69. Takei H, Edahiro Y, Mano S, Masubuchi N, Mizukami Y, Imai M, et al. Skewed megakaryopoiesis in human induced pluripotent stem cell-derived haematopoietic progenitor cells harbouring calreticulin mutations. *Br J Haematol.* (2018) 181:791–802. doi: 10.1111/bjh.15266
  70. Tulpule A, Kelley JM, Lensch MW, McPherson J, Park IH, Hartung O, et al. Pluripotent stem cell models of Shwachman-Diamond syndrome reveal a common mechanism for pancreatic and hematopoietic dysfunction. *Cell Stem Cell* (2013) 12:727–36. doi: 10.1016/j.stem.2013.04.002
  71. Varela I, Karagiannidou A, Oikonomakis V, Tzetzis M, Tzanoudaki M, Siapati EK, et al. Generation of human beta-thalassemia induced pluripotent cell lines by reprogramming of bone marrow-derived mesenchymal stromal cells using modified mRNA. *Cell Reprogram* (2014) 16:447–55. doi: 10.1089/cell.2014.0050
  72. Yamamoto S, Otsu M, Matsuzaka E, Konishi C, Takagi H, Hanada S, et al. Screening of drugs to treat 8p11 myeloproliferative syndrome using patient-derived induced pluripotent stem cells with fusion gene CEP110-FGFR1. *PLoS ONE* (2015) 10:e0120841. doi: 10.1371/journal.pone.0120841
  73. Ye Z, Liu CF, Lanikova L, Dowey SN, He C, Huang X, et al. Differential sensitivity to JAK inhibitory drugs by isogenic human erythroblasts and hematopoietic progenitors generated from patient-specific induced pluripotent stem cells. *Stem Cells* (2014) 32:269–78. doi: 10.1002/stem.1545
  74. Ye Z, Zhan H, Mali P, Dowey S, Williams DM, Jang YY, et al. Human-induced pluripotent stem cells from blood cells of healthy donors and patients with acquired blood disorders. *Blood* (2009) 114:5473–80. doi: 10.1182/blood-2009-04-217406
  75. Yung SK, Tilgner K, Ledran MH, Habibollah S, Neganova I, Singhapol C, et al. Brief report: human pluripotent stem cell models of fanconi anemia deficiency reveal an important role for fanconi anemia proteins in cellular reprogramming and survival of hematopoietic progenitors. *Stem Cells* (2013) 31:1022–9. doi: 10.1002/stem.1308
  76. Zou J, Mali P, Huang X, Dowey SN, Cheng L. Site-specific gene correction of a point mutation in human iPS cells derived from an adult patient with sickle cell disease. *Blood* (2011) 118:4599–608. doi: 10.1182/blood-2011-02-335554
  77. Maclean GA, Menne TF, Guo G, Sanchez DJ, Park IH, Daley GQ, et al. Altered hematopoiesis in trisomy 21 as revealed through *in vitro* differentiation of isogenic human pluripotent cells. *Proc Natl Acad Sci USA.* (2012) 109:17567–72. doi: 10.1073/pnas.1215468109
  78. Ma N, Liao B, Zhang H, Wang L, Shan Y, Xue Y, et al. Transcription activator-like effector nuclease (TALEN)-mediated gene correction in integration-free beta-thalassemia induced pluripotent stem cells. *J Biol Chem.* (2013) 288:34671–9. doi: 10.1074/jbc.M113.496174
  79. Hadoux J, Desterke C, Feraud O, Guibert M, De Rose RF, Opolon P, et al. Transcriptional landscape of a RET(C634Y)-mutated iPSC and its CRISPR-corrected isogenic control reveals the putative role of EGR1 transcriptional program in the development of multiple endocrine neoplasia type 2A-associated cancers. *Stem Cell Res.* (2018) 26:8–16. doi: 10.1016/j.scr.2017.11.015
  80. Song WJ, Sullivan MG, Legare RD, Hutchings S, Tan X, Kufrin D, et al. Haplinsufficiency of CBFA2 causes familial thrombocytopenia with propensity to develop acute myelogenous leukaemia. *Nat Genet.* (1999) 23:166–75. doi: 10.1038/13793
  81. Bellissimo DC, Speck NA. RUNX1 Mutations in Inherited and Sporadic Leukemia. *Front Cell Dev Biol.* (2017) 5:111. doi: 10.3389/fcell.2017.00111
  82. Salci KR, Lee JH, Laronde S, Dingwall S, Kushwah R, Fiebig-Comyn A, et al. Cellular reprogramming allows generation of autologous hematopoietic progenitors from AML patients that are devoid of patient-specific genomic aberrations. *Stem Cells* (2015) 33:1839–49. doi: 10.1002/stem.1994
  83. Raya A, Rodriguez-Piza I, Guenechea G, Vassena R, Navarro S, Barrero MJ, et al. Disease-corrected haematopoietic progenitors from Fanconi anaemia induced pluripotent stem cells. *Nature* (2009) 460:53–9. doi: 10.1038/nature08129
  84. Munoz-Lopez A, Romero-Moya D, Prieto C, Ramos-Mejia V, Agraz-Doblas A, Varela I, et al. Development refractoriness of MLL-rearranged human B cell acute leukemias to reprogramming into pluripotency. *Stem Cell Rep.* (2016) 7:602–18. doi: 10.1016/j.stemcr.2016.08.013
  85. Taniguchi TD, Andrea AD. Molecular pathogenesis of Fanconi anemia: recent progress. *Blood* (2006) 107:4223–33. doi: 10.1182/blood-2005-10-4240
  86. Vicente-Duenas C, Hauer J, Ruiz-Roca L, Ingenhag D, Rodriguez-Meira A, Auer F, et al. Tumoral stem cell reprogramming as a driver of cancer: Theory, biological models, implications in cancer therapy. *Semin Cancer Biol.* (2015) 32:3–9. doi: 10.1016/j.semcancer.2014.02.001
  87. Papp BP, Lath K. Reprogramming to pluripotency: stepwise resetting of the epigenetic landscape. *Cell Res.* (2011) 21:486–501. doi: 10.1038/cr.2011.28
  88. Hashimoto K, Yamada Y, Semi K, Yagi M, Tanaka A, Itakura F, et al. Cellular context-dependent consequences of Apc mutations on gene regulation and cellular behavior. *Proc Natl Acad Sci USA.* (2017) 114:758–63. doi: 10.1073/pnas.1614197114
  89. Hockemeyer D, Jaenisch R. Induced pluripotent stem cells meet genome editing. *Cell Stem Cell* (2016) 18:573–86. doi: 10.1016/j.stem.2016.04.013
  90. Chen S, Sun H, Miao KD, Deng CX. CRISPR-Cas9: from genome editing to cancer research. *Int J Biol Sci.* (2016) 12:1427–36. doi: 10.7150/ijbs.17421
  91. Moses C, Garcia-Bloj B, Harvey AR, Blancafort P. Hallmarks of cancer: The CRISPR generation. *Eur J Cancer* (2018) 93:10–8. doi: 10.1016/j.ejca.2018.01.002

92. Ratan ZA, Son YJ, Haidere MF, Uddin BMM, Yusuf MA, Zaman SB, et al. CRISPR-Cas9: a promising genetic engineering approach in cancer research. *Ther Adv Med Oncol.* (2018) 10:1758834018755089. doi: 10.1177/1758834018755089
93. Kim HS, Bernitz JM, Lee DF, Lemischka IR. Genomic editing tools to model human diseases with isogenic pluripotent stem cells. *Stem Cells Dev.* (2014) 23:2673–86. doi: 10.1089/scd.2014.0167
94. Brunet E, Simsek D, Tomishima M, DeKelver R, Choi VM, Gregory P, et al. Chromosomal translocations induced at specified loci in human stem cells. *Proc Natl Acad Sci USA.* (2009) 106:10620–5. doi: 10.1073/pnas.0902076106
95. Piganeau M, Ghezraoui H, De Cian A, Guittat L, Tomishima M, Perrouault L, et al. Cancer translocations in human cells induced by zinc finger and TALE nucleases. *Genome Res.* (2013) 23:1182–93. doi: 10.1101/gr.147314.112
96. Maddalo D, Manchado E, Concepcion CP, Bonetti C, Vidigal JA, Han YC, et al. *In vivo* engineering of oncogenic chromosomal rearrangements with the CRISPR/Cas9 system. *Nature* (2014) 516:423–7. doi: 10.1038/nature13902
97. Torres-Ruiz R, Martinez-Lage M, Martin MC, Garcia A, Bueno C, Castano J, et al. Efficient recreation of t(11;22) EWSR1-FLI1(+) in human stem cells using CRISPR/Cas9. *Stem Cell Rep.* (2017) 8:1408–20. doi: 10.1016/j.stemcr.2017.04.014
98. Lancaster MAK, Knoblich JA. Organogenesis in a dish: modeling development and disease using organoid technologies. *Science* (2014) 345:1247125. doi: 10.1126/science.1247125
99. Liu C, Oikonomopoulos A, Sayed NWU JC. Modeling human diseases with induced pluripotent stem cells: from 2D to 3D and beyond. *Development* (2018) 145:dev156166. doi: 10.1242/dev.156166
100. Sato T, Stange DE, Ferrante M, Vries RG, Van Es JH, Van den Brink S, et al. Long-term expansion of epithelial organoids from human colon, adenoma, adenocarcinoma, and Barrett's epithelium. *Gastroenterology* (2011) 141:1762–72. doi: 10.1053/j.gastro.2011.07.050
101. Gao D, Vela I, Sboner A, Iaquinta PJ, Karthaus WR, Gopalan A, et al. Organoid cultures derived from patients with advanced prostate cancer. *Cell* (2014) 159:176–87. doi: 10.1016/j.cell.2014.08.016
102. Boj SF, Hwang CI, Baker LA, Chio, II, Engle DD, Corbo V, et al. Organoid models of human and mouse ductal pancreatic cancer. *Cell* (2015) 160:324–38. doi: 10.1016/j.cell.2014.12.021
103. van de Wetering M, Frances HE, Francis JM, Bounova G, Iorio F, Pronk A, et al. Prospective derivation of a living organoid biobank of colorectal cancer patients. *Cell* (2015) 161:933–45. doi: 10.1016/j.cell.2015.03.053
104. Huang L, Holtzinger A, Jagan I, BeGora M, Lohse I, Ngai N, et al. Ductal pancreatic cancer modeling and drug screening using human pluripotent stem cell- and patient-derived tumor organoids. *Nat Med.* (2015) 21:1364–71. doi: 10.1038/nm.3973
105. Sachs N, de Ligt J, Kopper O, Gogola E, Bounova G, Weeber F, et al. A living biobank of breast cancer organoids captures disease heterogeneity. *Cell* (2018) 172:373–86 e10. doi: 10.1016/j.cell.2017.11.010
106. Mazzocchi AR, Rajan SAP, Votanopoulos KI, Hall ARSkardal A. *In vitro* patient-derived 3D mesothelioma tumor organoids facilitate patient-centric therapeutic screening. *Sci Rep.* (2018) 8:2886. doi: 10.1038/s41598-018-21200-8
107. Vlachogiannis G, Hediat S, Vatsiou A, Jamin Y, Fernandez-Mateos J, Khan K, et al. Patient-derived organoids model treatment response of metastatic gastrointestinal cancers. *Science* (2018) 359:920–26. doi: 10.1126/science.aao2774
108. Drost J, Clevers H. Organoids in cancer research. *Nat Rev Cancer* (2018) 18:407–18. doi: 10.1038/s41568-018-0007-6
109. Seidlitz T, Merker SR, Rothe A, Zakrzewski F, von Neubeck C, Grutzmann K, et al. Human gastric cancer modelling using organoids. *Gut* (2018). doi: 10.1136/gutjnl-2017-314549. [Epub ahead of print]
110. Mathur A, Loskill P, Shao K, Huebsch N, Hong S, Marcus SG, et al. Human iPSC-based cardiac microphysiological system for drug screening applications. *Sci Rep.* (2015) 5:8883. doi: 10.1038/srep08883
111. Giobbe GG, Michelin F, Luni C, Giulitti S, Martewicz S, Dupont S, et al. Functional differentiation of human pluripotent stem cells on a chip. *Nat Methods* (2015) 12:637–40. doi: 10.1038/nmeth.3411
112. Marsano A, Conficoni C, Lemme M, Occhetta P, Gaudiello E, Votta E, et al. Beating heart on a chip: a novel microfluidic platform to generate functional 3D cardiac microtissues. *Lab Chip* (2016) 16:599–610. doi: 10.1039/c5lc01356a
113. Musah S, Mammo A, Ferrante TC, Jeanty SSF, Hirano-Kobayashi M, Mammo T, et al. Mature induced-pluripotent-stem-cell-derived human podocytes reconstitute kidney glomerular-capillary-wall function on a chip. *Nat Biomed Eng.* (2017) 1:0069. doi: 10.1038/s41551-017-0069
114. Maschmeyer I, Lorenz AK, Schimek K, Hasenberg T, Ramme AP, Hubner J, et al. A four-organ-chip for interconnected long-term co-culture of human intestine, liver, skin and kidney equivalents. *Lab Chip* (2015) 15:2688–99. doi: 10.1039/c5lc00392j
115. Edington CD, Chen WLK, Geishecker E, Kassis T, Soenksen LR, Bhushan BM, et al. Interconnected microphysiological systems for quantitative biology and pharmacology studies. *Sci Rep.* (2018) 8:4530. doi: 10.1038/s41598-018-22749-0
116. Zhao WN, Cheng C, Theriault KM, Sheridan SD, Tsai LHHaggarty SJ. A high-throughput screen for Wnt/beta-catenin signaling pathway modulators in human iPSC-derived neural progenitors. *J Biomol Screen* (2012) 17:1252–63. doi: 10.1177/1087057112456876
117. Lapp H, Bruegmann T, Malan D, Friedrichs S, Kilgus C, Heidsieck A, et al. Frequency-dependent drug screening using optogenetic stimulation of human iPSC-derived cardiomyocytes. *Sci Rep.* (2017) 7:9629. doi: 10.1038/s41598-017-09760-7
118. Jung KB, Lee H, Son YS, Lee JH, Cho HS, Lee MO, et al. *In vitro* and *in vivo* imaging and tracking of intestinal organoids from human induced pluripotent stem cells. *FASEB J.* (2018) 32:111–22. doi: 10.1096/fj.201700504R
119. Bjork S, Ojala EA, Nordstrom T, Ahola A, Liljestrom M, Hyttinen J, et al. Evaluation of optogenetic electrophysiology tools in human stem cell-derived cardiomyocytes. *Front Physiol.* (2017) 8:884. doi: 10.3389/fphys.2017.00884
120. Tentler JJ, Tan AC, Weekes CD, Jimeno A, Leong S, Pitts TM, et al. Patient-derived tumour xenografts as models for oncology drug development. *Nat Rev Clin Oncol.* (2012) 9:338–50. doi: 10.1038/nrclinonc.2012.61
121. Siolas DHannon GJ. Patient-derived tumor xenografts: transforming clinical samples into mouse models. *Cancer Res.* (2013) 73:5315–9. doi: 10.1158/0008-5472.CAN-13-1069
122. Gao H, Korn JM, Ferretti S, Monahan JE, Wang Y, Singh M, et al. High-throughput screening using patient-derived tumor xenografts to predict clinical trial drug response. *Nat Med.* (2015) 21:1318–25. doi: 10.1038/nm.3954
123. Ben-David U, Ha G, Tseng YY, Greenwald NF, Oh C, Shih J, et al. Patient-derived xenografts undergo mouse-specific tumor evolution. *Nat Genet.* (2017) 49:1567–75. doi: 10.1038/ng.3967
124. DiMasi JA, Grabowski GH, Hansen RW. Innovation in the pharmaceutical industry: New estimates of R&D costs. *J Health Econ.* (2016) 47:20–33. doi: 10.1016/j.jhealeco.2016.01.012
125. Lee G, Ramirez CN, Kim H, Zeltner N, Liu B, Radu C, et al. Large-scale screening using familial dysautonomia induced pluripotent stem cells identifies compounds that rescue IKBKAP expression. *Nat Biotechnol.* (2012) 30:1244–8. doi: 10.1038/nbt.2435
126. Engle SJ, Puppala D. Integrating human pluripotent stem cells into drug development. *Cell Stem Cell* (2013) 12:669–77. doi: 10.1016/j.stem.2013.05.011
127. Engle SJ, Vincent F. Small molecule screening in human induced pluripotent stem cell-derived terminal cell types. *J Biol Chem.* (2014) 289:4562–70. doi: 10.1074/jbc.R113.529156
128. Wainger BJ, Kiskinis E, Mellin C, Wiskow O, Han SS, Sandoe J, et al. Intrinsic membrane hyperexcitability of amyotrophic lateral sclerosis patient-derived motor neurons. *Cell Rep.* (2014) 7:1–11. doi: 10.1016/j.celrep.2014.03.019
129. Naryshkin NA, Weetall M, Dakka A, Narasimhan J, Zhao X, Feng Z, et al. Motor neuron disease. SMN2 splicing modifiers improve motor function and longevity in mice with spinal muscular atrophy. *Science* (2014) 345:688–93. doi: 10.1126/science.1250127
130. Drawnel FM, Boccardo S, Prummer M, Delobel F, Graff A, Weber M, et al. Disease modeling and phenotypic drug screening for diabetic cardiomyopathy using human induced pluripotent stem cells. *Cell Rep.* (2014) 9:810–21. doi: 10.1016/j.celrep.2014.09.055

131. Miyauchi M, Koya J, Arai S, Yamazaki S, Honda A, Kataoka K, et al. ADAM8 is an antigen of tyrosine kinase inhibitor-resistant chronic myeloid leukemia cells identified by patient-derived induced pluripotent stem cells. *Stem Cell Rep.* (2018) 10:1115–30. doi: 10.1016/j.stemcr.2018.01.015
132. Liang P, Lan F, Lee AS, Gong T, Sanchez-Freire V, Wang Y, et al. Drug screening using a library of human induced pluripotent stem cell-derived cardiomyocytes reveals disease-specific patterns of cardiotoxicity. *Circulation* (2013) 127:1677–91. doi: 10.1161/CIRCULATIONAHA.113.001883
133. Chaudhari U, Nemade H, Wagh V, Gaspar JA, Ellis JK, Srinivasan SP, et al. Identification of genomic biomarkers for anthracycline-induced cardiotoxicity in human iPSC-derived cardiomyocytes: an *in vitro* repeated exposure toxicity approach for safety assessment. *Arch Toxicol.* (2016) 90:2763–77. doi: 10.1007/s00204-015-1623-5
134. Burridge PW, Li YF, Matsa E, Wu H, Ong SG, Sharma A, et al. Human induced pluripotent stem cell-derived cardiomyocytes recapitulate the predilection of breast cancer patients to doxorubicin-induced cardiotoxicity. *Nat Med.* (2016) 22:547–56. doi: 10.1038/nm.4087
135. Maillet A, Tan K, Chai X, Sadananda SN, Mehta A, Ooi J, et al. Modeling doxorubicin-induced cardiotoxicity in human pluripotent stem cell derived-cardiomyocytes. *Sci Rep.* (2016) 6:25333. doi: 10.1038/srep25333
136. Sharma A, Burridge PW, McKeithan WL, Serrano R, Shukla P, Sayed N, et al. High-throughput screening of tyrosine kinase inhibitor cardiotoxicity with human induced pluripotent stem cells. *Sci Transl Med.* (2017) 9:eaaf2584. doi: 10.1126/scitranslmed.aaf2584
137. Louise J, Wust RCI, Pistollato F, Palosaari T, Barilaro M, Macko P, et al. Assessment of acute and chronic toxicity of doxorubicin in human induced pluripotent stem cell-derived cardiomyocytes. *Toxicol In Vitro* (2017) 42:182–90. doi: 10.1016/j.tiv.2017.04.023
138. Blondel S, Egesipe AL, Picardi P, Jaskowiak AL, Notarnicola M, Ragot J, et al. Drug screening on Hutchinson Gilford progeria pluripotent stem cells reveals aminopyrimidines as new modulators of farnesylation. *Cell Death Dis.* (2016) 7:e2105. doi: 10.1038/cddis.2015.374

**Conflict of Interest Statement:** The authors declare that the research was conducted in the absence of any commercial or financial relationships that could be construed as a potential conflict of interest.

Copyright © 2018 Kim and Schaniel. This is an open-access article distributed under the terms of the Creative Commons Attribution License (CC BY). The use, distribution or reproduction in other forums is permitted, provided the original author(s) and the copyright owner(s) are credited and that the original publication in this journal is cited, in accordance with accepted academic practice. No use, distribution or reproduction is permitted which does not comply with these terms.



# Novel Antibody Drug Conjugates Targeting Tumor-Associated Receptor Tyrosine Kinase ROR2 by Functional Screening of Fully Human Antibody Libraries Using Transpo-mAb Display on Progenitor B Cells

## OPEN ACCESS

### Edited by:

Rhodri Ceredig,  
National University of Ireland Galway,  
Ireland

### Reviewed by:

Martin Bachmann,  
Universität Bern, Switzerland  
Hermen Spits,  
University of Amsterdam, Netherlands

### \*Correspondence:

Ulf Grawunder  
ulf.grawunder@nbe-therapeutics.com

### †Present Address:

Fabian I. Wolter,  
Celonic AG, Basel, Switzerland

### Specialty section:

This article was submitted to  
B Cell Biology,  
a section of the journal  
*Frontiers in Immunology*

Received: 22 July 2018

Accepted: 09 October 2018

Published: 02 November 2018

### Citation:

Hellmann I, Waldmeier L, Bannwarth-Escher M-C, Maslova K, Wolter FI, Grawunder U and Beerli RR (2018) Novel Antibody Drug Conjugates Targeting Tumor-Associated Receptor Tyrosine Kinase ROR2 by Functional Screening of Fully Human Antibody Libraries Using Transpo-mAb Display on Progenitor B Cells. *Front. Immunol.* 9:2490.  
doi: 10.3389/fimmu.2018.02490

Ina Hellmann, Lorenz Waldmeier, Marie-Christine Bannwarth-Escher, Kseniya Maslova, Fabian I. Wolter<sup>†</sup>, Ulf Grawunder\* and Roger R. Beerli

NBE-Therapeutics Ltd., Basel, Switzerland

Receptor tyrosine kinase-like orphan receptor 2 (ROR2) has been identified as a highly relevant tumor-associated antigen in a variety of cancer indications of high unmet medical need, including renal cell carcinoma and osteosarcoma, making it an attractive target for targeted cancer therapy. Here, we describe the *de novo* discovery of fully human ROR2-specific antibodies and potent antibody drug conjugates (ADCs) derived thereof by combining antibody discovery from immune libraries of human immunoglobulin transgenic animals using the Transpo-mAb mammalian cell-based IgG display platform with functional screening for internalizing antibodies using a secondary ADC assay. The discovery strategy entailed immunization of transgenic mice with the cancer antigen ROR2, harboring transgenic IgH and IgL chain gene loci with limited number of fully human V, D, and J gene segments. This was followed by recovering antibody repertoires from the immunized animals, expressing and screening them as full-length human IgG libraries by transposon-mediated display in progenitor B lymphocytes ("Transpo-mAb Display") for ROR2 binding. Individual cellular "Transpo-mAb" clones isolated by single cell sorting and capable of expressing membrane-bound as well as secreted human IgG were directly screened during antibody discovery, not only for high affinity binding to human ROR2, but also functionally as ADCs using a cytotoxicity assay with a secondary anti-human IgG-toxin-conjugate. Using this strategy, we identified and validated 12 fully human, monoclonal anti-human ROR2 antibodies with nanomolar affinities that are highly potent as ADCs and could be promising candidates for the therapy of human cancer. The screening for functional and internalizing antibodies during the early phase of antibody discovery demonstrates the utility of the mammalian cell-based Transpo-mAb Display platform to select for functional binders and as a powerful tool to improve the efficiency for the development of therapeutically relevant ADCs.

**Keywords:** antibody drug conjugate (ADC), transposition, mammalian IgG cell display, antibody discovery, functional screen, ROR2, human immune library, human IgG transgenic mice

## INTRODUCTION

Cancer is still a leading cause of death worldwide. While the landscape of cancer treatment has positively evolved recently with the advent of targeted, including antibody- and cell-based therapies, broadly effective and curative treatment options still remain limited. Classical chemotherapy with cytotoxic or cytostatic small molecules remains the standard of care in many anti-cancer treatments, although dose-limiting toxicities as well as limited selectivity against cancer cells result in only partial clinical efficacy (1). To increase the anti-tumor efficacy and to lower the toxicity on normal tissues, a targeted delivery of the cytotoxic agent to the tumor has long been desired. With the development of monoclonal antibodies (mAbs) (2), it became a possibility to use their specific binding to a tumor-associated antigen (TAA) to specifically target cancer cells. Naked antibodies either need to have an intrinsic capability to interfere with the growth of cancer cells, or they need to recruit other immune-system components to inhibit tumor growth and expansion. These activities of antibodies are often insufficient to effect complete eradication of targeted tumor cells. Therefore, selectively delivering a highly cytotoxic substance to the tumor by generating antibody drug conjugates (ADCs) has been considered an attractive concept for decades. ADCs consist of an antibody conjugated via a covalent linker to a potent cytotoxic payload, thereby combining the high selectivity of the antibody moiety to a TAA and the otherwise intolerably high cytotoxic potential of the payload (3). However, in order to generate not only potent, but also safe ADCs, many aspects of the molecule need to be optimal. This includes not only the tumor-selective binding of the antibody moiety to the targeted cancer cells, but also functional properties of the antibody moiety, such as its ability to internalize the ADC into the targeted cancer cell following binding of the ADC to the TAA. While the concept of antibody-mediated delivery of toxic payloads to cancer cells is known in the field for decades, due to the structural complexity of this class of molecules and the high functional requirements to achieve a favorable therapeutic index, only four ADCs have been approved to date by the regulatory authorities for treating cancer patients, while >60 ADCs are currently evaluated in clinical trials (4). In the field of targeted cancer therapies, ADCs will have an enormous potential for cancer treatment in the future, if engineered diligently with regard to linker stability and product homogeneity as well as optimal tumor selectivity and functionality.

It was the objective of this study to discover antibodies specifically targeting the TAA ROR2 with high internalization rates, eventually leading to potent cancer cell killing with anti-ROR2 antibody based ADCs. ROR2, along with ROR1, belongs to the receptor tyrosine kinase-like orphan receptor (ROR) family, both type I transmembrane proteins with a high degree of structural homology (5). The structure of both ROR1 and ROR2 includes an extracellular portion with three distinct domains, an N-terminal Ig-like domain, a Frizzled domain (or cysteine-rich repeat domain, CRD) and a membrane-proximal Kringle domain, followed by a transmembrane domain connecting to intracellular domains with a structural and amino acid

homology to receptor tyrosine kinases (6, 7). Here, we focused on human ROR2 and the identification of novel mAbs and ADCs against this promising cancer cell target. Like ROR1, ROR2 regulates cellular processes including cell proliferation, polarity, differentiation, migration, metabolism and survival (8–10). While ROR2 is expressed in a wide variety of tissues during early embryogenesis (11), it is mainly absent in adult normal tissues (7). In contrast, ROR2 is overexpressed in several human cancers, including renal cell carcinoma (11, 12), osteosarcoma (10), melanoma (13), stromal tumors (14), as well as breast (15, 16), colorectal (17), oral (18), and pancreatic cancer (19), and has been associated with a more aggressive disease state and poorer patient prognosis within these indications. Recently, it has been shown that ROR2 interacts with ligands Wnt5a and Wnt3a to activate a combination of noncanonical and canonical Wnt signaling pathways, respectively (9, 20–22). Upregulation of ROR2 is associated with mediating pro-tumorigenic activity (polarized cell migration, invasion, and tumor growth) via the noncanonical Wnt signaling pathway (7, 15, 23). In addition to its function as an oncogene, and in contrast to ROR1, ROR2 can also act as a suppressor of carcinogenesis in tumors driven by canonical Wnt signaling, where ROR2 expression is lost, as observed in colon cancer and hepatocellular carcinoma (6). Notably, the expression of ROR2 is largely mutually exclusive with its sister molecule ROR1 and only rare cases of ROR1 and ROR2 co-expression on tumors have been reported (5, 24).

To develop potent ADCs, antibodies with selectivity for the TAA and triggering high internalization rates are generally needed (4). This is particularly relevant for TAAs for which the level of expression on cancer cells is not extraordinarily high, like in the case of ROR2 (5, 6). The mode of action of ADCs requires specific binding to the TAA, upon which the ADC-TAA complex needs to be internalized by receptor-mediated endocytosis and directed toward lysosomal degradation, where the toxic payload is released intracellularly (25). Antibodies may vary in the rate and magnitude of internalization they are inducing, even if the same epitope on the cancer target antigen is recognized (26, 27). Hence, it is desirable to identify antibodies that are potent ADCs during early discovery. While antibody discovery technologies in eukaryotic cells are manifold, spanning from yeast (28, 29) to mammalian cell-based antibody expression platforms (30–33), these platforms typically do not allow a rapid and efficient screening for desired functional properties, e.g., potency as an ADC, without the need for cloning and reformatting of the antibody into a soluble form. In addition, many antibody discovery technologies yield non-human antibodies that require tedious humanization of the antibody in order to lower immunogenicity which could affect clinical safety and efficacy of the therapeutic (34, 35). Hence, a straightforward antibody screening platform to quickly identify functionally relevant fully human antibodies is highly desired.

In the present study, we describe the *de novo* discovery of fully human antibodies and potent ADCs derived thereof targeting the highly tumor selectively expressed human ROR2, using the Transpo-mAb Display (36) of immune antibody libraries isolated from immunized transgenic mice harboring transgenic IgH and IgL gene loci with human V, D, and J gene segments. The

straightforward functional screening of clonal supernatants from fully human immune cellular libraries allows for identification of mAbs suitable for the development of potent ADCs already during the early stages of antibody screening.

## MATERIALS AND METHODS

### Cell Lines

The origin and culturing conditions of murine progenitor B cell clone L11 derived from the Abelson-murine leukemia virus transformed progenitor B cell line 63-12 of a RAG2-deficient mouse and the murine breast cancer cell line EMT6 have been previously described (36). Human multiple myeloma cell line L363 (DSMZ) and human breast cancer cell line T47D (ATCC) were cultured in RPMI or DMEM, respectively, supplemented with 10% fetal calf serum (FCS), 2 mM L-glutamine, 100 IU penicillin, 0.1 mg/ml streptomycin and 0.25 µg/ml fungizone (all from Amimed) at 37°C in a humidified incubator at 5% CO<sub>2</sub> atmosphere.

### Mouse Strains

H2L2 mice were obtained from Harbor Biomed; H2L2 mice are a cross of the following mouse strains: F129, fvb/n and C57BL6, and upon immunization produce antibodies with a human variable domain and a rat constant domain, disclosed in patent application WO 2010/070263A1. Experimental procedures involving mice were performed at certified animal facilities at ETH-D-BSSE, Basel. All procedures involving animals were compliant with the guidelines and protocols for animal care and handling approved by the Basel-Stadt cantonal veterinary office.

### Immunization

Homozygous transgenic mice harboring transgenic IgH and IgL gene loci with a limited number of fully human V, D, and J gene segments back-crossed on IgH and IgkL chain double-knock-out background and designated H2L2 mice were obtained from Harbor BioMed in Cambridge, Massachusetts. While the V, D, and J gene segments in the transgenic IgH chain gene loci were fully human sequences, the coding region of the constant region exons were of rat origin, such that the mice primarily generate chimeric antibodies encoded by fully human V<sub>H</sub> and V<sub>L</sub> regions and rat constant regions. C57BL/6 wild-type mice were obtained from Janvier Laboratories (Saint-Berthevin Cedex, France). Mice were immunized with a soluble human ROR2 extracellular domain (ECD) fused to a Twin-Strep-tag (hROR2-ECD-Twin-Strep) using the following schedule: On day 0, mice were immunized intraperitoneally using 50 µg hROR2-ECD-Twin-Strep diluted in PBS and 20 µg monophosphoryl lipid A (MPLA) (Invivogen, tlr1-mpls) mixed 1:1 with Addavax adjuvant (Invivogen, vac-adx-10), creating an oil-in-water emulsion in 100 µl. On day 21, mice were boosted intraperitoneally using 20 µg hROR2-ECD-Twin-Strep diluted in PBS and 20 µg MPLA mixed 1:1 with Addavax adjuvant in 100 µl. On day 42, the mice were boosted intravenously using 10 µg hROR2-ECD-Twin-Strep without any adjuvants added in 100 µl. Blood sampling was performed from the tail vein of mice 7 days prior to the first immunization, and 7 days following each immunization

(days 7, 28), or by heart puncture on day 49, when the mice were sacrificed. Blood was allowed to clot for 15–60 min at room temperature, then spun down at 5,000 rpm for 15 min at 4°C. Serum was carefully transferred into a new tube and stored at –20°C until further use.

On day 49 following initial antigen injection, the mice were euthanized, spleens were collected, transferred into 1x PBS and stored on ice until processing. Each spleen was homogenized in a gentleMACS C-tube (Miltenyi Biotec) containing 2.4 ml of RPMI-10%FCS using the gentleMACS Octo Dissociator (Miltenyi Biotec). Cells were then filtered through a cell strainer to get a single cell suspension, frozen down in 90% FCS/10%DMSO, and stored in the vapor phase of liquid nitrogen until further use.

### Library Construction

For the isolation of antigen-specific B cells, splenocytes were thawed quickly at 37°C and washed twice in cold MACS buffer (0.5% BSA in PBS, 2 mM EDTA). Cell viability was assessed using 0.4% Trypan Blue (Amresco). Between  $1.9 \times 10^6$  and  $3.7 \times 10^6$  total viable cells were incubated with 20 µg/ml mouse IgG (ChromPure Mouse IgG, 015-000-003, Jackson Immunoresearch) for 15 min at 4°C. Isolation of antigen-specific B cells was performed in two consecutive steps: depletion of non-B cells, followed by positive selection for antigen-specific B cells. Magnetic labeling of non-B cells was performed using the Pan B Cell Isolation Kit Mouse (Miltenyi Biotec), according to the manufacturer's protocol. For the positive selection, 50 µl Strep-Tactin Magnetic Nanobeads (IBA Lifesciences) were coated with 12 µg hROR2-ECD-Twin-Strep over night at 4°C, followed by washing with MACS buffer in a magnetic field to remove unbound antigen and elution. Next, isolated B cells were incubated with hROR2-ECD-Twin-Strep-coated magnetic beads for 45 min, washed with MACS buffer and subjected to magnetic separation using LS columns (Miltenyi Biotec). The flow-through was discarded and elution was performed after removal from the magnetic field, yielding an enrichment of antigen-positive B cells. Cells were centrifuged and directly subjected to RNA extraction.

RNA was isolated using TRI-Reagent (Sigma-Aldrich) and reverse transcribed using Protoscript II Reverse Transcriptase (New England Biolabs) using random nonamers, following the manufacturer's instructions. Variable domains were amplified by semi-nested PCR using Q5 DNA polymerase (New England Biolabs). In general, in the first step of this PCR, a set of forward primers binding to the 5'-end of the framework (FR) 1 of human variable domains, thereby adding the 3'-portion of a universal leader peptide to the 5'-end of the amplicon, was paired with a reverse primer specific to the rat constant domain expressed in H2L2 mice. In the second PCR-step, a forward primer completing the N-terminal leader peptide and adding a restriction site for cloning at the 5'-end of the amplicon was paired with a set of reverse primers binding to the 3'-end of the FR4, thereby adding a restriction site for cloning to the 3'-end of the amplicon. The resulting amplicons contained the nucleotide sequences of restriction sites for cloning at the 5'-end and 3'-end, as well as a complete leader sequence followed by the entire human

variable V(D)J domain. The primer sequences are supplied in the Supplementary information (**Figure S1**).

In the first PCR step, human IgG and IgM heavy chain (HC) variable domains were amplified using human V<sub>H</sub>-specific forward primers (primer set: Set-huHC-FR1) paired with a reverse primer specific for the rat IgG (rat\_IgG12abc\_R) or IgM constant domain (rat\_IgM\_R). In the 2nd PCR step, forward primer Not-I-5'Leader and reverse primers specific to the human J<sub>H</sub>-domain (primer set: Set-huJH-R) were used to complete the PCR amplification. For amplification of Igκ light chain (LC) variable domains, a forward primer set specific to human V<sub>K</sub>-domains (primer set: Set-huKC-FR1) was paired with a reverse primer binding to the rat IgκLC constant domain (rat\_CK\_R) in the 1st PCR step. For the 2nd PCR step, forward primer Not-I-5'-Leader was paired with a primer set specific to human J<sub>K</sub>-domains (primer set: Set-huJK-R) to generate the final amplicon. In H2L2 mice, the endogenous mouse lambda light chain gene loci have not been knocked-out and remain intact, and no human lambda light chains are expressed. Therefore, the lambda light chain gene loci were not amplified. Cycling conditions were as follows: 98°C/30s -> 15-25x (98°C/10 s, 56°C/30 s, 72°C/60 s) -> 72°C, 2 min -> hold@ 4°C. For the first and second PCR, 25 or 15 cycles were performed, respectively.

Amplicons were then cloned into transposable vectors as previously described (36). In brief, IgG- and IgM-derived V<sub>H</sub> domains were cloned into pPB-Hygro-HCγ1-gen IgHC expression vector, encoding a genomic human IgG<sub>1</sub> constant domain, while kappa LC variable domains were cloned into pPB-Puro-LC, thereby complemented with a human Kappa constant domain, via NotI/NheI or NotI/BsiWI, respectively. Libraries were ligated, transformed into XL1-Blue electrocompetent cells, and at least 10 bacterial clones were analyzed by sequencing, as previously described (36). Library sizes ranged from  $6 \times 10^6$  to  $5 \times 10^7$  independent transformants.

Antibody protein sequences were annotated and assessed for their degree of identity to the closest human or mouse germline V gene sequence with using IgBLAST (<https://www.ncbi.nlm.nih.gov/igblast/>).

## Transposition, Staining and Sorting of Cellular Libraries

63-12 murine progenitor B cells, L11 cells, were transposed using a HC:LC:Transposase DNA weight ratio of 0.25:0.125:1, and selected using 1 μg/ml puromycin and 800 μg/ml hygromycin B, as previously described (36).

For staining and sorting of cellular libraries, 0.2–1 × 10<sup>7</sup> cells were stained with hROR2-ECD-Twin-Strep at concentrations between 0.25 and 2 μg/ml, Strep-MAB Oyster Classic 645 (IBA Lifesciences, 2-1555-050) diluted 1:500 and PE-labeled anti-human IgG (Fcγ-specific; ebioscience, 12-4998-82) diluted 1:250 in cold 2% FCS in PBS for 1 h on ice. For control stainings without antigen, hROR2-ECD-Twin-Strep was omitted in the staining. Following washing with 2% FCS in PBS, cells were either analyzed by flow cytometry using a FACSCalibur Instrument (Becton-Dickinson) or filtered using a cell strainer snap cap

FACS tube and single-cell sorted using a FACSAriaII instrument (Becton-Dickinson) with data analysis being performed using FlowJo analytical software (Tree Star, Ashland, OR). 288 hROR2-positive L11 clones per library were single-cell sorted into warm SF-IMDM medium supplemented with 2% FCS, 2 mM L-glutamine, 100 IU penicillin, 0.1 mg/ml streptomycin (all from Amimed), and 50 μM beta-mercaptoethanol (Amresco) at 37°C and 5% CO<sub>2</sub> atmosphere.

## Antigen Expression of Cell Lines

For determination of antigen expression on cell lines, 1 × 10<sup>6</sup> cells were stained with 2 μg/ml hROR2-specific antibody XBR2-401 (37) for 30 min on ice, detected using a PE-labeled anti-human IgG (Fcγ-specific) at 1:250 dilution for 30 min on ice and analyzed by flow cytometry using a FACSCalibur instrument (Becton-Dickinson), followed by data analysis using FlowJo analytical software (Tree Star, Ashland, OR).

## ELISA

For determination of serum titers and antigen-binding, Nunc-Immuno MaxiSorp 96-well plates (Thermo Fisher Scientific) were coated with 2 μg/ml antigen diluted in coating buffer (100 mM bicarbonate/carbonate buffer). For determination of IgG titers, plates were coated with 2 μg/ml AffiniPure donkey anti-human IgG F(ab')<sub>2</sub> fragment, Fcγ-specific (109-006-008) or AffiniPure goat anti-human IgG F(ab')<sub>2</sub> fragment, Fcγ-specific (109-006-098, both Jackson Immunoresearch) diluted in coating buffer overnight at 4°C. Plates were then washed twice with 0.05% Tween-20 in PBS (PBS-T), blocked at 37°C using PBS-T supplemented with 3% bovine serum albumin (BSA) (Carl Roth) for 1 h and washed again twice with PBS-T. Serum of the H2L2 and C57BL/6 mice was pre-diluted 1:100 in PBS-T/1% BSA. L11 clonal supernatants were pre-diluted 5-fold in PBS-T/1% BSA. Supernatants from transiently transfected HEK293T cells were pre-diluted 50-fold. Purified monoclonal antibodies were used at a starting concentration between 0.5–2 μg/ml. Samples were added to plates as serial dilutions (2.5-fold for serum titer; 3-fold for L11 and HEK293T cell supernatants; 3 to 20-fold for purified monoclonal antibodies) in PBS-T/1% BSA and were incubated for 1 h at 37°C. After six washes with PBS-T, horse radish peroxidase (HRP)-conjugated F(ab')<sub>2</sub> anti-human Fcγ (109-036-008, Jackson Immunoresearch) diluted 10,000-fold in PBS-T/1% BSA buffer was added, and plates were incubated for 1 h at 37°C. For assessment of serum titers in H2L2 and C57BL/6 mice, HRP-conjugated F(ab')<sub>2</sub> anti-rat Fcγ (112-036-071) or HRP-conjugated F(ab')<sub>2</sub> anti-mouse Fcγ (115-036-071, both Jackson Immunoresearch) was diluted 5,000-fold in PBS-T/1% BSA, respectively. After washing six times with PBS-T, Sigmafast OPD Peroxidase substrate (Sigma-Aldrich) was added, and reactions were stopped by adding 2 M H<sub>2</sub>SO<sub>4</sub>. Absorption was measured at 490 nm using a Spark™ 10M (Tecan Life Sciences). Half-maximal concentrations (EC50) values of standards with known concentrations and unknown samples were determined by 4-parameter curve fitting models in GraphPad Prism (GraphPad Software Inc.).

## In vitro Potency Assays

For the secondary ADC assay, 1,000 EMT6-hROR2 cells engineered to overexpress hROR2 were plated per well in 96-well plates. On the next day, clonal L11 cell supernatants were added undiluted with a final dilution on the plate of 10-fold (for single-well secondary killing assays) or using a 2-fold serial dilution using an IgG starting concentration adjusted to the IgG levels of the lowest expressing L11 clone (as determined by ELISA) for a titration curve assay, while control antibodies were 2-fold serially diluted resulting in a final concentration on the plate ranging from 1 µg/ml to 0.5 ng/ml. Following incubation at 37°C for 30 min, PNU-159682-coupled secondary ADC (HFc-CL-PNU, Moradec AH-102PN) was added with a final concentration of 0.5 nM and incubated for 3 days at 37°C.

For *in vitro* potency assays using purified ADCs, 1,000 hROR2-overexpressing T47D-hROR2 cells, or 10,000 L363 cells per well were plated in 96 well-plates. The following day ADC was added in 3.5-fold serial dilutions, with the final concentrations ranging from 20,000 to 0.25 ng/ml in duplicate, and incubated for 4 days at 37°C.

Following incubation at 37°C, cell viability was assessed using CellTiter-Glo® 2.0 Luminescence Assay (Promega G9243), according to the manufacturer's instructions, using a Tecan Infinite F200 or a Spark™ 10M (both Tecan Life Sciences) with an integration time of 250 ms per well. IC<sub>50</sub> values were determined by 4-point curve fitting models in GraphPad Prism (GraphPad Software Inc.).

## Expression and Purification of Antibodies and Antigens

Human V<sub>H</sub> and V<sub>L</sub> sequences recovered from L11 cell clones were obtained by sequence recovery as previously described and assembled into the pCB14b or pCB14g vector with the respective constant domains (36). The resulting antibody sequences contained a sortase A recognition motif and a Twin-Strep-tag as described previously (38) for subsequent conjugation to toxin. These tag sequences were: IgH chain, (LPETG-G-WSHPQFEK(G<sub>3</sub>S)<sub>3</sub>AWSHPQFEKGS); Igk chain, G<sub>4</sub>S-LPETG-G-WSHPQFEK(G<sub>3</sub>S)<sub>3</sub>AWSHPQFEKGS). In cases where more than one V<sub>H</sub> and/or V<sub>L</sub> were found, a deconvolution step was performed to identify the correct pairing, by expressing all possible HC/LC combinations in HEK293T cells and evaluating hROR2-ECD-Twin-Strep-binding by ELISA.

The antigens hROR2-ECD-Twin-Strep, cynomolgus monkey ROR2-ECD-Twin-Strep and mouse ROR2-ECD-Twin-Strep comprise the extracellular domain of human ROR2 (NP\_004551.2, amino acids 1-403), cynomolgus monkey ROR2 (XP\_005582291.1, amino acids 1-403) or mouse ROR2 (NP\_038874.3, amino acids 1-402), respectively, fused at the C-Termini to a Twin-Strep-tag (GSWSHPQFEK(G<sub>3</sub>S)<sub>2</sub>G<sub>2</sub>SAWSHPQFEKGS) for purification. The corresponding nucleotide sequences of the respective antigens flanked with 5'-NotI and 3'-BstBI sites were produced by total gene synthesis (GenScript), cloned into the expression vector pCB14b (36) and confirmed by DNA sequencing.

Transient and semi-stable expression of antibodies in HEK293T cells using Lipofectamine® LTX with Plus™ Reagent (Thermo Fisher Scientific), followed by FPLC-based purification using Amsphere™ Protein A columns (JSR Life Sciences) and Protein A HiTrap columns (GE Healthcare) on an ÄKTA pure (GE Healthcare) were performed as previously described (36).

For purification of antigens, harvested supernatants were subjected to FPLC-based affinity purification using Strep-Tactin columns (IBA Lifesciences), according to the manufacturer's protocol.

## Sortase-Mediated Antibody Conjugation (SMAC)

LPETG-tagged antibodies were site-specifically conjugated to glycine-modified toxins Gly<sub>3</sub>-EDA-PNU or Gly<sub>5</sub>-EDA-PNU using sortase-enzyme mediated antibody conjugation (SMAC-technology™), as previously described (38, 39). hROR2-specific ADCs were formulated in PBS. The drug-to-antibody-ratio (DAR) of the final ADCs ranged between 3 and 4, as determined by HPLC (38, 39).

## Surface Plasmon Resonance (SPR)

Affinities of anti-hROR2 antibodies to hROR2-ECD were measured by multi-cycle SPR on a Biacore T200 instrument (GE Healthcare), as described (36). Antibodies were captured using a CM5 Protein A chip (GE-Healthcare 29127556) or by Protein G immobilized on a CM5 sensor chip. hROR2-ECD-Twin-Strep was diluted in running buffer using 2-fold serial dilutions ranging from 40 nM to 2.5 nM. Capture levels ranged from 148 to 845 RU.

## RESULTS

### Outline of Functional Screening Strategy for Direct Identification of Novel mAbs With Optimal ADC Activity

We applied the Transpo-mAb mammalian cell IgG Display platform (36) (in short "Transpo-mAb Display") on immune libraries from Ig-transgenic mice with human V<sub>H</sub> and V<sub>L</sub> regions, to identify novel monoclonal antibodies against the extracellular domain of human ROR2 while concomitantly screening these antibodies for their suitability as ADCs without the need for prior sequence recovery, re-cloning and re-expression. An overview of the functional screening strategy is shown in **Figure 1**. Briefly, immunoglobulin transgenic mice expressing antibodies with fully human V<sub>H</sub> and V<sub>L</sub> sequences (called H2L2 mice), provided by Harbor BioMed, Cambridge, MA, were immunized with the extracellular domain of human ROR2 containing a C-terminal Twin-Strep-tag (hROR2-ECD-Twin-Strep). hROR2-specific B lymphocytes were enriched from the spleens of immunized mice using magnetic activated cell sorting (MACS), RNA was isolated from hROR2-ECD-Twin-Strep enriched B lymphocytes and libraries of coding regions for human V<sub>H</sub> and kappa V<sub>L</sub> variable domains were amplified by RT-PCR using specific primers. The variable region fragments were then cloned into separate transposable expression vectors for IgH and IgL chains in which the cloned V<sub>H</sub> and V<sub>L</sub> regions were

fused with IgG<sub>1</sub> HC and kappa LC constant regions, respectively, thus allowing for expression of fully human IgG<sub>1</sub>/κLC antibodies. The HC vector comprises a genomic version of the human HCγ 1 constant region including the two exons for the IgG membrane anchor and intracellular regions with complete intron sequences, thus allowing alternative splicing of a primary Ig-heavy chain transcript in certain B-lineage cells to allow for co-expression of high levels of both, membrane-bound and secreted antibody from the same expression vector (36). Following DNA library construction, cellular libraries were generated by stable transposition of HC and LC transposable vectors to stably display fully human IgG<sub>1</sub> antibodies on the surface of immortalized murine L11 pro-B cells derived by subcloning from the A-MuLV transformed RAG-2 knock-out cell line 63-12 (36), unable to express endogenous murine Ig components. Cells expressing hROR2-specific IgG were isolated by FACS using double staining for IgG and hROR2 binding followed by single-cell sorting of hROR2-binding cellular clones using FACS. Supernatants from single-cell sorted Transpo-mAb Display cell clones containing secreted antibodies were then used to perform functional screening for their binding to hROR2 by ELISA as well as their suitability as ADCs in a secondary cell killing assay. Sequences were only recovered upon confirmation of mAbs that showed efficient cell killing in the secondary ADC cell killing assay.

## Immunization of H2L2 Ig Transgenic and C57BL/6 Wild-Type Mice With Human ROR2-ECD

In order to generate novel monoclonal antibodies specific for human ROR2, five Ig transgenic H2L2 mice and five C57BL/6 wild-type mice (the latter as controls) were immunized with hROR2-ECD with a Twin-Strep-tag by one primary and two boost immunizations as described in the Materials and Methods. The Twin-Strep-tag appended to the C-terminus of the hROR2-ECD had been used for Strep-Tactin-mediated affinity purification of the recombinant hROR2-ECD-protein expressed in human HEK293T cells. Ig-transgenic H2L2 mice harbor small transgenic immunoglobulin gene loci with a limited set of human V, D, and J gene segments for V(D)J recombination with rat immunoglobulin constant regions on a homozygous knock-out background preventing expression of endogenous immunoglobulin heavy and kappa-light chain components. Immunization of C57BL/6 wild-type mice was included in order to benchmark the anti-hROR2-ECD-Twin-Strep humoral immune response in H2L2 Ig transgenic mice against that of wild-type mice. In the H2L2 Ig transgenic mice, serum titers against hROR2-ECD-Twin-Strep protein after primary and two boost immunizations were monitored by ELISA (**Figure 2A**). After primary immunization hardly any antibody titer specific for hROR2-ECD-Twin-Strep was detectable in the H2L2 Ig transgenic mice. Only after secondary (1st boost) and tertiary (2nd boost) immunization, antibody titers against the hROR2-ECD-Twin-Strep protein became detectable, reaching a mean level of approximately 1:7,700 (Standard deviation (SD): 1:2,011,  $n = 5$ ; individual values: mouse 1357: titer 1:9,911; mouse 1359: titer 1:9,323; mouse 1363: titer 1:8,002; mouse

1358: 1:5,926; mouse 1364: 1:5,374) on day 49, after the 3rd (2nd boost) immunization, indicating a successful immunization strategy. To assess whether the immunization generated titers against the Twin-Strep-tag, serum titers against a control antigen, unrelated to hROR2-ECD, but also containing the same tag were monitored. Significantly, titers against the Twin-Strep-tag were only observed following three immunizations on day 49 and were low (Mean: 1:779, SD: 1:863,  $n = 5$ ) in comparison to the hROR2-ECD-Twin-Strep-specific titers, indicating that only roughly 10% of hROR2-ECD-Twin-Strep-responses were specific for the tag. For benchmarking this immune response, five wild-type mice (C57BL/6) were also immunized in parallel with the identical immunization strategy and sampling schedule and serum titers of the different time points were assessed by ELISA as mentioned above. In wild-type mice, anti-hROR2-ECD-Twin-Strep-tag antibody titers followed the same pattern as in the H2L2 Ig transgenic mice, i.e., hardly detectable IgG anti-hROR2-ECD-Twin-Strep response after the first immunization, with increasing antigen-specific anti-IgG responses after 1st and 2nd boost immunization, but reaching higher levels of a mean of ca. 1:64,000 (SD 1:16,911,  $n = 5$ ) on day 49 following three immunizations (**Figure 2B**). Therefore, the antigen-specific serum titers against hROR2-ECD-Twin-Strep protein in C57BL/6 mice were about 9-fold higher than those observed in H2L2 mice. Significantly, the serum titers against the Twin-Strep portion of the recombinant hROR2-ECD-Twin-Strep protein were disproportionately higher than those in H2L2 mice (mean: ca. 1:31,000, SD: 1:22,159,  $n = 5$ ), indicating that in C57BL/6 mice roughly 50% of the antibody response was directed against the tag. Taken together, the immunizations in H2L2 Ig transgenic mice generated a hROR2-specific response which, although lower than in wild-type mice, was deemed sufficient for further antibody isolation. The three H2L2 Ig transgenic mice showing the highest IgG antibody serum titers after the 3rd immunization on day 49 (mice 1357, 1359, and 1363) were selected for isolation of hROR2-ECD-Twin-Strep-specific antibodies via V<sub>H</sub> and V<sub>L</sub> library cloning from spleen cells collected on day 49 of the experiment.

## Isolation of ROR2-Binders From Cellular Libraries

In a first step, B cell enriched splenocytes of the three H2L2 Ig transgenic mice with the highest serum titers were stained with recombinant hROR2-ECD-Twin-Strep in order to enrich antigen-reactive splenic B lymphocytes by MACS. From the hROR2-ECD-Twin-Strep MACS enriched splenic B cells, V<sub>H</sub> coding regions were amplified by RT-PCR using V<sub>H</sub> forward primers and either Fcγ-specific or Fcμ-specific reverse primers for the generation of IgG and IgM derived V<sub>H</sub> libraries. V<sub>L</sub> coding regions were amplified using V<sub>L</sub> (kappa) forward primers and Igκ light chain constant region-specific reverse primers for the generation of V<sub>L</sub> libraries. The V<sub>H</sub> amplicons (IgG and IgM derived) were then cloned into transposable expression vectors in frame with the coding region for human IgG<sub>1</sub> heavy chain constant domains. The V<sub>L</sub> amplicons were cloned into transposable expression vectors in frame with the coding region

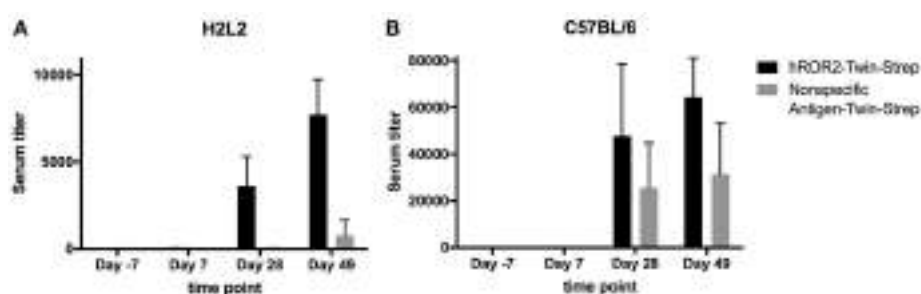
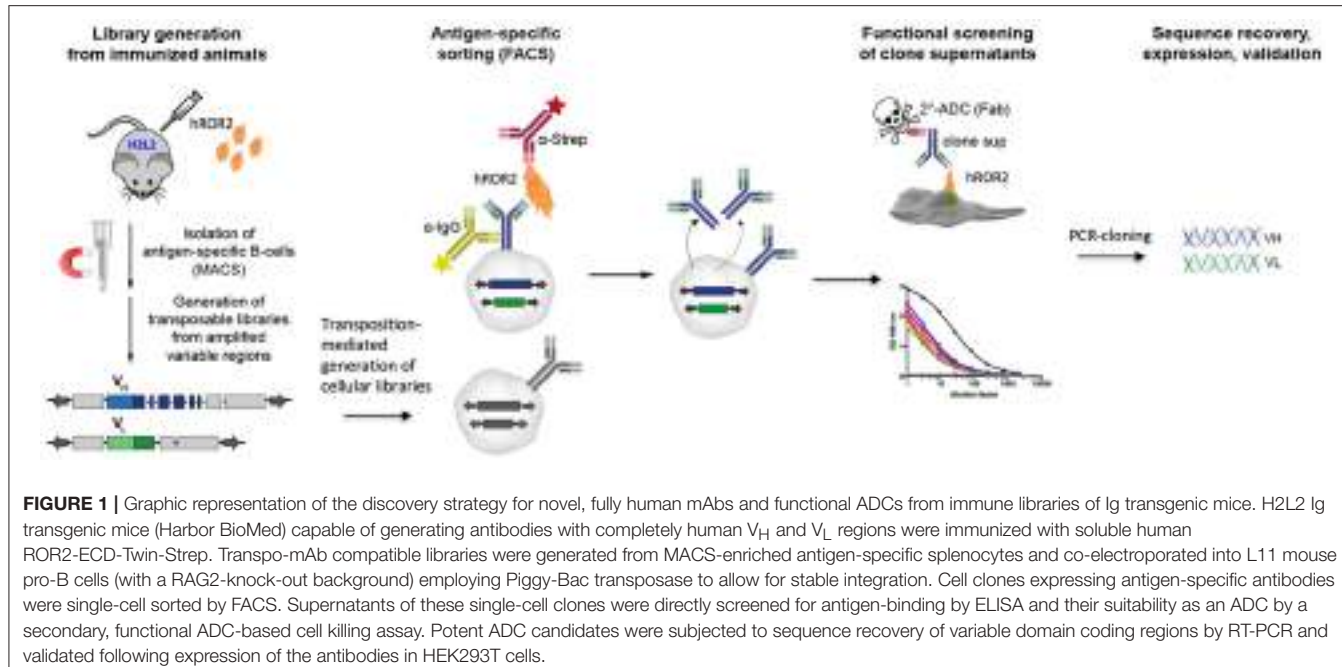


**FIGURE 2 |** hROR2-specific serum titers in H2L2 transgenic and in C57BL/6 wild-type mice. Five H2L2 Ig transgenic mice (**A**) and 5 wild-type C57BL/6 mice (**B**) were immunized with soluble hROR2-ECD-Twin-Strep. Serum samples were collected 7 days prior to immunization as well as on days 7, 28, and 49 post-immunization, i.e., always 7 days following each immunization. Titers in serum against hROR2-ECD-Twin-Strep as well as an unrelated soluble antigen also containing the same Twin-Strep-tag (Nonspecific Antigen-Twin-Strep) to assess tag-related responses were analyzed by ELISA. Bar graphs show mean values with standard deviation indicated.

for Igκ light chain constant domains. This resulted in libraries of expression vectors for fully human IgG<sub>1</sub> heavy chains (if IgG derived, designated HC<sub>γ</sub> library, and if IgM derived, designated HC<sub>μ</sub> library) and for fully human Igκ light chains (designated LC<sub>κ</sub> library), which were generated individually from each mouse. A sample of 10–15 individual plasmid clones from each library were analyzed by DNA sequencing and IgBLAST analysis to assess the quality of the transposable expression vector libraries, which confirmed that the majority of expression vectors contained *bona fide* V<sub>H</sub> (>80% of analyzed plasmid clones) and V<sub>L</sub> (>58% of analyzed plasmid clones) coding regions (Figure S2). This sequence analysis also confirmed that H2L2 mice indeed generated an antibody response involving the transgenic Ig heavy and light chain gene loci with fully human V<sub>H</sub> and V<sub>L</sub> coding regions. In addition, plasmid clones derived from HC<sub>μ</sub> libraries showed higher sequence identity to their

closest human germline V gene sequence than those derived from HC<sub>γ</sub> libraries, reflecting the expected lower frequency of somatic hypermutations in IgM compared to IgG antibodies (Figure S2).

Following successful quality control of the transposable IgG<sub>1</sub> heavy chain and Ig κ light chain expression libraries, cellular libraries were created by stably transposing the LC<sub>κ</sub>-library together with either the HC<sub>γ</sub>- or the HC<sub>μ</sub>-library derived from the same mouse into L11 progenitor B cells capable of efficiently expressing IgG<sub>1</sub>/κL antibodies as membrane-bound IgG as well as secreted IgG. This was achieved by co-electroporating the HC and LC expression libraries with a *Piggybac* transposase expression vector (36). As described previously, the three plasmids (HC-Library:LC-library:transposase vector) were electroporated at a ratio, at which roughly 50% of transfected cells contain only a single HC and LC integration, leading to expression of one mAb per

cell clone (36). Following antibiotic selection with hygromycin B and puromycin to select for clones expressing both, HC and LC, cellular libraries were stained for surface IgG expression and simultaneous binding to hROR2-ECD-Twin-Strep by FACS (**Figure 3**). In general, the majority of cellular library clones expressed surface IgG at varying levels, indicating a successful transposition and selection. More importantly, a fraction of these IgG-expressing cells showed variable binding to hROR2-ECD-Twin-Strep, with a correlation of cells expressing higher IgG levels also showing higher hROR2-ECD-Twin-Strep staining levels, detectable as a cell population in the upper-right quadrant of the FACS dot plots (**Figure 3**). From all three mice, libraries exhibiting high percentages of IgG-positive, hROR2-ECD-Twin-Strep-reactive cells were observed in the HC $\gamma$ /LC $\kappa$ -paired libraries (mouse 1357: 14.3%; mouse 1359: 35.8%, and mouse 1363: 12.0%) (**Figure 3**). In comparison to the HC $\gamma$ /LC $\kappa$ -libraries, HC $\mu$ /LC $\kappa$ -paired libraries showed lower percentages of IgG-expressing, hROR2-ECD-Twin-Strep-reactive cells in 2 out of 3 mice (mouse 1357: 1.71%, mouse 1359: 14.8%, mouse: 1363 1.17%). This is most likely a reflection of the higher expected occurrence of antigen binders among secondary and class-switched IgG antibodies derived from a boost response, as compared to IgM antibodies, which are either derived from a primary immune response, or potentially represent antibodies from T-cell independent re-stimulated non-class-switched B lymphocytes.

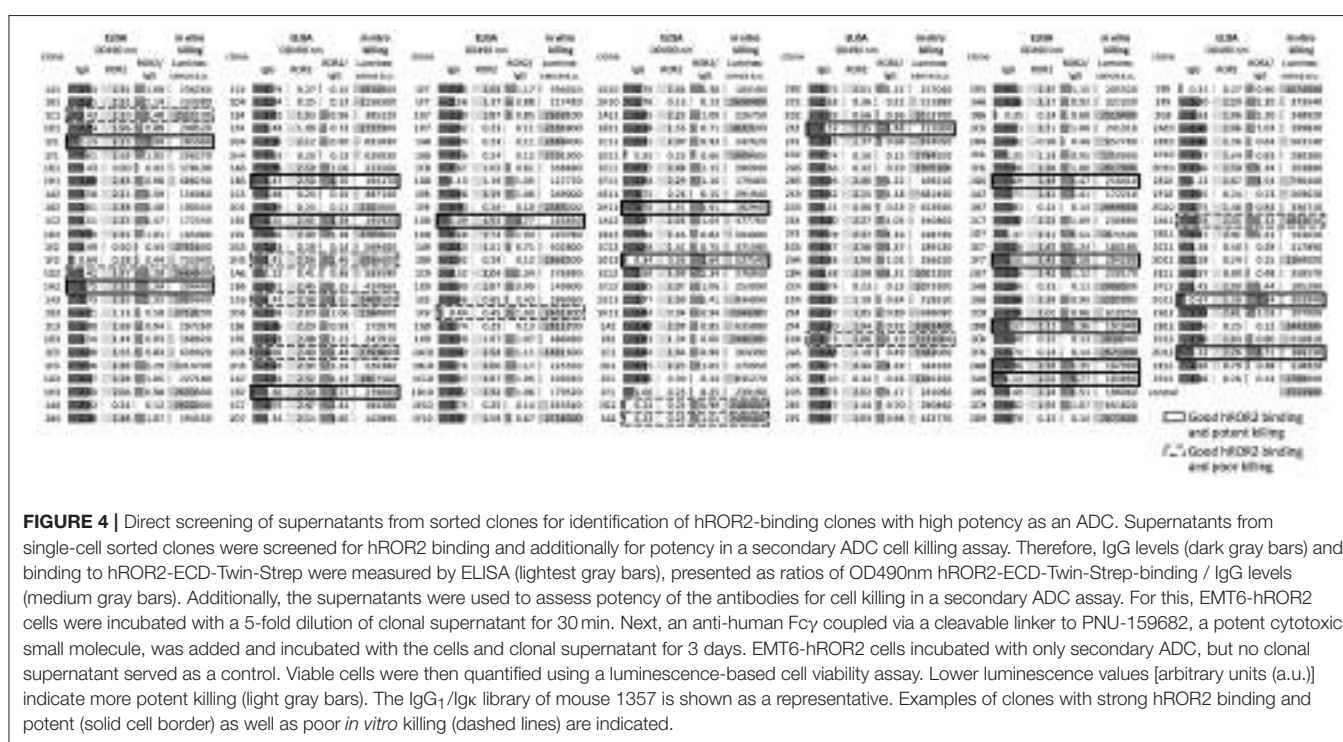
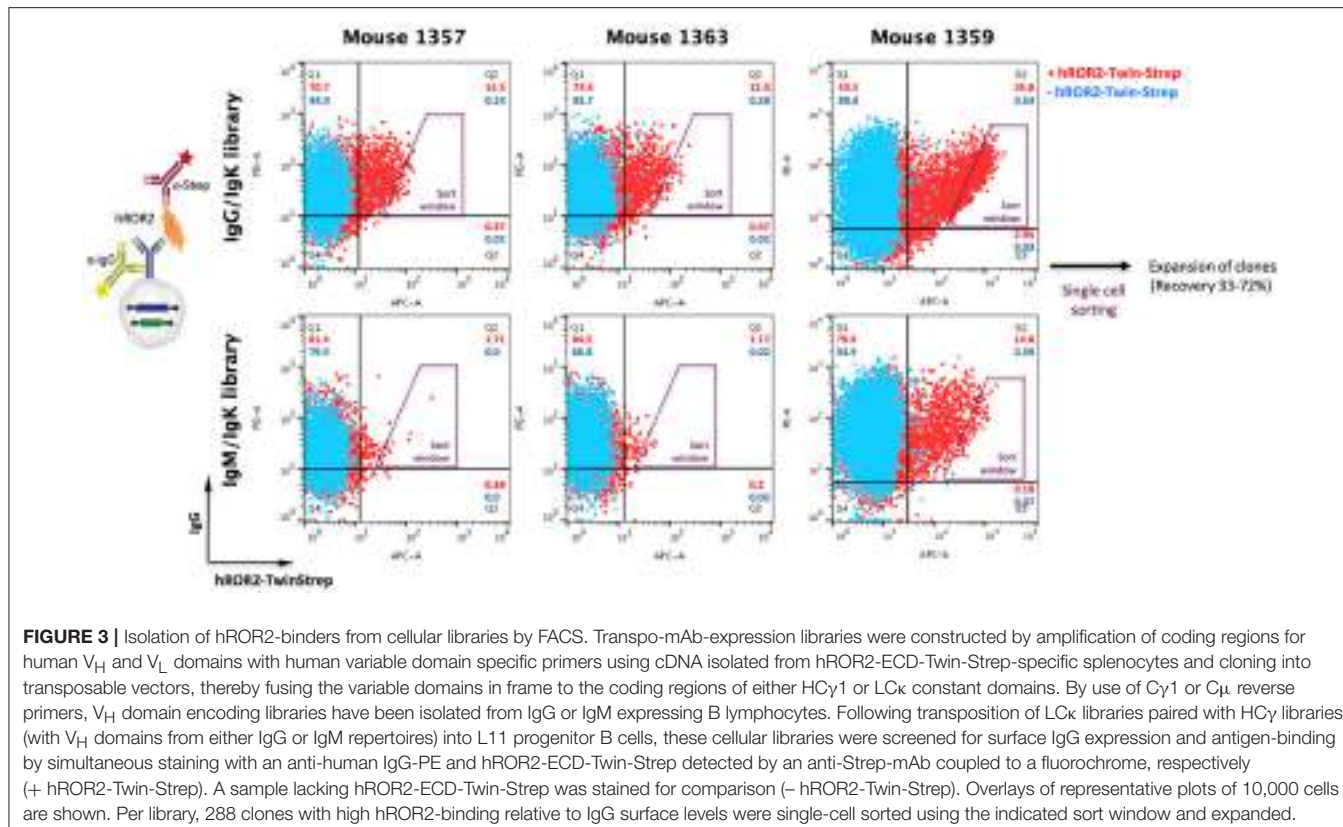
Based on the obtained IgG-hROR2-ECD-Twin-Strep double stainings, a trapezoid FACS sort window was set (see **Figure 3**), in order to sort cells with highest hROR2-ECD-Twin-Strep-reactivity and reasonable IgG expression levels. From each library, a total of 288 clones were single-cell sorted. Recovery following sorting was high, and at least 33% of clones isolated grew out as individual cell clones (mouse 1357: HC $\gamma$ /LC $\kappa$  62%, HC $\mu$ /LC $\kappa$  41%; mouse 1359: HC $\gamma$ /LC $\kappa$  69%, HC $\mu$ /LC $\kappa$  72%; mouse 1363: HC $\gamma$ /LC $\kappa$  44%, HC $\mu$ /LC $\kappa$  33%, **Figure S3**). All recovered individual cell clones obtained from the cellular libraries were selected for further binding and functional screening.

## Identification of Transpo-mAb Cell Clones Producing mAbs With hROR2-Reactivity and High Cell Killing Potency by Direct Functional ADC Screening

In the next step, all recovered individual cell clones were evaluated for their binding to hROR2-ECD-Twin-Strep, as well as for their activity in hROR2-specific cell killing using cells overexpressing hROR2 protein on the cell surface and a toxin-conjugated anti-IgG secondary reagent. To assess binding to hROR2-ECD-Twin-Strep, supernatants from sorted clones containing secreted antibodies were assessed for IgG expression and binding to hROR2-ECD-Twin-Strep by ELISA in a single-well measurement. Then, the ratio between OD = 490 nm (optical density at a wavelength of 490 nm) for hROR2-ECD-Twin-Strep-binding and OD = 490 nm for IgG expression was calculated to normalize hROR2-ECD-Twin-Strep-binding to antibody expression (**Figure 4**-medium gray bars). In the

HC $\gamma$ /LC $\kappa$  libraries, a large number of clonal supernatants showed high hROR2-ECD-Twin-Strep-binding/IgG-expression ratios, indicating that the majority of the single-cell sorted clones expressed antibodies with hROR2-ECD-Twin-Strep-reactivity (**Figure 4**, **Figure S4A**). In contrast, fewer clones with high hROR2-ECD-Twin-Strep-binding/IgG-expression ratios were observed in the HC $\mu$ /LC $\kappa$ -libraries (**Figure S4A**), demonstrating a lower prevalence of strong hROR2-ECD-Twin-Strep-binders in these libraries that were derived from non-class-switched B lymphocytes.

In addition to the measurement of hROR2-ECD-Twin-Strep-binding by ELISA, the supernatants were assessed for *in vitro* cell killing potency in a secondary ADC assay. In this approach, clonal supernatants containing secreted antibodies were incubated with EMT6 cells overexpressing hROR2, followed by addition of an anti-human Fc $\gamma$  IgG coupled to the potent cytotoxic anthracycline PNU-159682 via a cleavable linker, as described in the Materials and Methods. Viable cells were quantified following a 3 days incubation using a luminescence-based cell viability assay in a single-well measurement (**Figure 4**-light gray bars). In all libraries, luminescence signals ranging from low to high were observed, thus representing clonal supernatants with potent to poor *in vitro* cytotoxicity, respectively (**Figure 4**, **Figure S4B**). More importantly, the majority of cell clones exhibited both, strong hROR2-ECD-Twin-Strep-binding as assessed by ELISA, as well as high potency toward hROR2-expressing EMT6 cells by a secondary ADC *in vitro* cell killing assay, indicating suitability of the antibodies expressed by these clones as ADCs (**Figure 4**-solid border). Interestingly, several clones were identified that showed strong binding to hROR2-ECD-Twin-Strep in ELISA, but only poor cytotoxicity in the secondary ADC assay, indicating that not every hROR2-ECD-Twin-Strep-specific antibody is capable of mediating effective delivery of the cytotoxic payload of the secondary ADC to the hROR2-positive EMT6 cells (**Figure 4**-dashed line). This demonstrates that our functional assay is capable of distinguishing hROR2-specific antibodies with and without *in vitro* cell killing activity in a secondary ADC assay. While many clonal supernatants that induced strong *in vitro* cell killing were observed in the HC $\gamma$ /LC $\kappa$  libraries, there were only few potent mAbs in the HC $\mu$ /LC $\kappa$  libraries (**Figure S4B**). This matches the lower occurrence of strong hROR2-binders in these libraries. To confirm their *in vitro* cell killing potency, IgG levels of selected clonal supernatants were quantified and secondary ADC assays were then carried out using serial dilutions of clonal supernatants at defined antibody concentrations. This analysis confirmed the relative cell killing potencies of the selected clones (**Figure S5**). These results suggest that our functional screening not only allows the straightforward identification of antibodies that strongly bind hROR2, but also to rapidly differentiate between antigen-binding clones with or without activity in an *in vitro* ADC cell killing assay. Based on the antigen-reactivity, IgG expression and cell killing activity, 22 hROR2-reactive clones were selected for antibody sequence recovery. From these 22 clones, six clones each originated in mice 1357 and 1363, and 10 clones originated in mouse 1359.



## Recovery of $V_H$ And $V_L$ Coding Regions From Selected hROR2-Reactive Transpo-mAb Cell Clones and Characterization of Novel Fully Human Anti-hROR2 Antibodies

In the next step,  $V_H$  and  $V_L$  coding regions from 22 strongly hROR2-ECD-Twin-Strep-reactive cell clones that also showed potent *in vitro* cell killing activity in the functional ADC assay were recovered by RT-PCR from the stably Ig heavy chain and Ig light chain transposed cell clones, and cloned into an EBNA-based expression vector and sequenced (Figure 5). These clones displayed 12 distinct clonotypes as defined by their heavy chain CDR3 sequences with clonotypes GK-1E5, GK-2G8, and MK-3B12 originating in mouse 1357; clonotypes GK-5A1, GK-5E1, GK-5G12, GK-6B10, and MK-7C3 originating in mouse 1363; and clonotypes GK-21D3, GK-22G12, MK-24C10, and MK-24F9 originating in mouse 1359. While most of the corresponding light chain CDR3 sequences were also distinct, clones GK-1E5, GK-2G8 and MK-3B12, as well as GK-6B10 and MK-7C3, shared the same light chain CDR3 sequences, respectively. It was confirmed that all recovered sequences indeed represented fully human antibodies, as they shared a higher degree of sequence identity to their closest human than to their closest mouse germline V gene sequence, as assessed by IgBLAST. For the HC sequences, identities to the closest human or mouse germline V gene sequence ranged from 90.8–98 to 65.3–79.6%, respectively (Figure 6A). For the LC sequences, identities to the closest human or mouse germline V gene sequence ranged from 92.6–99 to 71.9–77.8%, respectively. This *in silico* IgBLAST analysis also revealed the germline V gene usage of the identified anti-hROR2-clonotypes (Table S1). In the HC sequences, the majority of clonotypes used the  $V_{H3}$ -33 gene segment ( $n = 9$ ), while one clonotype each used the  $V_{H4}$ -38,  $V_{H3}$ -7 or  $V_{H4}$ -34 gene segment. In the LC sequences, the most prevalent  $V_k$  gene segment was  $V_k1$ -5 ( $n = 8$ ), followed by  $V_k1$ -27 ( $n = 3$ ) and  $V_k2$ -28 ( $n = 1$ ). These identified V gene sequences are in line with frequently used human V gene sequences (40).

The 12 distinct clonotypes defined above were expressed at a larger scale in mammalian HEK293T cells and purified using Protein A. To assess the functional properties of the isolated, now recombinantly expressed monoclonal antibodies, affinity to hROR2-ECD-Twin-Strep was measured by Surface Plasmon Resonance (SPR) (Figure 6B, Figure S6). The SPR measurements confirmed that all recovered and recombinantly expressed antibodies showed hROR2-ECD-Twin-Strep binding by SPR with affinities ranging between 0.7 and 347 nM, with 6 of the 12 mAbs having affinities below 10 nM, 5 mAbs having affinities between 10 and 100 nM, and one mAb clone with 347 nM affinity. However, the clones displayed variable association and dissociation rates. 5 mAbs showed favorable and very slow dissociation rates (e.g. GK-22G12, MK-24F9, GK-5E1, GK-6B10, and GK-5B12), including some clones with the highest affinities.

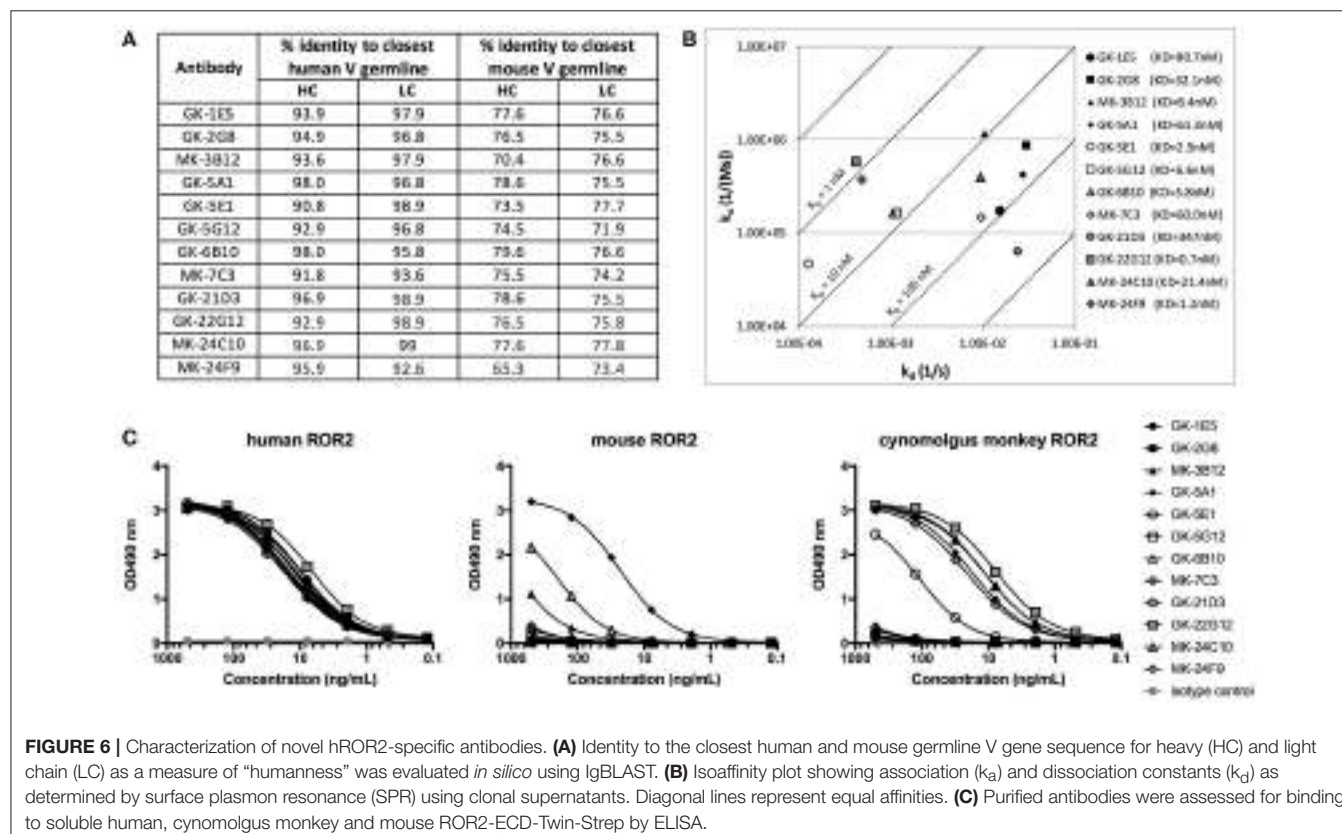
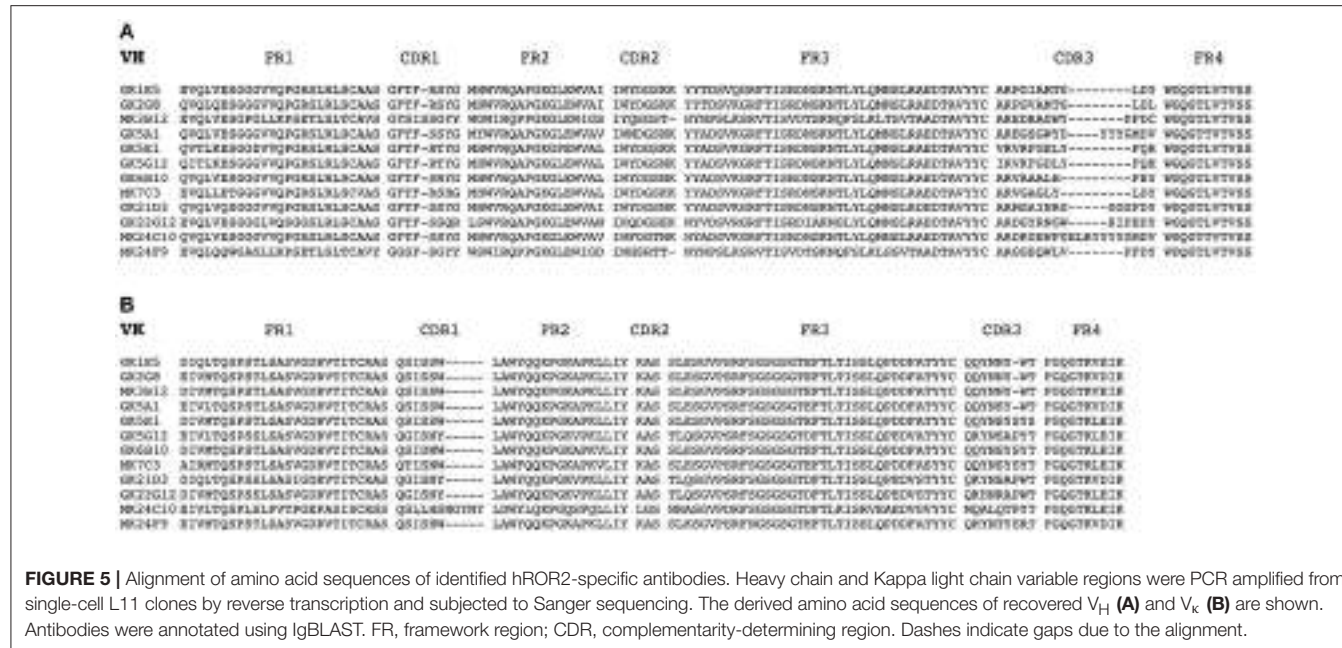
Another important characteristic of therapeutic monoclonal antibodies is their cross-reactivity to their specific antigen

in relevant toxicology species, e.g., mice and cynomolgus monkeys. Therefore, binding of the novel, fully human hROR2-specific mAbs to cynomolgus monkey as well as to mouse ROR2 was evaluated by ELISA (Figure 6C). While all tested antibodies strongly bound to human ROR2, only MK-3B12, GK-5A1, GK-5E1, MK-24C10, MK-24F9, and GK-22G12 were capable of binding cynomolgus monkey ROR2-ECD-Twin-Strep. Interestingly, GK-5A1 also strongly bound to mouse ROR2-ECD-Twin-Strep, with weaker binding observed also for MK-3B12 and MK-24F9. While the specific epitopes recognized by the identified antibodies have not yet been mapped, these results indicate that different epitopes are recognized by these different antibodies.

Taken together, the combined screening approach involving (1) immunization of human Ig-transgenic mice, (2) enrichment of antigen-reactive splenic B lymphocytes from immunized animals by MACS, and (3) concomitant screening of Transpo-mAb IgG display libraries for hROR2 binding and ADC functionality, resulted in the successful identification of a diverse panel of 12 novel, fully human anti-ROR2-specific monoclonal antibodies with nanomolar affinities to hROR2. Furthermore, some of these antibodies recognized ROR2 from relevant toxicology species.

## Generation and Evaluation of hROR2-Specific ADCs

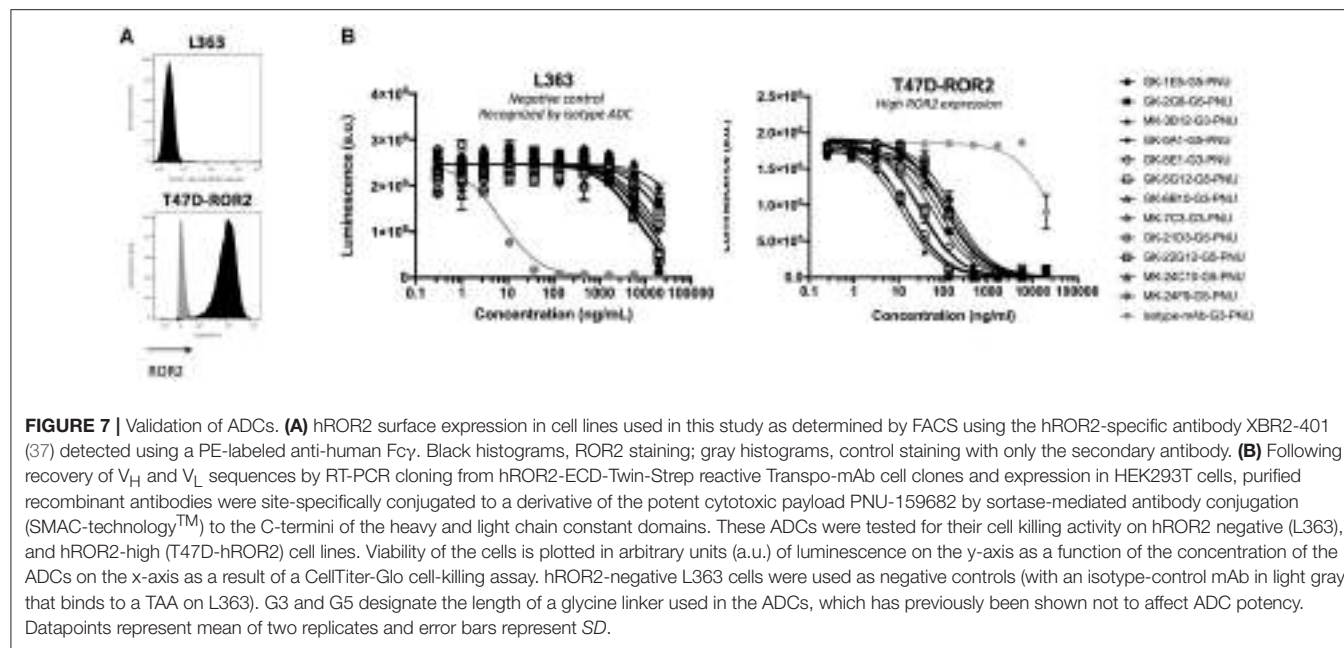
Finally, the activity of the 12 novel hROR2-specific monoclonal antibodies for *in vitro* cell killing was determined after conjugation of the recombinant mAbs to a derivative of the strong cellular toxin PNU-159682. For this, ADCs were generated by site-specific conjugation of a Gly<sub>3</sub>-EDA-PNU, or a Gly<sub>5</sub>-EDA-PNU linker toxin to the C-termini of the Ig heavy and light chains by SMAC-technology<sup>TM</sup> conjugation as described previously (39). The cell killing activity of these ADCs was then assessed on highly hROR2 expressing breast cancer cells T47D-hROR2, and, as a negative control, on hROR2-negative L363 multiple myeloma cells (Figure 7A), as described in the Materials and Methods. Highly potent killing of the highly hROR2-expressing cell line T47D-hROR2 cells was observed with all hROR2-specific ADCs, with IC<sub>50</sub> values ranging from 12.3 to 168 ng/ml (Table S2). In contrast, the ROR2-negative cell line L363 showed only minor cell killing at very high ADC concentrations. As a further control, a L363-reactive ADC (designated: isotype-mAb-G3-PNU) was included in the panel of ADCs tested for cell killing on the hROR2-negative and hROR2-positive cells, demonstrating that L363 cells, but not T47D-hROR2 cells could be killed with a L363-reactive ADC. Taken together, these data clearly demonstrate that the novel, fully human anti-hROR2 mAbs have favorable properties as ADCs for the specific targeting of hROR2 expressing cells. Interestingly, the ADC with the lowest cell killing activity (based on mAb GK-6B10) was among the higher affinity ADCs (K<sub>D</sub> of 5.8 nM). Conversely, the lowest affinity ADC (based on mAb GK-21D3 with a K<sub>D</sub> of 347 nM) had comparable cell killing activity as other, higher affinity ADCs, where the mAbs displayed single-digit nanomolar affinities.



## DISCUSSION

ADCs represent a promising therapeutic principle for cancer treatment, because cellular toxins can more specifically be

targeted to tumor cells via TAA-specific antibodies. A potent ADC kills tumor cells in a target-dependent manner by specifically binding a TAA via its antibody moiety, which at the same time needs to induce efficient internalization of the formed



antigen-ADC complex for efficient delivery of the cytotoxic payload into the tumor cell to release its cytotoxic potential. Because antibodies do not all internalize at the same rate (26, 27), ADC discovery would greatly benefit from functional screening for efficient internalization and eventually cell killing activity during the very early stages of antibody discovery, thereby reducing the time and costs for identification of suitable mAbs for ADC strategies and for pre-clinical development.

Here, we incorporated the functional screening for potent ADCs into the discovery process for novel, fully human hROR2-specific antibodies by combining immunization of transgenic mice with the Transpo-mAb display platform (36). Antigen binding capability and ADC potency with a secondary ADC killing assay was simultaneously evaluated by screening cell culture supernatants from single-cell sorted Transpo-mAb clones with an anti-human Fcγ antibody coupled to a derivative of the cytotoxic payload PNU-159682 via a Cathepsin-cleavable linker (41, 42). This secondary ADC reagent enters the cell by “piggybacking” onto the internalizing antibody, thereby allowing high-throughput screening for internalizing antibodies without prior cloning, re-expression of mAbs, and generation of ADCs from selected cell clones. Strategies for screening for internalizing antibodies using a secondary antibody to deliver a toxic payload have been described previously, including delivery of a protein toxin (43) or a small molecule cytotoxic agent such as Monomethyl auristatin E (MMAE) (44). However, it is important to note that these approaches employed hybridoma supernatants for functional screening, and that the recombinant cloning and sequence determination of hybridoma mAbs is often associated with significant challenges. In contrast, the approach described here involves recombinant libraries where the sequences of identified antibodies are readily available. In addition to the delivery of toxic payloads, other strategies to

functionally screen for internalizing antibodies using secondary reagents have been described, e.g., using a pH-sensitive dye such as Cy5Her5E (45) or a dual label consisting of the fluorophore DL650 and the quencher DL650-QC1 (46). Similar to these assays, our secondary ADC assay likely requires internalization of the antigen-secondary ADC complex by endocytosis and delivery of the complex to the lysosome for proper release and function of the payload in the low pH, protease-rich environment (44, 47). Thus, while both reported fluorescence-based high-throughput methods allow measuring antibody internalization, our assay more closely mimics a primary ADC as it contains a cytotoxic payload and is therefore more predictive of its function and potency as a directly conjugated ADC.

It is important to note that our assay uses an IgG-based rather than a Fab-based secondary reagent. Through the bivalence of the IgG, there is a potential risk for crosslinking of the antigen which could result in an enhanced internalization rate (48). However, these differences are expected to be minor, and it has been found that incubation of the naked antibody Herceptin with either Fab- or IgG-based secondary ADC reagents on HER2-expressing cell lines resulted in comparable IC<sub>50</sub> values (*personal communication from Moradec Inc., www.moradec.com*). While we used PNU-159682 as a model toxin due to its high potency (38, 49), the assay described herein is versatile and can be used with secondary ADC reagents conjugated to any other toxin, including tubulin-inhibitors, and using any suitable target-positive cell line.

In many library screening approaches, antibodies are screened for binding to their target, e.g., by ELISA. However, there is evidence that high affinity does not always correlate with good internalization (50). Similarly, we observed that affinity measured by SPR was not directly correlated with potency as an ADC. While some antibodies with low nanomolar K<sub>D</sub> values induced potent cytotoxicity, we also observed that an ADC based on

clone GK-6B10 ( $K_D = 5.8 \text{ nM}$ ) mediated the lowest potency on T47D-hROR2 cells, whereas an ADC based on the low affinity clone GK-21D3 (347 nM) was quite potent (Figures 6B, 7). These differences are likely to be related to the recognition of different epitopes, which is supported by the observation that 4 of the 5 cynomolgus monkey ROR2-crossreactive mAbs (MK-3B12, GK-22G12, MK-24C10, MK-24F9) give rise to ADCs ranking among the 5 most potent ADCs. This underlines that internalization is a complex process not only depending on binding affinity to the cognate target, but also on the epitope the antibody recognizes, the internalization rate of the antigen-ADC complex and the target surface expression (26, 51). This further highlights the importance of functionally screening antibodies for their ability to deliver a cytotoxic payload, rather than just for affinity, in a high-throughput setting during early discovery of ADCs.

One important aspect of our present study is the use of fully human immune libraries in the functional screening for ADC candidates. The discovery of fully human antibodies is highly desired for therapeutic use due to an expected lower risk of immunogenicity associated with a better efficacy and safety profile. Human antibodies can be obtained by numerous methods, including screening phage or yeast display libraries, identification of human mAbs from human PBMCs or antibody discovery from various human Ig transgenic mice (52–56). While some human antibody transgenic mouse strains achieve comparable serum titers to wild-type mice in response to antigen challenge, most transgenic mice have lower titers than wild-type mice (52, 57). We also observed lower serum titers in H2L2 Ig transgenic mice compared to wild-type mice following the same immunization strategy. Importantly, the serum titers in H2L2 mice we observed were in line with previous reports (Patent WO2017063593A1, WO2017016497A1), where titers around 1:10,000 as measured by ELISA were achieved using different antigens for immunization. This is possibly explained by the fact that the H2L2 transgenic mice harbor a small subset of variable, diversity and joining gene segments in comparison to the endogenous germline repertoire of variable, diversity and joining gene segments in the wild-type mouse genome. However, it is also possible that the human  $V_H$  and  $V_L$  coding regions assembled from the transgenic miniloci in combination with the rat constant regions contained in these transgenic constructs may not be able to generate the same signal quality during early B lymphopoiesis in the bone marrow of the transgenic mice, which may result in lower peripheral B cell numbers. During early pre-B cell development in the bone marrow of wild-type mice, V(D)J recombination on the heavy chain locus precedes V(D)J recombination on the light chain locus (58) and pre-B cells with a productive heavy chain rearrangement are expanded by expression of a pre-B cell receptor (pre-BCR) formed by the  $\mu H$  chain with the VpreB and  $\lambda_5$  surrogate light chain components (59, 60). This proliferative expansion of so-called pre-B-II cells with a signaling pre-BCR is critical for an effective generation of a full peripheral B cell compartment, as evidenced by mice with lack of either surrogate light chain components (61), or lack of the  $\mu H$  chain transmembrane anchor (62), or of the pre-BCR/BCR signaling components, B29 and mb-1. In addition, it is also possible that the human  $V_H$  and  $V_L$  regions following

productive rearrangements do not mediate proper association with the murine surrogate light chain components, VpreB and  $\lambda_5$ , thus compromising pre-BCR signaling and generation of a proliferating preB-II cell compartment. Equally, it is possible that the transgenic heavy and light chain gene loci do not mediate the proper sequential V(D)J recombination events on the heavy and the light chain gene loci and that IgMs from simultaneously rearranged transgenic heavy and light chain gene loci are expressed, which may not be able to trigger the proliferative expansion of pre-BCR expressing pre-B-II cells to the same extent as in wild-type mice. This would result in only a slow filling up of a normally sized peripheral B cell population, as observed in surrogate light chain knock-out mice (59), which depend on productive V to J gene rearrangements of conventional light chain loci, in the absence of the capacity to express a pre-BCR comprising a surrogate light chain (61). Without a detailed analysis of the pre-B and B cell subsets in H2L2 Ig transgenic mice it is not possible to predict, which of the discussed mechanisms accounts for the roughly 9-fold reduced antibody titers upon immunization of H2L2 mice vs. wild-type mice. Nevertheless, despite a weaker humoral immune response, we were able to identify a very diverse set of novel high affinity and fully-human anti-ROR2-specific antibodies from H2L2 mice for further characterization and development.

In summary, the combination of an immunization strategy of H2L2 transgenic mice with the IgG Transpo-mAb display platform expressing fully human antibodies has proven to be a powerful and effective method to identify novel hROR2 antibodies with potent cell killing activity as ADCs early during the antibody discovery process. Through the straightforward functional screening of soluble antibodies directly from the supernatants of sorted cells, we identified 12 fully human, monoclonal hROR2-specific antibodies with distinct characteristics with the potential to result in potent ADCs and the potential to be promising drug candidates for human tumor therapy. The functional screening approach presented here will be highly beneficial for the fast and efficient discovery of fully human antibodies and greatly help accelerate the development of ADCs.

## AUTHOR CONTRIBUTIONS

IH, LW, UG, and RB conceived the experiments. IH, M-CB-E, KM, and FW conducted the experiments and analyzed the data. IH, RB, and UG wrote the paper.

## ACKNOWLEDGMENTS

We would like to thank Sai T. Reddy, Gieri Camenisch and Daniel Zimmer from the D-BSSE of the ETH Zurich for their excellent technical support in planning and performing the mouse immunizations. We would also like to thank Henrik Schinke for valuable technical assistance and Romina Dörig and Christiane Zaborosch from the Zürcher Hochschule für Angewandte Wissenschaften (ZHAW) Wädenswil, Switzerland, for SPR measurements of selected ROR2 mAbs.

## SUPPLEMENTARY MATERIAL

The Supplementary Material for this article can be found online at: <https://www.frontiersin.org/articles/10.3389/fimmu.2018.02490/full#supplementary-material>

**Figure S1** | Primer sequences for library construction. Primers were either adapted from \*(1) Sblattero and Bradbury (63); (2) Tiller et al. (64); (3) Berry et al. (65); or (4) developed in-house.

**Figure S2** | Quality control analysis of the transposable expression vector libraries. 10–15 individual plasmids derived from the HC<sub>γ</sub>, HC<sub>μ</sub>, and LC<sub>κ</sub> libraries of mice 1357, 1359, and 1363 were analyzed using DNA sequencing and *in silico* IgBLAST analysis. IgBLAST was used to annotate the CDR3 sequences and to determine the sequence identities of the identified variable domains to their closest human germline V gene sequence. Sequences with an early stop codon were defined as incomplete.

**Figure S3** | Recovered clones following single-cell sorting for hROR2-binding cellular library clones. A total of 288 clones per library were sorted and expanded. The number and percentage of recovered clones are indicated.

**Figure S4** | Direct screening of supernatants from sorted clones allows identification of hROR2-binding clones with high potency as an ADC. **(A)** Supernatants from sorted single-cell cellular clones of the (GK) and (MK) libraries (GK = V<sub>H</sub> sequences cloned from IgGs, MK = V<sub>H</sub> sequences cloned from IgMs based on different reverse primers used) derived from mice 1357, 1359, and 1363 were functionally screened for IgG levels and hROR2-ECD-Twin-Strep binding by ELISA in a single-well measurement. Normalized hROR2 binding was expressed as the ratio of OD = 490 nm hROR2-ECD-Twin-Strep binding and OD = 490 nm IgG expression for all clones from the different libraries and is shown as box-plots. **(B)** All supernatants were also assessed for potency as an ADC using a secondary ADC assay. For this, EMT6-hROR2 cells were incubated with clonal supernatant without normalization for IgG levels for 30 min, before addition of an anti-human Fc<sub>Y</sub> coupled via a cleavable linker to PNU-159682. Viable cells were quantified following a 3 days incubation using a luminescence-based cell viability assay. Lower luminescence values in the box-plots indicate more potent killing.

**Figure S5** | Validation of *in vitro* killing potency of selected clones from functional ADC screening. Twelve clonal L11 supernatants with potent *in vitro* killing and four supernatants with poor *in vitro* killing (GK-1C6, GK-1G6, MK-3E5, and MK-3A11) were selected for testing in a secondary ADC assay using a range of defined concentrations to confirm their *in vitro* cell killing potency. To do so, IgG levels of the supernatants were quantified by ELISA and IgG concentration in all supernatants was adjusted to the lowest expressor. EMT6-hROR2 cells were incubated with 2-fold serial dilutions of these normalized clonal supernatants for 30 min, followed by the addition of an anti-human Fc<sub>Y</sub> coupled via a cleavable linker to PNU-159682. After a 3 days incubation, viable cells were quantified using a luminescence-based cell viability assay. **(A)** Viability of the EMT6-hROR2 cells plotted in arbitrary units (a.u.) of luminescence on the y-axis as a function of the IgG concentration in the supernatants on the x-axis. Clonal supernatants that had potent or poor *in vitro* cell killing potency in the initial functional ADC screening are shown in black or gray, respectively. **(B)** shows luminescence values that had been determined in the one-well secondary ADC assay during functional ADC screening compared to the IC<sub>50</sub> values which were determined in the secondary ADC assay using serial dilutions of normalized supernatants for the same clonal supernatants. IC<sub>50</sub> values were calculated using a four-parameter curve fitting model in GraphPad Prism. n/a indicates IC<sub>50</sub> values that could not be calculated due to a lack of *in vitro* killing.

**Figure S6** | SPR sensorgrams of anti-hROR2 antibodies. Affinities were measured by multi-cycle SPR on a Biacore T200 instrument (GE Healthcare). Antibodies were captured by Protein A or G immobilized on a CM5 sensor chip, followed by the addition of hROR2-ECD-Twin-Strep used as 2-fold serial dilutions ranging from 40 to 2.5 nM. KD values as a measure of binding affinity are indicated.

**Table S1** | Germline V gene usage of identified anti-hROR2-clonotypes. The closest human germline V gene sequences of heavy (HC) and light chain (LC) were identified *in silico* using IgBLAST.

**Table S2** | *In vitro* cell killing by anti-hROR2-ADCs. IC<sub>50</sub> values (ng/ml) reported here represent the IC<sub>50</sub> values of the hROR2-specific ADCs tested for their cell killing activity on hROR2-negative L363 and hROR2-high EMT6-hROR2 cell lines in **Figure 7**. IC<sub>50</sub> values were calculated from the mean of two replicates using a four-parameter curve fitting model in GraphPad Prism.

## REFERENCES

- Lambert JM, Morris CQ. Antibody-drug conjugates (ADCs) for personalized treatment of solid tumors: a review. *Adv Ther.* (2017) 34:1015–35. doi: 10.1007/s12325-017-0519-6
- Köhler G, Milstein C. Continuous cultures of fused cells secreting antibody of predefined specificity. *Nature* (1975) 256:495–7. doi: 10.1038/256495a0
- Beck A. Review of antibody-drug conjugates, methods in molecular biology series. *mabs* (2013) 6:30–3. doi: 10.4161/mabs.27005
- Beck A, Goetsch L, Dumontet C, Corvaia N. Strategies and challenges for the next generation of antibody-drug conjugates. *Nat Publish Group* (2017) 16:315–37. doi: 10.1038/nrd.2016.268
- Rebagay G, Yan S, Liu C, Cheung NK. ROR1 and ROR2 in Human malignancies: potentials for targeted therapy. *Front Oncol.* (2012) 2:34. doi: 10.3389/fonc.2012.00034
- Ford CE, Qian Ma SS, Quadrif A, Ward RL. The dual role of the novel Wnt receptor tyrosine kinase, ROR2, in human carcinogenesis. *Int J Cancer* (2013) 133:779–87. doi: 10.1002/ijc.27984
- Debebe Z, Rathmell WK. Ror2 as a Therapeutic target in cancer. *Pharmacol Ther.* (2015) 150:143–8. doi: 10.1016/j.pharmthera.2015.01.010
- DeChiara TM, Kimble RB, Poueymirou WT, Rojas J, Masiakowski P, Valenzuela DM, et al. Ror2, encoding a receptor-like tyrosine kinase, is required for cartilage and growth plate development. *Nat Genet.* (2000) 24:271–4. doi: 10.1038/73488
- Green JL, Kuntz SG, Sternberg PW. Ror receptor tyrosine kinases: orphans no more. *Trends Cell Biol.* (2008) 18:536–44. doi: 10.1016/j.tcb.2008.08.006
- Morioka K, Tanikawa C, Ochi K, Daigo Y, Katagiri T, Kawano H, et al. Orphan receptor tyrosine kinase ROR2 as a potential therapeutic target for osteosarcoma. *Cancer Sci.* (2009) 100:1227–33. doi: 10.1111/j.1349-7006.2009.01165.x
- Wright TM, Rathmell WK. Identification of Ror2 as a hypoxia-inducible factor target in von Hippel-Lindau-associated renal cell carcinoma. *J Biol Chem.* (2010) 285:12916–24. doi: 10.1074/jbc.M109.073924
- Yang CM, Ji S, Li Y, Fu LY, Jiang T, Meng FD. Ror2, a developmentally regulated kinase, is associated with tumor growth, apoptosis, migration, and invasion in renal cell carcinoma. *Oncol Res.* (2017) 25:195–205. doi: 10.3727/096504016X14732772150424
- O'Connell MP, Fiori JL, Xu M, Carter AD, Frank BP, Camilli TC, et al. The orphan tyrosine kinase receptor, ROR2, mediates Wnt5A signaling in metastatic melanoma. *Oncogene* (2009) 29:34–44. doi: 10.1038/onc.2009.305
- Edris B, Espinosa I, Mühlberg T, Mikels A, Lee CH, Steigen SE, et al. ROR2 is a novel prognostic biomarker and a potential therapeutic target in leiomyosarcoma and gastrointestinal stromal tumour. *J Pathol.* (2012) 227:223–33. doi: 10.1002/path.3986
- Baylerová M, Menck K, Klemm F, Wolff A, Pukrop T, Binder C, et al. Ror2 Signaling and Its Relevance in Breast Cancer Progression. *Front Oncol.* (2017) 7:135. doi: 10.3389/fonc.2017.00135
- Roarty K, Pfefferle AD, Creighton CJ, Perou CM, Rosen JM. Ror2-mediated alternative Wnt signaling regulates cell fate and adhesion during mammary tumor progression. *Oncogene* (2017) 36:5958–68. doi: 10.1038/onc.2017.206
- Mei H, Lian S, Zhang S, Wang W, Mao Q, Wang H. High expression of ROR2 in cancer cell correlates with unfavorable prognosis in colorectal cancer. *Biochem Biophys Res Commun.* (2014) 453:703–9. doi: 10.1016/j.bbrc.2014.09.141
- Kobayashi M, Shibuya Y, Takeuchi J, Murata M, Suzuki H, Yokoo S, et al. Ror2 expression in squamous cell carcinoma and epithelial dysplasia of the oral cavity. *YMOE* (2009) 107:398–406. doi: 10.1016/j.tripleo.2008.08.018

19. Huang J, Fan X, Wang X, Lu Y, Zhu H, Wang W, et al. High ROR2 expression in tumor cells and stroma is correlated with poor prognosis in pancreatic ductal adenocarcinoma. *Sci Rep.* (2015) 5:9. doi: 10.1038/srep12991
20. Oishi I, Suzuki H, Onishi N, Takada R, Kani S, Ohkawara B, et al. The receptor tyrosine kinase Ror2 is involved in non-canonical Wnt5a/JNK signalling pathway. *Genes Cells* (2003) 8:645–54. doi: 10.1046/j.1365-2443.2003.00662.x
21. Yamamoto H, Yoo SK, Nishita M, Kikuchi A, Minami Y. Wnt5a modulates glycogen synthase kinase 3 to induce phosphorylation of receptor tyrosine kinase Ror2. *Genes to Cells* (2007) 12:1215–23. doi: 10.1111/j.1365-2443.2007.01128.x
22. Rasmussen NR, Wright TM, Brooks SA, Hacker KE, Debebe Z, Sendor AB, et al. Receptor tyrosine kinase-like orphan receptor 2 (Ror2) expression creates a poised state of Wnt signaling in renal cancer. *J Biol Chem.* (2013) 288:26301–10. doi: 10.1074/jbc.M113.466086
23. Cheung NK. ROR1 and ROR2 in human malignancies: potentials for targeted therapy. *Front Oncol.* (2012) 2:1–8. doi: 10.3389/fonc.2012.00034/abstract
24. Henry C, Hacker N, Ford C. Silencing ROR1 and ROR2 inhibits invasion and adhesion in an organotypic model of ovarian cancer metastasis. *Oncotarget* (2017) 8:112727–38. doi: 10.18632/oncotarget.22559
25. Ritchie M, Tchistiakova L, Scott N. Implications of receptor-mediated endocytosis and intracellular trafficking dynamics in the development of antibody drug conjugates. *mAbs* (2014) 5:13–21. doi: 10.4161/mabs.22854
26. Rudnick SI, Lou J, Shaller CC, Tang Y, Klein-Szanto AJP, Weiner LM, et al. Influence of affinity and antigen internalization on the uptake and penetration of anti-HER2 antibodies in solid tumors. *Cancer Res.* (2011) 71:2250–9. doi: 10.1158/0008-5472.CAN-10-2277
27. Chaparro-Riggers J, Liang H, DeVay RM, Bai L, Sutton JE, Chen W, et al. Increasing serum half-life and extending cholesterol lowering in vivo by engineering antibody with pH-sensitive binding to PCSK9. *J Biol Chem.* (2012) 287:11090–7. doi: 10.1074/jbc.M111.319764
28. Boder ET, Wittrup KD. Yeast surface display for screening combinatorial polypeptide libraries. *Nat Biotechnol.* 15:553–537. doi: 10.1038/nbt0697-553
29. Gai SA, Wittrup KD. Yeast surface display for protein engineering and characterization. *Curr Opin Struct Biol.* (2007) 17:467–73. doi: 10.1016/j.sbi.2007.08.012
30. Smith ES, Shi S, Zauderer M. Construction of cDNA libraries in vaccinia virus. In: Isaacs SN, editor. *Vaccinia Virus and Poxvirology*. Totowa, NJ: Humana Press (2004). p. 65–75.
31. Ho M, Nagata S, Pastan I. Isolation of anti-CD22 Fv with high affinity by Fv display on human cells. *Proc Natl Acad Sci USA.* (2006) 103:9637–42. doi: 10.1073/pnas.0603653103
32. Beerli RR, Bauer M, Buser RB, Gwerder M, Muntwiler S, Maurer P, et al. Isolation of human monoclonal antibodies by mammalian cell display. *Proc Natl Acad Sci USA.* (2008) 105:14336–41. doi: 10.1073/pnas.0805942105
33. Breous-Nystrom E, Schultze K, Meier M, Flueck L, Holzer C, Boll M, et al. Retrocyte display® technology: generation and screening of a high diversity cellular antibody library. *Methods* (2014) 65:57–67. doi: 10.1016/j.ymeth.2013.09.003
34. Hughes B. Antibody-drug conjugates for cancer: poised to deliver? *Nat Publish Group* (2010) 9:665–7. doi: 10.1038/nrd3270
35. Hock MB, Thudium KE, Carrasco-Triguero M, Schwabe NF. Immunogenicity of antibody drug conjugates: bioanalytical methods and monitoring strategy for a novel therapeutic modality. *AAPS J.* (2014) 17:35–43. doi: 10.1208/s12248-014-9684-6
36. Waldmeier L, Hellmann I, Gutknecht CK, Wolter FI, Cook SC, Reddy ST, et al. Transpo-mAb display: Transposition-mediated B cell display and functional screening of full-length IgG antibody libraries. *mAbs* (2016) 8:726–40. doi: 10.1080/19420862.2016.1160990
37. Peng H, Nerreter T, Chang J, Qi J, Li X, Karunadharma P, et al. Mining naïve rabbit antibody repertoires by phage display for monoclonal antibodies of therapeutic utility. *J Mol Biol.* (2017) 429:2954–73. doi: 10.1016/j.jmb.2017.08.003
38. Stefan N, Gébleux R, Waldmeier L, Hell T, Escher M, Wolter FI, et al. Highly potent, anthracycline-based antibody-drug conjugates generated by enzymatic, site-specific conjugation. *Mol Cancer Ther.* (2017) 16:879–92. doi: 10.1158/1535-7163.MCT-16-0688
39. Beerli RR, Hell T, Merkel AS, Grawunder U. Sortase enzyme-mediated generation of site-specifically conjugated antibody drug conjugates with high *in vitro* and *in vivo* potency. *PLoS ONE* (2015) 10:e0131177–17. doi: 10.1371/journal.pone.0131177
40. Tiller T, Schuster I, Deppe D, Siegers K, Strohner R, Herrmann T, et al. A fully synthetic human Fab antibody library based on fixed VH/VL framework pairings with favorable biophysical properties. *mAbs* (2013) 5:445–70. doi: 10.4161/mabs.24218
41. Doronina SO, Toki BE, Torgov MY, Mendelsohn BA, Cerveny CG, Chace DF, et al. Development of potent monoclonal antibody auristatin conjugates for cancer therapy. *Nat Biotechnol.* (2003) 21:778–84. doi: 10.1038/nbt832
42. Francisco JA. cAC10-vcMMAE, an anti-CD30-monomethyl auristatin E conjugate with potent and selective antitumor activity. *Blood* (2003) 102:1458–65. doi: 10.1182/blood-2003-01-0039
43. Till M, May RD, Uhr JW, Thorpe PE, Vitetta ES. An assay that predicts the ability of monoclonal antibodies to form potent ricin A chain-containing immunotoxins. *Cancer Res.* (1988) 48:1119–23.
44. Klussman K, Mixan BJ, Cerveny CG, Meyer DL, Senter PD, Wahl AF. Secondary mAb-vcMMAE conjugates are highly sensitive reporters of antibody internalization via the lysosome pathway. *Bioconjugate Chem.* (2004) 15:765–73. doi: 10.1021/bc049969t
45. Riedl T, van Boxtel E, Bosch M, Parren PW, Gerritsen AF. High-throughput screening for internalizing antibodies by homogeneous fluorescence imaging of a pH-activated probe. *J Biomol Screen.* (2016) 21:12–23. doi: 10.1177/1087057115613270
46. Li Y, Liu PC, Shen Y, Snavely MD, Hiraga K. A cell-based internalization and degradation assay with an activatable fluorescence-quencher probe as a tool for functional antibody screening. *J Biomol Screen.* (2015) 20:869–75. doi: 10.1177/1087057115588511
47. Dubowchik GM, Mosure K, Knipe JO, Firestone RA. Cathepsin B-sensitive dipeptide prodrugs. 2. Models of anticancer drugs paclitaxel (Taxol), mitomycin C and doxorubicin. *Bioorg Med Chem Lett.* (1998) 8:3347–52.
48. Schmidt MM, Thurber GM, Wittrup KD. Kinetics of anti-carcinoembryonic antigen antibody internalization: effects of affinity, bivalence, and stability. *Cancer Immunol Immunother.* (2008) 57:1879–90. doi: 10.1007/s00262-008-0518-1
49. Quintieri L, Geroni C, Fantin M, Battaglia R, Rosato A, Speed W, et al. Formation and antitumor activity of PNU-159682, a major metabolite of nemorubicin in human liver microsomes. *Clin Cancer Res.* (2005) 11:1608–17. doi: 10.1158/1078-0432.CCR-04-1845
50. Lyon RP, Meyer DL, Setter JR, Senter PD. *Conjugation of Anticancer Drugs Through Endogenous Monoclonal Antibody Cysteine Residues*. 1st ed. Elsevier Inc (2012).
51. Andreev J, Thambi N, Perez Bay AE, Delfino F, Martin J, Kelly MP, et al. Bispecific antibodies and antibody-drug conjugates (ADCs) bridging HER2 and prolactin receptor improve efficacy of HER2 ADCs. *Mol Cancer Ther.* (2017) 16:681–93. doi: 10.1158/1535-7163.MCT-16-0658
52. Brüggemann M, Osborn MJ, Ma B, Hayre J, Avis S, Lundstrom B, et al. Human antibody production in transgenic animals. *Arch Immunol Ther Exp.* (2014) 63:101–8. doi: 10.1007/s00005-014-0322-x
53. Jones PT, Dear PH, Foote J, Neuberger MS, Winter G. Replacing the complementarity-determining regions in a human antibody with those from a mouse. *Nature* (1986) 321:522–5. doi: 10.1038/321522a0
54. Co MS, Queen C. Humanized antibodies for therapy. *Nature* (1991) 351:501–2. doi: 10.1038/351501a0
55. Chao G, Lau WL, Hackel BJ, Sazinsky SL, Lippow SM, Wittrup KD. Isolating and engineering human antibodies using yeast surface display. *Nat Protoc.* (2006) 1:755–68. doi: 10.1038/nprot.2006.94
56. Sblattero D, Bradbury A. Exploiting recombination in single bacteria to make large phage antibody libraries. *Nat Biotechnol.* (2000) 18:75–80. doi: 10.1038/71958
57. Lee EC, Liang Q, Ali H, Bayliss L, Beasley A, Bloomfield-Gerdes T, et al. Complete humanization of the mouse immunoglobulin loci enables efficient therapeutic antibody discovery. *Nat Biotechnol.* (2014) 1–12. doi: 10.1038/nbt.2825
58. Chen J, Alt FW. Gene rearrangement and B-cell development. *Curr Opin Immunol.* (1993) 5:194–200.

59. Kitamura D, Kudo A, Schaal S, Müller W, Melchers F, Rajewsky K. A critical role of  $\lambda$ 5 protein in B cell development. *Cell* (1992) 69:823–31. doi: 10.1016/0092-8674(92)90293-1
60. Melchers F, Haasner D, Grawunder U, Kalberer C, Karasuyama H, Winkler T, et al. Roles of IgH and L chains and of surrogate H and L chains in the development of cells of the B lymphocyte lineage. *Annu Rev Immunol.* (1994) 12:209–25. doi: 10.1146/annurev.jy.12.040194.001233
61. Rolink A, Karasuyama H, Grawunder U, Haasner D, Kudo A, Melchers F. B cell development in mice with a defective  $\lambda$ 5 gene. *Eur J Immunol.* (1993) 23:1284–8. doi: 10.1002/eji.1830230614
62. Kitamura D, Roes J, Kühn R, Rajewsky K. A B cell-deficient mouse by targeted disruption of the membrane exon of the immunoglobulin mu chain gene. *Nature* (1991) 350:423–26. doi: 10.1038/350423a0
63. Sblattero D, Bradbury A. A definitive set of oligonucleotide primers for amplifying human V regions. *Immunotechnology* (1998) 3:271–8.
64. Tiller T, Meffre E, Yurasov S, Tsuji M, Nussenzweig MC, Wardemann H. Efficient generation of monoclonal antibodies from single human B cells by single cell RT-PCR and expression vector cloning. *J Immunol Methods* (2008) 329:112–24. doi: 10.1016/j.jim.2007.09.017
65. Berry JD, Rutherford J, Silverman GJ, Kaul R, Elia M, Gobuty S, et al. Development of functional human monoclonal single-chain variable fragment antibody against HIV-1 from human cervical B cells. *Hybrid Hybridom.* (2003) 22:97–108. doi: 10.1089/153685903321948021

**Conflict of Interest Statement:** IH, LW, M-CB-E, UG, and RB are employees of NBE-Therapeutics Ltd and hold stocks or stock options of NBE-Therapeutics Ltd. This work has been included in a patent application by NBE-Therapeutics Ltd.

The remaining authors declare that the research was conducted in the absence of any commercial or financial relationships that could be construed as a potential conflict of interest.

Copyright © 2018 Hellmann, Waldmeier, Bannwarth-Escher, Maslova, Wolter, Grawunder and Beerli. This is an open-access article distributed under the terms of the Creative Commons Attribution License (CC BY). The use, distribution or reproduction in other forums is permitted, provided the original author(s) and the copyright owner(s) are credited and that the original publication in this journal is cited, in accordance with accepted academic practice. No use, distribution or reproduction is permitted which does not comply with these terms.



OPEN ACCESS

**Edited by:**

Hermann Eibel,

Universitätsklinikum Freiburg,  
Albert Ludwigs Universität  
Freiburg, Germany

**Reviewed by:**

Helmut Jonuleit,

Johannes Gutenberg-Universität  
Mainz, Germany  
Laurence Morel,  
University of Florida, United States

**\*Correspondence:**

Stefan Heiler  
s.heiler@unibas.ch

**†Present address:**

Jonas Lötscher,  
Immunobiology, Department of  
Biomedicine, University of Basel,  
Basel, Switzerland;  
Matthias Kreuzaler,  
Infection Biology, Department of  
Biomedicine, University of Basel,  
Basel, Switzerland

<sup>†</sup>These authors have contributed  
equally to this work.

<sup>§</sup>Deceased.

**Specialty section:**

This article was submitted  
to B Cell Biology,  
a section of the journal  
*Frontiers in Immunology*

**Received:** 18 December 2017

**Accepted:** 16 March 2018

**Published:** 04 April 2018

**Citation:**

Heiler S, Lötscher J, Kreuzaler M,  
Rolink J and Rolink A (2018)  
Prophylactic and Therapeutic Effects  
of Interleukin-2 (IL-2)/Anti-IL-2  
Complexes in Systemic Lupus  
Erythematosus-Like Chronic  
Graft-Versus-Host Disease.  
*Front. Immunol.* 9:656.  
doi: 10.3389/fimmu.2018.00656

# Prophylactic and Therapeutic Effects of Interleukin-2 (IL-2)/Anti-IL-2 Complexes in Systemic Lupus Erythematosus-Like Chronic Graft-Versus-Host Disease

Stefan Heiler<sup>\*,†</sup>, Jonas Lötscher<sup>†‡</sup>, Matthias Kreuzaler<sup>†</sup>, Johanna Rolink and Antonius Rolink<sup>§</sup>

Developmental and Molecular Immunology, Department of Biomedicine, University of Basel, Basel, Switzerland

Murine chronic graft-versus-host-disease (cGvHD) induced by injection of parental lymphocytes into F1 hybrids results in a disease similar to systemic lupus erythematosus. Here, we have used DBA/2 T cell injection into (C57BL/6 × DBA/2)F1 (BDF1) mice as a model system to test the prophylactic and therapeutic effects of interleukin-2 (IL-2)/anti-IL-2 immune complexes on the course of cGvHD. Our findings demonstrate that pretreatment with Treg inducing JES6/IL-2 complexes render BDF1 mice largely resistant to induction of cGvHD, whereas pretreatment with CD8<sup>+</sup> T cell/NK cell inducing S4B6/IL-2 complexes results in a more severe cGvHD. In contrast, treatment with JES6/IL-2 complexes 4 weeks after induction had no beneficial effect on disease symptoms. However, similar treatment with S4B6/IL-2 complexes led to a significant amelioration of the disease. This therapeutic effect seems to be mediated by donor CD8<sup>+</sup> T cells. The fact that a much stronger cGvHD is induced in BDF1 mice depleted of donor CD8<sup>+</sup> T cells strongly supports this conclusion. The contrasting effects of the two different IL-2 complexes are likely due to different mechanisms.

**Keywords:** chronic graft-versus-host-disease, interleukin-2/anti-interleukin-2 complexes, lupus, host regulatory T cells, donor CD8<sup>+</sup> T cells, interleukin-2 receptor, autoantibodies, immune complex-mediated glomerulonephritis

## INTRODUCTION

Systemic lupus erythematosus (SLE) is a complex, systemic autoimmune disease affecting multiple organs (1). High titers of autoantibodies binding to nuclear components, including histones and DNA, are characteristic of SLE and are routinely used as a disease marker in clinical diagnosis. Immune complex-mediated glomerulonephritis (ICGN), likely resulting from renal deposition of immune complexes and autoantibodies, is a common and severe clinical manifestation of SLE causing high mortality among affected individuals (2). Although the cellular and molecular events leading to breakdown of tolerance and the emergence of pathologic autoantibodies are still rather obscure, genetic traits clearly play a pivotal role in the susceptibility to SLE (3, 4). Once tolerance is broken either at the T cell or B cell level, self-amplifying/sustaining loops of antigen-presentation and lymphocyte-activation contribute to the generation of high-affinity autoantibodies (5, 6). Notably, the majority of pathogenic autoantibodies found in SLE are somatically hypermutated and class-switched, indicating differentiation and affinity maturation of autoreactive B cells in

the germinal centers of secondary lymphoid organs. Moreover, through somatic hypermutation, previously non-autoreactive precursors can also contribute to the pool of self-antigen reactive B cells (7, 8). Follicular helper T (Tfh) cells play important roles in germinal center reactions leading to the generation of high-affinity B cell clones and long-lived memory (9). There is accumulating evidence that aberrant Tfh responses contribute to SLE pathology, and new therapeutic approaches targeting Tfh-associated molecules are currently being tested (10). Up to now, standard SLE therapy depends on general immunosuppressive and anti-inflammatory drugs (11). More recently, the anti-BAFF monoclonal antibody (mAb) belimumab showed beneficial therapeutic effects in combination with standard drugs in clinical studies and has been approved for SLE therapy (12, 13). However, there is still an unmet clinical need for more specific therapies to improve the treatment of lupus.

Autoimmune-prone mice that spontaneously develop lupus-like disease have substantially contributed to a better understanding of genetics underlying disease development through identification of several loci contributing to disease susceptibility (14, 15). Moreover, spontaneously occurring mutations in, or targeted disruption of, specific genes in mice leading to SLE-like symptoms facilitate the identification of molecular events contributing to the pathogenesis of lupus (16).

The chronic graft-versus-host-disease (cGvHD) represents another commonly used mouse model for SLE-like disease and can be induced by transferring CD4<sup>+</sup> T cells into MHC-II mismatched recipients otherwise not prone to develop SLE-like autoimmunity (17). A well-established strain combination for the induction of cGvHD is the injection of parental DBA/2 (H2<sup>d/d</sup>) lymphocytes into semi-allogeneic (C57BL/6 × DBA/2)F1 (BDF1) (H2<sup>b/d</sup>) recipients (18). These mice develop symptoms closely resembling SLE, including high titers of anti-nuclear antibodies (ANA), anti-isologous erythrocyte (anti-RBC) antibodies, and fatal ICGN (19, 20). The known time point of disease induction facilitates studies on disease kinetics in this model. Moreover, the relatively easiness to manipulate the course of the disease and the rapid kinetics of disease development are, in our opinion, advantages to the spontaneous models mentioned above.

Interleukin-2 (IL-2) is a type I cytokine, produced primarily by conventional T cells, with pleiotropic effects on various cells of the immune system (21). Paradoxically, IL-2 can exert contradictory effects depending on the immunological context. On one hand, IL-2 exerts stimulatory effects on immune responses by expanding effector T cell populations. On the other hand, IL-2 can be immunosuppressive by inducing the proliferation of regulatory T cells (Tregs) that critically depend on IL-2 for homeostasis and to maintain their suppressive capacity (22). Thus, this property makes IL-2 an important regulator of peripheral self-tolerance by balancing the ratio of effector T cells and Tregs. Interestingly, T cells in some SLE patients were shown to be hyperactivated, but at the same time also produce less IL-2 compared to cells from healthy individuals (23, 24). Accordingly, impaired IL-2 production in some SLE patients might account for disturbed Treg homeostasis leading to a breakdown of tolerance to self-antigens.

Initially, IL-2 was discovered and described as growth factor for T cells due to its ability to induce activation and proliferation

of T cells *in vitro* (25, 26). Based on these findings, IL-2 was later on used as therapeutic treatment for renal cell carcinoma and metastatic melanoma. A major drawback, however, was the short half-life (~5 min) of IL-2 in the circulation and its toxicity at high doses. Thus, high-dose regimes necessary to achieve a clinical effect were accompanied by severe side effects, including a general vascular leakage syndrome. Additionally, response rates were rather poor at that time (5–10%) (27, 28). This might have in part contributed to the prevailing opinion that IL-2 has only a limited clinical potential. However, already by the 1990s, it was shown that autoimmune symptoms developing in MRL/lpr mice could be efficiently ameliorated by transfection with an IL-2-producing retroviral vector (29). Although this study provided evidence for IL-2 as potential treatment in autoimmune settings, this highly interesting finding was never followed up, likely due to the severe side effects of IL-2 observed in cancer immunotherapy.

More than 10 years ago, Boyman and co-workers elegantly demonstrated that the efficiency of IL-2 treatment could be readily enhanced and at the same time severe side effects could be prevented or largely reduced when IL-2 was administered as an immune complex bound to an anti-IL-2 mAb (30). Moreover, the authors showed that depending on the anti-IL-2 mAb used for the formation of the immune complexes different T cell subsets could be stimulated and expanded. Administration of IL-2 complexes generated with anti-IL-2 mAb JES6.1 (JES6/IL-2) selectively stimulate expansion of Tregs, whereas injection of IL-2 complexes formed by anti-IL-2 mAb S4B6 (S4B6/IL-2) induce predominantly an expansion of the CD8<sup>+</sup> T cell compartment and to a fewer extend an expansion of NK cells (31).

Structural analysis of IL-2 complexes suggests that mAb JES6.1 blocks epitopes of the IL-2 molecule involved in binding to IL-2 receptor β-chain (IL-2Rβ) and common γ-chain (γc) subunits, thus promoting interaction with IL-2 receptor α-chain (IL-2Rα). This in turn increases the biological availability to cells expressing high-affinity IL-2 receptors (IL-2Rαβγ) like Tregs. In contrast, mAb S4B6 blocks the epitope required for interactions with IL-2Rα, thus favoring interaction with low-affinity IL-2 receptors (IL-2Rβγ) expressed at high levels on CD8<sup>+</sup> T cells (32, 33). Up to now, the efficiency of IL-2 complexes in immunotherapy has been demonstrated in several murine models. It was shown that JES6/IL-2 complexes promote allograft survival, suppress the development of arthritis, and prevent the induction of experimental autoimmune encephalomyelitis (34–36). In contrast, S4B6/IL-2 complexes have been shown to enhance anti-tumor activity (37, 38). Whether IL-2 complexes might be equally efficient for the treatment of murine SLE-like autoimmune symptoms resulting from cGvHD has not yet been addressed in detail.

In this study, we examined the prophylactic and therapeutic effects of JES6/IL-2 and S4B6/IL-2 complexes on cGvHD. Our findings demonstrate that Treg expansion by JES6/IL-2 complexes, prior to disease induction, protects mice to a large extend from developing cGvHD. On the other hand, therapeutic administration of S4B6/IL-2 complexes 4 weeks after disease induction leads to significant amelioration of the disease. Interestingly, prophylactic treatment with S4B6/IL-2 complexes induces exacerbated cGvHD, whereas treatment of ongoing disease with JES6/IL-2 complexes has no significant effect on disease symptoms.

Moreover, we show that donor CD8<sup>+</sup> T cells are an important factor in cGvHD development. When cGvHD is induced in the absence of donor CD8<sup>+</sup> T cells, the disease is significantly aggravated, suggesting an inhibitory role of these cells on the course of cGvHD. The potential mechanism by which IL-2 complexes interfere with cGvHD and how donor CD8<sup>+</sup> T cells contribute to suppression of disease is discussed.

## MATERIALS AND METHODS

### Mice

(C57BL/6 × DBA/2)F1 (BDF1) and DBA/2 were bred in our animal facility and all mice were maintained under specific pathogen-free conditions. For experiments and analysis, age- and sex-matched mice between 8 and 12 weeks of age were used. Animal experiments were carried out within institutional guidelines (authorization number 1888 and 2434 from Cantonal Veterinarian Office, Basel).

### Preparation of Donor Cells and Induction of GvHD

For preparation of donor cells, spleens and LN (cervical, axillary, brachial, inguinal, and mesenteric) were removed from DBA/2 mice and gently passed through a 40 µm nylon mesh to obtain single cell suspensions in serum-free (SF) IMDM supplemented with 2% FCS (MP Biomedical, USA) and 0.5% Ciproxine (Bayer AG, CH). Spleen cell suspensions were treated with ACK buffer to lyse erythrocytes. Single cell suspensions were pooled, counted by Trypan blue exclusion, and washed in SF IMEM (Sigma-Aldrich, USA) prior to injection. GvHD was induced by i.v. injection of  $70 \times 10^6$  DBA/2 lymphocytes in a volume of 200 µl SF-IMEM.

### Depletion of Donor CD8<sup>+</sup> T Cells

In order to obtain donor cell suspensions depleted of CD8<sup>+</sup> T cells, DBA/2 mice were injected i.v. with 200 µl of 1 mg/ml YTS-156, a rat anti-mouse mAb specific for CD8β, 4 days before the mice were used to prepare cell suspensions. YTS-156 was purified from hybridoma culture supernatant according to standard procedures. The efficiency of CD8<sup>+</sup> T cell depletion was confirmed by flow cytometry using fluorescent-labeled anti-CD8α-specific mAb (53-6.7).

### Preparation of IL-2 Complexes

For a single injection, 2.5 µg rIL-2 and 7.5 µg anti-IL-2 mAb JES6.1A12 (BioXCell, USA) or S4B6 (purified from hybridoma culture supernatant by standard procedure) were mixed to prepare the IL-2 complexes. After a 30 min incubation at 37°C, the volume was adjusted to 200 µl with sterile PBS and injected i.p. into mice. Control mice were left untreated.

### Detection of Autologous IgG Anti-Erythrocyte Antibodies (Anti-RBC)

For the detection of anti-RBC antibodies in blood of cGvHD mice, Coombs test was performed as described elsewhere (18). Briefly, 100 µl heparinized blood was first diluted in the ratio of 1:20 in PBS containing 2% FCS and 0.1% of 1 M NaN<sub>3</sub>. 25 µl of

diluted blood was incubated with 50 µl of 1:200 diluted fluorescein isothiocyanate (FITC)-labeled goat anti-mouse IgG antibody (Jackson ImmunoResearch, USA) for 30 min at 4°C. Cells were washed and bound antibody was detected using a FACSCalibur (BD Bioscience, USA) flow cytometer. Mice were scored positive when the median of fluorescence intensity of staining was increased more than twofold compared to healthy controls.

### Detection of ANA

For the detection of ANA in the sera of cGvHD mice, 8 µm sections of snap-frozen kidneys obtained from RAG2<sup>-/-</sup> mice were used. Sections were first incubated with 80 µl serum from cGvHD mice diluted from 1:20 to 1:5,120 for 30 min at room temperature (RT) in the dark. After washing, bound ANA were detected by incubation with 80 µl of a 1:200 diluted FITC-labeled goat anti-mouse IgG antibody for 30 min at RT in the dark. The titer was determined by using a fluorescent microscope (Zeiss Axioscope) and was defined as the highest dilution that still gave a specific nuclear staining. Mice containing sera with titers lower than 1:20 were considered as negative for ANA.

### Measurement of Proteinuria

Proteinuria was determined semi quantitatively in weekly intervals using Albustix (Siemens Healthcare Diagnostics Inc., Newark, Delaware). Elevated protein levels in the urine are indicative of failure in kidney function (20). Mice were scored positive when a concentration >3 mg/ml was indicated by color change of the Albustix.

### Immunhistological Analysis

Kidneys from proteinuria positive mice were embedded in OCT-compound (Sakura Finetek, Netherlands) and snap-frozen on dry ice. 8 µm sections were prepared on glass slides, fixed in acetone for 10 min, and dried. For the detection of immune complex deposition in the glomeruli, sections were incubated with FITC-labeled goat anti-mouse IgG antibody for 30 min at RT. For the detection of complement deposition, kidney sections from cGvHD mice were incubated for 30 min at RT in the dark with FITC-labeled anti-C3 mAb (a kind gift of Dr. S. Izui, University of Geneva) diluted 1:100 in FACS buffer. Bound FITC-labeled mAb was detected by using a fluorescent microscope.

### Flow Cytometry

For analysis by flow cytometry, lymphoid organs were removed and single cell suspensions were prepared by gently passing the organs through a 40 µm nylon mesh into SF-IMDM containing 2% FCS and 0.5% Ciproxin. In order to lyse erythrocytes, spleen cell suspensions were treated with ACK buffer for approximately 1 min. Staining was performed in a 96-well round bottom plate in a total volume of 100 µl containing 50 µl cell suspension ( $1-2 \times 10^7$  cells/ml) and 50 µl diluted antibody mix. Cells were incubated for 30 min on ice in the dark. Cells were washed twice in FACS buffer. When biotinylated antibodies were used, a second staining step (20 min, 4°C, in the dark) was performed for the binding of streptavidin-coupled fluorochromes. If applicable, cells were resuspended in FACS buffer containing 5 µg/ml propidium iodide (Sigma-Aldrich, USA) to exclude dead cells. Intracellular

stainings were performed according to standard procedures. In brief, subsequent to surface staining, cells were fixed either with PBS containing 2% paraformaldehyde or with fix/perm buffer (eBioscience, USA) followed by the intracellular staining in FACS buffer containing 0.5% saponin (Sigma-Aldrich, USA) or in permeabilization buffer (eBioscience, USA). Intracellular stainings were incubated for 30 min at 4°C in the dark followed by washing steps in FACS buffer to remove unbound antibodies. Flow cytometry was performed on a FACSCalibur or LSRFortessa flow cytometer (BD Bioscience, USA) and data was analyzed using FlowJo (Tree Star, USA) software. Donor and host cell populations were distinguished by the expression of H2-K<sup>b</sup> and H2-K<sup>d</sup>. Representative plots of presented key populations are provided in Figure S1 in Supplementary Material.

### Phorbol-12-Myristate-13-Acetate (PMA)/Ionomycin Stimulation for Detection of IFN- $\gamma$

Single cell suspensions were stimulated during 4 h using 1  $\mu$ g/ml ionomycin (Sigma-Aldrich, USA) and 5 ng/ml PMA (Calbiochem, USA) in the presence of 10  $\mu$ g/ml brefeldin A (Sigma-Aldrich, USA). Cells were harvested and stained by standard intracellular staining procedures (see above).

### Antibodies

Fluorescein isothiocyanate-, phycoerythrin- (PE), allophycocyanin-, Pacific Blue- (PB), Brilliant Violet- (BV), PE-Cy7-, PerCP-Cy5.5, or biotin-labeled monoclonal antibodies specific for CD4 (GK1.5), CD8 $\alpha$  (53-6.7), CD8 $\beta$  (YTS-156.7.7), CD25 (PC61), CD44 (IM7), H2-K<sup>b</sup> (Y3), H2-K<sup>d</sup> (19.191), TCR $\beta$ c (H57-597), CD62L (Mel-14), CXCR5 (L138D7), PD-1 (RMP1-30), IFN- $\gamma$  (XMG1.2), or FoxP3 (FJK-16s) were purchased from BD Bioscience, eBioscience, or BioLegend, or purified from hybridoma culture supernatant and fluorescently labeled in our laboratory according to standard procedures. Antibodies were titrated and used at the lowest dilution that gave the best separation.

## RESULTS

### Prophylactic Administration of IL-2 Complexes

To investigate the effect of prophylactic administration of IL-2 complexes on the development of SLE-like murine cGvHD, BDF1 mice received i.p. injections of IL-2 complexes (either S4B6/IL-2 or JES6/IL-2) on three consecutive days before disease induction. The cGvHD was induced by i.v. injection of parental (DBA/2) lymphocytes from pooled preparations of splenocytes and LN cells. Disease development was followed by measuring the presence of anti-RBC antibodies in the blood, the titers of ANA in the serum, and the incidence of proteinuria over a period of 12 weeks.

Prophylactic treatment with JES6/IL-2 complexes (pJES6/IL-2) was highly efficient in ameliorating the SLE-like symptoms of murine cGvHD throughout the observation period. As shown in **Figure 1**, prophylactic JES6/IL-2 treatment results in reduced frequency of anti-RBC positive mice in the Coombs test as well as decreased titers of ANA in the serum (**Figures 1A,B**). This was

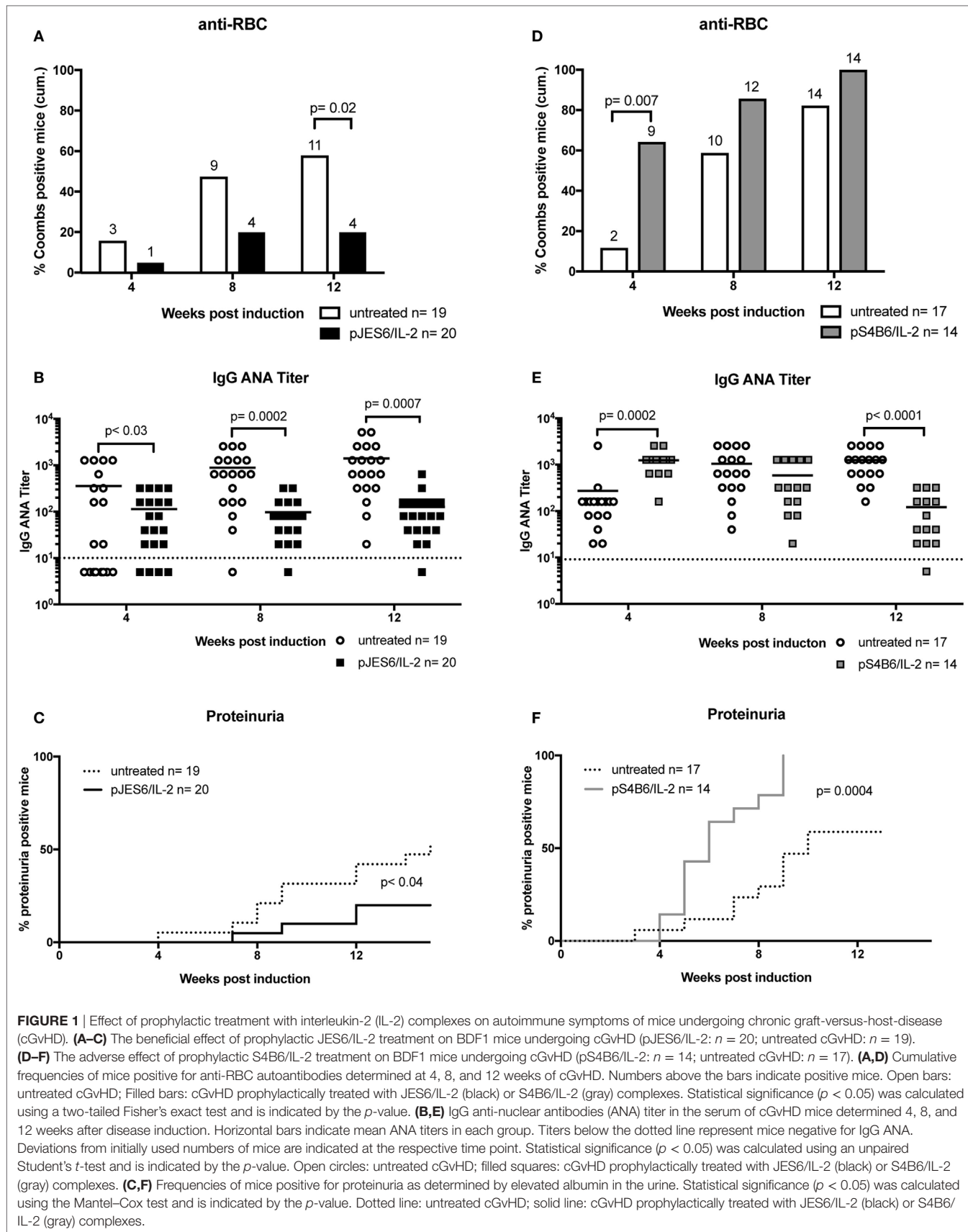
evident at all measured time points. Mice receiving a prophylactic JES6/IL-2 treatment showed delayed onset and reduced incidence of proteinuria (**Figure 1C**). Analysis of kidneys of proteinuria positive mice by immunohistochemistry showed reduced deposition of immune complexes and complement in those mice that were pretreated with JES6/IL-2 complexes (**Figure 2B**) compared to untreated cGvHD mice (**Figure 2A**).

Surprisingly, prophylactic treatment with the S4B6/IL-2 complexes (pS4B6/IL-2) induced stronger autoimmune symptoms and a more aggressive course of disease. At all measured time points, a higher fraction of mice was positive for the production of anti-RBC antibodies in the group receiving prophylactic S4B6/IL-2 treatment (**Figure 1D**). These mice also had significantly elevated ANA titers in the serum at 4 weeks after disease induction compared to the controls (**Figure 1E**). The decreased ANA titers measured at 12 weeks after disease induction might be a consequence of the faster kinetics and higher incidence of ICGN in that group. Pretreatment with S4B6/IL-2 complexes resulted in full penetrance of proteinuria by 9 weeks after disease induction (**Figure 1F**). Moreover, mice pretreated with S4B6/IL-2 complexes showed increased renal deposition of immune complexes and complement (**Figure 2C**) compared to mice with untreated cGvHD. Besides the significant amounts of albumin secreted by the urine of mice undergoing cGvHD, there is likely a considerable loss of immune globulins that might explain the decreased ANA titers at 12 weeks after disease induction. Despite the reduced number of experimental animals receiving prophylactic S4B6/IL-2 treatment, a statistically significant effect on disease symptoms could be observed that clearly contrasts to the observations in the control group. Although not compared directly within one experiment, the effects of prophylactic S4B6/IL-2 or JES6/IL-2 treatment were in marked contrast to each other and do not arise from variations in the control groups.

In summary, prophylactic treatment with JES6/IL-2 complexes leads to an amelioration of SLE-like symptoms, whereas the prophylactic treatment with S4B6/IL-2 markedly aggravates disease symptoms when compared to mice with the untreated form of murine cGvHD.

### Cellular Mechanism Underlying the Opposing Effects of JES6/IL-2 Versus S4B6/IL-2 Prophylactic Treatments

To gain further insight into how prophylactic administration of IL-2 complexes modifies cellular responses during cGvHD, we performed multicolor flow cytometry analysis on mice, prophylactically treated with IL-2 complexes, 2 weeks after disease induction. Total spleen size was similar to untreated mice (**Figure 3A**), but numbers of engrafted donor CD4 $^+$  T cells recovered from the spleens of mice prophylactically treated with JES6/IL-2 complexes was significantly reduced compared to those of the controls (**Figure 3B**). Moreover, donor CD4 $^+$  T cells were less activated (**Figure 3C**) and the population of donor CD4 $^+$  T cells with a central memory phenotype (CD44 $^+$ /CD62L $^+$ ) was significantly reduced (**Figure 3D**). Interestingly, there was no significant difference in Tfh cells, identified by staining for the surface markers, PD1 and CXCR5, in the prophylactically JES6/IL-2-treated



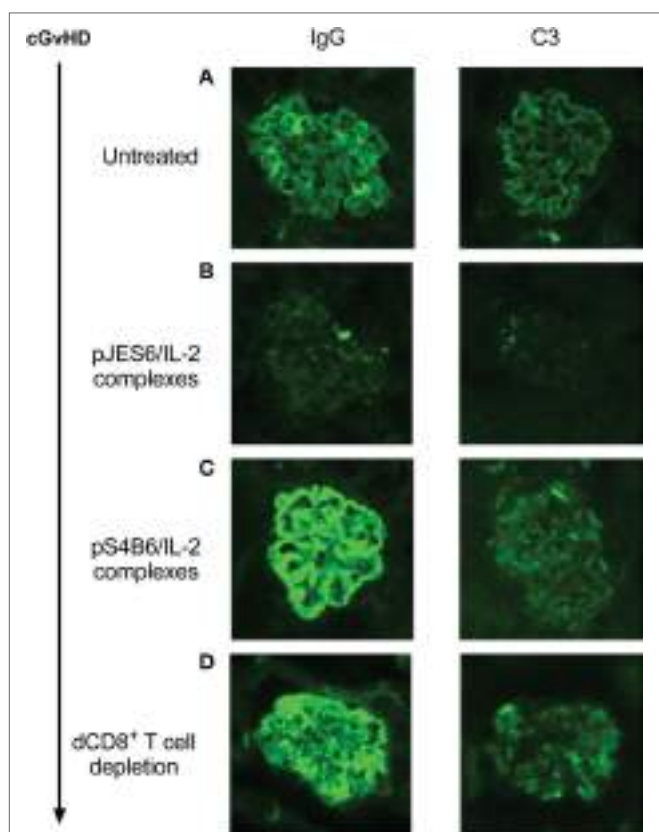


**FIGURE 2 |** Immunohistological staining of IgG and C3 deposition in glomeruli of proteinuria positive chronic graft-versus-host-disease (cGvHD) mice. Kidneys were obtained from mice positive for proteinuria for <1 week. Cryo sections were prepared and stained for IgG deposition (left panel) or C3 deposition (right panel). Stained sections were analyzed by using a Zeiss Axioscope mounted with a Nikon digital camera DXM 1200F in combination with imaging software (Nikon ACT-1). Photos show representative stainings of kidneys from different experiments. **(A)** Untreated cGvHD mice induced with DBA/2 lymphocytes. **(B)** cGvHD mice as in **(A)**, but prophylactically treated with JES6/interleukin-2 (IL-2). **(C)** cGvHD mice as in **(A)**, but prophylactically treated with S4B6/IL-2. **(D)** Untreated cGvHD mice whose disease was induced with DBA/2 lymphocytes depleted of CD8<sup>+</sup> T cells.

group compared to controls (Figure 3E). Host Treg compartment expressing the lineage-specific transcription factor FoxP3 was significantly expanded compared to untreated mice (Figure 3F), and absolute numbers of host Tregs were sustained during the first 2 weeks of cGvHD (Figure 4G). The reduced engraftment/expansion as well as decreased activation of donor CD4<sup>+</sup> T cells might be a consequence of the expanded host Treg compartment (40-fold compared to control group). The finding that prophylactic JES6/IL-2 treatment induced marked increase in FoxP3 expression in host Tregs further supports this assumption (Figure 4H).

Mice treated prophylactically with the S4B6/IL-2 complexes had significantly increased total cellularity of their spleens compared to cGvHD mice in the control group (Figure 4A). In contrast to mice treated prophylactically with JES6/IL-2 complexes, the numbers of total engrafted donor CD4<sup>+</sup> T cells (Figure 4B) and numbers of activated donor CD4<sup>+</sup> T cells in cGvHD mice treated prophylactically with S4B6/IL-2 complexes were similar to those

found in untreated mice (Figure 4C). On the other hand, central memory donor CD4<sup>+</sup> T cells were significantly expanded in mice pretreated with S4B6/IL-2 complexes (Figure 4D). Moreover, in these mice, the population of donor CD4<sup>+</sup> Tfh cells was increased more than fourfold (Figure 4E). Unexpectedly, the extent of host Treg expansion in response to prophylactic treatment with S4B6/IL-2 complexes was even greater compared to the expansion induced by prophylactic JES6/IL-2 treatment (Figure 4F). However, the expansion of host Tregs upon prophylactic S4B6/IL-2 treatment did not ameliorate autoimmune symptoms in contrast to Tregs expanded by prophylactic treatment with JES6/IL-2 complexes. Although we also observed increased FoxP3 expression in S4B6/IL-2 expanded host Tregs (Figure 4H) these cells are unable to efficiently control the induced disease. In these mice elevated numbers of activated donor cells of the CD4<sup>+</sup> central memory and Tfh subsets might account for the augmented production of autoantibodies and more severe cGvHD observed.

## Therapeutic Administration of IL-2 Complexes

Next, we investigated the influence of the IL-2 complexes on SLE-like symptoms when administrated during ongoing disease. Therefore, we injected either JES6/IL-2 or S4B6/IL-2 complexes therapeutically on three consecutive days starting 4 weeks following the induction of cGvHD by transfer of parental DBA/2 lymphocytes.

The therapeutic treatment with JES6/IL-2 complexes (tJES6/IL-2) had no significant effect on the development of the monitored autoimmune symptoms. Apart from a mild effect on the frequency of anti-RBC positive mice (Figure 5A) ANA titers and frequencies of mice developing proteinuria were comparable in both groups (Figures 5B,C).

In contrast, S4B6/IL-2 complexes, when administrated therapeutically, showed an ameliorating effect on autoimmune symptoms in mice undergoing cGvHD. Following injection of S4B6/IL-2 complexes, the frequency of mice producing anti-RBC antibodies remained constant, whereas the frequency of anti-RBC-producing mice in the control group increased over time (Figure 5D). Moreover, ANA titers measured at time points after the initiation of S4B6/IL-2 therapy were significantly lower compared to the control group that showed a steady increase of ANA titers over time (Figure 5E). The incidence of proteinuria was significantly reduced following S4B6/IL-2 therapy (Figure 5F), most likely as a result of decreased autoantibody production.

Taken together, the data indicate that therapeutic administration of JES6/IL-2 complexes has no significant effect on the symptoms of lupus-like murine cGvHD. This is in contrast to therapeutic administration of S4B6/IL-2 complexes that induce an amelioration of disease symptoms. These results also contrast with the effects of prophylactic administration of these two IL-2 complexes. JES6/IL-2 complexes are effective in prophylactic, but not therapeutic treatment of cGvHD. The reverse is true for S4B6/IL-2 complexes.

## Donor CD8<sup>+</sup> T Cells Modulate the Pathogenesis of Murine cGvHD

CD8<sup>+</sup> T cells are suggested to play an important role in the development of SLE and murine cGvHD (39). The potent capacity

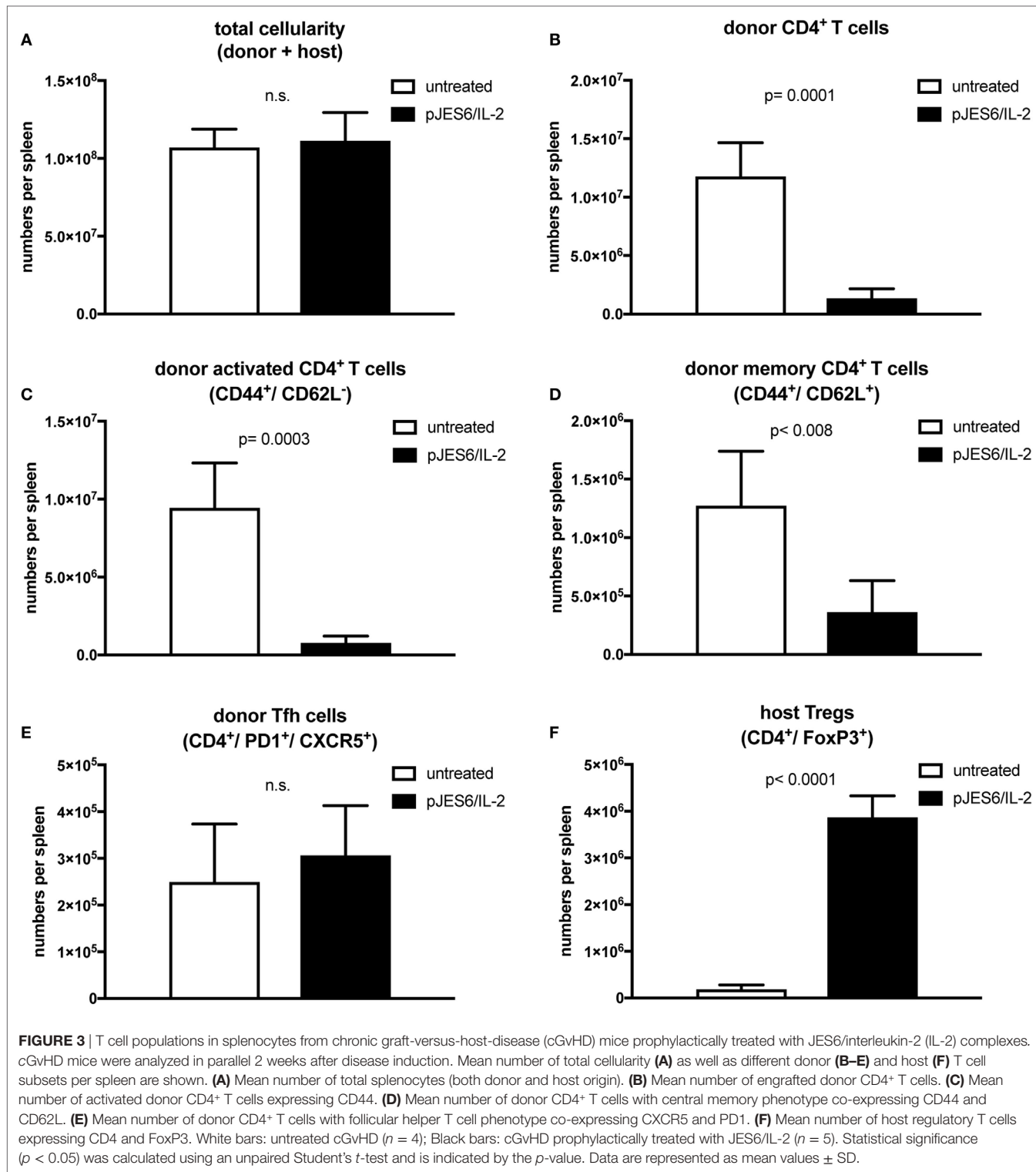


**FIGURE 3 |** T cell populations in splenocytes from chronic graft-versus-host-disease (cGvHD) mice prophylactically treated with JES6/interleukin-2 (IL-2) complexes. cGvHD mice were analyzed in parallel 2 weeks after disease induction. Mean number of total cellularity (A) as well as different donor (B–E) and host (F) T cell subsets per spleen are shown. (A) Mean number of total splenocytes (both donor and host origin). (B) Mean number of engrafted donor CD4<sup>+</sup> T cells. (C) Mean number of activated donor CD4<sup>+</sup> T cells expressing CD44. (D) Mean number of donor CD4<sup>+</sup> T cells with central memory phenotype co-expressing CD44 and CD62L. (E) Mean number of donor CD4<sup>+</sup> T cells with follicular helper T cell phenotype co-expressing CXCR5 and PD1. (F) Mean number of host regulatory T cells expressing CD4 and FoxP3. White bars: untreated cGvHD ( $n = 4$ ); Black bars: cGvHD prophylactically treated with JES6/IL-2 ( $n = 5$ ). Statistical significance ( $p < 0.05$ ) was calculated using an unpaired Student's *t*-test and is indicated by the *p*-value. Data are represented as mean values  $\pm$  SD.

of S4B6/IL-2 complexes to expand CD8<sup>+</sup> T cells (31) and the observation of the beneficial clinical effect of therapeutic S4B6/IL-2 treatment prompted us to further examine the CD8<sup>+</sup> T cell compartment in mice undergoing cGvHD. Analysis of IFN- $\gamma$  production in untreated cGvHD mice showed that CD8<sup>+</sup> T cells

of both, donor and host origin, were highly activated irrespective of the time point of the analysis after disease induction. On average, 80% of donor CD8<sup>+</sup> T cells produced IFN- $\gamma$  after *in vitro* stimulation, whereas the frequency of IFN- $\gamma$ -producing cells in the host population was about 40% (Figure 6A). These findings

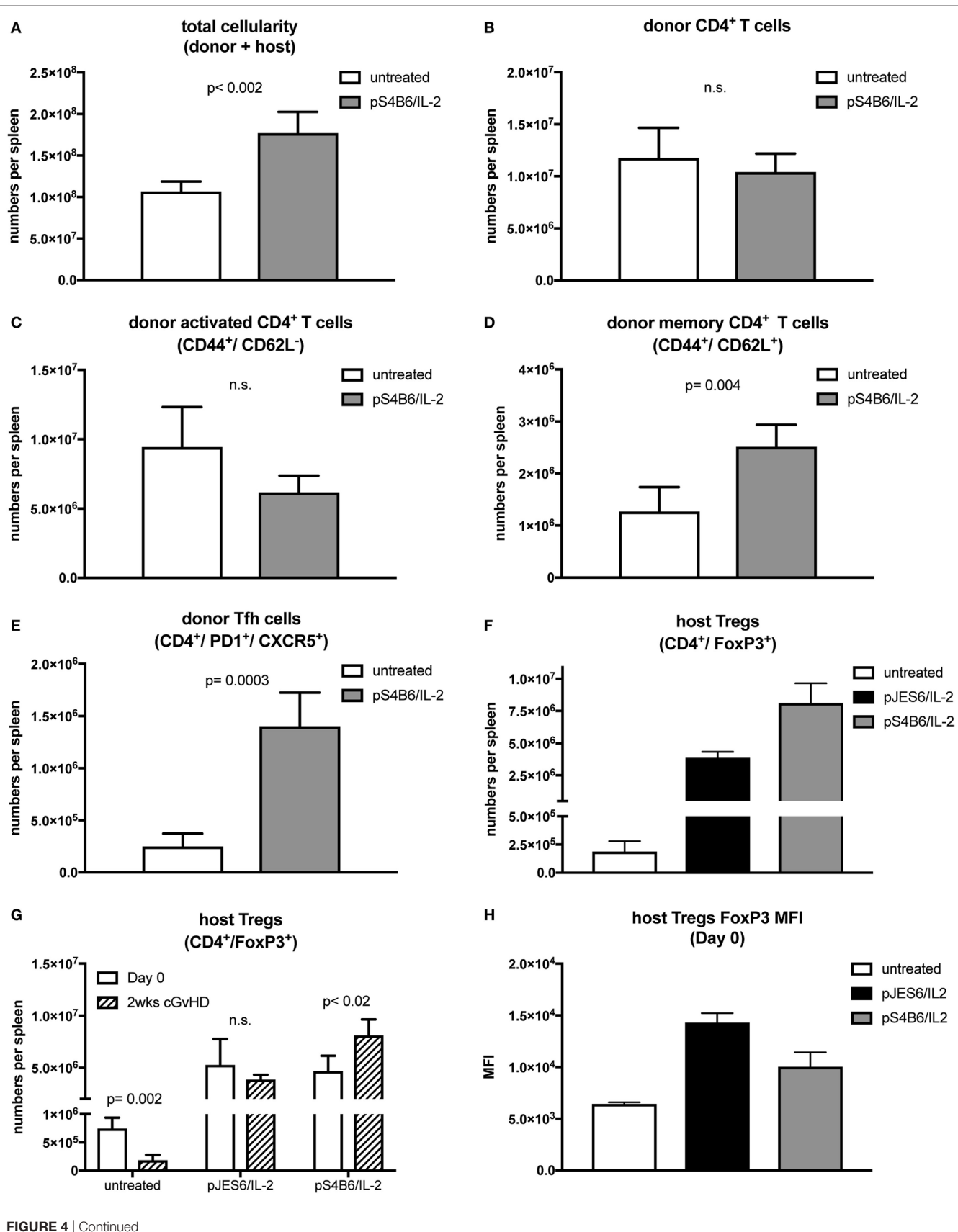


FIGURE 4 | Continued

**FIGURE 4 |** T cell populations in splenocytes from chronic graft-versus-host-disease (cGvHD) mice prophylactically treated with S4B6/interleukin-2 (IL-2) complexes. Mean number of total cellularity (**A**) as well as different donor (**B–E**) and host (**F,G**) T cell subsets per spleen are shown. (**A**) Mean number of total splenocytes (donor and host origin). (**B**) Mean number of engrafted donor CD4<sup>+</sup> T cells. (**C**) Mean number of activated donor CD4<sup>+</sup> T cells expressing CD44. (**D**) Mean number of donor CD4<sup>+</sup> T cells with central memory phenotype co-expressing CD44 and CD62L. (**E**) Mean number of donor CD4<sup>+</sup> T cells with follicular helper T cell phenotype co-expressing CXCR5 and PD1. (**F**) Mean number of host regulatory T cells (Tregs) expressing CD4 and FoxP3. White bars: untreated cGvHD ( $n = 4$ ); gray bars: cGvHD prophylactically treated with S4B6/IL-2 ( $n = 5$ ); black bars: cGvHD mice prophylactically treated with JES6/IL-2 ( $n = 5$ ). (**G**) Mean numbers of host Tregs in mice left untreated or pretreated with JES6/IL-2 or S4B6/IL-2 at day 0 (just before cGvHD induction) and after 2 weeks of cGvHD. White bars: day 0 ( $n = 4$ ); black patterned bars: 2 weeks cGvHD ( $n = 4\text{--}5$ ). (**H**) FoxP3 median fluorescence intensity in host Tregs in mice left untreated or pretreated for 3 days with JES6/IL-2 or S4B6/IL-2 complexes. Statistical significance ( $p < 0.05$ ) was calculated using an unpaired Student's *t*-test and is indicated by the *p*-value. Data are represented as mean values  $\pm$  SD.

further support the contribution of CD8<sup>+</sup> T cells during the development of cGvHD. In order to confirm a potential involvement of CD8<sup>+</sup> T cells and to test the particular contribution of donor and host T cells in the pathogenesis of cGvHD, we followed the development of SLE-like symptoms in the absence of donor CD8<sup>+</sup> T cells. For this, CD8<sup>+</sup> T cells were depleted from donor DBA/2 mice by i.v. injection of 200 µg YTS-156, a monoclonal anti-CD8β antibody, 4 days prior to harvesting donor cells for cGvHD induction. The high efficiency of *in vivo* donor CD8<sup>+</sup> T cell depletion was confirmed by flow cytometry analysis of the donor lymphocyte preparation (data not shown).

The results show that depletion of donor CD8<sup>+</sup> T cells results in a much more severe cGvHD. Almost all mice induced with CD8<sup>+</sup> T cell-depleted donor inoculum were positive for the presence of anti-RBC antibodies already after 3 weeks of cGvHD, whereas in the control group, receiving non-depleted donor cells, the frequency of anti-RBC positive mice reached 80% with delayed kinetics (Figure 6B). ANA titers in the two groups were not significantly different during the first 6 weeks of cGvHD. However, at later time points, ANA titers of mice induced with donor CD8<sup>+</sup> T cell depleted cells decrease, whereas the titers of the other group continued to increase (Figure 6C). Again, decreased ANA titers at 12 weeks of cGvHD might be due to the greater incidence of proteinuria in this group, showing earlier onset and full penetrance by 9 weeks after disease induction. Immunohistological analysis of kidneys of cGvHD mice induced with donor inoculum depleted of CD8<sup>+</sup> T cells revealed a marked increase of immune complex and complement deposition (Figure 2D) in contrast to untreated cGvHD mice induced with non-depleted donor cells (Figure 2A).

## Beneficial Effect of Therapeutic S4B6/IL-2 Treatment Depends on Donor CD8<sup>+</sup> T Cells

The importance of the donor CD8<sup>+</sup> T cell compartment in determining the severity of disease symptoms raised the following questions: (i) To what extent can the observed effect of S4B6/IL-2 complexes be attributed to donor or host CD8<sup>+</sup> T cells and (ii) whether the effect is reproducible in the absence of donor CD8<sup>+</sup> T cells? To test this, cGvHD was induced by transfer of donor lymphocytes from DBA/2 mice previously injected with the CD8β-depleting mAb YTS-156. After 4 weeks of ongoing disease, one group of mice was treated with S4B6/IL-2 complexes on three consecutive days. No significant improvement of the disease symptoms was observed upon therapeutic S4B6/IL-2 treatment

in cGvHD mice injected with CD8<sup>+</sup> T cell-depleted donor lymphocytes. We failed to observe any significant difference, in any measured parameter, throughout the experiment between the two experimental groups (Figures 6E–G). These results provide strong evidence for the idea that donor CD8<sup>+</sup> T cells are required for S4B6/IL-2 complexes to ameliorate SLE-like symptoms in mice undergoing cGvHD.

## DISCUSSION

Murine chronic GvHD resulting from the injection of DBA/2 lymphocytes into BDF1 mice leads to autoimmune symptoms closely resembling SLE in man. Although the beneficial effect of IL-2 in autoimmunity has been established some time ago (29), severe side effects impeded its application in the clinics. The discovery that such adverse reactions could be prevented when IL-2 was administered as immune complex bound to anti-IL-2 mAb opened up new therapeutic approaches for the treatment of autoimmune diseases like SLE. Herein, we investigated the prophylactic and therapeutic effect of two IL-2 complexes (JES6/IL-2 and S4B6/IL-2) on SLE-like symptoms resulting from chronic GvHD.

Prophylactic administration of JES6/IL-2 complexes ameliorated cGvHD symptoms and protected BDF1 mice to a large extent from developing fatal ICGN. In these treated mice, fewer donor CD4<sup>+</sup> T cells had engrafted in the spleen 2 weeks after transfer. Donor CD4<sup>+</sup> T cells are central in the pathogenesis of cGvHD by providing help to host B cells; this leads to the production of disease driving autoantibodies (40). Hence, amelioration of disease upon JES6/IL-2 pretreatment is a likely consequence of the reduced engraftment and/or functioning of donor CD4<sup>+</sup> T cells. Moreover, donor CD4<sup>+</sup> T cells in JES6/IL-2-pretreated mice were phenotypically less activated and generated reduced numbers of central memory T cells. This may result from enhanced suppressive capacity of the host Treg compartment following the prophylactic treatment with JES6/IL-2 complexes. It is well established that Tregs can regulate effector T cell responses by suppressing their activation and differentiation into effector subsets (41). In this regard, it is conceivable that prophylactic treatment with JES6/IL-2 complexes expands a host Treg population capable of suppressing alloreactive donor CD4<sup>+</sup> T cells.

In marked contrast, prophylactic treatment with S4B6/IL-2 complexes significantly enhanced SLE-like symptoms and induced a more severe course of the disease. Mice pretreated with S4B6/IL-2 complexes had increased splenomegaly as well as significantly higher numbers of donor CD4<sup>+</sup> T cells with a

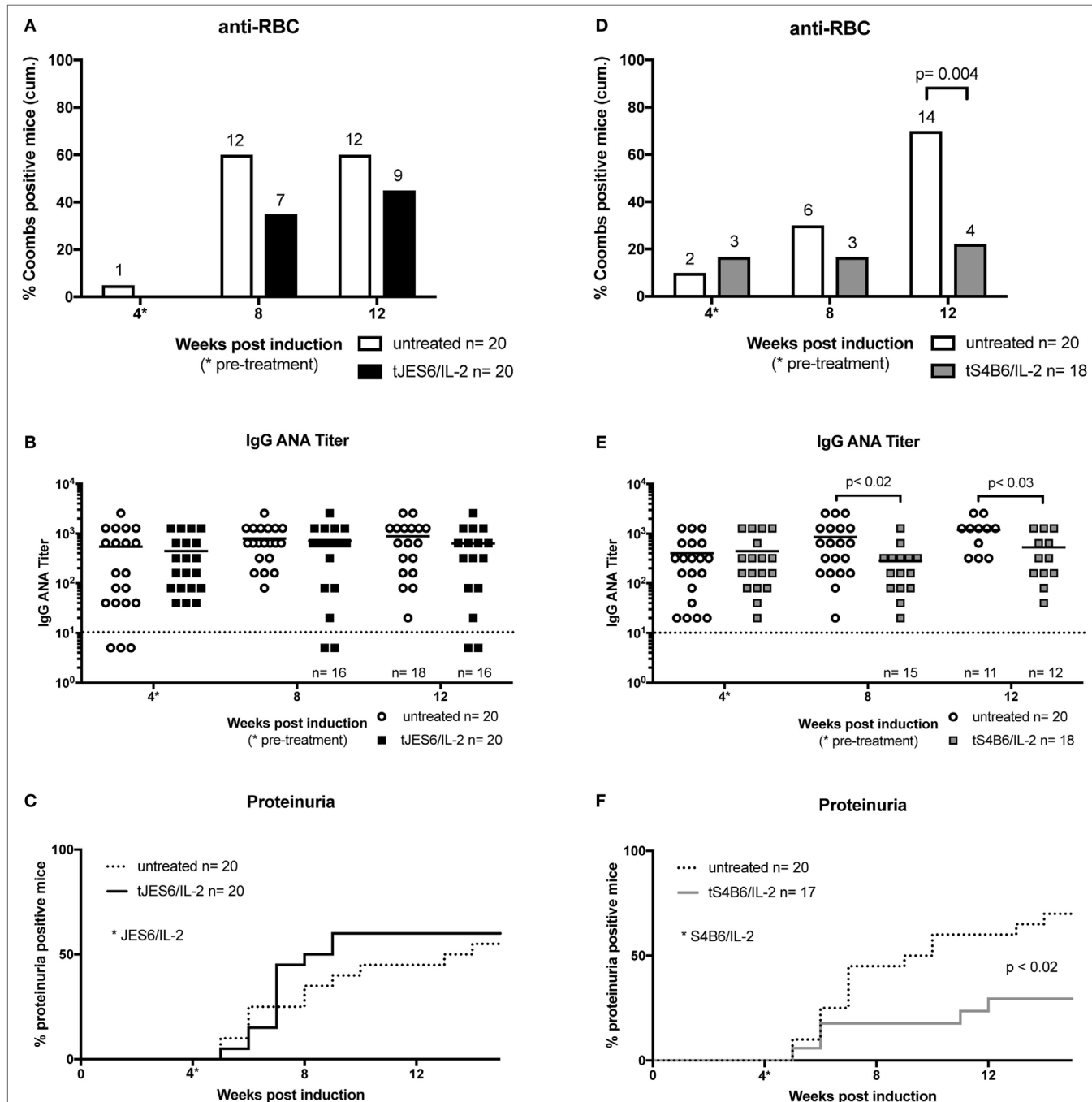


**FIGURE 5 |** Effect of therapeutic treatment with interleukin-2 (IL-2) complexes on autoimmune symptoms of mice undergoing chronic graft-versus-host-disease (cGvHD). **(A–C)** The efficiency of therapeutic JES6/IL-2 treatment of cGvHD is confined to the production of anti-RBC (tJES6/IL-2:  $n = 20$ ; untreated cGvHD:  $n = 19$ ). **(D–F)** The beneficial effects of therapeutic S4B6/IL-2 treatment of cGvHD (tS4B6/IL-2:  $n = 18$ ; untreated cGvHD:  $n = 20$ ). **(A,D)** Cumulative frequencies of mice positive for anti-RBC autoantibodies determined at 4, 8, and 12 weeks of cGvHD. Numbers above the bars indicate positive mice. White bars: untreated cGvHD; filled bars: cGvHD therapeutically treated with JES6/IL-2 (black) or S4B6/IL-2 (gray) complexes. Statistical significance ( $p < 0.05$ ) was calculated using a two-tailed Fisher's exact test and is indicated by the  $p$ -value. **(B,E)** IgG anti-nuclear antibodies (ANA) titer in the serum of cGvHD mice determined 4, 8, and 12 weeks after disease induction. Horizontal bars indicate mean ANA titers in each group. Titers below the dotted line represent mice negative for IgG ANA. Deviations from initially used numbers of mice are indicated at the respective time point. Statistical significance ( $p < 0.05$ ) was calculated using an unpaired Student's *t*-test and is indicated by the  $p$ -value. Open circles: untreated cGvHD; filled squares: cGvHD therapeutically treated with JES6/IL-2 (black) or S4B6/IL-2 (gray) complexes. **(C,F)** Frequencies of mice positive for proteinuria as determined by elevated albumin in the urine. Statistical significance ( $p < 0.05$ ) was calculated using the Mantel-Cox test and is indicated by the  $p$ -value. Dotted line: untreated cGvHD; solid line: cGvHD prophylactically treated with JES6/IL-2 (black) or S4B6/IL-2 (gray) complexes.

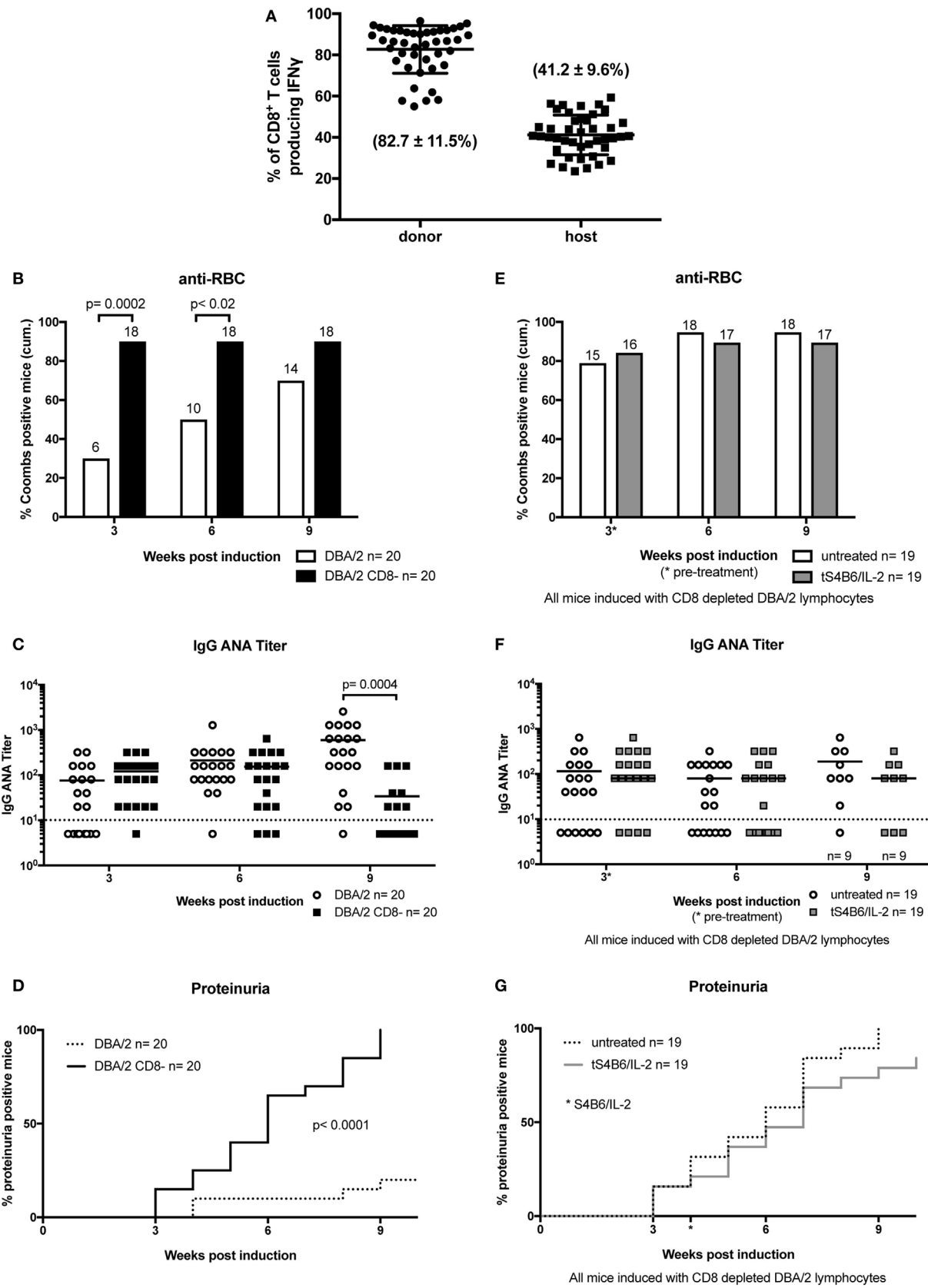


FIGURE 6 | Continued

**FIGURE 6 |** Donor CD8<sup>+</sup> T cells are important modulators of chronic graft-versus-host-disease (cGvHD) and mediate the beneficial effect of therapeutic S4B6/interleukin-2 (IL-2) therapy. **(A)** Frequencies of IFN- $\gamma$  producing CD8<sup>+</sup> T cells of donor (circles) and host (squares) origin in splenocytes of untreated cGvHD mice analyzed at various time points between 2 and 12 weeks after disease induction. **(B–D)** A more severe cGvHD develops when induced with DBA/2 lymphocytes depleted of CD8<sup>+</sup> T cells (DBA/2 CD8<sup>-</sup>) (DBA/2:  $n = 20$ ; DBA/2 CD8<sup>-</sup>:  $n = 20$ ). **(E–G)** No effect on cGvHD severity with S4B6/IL-2 therapy in the absence of donor CD8<sup>+</sup> T cells (untreated cGvHD:  $n = 19$ ; tS4B6/IL-2:  $n = 19$ ). **(B,E)** Cumulative frequencies of mice positive for anti-RBC autoantibodies determined at 3, 6, and 9 weeks of cGvHD. Numbers above the bars indicate positive mice. Statistical significance ( $p < 0.05$ ) was calculated using a two-tailed Fisher's exact test and is indicated by the  $p$ -value. **(B)** White bars: cGvHD mice induced with DBA/2 lymphocytes; black bars: cGvHD induced with DBA/2 lymphocytes depleted of CD8<sup>+</sup> T cells. **(E)** White bars: cGvHD induced with DBA/2 lymphocytes depleted of CD8<sup>+</sup> T cells. **(C,F)** IgG anti-nuclear antibodies (ANA) titer in the serum of cGvHD mice determined 3, 6, and 9 weeks after disease induction. Horizontal bars indicate mean of ANA titers in each group. Titers below the dotted line represent mice negative for IgG ANA. Deviations from initially used number of mice are indicated at the respective time point. Statistical significance ( $p < 0.05$ ) was calculated using an unpaired Student's *t*-test and is indicated by the  $p$ -value. **(C)** Open circles: cGvHD induced with DBA/2 lymphocytes; filled squares: cGvHD induced with DBA/2 lymphocytes depleted of CD8<sup>+</sup> T cells. **(F)** Open circles: untreated cGvHD mice induced with DBA/2 lymphocytes depleted of CD8<sup>+</sup> T cells and therapeutically treated with S4B6/IL-2 complexes. **(D,G)** Frequencies of mice positive for proteinuria as determined by elevated albumin in the urine. Statistical significance ( $p < 0.05$ ) was calculated using the Mantel-Cox test and is indicated by the  $p$ -value. **(D)** Dotted line: cGvHD induced with DBA/2 lymphocytes; solid line: cGvHD induced with DBA/2 lymphocytes depleted of CD8<sup>+</sup> T cells. **(G)** Dotted line: cGvHD induced with DBA/2 lymphocytes depleted of CD8<sup>+</sup> T cells and therapeutically treated with S4B6/IL-2 complexes.

central memory phenotype. Memory T cells have lower activation thresholds and respond to secondary antigenic stimulation with augmented effector function (42), thereby possibly enhancing autoimmunity. Moreover, only pretreatment with S4B6/IL-2 complexes induced differentiation of donor CD4<sup>+</sup> Tfh cells expressing PD1 and CXCR5. Expression of CXCR5 facilitates the localization of Tfh cells to CXCL13 producing B cells and the initiation of germinal center. As Tfh cells contribute to survival, affinity maturation, isotype class-switching, and differentiation of germinal center B cells (9), it is likely that exacerbated SLE-like symptoms in S4B6/IL-2-pretreated mice resulted from enhanced germinal center reactions leading to augmented production of pathogenic autoantibodies. In support of this hypothesis, a pathogenic role of Tfh cells has been recently established in other murine lupus models and in human SLE (43).

Whether administration of S4B6/IL-2 complexes directly promotes differentiation of donor CD4<sup>+</sup> T cells into Tfh cells is unclear. First, the biological half-life of IL-2 complexes is relatively short (<4 h) (31), thereby arguing against a direct contribution on donor CD4<sup>+</sup> T cell differentiation, since donor cells were transferred approximately 24 h after the last injection of IL-2 complexes. Second, S4B6/IL-2 complexes failed to induce expression of Tfh cell-specific markers in normal mice not undergoing cGvHD (data not shown). For these reasons, we expect the effect of S4B6/IL-2 pretreatment on donor Tfh differentiation is indirect and likely involves cells of the host. Moreover, consistent with previous reports (37), we found that pretreatment with S4B6/IL-2 complexes leads to marked expansion of dendritic cells expressing CD11c and MHC-II (data not shown). Whether the expanded dendritic cell compartment contributes to exacerbated cGvHD in S4B6/IL-2 pretreated mice, perhaps by providing enhanced co-stimulation factors, requires further investigation.

Another surprising finding was the effect of S4B6/IL-2 pretreatment on the host Treg compartment. As previously reported (31) and in agreement with our own data, at the time of cGvHD induction, host Treg compartments were expanded equally, efficiently upon prophylactic treatment with JES6/IL-2

or S4B6/IL-2 complexes. Nevertheless, mice pretreated with S4B6/IL-2 complexes developed exacerbated cGvHD symptoms, whereas JES6/IL-2 pretreated mice were largely protected from disease. Although mice pretreated with S4B6/IL-2 or JES6/IL-2 complexes have not been compared directly in one experiment, the observed effects on the course of the disease induced by either complex are strikingly different and it is highly unlikely that these differences are artifacts resulting from variations in the control groups. Surprisingly, the host Treg compartment in the first 2 weeks of cGvHD in S4B6/IL-2 pretreated mice markedly expanded, but was unable to control the disease. These rather contradictory findings suggest functional differences in the capacity of Tregs stimulated either by S4B6/IL-2 or JES6/IL-2 complexes. Since mAb S4B6 blocks the epitope necessary for the interaction of IL-2 with CD25, S4B6/IL-2 complexes largely prevent signaling *via* high-affinity IL-2 receptors, but allow for signal transduction through low-affinity IL-2 receptors. This stimulation through low-affinity IL-2 receptor might induce Treg survival and expansion, but may not maintain suppressive functionality. Interestingly, Tregs from CD25<sup>-/-</sup> Bim<sup>-/-</sup> mice, where IL-2-dependent survival and function have been uncoupled, were shown to be less suppressive *in vitro* and unable to prevent autoimmunity *in vivo* (44). Thus, maintenance of Treg functionality in our model seems to be critically dependent on IL-2 signals transduced by high-affinity IL-2 receptors, which apparently cannot be substituted by IL-2 signaling *via* the low-affinity receptor. Therefore, it is likely that Tregs expanded upon pretreatment with S4B6/IL-2 complexes are poorly functional and unable to control alloreactive donor CD4<sup>+</sup> T cells compared to those expanded by prophylactic JES6/IL-2 treatment. Notably, the ratio of host Tregs to donor CD4<sup>+</sup> T cells in S4B6/IL-2 complex-pretreated mice was decreased compared to the ratio in mice pretreated with JES6/IL-2 complexes. Since these ratios were similar in both groups at the initiation of cGvHD (day 0), these differences must have accumulated during the first 2 weeks of cGvHD (compare Figures 3B and 4B,F). These differences may be a result of differences in suppressive capacity in host Tregs in the two different groups at the time of donor cell transfer.

Therapeutic administration of JES6/IL-2 complexes following the induction of cGvHD, on the other hand, showed no significant effect on cGvHD symptoms and the general course of the disease. Our findings demonstrate a critical timing for JES6/IL-2 treatment in the cGvHD model of lupus. Since pathogenic mechanisms are already well established at the time of JES6/IL-2 therapy (4 weeks after cGvHD induction), Treg expansion was not able to ameliorate the ongoing autoimmunity. In this regard, it has to be considered that, in an ongoing disease, JES6/IL-2 complexes may stimulate not only Treg, but also engrafted alloreactive donor CD4<sup>+</sup> T cells that have been previously activated and express high-affinity IL-2 receptors. However, while therapeutic administration of JES6/IL-2 complexes stimulated donor CD4<sup>+</sup> T cells expressing the high-affinity IL-2 receptor, this did not result in aggravated disease symptoms. It is conceivable that a parallel increase of the suppressive capacity in the Treg compartment might counteract the stimulatory effect on donor CD4<sup>+</sup> T cells and thereby prevented disease exacerbation. Notably, therapeutic administration of JES6/IL-2 complexes in a spontaneous model of lupus was shown to ameliorate ICGN (45), arguing in favor for our hypothesis that stimulation of donor CD4<sup>+</sup> T cells by JES6/IL-2 complexes canceled out the beneficial effect of Treg stimulation. Moreover, in contrast to cGvHD, spontaneous lupus is a slowly developing disease that is not driven by a high number of alloreactive donor cell populations and, therefore, might be more susceptible to therapeutic intervention with JES6/IL-2 complexes. Another explanation for the inefficiency of therapeutic JES6/IL-2 treatment to control the disease might be linked to the fact that during the course of cGvHD, the numbers of host Tregs significantly decrease as shown for untreated cGvHD mice at 2 weeks. Thus, fewer host Tregs are present to respond to JES6/IL-2 complexes resulting in a smaller expanded regulatory compartment with poor suppressive capacity.

Finally, therapeutic administration of S4B6/IL-2 complexes significantly ameliorated SLE-like symptoms in ongoing cGvHD. Our findings strongly suggest that this improvement is dependent on donor CD8<sup>+</sup> T cells, since mice injected with CD8<sup>+</sup> T cell-depleted donor cells were not affected by therapeutic S4B6/IL-2 treatment. It might well be envisaged that S4B6/IL-2 complexes stimulate the activation and differentiation of host-reactive donor CD8<sup>+</sup> T cells into functional cytotoxic T lymphocytes (CTLs), thereby inducing a mild form of acute GvHD. B cells are known to be one of the first host lymphocyte population targeted by alloreactive CTLs in acute GvHD (46). Thus, therapeutic S4B6/IL-2 might have ameliorated cGvHD symptoms by enhancing a donor CD8<sup>+</sup> T cell-mediated alloresponse against autoreactive host B cells leading to reduced production of autoantibodies. In support of our hypothesis it was recently shown that IL-21 could also induce the stimulation of such anti-host responses of donor CD8<sup>+</sup> T cells resulting in amelioration of cGvHD symptoms (47). The fact that a more severe cGvHD results from the injection of CD8<sup>+</sup> T cell-depleted donor cells further supports a regulatory role of this population in murine cGvHD.

In conclusion, JES6/IL-2 complexes efficiently ameliorated cGvHD in our model only when administrated prophylactically, possibly by acting during priming and initiation of the disease.

Due to improved diagnosis of SLE and a considerable lag time until clinical manifestation of severe lupus, JES6/IL-2 complexes might be considered as potential approach to prevent more severe symptoms in those patients, where SLE is recognized early enough. In contrast, S4B6/IL-2 aggravated SLE-like symptoms when administrated prophylactically and ameliorated disease only when given therapeutically. With prophylactic treatment, we propose an indirect effect of S4B6/IL-2 complexes on donor CD4<sup>+</sup> T cell differentiation leading to more severe disease symptoms. With therapeutic treatment of an ongoing cGvHD, the ameliorating effect was likely due to direct effects of S4B6/IL-2 complexes on donor CD8<sup>+</sup> T cells inducing their activation and subsequent enhancement of alloresponses directed against host lymphocytes, e.g., host B cells. Results obtained from therapeutic treatment with S4B6/IL-2 complexes may not be directly relevant for the treatment of SLE. While SLE patients exhibit an increased cytotoxicity among their CD8<sup>+</sup> T cells, this has been correlated with increased disease activity. Increased cytotoxic activity of (autoimmune) CD8<sup>+</sup> T cells would release self-antigens from target cells resulting in further stimulation of autoreactive lymphocytes. Nevertheless, the therapeutic administration of S4B6/IL-2 complexes and experiments using CD8<sup>+</sup> T cell-depleted donor cells point to a potential regulatory role of donor CD8<sup>+</sup> T cells in the pathogenesis of murine cGvHD. In summary, the administration of IL-2/mAb complexes has marked effects on the course of cGvHD in this murine model. Whether our findings can be adapted to a treatment of autoimmune diseases in humans is an area for further investigation.

## ETHICS STATEMENT

Animal experiments were carried out within institutional guidelines (authorization number 1888 and 2434 from Cantonal Veterinarian Office, Basel).

## AUTHOR CONTRIBUTIONS

AR conceived the study and designed experiments. All authors performed experiments and analyzed the data. AR and SH wrote the paper.

## ACKNOWLEDGMENTS

We thank Drs. Ed Palmer and Jan Andersson for helpful comments and critical reading of the manuscript. We thank Mike Rolink for skillful technical assistance. This paper is dedicated to the memory of Antonius (Ton) Rolink, our principal investigator and professor, who unexpectedly died during the preparation of this manuscript.

## FUNDING

AR is holder of the chair in Immunology endowed by F. Hoffmann-La Roche Ltd., Basel to the University of Basel. This study was supported by the Swiss National Science Foundation and JL was supported by personal grant (323530\_171148) of Swiss National Science Foundation.

## SUPPLEMENTARY MATERIAL

The Supplementary Material for this article can be found online at <https://www.frontiersin.org/article/10.3389/fimmu.2018.00656/full#supplementary-material>.

## REFERENCES

1. Tsokos GC. Mechanisms of disease systemic lupus erythematosus. *N Engl J Med* (2011) 365(22):2110–21. doi:10.1056/NEJMra1100359
2. van der Vlag J, Berden JH. Lupus nephritis: role of antinucleosome autoantibodies. *Semin Nephrol* (2011) 31(4):376–89. doi:10.1016/j.semephrol.2011.06.009
3. Relle M, Schwarting A. Role of MHC-linked susceptibility genes in the pathogenesis of human and murine lupus. *Clin Dev Immunol* (2012) 2012:1–15. doi:10.1155/2012/584374
4. Tsao BP. An update on genetic studies of systemic lupus erythematosus. *Curr Rheumatol Rep* (2002) 4(4):359–67. doi:10.1007/s11926-002-0046-5
5. Foster MH. T cells and B cells in lupus nephritis. *Semin Nephrol* (2007) 27(1):47–58. doi:10.1016/j.semephrol.2006.09.007
6. Shlomchik MJ, Craft JE, Mamula MJ. From T to B and back again: positive feedback in systemic autoimmune disease. *Nat Rev Immunol* (2001) 1(2):147–53. doi:10.1038/35100573
7. Schroeder K, Herrmann M, Winkler TH. The role of somatic hypermutation in the generation of pathogenic antibodies in SLE. *Autoimmunity* (2013) 46(2):121–7. doi:10.3109/08916934.2012.748751
8. Faderl M, Klein F, Wirz OF, Heiler S, Alberti-Servera L, Engdahl C, et al. Two distinct pathways in mice generate antinuclear antigen-reactive B cell repertoires. *Front Immunol* (2018):9. doi:10.3389/fimmu.2018.00016
9. Crotty S. Follicular helper CD4 T cells (T-FH). *Annu Rev Immunol* (2011) 29:621–63. doi:10.1146/annurev-immunol-031210-101400
10. Sawaf M, Dumortier H, Monneaux F. Follicular helper T cells in systemic lupus erythematosus: why should they be considered as interesting therapeutic targets? *J Immunol Res* (2016) 2016:1–13. doi:10.1155/2016/5767106
11. Yildirim-Toruner C, Diamond B. Current and novel therapeutics in the treatment of systemic lupus erythematosus. *J Allergy Clin Immunol* (2011) 127(2):303–12. doi:10.1016/j.jaci.2010.12.1087
12. Navarra SV, Guzmán RM, Gallacher AE, Hall S, Levy RA, Jimenez RE, et al. Efficacy and safety of belimumab in patients with active systemic lupus erythematosus: a randomised, placebo-controlled, phase 3 trial. *Lancet* (2011) 377(9767):721–31. doi:10.1016/S0140-6736(10)61354-2
13. Jacobi AM, Huang WQ, Wang T, Freimuth W, Sanz I, Furie R, et al. Effect of long-term belimumab treatment on B cells in systemic lupus erythematosus. *Arthritis Rheum* (2010) 62(1):201–10. doi:10.1002/art.27189
14. Crampton SP, Morawski PA, Bolland S. Linking susceptibility genes and pathogenesis mechanisms using mouse models of systemic lupus erythematosus. *Dis Model Mech* (2014) 7(9):1033–46. doi:10.1242/dmm.016451
15. Andrews BS, Eisenberg RA, Theofilopoulos AN, Izui S, Wilson CB, McConahey PJ, et al. Spontaneous murine lupus-like syndromes. Clinical and immunopathological manifestations in several strains. *J Exp Med* (1978) 148(5):1198–215. doi:10.1084/jem.148.5.1198
16. Perry D, Sang A, Yin Y, Zheng YY, Morel L. Murine models of systemic lupus erythematosus. *J Biomed Biotechnol* (2011) 2011:1–19. doi:10.1155/2011/271694
17. Eisenberg R. The chronic graft-versus-host model of systemic autoimmunity. *Curr Dir Autoimmun* (2003) 6:228–44. doi:10.1159/000066864
18. Gleichmann E, Vanelven EH, Vanderveen JPW. A systemic lupus-erythematosus (SLE)-like disease in mice induced by abnormal T-B-cell cooperation – preferential formation of autoantibodies characteristic of SLE. *Eur J Immunol* (1982) 12(2):152–9. doi:10.1002/eji.1830120210
19. Van der Veen F, Rolink AG, Gleichmann E. Diseases caused by reactions of T lymphocytes to incompatible structures of the major histocompatibility complex. IV. Autoantibodies to nuclear antigens. *Clin Exp Immunol* (1981) 46(3):589–96.
20. Rolink AG, Gleichmann H, Gleichmann E. Diseases caused by reactions of T lymphocytes to incompatible structures of the major histocompatibility complex. VII. Immune-complex glomerulonephritis. *J Immunol* (1983) 130(1):209–15.
21. Malek TR. The biology of interleukin-2. *Annu Rev Immunol* (2008) 26:453–79. doi:10.1146/annurev.immunol.26.021607.090357
22. Létourneau S, Krieg C, Pantaleo G, Boyman O. IL-2-and CD25-dependent immunoregulatory mechanisms in the homeostasis of T-cell subsets. *J Allergy Clin Immunol* (2009) 123(4):758–62. doi:10.1016/j.jaci.2009.02.011
23. Alcercovarela J, Alarcón-Segovia D. Decreased production of and response to interleukin-2 by cultured lymphocytes from patients with systemic lupus erythematosus. *J Clin Invest* (1982) 69(6):1388–92. doi:10.1172/JCI110579
24. Lieberman LA, Tsokos GC. The IL-2 defect in systemic lupus erythematosus disease has an expansive effect on host immunity. *J Biomed Biotechnol* (2010) 2010:1–6. doi:10.1155/2010/740619
25. Gillis S, Smith KA. Long term culture of tumour-specific cytotoxic T cells. *Nature* (1977) 268(5616):154–6. doi:10.1038/268154a0
26. Rosenberg SA, Mule JJ, Spiess PJ, Reichert CM, Schwarz SL. Regression of established pulmonary metastases and subcutaneous tumor mediated by the systemic administration of high-dose recombinant interleukin-2. *J Exp Med* (1985) 161(5):1169–88. doi:10.1084/jem.161.5.1169
27. Rosenstein M, Ettinghausen SE, Rosenberg SA. Extravasation of intravascular fluid mediated by the systemic administration of recombinant interleukin-2. *J Immunol* (1986) 137(5):1735–42.
28. Fyfe GA, Fisher RI, Rosenberg SA, Sznol M, Parkinson DR, Louie AC. Long-term response data for 255 patients with metastatic renal cell carcinoma treated with high-dose recombinant interleukin-2 therapy. *J Clin Oncol* (1996) 14(8):2410–1. doi:10.1200/JCO.1996.14.8.2410
29. Gutierrez-Ramos JC, Andreu JL, Revilla Y, Viñuela E, Martínez C. Recovery from autoimmunity of MRL/lpr mice after infection with an interleukin-2/vaccinia recombinant virus. *Nature* (1990) 346(6281):271–4. doi:10.1038/346271a0
30. Boyman O, Surh CD, Sprent J. Potential use of IL-2/anti-IL-2 antibody immune complexes for the treatment of cancer and autoimmune disease. *Expert Opin Biol Ther* (2006) 6(12):1323–31. doi:10.1517/14712598.6.12.1323
31. Boyman O, Kovar M, Rubinstein MP, Surh CD, Sprent J. Selective stimulation of T cell subsets with antibody-cytokine immune complexes. *Science* (2006) 311(5769):1924–7. doi:10.1126/science.1122927
32. Spangler JB, Tomala J, Luca VC, Jude KM, Dong S, Ring AM, et al. Antibodies to interleukin-2 elicit selective T cell subset potentiation through distinct conformational mechanisms. *Immunity* (2015) 42(5):815–25. doi:10.1016/j.jimmuni.2015.04.015
33. Létourneau S, Leeuwen EM, Krieg C, Martin C, Pantaleo G, Sprent J, et al. IL-2/anti-IL-2 antibody complexes show strong biological activity by avoiding interaction with IL-2 receptor alpha subunit CD25. *Proc Natl Acad Sci U S A* (2010) 107(5):2171–6. doi:10.1073/pnas.0909384107
34. Boyman O, Krieg C, Létourneau S, Webster K, Surh CD, Sprent J. Selectively expanding subsets of T cells in mice by injection of interleukin-2/antibody complexes: implications for transplantation tolerance. *Transplant Proc* (2012) 44(4):1032–4. doi:10.1016/j.transproceed.2012.01.093
35. Lee SY, Cho ML, Oh HJ, Ryu JG, Park MJ, Jhun JY, et al. Interleukin-2/anti-interleukin-2 monoclonal antibody immune complex suppresses collagen-induced arthritis in mice by fortifying interleukin-2/STAT5 signalling pathways. *Immunology* (2012) 137(4):305–16. doi:10.1111/imrn.12008
36. Webster KE, Walters S, Kohler RE, Mrkvan T, Boyman O, Surh CD, et al. In vivo expansion of Treg cells with IL-2-mAb complexes: induction of resistance to EAE and long-term acceptance of islet allografts without immunosuppression. *J Exp Med* (2009) 206(4):751–60. doi:10.1084/jem.20082824
37. Jin GH, Hirano T, Murakami M. Combination treatment with IL-2 and anti-IL-2 mAbs reduces tumor metastasis via NK cell activation. *Int Immunopharmacol* (2008) 20(6):783–9. doi:10.1093/intimm/dxn036

**FIGURE S1 |** Representative FACS plots of key populations shown in Figures 3 and 4. Top row indicates the ancestor gating of plots shown below. Squares within plots indicate population gates. Numbers adjacent to population gates indicate frequency of gated population in the ancestor gates. First row: untreated chronic graft-versus-host-disease mice. Second row: prophylactically JES6/IL-2 treated mice. Third row: prophylactically S4B6/IL-2 treated mice.

38. Krieg C, Létourneau S, Pantaleo G, Boyman O. Improved IL-2 immunotherapy by selective stimulation of IL-2 receptors on lymphocytes and endothelial cells. *Proc Natl Acad Sci U S A* (2010) 107(26):11906–11. doi:10.1073/pnas.1002569107
39. Puliaeva I, Puliaev R, Via CS. Therapeutic potential of CD8+ cytotoxic T lymphocytes in SLE. *Autoimmun Rev* (2009) 8(3):219–23. doi:10.1016/j.autrev.2008.07.045
40. Rolink AG, Gleichmann E. Allosuppressor- and allohelper-T cells in acute and chronic graft-vs-host (GVH) disease. III. Different Lyt subsets of donor T cells induce different pathological syndromes. *J Exp Med* (1983) 158(2):546–58. doi:10.1084/jem.158.2.546
41. Itoh M, Takahashi T, Sakaguchi N, Kuniyasu Y, Shimizu J, Otsuka F, et al. Thymus and autoimmunity: production of CD25(+)CD4(+) naturally anergic and suppressive T cells as a key function of the thymus in maintaining immunologic self-tolerance. *J Immunol* (1999) 162(9):5317–26.
42. Sallusto F, Geginat J, Lanzavecchia A. Central memory and effector memory T cell subsets: function, generation, and maintenance. *Annu Rev Immunol* (2004) 22:745–63. doi:10.1146/annurev.immunol.22.012703.104702
43. Blanco P, Ueno H, Schmitt N. T follicular helper (Tfh) cells in lupus: activation and involvement in SLE pathogenesis. *Eur J Immunol* (2016) 46(2):281–90. doi:10.1002/eji.201545760
44. Barron L, Dooms H, Hoyer KK, Kuswanto W, Hofmann J, O'Gorman WE, et al. Cutting edge: mechanisms of IL-2-dependent maintenance of functional regulatory T cells. *J Immunol* (2010) 185(11):6426–30. doi:10.4049/jimmunol.0903940
45. Yan JJ, Lee JG, Jang JY, Koo TY, Ahn C, Yang J. IL-2/anti-IL-2 complexes ameliorate lupus nephritis by expansion of CD4(+)CD25(+)Foxp3(+) regulatory T cells. *Kidney Int* (2017) 91(3):603–15. doi:10.1016/j.kint.2016.09.022
46. Puliaev R, Puliaeva I, Welniak LA, Ryan AE, Haas M, Murphy WJ, et al. CTL-promoting effects of CD40 stimulation outweigh B cell-stimulatory effects resulting in B cell elimination and disease improvement in a murine model of lupus. *J Immunol* (2008) 181(1):47–61. doi:10.4049/jimmunol.181.1.47
47. Nguyen V, Rus H, Chen C, Rus V. CTL-promoting effects of IL-21 counteract murine lupus in the parent -> F1 graft-versus-host disease model. *J Immunol* (2016) 196(4):1529–40. doi:10.4049/jimmunol.1501824

**Conflict of Interest Statement:** The authors declare no financial or commercial conflicts of interest.

The handling Editor declared a past co-authorship with one of the authors (AR).

Copyright © 2018 Heiler, Lötscher, Kreuzaler, Rolink and Rolink. This is an open-access article distributed under the terms of the Creative Commons Attribution License (CC BY). The use, distribution or reproduction in other forums is permitted, provided the original author(s) and the copyright owner are credited and that the original publication in this journal is cited, in accordance with accepted academic practice. No use, distribution or reproduction is permitted which does not comply with these terms.



# DN2 Thymocytes Activate a Specific Robust DNA Damage Response to Ionizing Radiation-Induced DNA Double-Strand Breaks

Irene Calvo-Asensio<sup>1†</sup>, Tara Sugrue<sup>1†</sup>, Nabil Bosco<sup>2</sup>, Antonius Rolink<sup>2</sup> and Rhodri Ceredig<sup>1\*</sup>

<sup>1</sup>National University of Ireland, Galway, Ireland, <sup>2</sup>Department of Biomedicine, University of Basel, Basel, Switzerland

## OPEN ACCESS

### Edited by:

Bernard Malissen,  
INSERM U1104 Centre  
d'immunologie de Marseille-Luminy,  
France

### Reviewed by:

Graham Anderson,  
University of Birmingham,  
United Kingdom  
Avinash Bhandoola,  
National Institutes of Health (NIH),  
United States

### \*Correspondence:

Rhodri Ceredig  
[rhodri.ceredig@nuigalway.ie](mailto:rhodri.ceredig@nuigalway.ie)

<sup>†</sup>These authors have contributed  
equally to this work.

### Specialty section:

This article was submitted  
to *T Cell Biology*,  
a section of the journal  
*Frontiers in Immunology*

Received: 10 April 2018

Accepted: 28 May 2018

Published: 11 June 2018

### Citation:

Calvo-Asensio I, Sugrue T, Bosco N,  
Rolink A and Ceredig R (2018) DN2  
Thymocytes Activate a Specific  
Robust DNA Damage Response to  
Ionizing Radiation-Induced DNA  
Double-Strand Breaks.  
*Front. Immunol.* 9:1312.  
doi: 10.3389/fimmu.2018.01312

For successful bone marrow transplantation (BMT), a preconditioning regime involving chemo and radiotherapy is used that results in DNA damage to both hematopoietic and stromal elements. Following radiation exposure, it is well recognized that a single wave of host-derived thymocytes reconstitutes the irradiated thymus, with donor-derived thymocytes appearing about 7 days post BMT. Our previous studies have demonstrated that, in the presence of donor hematopoietic cells lacking T lineage potential, these host-derived thymocytes are able to generate a polyclonal cohort of functionally mature peripheral T cells numerically comprising ~25% of the peripheral T cell pool of euthymic mice. Importantly, we demonstrated that radioresistant CD44<sup>+</sup> CD25<sup>+</sup> CD117<sup>+</sup> DN2 progenitors were responsible for this thymic auto-reconstitution. Until recently, the mechanisms underlying the radioresistance of DN2 progenitors were unknown. Herein, we have used the *in vitro* "Plastic Thymus" culture system to perform a detailed investigation of the mechanisms responsible for the high radioresistance of DN2 cells compared with radiosensitive hematopoietic stem cells. Our results indicate that several aspects of DN2 biology, such as (i) rapid DNA damage response (DDR) activation in response to ionizing radiation-induced DNA damage, (ii) efficient repair of DNA double-strand breaks, and (iii) induction of a protective G<sub>1</sub>/S checkpoint contribute to promoting DN2 cell survival post-irradiation. We have previously shown that hypoxia increases the radioresistance of bone marrow stromal cells *in vitro*, at least in part by enhancing their DNA double-strand break (DNA DSB) repair capacity. Since the thymus is also a hypoxic environment, we investigated the potential effects of hypoxia on the DDR of DN2 thymocytes. Finally, we demonstrate for the first time that *de novo* DN2 thymocytes are able to rapidly repair DNA DSBs following thymic irradiation *in vivo*.

**Keywords:** DN2 pro-T cells, DNA damage response, ionizing radiation, hypoxia, thymic auto-reconstitution, bone marrow transplantation

## INTRODUCTION

In adults, the bone marrow is the main organ in which hematopoiesis takes place. There, self-renewing, multipotent hematopoietic stem cells (HSCs) reside in a specialized niche and are responsible for continually giving rise to all types of hematopoietic cells (1–4). However, unlike other hematopoietic cells, T lymphocytes are not produced in the bone marrow but rather in the thymus (5, 6),

an organ that provides the optimal microenvironment for supporting all stages of T cell development and selection (7, 8). Under normal physiological conditions, the thymus does not contain self-renewing HSCs. Instead, it is continuously seeded by bone marrow-derived multipotent progenitors that migrate there through the blood (9, 10). Once within the thymus, these progenitors receive signals from the thymic stroma that induce them to proliferate and to undergo progressive differentiation into mature, functional, and self-tolerant T cells (11, 12).

Within the thymus, developing T cells, i.e., immature thymocytes, undergo a series of developmental stages that can be distinguished according to the surface expression pattern of the CD4 and CD8 co-receptors. In a normal thymus, ~5% of thymocytes express neither CD4 nor CD8 (double-negative, DN cells); ~80% express both CD4 and CD8 (double-positive, DP cells); ~10% are CD4 single-positive (CD4SP), and ~5% CD8 single-positive (CD8SP) (13). The most immature intra-thymic T cell progenitors are contained within the DN population (14) and according to their surface expression of CD25, CD44, and CD117, DN cells can be further subdivided into four major cellular subsets known as DN1 to DN4. DN1 cells, the most undifferentiated DN subset, can be identified as CD25<sup>-</sup>CD44<sup>+</sup>CD117<sup>+</sup>; DN2 cells are CD25<sup>+</sup>CD44<sup>+</sup>CD117<sup>+</sup>; DN3 cells are CD25<sup>+</sup>CD44<sup>low</sup>CD117<sup>low</sup>, and finally DN4 cells, the most differentiated DN subpopulation, are negative for all three markers (CD25<sup>-</sup>CD44<sup>-</sup>CD117<sup>-</sup>) (10, 14).

Upon irradiation, thymic cellularity is dramatically reduced due to the high radiosensitivity of thymocytes (15). However, shortly after exposure to a lethal dose of ionizing radiation (IR), unlike all other hematopoietic and lymphoid organs, there is a single wave of thymic auto-reconstitution that results from the proliferation and differentiation of host-derived intra-thymic radioresistant T cell precursors (16–19). These cells would also appear to be resistant to the administration of hydrocortisone acetate (20) and were identified by Bosco et al. as DN2 thymocytes (21). These DN2 thymocytes were able to give rise to a cohort of functional mature T lymphocytes capable of re-constituting ~25% of the normal peripheral T cell compartment, and displaying a polyclonal T cell receptor (TCR) repertoire (21). However, the reasons why specifically these DN2 thymocytes are able to survive following thymic irradiation and subsequently resume their normal intra-thymic development post-IR is currently unknown. Therefore, further investigation is required to define the molecular mechanisms underlying the radioresistance of DN2 thymocytes.

Historically, different systems have been developed to study T cell development, including (i) fetal thymus organ culture (FTOC), (ii) re-aggregated FTOC, (iii) bone marrow chimeras, and (iv) transgenesis (22, 23). More recently, *in vitro*-based expansion and differentiation of immature thymocytes using stromal cell lines ectopically expressing Notch ligands have been used to dissect the signaling events required for T cell development (24–27). However, in these *in vitro* systems, the exact combination and intensity of signals delivered by stromal cells are difficult to control. In addition, the presence of stromal cells in these cultures makes detailed genetic and molecular analysis of uniquely T cell-specific events occurring within cultured progenitors difficult to dissect. The recent development of a stromal cell-free pro-T cell

culture system in the laboratory of Prof. Antonius Rolink has proven to be a very useful tool for studying the minimal requirements necessary for T-cell commitment and differentiation (28). This stromal cell-free culture system commonly known as “*The Plastic Thymus*” is based on the immobilization of a DL4-human IgG<sub>1</sub>-Fc (DL4-Fc) fusion protein to the surface of plastic tissue culture plates pre-coated with a monoclonal anti-human IgG<sub>1</sub>-Fc antibody (28). In addition, the culture medium is supplemented with IL-7 and SCF, allowing the long-term *in vitro* maintenance and expansion of purified DN2 thymocytes (29). Importantly, the pro-T cells generated and expanded *in vitro* using this methodology (i) retain their normal functionality, (ii) can be genetically manipulated, and (iii) are able to reconstitute T cell compartments of irradiated recipient mice (29). Therefore, “*The Plastic Thymus*” represents a novel technology with which to study purified DN2 thymocytes at the molecular level, something that is otherwise technically difficult to do in the normal mouse thymus *in vivo* due to the limited numbers of pro-T cells, particularly DN1 and DN2 cells.

Cellular responses to IR exposure mainly occur due to its detrimental impact on the genome integrity of exposed cells. IR-induced DNA damage can occur due to energy deposited directly onto DNA, or indirectly due to the generation of free radicals within cells, which collectively lead to the modification and/or breakage of DNA strands. The most genotoxic IR-induced DNA lesions are DNA double-strand breaks (DNA DSBs). The maintenance of genomic integrity is essential for cellular survival and for preventing carcinogenesis. Consequently, cells have developed an integrated series of signaling networks, known collectively as the DNA damage response (DDR), to mount biological responses to genotoxic insult. At the molecular level, the DDR consists of (i) sensor proteins that recognize sites of damaged DNA, (ii) transducer proteins that amplify DNA damage signals, and (iii) effector proteins, required for the desired biological response(s) including DNA repair, transient delays in cell cycle progression (termed checkpoints), transcriptional and epigenetic programs, apoptosis, and senescence (30, 31).

Similar to DN2 thymocytes, mesenchymal stromal cells (MSCs) that support hematopoiesis in the bone marrow, and thymic epithelial cells (TECs), which support thymopoiesis in the thymus, are also relatively radioresistant (32–34). In previous studies, we have demonstrated that the activation of the DDR plays important roles in enabling *in vitro* irradiated MSCs and TECs to quickly respond to IR-induced DNA damage and to engage molecular pathways that promote rapid DNA DSB repair, DNA damage checkpoint activation, and cell survival (34, 35). Therefore, using the methods we have previously applied to investigate the DDR of irradiated MSCs, we aimed herein to investigate the role of the DDR in mediating the radioresistance of DN2 thymocytes.

In this study, we have used the “*Plastic Thymus*” culture system to dissect DN2 radiobiology at the molecular level. For comparative purposes, and as a model of a radiosensitive hematopoietic cell type, we have also used a NUP98-HOXB4 expressing HSC line (refer to Section “Materials and Methods” for further information). We demonstrate for the first time that in response to IR-induced DNA DSBs, DN2 thymocytes execute a robust DDR

leading to the resolution of these lesions and to cell survival. Furthermore, we also demonstrate that this robust DDR is also executed by DN2 thymocytes *in vivo* following thymic irradiation. Taken together, our results from both *in vitro* and *in vivo*-derived cells indicate that the DDR of DN2 thymocytes harbors characteristic features favoring their ability to rapidly respond to IR-induced DNA damage and repair DNA lesions, likely playing a key role in their relative radioresistance.

## MATERIALS AND METHODS

### Cell Culture and Treatments

DN2 thymocytes (CD4<sup>-</sup> CD8<sup>-</sup> CD44<sup>+</sup> CD25<sup>+</sup> c-kit<sup>+</sup> CD127<sup>+</sup>) were isolated from the thymi of 4- to 6-week-old C57BL/6 mice as previously described (10) and sorted using a BD FACS Aria<sup>®</sup> cell sorter. As previously discussed, the “*Plastic Thymus*” culture system allows long-term expansion of DN2 pro-T cells *in vitro* in the absence of stromal cells (29). Details of this culture system are described in Section Supplementary Methods in Supplementary Material and shown graphically in Figure S1 in Supplementary Material. DN2 thymocytes were shown to maintain their characteristic cell surface phenotype (CD44<sup>+</sup> CD25<sup>+</sup> CD117<sup>+</sup>) when cultured long-term in 21% O<sub>2</sub> (Figure S2 in Supplementary Material).

To study HSCs, a NUP98-HOXB4 HSC (NH-HSC) line was generated from C57BL/6 mice following the protocol established by Sauvageau et al. (36) and subsequently optimized by Ruedl et al. (37). The NH-HSC line obtained following this protocol was confirmed to display the surface phenotype: CD45<sup>+</sup> Lin<sup>-</sup> c-kit<sup>+</sup> Sca-1<sup>+</sup> CD11c<sup>-</sup> CD19<sup>-</sup> B220<sup>-</sup> CD4<sup>-</sup> CD8<sup>-</sup> and to be capable of successfully re-constituting all hematopoietic lineages in sub-lethally irradiated mice (38). For the purposes of this study, NH-HSCs were maintained in SF-IMDM (Gibco) supplemented with 5% forward light scatter (FCS) (Gibco), 3% v/v IL-6-containing supernatant, 0.1 µg/ml SCF and 0.2% v/v Ciproxin<sup>®</sup> (Bayer Pharmaceutical) at 37°C [as described in Ref. (38)], in either normoxia (21% O<sub>2</sub>) or hypoxia (5% O<sub>2</sub>).

γ-Irradiation at the indicated doses was performed using a Gammacell 40 irradiator containing a <sup>137</sup>Cs source at a dose rate of ~80 cGy/min.

### Mice

C57BL/6 mice were bred under pathogen-free conditions at the Centre for Biomedicine at the University of Basel. All animal experiments were carried out within institutional guidelines (authorization numbers 1886 and 1888 from Kantonales Veterinäramt, Basel).

### Isolation and Sorting of Mouse CD4/CD8 DN 1–3 Subpopulations

Double-negative cells were isolated from 5 thymi per time point after irradiation (9 Gy) and sorted according to their cell surface phenotypes as previously described (10) and outlined in Section Supplementary Methods and Figure S3 in Supplementary Material. DN1 were sorted as CD117<sup>high</sup>, CD25<sup>-</sup> and CD44<sup>high</sup>, DN2 as CD117<sup>high</sup>, CD25<sup>+</sup> and CD44<sup>high</sup> and DN3 as CD117<sup>low</sup>,

CD25<sup>+</sup> and CD44<sup>low</sup> (Figure S3 in Supplementary Material) (10). Sorted cells were pelleted, re-suspended in 100 µl IMDM, and centrifuged onto poly-L-lysine-coated microscope slides using a Cytospin<sup>®</sup> centrifuge (Shandon) for immunofluorescence staining as described below.

### Clonogenic Survival Assay

DN2 and NH-HSC were irradiated at 0.5–4 Gy, seeded into 6-well plates at a concentration of 50,000 cells/well, harvested 3 or 5 days post-irradiation (for NH-HSCs and DN2 cells, respectively) and viable cell numbers were counted in duplicate using a hemocytometer and Trypan blue for exclusion of dead cells. The time-points for cell counting were selected based on the fact that DN2 thymocytes proliferated more slowly than NH-HSCs (Figure S4 in Supplementary Material). The percentage survival of each cell type was then determined by normalizing the number of cells quantified from irradiated versus control (un-irradiated) cultures.

### Flow Cytometry Methods

Cells were harvested and counted prior to staining following the different protocols described below. Cells were then analyzed using a BD FACS Canto<sup>®</sup> or BD FACS Calibur flow cytometer (BD Biosciences) and FlowJo<sup>®</sup> data analysis software (Tree Star Inc., OR, USA). For surface labeling, cells were pelleted and re-suspended in FACS buffer (2% FCS, 0.05% Sodium Azide, PBS) at 5 × 10<sup>6</sup> cells/ml. Then, 5 × 10<sup>5</sup> cells/sample were stained for 20 min with the appropriate primary antibodies or isotype controls. To reveal cells stained with biotin-labeled antibodies, the cells were subsequently washed in FCS-free FACS buffer, stained for 10 min with fluorescently labeled streptavidin, washed, and then analyzed.

For cell cycle analysis, cells were labeled for 1 h with 25 µM 5'-bromo-deoxyuridine (BrdU) (Sigma-Aldrich), washed with PBS, and re-suspended in growth medium. Cells were harvested at the indicated time points post-irradiation (4 Gy), fixed in ice-cold 70% ethanol, and stained with anti-BrdU and FITC-conjugated anti-mouse IgG antibodies and propidium iodide (PI)/RNase staining buffer (BD Biosciences) as previously described (35). The progression of cells through the cell cycle was analyzed by measuring the percentage BrdU-positive cells in each G<sub>1</sub> phase until 24 h post IR using a BD FACS Canto<sup>®</sup> flow cytometer (BD Biosciences) and FlowJo<sup>®</sup> software (Tree Star Inc., OR, USA).

Information regarding all antibodies used for flow cytometry can be found in Section Supplementary Methods in Supplementary Material.

### Real-Time PCR

Total RNA was isolated from cells by TRIzol<sup>®</sup> Reagent (Life Technologies)—and cDNA was generated using Applied Biosystems’ High-Capacity cDNA Reverse Transcription Kit according to the manufacturer’s instructions. 10–20 ng of cDNA was used as template in semi-quantitative real-time PCR reactions with specific primers on a Step One Plus Real-Time PCR System (Applied Biosystems). Reactions were prepared with TaqMan<sup>®</sup> gene expression master mix (Thermo Fisher Scientific) using predesigned TaqMan<sup>®</sup> gene expression assays for amplification

of mouse Lig4 (DNA Ligase 4), Prkdc (DNA-PKcs), Rad51, and β-actin (Thermo Fisher Scientific). Gene expression changes were determined using the ΔΔCt method, using β-actin as a housekeeping gene for normalization according to the primer efficiencies previously calculated.

## Western Blotting

Whole cell extracts were prepared from control or irradiated cells at the indicated time points post-irradiation by direct addition of 5 µl of 4× Laemmli buffer per 100,000 cells that we previously harvested from culture by centrifugation, washed with ice-cold PBS, and counted. Cells were disaggregated into the Laemmli buffer, heated at 95°C for 5 min, and sonicated (20% amplitude for 3 s) prior to separation using SDS-PAGE gels and transferred to nitrocellulose membranes. Chemiluminescence was detected using SuperSignal West Pico Chemiluminescent Substrate (Thermo Fisher Scientific) and medical x-ray film (Konica Minolta Medical and Graphic Imaging Inc.). Information regarding all antibodies used for western blotting can be found in Section Supplementary Methods in Supplementary Material.

## Immunofluorescence Staining and Microscopy

Double-negative cells were spun onto poly-L-lysine-coated microscope slides using a Cytospin® centrifuge (Shandon), fixed in 4% paraformaldehyde (Sigma-Aldrich), and subsequently permeabilized in 0.1% Triton®-X 100 solution. Nuclei were then stained for γH2AX IR-induced foci (IRIF) as previously described (35). Image Z-stacks were captured using 60× magnification on a Leica SP5 integrated microscope system (Leica Microsystems). Images were deconvoluted using the Huygens Software by Scientific Volume Imaging. Image Z-stacks were projected using the maximal intensity method using Fiji (39). Customized macros for Fiji were used to adjust the projected images and the number of γH2AX IRIF per nucleus were counted blind. Information regarding all antibodies used for western blotting can be found in Section Supplementary Methods in Supplementary Material.

## RESULTS

### DN2 Thymocytes Are Relatively Radioresistant *In Vitro*

We first investigated the effects of irradiation on the survival of DN2 thymocytes *in vitro*, using NH-HSCs as a radiosensitive control. To do so, DN2 and NH-HSC were irradiated at 0–4 Gy and cultured for 3 (NH-HSC) or 5 days (DN2) before counting surviving cells. As shown in **Figure 1**, the radioresistance of DN2 and NH-HSC was comparable at IR doses of 0.5–2 Gy. However, at 4 Gy, the radioresistance of DN2 cells was found to be 10-fold greater than that of NH-HSC (~18.7% DN2 survival versus ~1.8% NH-HSC survival) (**Figure 1**).

### DN2 Thymocytes Activate DNA Damage Checkpoints *In Vitro*

As previously mentioned, the DDR plays a key role in determining whether a cell survives or dies following exposure to genotoxic

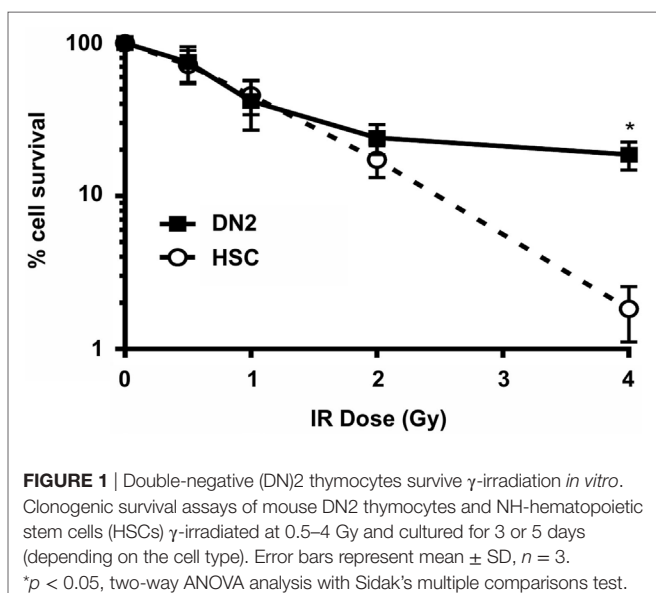


**FIGURE 1 |** Double-negative (DN)2 thymocytes survive γ-irradiation *in vitro*. Clonogenic survival assays of mouse DN2 thymocytes and NH-hematopoietic stem cells (HSCs) γ-irradiated at 0.5–4 Gy and cultured for 3 or 5 days (depending on the cell type). Error bars represent mean  $\pm$  SD,  $n = 3$ . \* $p < 0.05$ , two-way ANOVA analysis with Sidak's multiple comparisons test.

agents, such as IR. The activation of DNA damage checkpoints during the cell cycle acts to prolong the time in which a given cell can execute mechanisms to try and resolve genomic damage and promote its survival. The difference in the long-term survival between DN2 and NH-HSC suggested that these DNA damage checkpoints may be differentially executed between these two cell types. To investigate this, the cell cycle progression of BrdU pulse-labeled DN2 and NH-HSCs was analyzed at various time points post 4 Gy irradiation by flow cytometry (**Figure 2A**). By co-staining these cells with an anti-BrdU antibody and PI, the G<sub>1</sub>, S, and G<sub>2</sub>/M phases of the cell cycle (**Figure 2A**, top left panel) can be clearly distinguished. Furthermore, the progression of BrdU-labeled (S phase) cells through the cell cycle and their return to the G<sub>1</sub> phase can be monitored (**Figure 2A**). Importantly, under control conditions (no irradiation, 0 Gy), BrdU labeling itself did not cause significant toxicity to either DN2 or NH-HSCs (Figure S4 in Supplementary Material). Under normal conditions (0 h), ~16% DN2 population were in S phase (BrdU-positive) compared with ~56% NH-HSC (**Figure 2B**). Furthermore, ~78% DN2 population was found to be in G<sub>1</sub> phase, compared with ~41% NH-HSC population (**Figure 2B**). These results correlate with the increased rate of cell cycle progression observed in NH-HSCs, compared with DN2 cells (Figure S4 in Supplementary Material).

Dramatic differences in the ability of DN2 and NH-HSC to activate cell cycle arrest were observed post-irradiation. Strikingly, DN2 thymocytes that were in G<sub>1</sub> phase at the time of irradiation were largely maintained over time (~78% in G<sub>1</sub> at 0 h versus ~68.4% in G<sub>1</sub> at 36 h post IR) (**Figure 2C**). This strongly contrasted with NH-HSCs whose G<sub>1</sub> population reduced rapidly post-irradiation from ~41% at 0 h to ~0.8% at 36 h post IR (**Figure 2C**). This reduction in % G<sub>1</sub> cells was likely due to the activation of cell death as evidenced by the appearance of a large sub-G<sub>1</sub> population in NH-HSC profiles post-irradiation (**Figure 2E** and indicated in **Figure 2A** by black arrows in bottom panels). BrdU-labeled DN2 cells accumulated as a cohort in late S/G<sub>2</sub> phases until 8 h post IR, indicative of the activation

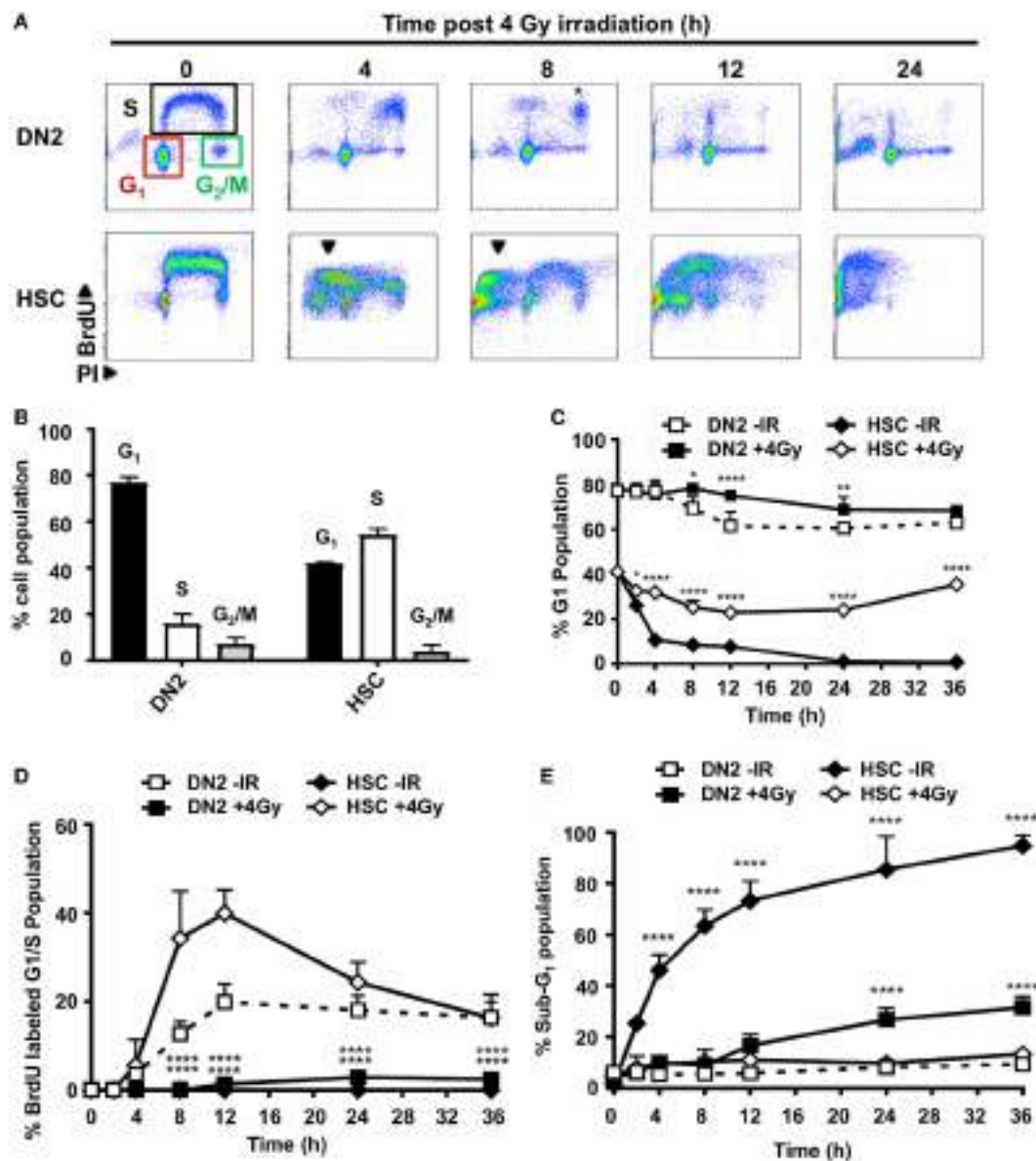


**FIGURE 2 |** Double-negative (DN2) thymocytes activate DNA damage checkpoints. **(A)** Representative cytograms of DN2 and NH-hematopoietic stem cells (HSCs) at 0–24 h post 4 Gy irradiated and stained for bromo-deoxyuridine (BrdU) incorporation and DNA content using propidium iodide (PI). Colored boxes are used to indicate G<sub>1</sub>, S, and G<sub>2</sub>/M phase cells under control conditions; black arrowheads indicate sub-G<sub>1</sub> cells and \* indicates cohort of BrdU-labeled DN2 cells accumulated in late S/G<sub>2</sub>. **(B)** Quantification of the percentage DN2 and NH-HSCs in each phase of the cell cycle under normal conditions. **(C)** Quantification of the percentage G<sub>1</sub> DN2 cells and NH-HSCs at 0–36 h post-irradiation or under normal conditions. **(D)** Quantification of the percentage BrdU-labeled G<sub>1</sub>/early S phase DN2 cells and NH-HSCs at 0–36 h post-irradiation or under normal conditions. **(E)** Quantification of the percentage sub-G<sub>1</sub> DN2 cells and NH-HSCs at 0–36 h post-irradiation or under normal conditions. All cytograms and graphs are representative of three independent experiments. Error bars represent mean  $\pm$  SD,  $n = 3$ , \* $p < 0.05$ , \*\* $p < 0.01$ , \*\*\* $p < 0.0001$ . Two-way ANOVA analysis with Tukey's multiple comparisons test was performed on the following conditions (i) DN2-ionizing radiation (IR) versus DN2 + 4 Gy and (ii) HSC-IR versus HSC + 4 Gy.

of intra-S-phase and G<sub>2</sub> checkpoints (32) (Figure 2A, \* in top 8 h panel). However, BrdU labeled DN2 thymocytes did not re-enter cell cycle following G<sub>2</sub> checkpoint activation and likely entered cell death, similar to NH-HSCs (Figure 2B, top 24 h panel). Similar to the G<sub>1</sub> NH-HSC population, BrdU labeled NH-HSCs also underwent cell death post IR (Figures 2A,E). Taken together, these results indicate that in the immediate

response to irradiation, DN2 thymocytes activate DNA damage checkpoints more robustly than NH-HSCs which instead seem to directly revert to activating cell death. Interestingly, these results also demonstrate that DN2 thymocytes that survive long-term post IR originate primarily from cells in G<sub>1</sub> phase of the cell cycle, indicating that DN2 thymocytes induce a protective G<sub>1</sub>/S checkpoint in response to IR-induced DNA damage.

## DN2 Thymocytes Activate a Robust DDR Post-Irradiation

The contrasting cellular responses of DN2 thymocytes versus NH-HSCs to IR-induced DNA Damage (strong induction of G<sub>1</sub> arrest in irradiated DN2 thymocytes versus apoptosis in NH-HSCs) suggested that the molecular DDR pathways may be differentially executed in these two cell types. To determine whether DN2 and HSC differentially activate the DDR in response to IR-induced DNA DSBs, H2AX Ser139 phosphorylation ( $\gamma$ H2AX, DNA DSB marker); p53 stabilization; and p21 and Puma expression were analyzed over a 24-h time-course (Figure 3A). Maximal H2AX phosphorylation was detected in DN2 at 1 h post IR, whereas it was delayed in HSC and accumulated until 4 h post IR (Figure 3A). p53 was stabilized, and p21 and Puma expression were induced, in irradiated DN2 and HSC, indicating that DDR pathways were intact in these cell types *in vitro*. However, in contrast to HSC, p53 stabilization and induced expression of the pro-apoptotic protein, Puma, were transient in irradiated DN2 (Figure 3A). Furthermore, p21 expression was strongly induced in DN2 at early (1–4 h) time-points post IR whereas it was weakly induced

in HSC at later time-points (12 and 24 h) (Figure 3A). Taken together, these results indicate that irradiated DN2 thymocytes rapidly induce the p53/p21 signaling cascade following DNA DSB generation which likely contributes to the ability of this cell type to induce a protective G<sub>1</sub>/S checkpoint, promoting their survival. Similar to previous observations seen in other radiosensitive cell types such as DP thymocytes (35), NH-HSCs appear to rapidly revert to inducing apoptosis, rather than protective DNA damage checkpoints, as evidenced by the long-term persistence of Puma and p53 stabilization in the presence of DNA DSBs (Figure 3A).

Western blot analysis of control DN2 and HSC whole cell extracts revealed that DN2 expressed higher endogenous levels of the DNA DSB sensor protein, ATM (Figure 3B) and of the DNA DSB repair *via* NHEJ proteins, DNA-PK<sub>cs</sub> and 53BP1, than NH-HSCs (Figures 3B,C). The expression levels of the DNA DSB mediator protein, Chk2, were found to be comparable between DN2 and NH-HSCs, whereas endogenous levels of Rad51, a protein playing a key role in DNA DSB repair *via* homologous recombination was increased in NH-HSCs in comparison with DN2 cells (Figure 3C). In addition, compared with NH-HSC, DN2 cells were found to

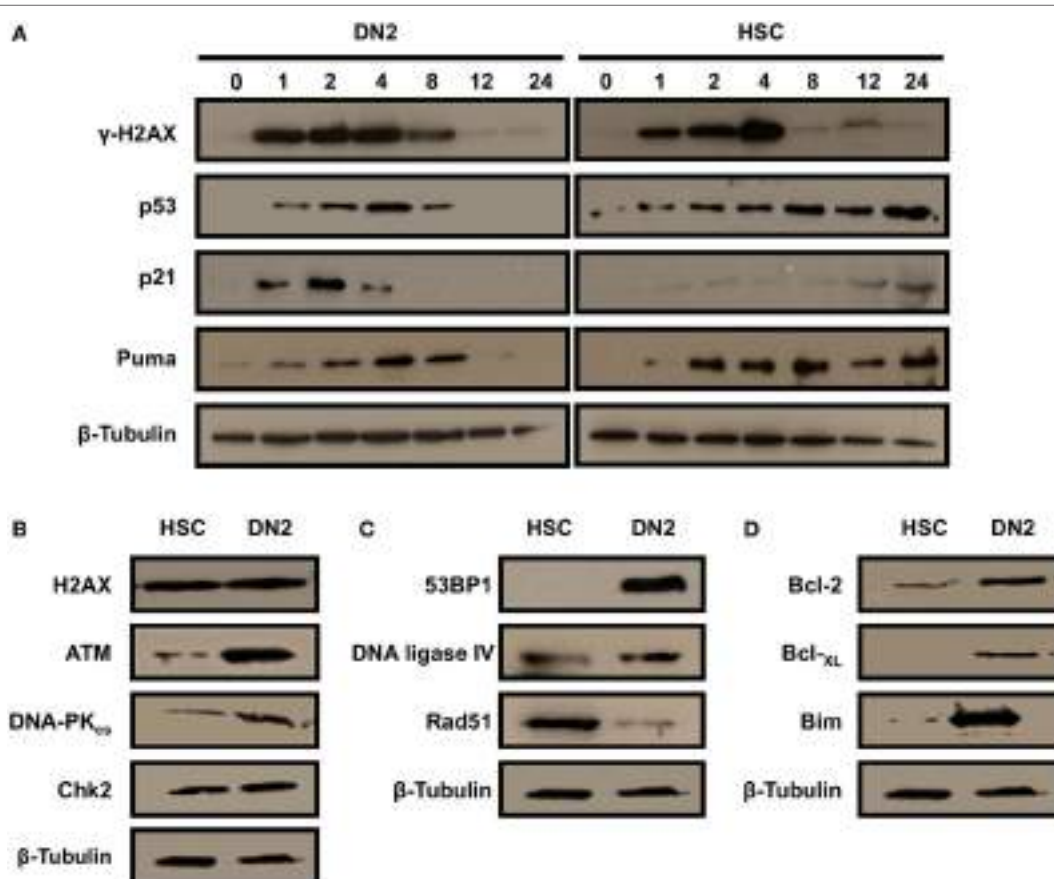


**FIGURE 3 |** DN2 thymocytes activate a robust DNA damage response following  $\gamma$ -irradiation. Western blot analysis of (A) H2AX (Ser139) phosphorylation ( $\gamma$ H2AX—marker of DNA double-strand breaks), p53 stabilization; and p21 and Puma expression in DN2 cells and NH-hematopoietic stem cells (HSCs) at 0–24 h post 4 Gy irradiation. Western blot analysis of total endogenous levels of (B) of H2AX, ATM, DNA-PK<sub>cs</sub> and Chk2; (C) of 53BP1, DNA ligase IV and Rad51; and (D) of Bcl-2, Bcl-XL, and Bim in un-irradiated (control) DN2 cells and NH-HSCs.  $\beta$ -Actin and  $\beta$ -tubulin were used as internal controls. All images are representative of one of three independent experiments.

express higher levels of anti-apoptotic proteins, Bcl-2 and Bcl-XL, and of the pro-apoptotic protein, Bim (Figure 3D).

## Hypoxia Differentially Impacts on the DNA DSB Repair Capacity of DN2 Thymocytes and NH-HSCs

Our group has previously shown that the capacity of irradiated mouse MSCs and TECs to repair DNA DSBs is modulated by hypoxia, correlating with an effect on their intrinsic radioresistance (34, 40). Similar to the bone marrow, the thymus also consists of a hypoxic environment and therefore we were interested

in investigating whether hypoxia may affect the radiobiology of DN2 thymocytes. To this end, we first investigated the effect of hypoxia on cell cycle checkpoint activation in irradiated DN2 thymocytes and NH-HSCs using the irradiation conditions studied previously. Culture in hypoxia did not affect the cell cycle progression of neither DN2 thymocytes nor NH-HSCs in normal growth conditions (Figure 4A). In addition, hypoxia exposure did not significantly impact on DNA damage checkpoint activation and recovery of DN2 thymocytes in response to irradiation (Figures 4B,D). However, culture under hypoxic conditions resulted in a significantly higher proportion of NH-HSCs being able to survive and resume the cell cycle,

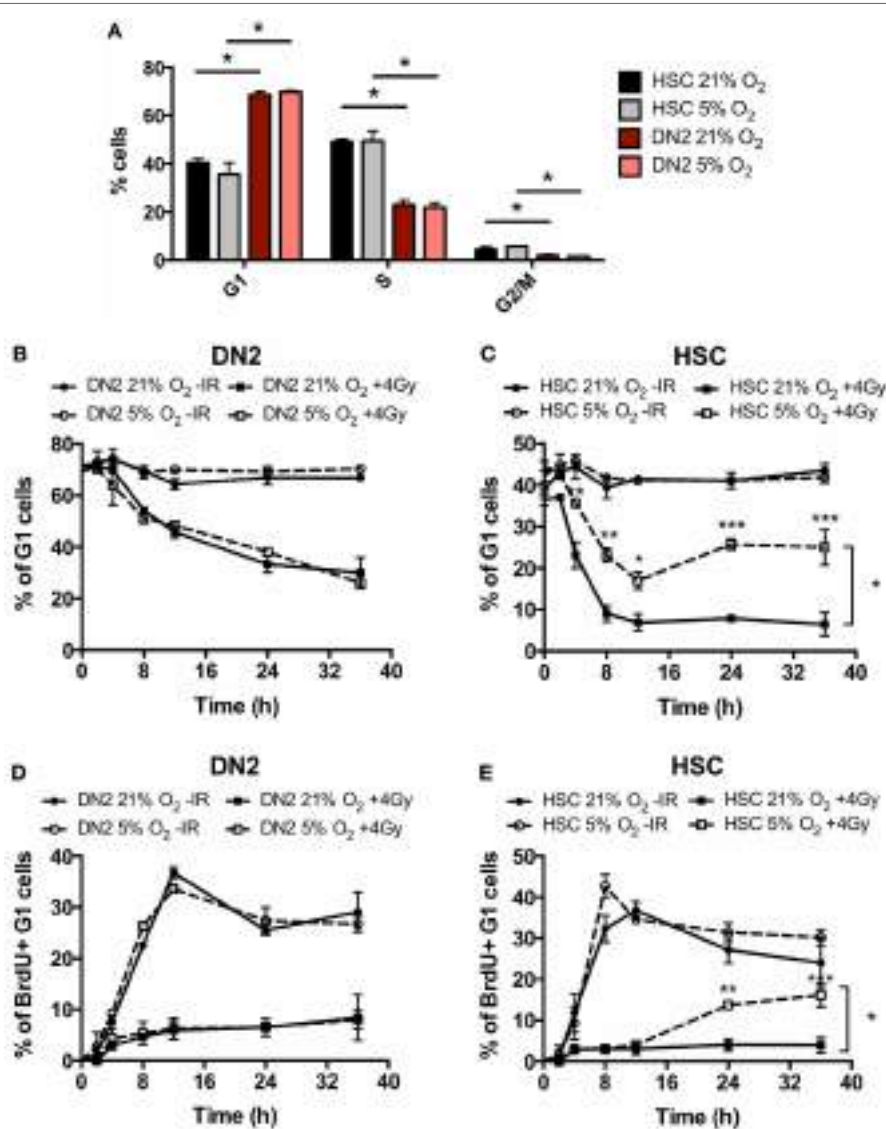


**FIGURE 4 |** Cell cycle checkpoint activation of normoxic and hypoxic DN2 thymocytes. **(A)** Comparison of the percentage of cells in each phase of the cell cycle in NH-hematopoietic stem cell (HSC) and DN2 cells cultured in 21 or 5% O<sub>2</sub>. \*p < 0.05, multiple t-tests with Holm–Sidak post-test correction. Quantification of average percentage of G<sub>1</sub> phase **(B)** DN2 and **(C)** NH-HSC cells cultured in either 21 or 5% O<sub>2</sub>, 0–36 h post bromo-deoxyuridine (BrdU) pulse, with or without treatment with 4 Gy of ionizing radiation (IR). \*p < 0.05, \*\*p < 0.01, \*\*\*p < 0.001, two-way ANOVA analysis with Bonferroni post-test correction, n = 3. Quantification of average percentage of BrdU-labeled G<sub>1</sub> phase **(D)** DN2 and **(E)** NH-HSC cells cultured in either 21 or 5% O<sub>2</sub>, 0–36 h post BrdU pulse, with or without treatment with 4 Gy of IR. \*\*p < 0.01, \*\*\*p < 0.001, two-way ANOVA analysis with Bonferroni post-test correction, n = 3.

compared to their normoxic counterparts (**Figures 4C,E**; **Figure S5** in Supplementary Material).

In addition, the kinetics of γH2AX induction and resolution in DN2 and NH-HSC cultured in normoxia and hypoxia was analyzed at different time-points post-irradiation (**Figure 5A**). The kinetics of γH2AX induction in both cell types at early time-points post-irradiation were found to be unaffected by oxygen tension (**Figure 5A**). However, in hypoxia, faster resolution of γH2AX phosphorylation was observed in the case of NH-HSCs, which may indicate faster repair of DNA DSBs. By contrast, although as previously shown the peak of γH2AX levels in DN2 cells occurs earlier, culture under hypoxic conditions results in slower kinetics of DSB repair in these cells, opposite to the results obtained with NH-HSCs.

In light of the previous results (**Figure 3B**), the effects of hypoxia on the endogenous expression levels of DNA repair and

apoptotic factors in NH-HSCs and DN2 cells were also analyzed (**Figures 5B,D**). Culture under different oxygen levels did not cause significant changes in mRNA expression level of any of the DNA repair factors analyzed (DNA-PKcs, DNA ligase IV, and Rad51) in both cell types (**Figure 5B**). Similar to previous results (**Figure 3B**), DN2 thymocytes expressed (i) higher endogenous levels of DNA Ligase IV and 53BP1 and (ii) lower levels of Rad51 compared with NH-HSCs (**Figures 5B,C**). However, hypoxic DN2 cells had decreased levels of both proteins in comparison to their normoxic counterparts, correlating with the lower DSB repair efficiency detected in these cells in hypoxia (**Figure 5A**).

Protein levels of the anti-apoptotic factors Bcl-2 and Mcl-1 and the pro-apoptotic factors Bim and Puma were also analyzed. Interestingly, compared with normoxic cultures, culture of NH-HSCs under hypoxic conditions resulted in a large increase

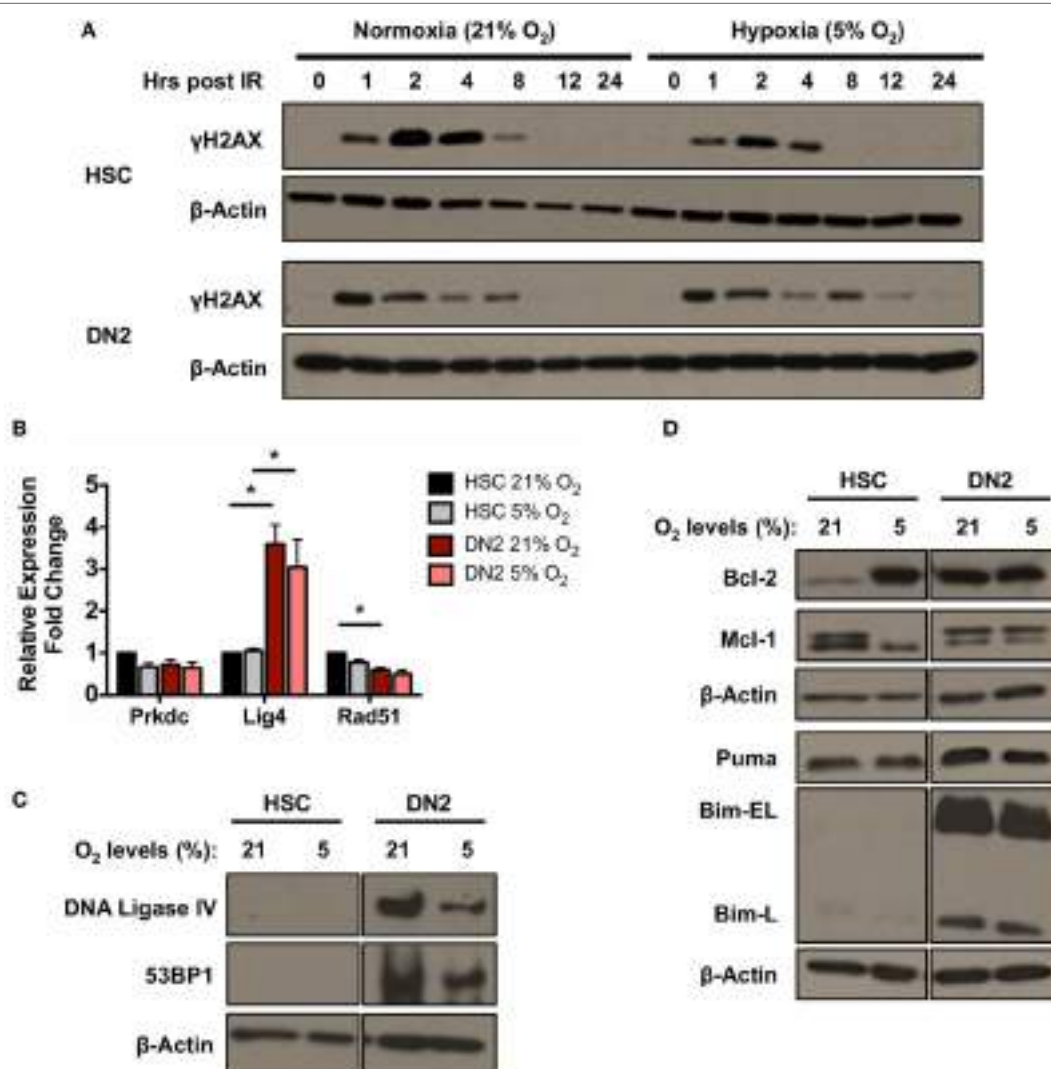


**FIGURE 5 |** DNA repair and apoptotic proteins expression in normoxic and hypoxic NH-hematopoietic stem cell (HSC) and DN2 thymocytes. **(A)** Western blot analysis of H2AX (Ser139) phosphorylation in DN2 cells and NH-HSCs cultured in either normoxia (21% O<sub>2</sub>) or hypoxia (5% O<sub>2</sub>) at 0–24 h post 4 Gy irradiation. **(B)** mRNA expression levels of DNA repair factors DNA-PKcs (Prkdc), DNA Ligase IV (Lig4) and Rad51 in NH-HSC and DN2 cells in normoxia (21% O<sub>2</sub>) and hypoxia (5% O<sub>2</sub>). All values were normalized against β-actin and expressed relative to the NH-HSC normoxic sample. Representative western blots of **(C)** DNA damage response factors DNA ligase IV and 53BP1; and **(D)** pro- and anti-apoptotic proteins in NH-HSC and DN2 cells in normoxia (21% O<sub>2</sub>) and hypoxia (5% O<sub>2</sub>). All graphs show the average of three biological replicates. (\*p < 0.05, multiple t-tests with Holm–Sidak post-test correction).

in endogenous Bcl-2 protein levels (**Figure 5D**). In line with this, the radioresistance of NH-HSCs was found to be increased in hypoxic conditions (Figure S5 in Supplementary Material). In normoxia, DN2 cells expressed high levels of endogenous Bcl-2 protein, similar to those of hypoxic NH-HSCs, but this was not affected by oxygen tension. Interestingly, NH-HSCs and DN2 cells showed different patterns of expression of the two Mcl-1 bands detected by Western blotting. While DN2 cells express higher levels of the upper band regardless of the oxygen levels, NH-HSC express equal levels of both bands in normoxia, but show preferential expression of the lower one in hypoxia (**Figure 5D**). With regard to the pro-apoptotic proteins, while the levels of Puma were similar between DN2 and HSC, DN2 showed much higher levels of the Bim-EL and Bim-L isoforms.

## In Vivo Response of DN Pro-T Cell Subpopulations to IR

Until now, we have demonstrated that the execution of the DDR and DNA DSB repair plays important roles in mediating the radioresistance of DN2 thymocytes *in vitro*. Therefore, our final

objective was to determine whether DN2 thymocytes activate the DDR *in vivo* in response to irradiation. To do so, DN2 pro-T cells and their radiosensitive progenitors (DN1 cells) and progeny (DN3 cells) were isolated from either control or irradiated mice at different time-points following 9 Gy of whole body irradiation as graphically described in Figure S3A in Supplementary Material. The isolated cells were subsequently stained with specific antibodies to CD25, CD44, cKit, and CD3 and sorted into DN1, DN2, and DN3 subpopulations (Figure S3B in Supplementary Material). The numbers of both DN1 and DN3 pro-T cells recovered from the thymi dramatically dropped after IR treatment, whereas the number of DN2 pro-T cells remained higher in proportion at all time-points post-IR (**Figures 6A,B**). Interestingly, CD117 (cKit) surface expression by DN cells decreased over time following the IR treatment, an effect that was not correlated with changes in cell size, as measured by FCS measurements (Figure S6 in Supplementary Material). Sorted DN subpopulations were then analyzed at different time-points post IR for the appearance and resolution of  $\gamma$ H2AX IRIF (**Figures 6C,D**). Similar to our findings *in vitro* (**Figure 3A**), *in vivo*-derived DN2 cells activated the DDR very quickly post IR, as evidenced by the peak in  $\gamma$ H2AX

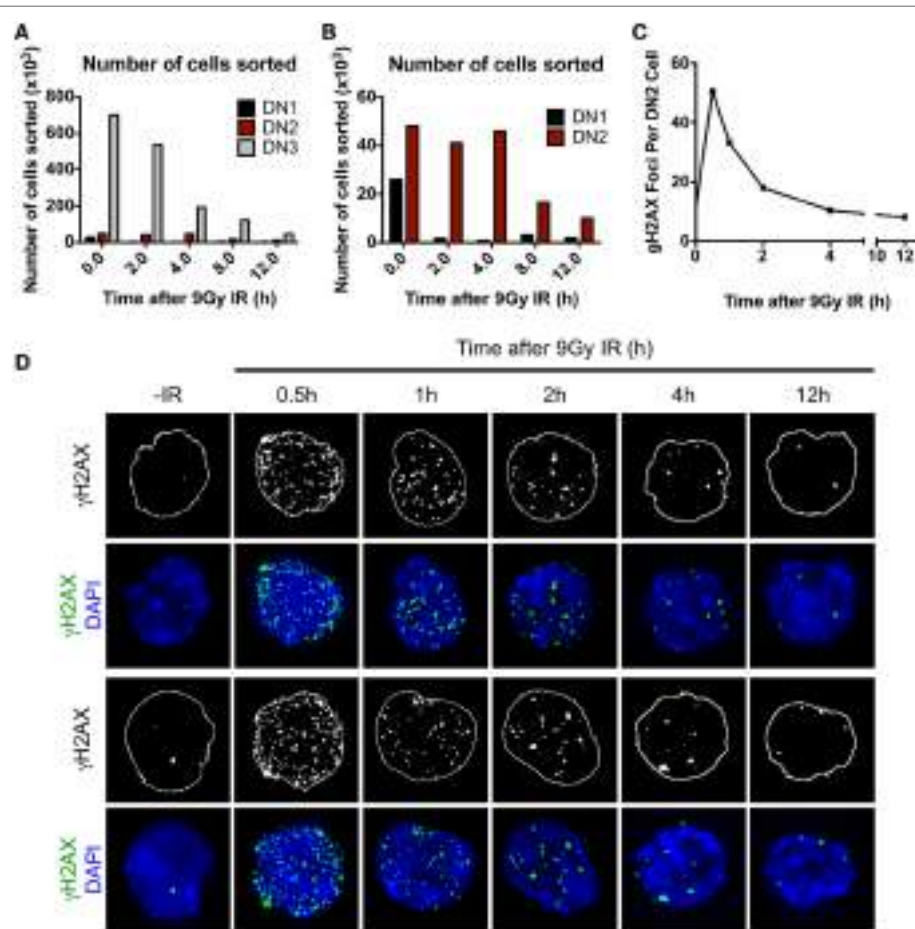


**FIGURE 6 |** Characterization of DN pro-T cells *in vivo* response to ionizing radiation (IR). **(A)** Number of DN1, DN2, and DN3 pro-T cells; **(B)** number of DN1 and DN2 pro-T cells only that were recovered at different time points 0–12 h after irradiation with 9 Gy. **(C)** Average number of  $\gamma$ H2AX IR-induced foci (IRIF) per nucleus and **(D)** representative images of DN2 nuclei stained for  $\gamma$ H2AX IRIF and DAPI, corresponding to cells irradiated *in vivo* and isolated 0–12 h post IR.

IRIF formation at only 30 min post IR. Remarkably, irradiated DN2 cells rapidly resolved these DNA DSBs, as indicated by the resolution of the majority of  $\gamma$ H2AX IRIFs by 4 h. As previously shown (**Figures 6A,B**), the numbers of DN1 and DN3 cells decreased dramatically post-IR due to cell death, and for DN1 cells, sufficient cells could not be recovered to carry out IRIF experiments. Since DN3 cells rapidly undergo apoptosis following IR, causing generalized  $\gamma$ H2AX staining in their apoptotic nuclei, accurately quantifying  $\gamma$ H2AX foci was not possible. In addition, it must be noted that all time-points referred to in this experiment correspond to the time when the thymi were isolated post IR and cell suspensions placed at 4°C. The time elapsed during sample preparation and sorting until cells were fixed (~2 h) is likely to underestimate the early kinetics of DNA damage repair in DN2 cells.

## DISCUSSION

Following bone marrow transplantation (BMT), patients undergo a period of lymphopenia until their immune system is successfully regenerated. This lymphopenia renders them susceptible to life-threatening opportunistic infections and reactivation of endogenous viruses (41, 42). Although thymic cellularity drops drastically following irradiation due to the high radiosensitivity of the majority of thymocytes (15), many authors have reported a single wave of thymic auto-reconstitution occurring shortly after radiation exposure (16–20). Bosco et al. (21) determined that auto-reconstitution of the thymus was due to the survival of relatively radioresistant CD25<sup>+</sup>, CD44<sup>+</sup>, CD117<sup>high</sup> conventional DN2 pro-thymocytes capable of recapitulating normal thymic differentiation and generating a cohort of cells exported to the periphery. In addition, they suggested that their mature peripheral T cell progeny may act as a first barrier against infections during the lymphopenic periods that follow BMT (21). In fact, it has been shown that in some cases, host-derived anti-cytomegalovirus-specific T cells are able to protect patients against viral infection during the lymphopenic period following BMT (43). As shown by Bosco et al. (21) in mouse BM chimeras, host-derived T cells survive for at least 6 months (21), display a polyclonal TCR V $\beta$  repertoire, and appear to be functional both *in vitro* (17) and *in vivo* (21). To positively identify the DN2-derived cohort of T cells and distinguish them from their extra-thymically derived partners is difficult. However, since the thymic stroma is also irradiated in BM chimeras, it would be of interest to investigate the efficiency of negative selection of the TCR V $\beta$  repertoire amongst host thymus-derived T cells.

The mechanisms that mediate the radioresistance of DN2 thymocytes, in contrast to radiosensitive DN1 and DN3 thymocytes, are so far poorly characterized. One of the main difficulties to overcome in studying the radiobiology of DN cells at the molecular level is their low number (especially DN1 and DN2) in the normal mouse thymus. Therefore, in this study, we utilized “*The Plastic Thymus*” culture system to expand purified DN2 pro-T cells *in vitro* to study the role of the DDR in mediating their radioresistance. Overall, this study has demonstrated that (i) DN2 thymocytes activate a rapid DDR in response to IR-induced DNA DSBs, which in turn, (ii) is likely to contribute to their ability to

induce a protective G<sub>1</sub>/S checkpoint and thereby, provide DN2 cells with a time window for repairing DNA DSBs, promoting their survival.

Developing T cells undergo a process of rearrangement of their TCR *via* V(D)J recombination, which begins during the DN1 to DN2 transition (44). V(D)J recombination is initiated by Rag-mediated DNA DSBs (45) that trigger the activation of the DDR and the subsequent repair of the lesions *via* NHEJ (46–48). The DDR pathway is crucial for lymphocyte development as demonstrated by the fact that deficiency or loss-of-function mutations in important DDR genes such as ATM, Nbs1, 53BP1, TopBP1, and DNA ligase IV cause multiple defects in lymphocyte development and function, resulting in aberrant V(D)J rearrangements, lymphopenia, and increased susceptibility to hematological malignancies (49–54). Interestingly, in this study, compared with HSC, DN2 thymocytes were found to express higher endogenous levels of key DDR sensor and NHEJ proteins, including ATM, 53BP1, DNA ligase IV, and DNA-PK<sub>cs</sub> (**Figures 3B,C**). This may reflect the need for DN2 thymocytes to have a robust DDR in place for effective regulation of TCR gene rearrangements during early thymic development. Also, in lymphocytes, ATM and p53 have been directly implicated in limiting DSBs caused by V(D)J recombination exclusively to the G<sub>1</sub> phase of the cell cycle (55), *via* the repression of Cyclin D3 expression (56). This mechanism, which is specific for developing lymphocytes and not observed in mature T cells, may explain the preferential activation of the G<sub>1</sub>/S checkpoint in DN2 pro-T cells in response to DNA damage. However, the V(D)J recombination process not only occurs in DN2 cells but also in more advanced stages of T cell development, as well as in pro-B cells (10), which are highly radiosensitive. Therefore, gene rearrangement alone is not sufficient to explain the unique radioresistance of DN2 cells, compared with other lymphoid progenitors that also execute V(D)J recombination.

In addition, in comparison with HSCs, DN2 cells also expressed particularly high levels of the pro-apoptotic factor Bim (**Figure 5D**). Bim is an important apoptotic mediator in thymocyte biology that has been shown to be crucial in many stages of T cell development, such as for the regulation of lymphocyte progenitor survival and negative selection (57–60). Furthermore, Bim activity is known to be crucial for inducing apoptosis in thymocytes in response to IR (61), and it has been shown to be highly expressed in thymocytes prior to pre-TCR expression, that is, at the DN3 stage, and is downregulated upon signaling through the pre-TCR (62). Therefore, our observation of high levels of Bim being expressed in DN2 thymocytes is in line with the literature in the field. These high levels of Bim would be lethal for the cells if they were not counteracted by high expression of anti-apoptotic proteins such as Bcl-2 [also in line with our results (**Figure 3B**), which is also highly expressed in DN pro-T cells and is downregulated at the DP stage (63, 64)]. Interestingly, this high Bcl-2 expression is dependent on IL-7, an indispensable cytokine for T lymphopoiesis, whose receptor IL7R $\alpha$  (CD127) is under the control of Notch1 signaling (65, 66), two of the main components in “*The Plastic Thymus*” culture system.

In contrast to DN2 pro-T cells, HSCs are highly radiosensitive (67, 68). Here, we have characterized the DDR of NH-HSCs cultured *in vitro* and compared it to that of DN2 cells, showing

that NH-HSCs display higher radiosensitivity than DN2 cells particularly at high IR doses (closer to those used as cytoreductive regimens prior to BMT) (**Figure 1**). Several aspects of their biology may be contributing to this effect, such as (i) their slower activation of the DDR pathway in response to IR, (ii) lower levels of expression of DDR factors that are important for NHEJ, (iii) differential DNA damage checkpoint activation compared with DN2 cells (**Figures 2** and **3**), and (iv) more rapid cell cycle kinetics. It would appear that cell cycle kinetics alone cannot explain the increased susceptibility of NH-HSCs to irradiation. Strikingly, NH-HSCs from Bcl-2 transgenic mice, although retaining the same cell cycle kinetics as their non-Bcl-2 partners, did not undergo apoptosis following irradiation (unpublished observation). This indicates that the more rapid cell cycle kinetics of NH-HSC compared with DN2 cells was not responsible for their susceptibility to apoptosis. As previously shown by Bosco et al. (21), DN2 cells from Bcl-2 transgenic mice also showed dramatic changes in survival *in vitro*. Taken together, while the proliferation status of a given cell type may affect its radiosensitivity, we believe that our studies collectively suggest that the intrinsic orchestration of the DDR signaling pathway choice (i.e., induction of DNA damage checkpoints and DNA DSB repair versus cell death) plays a more important role in determining radiosensitivity. It would be of interest to compare the *in vitro* sensitivity of NH-HSC and DN2 thymocytes to glucocorticoids to help separate differences in their survival and DDR pathways. Previous experiments (20) had shown that host (presumably DN2)-derived thymocytes were seen in BM chimeras where recipient mice had been treated with hydrocortisone acetate 48 h prior to irradiation and BM reconstitution. This suggests that DN2 cells are glucocorticoid resistant *in vivo*. Animals treated with glucocorticoids and left to recover showed no sign of hematopoietic failure, suggesting indirectly that HSC and/or multipotent progenitors do not appear to be glucocorticoid sensitive *in vivo* (20).

Interestingly, culturing NH-HSCs under hypoxic conditions (5% O<sub>2</sub>) increased the efficiency of DNA repair (**Figure 5A**) and survival capacity (**Figure 4**; Figure S5 in Supplementary Material) in these cells, as well as inducing an important up-regulation of Bcl-2 protein levels (**Figure 5D**). By contrast, culture of DN2 cells in hypoxia resulted in less efficient DNA repair (**Figure 5A**) and decreased levels of DNA ligase IV and 53BP1 (**Figure 5C**) were detected in this condition. However, surface marker analysis of normoxic and hypoxic *in vitro* DN2 cultures demonstrated that, while DN2 cells cultured in normoxia maintain a stable phenotype, culturing the same cells in hypoxia results in the accumulation of a CD25<sup>-</sup> subpopulation that increases in number over time (data not shown). This fact makes it impossible to compare the DDR of DN2 cells in normoxia and in hypoxia, since in this last condition, a mixed population of CD25<sup>+</sup> DN2-like cells and CD25<sup>-</sup> cells of unknown nature are analyzed jointly and it is impossible to distinguish the specific contributions of each one to the overall result.

Despite these previous observations, DN2 pro-T cells cultured *in vitro* under normoxia retain many of their phenotypic and functional characteristics, which makes this culture system a very useful tool for the study of DN2 cells at the molecular level.

For this reason, it was important to also investigate whether the robust DDR activation and DNA DSB repair by DN2 thymocytes observed *in vitro* also occurs within the thymus itself (**Figure 6**). Cell numbers recovered from the thymus at different time-points post IR indicated that a higher proportion of DN2 thymocytes remain viable, in comparison with DN1 and DN3 thymocytes, whose numbers dropped quickly following IR exposure (**Figures 6A,B**). Surprisingly, cKit surface expression by DN cells was observed to decrease over time after IR (Figure S6 in Supplementary Material). Previous studies (69) have indicated that *ckit* is a target gene for Notch signaling. Therefore, the decrease in CD117 expression may be the result of decreased Notch ligand expression by TECs following irradiation (34).

Interestingly, DN2 pro-T cells displayed discrete, single, γH2AX IRIF in the absence of IR treatment (**Figure 6D**), which according to the observations from Chen et al. (52), may correspond to sites of V(D)J recombination-induced DSBs. Similar to the results obtained from DN2 cells *in vitro*, DN2 thymocytes *ex vivo* displayed fast activation of their DDR following IR, with γH2AX IRIF numbers peaking at 30 min post-IR. The quick disappearance of γH2AX IRIF, which was largely complete by 4 h after IR, is an indicator of the high efficiency in DSB repair displayed by DN2 cells *in vivo*. This is, to the best of our knowledge, the first time that the *in vivo* DNA repair efficiency of DN2 cells has been characterized.

In conclusion, we have used “*The Plastic Thymus*” *in vitro* culture system to investigate in detail the mechanisms responsible for the relatively high DN2 radioresistance that allows thymic auto-reconstitution following radiation exposure. We have shown that multiple facets of their DDR are likely to contribute to their enhanced survival in contrast to radiosensitive HSCs. Finally, we have demonstrated that DN2 pro-thymocytes are capable of efficiently repairing DNA DSBs *in vivo* following lethal thymic irradiation.

## ETHICS STATEMENT

All animal experiments were carried out within institutional guidelines (authorization numbers 1886 and 1888 from Kantonales Veterinäramt, Basel).

## AUTHOR CONTRIBUTIONS

IC-A and TS: conception and design, collection and assembly of data, data analysis and interpretation, and manuscript writing. NB: conception and design, data analysis and interpretation, manuscript writing, and final approval of manuscript. AR: conception and design, financial support, data analysis, and interpretation. RC: conception and design, financial support, data analysis and interpretation, manuscript writing, and final approval of manuscript.

## ACKNOWLEDGMENTS

We dedicate this paper to the memory of our colleague, friend, group leader, and mentor Antonius Rolink. We would also like to acknowledge the support and generosity provided by the

lab members of research groups based at NUI Galway and the University of Basel which made this highly fruitful collaboration possible.

## FUNDING

The research leading to these results has been supported by the European Community's Seventh Framework Programme FP7/2007-2013 under grant agreement number 315902. TS and RC were supported by Science Foundation Ireland under grant numbers SFI09/SRC/B1794 and SFI07/SK/B1233b. TS

## REFERENCES

- Rieger MA, Schroeder T. Hematopoiesis. *Cold Spring Harb Perspect Biol* (2012) 4:1–18. doi:10.1101/cshperspect.a008250
- Jagannathan-Bogdan M, Zon LI. Hematopoiesis. *Development* (2013) 140:2463–7. doi:10.1242/dev.083147
- Chi AW, Bell JJ, Zlotoff DA, Bhandoola A. Untangling the T branch of the hematopoiesis tree. *Curr Opin Immunol* (2009) 21:121–6. doi:10.1016/j.coim.2009.01.012
- Zhao M, Li LH. Regulation of hematopoietic stem cells in the niche. *Sci China Life Sci* (2015) 58:1209–15. doi:10.1007/s11427-015-4960-y
- Miller JFAP. Immunological function of the thymus. *Lancet* (1961) 2:748–9. doi:10.1016/S0140-6736(61)90693-6
- Miller JFAP. The discovery of thymus function and of thymus-derived lymphocytes. *Immunol Rev* (2002) 185:7–14. doi:10.1034/j.1600-065X.2002.18502.x
- Manley NR, Richie ER, Blackburn CC, Condie BG, Sage J. Structure and function of the thymic microenvironment. *Front Biosci* (2011) 16:2461–77. doi:10.2741/3866
- Alves NL, Takahama Y, Ohigashi I, Ribeiro AR, Baik S, Anderson G, et al. Serial progression of cortical and medullary thymic epithelial microenvironments. *Eur J Immunol* (2014) 44:16–22. doi:10.1002/eji.201344110
- Boehm T, Bleul CC. Thymus-homing precursors and the thymic microenvironment. *Trends Immunol* (2006) 27:477–84. doi:10.1016/j.it.2006.08.004
- Ceredig R, Rolink T. A positive look at double-negative thymocytes. *Nat Rev Immunol* (2002) 2:888–97. doi:10.1038/nri937
- Alves NL, Huntington ND, Rodewald HR, Di Santo JP. Thymic epithelial cells: the multi-tasking framework of the T cell “cradle”. *Trends Immunol* (2009) 30:468–74. doi:10.1016/j.it.2009.07.010
- Anderson G, Takahama Y. Thymic epithelial cells: working class heroes for T cell development and repertoire selection. *Trends Immunol* (2012) 33:256–63. doi:10.1016/j.it.2012.03.005
- Ceredig R, Dialynas DP, Fitch FW, MacDonald HR. Precursors of T cell growth factor producing cells in the thymus: ontogeny, frequency, and quantitative recovery in a subpopulation of phenotypically mature thymocytes defined by monoclonal antibody GK-1.5. *J Exp Med* (1983) 158:1654–71. doi:10.1084/jem.158.5.1654
- Godfrey DI, Zlotnik A, Suda T. Phenotypic and functional characterization of c-kit expression during intrathymic T cell development. *J Immunol* (1992) 149:2281–5.
- Takada A, Takada Y, Huang CC, Ambrus JL. Biphasic pattern of thymus regeneration after whole-body irradiation. *J Exp Med* (1969) 129:445–57. doi:10.1084/jem.129.3.445
- Kadish JL, Basch RS. Thymic regeneration after lethal irradiation evidence for an intra-thymic radioresistant T cell precursor. *J Immunol* (1975) 114:452–8.
- Ceredig R, MacDonald HR. Phenotypic and functional properties of murine thymocytes. II. Quantitation of host- and donor-derived cytolytic T lymphocyte precursors in regenerating radiation bone marrow chimeras. *J Immunol* (1982) 128:614–20.
- Zúñiga-Pflücker JC, Kruisbeek AM. Intrathymic radioresistant stem cells follow an IL-2/IL-2R pathway during thymic regeneration after sublethal irradiation. *J Immunol* (1990) 144:3736–40.
- Thomas DB, Congdon CC. Spontaneous recovery in the thymus after supra-lethal whole-body x-irradiation. *J Physiol* (1967) 188:28–9.
- Ceredig R, Cummings DE. Phenotypic and functional properties of murine thymocytes. III. Kinetic analysis of the recovery of intrathymic cytolytic T lymphocyte precursors after in vivo administration of hydrocortisone acetate. *J Immunol* (1983) 130:33–7.
- Bosco N, Swee LK, Bénard A, Ceredig R, Rolink A. Auto-reconstitution of the T-cell compartment by radioresistant hematopoietic cells following lethal irradiation and bone marrow transplantation. *Exp Hematol* (2010) 38:222–32. doi:10.1016/j.exphem.2009.12.006
- Hare KJ, Jenkinson EJ, Anderson G. In vitro models of T cell development. *Semin Immunol* (1999) 11:3–12. doi:10.1006/smim.1998.0151
- Basson MA, Zamyska R. Insights into T-cell development from studies using transgenic and knockout mice. *Methods Mol Biol* (2000) 134:3–22. doi:10.1385/1-59259-682-7:3
- Mohtashami M, Shah DK, Kianizad K, Awong G, Zúñiga-Pflücker JC. Induction of T-cell development by delta-like 4-expressing fibroblasts. *Int Immunol* (2013) 25:601–11. doi:10.1093/intimm/dxt027
- Schmitt TM, Ciofani M, Petrie HT, Zúñiga-Pflücker JC. Maintenance of T cell specification and differentiation requires recurrent notch receptor-ligand interactions. *J Exp Med* (2004) 200:469–79. doi:10.1084/jem.20040394
- Schmitt TM, Zúñiga-Pflücker JC. Induction of T cell development from hematopoietic progenitor cells by delta-like-1 in vitro. *Immunity* (2002) 17:749–56. doi:10.1016/S1074-7613(02)00474-0
- Wang H, Pierce LJ, Spangrude GJ. Distinct roles of IL-7 and stem cell factor in the OP9-DL1 T-cell differentiation culture system. *Exp Hematol* (2006) 34:1730–40. doi:10.1016/j.exphem.2006.08.001
- Tussiwand R, Engdahl C, Gehre N, Bosco N, Ceredig R, Rolink AG. The preT-CR-dependent DN3 to DP transition requires Notch signaling, is improved by CXCL12 signaling and is inhibited by IL-7 signaling. *Eur J Immunol* (2011) 41:3371–80. doi:10.1002/eji.201141824
- Gehre N, Nusser A, von Muenchow L, Tussiwand R, Engdahl C, Capoferra G, et al. A stromal cell free culture system generates mouse pro-T cells that can reconstitute T-cell compartments in vivo. *Eur J Immunol* (2015) 45:932–42. doi:10.1002/eji.201444681
- Kastan MB, Bartek J. Cell-cycle checkpoints and cancer. *Nature* (2004) 432:316–23. doi:10.1038/nature03097
- Harper JW, Elledge SJ. The DNA damage response: ten years after. *Mol Cell* (2007) 28:739–45. doi:10.1016/j.molcel.2007.11.015
- Sugrue T, Calvo-Asensio I, Ceredig R. The radio-resistance of mesenchymal stromal cells and their potential role in the management of radiation injury. In: Atkinson K, editor. *The Biology and Therapeutic Application of Mesenchymal Cells*. Hoboken, New Jersey: John Wiley and Sons Inc. (2016). p. 391–414.
- Sugrue T, Lowndes NF, Ceredig R. Mesenchymal stromal cells: radio-resistant members of the bone marrow. *Immunol Cell Biol* (2013) 91:5–11. doi:10.1038/icb.2012.61
- Calvo-Asensio I, Barthlott T, von Muenchow L, Lowndes NF, Ceredig R. Differential response of mouse thymic epithelial cell types to ionizing radiation-induced DNA damage. *Front Immunol* (2017) 8:418. doi:10.3389/fimmu.2017.00418
- Sugrue T, Brown JAL, Lowndes NF, Ceredig R. Multiple facets of the DNA damage response contribute to the radioresistance of mouse mesenchymal stromal cell lines. *Stem Cells* (2013) 31:137–45. doi:10.1002/stem.1222
- Sauvageau G, Thorsteinsdottir U, Eaves CJ, Lawrence HJ, Largman C, Lansdorp PM, et al. Overexpression of HOXB4 in hematopoietic cells causes

was supported by an EMBO Short-Term Fellowship (ASTF 339-2012) and an Irish Research Council Government of Ireland Embark Postgraduate Scholarship in Science, Engineering, and Technology (Grant No. RS20102702). AR was holder of the chair in immunology endowed by F. Hoffmann—La Roche Ltd., Basel.

## SUPPLEMENTARY MATERIAL

The Supplementary Material for this article can be found online at <https://www.frontiersin.org/articles/10.3389/fimmu.2018.01312/full#supplementary-material>.

- the selective expansion of more primitive populations in vitro and in vivo. *Genes Dev* (1995) 9:1753–65. doi:10.1101/gad.9.14.1753
37. Ruedl C, Khameneh HJ, Karjalainen K. Manipulation of immune system via immortal bone marrow stem cells. *Int Immunol* (2008) 20:1211–8. doi:10.1093/intimm/dxn079
  38. von Muenchow L, Engdahl C, Karjalainen K, Rolink AG. The selection of mature B cells is critically dependent on the expression level of the co-receptor CD19. *Immunol Lett* (2014) 160:113–9. doi:10.1016/j.imlet.2014.01.011
  39. Schindelin J, Arganda-Carreras I, Frise E, Kaynig V, Longair M, Pietzsch T, et al. Fiji: an open-source platform for biological-image analysis. *Nat Methods* (2012) 9:676–82. doi:10.1038/nmeth.2019
  40. Sugrue T, Lowndes NF, Ceredig R. Hypoxia enhances the radioresistance of mouse mesenchymal stromal cells. *Stem Cells* (2014) 32:2188–200. doi:10.1002/stem.1683
  41. Wingard JR, Hsu J, Hiemenz JW. Hematopoietic stem cell transplantation: an overview of infection risks and epidemiology. *Infect Dis Clin North Am* (2010) 24:257–72. doi:10.1016/j.idc.2010.01.010
  42. Daikeler T, Tichelli A, Passweg J. Complications of autologous hematopoietic stem cell transplantation for patients with autoimmune diseases. *Pediatr Res* (2012) 71:439–44. doi:10.1038/pr.2011.57
  43. Chalandon Y, Degermann S, Villard J, Arlettaz L, Kaiser L, Vischer S, et al. Pretransplantation CMV-specific T cells protect recipients of T-cell-depleted grafts against CMV-related complications. *Blood* (2006) 107:389–96. doi:10.1182/blood-2005-07-2746
  44. Balciunaite G, Ceredig R, Fehling HJ, Zúñiga-Pflücker JC, Rolink AG. The role of Notch and IL-7 signaling in early thymocyte proliferation and differentiation. *Eur J Immunol* (2005) 35:1292–300. doi:10.1002/eji.200425822
  45. Fugmann SD, Lee AI, Shockett PE, Villey IJ, Schatz DG. The RAG proteins and V(D)J recombination: complexes, ends, and transposition. *Annu Rev Immunol* (2000) 18:495–527. doi:10.1146/annurev.immunol.18.1.495
  46. Bednarski JJ, Sleckman BP. Lymphocyte development: integration of DNA damage response signaling. *Adv Immunol* (2012) 116:175–204. doi:10.1016/B978-0-12-394300-2.00006-5
  47. Bednarski JJ, Sleckman BP. Integrated signaling in developing lymphocytes: the role of DNA damage responses. *Cell Cycle* (2012) 11:4129–34. doi:10.4161/cc.22021
  48. Helmink BA, Sleckman BP. The response to and repair of RAG-mediated DNA double-strand breaks. *Annu Rev Immunol* (2012) 30:175–202. doi:10.1146/annurev-immunol-030409-101320
  49. Bredemeyer AL, Sharma GG, Huang C-Y, Helmink BA, Walker LM, Khor KC, et al. ATM stabilizes DNA double-strand-break complexes during V(D)J recombination. *Nature* (2006) 442:466–70. doi:10.1038/nature04866
  50. Huang C-Y, Sharma GG, Walker LM, Bassing CH, Pandita TK, Sleckman BP. Defects in coding joint formation in vivo in developing ATM-deficient B and T lymphocytes. *J Exp Med* (2007) 204:1371–81. doi:10.1084/jem.20061460
  51. Bowen S, Wangsa D, Ried T, Livak F, Hodges RJ. Concurrent V(D)J recombination and DNA end instability increase interchromosomal trans-rearrangements in ATM-deficient thymocytes. *Nucleic Acids Res* (2013) 41:4535–48. doi:10.1093/nar/gkt154
  52. Chen HT, Bhandoora A, Difilippantonio MJ, Zhu J, Brown MJ, Tai X, et al. Response to RAG-mediated VDJ cleavage by NBS1 and gamma-H2AX. *Science* (2000) 290:1962–5. doi:10.1126/science.290.5498.1962
  53. Nijnik A, Dawson S, Crockford TL, Woodbine L, Visetnoi S, Bennett S, et al. Impaired lymphocyte development and antibody class switching and increased malignancy in a murine model of DNA ligase IV syndrome. *J Clin Invest* (2009) 119:1696–705. doi:10.1172/JCI32743
  54. Kim J, Lee SK, Jeon Y, Kim Y, Lee C, Jeon SH, et al. TopBP1 deficiency impairs V(D)J recombination during lymphocyte development. *EMBO J* (2014) 33: 217–28. doi:10.1002/embj.201284316
  55. Dujka ME, Puebla-Osorio N, Tavana O, Sang M, Zhu C. ATM and p53 are essential in the cell-cycle containment of DNA breaks during V(D)J recombination in vivo. *Oncogene* (2010) 29:957–65. doi:10.1038/onc.2009.394
  56. DeMicco A, Reich T, Arya R, Rivera-Reyes A, Fisher MR, Bassing CH. Lymphocyte lineage-specific and developmental stage specific mechanisms suppress cyclin D3 expression in response to DNA double strand breaks. *Cell Cycle* (2016) 15:2882–94. doi:10.1080/15384101.2016.1198861
  57. Hernandez JB, Newton RH, Walsh CM. Life and death in the thymus – cell death signaling during T cell development. *Curr Opin Biol* (2011) 22:865–71. doi:10.1016/j.celb.2010.08.003
  58. Bouillet P, Purton JF, Godfrey DI, Zhang L-C, Coultras L, Puthalakath H, et al. BH3-only Bcl-2 family member Bim is required for apoptosis of autoreactive thymocytes. *Nature* (2002) 415:922–6. doi:10.1038/415922a
  59. Gray DHD, Kupresanin F, Berzins SP, Herold MJ, O'Reilly LA, Bouillet P, et al. The BH3-only proteins Bim and Puma cooperate to impose deleterious tolerance of organ-specific antigens. *Immunity* (2012) 37:451–62. doi:10.1016/j.immuni.2012.05.030
  60. Pellegrini M, Bouillet P, Robati M, Belz GT, Davey GM, Strasser A. Loss of Bim increases T cell production and function in interleukin 7 receptor-deficient mice. *J Exp Med* (2004) 200:1189–95. doi:10.1084/jem.20041328
  61. Erlacher M, Michalak EM, Kelly PN, Labi V, Niederegger H, Coultras L, et al. BH3-only proteins Puma and Bim are rate-limiting for gamma-radiation- and glucocorticoid-induced apoptosis of lymphoid cells in vivo. *Blood* (2005) 106:4131–8. doi:10.1182/blood-2005-04-1595
  62. Mandal M, Crusio KM, Meng F, Liu S, Kinsella M, Clark MR, et al. Regulation of lymphocyte progenitor survival by the proapoptotic activities of Bim and Bid. *Proc Natl Acad Sci U S A* (2008) 105:20840–5. doi:10.1073/pnas.0807557106
  63. Gratiot-Deans J, Merino R, Nuñez G, Turka LA. Bcl-2 expression during T-cell development: early loss and late return occur at specific stages of commitment to differentiation and survival. *Proc Natl Acad Sci U S A* (1994) 91:10685–9. doi:10.1073/pnas.91.22.10685
  64. Gratiot-Deans J, Ding L, Turka LA, Nuñez G. bcl-2 proto-oncogene expression during human T cell development. Evidence for biphasic regulation. *J Immunol* (1993) 151:83–91.
  65. Ceredig R, Rolink AG. The key role of IL-7 in lymphopoiesis. *Semin Immunol* (2012) 24:159–64. doi:10.1016/j.smim.2012.02.004
  66. González-García S, García-Peydró M, Martín-Gayo E, Ballestar E, Esteller M, Bornstein R, et al. CSL-MAML-dependent Notch1 signaling controls T lineage-specific IL-7R $\alpha$  gene expression in early human thymopoiesis and leukemia. *J Exp Med* (2009) 206:779–91. doi:10.1084/jem.20081922
  67. Meijne EI, van der Winden-van Groenewegen RJ, Ploemacher RE, Vos O, David JA, Huiskamp R. The effects of X-irradiation on hematopoietic stem cell compartments in the mouse. *Exp Hematol* (1991) 19:617–23.
  68. Harfouche G, Martin MT. Response of normal stem cells to ionizing radiation: a balance between homeostasis and genomic stability. *Mutat Res* (2010) 704:167–74. doi:10.1016/j.mrrev.2010.01.007
  69. Massa S, Balciunaite G, Ceredig R, Rolink AG. Critical role for c-kit (CD117) in T cell lineage commitment and early thymocyte development in vitro. *Eur J Immunol* (2006) 36:526–32. doi:10.1002/eji.200535760

**Conflict of Interest Statement:** Co-author NB is currently employed by Nestlé Research Center Asia. All other authors declare no competing interests. Co-author TS declares her affiliation with Frontiers and the handling Editor states that the process nevertheless met the standards of a fair and objective review. All other authors declare they have no potential conflicts of interests to disclose.

Copyright © 2018 Calvo-Asensio, Sugrue, Bosco, Rolink and Ceredig. This is an open-access article distributed under the terms of the Creative Commons Attribution License (CC BY). The use, distribution or reproduction in other forums is permitted, provided the original author(s) and the copyright owner are credited and that the original publication in this journal is cited, in accordance with accepted academic practice. No use, distribution or reproduction is permitted which does not comply with these terms.



# Getting in and Staying Alive: Role for Coronin 1 in the Survival of Pathogenic Mycobacteria and Naïve T Cells

Mayumi Mori and Jean Pieters\*

Biozentrum, University of Basel, Basel, Switzerland

## OPEN ACCESS

**Edited by:**

Rhodri Ceredig,  
National University of Ireland  
Galway, Ireland

**Reviewed by:**

Salvatore Valitutti,  
Institut National de la Santé et  
de la Recherche Médicale  
(INSERM), France  
Martin Turner,  
Babraham Institute (BBSRC),  
United Kingdom  
Nick Gascoigne,  
National University of Singapore,  
Singapore

**\*Correspondence:**

Jean Pieters  
jean.pieters@unibas.ch

**Specialty section:**

This article was submitted  
to *T Cell Biology*,  
a section of the journal  
*Frontiers in Immunology*

**Received:** 01 May 2018

**Accepted:** 27 June 2018

**Published:** 10 July 2018

**Citation:**

Mori M and Pieters J (2018) Getting in and Staying Alive: Role for Coronin 1 in the Survival of Pathogenic Mycobacteria and Naïve T Cells. *Front. Immunol.* 9:1592.  
doi: 10.3389/fimmu.2018.01592

There are many different pathogenic stimuli that are able to activate the immune system, ranging from microbes that include bacteria, viruses, fungi, and parasites to host-derived triggers such as autoantigens that can induce autoimmunity as well as neoantigens involved in tumorigenesis. One of the key interactions shaping immunity toward these triggers involves the encounter of antigen-processing and -presenting cells such as macrophages and dendritic cells with T cells, resulting in immune responses that are highly selective for the antigenic trigger. Research over the past few years has implicated members of the coronin protein family, in particular coronin 1, in responses against several pathogenic triggers. While coronin 1 was initially described as a host factor allowing the intracellular survival of the pathogen *Mycobacterium tuberculosis*, subsequent work showed it to be a crucial factor for naïve T cell homeostasis. The activity of coronin 1 in allowing the intracellular survival of pathogenic mycobacteria is relatively well characterized, involving the activation of the Ca<sup>2+</sup>/calcineurin pathway, while coronin 1's role in modulating naïve T cell homeostasis remains more enigmatic. In this mini review, we discuss the knowledge on the role for coronin 1 in immune cell functioning and provide a number of potential scenarios via which coronin 1 may be able to regulate naïve T cell homeostasis.

**Keywords:** coronin 1, macrophages, *Mycobacterium tuberculosis*, naïve T cell homeostasis, interleukin 7, T cell receptor

## INTRODUCTION

The vertebrate immune system has evolved to efficiently deal with both intracellular and extracellular pathogens to ensure a battery of defense strategies, both through innate and adaptive mechanisms. The innate immune defense arm can react rapidly as a result of the recruitment of neutrophils, natural killer cells, dendritic cells, and macrophages to the site of infection. These cells not only ensure the direct elimination of the pathogens but also aid in the activation of adaptive immunity by inducing the proliferation, maturation, and expansion of B and T lymphocytes. The concerted action of innate and adaptive immune cells results in an effective clearance of microbial and parasitic pathogens; however, several pathogens have evolved to withstand such immune detection, sometimes by hijacking the immune system at several levels.

For many bacterial pathogens, the initial and often fatal encounter is their interaction with macrophages. These cells are the scavengers of the vertebrate immune system, and typically digest any microbe following their internalization through phagocytosis and delivery to lysosomes and/or

autophagosomes (1, 2). Following digestion, pathogen-derived antigens (peptides, lipids, and metabolites) can be bound to the so-called antigen-presenting molecules of the major histocompatibility complex (MHC) class I and class II, cluster of differentiation 1 (CD1), or MHC class I-related protein MR1 complexes, which are then re-routed to the plasma membrane where these antigens can be presented to T lymphocytes. This interaction between antigen-presenting cells and T cells subsequently triggers T cell proliferation/expansion in an antigen-specific manner (3–6). One particularly notorious pathogen, *Mycobacterium tuberculosis*, which is transmitted through aerosols and is phagocytosed by alveolar macrophages, has evolved to hijack this process of intracellular degradation, thereby converting the normal hostile environment of the macrophage into a safe haven. *M. tuberculosis* does so using multiple strategies, including the attenuation of macrophage inflammatory signaling cascades, neutralization of reactive oxygen and nitrogen species, as well as altering its metabolic state (7–10). As a result, instead of being degraded within macrophages, *M. tuberculosis* manages to survive for a prolonged time within these cells, often in a so-called dormant state, and can become reactivated when the health of an infected person deteriorates, for example, following food deprivation or inflammatory stress, such as co-infection by HIV. Apart from its ability to survive within macrophage phagosomes, *M. tuberculosis* has been reported to be released into the macrophage cytosol, where it can activate a number of mechanisms leading to cell death, allowing the dissemination of the bacilli to neighboring cells (11). The capacity of *M. tuberculosis* to withstand intracellular delivery to lysosomes and degradation was initially realized from electron micrographs of *M. tuberculosis*-infected macrophages (12) and has been widely recognized as a major strategy employed by *M. tuberculosis* to establish long-term infections.

## IDENTIFICATION OF CORONIN 1 AS A SURVIVAL FACTOR FOR INTRACELLULARLY RESIDING MYCOBACTERIA

Given the central importance for *M. tuberculosis* to prevent intracellular delivery to lysosomes for the establishment of a long-term infection, it is not surprising that mycobacteria utilize a number of different strategies to achieve this (8, 9, 13). One of these strategies was found to be the recruitment and retention of a host protein, coronin 1 (also known as P57 or TACO, for Tryptophan Aspartate containing Coat protein), to the cytosolic side of the mycobacterial phagosome. Coronin 1 is expressed in all hematopoietic cell types and is a member of the widely conserved coronin protein family, members of which are expressed in virtually all eukaryotic species (14, 15). The recruitment of coronin 1 activates the calcium/calcineurin pathway that was shown to block phagosome–lysosome fusion and the degradation of the internalized mycobacteria (16, 17). The precise mechanism *via* which calcineurin, a ubiquitously expressed phosphatase, modulates intracellular mycobacterial survival remains to be identified, and it is possible that calcineurin acts in

concert with several of the other factors that have been identified to allow *M. tuberculosis* survival within macrophages, including kinases, lipids, metabolites, and signaling molecules (18–23). Coronin 1-dependent modulation of lysosomal trafficking appears to be specific for mycobacteria, since several other types of cargo are readily delivered to lysosomes in a coronin 1-independent manner (16).

The role for coronin 1 in protecting *M. tuberculosis* from intracellular death within macrophages was corroborated by analyzing mice that lack the gene coding coronin 1 (*coro1a*). In macrophages derived from these mice, mycobacteria are readily transferred to lysosomes followed by their destruction (16). However, other than the inability of coronin 1-deficient macrophages to support the intracellular survival of pathogenic mycobacteria, macrophages devoid of coronin 1 appear to be fully functional in terms of phagocytosis, endocytosis, motility, membrane ruffling, and migration (16, 24). This is also notable because coronin family members have been widely implicated in regulation of the F-actin cytoskeleton (25). The reasons for the absence of F-actin-dependent phenotypes in macrophages devoid of coronin 1 may lie within (i) the fact that other coronin family members with redundant roles are co-expressed in macrophages, (ii) a function for coronin 1 upstream of F-actin modulation, or (iii) differences in experimental protocols used to analyze coronin 1's function in macrophages. Interestingly, upon macrophage activation as occurs during an inflammatory stimulus, coronin 1 functions to switch the mode of uptake from phagocytosis to macropinocytosis, thereby enabling macrophages to rapidly internalize large amount of cargo and shuttling these to lysosomes for degradation (26, 27). Thus, it appears that *M. tuberculosis*, perhaps in the course of its long-term co-evolution with their mammalian hosts, has gained the capacity to utilize coronin 1-dependent arrest of phagosome–lysosome fusion to allow long-term survival within macrophages, that are precisely those cells destined to destroy any incoming bacilli.

## PERIPHERAL T CELL SURVIVAL AND CORONIN 1

The availability of mice lacking coronin 1 also allowed the analysis of other hematopoietic cell types with respect to their dependence on coronin 1 for proper functioning. Strikingly, whereas virtually all other cell types appear to be unaffected by the absence of coronin 1, there is one notable exception: mice devoid of coronin 1 are profoundly deficient in T cells (28–31). Interestingly, this T cell deficiency is exclusively found in peripheral lymphoid organs: T cell development and selection, as for example occurring in the thymus, is not affected by the absence of coronin 1 (32). Several explanations have been put forward to explain the peripheral T cell deficiency in mice lacking coronin 1: first, the above-mentioned role for coronin proteins in modulating F-actin was suggested to be responsible for inducing T cell death, *via* a proposed role for coronin 1 in reducing F-actin levels, in the absence of which elevated F-actin may act to induce cell death (28). However, subsequent work showed that in leukocytes coronin 1 does not modulate F-actin,

and furthermore that accumulation of F-actin does not correlate with the induction of cell death (30, 33). Alternatively, coronin 1 may be involved in the transduction of signals downstream of the T cell receptor (TCR), in the absence of which pro-apoptotic, rather than pro-survival signals, are being activated (29, 30, 33). Such a pro-survival role for coronin 1 must be selective for peripheral naïve T cells, since both thymic selection and effector/memory T cells do not depend on coronin 1 for either survival or functionality (29, 32).

## HOMEOSTATIC CONTROL OF PERIPHERAL NAÏVE T CELL NUMBERS

As mentioned above, while peripheral CD4 and CD8 positive T cells are profoundly depleted upon coronin 1 inactivation, T cell development and selection in bone marrow and thymus is virtually undisturbed. This is a surprising observation since two of the main drivers of naïve T cell homeostasis, namely, MHC:TCR signaling and interleukin (IL)-7:IL-7 receptor (IL7R) signaling are both important for thymic T-cell survival (34). Thus, either these signaling pathways require coronin 1 exclusively in peripheral lymphoid organs or, alternatively, coronin 1 is involved in an as yet undefined pathway responsible for peripheral naïve T cell survival.

Homeostatic proliferation and survival are differently controlled between naïve and memory T cells and between CD4 and CD8 T cells (35). For the discussion here, we focus on the naïve CD4 T cell subset, which is most severely suppressed in coronin 1-deficient mice. The mechanisms that have been suggested to maintain naïve CD4 T cells include, besides the aforementioned IL-7 signaling and MHC-TCR interaction, other signaling pathways such as those involving IL-2, 15, and type I interferons, although these appear to be involved to a lesser extent (34, 36–38).

Interleukin-7 has a central role in early lymphopoiesis in the thymus to drive the selection of CD8 lineage-committed cells (39–41). IL-7 does so, *via* activation of the IL7R pathway, through induction of the expression of the pro-survival factor Bcl2 and inhibiting the pro-apoptotic factors Bad and Bax. Regarding the role for IL-7 on maintenance of the peripheral naïve CD4 T cell pool, there are conflicting data in the literature. In support of a role for IL-7 in naïve CD4 T cell survival, Tan et al. demonstrated a failure of transferred T cells to survive when adoptively transferred to IL-7-deficient mice (42). Also, overexpression of IL-7 was shown to enhance T cell proliferation in a lymphopenic mouse model (43). Furthermore, several studies documented enhanced peripheral T cell proliferation upon overexpression of IL-7 or the IL7R (44, 45), although this was not observed in all animal models (46). Furthermore, *in vivo* infusion of IL-7 results in increased naïve CD4 T cell numbers, although the effect on CD8 T cells is many-fold higher (47–49). On the other hand, a number of studies have reported that IL-7 is dispensable for CD4 T cell proliferation and survival; for example, blockade of the IL-7 receptor alpha chain (IL-7Ra) inhibits only a minor population of low-rate proliferating naïve CD4 T cells after transfer to RAG2-deficient recipients, without affecting the high-rate proliferating cells (50). Also, while administration

of anti-IL-7 antibodies reduces the survival of peripheral CD4 positive T cell numbers (51), it does so only when IL-4 is also depleted (52), suggesting redundant roles for cytokines sharing the common receptor gamma chain ( $\gamma$ ). Conversely, more recent work using a xenogeneic model suggests that increasing IL-7 signaling does not affect peripheral T cell numbers while it does modulate T cell development in the thymus (53). Furthermore, conditional genetic deletion of IL-7Ra or  $\gamma$  at the late-stage of thymic development, circumventing the suppressive effect on early lymphopoiesis, showed only minimal reduction in CD4 single positive thymocytes, compared with a profound reduction of CD8 single positive T cells, whereas peripheral naïve CD4 T cell numbers have not been addressed in these studies (54, 55). Finally, it has been proposed that rather than a direct availability of IL-7 to CD4 T cells, IL-7 signaling on antigen-presenting cells may be the main driver of homeostatic proliferation of naïve CD4 T cells *in vivo* (56, 57).

Thus, while the role for IL-7 in CD8 T cell lineage selection in the thymus is clearly established, it appears to be dispensable for CD4 T cell lineage selection, and an exclusive role for this cytokine in the maintenance of peripheral naïve CD4 T cell survival is unclear. Perhaps, IL-7 is mainly required for depletion-induced (“homeostatic”) proliferation rather than maintenance of T cell numbers under non-perturbed situations. Given the normal thymic T cell development observed in mice lacking coronin 1 (32), it is unlikely that coronin 1 plays a role directly downstream of IL-7 signaling. However, it is possible that coronin 1 works in concert with IL-7 signaling to allow peripheral naïve CD4 T cell survival.

The second trigger that is widely reported to be involved in naïve CD4 T cell survival is TCR signaling by MHC:peptide complexes. While, similar to IL-7 signaling, MHC molecules play a crucial role during thymic selection (58, 59), several studies have reported that MHC molecules are important for peripheral T cell survival and proliferation (60–62). In particular, peptides loaded on MHC, possibly self-ligands, were considered to be crucial for homeostatic expansion of CD4 T cells, as shown by reduced expansion in hosts that lack peptide presentation on MHCII (63, 64), suggesting that specific TCR–MHC interaction is important.

Besides the aforementioned studies that report a role for MHC molecules in the survival and proliferation of naïve T cells, there are several studies suggesting that naïve T cell survival is MHC independent. For example, both survival and proliferation of peripheral CD4 T cells have been reported to occur in the absence of MHC class II molecules (65, 66). In addition, another study indicates that MHC may be important for proliferation but not for survival of naïve CD4 T cells (67), considering also the long half-life of T cells after depletion of MHC class II molecules (68, 69).

Regarding the role for peptide presentation on MHC class II molecules, one study using the same H2M-deficient system as Viret et al. (63) have shown dispensability of peptide ligands for peripheral T cell survival (68). Moreover, DC-T cell synapse accompanied with polarized PKC $\theta$  phosphorylation, indicating the existence of TCR signaling, was detected without antigens or MHC itself (66). Thus, T cell responses supposed

to be important for peripheral T cell survival and homeostatic proliferation may not require interaction with cognate peptide–MHC complexes.

As described above, arguments have been brought forward both in favor of and against a role for MHC class II molecules in naïve T cell survival. What exactly underlies the discrepancy between these opposing results, that in part were obtained using the same experimental model [for example, the same H2M-deficient mouse was used to conclude for and against a role of MHC class II in T cell survival, see Ref. (63, 68)], remains to be analyzed and could lie within an inability to distinguish survival and proliferation, the usage of mice deficient in different components of MHC, or the subtype of peripheral T cells analyzed (e.g., naïve versus memory) (70–72). Interestingly, even in the complete absence of MHC class II molecules in both mice and man, peripheral naïve T cells can be maintained, even for prolonged times (72–74).

Thus, the extent to which MHC–peptide:TCR interaction is important for peripheral naïve CD4 T cell survival remains unclear. Given the normal thymic development of T cell precursors in mice deficient in coronin 1 and the important role for MHC–TCR signaling in that process, it is unlikely that coronin 1 plays a prominent role in MHC-dependent T cell activation to generate mature T cells. Whether the role for coronin 1 in the maintenance of peripheral T cells involves intracellular events downstream of TCR remains to be analyzed (29). Coronin 1 has been suggested to act through activation

of calcium/calcineurin signaling and through modulation of the cytoskeleton (16, 28–31, 33), but how, exactly, defects in these pathways would result in such a selective phenotype (peripheral naïve T cell deficiency) remains unclear. It should also be mentioned that little is known about the molecular mechanisms underlying the transition from semi-mature single positive thymocytes to mature naïve T cells in the periphery (75). Future work exploring a possible role for coronin 1 in both the above described IL-7 and MHC–TCR signaling as well as yet unexplored pathways may allow to shed light not only on the molecular mechanisms in which coronin 1 is involved but also possibly contribute to a better understanding of peripheral naïve T cell homeostasis.

## AUTHOR CONTRIBUTIONS

MM and JP conceived and wrote the paper.

## ACKNOWLEDGMENTS

We thank Rajesh Jayachandran, Ravindra Mode, and Tohnyui Ndinyanka Fabrice for critical comments on the manuscript. Work in the Pieters Laboratory is supported by the Swiss National Science Foundation, the Swiss Multiple Sclerosis Society, the Novartis Foundation for Medical-Biological Research, the Gebert Ruef Foundation, and the Canton of Basel.

## REFERENCES

1. Weiss G, Schaible UE. Macrophage defense mechanisms against intracellular bacteria. *Immunol Rev* (2015) 264:182–203. doi:10.1111/imr.12266
2. Taylor PR, Martinez-Pomares L, Stacey M, Lin HH, Brown GD, Gordon S. Macrophage receptors and immune recognition. *Annu Rev Immunol* (2005) 23:901–44. doi:10.1146/annurev.immunol.23.021704.115816
3. Blum JS, Wearsch PA, Cresswell P. Pathways of antigen processing. *Annu Rev Immunol* (2013) 31:443–73. doi:10.1146/annurev-immunol-032712-095910
4. Roche PA, Furuta K. The ins and outs of MHC class II-mediated antigen processing and presentation. *Nat Rev Immunol* (2015) 15:203–16. doi:10.1038/nri3818
5. Major AS, Joyce S, Van Kaer L. Lipid metabolism, atherogenesis and CD1-restricted antigen presentation. *Trends Mol Med* (2006) 12:270–8. doi:10.1016/j.molmed.2006.04.004
6. Mori I, Lepore M, De Libero G. The immunology of CD1- and MR1-restricted T cells. *Annu Rev Immunol* (2016) 34:479–510. doi:10.1146/annurev-immunol-032414-112008
7. Nathan C. Role of iNOS in human host defense. *Science* (2006) 312:1874–5; author reply 1874–5. doi:10.1126/science.312.5782.1874b
8. Rohde K, Yates RM, Purdy GE, Russell DG. *Mycobacterium tuberculosis* and the environment within the phagosome. *Immunol Rev* (2007) 219:37–54. doi:10.1111/j.1600-065X.2007.00547.x
9. Pieters J. *Mycobacterium tuberculosis* and the macrophage: maintaining a balance. *Cell Host Microbe* (2008) 3:399–407. doi:10.1016/j.chom.2008.05.006
10. Zondervan NA, van Dam JCJ, Schaap PJ, Martins Dos Santos VAP, Suarez-Diez M. Regulation of three virulence strategies of *Mycobacterium tuberculosis*: a success story. *Int J Mol Sci* (2018) 19:347. doi:10.3390/ijms19020347
11. Stutz MD, Clark MP, Doerflinger M, Pellegrini M. *Mycobacterium tuberculosis*: rewiring host cell signaling to promote infection. *J Leukoc Biol* (2018) 103:259–68. doi:10.1002/JLB.4MR0717-277R
12. Armstrong JA, Hart PD. Phagosome-lysosome interactions in cultured macrophages infected with virulent tubercle bacilli. Reversal of the usual nonfusion pattern and observations on bacterial survival. *J Exp Med* (1975) 142:1–16. doi:10.1084/jem.142.1.1
13. Warner DF, Mizrahi V. The survival kit of *Mycobacterium tuberculosis*. *Nat Med* (2007) 13:282–4. doi:10.1038/nm0307-282
14. Eckert C, Hammesfahr B, Kollmar M. A holistic phylogeny of the coronin gene family reveals an ancient origin of the tandem-coronin, defines a new subfamily, and predicts protein function. *BMC Evol Biol* (2011) 11:268. doi:10.1186/1471-2148-11-268
15. Pieters J, Muller P, Jayachandran R. On guard: coronin proteins in innate and adaptive immunity. *Nat Rev Immunol* (2013) 13:510–8. doi:10.1038/nri3465
16. Jayachandran R, Sundaramurthy V, Combaluzier B, Mueller P, Korf H, Huygen K, et al. Survival of mycobacteria in macrophages is mediated by coronin 1-dependent activation of calcineurin. *Cell* (2007) 130:37–50. doi:10.1016/j.cell.2007.04.043
17. Ferrari G, Langen H, Naito M, Pieters J. A coat protein on phagosomes involved in the intracellular survival of mycobacteria. *Cell* (1999) 97:435–47. doi:10.1016/S0092-8674(00)80754-0
18. Scherr N, Pieters J. The eukaryotic-like serine/threonine protein kinase family in mycobacteria. In: Parish T, Brown A, editors. *Mycobacterium: Genomics and Molecular Biology*. Poole: Horizon Scientific Press (2009). p. 171–88.
19. Vergne I, Fratti RA, Hill PJ, Chua J, Belisle J, Deretic V. *Mycobacterium tuberculosis* phagosome maturation arrest: mycobacterial phosphatidylinositol analog phosphatidylinositol mannoside stimulates early endosomal fusion. *Mol Biol Cell* (2004) 15:751–60. doi:10.1091/mbc.e03-05-0307
20. Walburger A, Koul A, Ferrari G, Nguyen L, Prescianotto-Baschong C, Huygen K, et al. Protein kinase G from pathogenic mycobacteria promotes survival within macrophages. *Science* (2004) 304:1800–4. doi:10.1126/science.1099384
21. Agarwal N, Lamichhane G, Gupta R, Nolan S, Bishai WR. Cyclic AMP intoxication of macrophages by a *Mycobacterium tuberculosis* adenylate cyclase. *Nature* (2009) 460:98–102. doi:10.1038/nature08123
22. Shenoy AR, Visweswariah SS. New messages from old messengers: cAMP and mycobacteria. *Trends Microbiol* (2006) 14:543–50. doi:10.1016/j.tim.2006.10.005
23. Chao J, Wong D, Zheng X, Poirier V, Bach H, Hmama Z, et al. Protein kinase and phosphatase signaling in *Mycobacterium tuberculosis* physiology and pathogenesis. *Biochim Biophys Acta* (2010) 1804:620–7. doi:10.1016/j.bbapap.2009.09.008

24. Jayachandran R, Gatfield J, Massner J, Albrecht I, Zanolari B, Pieters J. RNA interference in J774 macrophages reveals a role for coronin 1 in mycobacterial trafficking but not in actin-dependent processes. *Mol Biol Cell* (2008) 19:1241–51. doi:10.1091/mbc.e07-07-0640
25. de Hostos EL. The coronin family of actin-associated proteins. *Trends Cell Biol* (1999) 9:345–50. doi:10.1016/S0962-8924(99)01620-7
26. BoseDasgupta S, Moes S, Jenoe P, Pieters J. Cytokine-induced macropinocytosis in macrophages is regulated by 14-3-3zeta through its interaction with serine-phosphorylated coronin 1. *FEBS J* (2015) 282:1167–81. doi:10.1111/febs.13214
27. Bozedasgupta S, Pieters J. Inflammatory stimuli reprogram macrophage phagocytosis to macropinocytosis for the rapid elimination of pathogens. *PLoS Pathog* (2014) 10:e1003879. doi:10.1371/journal.ppat.1003879
28. Foger N, Rangell L, Danilenko DM, Chan AC. Requirement for coronin 1 in T lymphocyte trafficking and cellular homeostasis. *Science* (2006) 313:839–42. doi:10.1126/science.1130563
29. Mueller P, Massner J, Jayachandran R, Combaluzier B, Albrecht I, Gatfield J, et al. Regulation of T cell survival through coronin-1-mediated generation of inositol-1,4,5-trisphosphate and calcium mobilization after T cell receptor triggering. *Nat Immunol* (2008) 9:424–31. doi:10.1038/ni1570
30. Haraldsson MK, Louis-Dit-Sully CA, Lawson BR, Sternik G, Santiago-Raber ML, Gascoigne NR, et al. The lupus-related Lmb3 locus contains a disease-suppressing coronin-1A gene mutation. *Immunity* (2008) 28:40–51. doi:10.1016/j.jimmuni.2007.11.023
31. Shiow LR, Roadcap DW, Paris K, Watson SR, Grigorova IL, Lebet T, et al. The actin regulator coronin 1A is mutant in a thymic egress-deficient mouse strain and in a patient with severe combined immunodeficiency. *Nat Immunol* (2008) 9:1307–15. doi:10.1038/ni.1662
32. Lang MJ, Mori M, Ruer-Laventie J, Pieters J. A coronin 1-dependent decision switch in juvenile mice determines the population of the peripheral naïve T cell compartment. *J Immunol* (2017) 199:2421–31. doi:10.4049/jimmunol.1700438
33. Mueller P, Liu X, Pieters J. Migration and homeostasis of naïve T cells depends on coronin 1-mediated prosurvival signals and not on coronin 1-dependent filamentous actin modulation. *J Immunol* (2011) 186:4039–50. doi:10.4049/jimmunol.1003352
34. Surh CD, Sprent J. Homeostasis of naïve and memory T cells. *Immunity* (2008) 29:848–62. doi:10.1016/j.jimmuni.2008.11.002
35. Boyman O, Letourneau S, Krieg C, Sprent J. Homeostatic proliferation and survival of naïve and memory T cells. *Eur J Immunol* (2009) 39:2088–94. doi:10.1002/eji.200939444
36. Purton JE, Sprent J, Surh CD. Staying alive – naïve CD4(+) T cell homeostasis. *Eur J Immunol* (2007) 37:2367–9. doi:10.1002/eji.200737721
37. Sprent J, Surh CD. Normal T cell homeostasis: the conversion of naïve cells into memory-phenotype cells. *Nat Immunol* (2011) 12:478–84. doi:10.1038/ni.2018
38. Boyman O, Krieg C, Homann D, Sprent J. Homeostatic maintenance of T cells and natural killer cells. *Cell Mol Life Sci* (2012) 69:1597–608. doi:10.1007/s00018-012-0968-7
39. Singer A, Adoro S, Park JH. Lineage fate and intense debate: myths, models and mechanisms of CD4- versus CD8-lineage choice. *Nat Rev Immunol* (2008) 8:788–801. doi:10.1038/nri2416
40. Peschon JJ, Morrissey PJ, Grabstein KH, Ramsdell FJ, Maraskovsky E, Gliniak BC, et al. Early lymphocyte expansion is severely impaired in interleukin 7 receptor-deficient mice. *J Exp Med* (1994) 180:1955–60. doi:10.1084/jem.180.5.1955
41. Hong C, Luckey MA, Park JH. Intrathymic IL-7: the where, when, and why of IL-7 signaling during T cell development. *Semin Immunol* (2012) 24:151–8. doi:10.1016/j.smim.2012.02.002
42. Tan JT, Dudd E, LeRoy E, Murray R, Sprent J, Weinberg KI, et al. IL-7 is critical for homeostatic proliferation and survival of naïve T cells. *Proc Natl Acad Sci U S A* (2001) 98:8732–7. doi:10.1073/pnas.161126098
43. Bosco N, Agenes F, Ceredig R. Effects of increasing IL-7 availability on lymphocytes during and after lymphopenia-induced proliferation. *J Immunol* (2005) 175:162–70. doi:10.4049/jimmunol.175.1.162
44. Ceredig R, Rolink AG. The key role of IL-7 in lymphopoiesis. *Semin Immunol* (2012) 24:159–64. doi:10.1016/j.smim.2012.02.004
45. Mertsching E, Burdet C, Ceredig R. IL-7 transgenic mice: analysis of the role of IL-7 in the differentiation of thymocytes in vivo and in vitro. *Int Immunopharmacol* (1995) 7:401–14. doi:10.1093/intimm/7.3.401
46. Rich BE, Campos-Torres J, Tepper RI, Moreadith RW, Leder P. Cutaneous lymphoproliferation and lymphomas in interleukin 7 transgenic mice. *J Exp Med* (1993) 177:305–16. doi:10.1084/jem.177.2.305
47. Boyman O, Ramsey C, Kim DM, Sprent J, Surh CD. IL-7/anti-IL-7 mAb complexes restore T cell development and induce homeostatic T cell expansion without lymphopenia. *J Immunol* (2008) 180:7265–75. doi:10.4049/jimmunol.180.11.7265
48. Komschlies KL, Gregorio TA, Gruys ME, Back TC, Faltynek CR, Wiltrot RH. Administration of recombinant human IL-7 to mice alters the composition of B-lineage cells and T cell subsets, enhances T cell function, and induces regression of established metastases. *J Immunol* (1994) 152:5776–84.
49. Geiselhart LA, Humphries CA, Gregorio TA, Mou S, Subleski J, Komschlies KL. IL-7 administration alters the CD4:CD8 ratio, increases T cell numbers, and increases T cell function in the absence of activation. *J Immunol* (2001) 166:3019–27. doi:10.4049/jimmunol.166.5.3019
50. Min B, Yamane H, Hu-Li J, Paul WE. Spontaneous and homeostatic proliferation of CD4 T cells are regulated by different mechanisms. *J Immunol* (2005) 174:6039–44. doi:10.4049/jimmunol.174.10.6039
51. Seddon B, Zamoyska R. TCR and IL-7 receptor signals can operate independently or synergize to promote lymphopenia-induced expansion of naïve T cells. *J Immunol* (2002) 169:3752–9. doi:10.4049/jimmunol.169.7.3752
52. Boursaliان TE, Bottomly K. Survival of naïve CD4 T cells: roles of restricting versus selecting MHC class II and cytokine milieu. *J Immunol* (1999) 162:3795–801.
53. van Lent AU, Dontje W, Nagasawa M, Siamari R, Bakker AQ, Pouw SM, et al. IL-7 enhances thymic human T cell development in “human immune system” Rag2<sup>-/-</sup>IL-2R<sup>gamma</sup>mac<sup>-/-</sup> mice without affecting peripheral T cell homeostasis. *J Immunol* (2009) 183:7645–55. doi:10.4049/jimmunol.0902019
54. McCaughtry TM, Etzensperger R, Alag A, Tai X, Kurtulus S, Park JH, et al. Conditional deletion of cytokine receptor chains reveals that IL-7 and IL-15 specify CD8 cytotoxic lineage fate in the thymus. *J Exp Med* (2012) 209:2263–76. doi:10.1084/jem.20121505
55. Kimura MY, Pobezinsky LA, Guinter TI, Thomas J, Adams A, Park JH, et al. IL-7 signaling must be intermittent, not continuous, during CD8(+) T cell homeostasis to promote cell survival instead of cell death. *Nat Immunol* (2013) 14:143–51. doi:10.1038/ni.2494
56. Guimond M, Veenstra RG, Grindler DJ, Zhang H, Cui Y, Murphy RD, et al. Interleukin 7 signaling in dendritic cells regulates the homeostatic proliferation and niche size of CD4+ T cells. *Nat Immunol* (2009) 10:149–57. doi:10.1038/ni.1695
57. Osborne LC, Patton DT, Seo JH, Abraham N. Elevated IL-7 availability does not account for T cell proliferation in moderate lymphopenia. *J Immunol* (2011) 186:1981–8. doi:10.4049/jimmunol.1002224
58. Kisielow P, Teh HS, Bluthmann H, von Boehmer H. Positive selection of antigen-specific T cells in thymus by restricting MHC molecules. *Nature* (1988) 335:730–3. doi:10.1038/335730a0
59. Jameson SC, Hogquist KA, Bevan MJ. Positive selection of thymocytes. *Annu Rev Immunol* (1995) 13:93–126. doi:10.1146/annurev.iy.13.040195.000521
60. Kirberg J, Berns A, von Boehmer H. Peripheral T cell survival requires continual ligation of the T cell receptor to major histocompatibility complex-encoded molecules. *J Exp Med* (1997) 186:1269–75. doi:10.1084/jem.186.8.1269
61. Fischer UB, Jacovetty EL, Medeiros RB, Goudy BD, Zell T, Swanson JB, et al. MHC class II deprivation impairs CD4 T cell motility and responsiveness to antigen-bearing dendritic cells in vivo. *Proc Natl Acad Sci U S A* (2007) 104:7181–6. doi:10.1073/pnas.0608299104
62. Do JS, Min B. Differential requirements of MHC and of DCs for endogenous proliferation of different T-cell subsets in vivo. *Proc Natl Acad Sci U S A* (2009) 106:20394–8. doi:10.1073/pnas.0909954106
63. Viret C, Wong FS, Janeway CA Jr. Designing and maintaining the mature TCR repertoire: the continuum of self-peptide:self-MHC complex recognition. *Immunity* (1999) 10:559–68. doi:10.1016/S1074-7613(00)80055-2
64. Bender J, Mitchell T, Kappler J, Marrack P. CD4+ T cell division in irradiated mice requires peptides distinct from those responsible for thymic selection. *J Exp Med* (1999) 190:367–74. doi:10.1084/jem.190.3.367
65. Takeda S, Rodewald HR, Arakawa H, Bluthmann H, Shimizu T. MHC class II molecules are not required for survival of newly generated CD4+ T cells, but affect their long-term life span. *Immunity* (1996) 5:217–28. doi:10.1016/S1074-7613(00)80317-9

66. Revy P, Sospedra M, Barbour B, Trautmann A. Functional antigen-independent synapses formed between T cells and dendritic cells. *Nat Immunol* (2001) 2:925–31. doi:10.1038/ni713
67. Grandjean I, Duban L, Bonney EA, Corcuff E, Di Santo JP, Matzinger P, et al. Are major histocompatibility complex molecules involved in the survival of naïve CD4+ T cells? *J Exp Med* (2003) 198:1089–102. doi:10.1084/jem.20030963
68. Clarke SR, Rudensky AY. Survival and homeostatic proliferation of naïve peripheral CD4+ T cells in the absence of self peptide:MHC complexes. *J Immunol* (2000) 165:2458–64. doi:10.4049/jimmunol.165.5.2458
69. Witherden D, van Oers N, Waltzinger C, Weiss A, Benoist C, Mathis D. Tetracycline-controllable selection of CD4(+) T cells: half-life and survival signals in the absence of major histocompatibility complex class II molecules. *J Exp Med* (2000) 191:355–64. doi:10.1084/jem.191.2.355
70. Dorfman JR, Germain RN. MHC-dependent survival of naïve T cells? A complicated answer to a simple question. *Microbes Infect* (2002) 4:547–54. doi:10.1016/S1286-4579(02)01571-X
71. Jameson SC. T cell homeostasis: keeping useful T cells alive and live T cells useful. *Semin Immunol* (2005) 17:231–7. doi:10.1016/j.smim.2005.02.003
72. Martin B, Bourgeois C, Dautigny N, Lucas B. On the role of MHC class II molecules in the survival and lymphopenia-induced proliferation of peripheral CD4+ T cells. *Proc Natl Acad Sci U S A* (2003) 100:6021–6. doi:10.1073/pnas.1037754100
73. Martin B, Becourt C, Bienvenu B, Lucas B. Self-recognition is crucial for maintaining the peripheral CD4+ T-cell pool in a nonlymphopenic environment. *Blood* (2006) 108:270–7. doi:10.1182/blood-2006-01-0017
74. Al-Herz W, Alsmadi O, Melhem M, Recher M, Frugoni F, Notarangelo LD. Major histocompatibility complex class II deficiency in Kuwait: clinical manifestations, immunological findings and molecular profile. *J Clin Immunol* (2013) 33:513–9. doi:10.1007/s10875-012-9831-8
75. Hogquist KA. Immunodeficiency: when T cells are stuck at home. *Nat Immunol* (2008) 9:1207–8. doi:10.1038/ni1108-1207

**Conflict of Interest Statement:** The authors declare that the research was conducted in the absence of any commercial or financial relationships that could be construed as a potential conflict of interest.

Copyright © 2018 Mori and Pieters. This is an open-access article distributed under the terms of the Creative Commons Attribution License (CC BY). The use, distribution or reproduction in other forums is permitted, provided the original author(s) and the copyright owner(s) are credited and that the original publication in this journal is cited, in accordance with accepted academic practice. No use, distribution or reproduction is permitted which does not comply with these terms.

# Advantages of publishing in Frontiers



## OPEN ACCESS

Articles are free to read for greatest visibility and readership



## FAST PUBLICATION

Around 90 days from submission to decision



## HIGH QUALITY PEER-REVIEW

Rigorous, collaborative, and constructive peer-review



## TRANSPARENT PEER-REVIEW

Editors and reviewers acknowledged by name on published articles



## REPRODUCIBILITY OF RESEARCH

Support open data and methods to enhance research reproducibility



## DIGITAL PUBLISHING

Articles designed for optimal readership across devices



FOLLOW US  
@frontiersin



IMPACT METRICS  
Advanced article metrics track visibility across digital media



EXTENSIVE PROMOTION  
Marketing and promotion of impactful research



LOOP RESEARCH NETWORK  
Our network increases your article's readership

### Frontiers

Avenue du Tribunal-Fédéral 34  
1005 Lausanne | Switzerland

Visit us: [www.frontiersin.org](http://www.frontiersin.org)

Contact us: [info@frontiersin.org](mailto:info@frontiersin.org) | +41 21 510 17 00